EGG-WM-8949
July 1990

INFORMAL REPORT

FY 89 REPORT RWMC VADOSE ZONE BASALT CHARACTERIZATION

C. F. Knutson
K. A. McCormick
R. P. Smith
W. R. Hackett[a]
J. P. O'Brien[a]
J. C. Crocker[a]

a. Idaho State University

Idaho National Engineering Laboratory

Managed by the U.S. Department of Energy

EG&G Idaho

Work performed under DOE Contract No. DE-AC07-76ID01570

EGG-WM--8949

DE90 015420

FY 89 REPORT

RWMC VADOSE ZONE BASALT CHARACTERIZATION

C. F. Knutson
K. A. McCormick
R. P. Smith
W. R. Hackett[a]
J. P. O'Brien[a]
J. C. Crocker[a]

Published July 1990

EG&G Idaho, Inc.
Idaho Falls, Idaho 83415

Prepared for the
U. S. Department of Energy
Idaho Operations Office
Under DOE Contract No. DE-AC07-76ID01570

a. Idaho State University

ABSTRACT

The studies discussed in this report were conducted for the Department of Energy (DOE) at the Idaho National Engineering Laboratory (INEL). This report summarizes the petrological information developed as an initial step in the characterization of basalt in the vadose zone beneath the Radioactive Waste Management Complex (RWMC). The study was based on the concept of modified plains volcanism, which explains the emplacement of basalt lava flows on the Eastern Snake River Plain. A petrologic study, including lithologic logging of the core and representative samples of basalt, was performed. Subsequent studies of the core samples were also conducted. Petrophysical studies were performed measuring porosity, permeability, grain density, equilibrium water saturation, and pore-size distribution of flow groups. Thin cylindrical slices were cut from the petrophysical plugs, and petrographic studies analyzing texture and mineralogy were accomplished using a petrographic microscope. These studies, along with geostatistical studies of Box Canyon of the Big Lost River and Hell's Half Acre, resulted in a conceptual geologic model of the basalt of the vadose zone under the RWMC. The evaluation of this preliminary model was used as a basis for recommendations of subsequent data acquisition efforts.

EXECUTIVE SUMMARY

This document summarizes the geostatistical information developed in an initial step toward the characterization of basalt in the vadose zone beneath the Radioactive Waste Management Complex (RWMC). This is considered a preliminary effort since significant future efforts will be required before an adequate characterization of this complex geological system is accomplished.

The emplacement of basalt lava flows can be understood in the context of a modified version of the plains volcanism of Greeley (1982). His model must be modified to account for concentration of volcanic activity in rift zones and for deposition of sedimentary interbeds in the basalt sequence between the rift zones. Sedimentary interbeds were deposited under climatic conditions that ranged from humid glacial to subarid.

The RWMC is located in an inter-rift zone area and the basalts encountered there are from the medial and distal flow facies. The uppermost flow group at the RWMC originated at Quaking Aspen Butte to the southwest. At the RWMC, the flow direction of this ~100 Ka unit is to the south and southeast. The flow group underlying this is a ~200 Ka unit that originated at Butte 5206 to the south-southeast. The origin of the successively deeper flow groups is undetermined at this time.

The quantitative data presented in this report were gleaned from descriptions and measurements made on the cores from 15 RWMC wells. Existing geophysical logs are not of sufficient quality to yield quantitative interpretations. The general stratigraphic nomenclature adopted is consistent with that of Anderson and Lewis (1989). Their stratigraphic hierarchy consists of flow groups separated by interbeds. The flow groups are composed of two or more overlying flow units having consistent petrologic properties. These flow units are made up of one to five individual flows, flow lobes, or "fingers." The median thickness of

an individual flow is 15 ft (4.6 m). The individual flows ideally consist of four elements: a substratum, a bottom vesicular element, a central nonvesicular element, and an upper vesicular element. The observed median thicknesses of the three upper elements are 1.5, 7.5, and 6 ft (0.5, 2.3, 1.8 m). Thus, the central element is usually the thickest, and the lower element the thinnest.

The flow units are frequently correlatable on the basis of their phenocrysts and groundmass textures. For example, flow unit B-1 is intergranular, B-2 is prophyritic, and B-3 is intergranular. The principal minerals are plagioclase, olivine, clinopyroxene, and minor Fe-Ti oxides. In addition, glass and opaque oxide masses are common constituents of the vesicular elements. Plagioclase laths and bundles, aggregates of olivine crystals, and ophitic and sub-ophitic clinopyroxenes are the most common phenocrysts. Correlations are generally made by relating the sizes and amounts of the plagioclase phenocrysts.

Permeabilities, porosities, and densities were measured both in the field on full cores and in the laboratory on 1 by 1.1 in. (25 by 28 mm) cylinders. Permeability is generally controlled by the matrix characteristics. The median permeabilities of the lower, central, and upper elements are 4, 8, and 7 md (md$\simeq\mu m^2$). The lower permeability of the vesicular elements is a function of the less crystalline state of the matrix. The median porosities of the lower vesicular, central, and upper vesicular elements are 21, 10, and 22%, respectively. The porosity of the vesicular elements is controlled by the fraction of vesicles present. The median grain densities for the lower, central, and upper elements are 3.045, 3.055, and 3.045 g/cm^3, respectively. The slightly lower median grain density of the vesicular elements is also probably a function of the slightly less crystalline state of the rock matrix. Since the grain densities are similar, the bulk densities are strictly a function of the porosity.

The capillary pressure, pore-size distribution, and surface area are currently being determined on 45 representative basalt samples. This is

being carried out using the equilibrium saturation method. The final results will be available early in 1990. Preliminary data are presented in this report.

Geostatistical studies were carried out at Box Canyon of the Big Lost River to develop insight into the three-dimensional variability of the basalt flows. The basic geometry of the flows is not planar stratified, but rather, a complex interfingering of lobes. The ratios of thickness to length of the flow lobes exposed on the canyon walls were measured. The median length to width to thickness (or height) ratio is >8.4:4.6:1. Thus, the median flow thickness from the core data result in flow dimensions of the order of >130:69:15 ft (>40:21:4.6 m). The general flow direction of the H to R segments of the Box Canyon flows is northeast-southwest.

Additional work, performed at the Hell's Half Acre flow, resulted in variograms that can be used to evaluate kriging results for flow top geometries and flow thickness variations at the RWMC. Measurements of flow top characteristics also resulted in insight into expected substratum conditions. Smooth/uneven surfaces occur 51%, fracture/fissures 19%, rubble 17%, and bouldery/blocky/broken surfaces 13% of the time.

At this point in time, we have a good deal of geostatistical data available that could be used, by stochastic interpolation, to construct a three-dimensional subsurface model at the RWMC. However, the quantitative data for the departure points for such an interpolation are missing. Thus, we have recommendations for future programs:

- A quantitative data set should be developed for all future wells. This should include:
  - An appropriate suite of quantitative geophysical logs;
  - Detailed lithologic logging of continuous core;
  - Flow or performance tests.

These data should be archived in a generally available data base (such as ERIS).

- The remainder of the currently available RWMC core should be lithologically logged to provide additional subsurface stratigraphy.

- The petrography of the surface flow groups should be determined to allow the source identification for the flows below flow group B.

- Flow tests of the high transmissivity elements at outcrops near RWMC should be made to provide insight into the flow capability of these elements.

- Several tomographic characterization techniques should be evaluated.

- Other correlation techniques should be evaluated, such as:

  - Paleomagnetism;

  - Magnetics;

  - Trace element geochemistry;

  - Major element geochemistry;

  - Mineral composition;

  - Better radiometric age dating techniques, etc.

ACKNOWLEDGMENTS

We would like to thank members of DOE-ID Buried Waste Division and EG&G Idaho Buried Waste Management for support and assistance with this project.

This work was performed under auspices of the U. S. Department of Energy, DOE Contract No. DE-AC07-761D01570.

CONTENTS

APPENDIXES

FIGURES

TABLES

FY 89 REPORT--RWMC VADOSE ZONE BASALT CHARACTERIZATION

INTRODUCTION

The purpose of this study is to provide geologic data that can be used to construct a three-dimensional subsurface model of the vadose zone beneath the Radioactive Waste Management Complex (RWMC). The type of modeling effort that is envisioned is the development of a hybrid stochastic simulation. A hybrid model is necessary because of the requirements to treat both (1) discrete parameters, such as the geometry of individual flows, and (2) continuous parameters, such as the permeability variation within a flow.[a]

The procedures being used in this study are to:

- Review the general geologic picture to understand the paleoenvironment of the RWMC area.
- Develop parameter distribution and variations through geostatistical studies of medial and distal facies of analogous flow units that are available for examination at Box Canyon and Hell's Half Acre.
- Carefully measure the lithologic and petrophysical parameter of the available cores taken during previous investigations at the RWMC.

The effort of the Radioactive Waste Management Complex (RWMC) Basalt Characterization (work package 3X1EN5500) in FY-1989 was largely to acquire quantitative data for parameters that can be used to develop a conceptual

---

a. See Haldorsen and Damsleth, 1990, for an excellent description of hybrid stochastic modeling.

model of the near-surface basalts in the area. These data acquisition efforts can be summarized in the following categories:

- Regional geologic analysis and literature search. Basalts of the Eastern Snake River Plain (ESRP) were evaluated, and a literature search of GEOREF and other data bases was conducted.

- Petrologic descriptions of a suite of available, but unprocessed cores from old RWMC wells. This study, carried out largely by J. P. O'Brien (an ISU graduate student), included the detailed lithologic logging of the core and the selection of representative samples from each recognizable basalt flow. The samples were used in subsequent petrographic and petrophysical studies.

- Petrophysical studies of core samples. These studies used 25 x 28 mm cylindrical plugs cut from the representative samples of each flow. Parameters measured were porosity, permeability, grain density, bulk density, equilibrium water saturation, and pore-size distribution.

- Petrographic studies of core samples. These studies used thin, cylindrical slices cut from the ends of the petrophysical plugs. The slices were petrographically examined and approximately 150 were selected for thin sectioning and subsequent detailed statistical analysis using a petrographic microscope. The petrographic analysis was carried out by John C. Crocker (an ISU graduate student).

- Statistical studies of surface and near-surface basalts at Hell's Half Acre near the southeastern margin of the INEL (Idaho National Engineering Laboratory) and Box Canyon of the Big Lost River near the southwestern margin of the INEL. These geostatistical studies were carried out to provide a framework for the evaluation of flow morphology and other discrete modeling parameters. These studies complimented the continuous parameter interpretation of the petrologic, petrophysical, and petrographic efforts.

- Development of a preliminary conceptual model. The evaluation of this model was used as a basis for recommendations concerning subsequent data acquisition efforts.

The procedures used and the results of the studies will be discussed in the following sections of the report.

REGIONAL BASALT GEOLOGY

RWMC Basalt Lava Flows in Regional Context

The basalt lava flows at RWMC and throughout the INEL are thought to have been formed by "plains-style" volcanism, as shown in Figure 1 (Greeley, 1982). This style is intermediate between flood basalt volcanism like that of the Columbia Plateau, and basaltic shield volcanism like that of the Hawaiian Islands. The very low shield volcanoes, with slopes of about one degree dip, form in an overlapping manner, and this overlapping and coalescing of flows form the low relief surface of the Eastern Snake River Plain (ESRP). Tube-fed lava flows travel long distances and minor fissure-fed flows help to fill in low areas between shields, producing subdued topography.

Interpretation of INEL- and ESRP-wide subsurface geology obtained from drill hole information suggests that for this study the concept of plains volcanism be modified in two ways. First, volcanic vents are not randomly distributed over the plain, but are more or less restricted to volcanic rift zones (Figure 2). Almost all the vents in the INEL region of the ESRP are located in one of the rift zones. The rift zones are characterized by fissuring and minor faulting that result from emplacement of dikes which feed the vents (Smith et al., 1989a, 1989b). Since volcanic eruptions occur in rift zones more commonly than elsewhere, the rift zones persist as "ridges" of high elevation. Second, deposition of sediments is a major contributor to maintaining a low topographic relief by filling in low areas between shields and rift zones. These sediments are of several types: loess, alluvial silts, sands, and gravels, and lacustrine clays and silts. Sediments on the INEL were deposited from (1) the Big Lost River and other streams that enter the plain from the intermountain valleys to the north, (2) the waxing and waning of Lake Terreton during the last few million years, and (3) loess deposition.

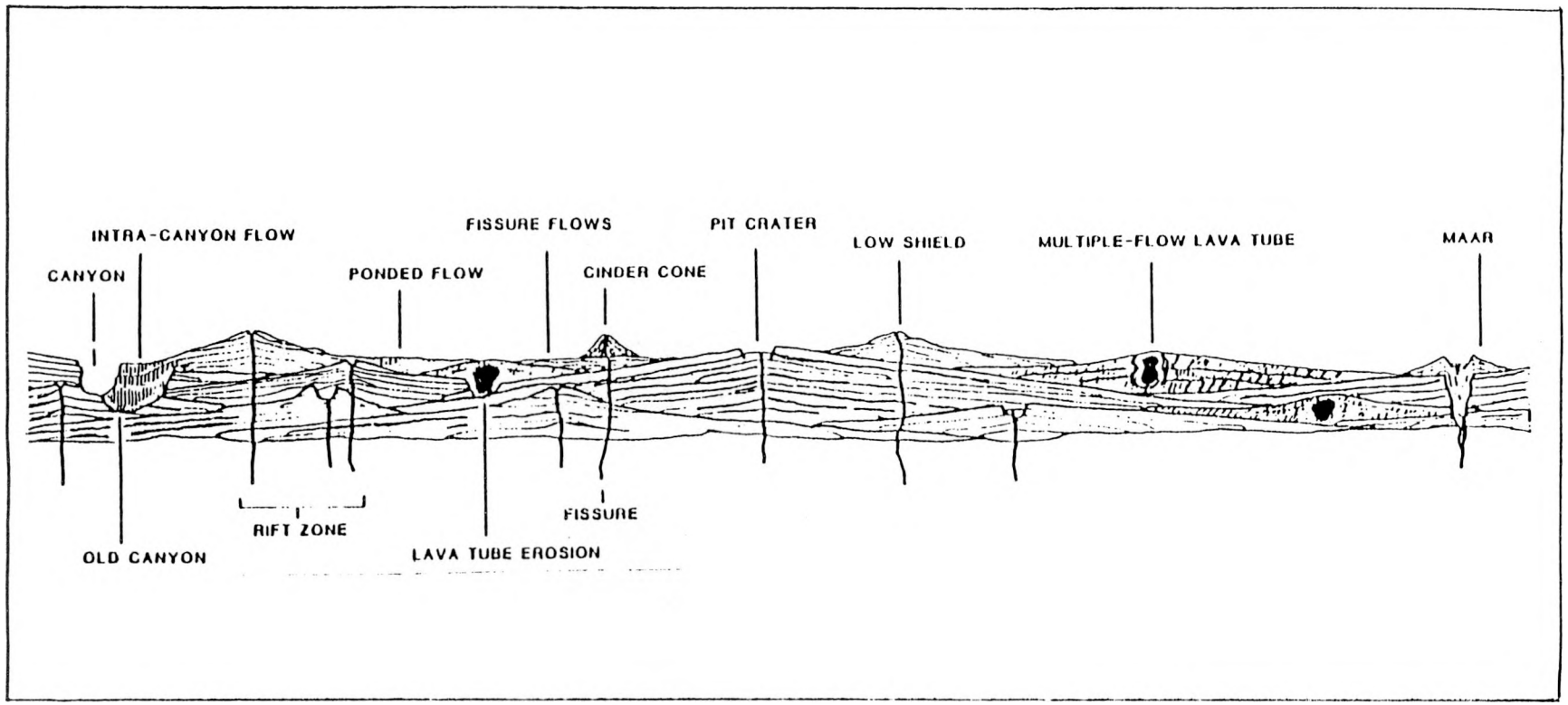

Figure 1. Schematic cross section showing the salient features of a "plains" basalt region, typified by the Snake River Plain.

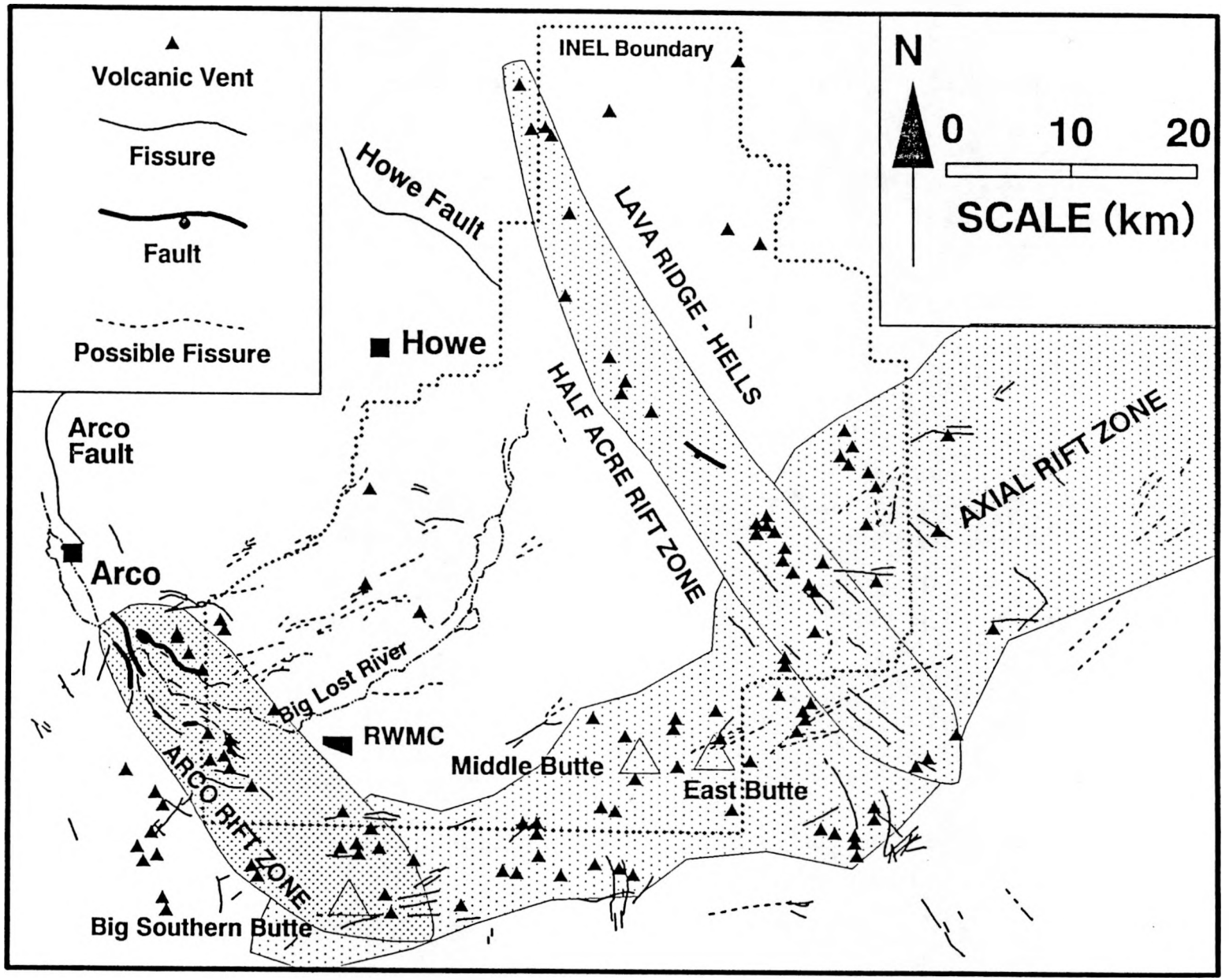

Figure 2. Volcanic rift zones near the INEL.

Figure 3 shows the proposed volcanic-sedimentological model for the INEL area. Here, we see the complex intercalation of basalt lava flows from vents in rift zones with sedimentary material between rift zones. On the INEL, the course of the Big Lost River has been partly controlled by the existing rift zones so that it flows into the basin between rifts.

The RWMC is located near the southwestern margin of the inter-rift basin near the Arco Rift Zone and the Axial Rift Zone. The area has received lava flows from both rift zones, alluvial sediments from the Big Lost River, and loess deposits from sources to the southwest. The volcanism has been episodic, so that one or several lava flows are emplaced over a short period of time (a few centuries to a few thousand years), with little interflow sedimentary accumulation. These volcanic episodes are separated by long periods of time (tens to hundreds of thousands of years), during which sedimentary interbeds accumulate (Kuntz et al., 1986; Champion et. al., 1988).

Source Vents and Flow Directions for Lava Flows at RWMC

Near-surface basalt lava flows at the RWMC were erupted from several volcanic vents in the southwest part of the INEL. Most of the lava flows above the water table are younger than 500 Ka[a] (Champion et al., 1988) and were erupted from vents in the Arco Rift Zone.

Drill hole (DDH) 77-1 (Figure 4), located on the north side of the RWMC, penetrated a number of different lava flows above the water table. The topmost one (flow group A, flow units A-1 and A-2, see Figures 10 and 11) is about 100,000 years old and flowed many miles from its source vent at Quaking Aspen Butte to the southwest of the RWMC. The overall direction of the flow is northeastward, but in the local area of the RWMC the flow direction curves toward the south and southeast (Figure 4).

---

a. Ka is the dimensional abbreviation for "thousands of years before the present".

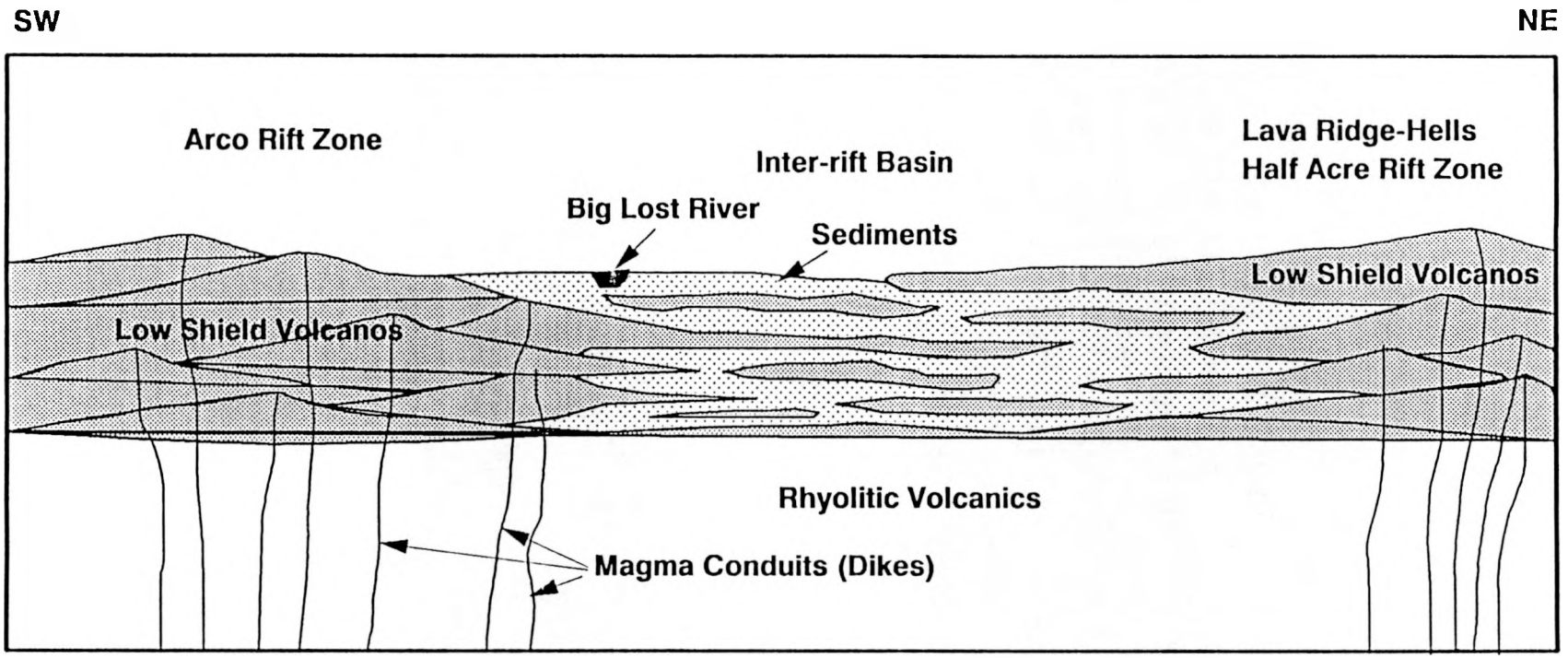

Figure 3. Schematic diagram of modified "plains-style" volcanism (RWMC lies south of this cross section near Arco Rift Zone).

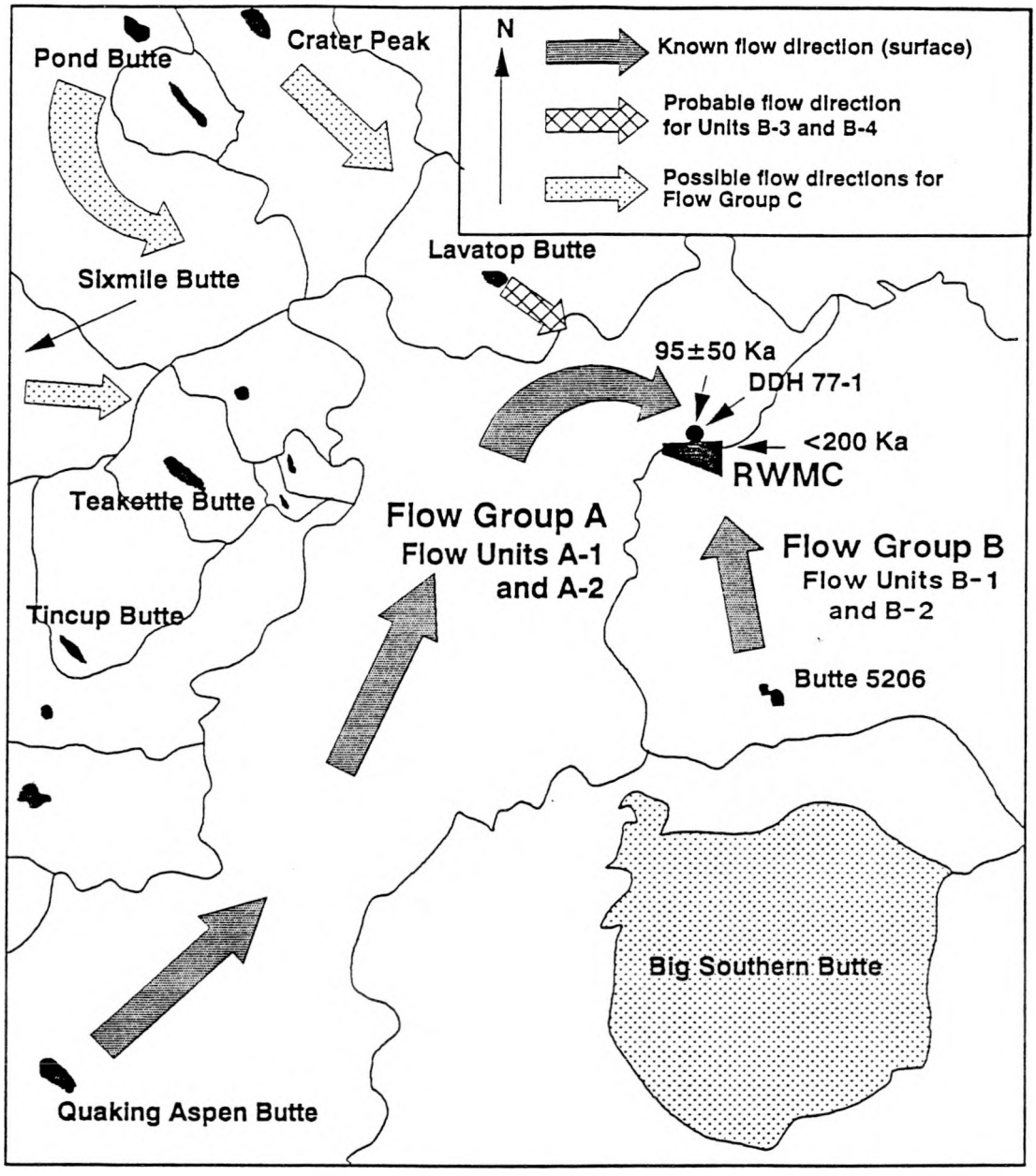

Figure 4. Inferred source vents and flow directions for lava flows at the RWMC.

The first two lava flows of group B (flow units B-1 and B-2) in DDH 77-1[a] are also exposed in the Subsurface Disposal Area (SDA) burial pit. These flows came from Butte 5206, just north of Big Southern Butte (Figure 4). Their flow direction at the RWMC is almost due north. They have been dated at <200 Ka (Champion et al., 1988).

The source(s) of flow units B-3 and B-4 in DDH 77-1 are more problematic. The most likely source is Lavatop Butte (Figure 4). If that is the case, then the flow direction at the RWMC is most probably southeastward, but local topographic conditions could have influenced the direction. Their radiometric age is also about 200 Ka (Kuntz, et al., 1980).

Lava flows below flow group B in DDH 77-1 could have been erupted from numerous vents in the RWMC area. The most likely ones are Crater Peak, Pond Butte, and Sixmile Butte. These are all large vents with lava flows that could have travelled many miles. Comparison of the detailed hand specimen and petrographic descriptions of RWMC core developed by J. P. O'Brien and John Crocker (Appendixes A and B) with the lavas from these possible vents could help define the source vents and flow directions of lava flows older than flow unit B-2 at the RWMC.

Idealized Volcanic Facies of Basalt Lava Flows

Lava flows exhibit varying characteristics dependent on the distance from their source. The proximal volcanic facies of a basalt lava flow is a zone of thin lava, cavernous flows (termed shelly pahoehoe) with interlayered vent facies of pyroclastics and agglutinate (Figure 5). The thin lava grades outward into thicker flows with upper and lower crusts, upper and lower vesicular zones, and columnar-jointed, massive interiors. The distal facies exhibit numerous terminations of lava flows and

---

a. The DDH 77-1 well is the deepest well near the RWMC (720 ft, 219 m) and was studied by the USGS to determine flow group ages, paleomagnetic characteristics, and sources.

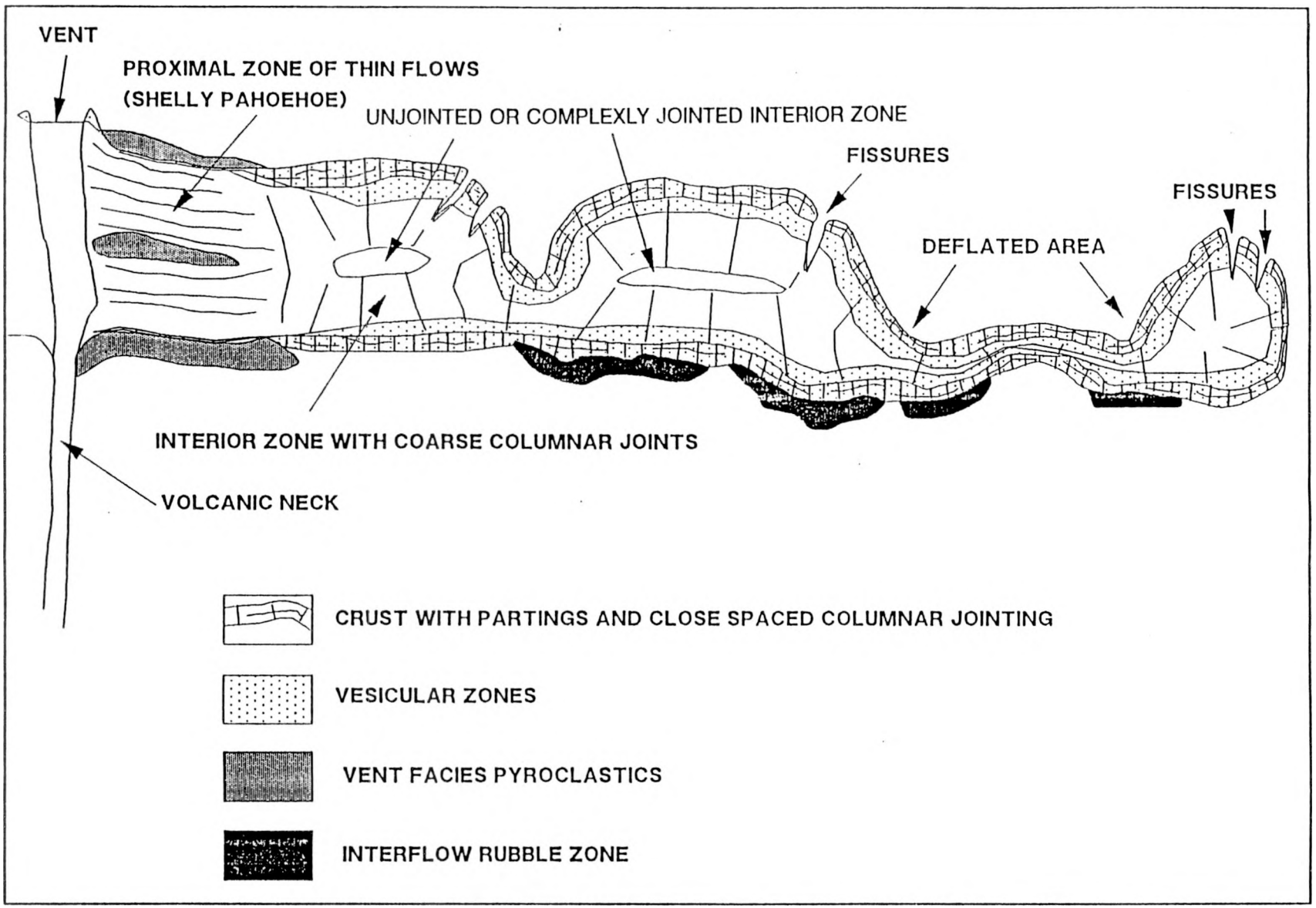

Figure 5. Idealized section of a basalt lava flow on the ESRP.

irregularly-shaped lobes or "fingers" that extend outward from the main body of the flow. The intermediate and distal facies contain areas from which lava has flowed to lower areas, causing the upper crust to collapse into irregular depressions. Fissures have developed in buckled crust around the collapsed areas and near the distal ends of the flow.

In the RWMC area, none of the lava flows observed at the surface or at depth in drill core exhibit proximal facies characteristics. From surface observations (Figure 6), we see that the two uppermost lava flows represent distal facies. It is likely that deeper flows at the RWMC are also distal or intermediate facies since the area is just outside the rift zones and within the inter-rift basin.

Bibliography

A bibliography for ESRP basalts, developed during a search of the geologic data bases, is presented as Appendix C.

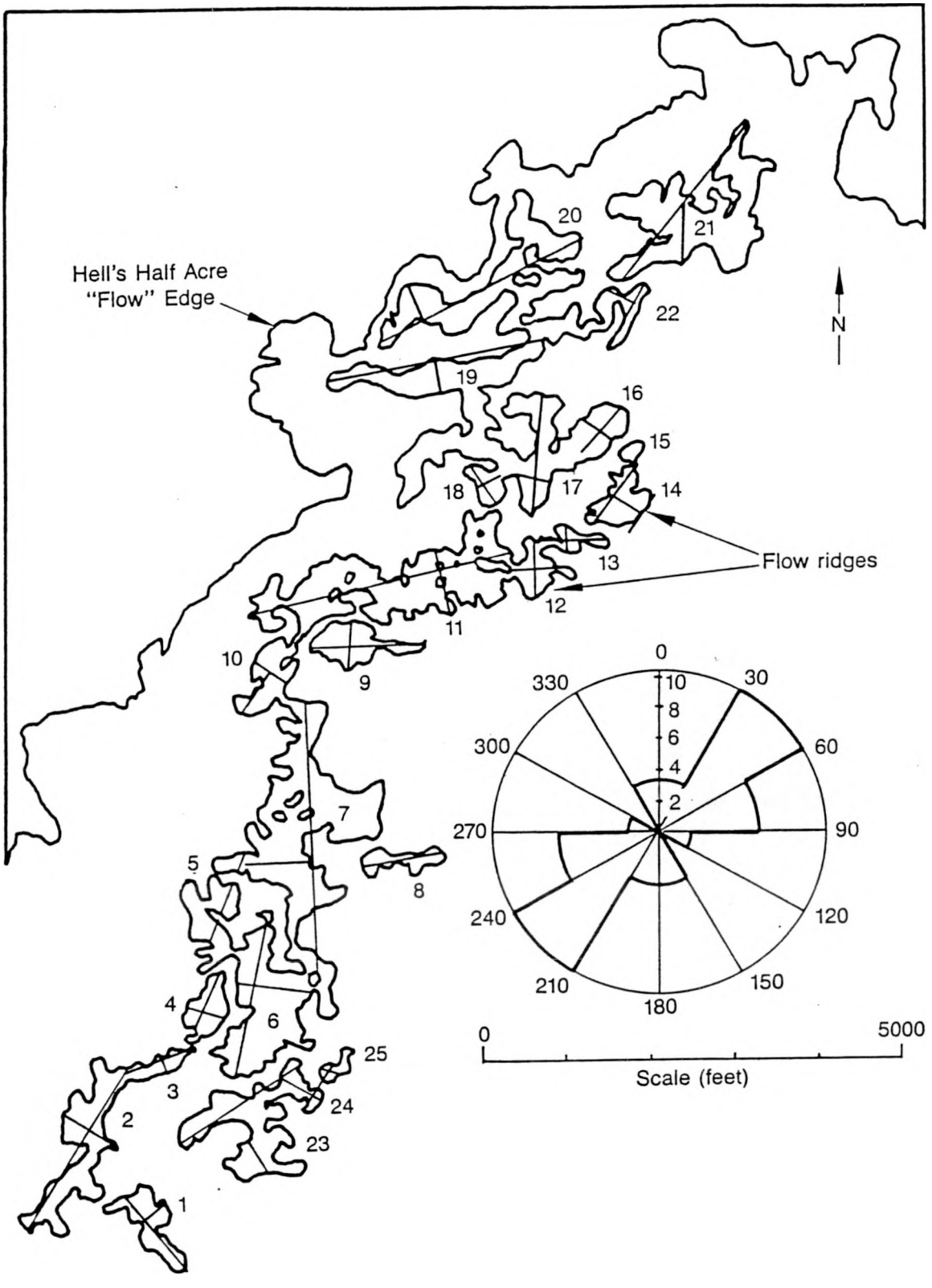

Figure 6. Hell's Half Acre flow ridges sketched from stereo photos (rose diagram shows orientation of long axis of ridges).

DETAILED CORE DESCRIPTIONS

Procedure

The core stored in CFA-649 was inventoried and cores from 15 wells, which provided reasonable areal coverage of the RWMC, were selected for detailed descriptions (Figure 7). A core logging form and protocol were developed by R. P. Smith, C. F. Knutson, and W. R. Hackett (Figure 8). The majority of the core was logged by J. P. O'Brien.

The core was removed from the 10-ft (3-m) boxes or plastic tubes and carefully assembled on a 12-ft (3.7-m) tray. The geophysical logs were used to attempt to correctly locate the sedimentary interbeds (the logs were generally inadequate for the evaluation of the basalt properties). The best estimate of the depths of the core was made from the information on the boxes and from the geophysical logs. The estimated depth was marked on the core at 1-ft (0.3-m) intervals. Parallel red and blue lines were drawn longitudinally down the core, with the red line on the right when looking toward shallower core depths. This provided a definite up/down reference for pieces of core removed from the tray for examination or measurement.

A field permeameter and porosimeter were developed to provide the capability for making quantitative measurements during the core examination phase (see Appendix D for descriptions and procedures for use of the field equipment).

The 10-ft (3-m) section of core was petrologically logged. Samples were selected from each identified flow event and were sent to the EG&G Geosciences Core Laboratory for additional studies. The core was then boxed in 3-ft (1-m) cardboard boxes, which were labeled and stored on shelves in the west room of building CFA-649.

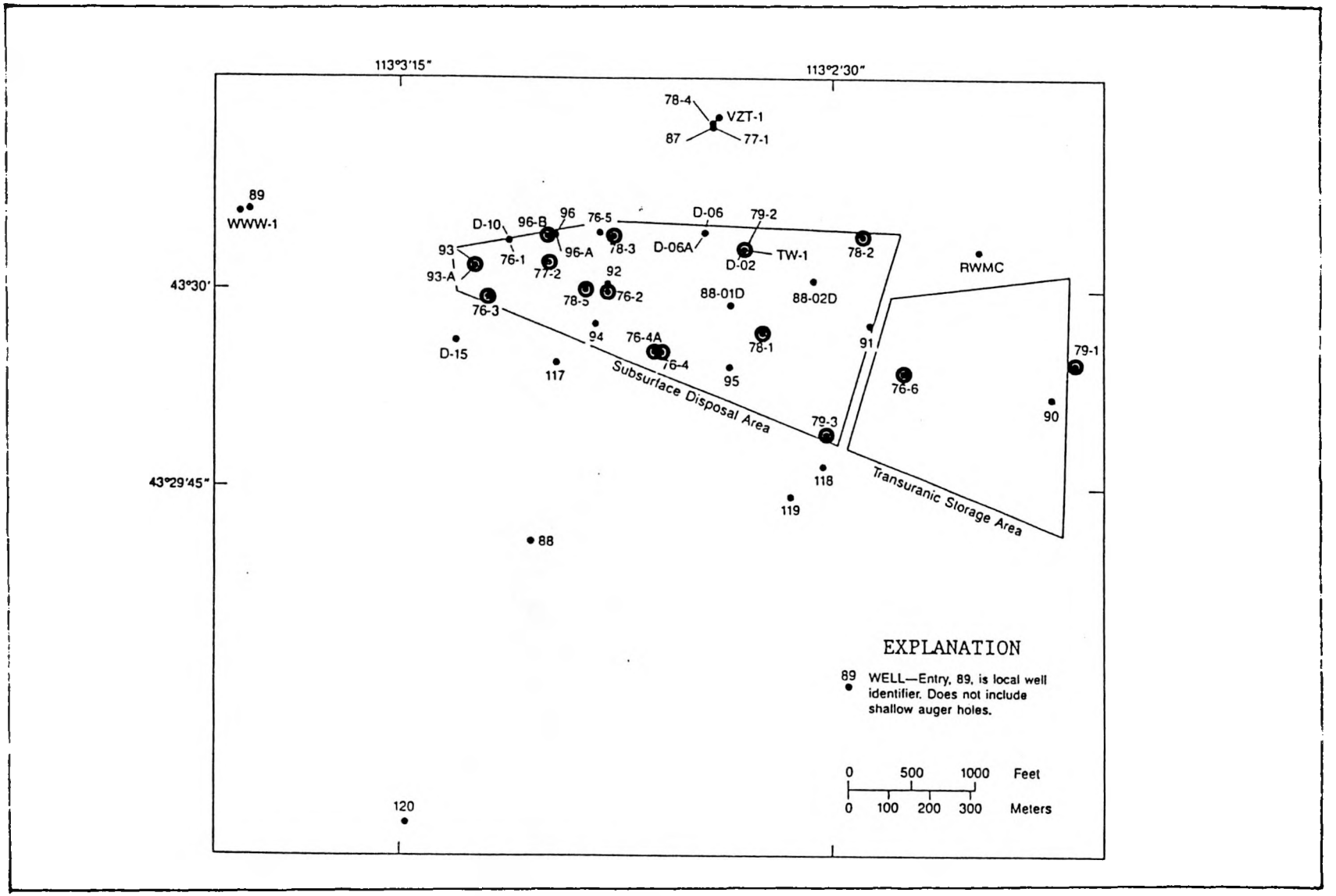

Figure 7. Location of wells at the RWMC (wells with core logged in project are circled).

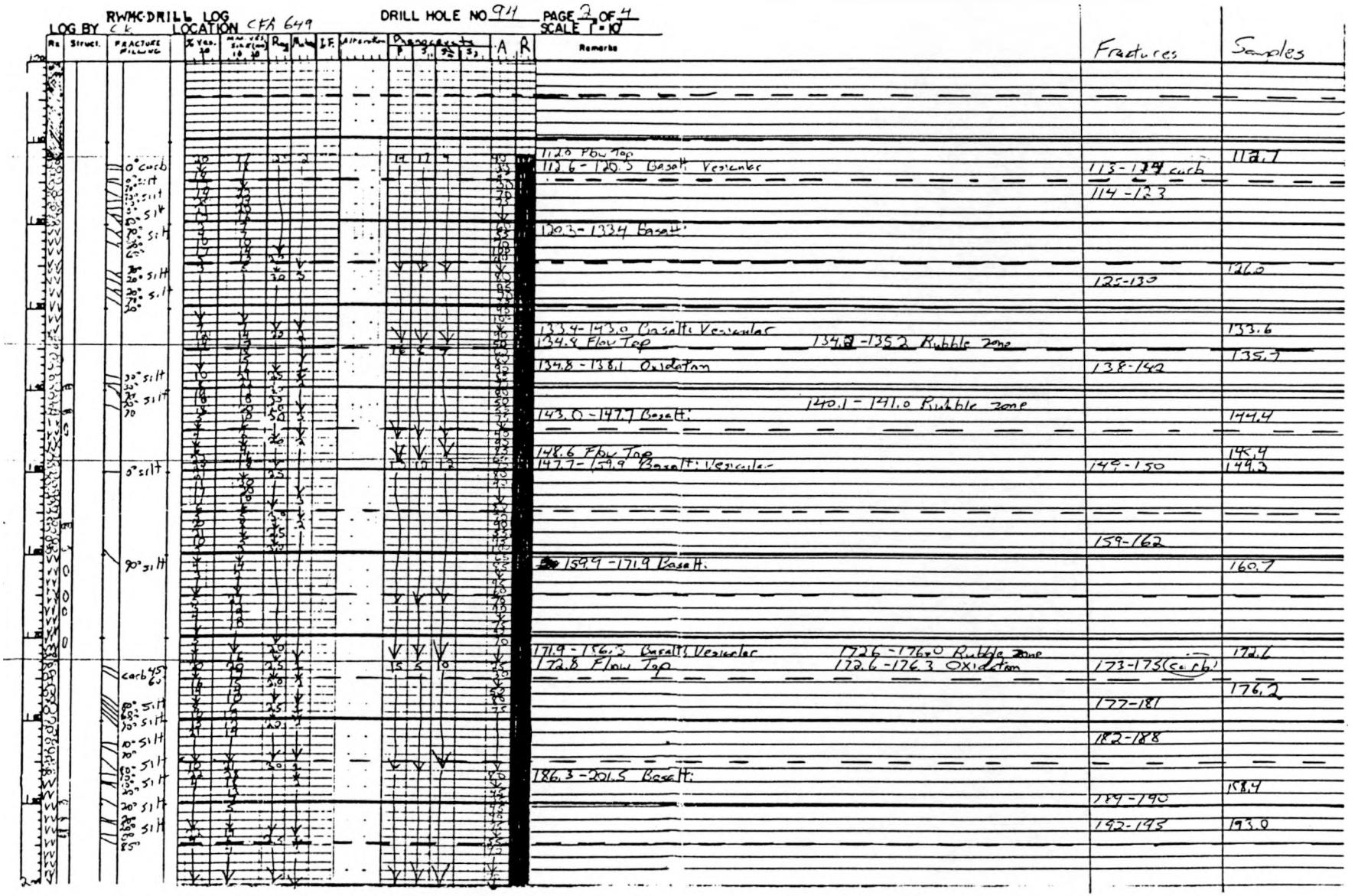

Figure 8. Example core logging sheet for Drill Hole 94.

Description of Core

The core logging information was evaluated in the general stratigraphic framework of flow groups and interbeds developed by Anderson, Lewis, and others (Anderson and Lewis, 1989). These flow groups can be differentiated into flow units exhibiting similar lithologies. The flow units are constructed of one or more flows or flow lobes.

In general, each flow is composed of four elements: (1) an upper vesicular zone, (2) a central massive zone, (3) a lower vesicular zone, and (4) a substratum. The flows can be integrated into flow units on the basis of composition and mineralogy, grain/phenocryst size, oxidation, and color. The flow units can be assigned to the complex flow group stratigraphy (groups A, B, C, etc.) of Anderson and Lewis (Anderson and Lewis, 1989), on the basis of the intervening sedimentary interbeds (Anderson and Lewis' surficial layer, interbed AB, BC, etc.).

Correlation of flows between wells is questionable; however, tentative correlations of flow units have been made (Anderson and Lewis, 1989). East-west correlations of flow units are presented in Figure 9 through 11. Figure 9 presents the location map for cross sections A-A′ and B-B′. Figure 10 is east-west cross section A-A′ across the northern tier of wells at the RWMC, and Figure 11 is east-west cross section B-B′ across the southern tier of wells.

The individual flow groups can be divided into one or more flow units, e.g., A-1 and -2, B-1, -2, and -3, etc., and these units can be divided into 1 to 5 individual flows.

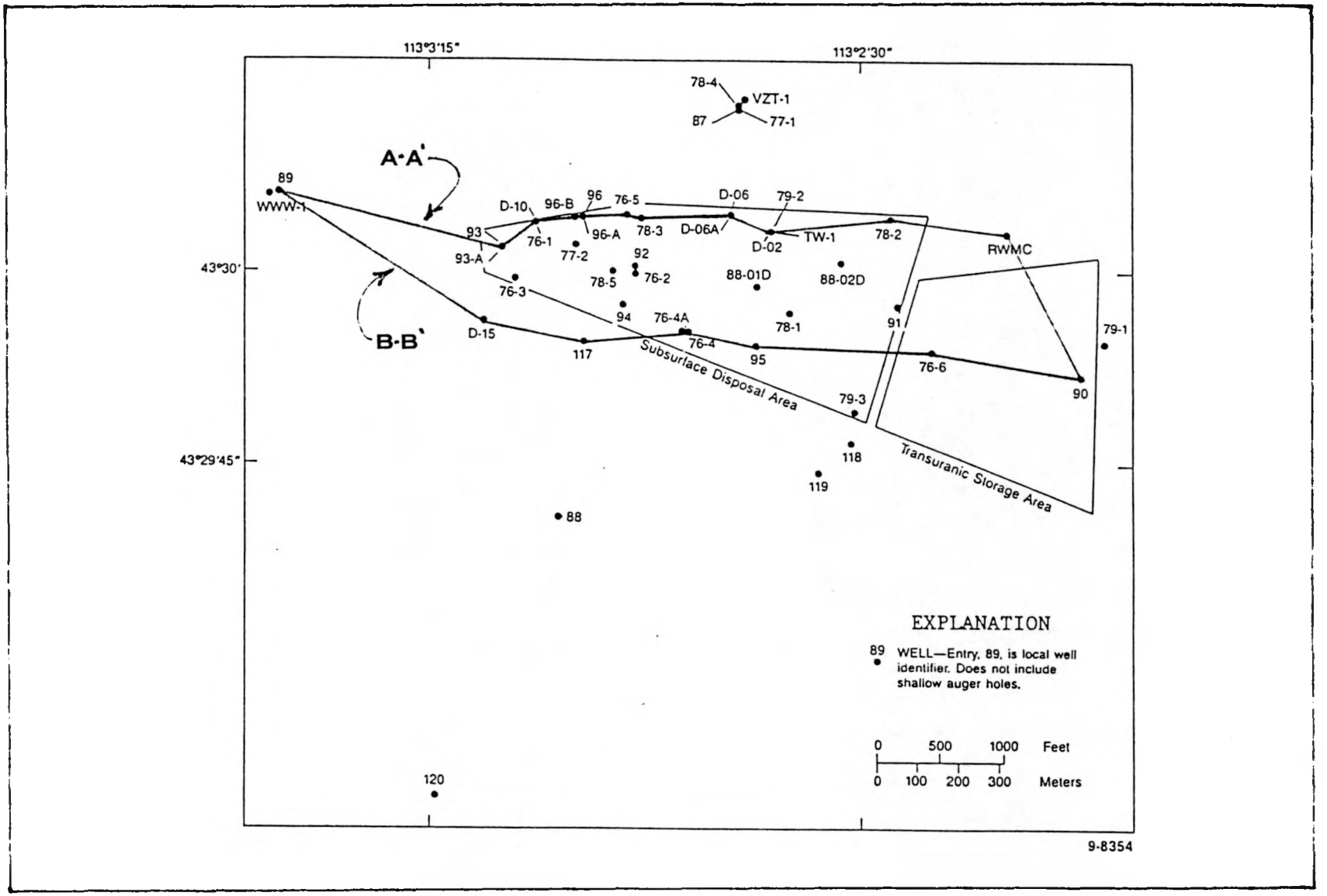

Figure 9. Location of wells and cross sections A-A′ and B-B′ at the RWMC (Anderson and Lewis, 1989).

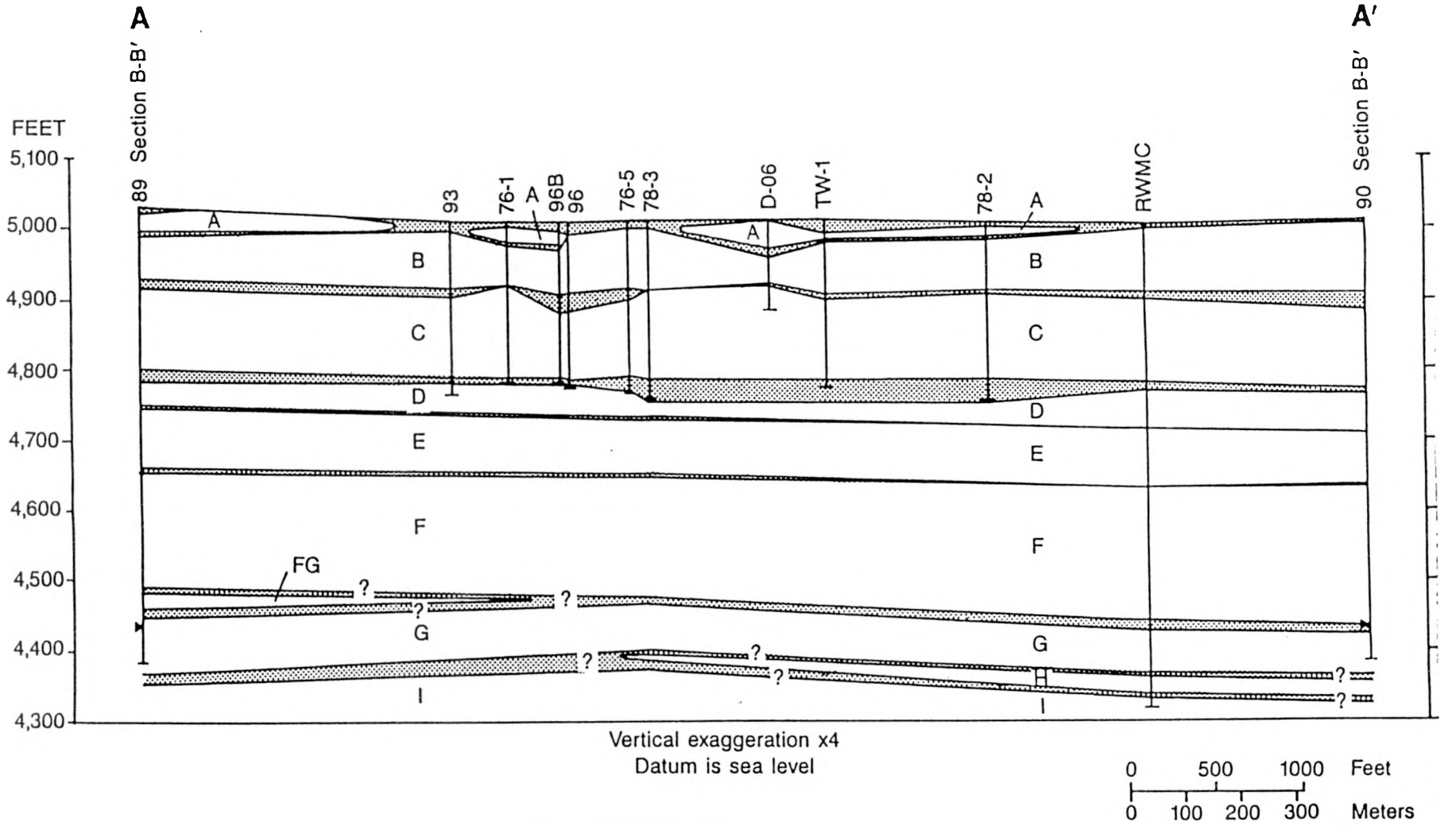

Figure 10. Schematic cross section A-A′ showing configuration of flow groups (Anderson and Lewis, 1989).

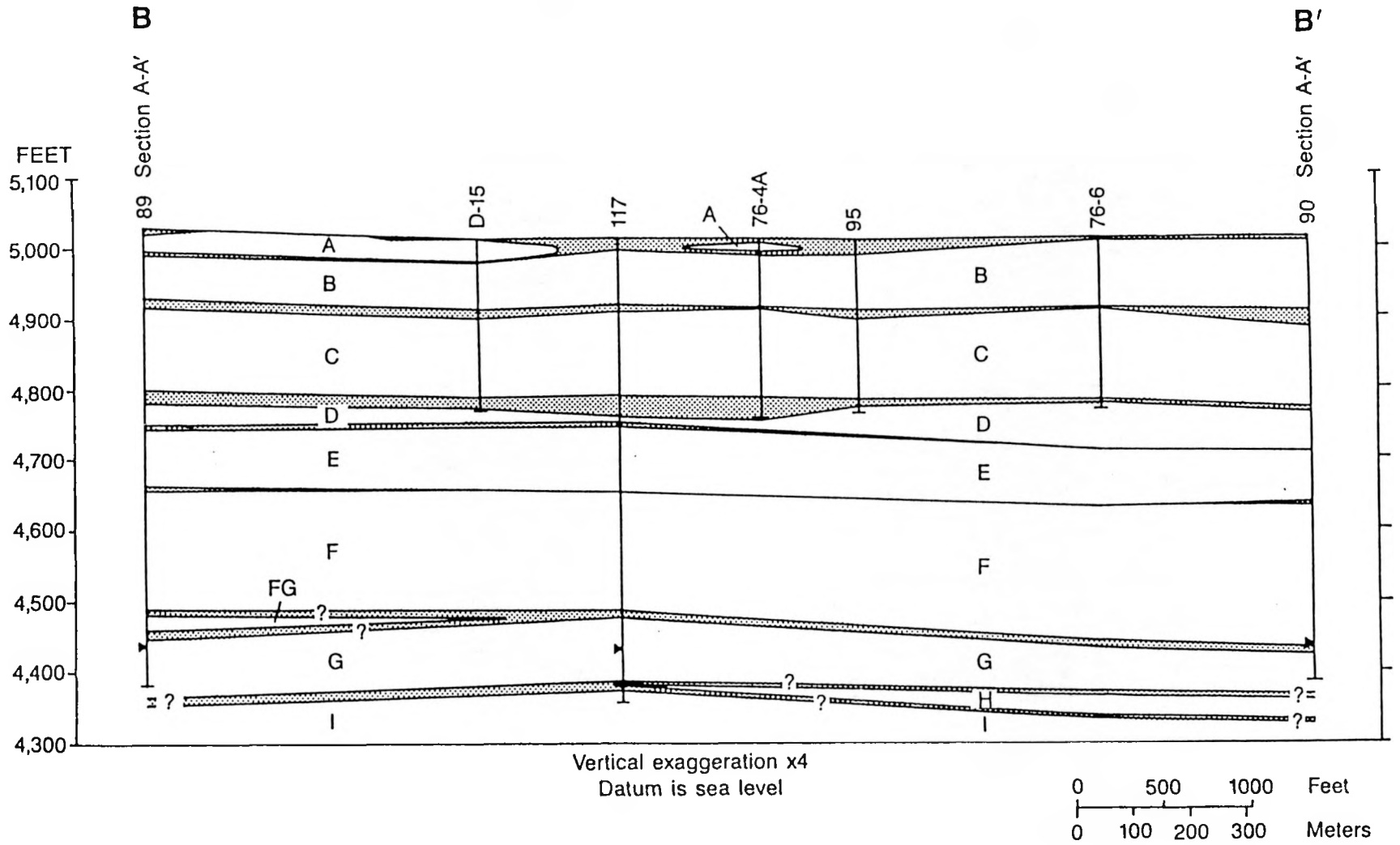

Figure 11. Schematic cross section B-B′ showing configuration of flow groups (Anderson and Lewis, 1989).

An analysis of the thicknesses of individual flow elements indicated the following:

Flow Element	Median Thickness (ft)	Range (ft)	Number of Measurements
Top Vesicular Element	6	1-28	114
Central Element	7.5	0-44	114
Bottom Vesicular Element	1.5	1-6	114
Intermediate Vesicular Element	3	0-8	8
Collapse/Rubble Element	4	0-12	13
Complete Flow	15	1-56	114

Thus, the central zone is generally the thickest, with the top vesicular zone next, and the bottom vesicular zone the thinnest of the commonly occurring components. The size distribution plots of the individual flow elements, as well as that of the total flow thickness are presented as Figure 12. The size distributions were normalized to determine if the individual elements were a characteristic fraction of the flow thickness. The resulting fractional distributions were similar to the thickness values.

Flow Element	Median Thickness (%)	Range (%)	Number of Measurements
Top Vesicular Element	35	9-76	114
Central Element	49	11-84	114
Intermediate Vesicular Element	17	0-32	8
Bottom Vesicular Element	11	1-42	114

The normalized distribution plots are presented as Figure 13.

The collapse/rubble zone is the name given to a single complex vesicular zone, often rubblized, that occurs between two flow breaks. These elements may be one of the most transmissive portions of the basalt sequence. They occur relatively frequently and about 13% of the basalt-basalt contacts are of this type (119 flows were used in the analysis; 20 basalt flow contacts were with sediments, and 13 were with a collapse/rubble element).

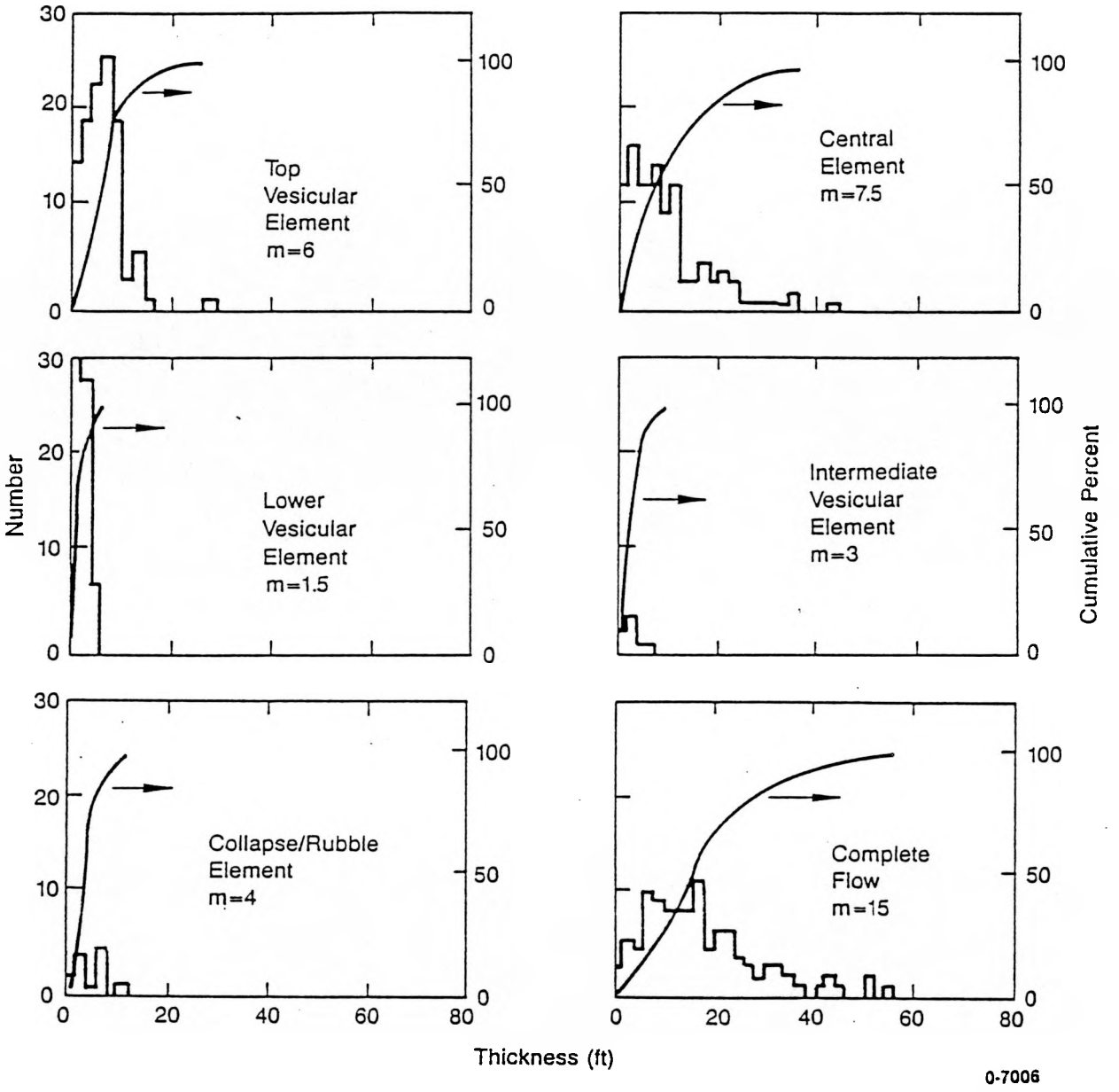

Figure 12. Thickness distributions for flow elements and complete flows (m = median value).

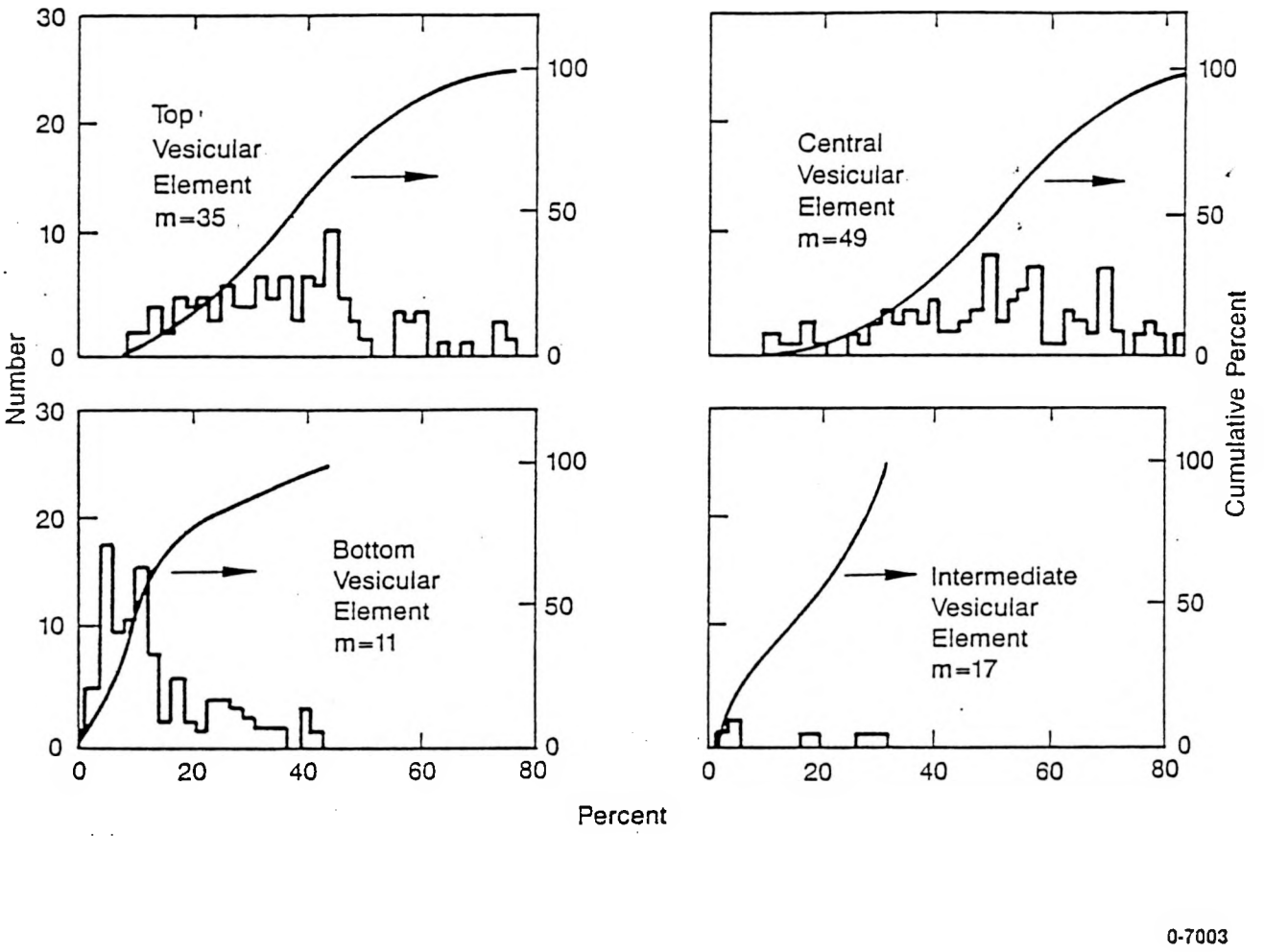

Figure 13. Normalized thickness distribution of flow elements in percent of total flow height (m = median value).

It was not possible to make any, even semi-qualitative, measurements of the transmissivity, porosity, or bulk density of these collapse/rubble zones from either the core or the available logs. The core recovery is generally less than 50% in these zones, and the logs are very qualitative (the noise in the log traces is greater than the difference between 5% porosity central and 30% vesicular elements). This represents an important area in which more work should be done.

Petrographic Descriptions

A brief petrographic description of the flow units is presented in this portion of the report. The information presented is restricted to that obtained from the analysis of core from the 15 RWMC wells under discussion.

Flow Group A

Flow group A consists of one flow unit and two flows. The rock is very fine- to medium-grained and light gray in color. The flows are generally equigranular with minor sporadic occurrences of feldspar and olivine phenocrysts. Plagioclase phenocrysts average about 3% of the rock; olivine about 5% (both with mean size of about 2 mm), and the fine crystalline matrix (<0.05 mm) occupies about 92% of the rock. The core is not heavily oxidized and, where oxidation occurs, it is generally limited to vesicle walls and surfaces of the intergranular pores. The flow is lightly fractured, generally with low fracture angles less than 30 degrees from the horizontal. The fractures are filled with only traces of silt.

Flow Group B

Flow group B is represented by three flow units that are distinguishable on the basis of textural differences.

Flow unit B-1 is light gray with a fine- to medium-grained equigranular groundmass, and is moderately porphyritic. Plagioclase phenocrysts (~2.5 mm) average 15%, olivine (~1 mm) about 4%, and the groundmass (<0.5 mm) about 81% of the rock. The core is moderately fractured throughout.

The fractures are predominately less than 30 degrees from the horizontal and contain minor amounts of sedimentary filling. The top vesicular zone is typified by dark oxide vesicle linings.

Flow unit B-2 is typified by two flows in all but three wells, where three, four, and six flows are found. All flows have nearly identical appearances. The rock is dark gray to purplish-gray in color, with prominent plagioclase phenocrysts (~4.4 mm) making up about 17% of the rock. Subordinate olivine (~1.4 mm) and subophitic clinopyroxene phenocrysts are common (each about 6%), and the fine-grained groundmass constitutes about 72% of the rock. Fracturing is locally heavy and displays silt filling. The upper 3 ft (1 m) of the flows are lightly oxidized.

Flow unit B-3 is represented by a single flow in all but two cores, where two flows are noted. This flow unit is light gray in color and has distinctive orange-colored flow tops that are commonly stained and coated with carbonates. The flow is porphyritic with plagioclase (~3.3 mm) as the most common phenocryst (18%). Olivine (~1.3 mm) and ophitic to subophitic clinopyroxenes are also common (~6%). The groundmass (~76%), has an unusually high fraction of opaques. The cores are moderately to highly fractured with very little silt filling the fractures.

Flow Group C

Flow group C is represented by at least three flow units which may have up to five individual flows. However, the amount of continuous core from flow group C is very limited and the correlations, based on the petrologic evaluation, are tentative.

All of the basalt flow units have intergranular textures with a few plagioclase phenocrysts and with small olivine phenocrysts and clusters. Differentiation between individual flow units is dependent on subtle changes in groundmass textures and the state of olivine phenocryst oxidation.

Flow unit C-1 has a fine-to-coarse intergranular groundmass with ~10% large plagioclase phenocrysts (2.2 mm average) and similarly sized (~5%) olivine grains. Flow tops are frequently oxidized to an orange color, commonly contain silt fracture filling, and have carbonate encrustations. The vesicular zones have a dark groundmass with common opaque oxide wall coatings. Olivine grains in these zones are frequently oxidized, with a brassy-appearing surface. This flow unit is highly fractured. However, except for the upper portion of the top vesicular zone, these fractures are generally free of silt.

Flow unit C-2 has a coarse, intergranular groundmass. Aggregates of ~2.2 mm olivine crystals are prominent, and the plagioclase phenocrysts and coarse plagioclase of the groundmass yield a mildly porphyritic texture. Flow tops are somewhat oxidized, but do not display an orange color, and the olivine phenocrysts are relatively unoxidized.

Flow unit C-3 has a medium-grained, intergranular groundmass with subordinate plagioclase and olivine phenocrysts. The upper flow surfaces are commonly oxidized, colored orange, and have clay fillings and carbonate encrustations. The olivine phenocrysts commonly occur in aggregates and are oxidized. The ophitic clinopyroxenes are conspicuous. This unit is distinguished from the overlying unit, predominately on the basis of its more advanced oxidation.

Petrologic characteristics are summarized in the following sections of this report. Detailed information, including the computer-drafted logs with the field and laboratory porosity and permeability data, is presented in Appendix A. Appendix A includes J. P. O'Brien's summary of his core logging assignment, as well as a discussion of the procedure used to transform the field core logs to a computerized logging file that can be printed out at any scale by the commercial Logger^{tm} program (the logs provided with this report are to a scale of 1 inch equals 10 feet, i.e., 1:120).

PETROPHYSICS

The term "petrophysics" is used by some authors as a synonym for quantitative geophysical log analysis (Elphick, 1989). A more general definition will be used in this report - "petrophysics - a study of the physical properties of reservoir/aquifer rocks" (Bates and Jackson, 1980). At present, geophysical logs suitable for evaluation of the physical properties of the vadose zone basalts are unavailable. Thus, the physical properties measured and reported here are porosity, permeability, density, equilibrium saturation, and pore-size distribution, as determined from the core analysis.

Procedures

The permeability and bulk density of usable, representative pieces of core were measured during the core description phase carried out at CFA-649.

The permeameter was designed and built at the INEL. A description of the hardware, calculation procedures, and programs are presented in Appendix D. In general, the flow rates and pressure drops obtained when using this permeameter and 3.5 in. (8.9 cm) diameter cores, were about one-fifth of that to be expected from a cylinder of rock having an outside diameter of the stopper, an inside diameter of the stopper hole, a length equal to the core radius, and the same permeability as the core.

The bulk density (density of the dry basalt, including pore space) was obtained by measuring the weight, length, and diameter of regularly shaped pieces of core. The grain density of the rock (density of the solid

basalt rock matrix) was near 3.05 g/cm^3. A porosity can be approximated from the bulk density by using the following equation:

$$\phi = [BV - (WT/3.05)]/BV \quad (1)$$

where

ϕ = porosity (fractional)

BV = bulk volume, cm^3

WT = weight of sample, g.

The distribution of grain densities, as determined from helium porosities, is presented as Figure 14. The grain density distribution has a low standard deviation (~0.02 g/cm^3). Thus, 95% of the time, the error associated with using a 3.05 g/cm^3 grain density will be less than ~1.0%. Sixty-seven percent of the time the grain density is between 3.03 and 3.07 g/cm^3, and 95% of the time it is between 3.01 and 3.09 g/cm^3.

Representative pieces of core were selected for laboratory studies. Cylindrical plugs were cut from the core samples and the air permeability and helium porosity of the plugs were determined.

The laboratory porosity and permeability for each plug were used to generate a scatter plot, and 45 plugs were selected covering the permeability range and within $\pm$ 25% of the curve fitted through the data. These representative plugs were used in a capillary pressure/pore-size distribution study, using an equilibrium saturation technique. This technique was pioneered in cement characterization and is not widely known or used in petrophysical studies. The basic process is the adsorption/desorption of water from an atmosphere with a carefully controlled, partial water vapor pressure (Daian, 1988). The partial pressures can be controlled by hygrostat solutions and related to capillary pressure. The surface area can also be calculated from the equilibrium saturation data.

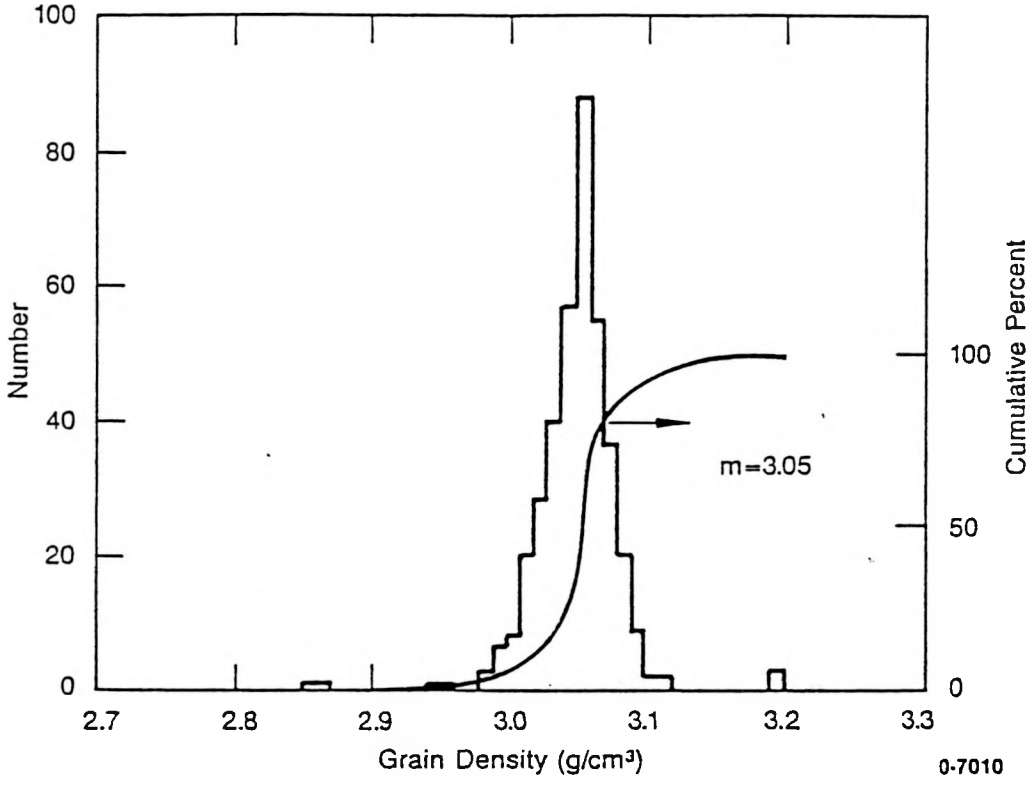

Figure 14. Distribution plot of grain density (m = median value).

Slices from the end of the core plugs were labeled and bagged and approximately 150 were sent for thin sectioning and used in the petrographic evaluation discussed later.

Porosity/Permeability/Density

The porosity and permeability information is included as part of the computer-drawn individual well logs presented as part of Appendix A. The information can also be summarized as one of the continuous distribution characteristics of the flow elements. The flow elements used were: (1) the upper vesicular, (2) the central, (3) intermediate vesicular (infrequently encountered) intervals, which represent bubble trains and bubble plumes incorporated into vesicular intervals by the viscous flow of the cooling, but still plastic basalt, and rising via density differentials, and (4) the lower vesicular element.

Porosity

The porosity data are summarized by flow groups, flow units (A, B-1, C-2, etc), and flow elements (top vesicular, central nonvesicular, etc.) in Table 1. Both the field and laboratory values are integrated into this data set. The median porosities for the upper, central, and lower elements or zones for flow group A were 19, 8, and 23%; for flow group B they were 22, 10, and 21%; and for flow group C they were 21, 11, and 18%. The medians for all samples were 22, 10, and 21%.

A reasonable generalization for the vadose zone basalt porosity can be made. The maximum porosity for the nonvesicular elements is <15% and the minimum porosity for the vesicular elements is >15%. Thus, the vesicular and nonvesicular elements can be separated merely on the basis of their porosity. The porosity distribution plots for all the data are presented as Figure 15, and for flow groups A, B, and C as Figures 16, 17, and 18. The generally peaked distributions for the nonvesicular elements and the broader distributions for the vesicular elements can be noted in these figures.

Table 1. Porosity distribution by elements for flow units, flow groups, and all samples (values are in percent)

Element	Flow Units				Flow Groups			
	Minimum	Media	Maximum	Number	Minimum	Median	Maximum	Number
A TV	14	19	27	9	14	19	27	9
C	3	8	8	13	3	8	14	13
BV	14	23	33	5	14	23	33	5
B-1TV	14	22	26	13				
C	5	10	14	16				
BV	15	20	24	9				
B-2TV	16	23.5	38	38	12	22	38	86
C	3	10	17	70	3	10	17	144
BV	13	22	33	16	12	21	39	32
B-3TV	12	21	29	35				
C	4	11	16	58				
BV	12	14	40	7				
C-1TV	15	21	29	28				
C	6	12	14	34				
BV	13	18	26	5				
C-2TV	11	20.5	33	18	11	21	43	68
C	6	11	17	17	6	11	17	109
VI								
BV	14	21.5	34	8	12	18	35	25
C-3TV	15	23	43	22				
C	6	10.5	17	58				
VI								
BV	12	17.5	26	12				
All Samples								
ALLTV	11	22	43	163				
C	3	10	17	261				
VI								
BV	12	21	39	62				

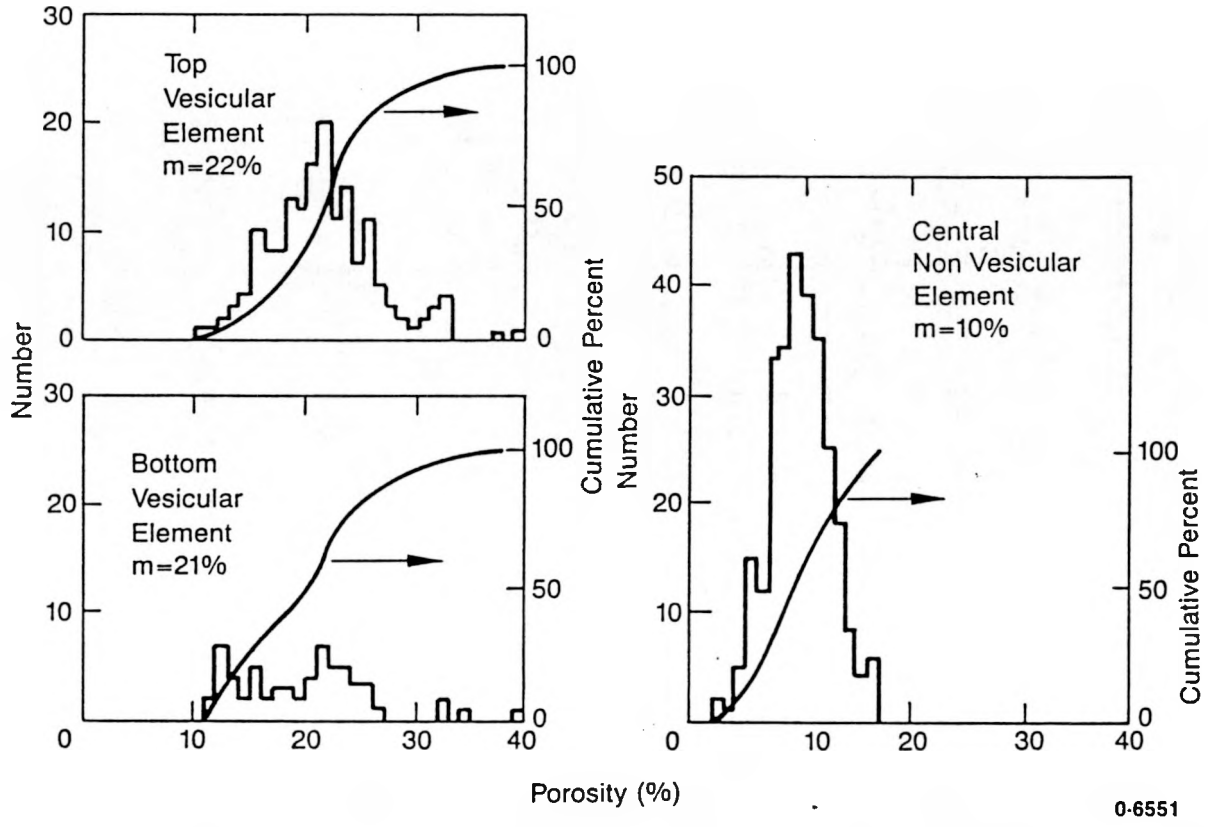

Figure 15. Porosity distribution for the vesicular and nonvesicular portions of all flows (m = median value).

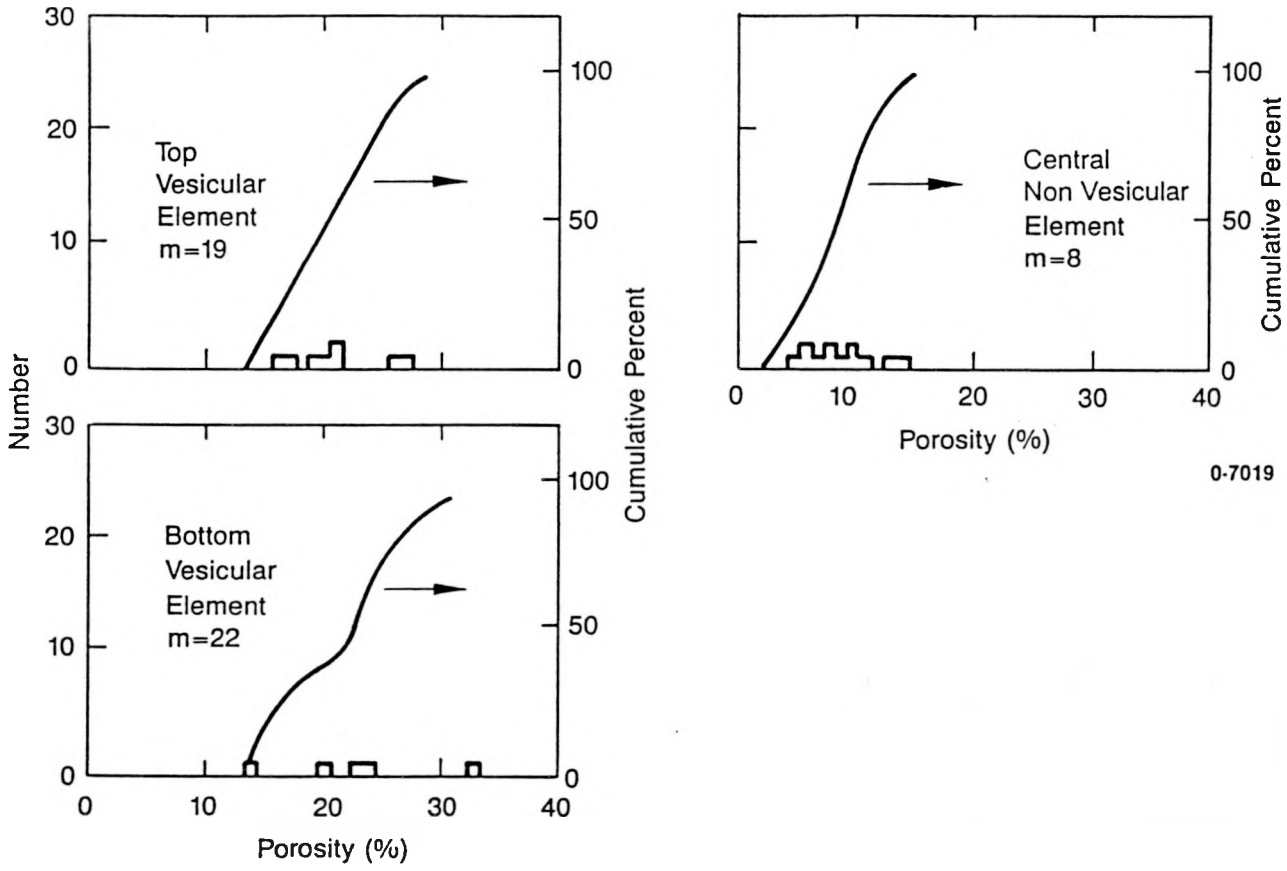

Figure 16. Porosity distribution for the vesicular and nonvesicular elements of flow group A (m = median value).

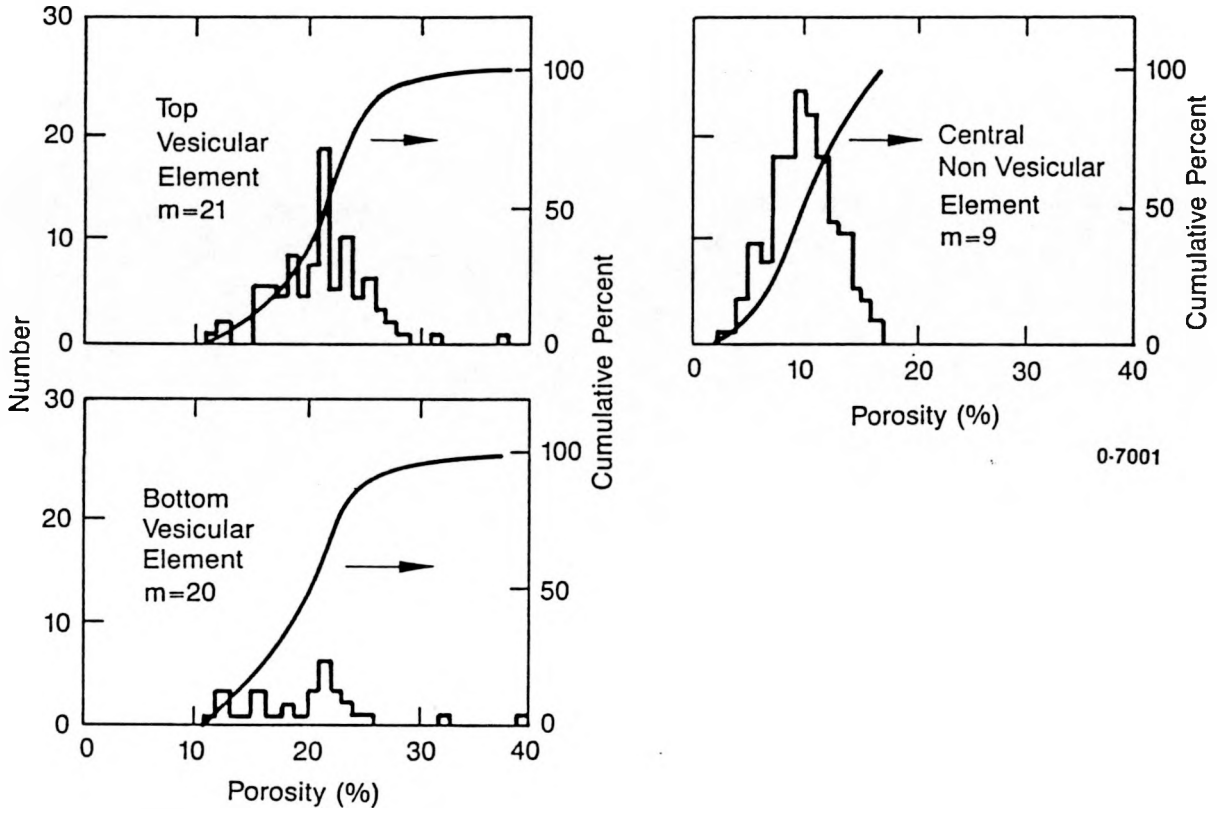

Figure 17. Porosity distribution for the vesicular and nonvesicular elements of flow group B (m = median value).

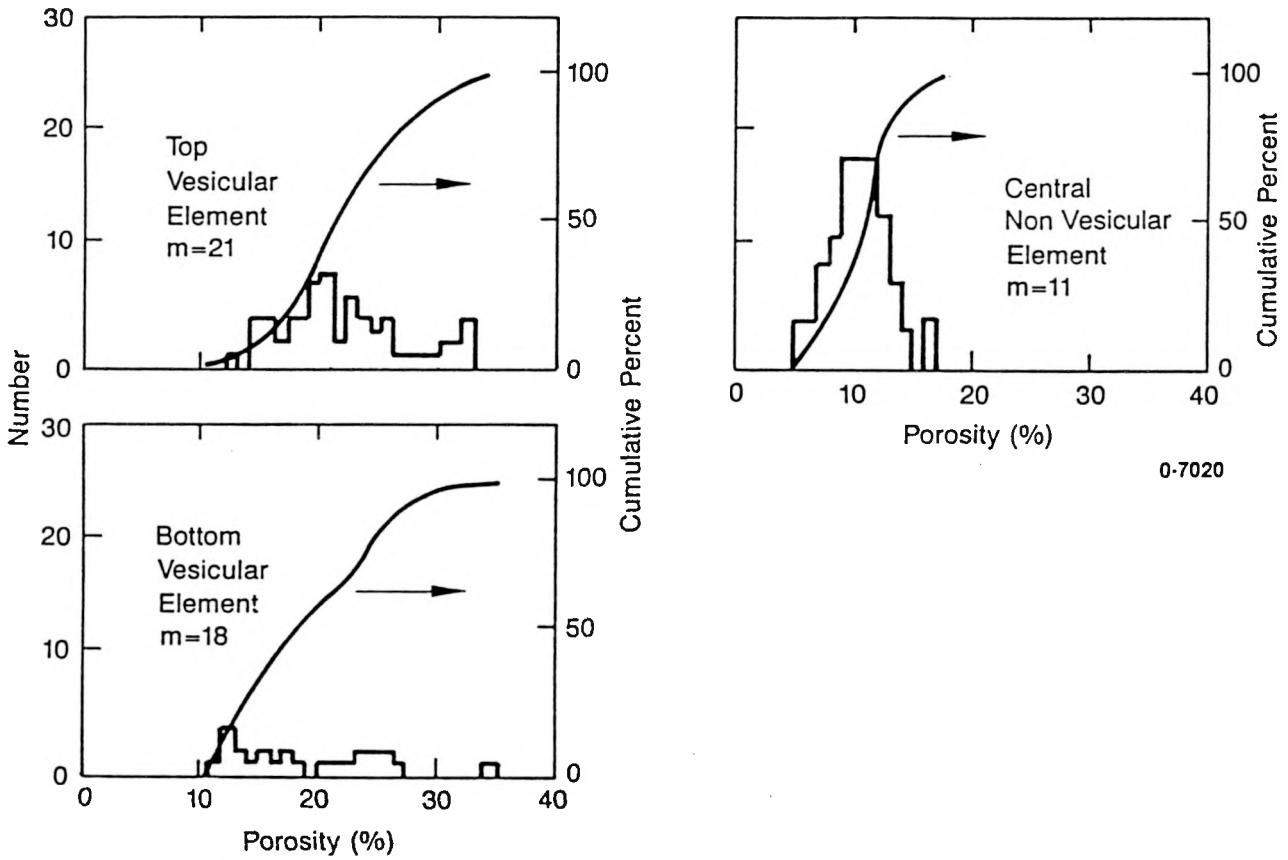

Figure 18. Porosity distribution for the vesicular and nonvesicular elements of flow group C (m = median value).

Permeability

The permeability data are summarized in Table 2. This data set includes both lab and field values. The median permeabilities for the upper, central, and lower elements for flow group A were 16, 22, and 8 md; for flow group B were 6, 9, and 4 md; and for flow group C were 7, 9, and 4 md (the intermediate vesicular element in group C had a median permeability of 5 md).

The permeabilities are generally controlled by the characteristics of the rock matrix. Although the highest maximum permeabilities occurred in the vesicular elements in samples where good local connection between the vesicles occurred, generally the median permeability of the vesicular elements was less than that of the central nonvesicular element. The permeability distribution plots for all the data are presented as Figure 19, and for flow groups A, B, and C as Figures 20, 21, and 22. The permeability distributions, even when plotted as logarithmic functions, are generally broader than the porosity distributions. The lowest permeabilities generally occurred in very tight, low porosity, nonvesicular material.

The permeability-porosity relation is quite complex. A permeability-porosity plot, for samples less than 100 md, is presented as Figure 23. This figure illustrates the poor correlation between the two parameters. A manageable permeability-porosity relation is a desirable condition because permeabilities are difficult to determine indirectly. The porosities can be estimated from quantitative geophysical logging measurements. If permeability can be estimated from porosity via a Kozeny-type equation, then continuous estimates of porosity and permeability can be calculated from the logging data.

Table 2. Permeability distribution by elements for flow units, flow groups, and all samples (values are in millidarcys)

Element	Flow Units				Flow Groups			
	Minimum	Media	Maximum	Number	Minimum	Median	Maximum	Number
1 TV	1	3	16	8	1	3	16	8
C	<0.05	5	22	12	<0.05	5	22	12
BV	0.20	7	8	3	0.20	7	8	3
2-1TV	1	3	415	14				
C	0.30	5	48	22				
BV	1	3	7	9				
2-2TV	0.7	8	5000	44	0.3	55	5000	86
C	0.1	5	253	71	0.3	9	253	148
BV	0.36	4	873	17	0.3	4	1649	33
2-3TV	0.3	8	395	28				
C	0.3	15	112	53				
BV	0.1	6		1649				
3-1TV	0.4	7	437	38				
C	1	10	31	28				
BV	1	5	36	9				
3-2TV	0.1	5	1574	24	0.1	7	4824	91
C	2	10	47	27	<0.05	9	175	122
VI	117	117	117	1	0.2	5	984	9
BV	0.3	15	241	10	<0.05	4	241	35
3-3TV	0.3	4	4824	29				
C	<0.05	9	175	67				
VI	0.2	3.5	984	8				
BV	<0.05	4.5	81	16				
All Samples								
ALLTV	0.1	7	5000	185				
C	<0.05	8	253	282				
VI	0.2	5	984	9				
BV	<0.05	4	1649	71				

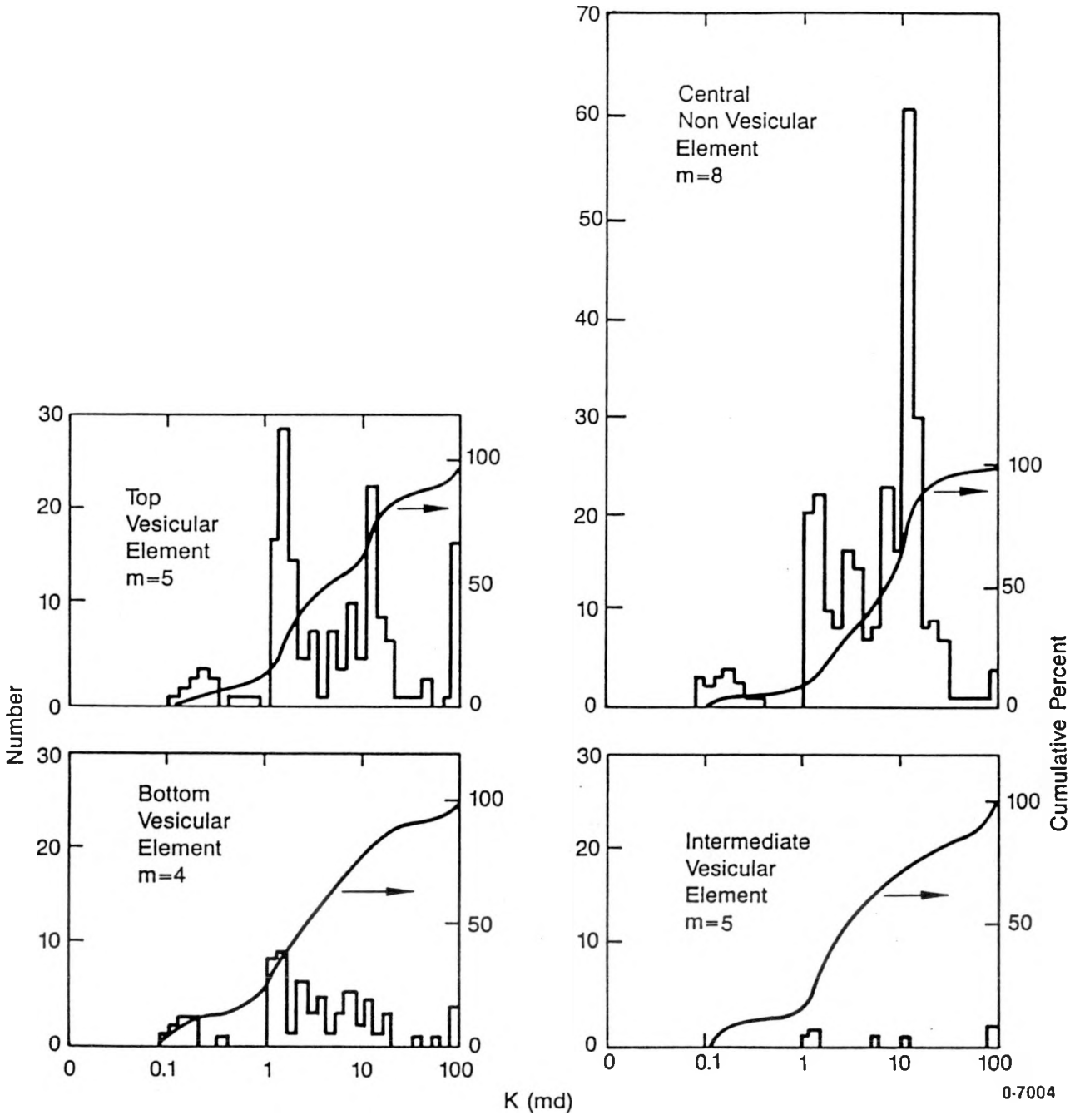

Figure 19. Permeability distribution for the vesicular and nonvesicular portions of all flows (m = median value).

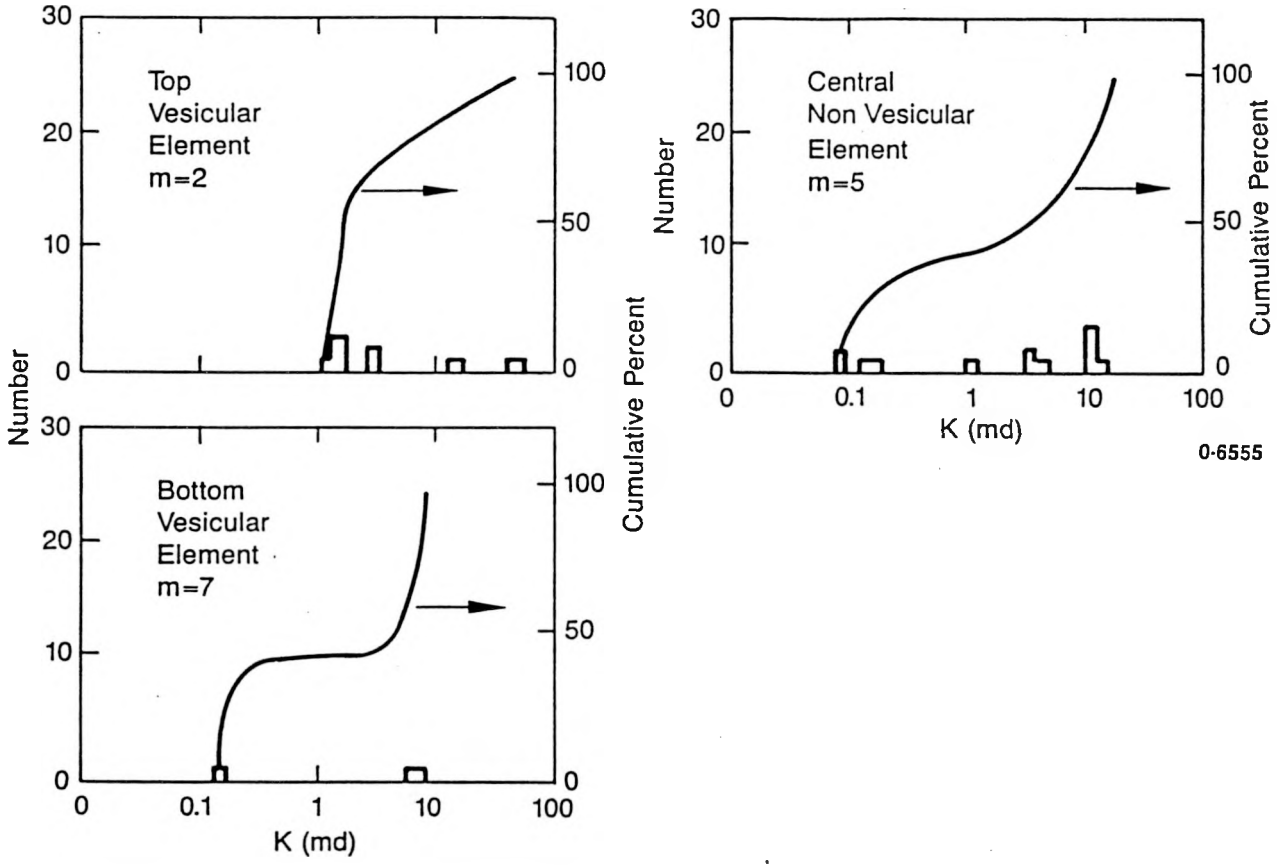

Figure 20. Permeability distribution for the vesicular and nonvesicular elements of flow group A (m = median value).

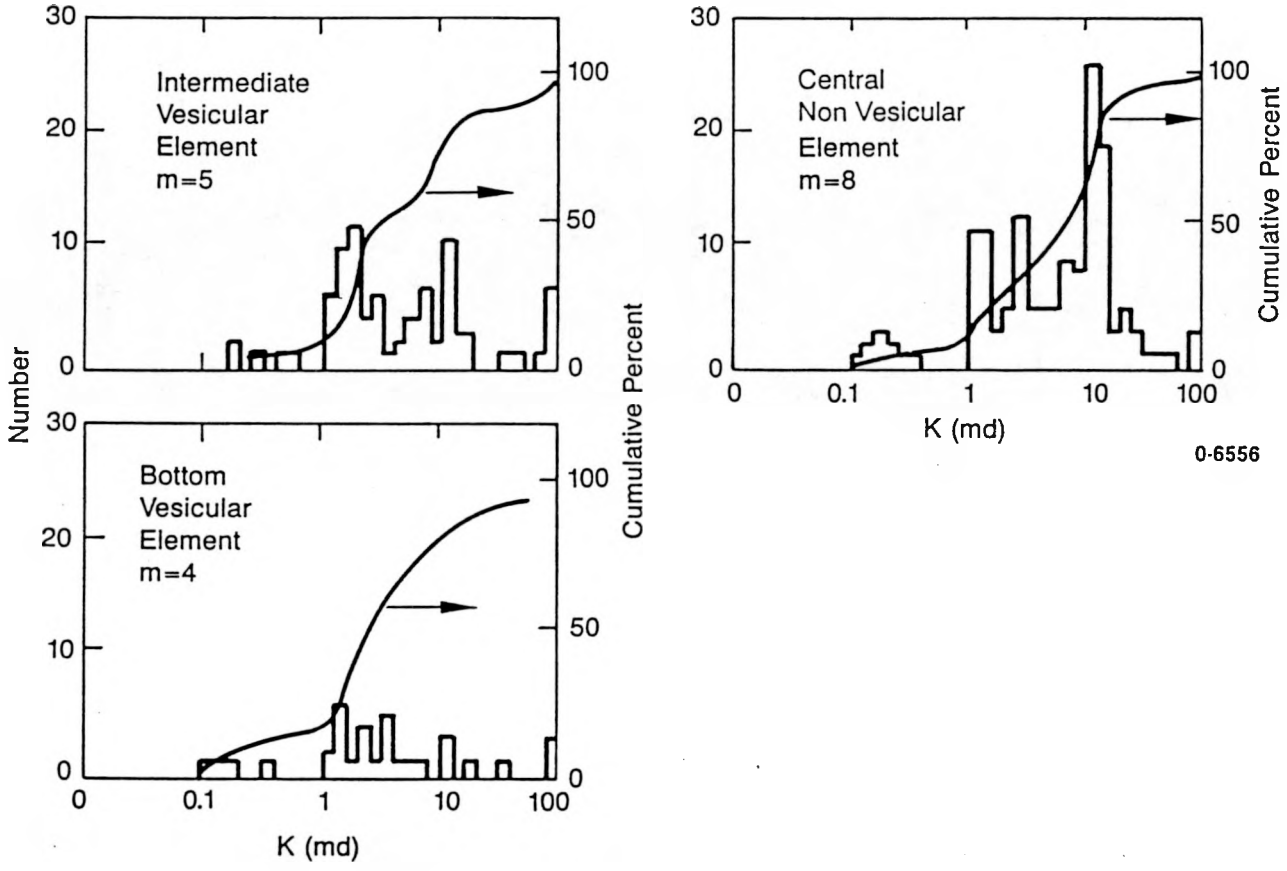

Figure 21. Permeability distribution for the vesicular and nonvesicular elements of flow group B (m = median value).

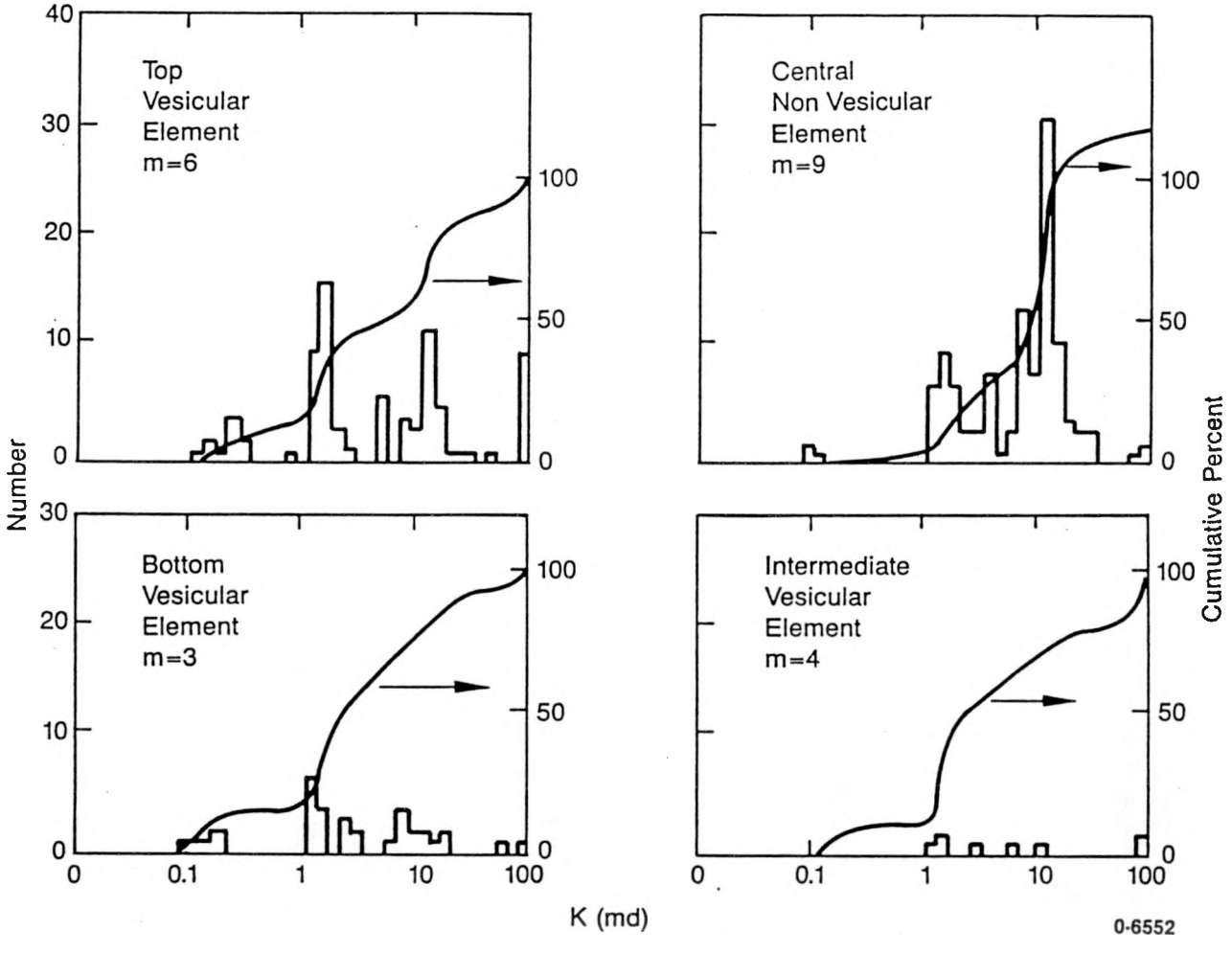

Figure 22. Permeability distribution for vesicular and nonvesicular elements of flow group C (m = median value).

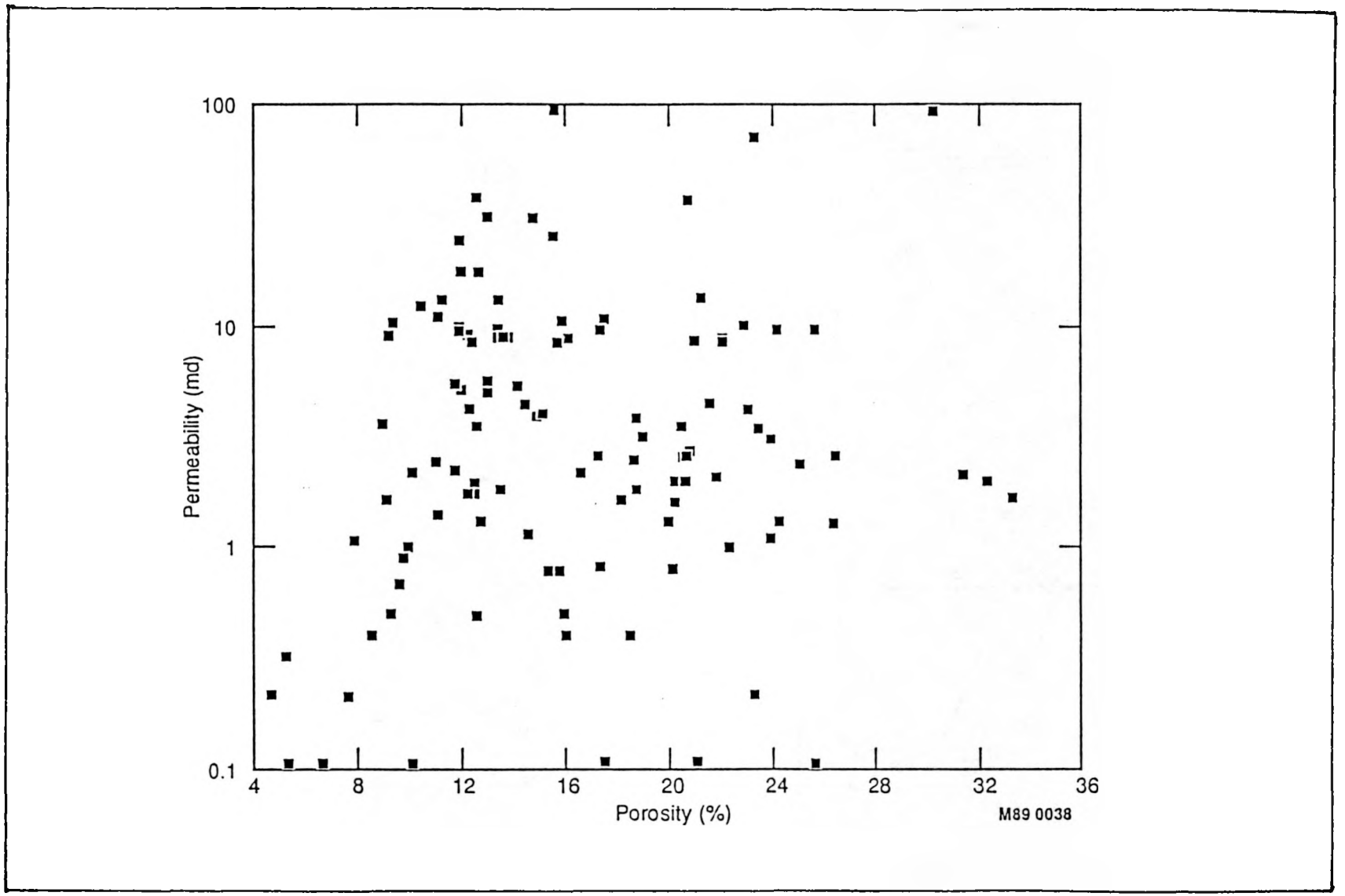

Figure 23. Scatter plot of permeabilities less than 100 md and their associated porosities.

Density

The median grain density for all the samples is 3.05 g/cm^3 and the grain density distribution is relatively peaked (Figure 14). However, when the data are evaluated by elements, there is a small, consistent median density difference between the vesicular and nonvesicular material (Table 3). In general, the nonvesicular elements have a median grain density of 3.05 g/cm^3, and the vesicular elements, a median grain density of 3.04 g/cm^3. The intermediate vesicular elements have a median grain density of 3.05 g/cm^3. This affinity with the nonvesicular element median may be because the intermediate element is physically in the central nonvesicular area. However, the intermediate element sample set is quite small (8 samples) and has little statistical significance.

The grain density distribution for the complete data set is presented as Figure 24, and for flow groups A, B, and C as Figures 25, 26, and 27. In general, the distributions are rather peaked and the vesicular and nonvesicular elements have medians that are displaced by only about 0.01 g/cm^3.

In general, the bulk density distributions are similar to the porosity distribution, with vesicular median bulk densities near 2.40 g/cm^3 and nonvesicular median bulk densities near 2.70 g/cm^3 (Table 4). The distributions for all samples are presented as Figure 28, and for flow groups A, B, and C as Figures 29, 30, and 31. In general, the vesicular element bulk densities are less than 2.60 g/cm^3 and the nonvesicular element bulk densities are greater than 2.60 g/cm^3.

Limitations Inherent in the Data Set

A severe limitation exists because of the size of the sample set used. This same caveat is true for all of the measurements that utilize core porosity, permeability, and density. The problem is that the core is retrieved from only the most competent portion of the formation. The more transmissive features, rubble piles, lava tubes, partially collapsed

Table 3. Grain density distribution by elements for flow units, flow groups, and all samples (values are g/cm^3)

Element	Flow Units				Flow Groups			
	Minimum	Media	Maximum	Number	Minimum	Median	Maximum	Number
1 TV	3.02	3.04	3.06	5	3.02	3.04	3.06	5
C	3.03	3.05	3.07	8	3.03	3.05	3.07	8
BV	2.99	3.04	3.05	4	2.99	3.04	3.05	4
2-1TV	3.02	3.05	3.07	12				
C	3.02	3.05	3.09	12				
BV	2.98	3.05	3.09	7				
2-2TV	2.99	3.04	3.19	40	2.98	3.04	3.09	72
C	3.00	3.05	3.08	51	3.00	3.05	3.11	109
BV	2.96	3.04	3.09	15	2.96	3.04	3.09	27
2-3TV	2.98	3.04	3.08	20				
C	3.00	3.06	3.11	46				
BV	3.00	3.05	3.08	5				
3-1TV	2.94	3.02	3.05	21				
C	3.00	3.04	3.11	24				
BV	2.98	3.03	3.07	6				
3-2TV	2.97	3.04	3.19	29	2.94	3.04	3.21	78
C	3.00	3.04	3.07	20	3.00	3.05	3.11	79
VI		3.05		1	2.99	3.05	3.10	6
BV	2.99	3.02	3.07	13	2.98	3.04	3.08	30
3-3TV	2.99	3.05	3.19	28				
C	3.01	3.07	3.11	35				
VI	2.99	3.05	3.10	51				
BV	3.00	3.06	3.08	11				
All Samples								
ALLTV	2.94	3.04	3.21	155				
C	3.00	3.05	3.11	196				
VI	2.99	3.05	3.10	8				
BV	2.96	3.04	3.09	61				

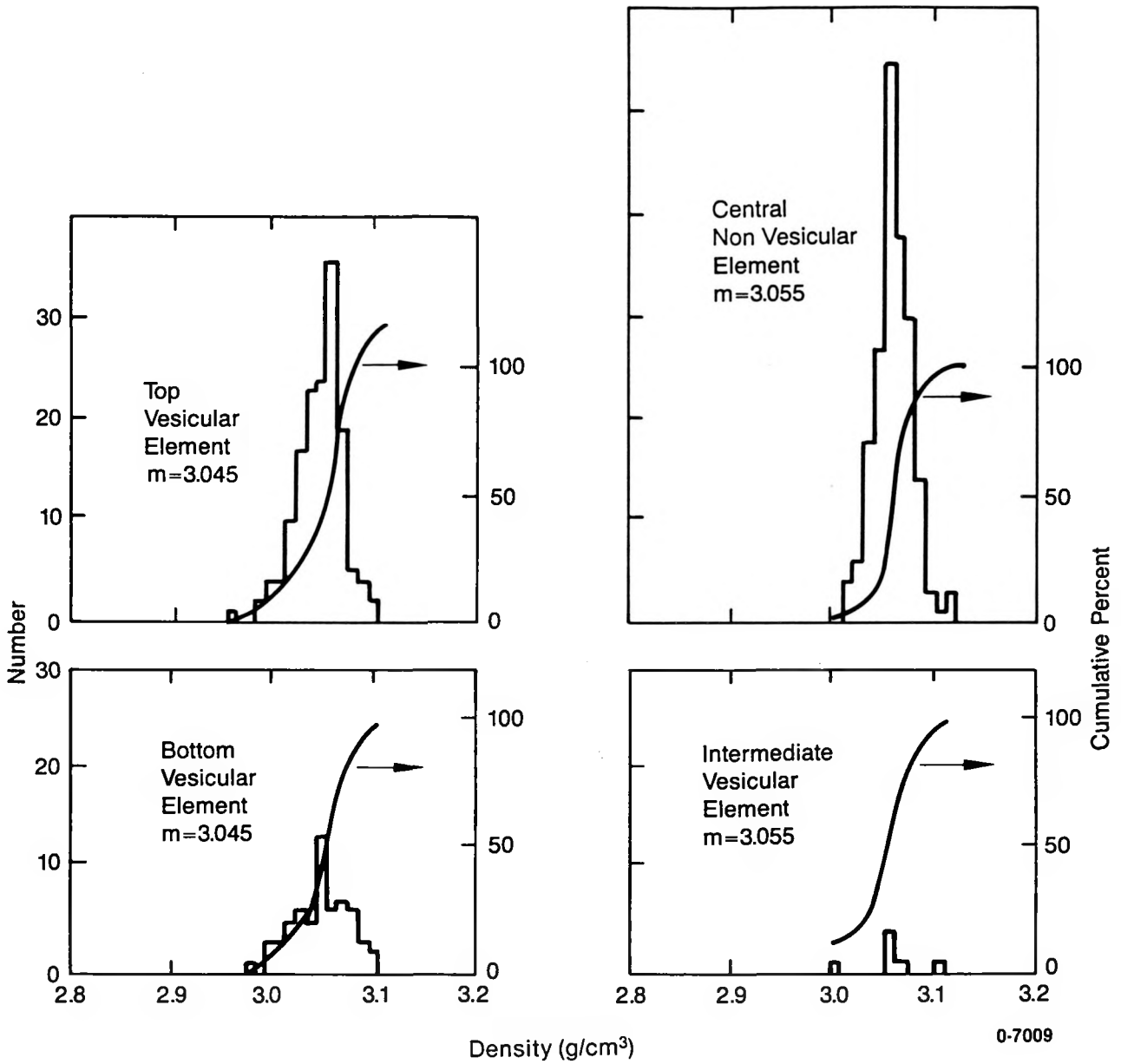

Figure 24. Grain density distribution for vesicular and nonvesicular elements, all samples (m = median value).

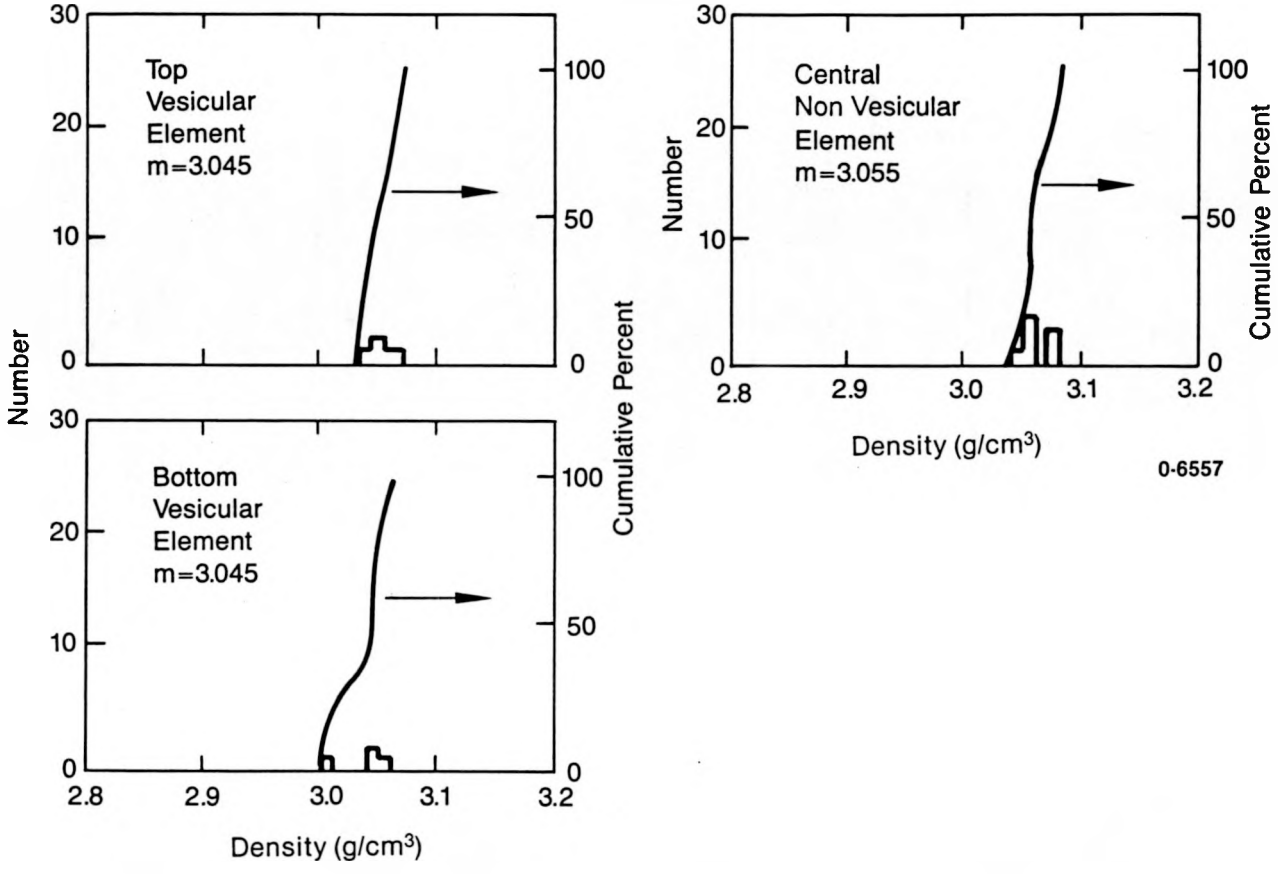

Figure 25. Grain density distribution for vesicular and nonvesicular elements of flow group A (m = median value).

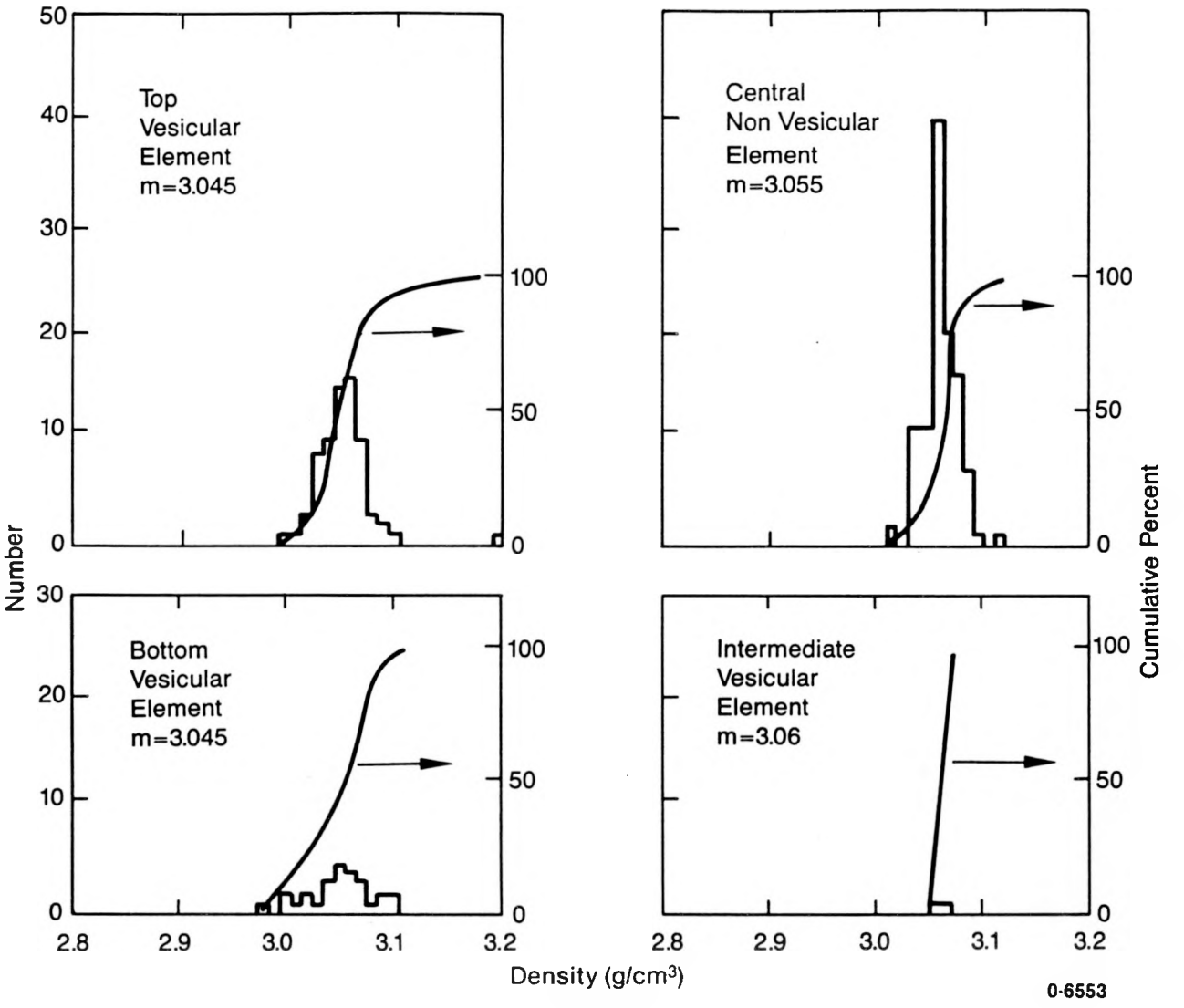

Figure 26. Grain density distribution for vesicular and nonvesicular elements of flow group B (m = median value).

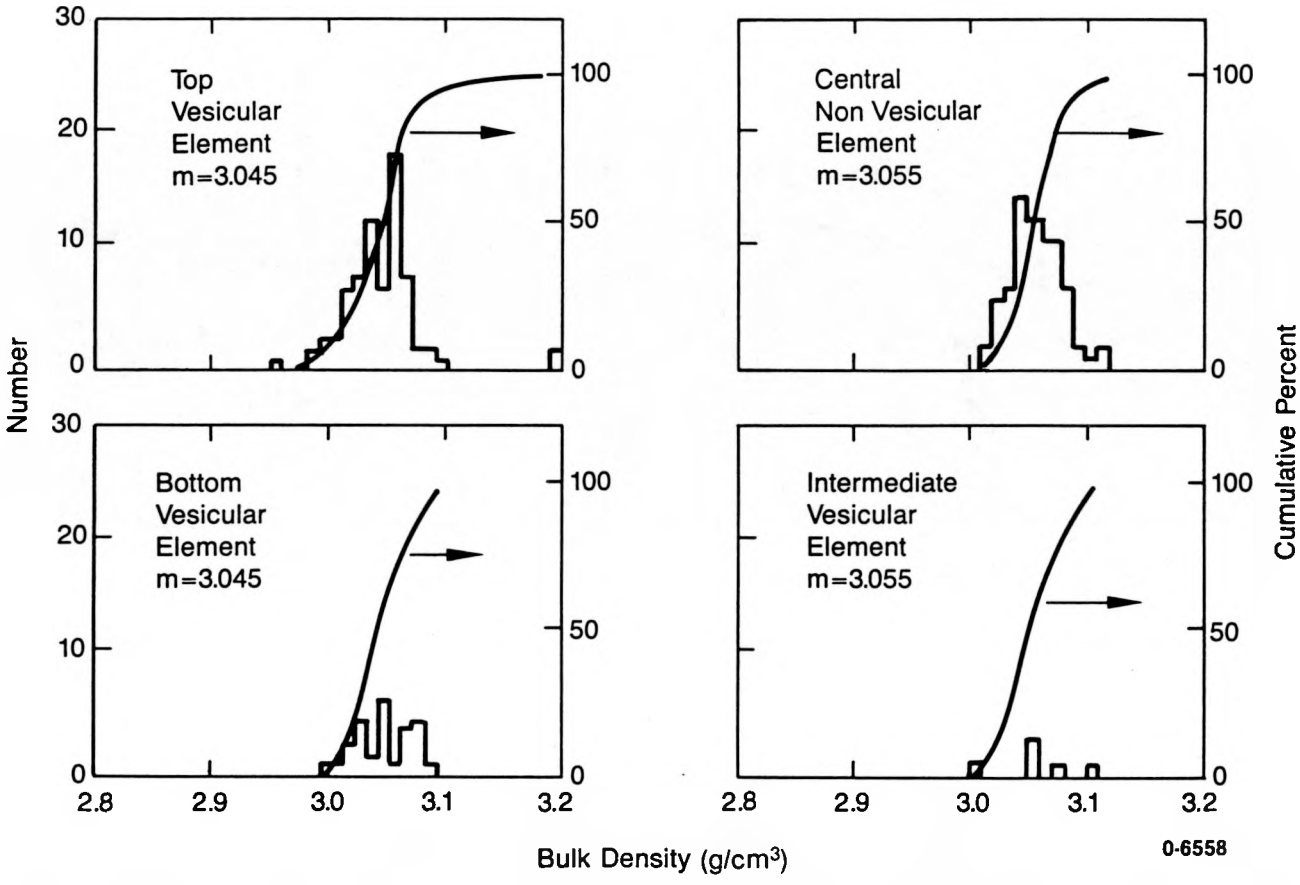

Figure 27. Grain density distribution for vesicular and nonvesicular elements of flow group C (m = median value).

Table 4. Bulk density distribution by elements for flow units, flow groups, and all samples (values are g/cm^3)

Element	Flow Units				Flow Groups			
	Minimum	Media	Maximum	Number	Minimum	Median	Maximum	Number
1 TV	<2.20	2.40	2.61	11	<2.20	2.40	2.61	11
C	2.54	2.73	2.97	20	2.54	2.73	2.97	20
BV	<2.20	2.30	2.45	6	<2.20	2.30	2.45	6
2-1TV	<2.20	2.42	2.61	21				
C	2.57	2.76	2.95	30				
BV	2.29	2.37	2.61	12				
2-LTV	<2.20	2.38	2.61	71	<2.20	2.38	2.65	140
C	2.51	2.75	>3.00	87	2.43	2.73	>3.00	220
BV	<2.20	2.42	2.65	22	2.33	2.45	2.57	2
2-3TV	<2.20	2.39	2.65	48				
C	2.43	2.72	2.93	103				
BV	<2.20	2.39	2.65	6				
3-1TV	<2.20	2.38	2.67	49				
C	2.51	2.69	2.87	56				
BV	<2.20	2.24	2.65	9				
3-2TV	<2.20	2.39	2.65	40	<2.20	2.38	2.67	142
C	2.53	2.72	2.87	39	2.51	2.71	2.93	194
VI					<2.20	2.29	2.59	8
BV	<2.20	2.30	2.59	13	<2.20	2.36	2.65	35
3-3TV	<2.20	2.40	2.65	53				
C	2.51	2.73	2.93	99				
VI	<2.20	2.27	2.59	7				
BV	2.23	2.45	2.59	13				
All Samples								
ALLTV	<2.20	2.39	2.67	293				
C	2.43	2.72	>3.30	434				
VI	<2.20	2.34	2.58	10				
BV	<2.20	2.39	2.65	81				

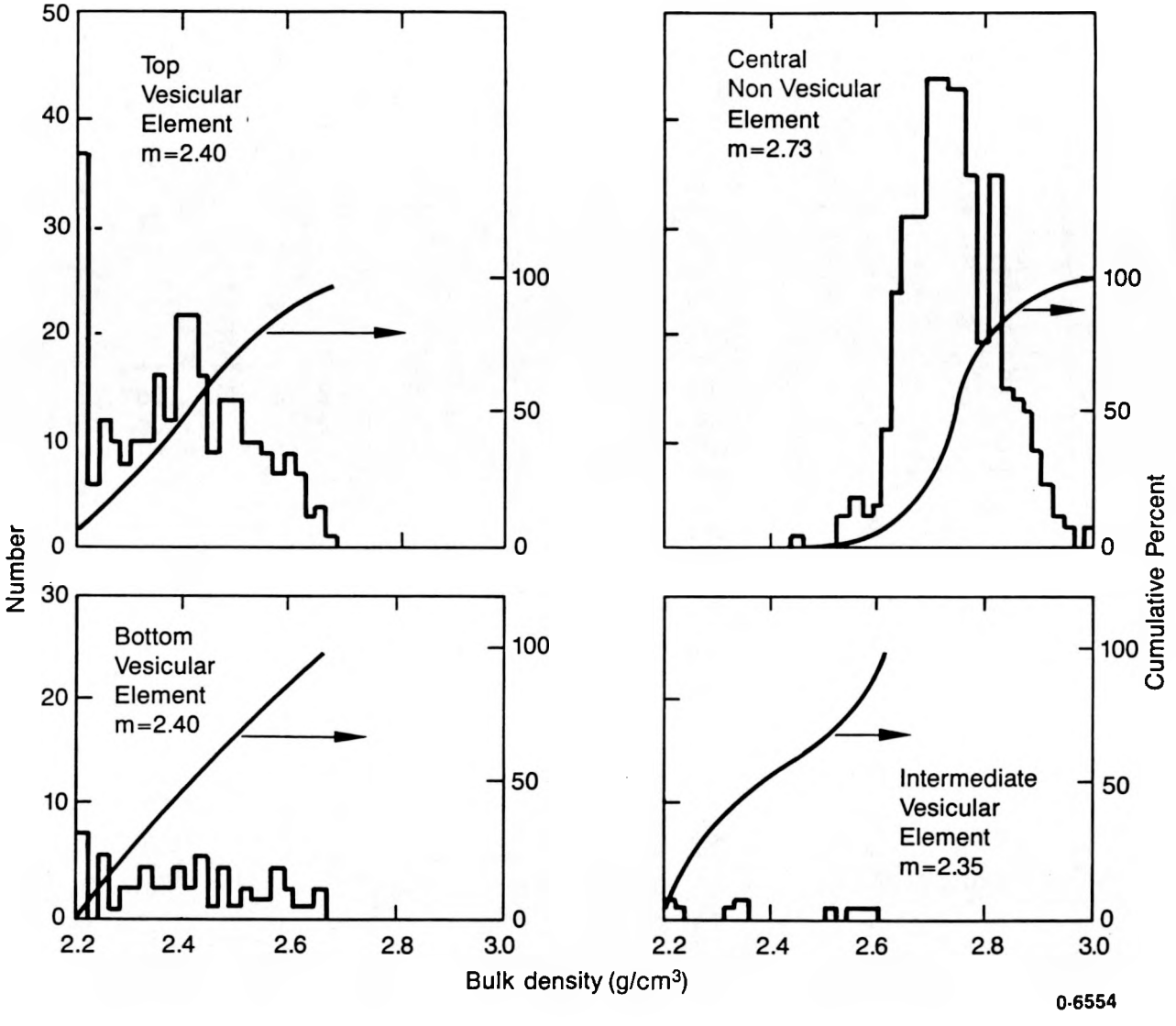

Figure 28. Bulk density distribution for vesicular and nonvesicular elements for the complete sample set (m = median value).

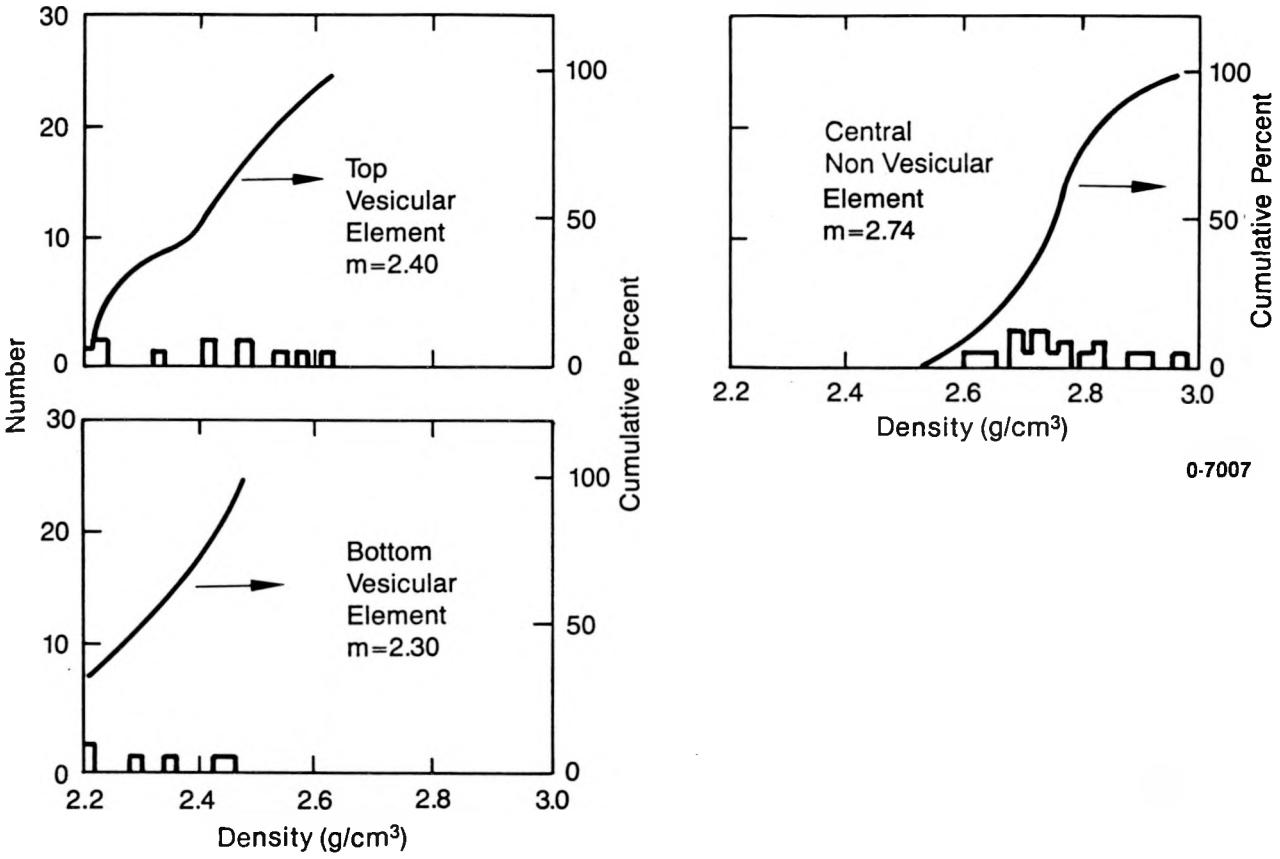

Figure 29. Bulk density distribution for vesicular and nonvesicular elements of flow group A (m = median value).

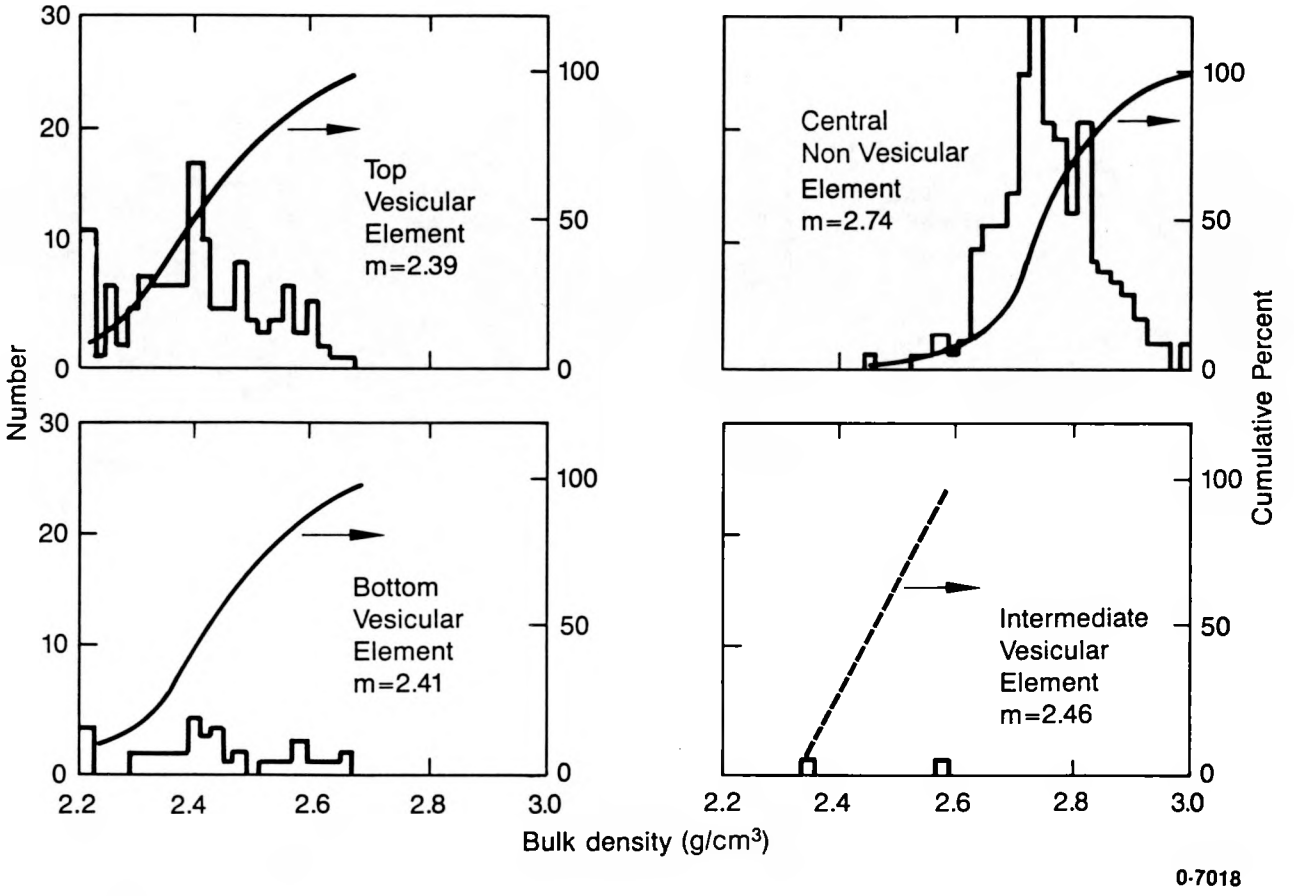

Figure 30. Bulk density distribution for vesicular and nonvesicular elements of flow group B (m = median value).

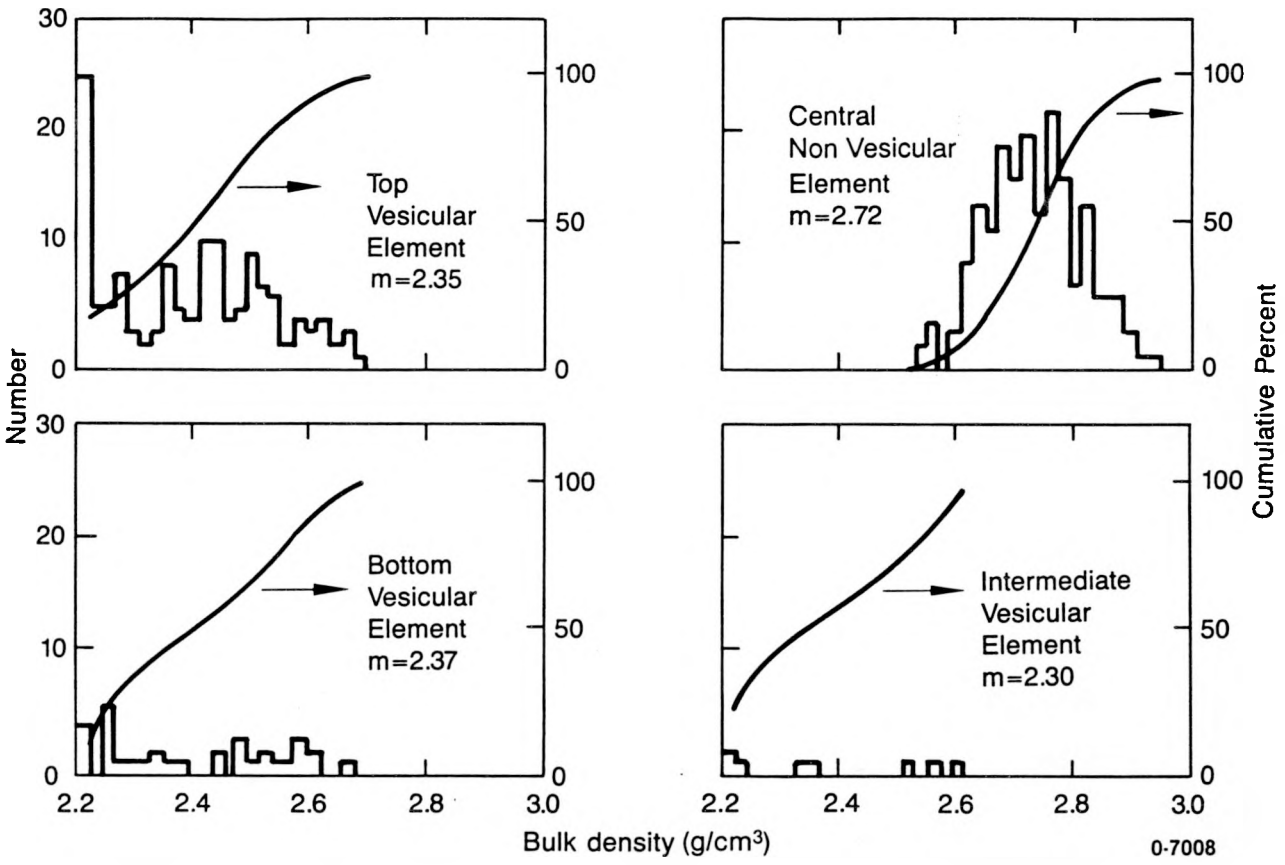

Figure 31. Bulk density distribution for vesicular and nonvesicular elements of flow group C (m = median value).

elements, and intensely fractured areas are not represented by the core that is available, nor can they be analyzed by the logging suite that was used. Hence, the evaluation of some of the important features remain to be made using more sophisticated logging techniques and equipment, and tests that are designed to specifically retrieve information from these elements.

Equilibrium Water Saturation

Water saturation data from each of the 45 basalt plugs in the equilibrium water saturation experiment are summarized in Table 5. The water content (in grams) for each plug is obtained by subtracting the initial dry weight of the sample from the weight of the sample at equilibrium with the given relative humidity. The percent water saturation (i.e., the percent of total pore volume occupied by water) is then calculated using the following equation:

$$\%PV = 100 * Ww/(\rho_w * PV_{tot}) \quad (2)$$

where:

%PV = percent water saturation

W_w = weight of water, g

ρ_w = density of water, g/cm^3 at temperature T

PV_{tot} = total pore volume, cm^3.

In Figure 32, the water saturation data at 12% relative humidity is plotted against the permeability using a semi-logarithmic scale. In an intergranular system, permeability and water saturation are inversely related; these data should define a curve (on a logarithmic scale). However, Figure 32 shows that there is considerable scatter. Thus, the effects of vesicles, the amount of spongy black oxide material, and the ultimate breakover relative humidity need to be more clearly defined before generalizations about saturation and permeability can be made.

Table 5. Equilibrium water saturation adsorption data

Well	Sample	Laboratory Por. (%)	Laboratory Perm. (md)	Rh:	% Water Saturation at Given Relative Humidity (Rh in %) 12.2	32	75.7	94.3	95.7	96.6	97.7	98.4	99.30	99.80	100.00
79-1	A 2	23.48	3.50		0.16	0.53	0.46	0.89	1.02	1.18	1.31	1.35	1.38	1.22	75.01
79-2	B 2	23.60	1.10		0.13	0.29	0.58	1.26	1.48	1.64	1.71	1.81	1.87	1.71	65.69
	B 4	13.04	10.55		0.29	0.58	1.40	2.45	2.74	2.97	3.20	3.32	3.32	3.26	82.33
	B 9	26.63	2.63		0.09	0.32	0.43	0.84	0.92	1.01	1.15	1.21	1.21	1.27	49.57
79-3	C 1	24.98	3.38		0.06	0.18	0.18	0.58	0.68	0.86	0.92	0.95	0.92	0.73	47.27
	C 5	14.78	1.07		0.20	0.36	0.72	1.48	1.74	1.99	2.25	2.35	2.35	2.10	73.79
	C 9	8.85	0.21		0.60	1.12	2.07	4.15	5.01	5.61	5.96	6.22	6.48	5.88	72.19
	C 11	21.64	1.79		0.10	0.24	0.38	0.73	0.80	0.91	1.05	1.12	1.12	1.26	55.28
	C 14	15.59	1.67		0.29	0.48	1.07	2.28	2.61	2.95	3.19	3.44	3.39	3.29	71.76
76-2	D 3	26.90	11.21		0.00	0.11	0.25	0.56	0.62	0.68	0.73	0.76	0.76	0.62	60.46
	D 7	22.93	2.73		0.13	0.20	0.30	0.63	0.76	0.86	0.96	1.03	1.03	1.00	68.71
	D 10	10.56	1.20		0.29	0.51	0.94	1.89	1.96	2.18	2.25	2.40	2.47	2.47	70.93
	D 15	16.53	2.22		0.14	0.32	0.46	1.05	1.14	1.32	1.46	1.55	1.50	1.41	86.34
	D 17	26.29	873.74		0.20	0.93	1.45	3.77	4.98	5.70	--	--	--	--	--
79-3	E 2	12.82	33.59		0.18	0.24	0.59	1.25	1.30	1.48	1.72	1.90	2.02	1.96	88.37
	E 5	22.07	2.56		0.14	0.20	0.31	0.61	0.68	0.78	0.82	0.89	0.92	0.89	57.38
	E 7	22.26	4.07		0.10	0.17	0.37	0.78	0.91	1.08	1.18	1.22	1.28	1.15	58.15
	E 11	17.07	4.77		0.22	0.44	0.71	1.55	1.72	2.03	2.16	2.30	2.34	2.43	78.25
	E 17	11.01	12.33		0.34	0.76	1.58	3.50	3.64	3.98	4.25	4.88	4.87	5.15	81.40
	E 18	12.06	9.36		0.31	0.50	0.81	1.56	1.80	1.99	2.18	2.30	2.37	2.12	84.16
	E 20	12.21	8.92		0.19	0.31	0.74	1.49	1.73	1.92	2.10	2.23	2.35	1.73	90.39
	E 24	21.25	0.42		0.11	0.18	0.53	1.10	1.24	1.45	1.49	1.56	1.63	1.56	68.86
	E 26	6.48	0.18		0.47	0.82	1.86	3.85	4.19	5.01	5.47	5.83	5.94	5.83	82.10
	E 27	10.89	46.79		0.21	0.28	0.90	1.80	1.93	2.14	2.49	2.63	2.63	2.83	93.45
	E 30	43.24	4824.28		0.04	0.44	0.91	1.65	1.77	1.96	2.05	2.28	2.31	2.45	64.09
	E 32	20.94	19.75		0.21	0.43	1.04	1.97	2.47	2.72	2.86	3.12	3.15	3.04	69.56
	E 34	23.44	0.16		0.26	0.58	1.19	2.18	2.51	2.79	2.89	3.18	3.24	3.98	67.54
	E 38	12.55	0.00		0.84	1.98	3.48	6.06	7.38	8.10	8.64	8.95	8.94	9.31	68.52

Table 5. (continued)

Well	Sample	Laboratory Por. (%)	Laboratory Perm. (md)	Rh:	% Water Saturation at Given Relative Humidity (Rh in %) 12.2	32	75.7	94.3	95.7	96.6	97.7	98.4	99.30	99.80	100.00
78-5	F 1	19.43	3.35		0.12	0.31	0.43	0.78	0.89	1.09	1.16	1.20	1.09	1.17	71.92
	F 2	11.76	4.05		0.26	0.64	1.09	1.85	2.04	2.30	2.42	2.55	2.55	2.62	83.49
	F 3	22.51	1.04		0.13	0.30	0.53	1.10	1.24	1.40	1.47	1.50	1.54	1.54	65.71
	F 6	16.07	8.77		0.19	0.42	0.66	1.36	1.55	1.74	1.88	2.02	2.02	1.93	71.95
	F 10	25.87	395.47		0.09	0.20	0.29	0.58	0.73	0.84	0.93	1.02	0.99	0.87	63.59
	F 13	11.68	29.22		0.19	0.39	0.84	1.75	1.87	2.13	2.33	2.46	2.52	2.33	81.21
	F 17	25.15	2.42		0.18	0.42	0.72	1.26	1.35	1.44	1.59	1.71	1.74	1.89	51.98
	F 22	12.80	19.92		0.29	0.47	1.00	1.95	2.24	2.47	2.59	2.65	2.77	2.36	81.71
	F 23	10.82	5.54		0.28	0.77	1.53	3.06	3.48	3.90	4.24	4.39	4.45	4.18	91.17
	F 24	21.42	123.82		0.14	0.32	0.71	1.34	1.55	1.73	1.83	1.98	2.01	2.05	65.72
	F 27	31.56	2.17		0.12	0.38	0.84	1.44	1.63	1.82	1.92	2.09	2.01	2.28	67.81
	F 28	17.94	11.22		0.55	1.10	2.19	3.62	4.08	4.50	4.92	5.31	5.31	6.23	74.29
	F 32	13.73	9.47		0.77	1.48	2.68	4.77	5.58	6.08	6.46	6.96	7.01	7.94	82.04
93-A	G 2	11.26	1.37		0.40	0.67	1.28	2.22	2.35	2.55	2.69	2.83	3.03	3.03	82.99
	G 5	16.68	0.53		0.27	0.59	1.04	1.85	2.03	2.17	2.35	2.48	2.53	2.48	75.04
96-A	H 2	12.50	9.58		0.24	0.36	0.78	1.63	1.75	1.93	2.23	2.36	2.35	2.42	77.76
76-3	I 2	13.19	32.46		0.29	0.63	1.15	2.65	2.94	3.28	3.40	3.57	3.69	3.80	83.81

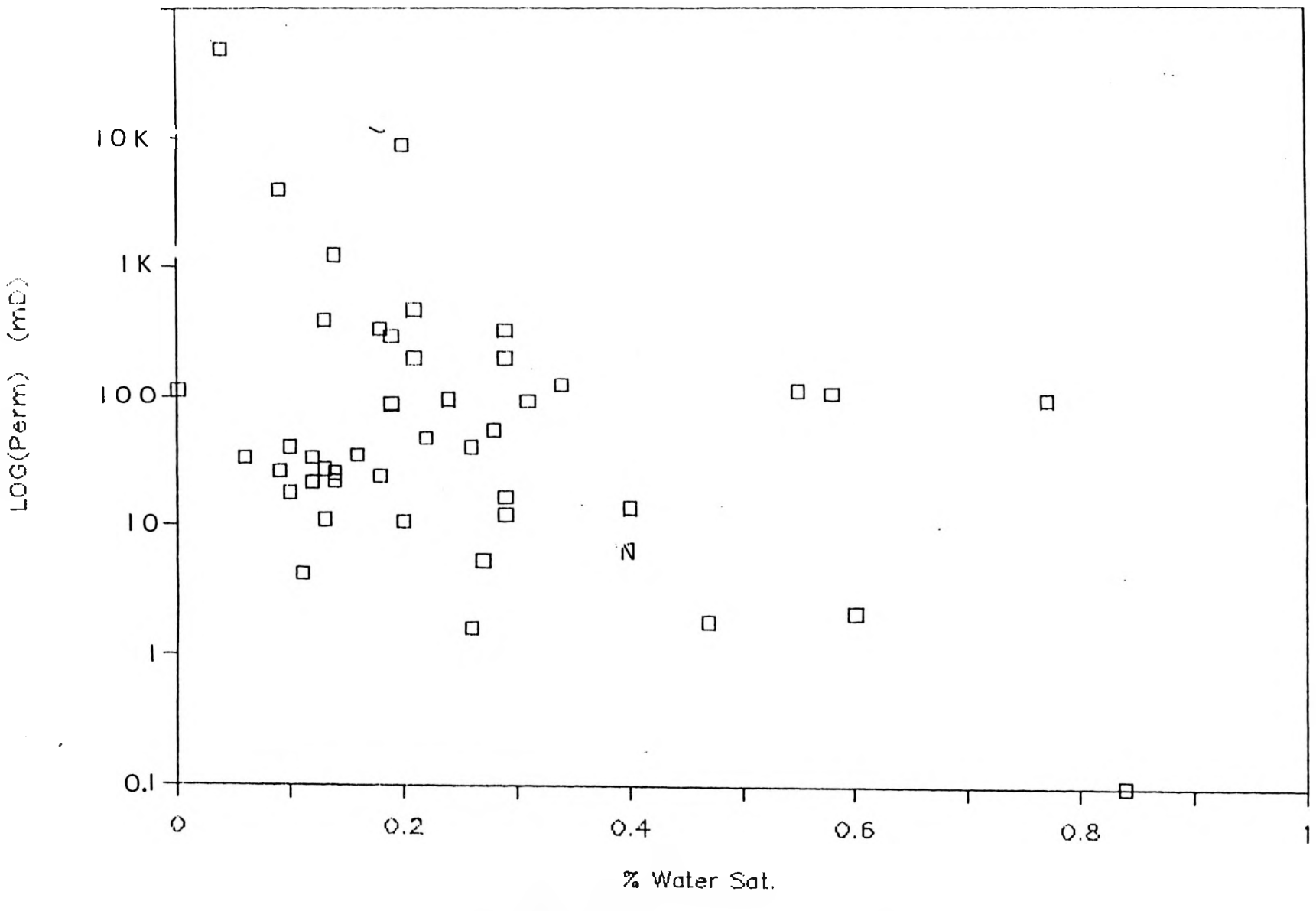

Figure 32. Air permeability versus water saturation at 12% relative humidity.

A number of checks were made on possible effects on saturation caused by the geometry of the physical saturation environment. Both location above the salt solution and the possibility that equilibrium was not reached for these samples have been evaluated. However, no correlation has been found between distance above the salt solution and deviations in saturation behavior (the low-output fan apparently provides adequate air circulation). Furthermore, the same saturation pattern from these plugs is preserved at the higher relative humidities, when greater time is allowed for the plugs to reach equilibrium, and distances above the salt solution are varied. It must be concluded then, that either there is an as-yet unrecognized bias in the experimental setup or the scatter in these data are real.

The percent water saturation data available to date for each basalt plug was also plotted against relative humidity. It is common in adsorption/desorption studies to relate water saturation to either capillary pressure (matric potential) or relative humidity. To convert relative humidity to capillary pressure (-Pc), or vice versa, the following equation is used:

$$-Pc = RT\ (\rho_w \times 10^6)\ \ln(h_r)/(m \times 10^3) \qquad (3)$$

where:

R = gas constant = 8.3144 J/K-mol

T = temperature in K

ρ_w = density of water, g/cm^3 at temperature T

h_r = relative humidity in fraction form

m = molecular weight of water, g/mol

Both the percent water saturation and the capillary pressure equations are used in the program EQWSAT.BAS (Appendix D), which calculates vapor pressure, water volume, and percent water saturation.

In Figure 33, the range of adsorption curve shapes of the 45 basalt plugs at increasing relative humidity is represented by samples C14, F10, and E38. The F10 adsorption curve (Figure 33a) is typical of samples with the lowest percent water saturation, and has a permeability of 395.47 md. The E38 adsorption curve (Figure 33b) is typical of those samples with the highest percent water saturation, and has a permeability of less than 0.01 md. The C14 adsorption curve (Figure 33c) is an intermediate type between the F10 and E38 extremes. The C14 adsorption curve has a permeability of 1.67, which is a little below the average for this sample group.

The adsorption curve shapes represented by F10, E38, and C14 were compared to standard hysteresis loop types used to classify experimentally derived hysteresis loops. Based strictly on the absorption curve, the curve shapes illustrated in Figure 33 are all a variation of de Boer's Type A hysteresis loop (Figure 33d). This is fortunate because some curve types [i.e, de Boer's Type B, (Figure 33d)] do not allow surface area to be calculated.

Pore-Size Distribution and Surface Area

The pore-size distribution and surface area for each basalt plug cannot be calculated until the desorption or drying curve is completed. Data for the desorption or drying curve are still being collected, thus there are no data to report at this time. The program PORSFC.BAS (included in Appendix D) will be used to calculate pore-size distribution and surface area. The nature of adsorption in this context actually involves both adsorption and condensation of water. For humidities less than the critical humidity (the humidity at which condensation can begin), there are no pores small enough to allow capillary condensation, so it is a domain of pure adsorption, where the adsorbed water layer grows only by vapor diffusion (Daian, 1988). At the capillary condensation threshold, i.e., at the point

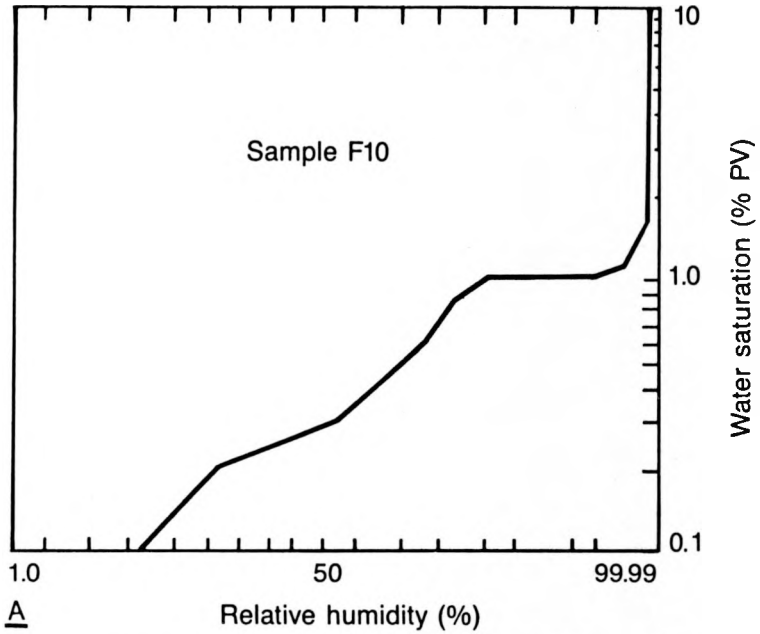

A

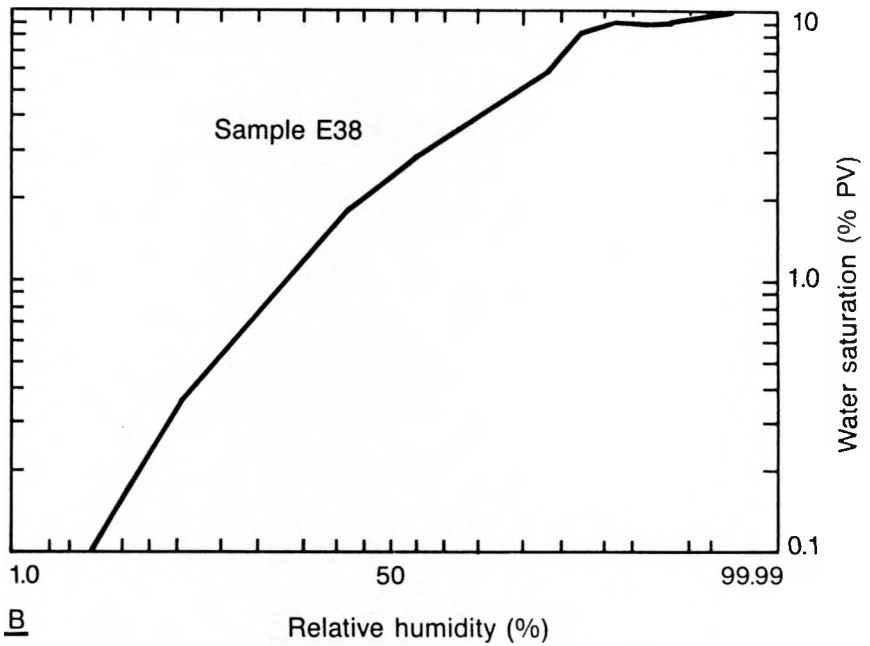

B

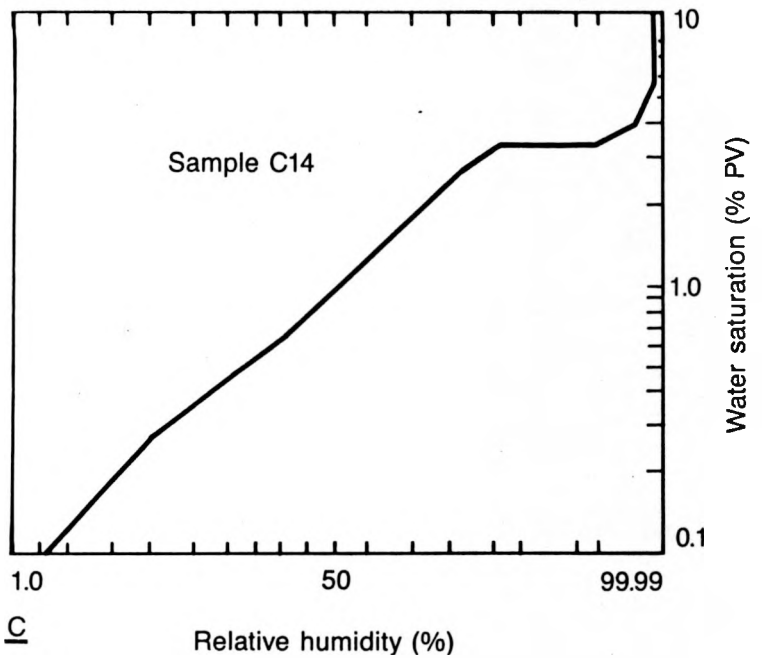

C

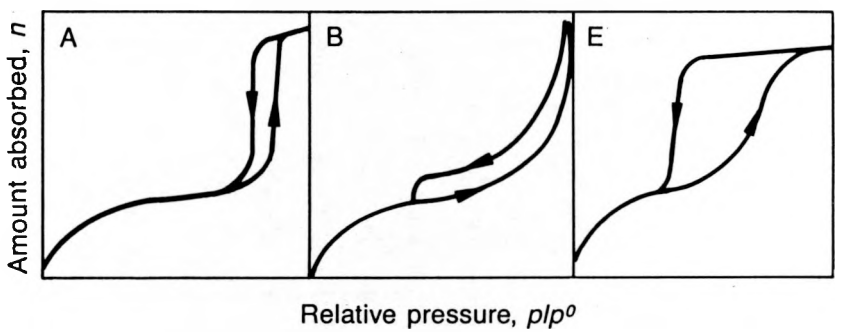

D (from de Boer's)

0-6897

Figure 33. Water saturation versus relative humidity.

where the critical humidity is reached, capillary water will begin to appear in all pores of the smallest radius. As the meniscus of the adsorbed layer becomes larger, the capillary water will appear in an increasingly larger class (size) of pores (Gregg and Sing, 1982; Daian, 1988). (The nearly discontinuous capillary islands that are subsequently formed are provided by both direct capillary migration of liquid water and vapor diffusion.)

The method used here to calculate both pore-size distribution and surface area was first proposed by A. Wheeler in 1945 and developed by C. G. Shell, E. P. Barrett, et al., and R. W. Cranston and F. A. Inkley, among others (Gregg and Sing, 1982). This method was later simplified by D. Dollimore and G. R. Heal (Dollimore and Heal, 1970) and it is Dollimore and Heal's version as presented by Gregg and Sing (1982) that is used in PORSFC.BAS and presented in Appendix D.

PETROGRAPHY

Procedures

The wafers cut from the ends of the 25-mm porosity/permeability plugs were placed in labeled "ziplock" bags. These bags were placed, in sequence by wells, in core boxes and taken to Idaho State University. From the total of about 400 samples, approximately 150 representative samples were chosen for thin sectioning (after a careful hand lens and/or binocular microscopic examination). The wafers selected for thin sections from 11 wells were petrographically analyzed for texture and mineralogy. Quantitative analysis of phenocrysts, matrix, and voids, were made by counting at least 1,000 points on 75 of the 150 thin sections. The porosity and permeability data from the plug, adjacent to the thin section, were compared to the petrographic analysis results.

The petrographic correlations of the flows were used to provide a grouping of core into specific flow groups, flow units, and flows. The petrographic analyses were made by J. C. Crocker. His complete report is included as Appendix B.

Petrographic Results

The flow group boundaries used in this analysis were those developed by Anderson and Lewis (1989). The flow unit correlations were attempted using petrographic analysis results. The correlations were inconclusive in flow group C because of the lack of relatively continuous core in a significant number of wells. Summaries of the individual flow unit characteristics follow.

Flow Group A

Flow group A is found only in the cores from the northern tier of wells, 76-2, 76-3, 76-4, 76-4A, 77-2, 78-2, 79-2, and 96-A (Figure 8). Two flows are recognized in the samples and are designated 1 and 1a.

Kuntz and others (1980) correlated this flow group on the basis of ubiquitous heavy oxidation of hand specimens. This characteristic is not discernible in the group of samples used for petrographic analysis. The identifying parameters are as follows:

- Phenocrysts are minor constituents. Small olivine phenocrysts occur as aggregates and individual grains. The plagioclase and olivine phenocrysts that do occur are unaltered and set in a fine-grained intergranular matrix with abundant, dark-opaque oxides in the flow tops and bottoms, and in an intergranular fine to coarse matrix in the flow centers.

- Matrix plagioclase is <0.5 mm and olivine is <0.5 mm. The clinopyroxenes are commonly intergranular, but may be locally ophitic and/or subophitic.

- Vesicle borders are frequently composed of glasses or opaques in flow tops and bottoms, but are commonly diktytaxitic, i.e., the vesicle surfaces are made up of crystal ends or edges in the flow centers.

This flow group is differentiated from the underlying group B by the lack of large feldspar phenocrysts. The statistical point count results are summarized in Table 6.

Flow Group B

Flow unit B-1 is of limited extent within the RWMC area. It probably filled a topographical low on the flow unit B-2 surface. This low was apparently filled to a topographic high in most places by B-1 when the overlying flow group A was emplaced, because flow group A is not found where flow unit B-1 is present, except in Well 76-2.

Table 6. Volume-percent ranges and averages of thin-section measured values for flow group A

	Flow Unit A		
	Minimum	Maximum	Mean
% Plagioclase (2)[a]	2.7	2.5	2.6
% Olivine (2)	4.3	5.8	5.1
% Matrix (2)	91.5	93.2	92.4
% Voids (2)	8.6	15.7	12.2
% Porosity (8)	4.8	26.5	14.5
Permeability (8)	0.0	18.0	4.5
Maximum size in mm			
Max plagioclase (8)	1.6	2.7	2.1
Max olivine (8)	1.15	4.15	2.0
Max vesicle (8)	3.6	5.2	4.5

a. Values in parentheses are total number of samples measured.

B-1 is a light gray rock with a fine- to medium-grained matrix. Plagioclase, the predominant phenocryst, increases in size from the top to the bottom of the flow. The amount of oxidation also increases towards the bottom of the flow.

The flow top and bottom matrix is dark, with a high percentage of opaque oxides, and has intergranular, fine plagioclase and olivine crystals <0.5 mm in size. Clinopyroxene phenocrysts are uncommon. However, ophitic clinopyroxene is found near the flow bottom.

The midflow matrix has a coarse intergranular texture and diktytaxitic vesicle walls. The matrix mineralogy consists of plagioclase, olivine, intergranular to subophitic clinopyroxene, and opaques with a general size <0.5 mm.

The B-1 flow can be differentiated from the underlying B-2 flow by its rare large phenocrysts. The statistical point count data are summarized in Table 7. The contrast in size between the mean plagioclase and olivine phenocryst size in flow B-1 (2.5 and 0.9 mm) and that displayed by the underlying B-2 flow (4.3 and 1.5 mm) is an important aspect of the Table 7 data set.

Flow unit B-2 is generally represented by two flows (B-2a and B-2b), separated by a flow interface. The physical appearance of the two flows is identical. Thus, the following description applies to the B-2 flow, as a whole.

The rock is distinctly porphyritic, with a dark gray to purplish-gray matrix. Although the plagioclase is the predominant phenocryst, olivine crystals, as large as 1.5 mm, and clusters of olivine crystal aggregates are common.

Flow tops are lightly oxidized, lending a reddish tint to the rock. This color change disappears about 1 m below the flow surface. Below this point, oxidation is limited to vesicle and matrix walls.

Table 7. Ranges in measured values for flow group B

	Minimum	Maximum	Mean
Flow Unit B-1			
% Plagioclase (17)[a]	6.4	24.5	14.6
% Olivine (17)	0.4	10.0	3.5
% Matrix (17)	70.9	92.9	81.8
% Voids (17)	0.1	12.2	5.3
% Porosity (22)	5.2	30.7	17.1
Permeability (22)	0.1	6.8	9.8
Maximum size in mm			
Max plagioclase (22)	1.2	6.8	2.5
Max olivine (22)	0.3	2.1	0.9
Max vesicle (22)	2.8	11.2	5.7
Flow Unit B-2a			
% Plagioclase (7)	10.3	26.7	17.5
% Olivine (7)	2.3	8.2	5.3
% Matrix (7)	69.8	87.4	77.2
% Voids (7)	0.0	13.9	7.6
% Porosity (8)	4.6	32.4	16.5
Permeability (8)	0.2	18.0	5.0
Maximum size in mm			
Max plagioclase (8)	3.2	6.3	4.3
Max olivine (8)	0.9	1.8	1.5
Max vesicle (8)	1.1	16.0	5.8
Flow Unit B-2b			
% Plagioclase (7)	9.0	21.4	16.6
% Olivine (7)	3.1	7.5	5.4
% Matrix (7)	72.8	87.9	77.9
% Voids (7)	0.9	10.5	5.1
% Porosity (9)	5.2	26.3	15.0
Permeability (9)	0.0	4448.0	414.0
Maximum size in mm			
Max plagioclase (9)	2.3	5.8	4.4
Max olivine (9)	0.9	2.3	1.4
Max vesicle (9)	1.7	8.4	4.4

Table 7. (continued)

	Minimum	Maximum	Mean
Flow Unit B-3			
% Plagioclase (8)[a]	6.9	27.1	18.5
% Olivine (8)	4.0	6.0	5.1
% Matrix (8)	67.4	89.1	76.5
% Voids (8)	2.2	16.2	9.2
% Porosity (13)	7.6	25.9	14.9
Permeability (13)	0.2	39.5	33.1
Maximum size in mm			
Max plagioclase (13)	1.3	6.9	3.3
Max olivine (13)	0.7	3.4	1.3
Max vesicle (13)	1.6	8.6	4.4

a. Value in parentheses is the number of samples measured.

The flow top matrix has a large fraction of opaque oxides. The discernible matrix minerals are plagioclase and olivine, and some oxidized clinopyroxene, and the crystals are very fine-grained.

The midflow matrix is more coarsely grained, has a higher clinopyroxene fraction, and lacks the significant opaque oxide fraction compared to the flow tops and bottoms. Approximately half of the B-2 samples counted had significant amounts of subophitic clinopyroxenes.

The phenocryst morphology is common to all B-2 elements. Plagioclase phenocrysts occur as individual laths, subparallel bundles, crosses, and radial crystal assemblages. Interstitial olivine and clinopyroxene are ubiquitously associated with the plagioclase phenocrysts. Olivine phenocrysts are also common in all samples.

Flow units B-2 and B-3 are easily distinguishable because B-3 is intergranular. The point count statistics for flow unit B-2 are also summarized in Table 7.

Flow unit B-3 is present in all cores as a single flow. It is predominately light gray in color and equigranular and intergranular. Flow tops are oxidized and have a distinctive orange color.

The matrix of the upper flow element is fine-grained with rare phenocrysts that are much smaller than those found in flow unit B-2. Rare olivine phenocrysts also occur, as does ophitic clinopyroxene. Some of the olivine is in aggregates as large as 3-4 mm in diameter.

The flow top matrix has such a large fraction of dark opaque constituents, that it is nearly opaque when viewed in thin section. The discernible grains are plagioclase and olivine with some clinopyroxene, all having a grain size <0.5 mm.

The flow bottoms have a texture similar to that of the flow tops. However, bottoms are slightly finer and lack the rare ophitic clinopyroxenes.

The midflow matrix consists of intergranular plagioclase, olivine, opaques, and clinopyroxene. Some subophitic clinopyroxene is generally present in about half of the samples.

It is not easy to differentiate B-3 from C-1 where the BC interbed is not present. The subtle differences are that the rare B-3 plagioclase phenocrysts are larger and the rare olivine phenocrysts are smaller than in C-1. In addition, the olivine aggregates are more common in C-1. The point count data from flow unit B-3 is also summarized in Table 7.

Flow Group C

An attempt was made to correlate flow units C-1 and C-2. So little core is available below C-2 and so many gaps are present in this core, that it is not practical to attempt correlation below this point.

Flow unit C-1 is classified as equigranular and ranges from intergranular fine to coarse. Flow tops are locally oxidized orange and have fine to aphanitic matrix grain size. These oxidized areas often have a slightly porphyritic texture. The flow bottoms generally have an aphanitic matrix and matrix voids that are relatively small in size.

The flow top and bottom matrix have abundant opaque oxides and glassy or oxide-dominant vesicle walls. Matrix mineralogy consists of unaltered plagioclase and olivine, with the associated opaque oxides and small grains of oxidized clinopyroxene. Olivine grains are locally oxidized along crystal faces.

The midflow matrices are fine to coarse equigranular, but with occasional prominent individual grains and aggregates of olivine. The olivine grains are locally oxidized along fracture surfaces. Where vesicles

occur, they have diktytaxitic walls. The grains are <0.5 mm in size. About one-third of the midflow thin sections display ophitic texture, and examples of subophitic texture were found in most of the thin sections.

The C-1 flow can be differentiated from the underlying C-2 flow by the smaller plagioclase grains found in C-1. The point count statistics for the C-1 flow are summarized in Table 8.

Flow unit C-2 is predominately intergranular and coarse in texture. Some examples of fine texture are found in chilled flow tops. Flow tops and bottoms have abundant opaque oxide grains and clinopyroxenes are represented by small oxidized matrix grains. Matrix plagioclase grains are generally <0.1 mm and olivine is <0.5 mm. Diktytaxitic textures are found in the flow tops and bottoms, but this is not the dominant texture, as typified by all the midflow samples.

The phenocrysts that occur are predominately plagioclase laths or subparallel bundles with some crosses and occasional radial aggregates. The olivine phenocrysts are generally large aggregates (<0.5 mm) and are generally associated with the plagioclase phenocrysts.

The main parameter differentiating the C-2 from the underlying flow unit is the generally unoxidized or poorly oxidized state of olivine crystals in the C-2 flow. The point count statistics for the C-2 flow are also summarized in Table 8.

Correlation of flow units below C-2 is tenuous because of the lack of continuous core from any one well and the more common, general lack of a reasonable amount of core from the sub C-2 to CD interbed in any of the sampled wells. Two general flow unit types might be present in sub C-2. However, the overlap of textures from these is so great that they will be discussed as a single, general entity.

Table 8. Ranges in measured values for flow group C

	Minimum	Maximum	Mean
Flow Unit C-1			
% Plagioclase (12)[a]	2.3	17.5	11.3
% Olivine (12)	2.0	8.9	5.0
% Matrix (12)	76.9	95.7	83.5
% Voids (12)	10.0	12.0	10.2
% Porosity (14)	10.0	33.1	17.0
Permeability (14)	0.1	1575.0	133.0
Maximum size in mm			
Max plagioclase (14)	1.3	3.0	2.2
Max olivine (14)	0.8	4.0	2.3
Max vesicle (10)	1.7	8.1	4.0
Flow Unit C-2			
% Plagioclase (10)	3.1	17.2	10.8
% Olivine (10)	0.2	10.9	5.0
% Matrix (10)	75.0	96.7	84.2
% Voids (10)	8.3	26.7	18.7
% Porosity (13)	12.7	33.4	12.7
Permeability (13)	0.0	379.0	53.9
Maximum size in mm			
Max plagioclase (13)	1.9	3.1	2.4
Max olivine (13)	0.7	3.7	2.2
Max vesicle (13)	0.5	13.0	4.8

a. Value in parentheses is the number of samples measured.

The sub C-2 interval (understood to be from the bottom of flow unit C-2 to the top of interbed CD) is represented by one to six individual flows. These flows are classified as intergranular, and fine to coarse in texture. In general, the C-3 flows have smaller plagioclase crystals than C-2. The flow tops are oxidized a distinctive orange color, with many vesicles filled with clay/silts and caliche. The flow top and bottom matrix is generally fine-grained, and the vesicles usually have glassy or opaque oxide walls. The flow bottom oxidation results in a rusty coloration.

Midflow samples are generally intergranular-coarse in texture. Olivine occurs as rare, large grains and aggregates. The olivine generally has a surface oxidation layer that gives it a brassy appearance. The clinopyroxene is commonly ophitic in texture, but subophitic and intergranular varieties were also observed. Diktytaxitic texture is normal in midflow samples and rare in flow tops and bottoms.

The general configuration of the flow groups, units, and flows is displayed by fence diagrams in Figures 34a and 34b. Flow group A is a single flow except in Well 76-2 where two flows are present.

Flow groups B and C are more complex. Flow unit B-1 is a single event. However, flow unit B-2 is represented by two flows in the northern tier of wells, and is differentiated into as many as six flows in Well 79-3 at the southern margin of the area of interest. The actual complexity can be shown by contrasting the two flows in Well 76-4A with the five flows in its twin well, 76-4.

Flow unit B-3 is a single flow in all but three wells where it is broken into two flows. Flow unit C-1 is a single flow, while C-2 changes from one (two wells) or two (three wells) flows in the northern tier of wells to as many as four flows (two wells) in the southern tier of wells. The sub C-2 flow units in flow group C are represented by the least amount of core. This group of flows varies in complexity. It is represented by

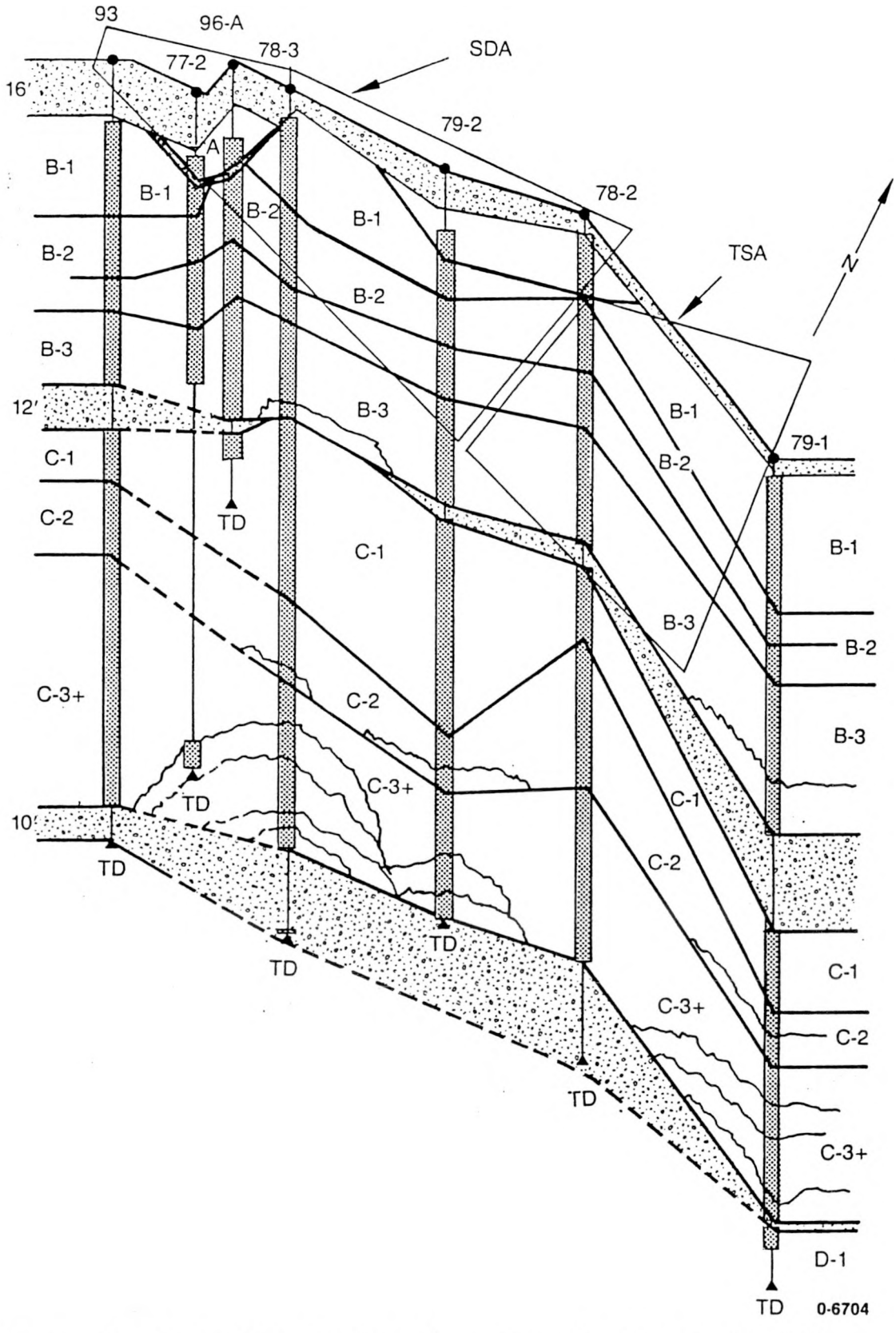

Figure 34a. Fence diagram of northern tier of wells at the RWMC.

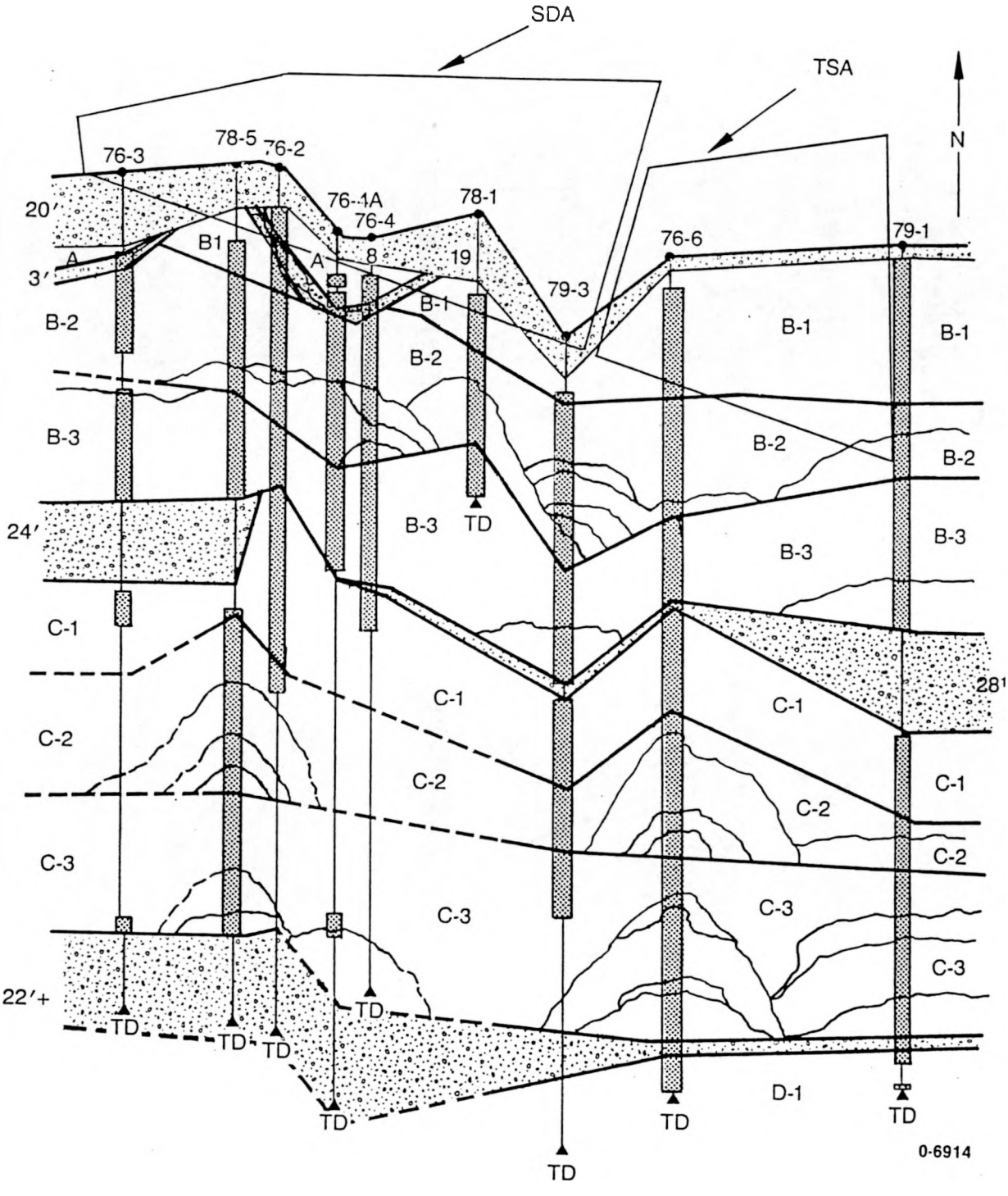

Figure 34b. Fence diagram of southern tier of wells at the RWMC.

single flows in two northern tier wells (93-A and 78-2), but displays three, four, and five flows in the other three northern tier wells and either four or five flows in the southern tier wells.

The distribution of flow heights from each of the flow units is presented graphically as Figures 35 and 36, and is summarized in Table 9. The median thickness from the core data for all the flows is 15 ft (4.6 m). The minimum and maximum thickness is 3 and 76 ft (0.9 and 23.2 m). This data is from a data set of 124 flows.

Textural Control for Permeability/Porosity

The thin section analysis provides some insight into the porosity and permeability relationships of the RWMC basalts. The main porosity components are (1) the intergranular voids and (2) the vesicles. The porosity of the matrix (intergranular porosity) can be roughly estimated from the visible pinpoint porosity in the rock: low ~6%, medium ~9%, and high ~12% porosity. There is a lot of scatter around these values, but they can serve as the general rule. Thus, the total porosity can be estimated to a reasonable level by summing the vesicle and median matrix porosities.

It would be fortunate if there were a well-behaved relationship between the porosity and the permeability that could be visually estimated. Unfortunately, the relationship is quite complex. Basically, the permeability of the rock is usually controlled by the permeability of the matrix. The flow tops and, to a lesser extent, the flow bottoms have matrices with large fractions of opaque oxides and some glass, and a generally lower visible matrix porosity. The vesicular portion of the rock has vesicle walls that are, for the most part, glassy/opaque oxide, as is an appreciable fraction of the matrix. Thus, the material connecting the vesicles has a lower permeability than the central portions of the flows. This relationship can be seen in the median permeabilities, where the median permeability of the top and bottom vesicular zones, 7 and 4 md, are lower than the median permeability of the central zone, which is 8 md. This is

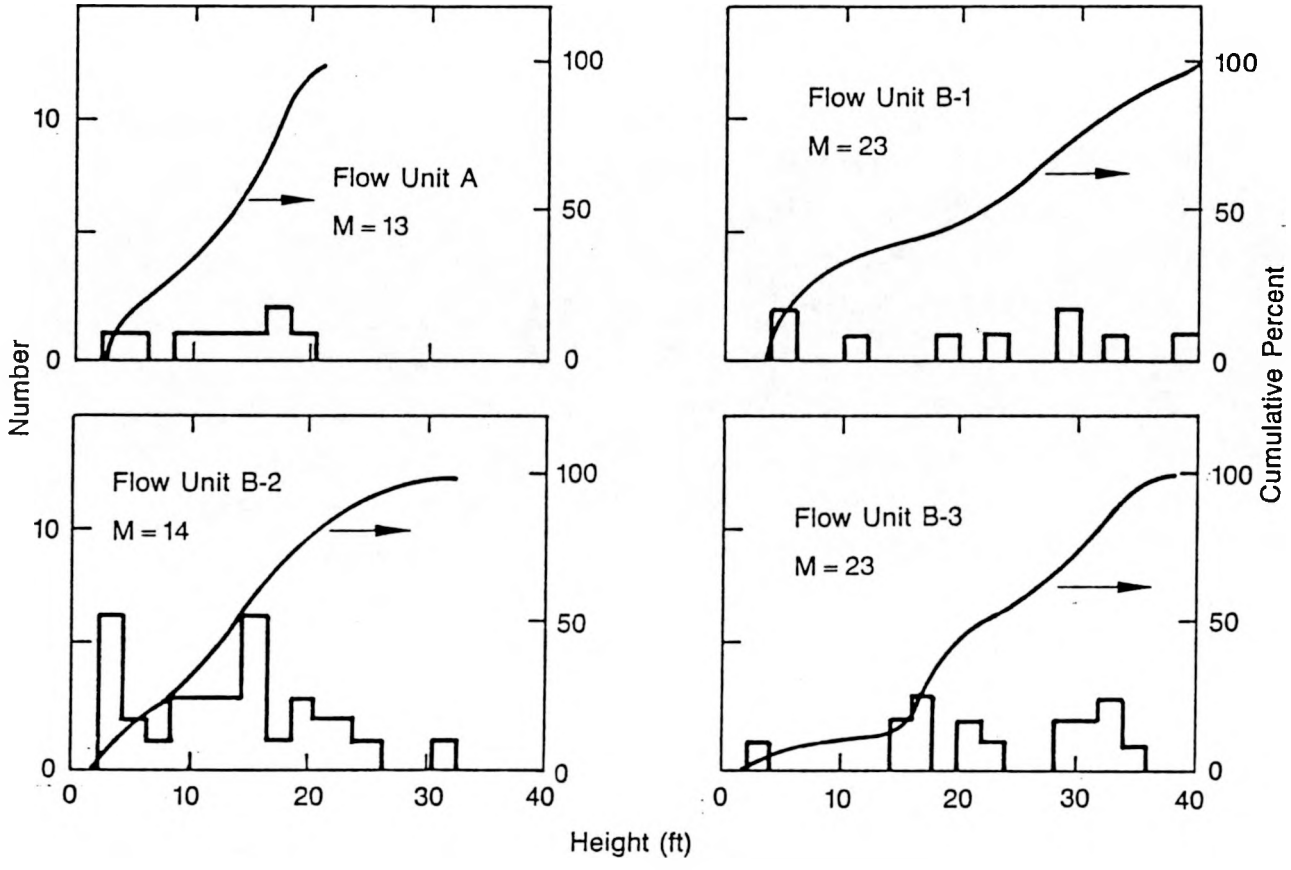

Figure 35. Thickness distribution of flow units in flow groups A and B (m = median value).

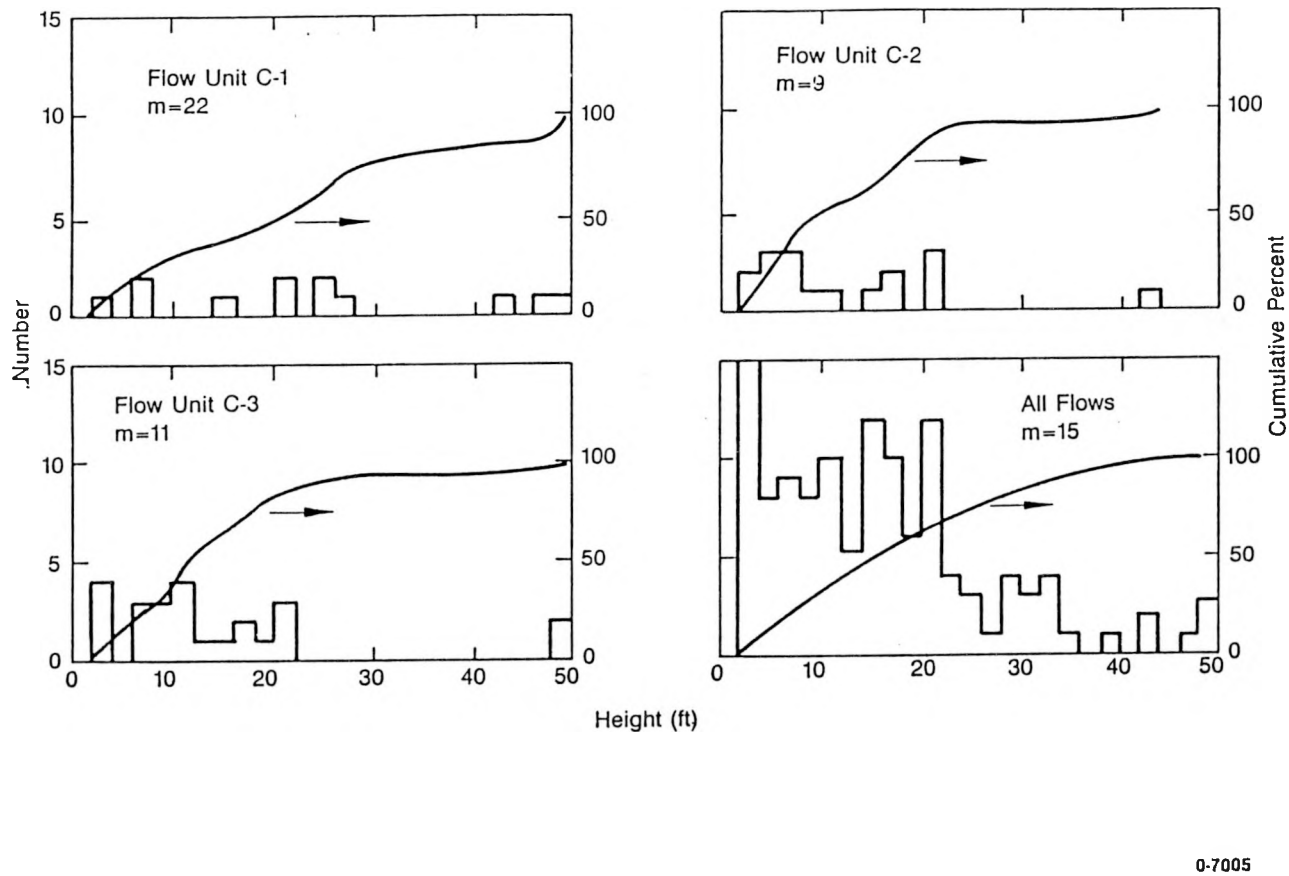

Figure 36. Thickness distributions for flow units in flow group C and for all flow units (m = median value).

Table 9. Thickness distributions of flows based on core data

	Thickness (ft)			
Group/Unit	Minimum	Median	Maxima	Number
Flow Group A	4	13	19	9
Flow Group B				
Unit B-1	5	22	34	9
Unit B-2	3	14	26	36
Unit B-3	4	22	36	17
Flow Group C				
Unit C-1	4	22	52	12
Unit C-2	3	10	44	17
Unit C-3	3	14	76	24
All Flows	3	15	76	124

quite impressive when we consider that there are a large number of spuriously high permeabilities from the vesicular rock (where, because of the small physical size of the sample compared to the vesicle sizes, the flow path through the rock may encounter 90% or more open space than rock).

The opaque oxide material grades into intergranular magnetite and ilmenite in the central portion of the rock. The magnetic properties of the two zones are quite different, and reasonably well known. The crystalline magnetite has much higher susceptibilities. This factor is used in mineral separation, and the magnetic constants, etc., had been measured as early as 1935 (Dean et al., 1935). The magnetic susceptibility is currently being used in ash flow correlations (Eick and Schlinger, 1989) and magnetic domain studies in magnetite are currently a part of the international geomagnetism effort (Worm et al., 1989). This flow parameter should provide characterization information from a magnetic log (one has been developed by the DOE-ID group at the Grand Junction, Colorado office and is available).[a]

Thus, insight into the petrography of the rock can provide ideas on how the basalt flows could be characterized using remote sensing techniques, such as geophysical logging. From a characterization standpoint, every well drilled at the INEL should be logged. Enough core should be cut during the drilling program to verify the logging calculations and to provide feedback for maintaining the optimum suite of logs to be used.

Density logs can provide information about porosity and bulk density, sonic logs yield information on fracturing, neutron, and dielectric constant, and resistivity logs can yield information on water content (which relates to the subcapillary/capillary pore fraction in the vadose zone).

---

a. Private communication, D.A. Emilia, Grand Junction DOE-ID Office, February, 1990.

SURFACE/NEAR SURFACE STATISTICAL STUDIES

The effort to provide geostatistical data that could be used to construct the conceptual geological model for the vadose zone under the RWMC was collected from the Hell's Half Acre flow to the southeast of the INEL and the Box Canyon of the Big Lost River at the southwest corner of the INEL (Figure 2). These sites were the ones closest to the RWMC that could provide the large volume of data necessary for statistical studies. The Box Canyon outcrop study determined the flow geometry in the X-Z or vertical sense, while the Hell's Half Acre study looked at the flow properties in a horizontal sense.

Box Canyon Study

The Box Canyon site was selected after an overflight of the Big Lost River from near the Central Facilities Area (CFA) to the upstream end of Box Canyon. The section of the canyon selected was from the river bend at 1,700 ft (518 m) from the north and west lines of Section 35, Range 27 East, Township 3 North to a fence across the river located approximately on the east line of Section 1, Range 27 East, Township 2 North. This stretch of the river is on the USGS Butte City, Idaho 7 1/2 minute (1972) topographic map. Access to the site is by gravel and dirt roads that parallel the river on the south bank. This access starts at the turnoff from U.S. Highway 20/26 at mileage 265.6. Access from Arco is also possible along the Gooddale cutoff.

Thirty-eight stations were established along the 2 1/2-mile section of the canyon chosen for the study. The station locations were plotted on a base map and all photo points and measurements were referenced to these locations. The section of canyon was divided into 10 segments, labeled H through R, by drawing a line across selected bends perpendicular to the river. Approximately 120 photographic stations were located along the canyon (Figure 37). Two or three bearings were taken from each station, as well as a distance to some prominent point near the center of the photo group (distances were measured with an optical rangefinder). The

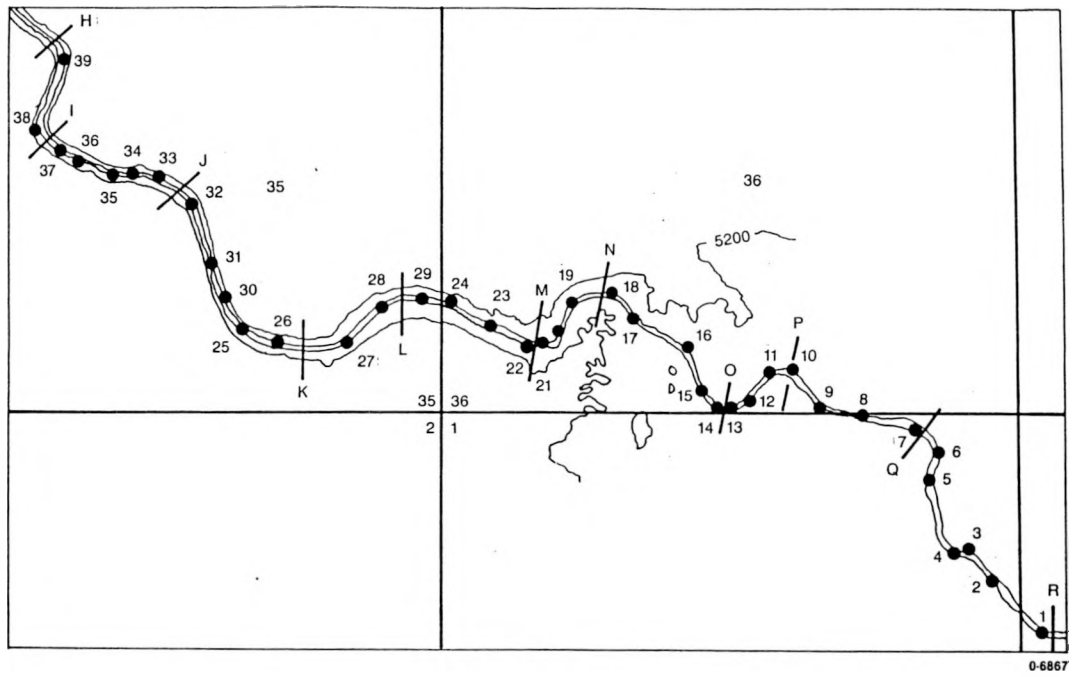

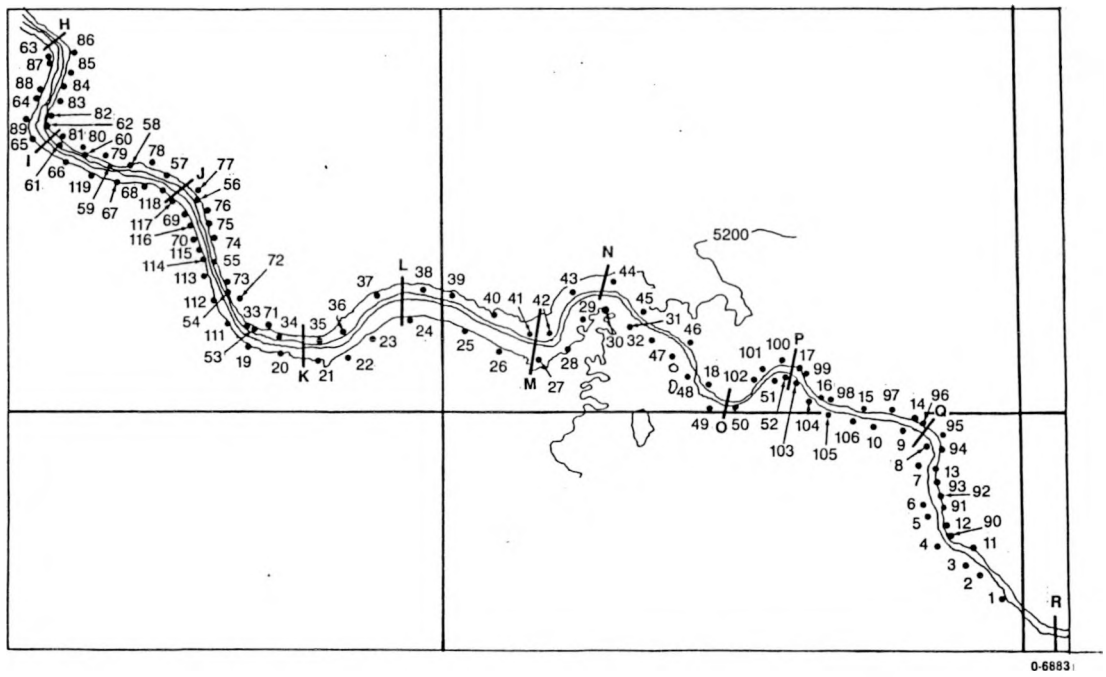

Figure 37. Photographic stations (locations of reference stations are displayed in upper figure, and photo stations in lower figure. The alphabetic designations H through R divide this section of Box Canyon into reference segments).

camera-lens-enlargement system was calibrated so that a length measured on the photographic print could be related to the length of the object using the relationship:

$$L = 25.6 * D1 * D2 \quad (4)$$

where:

L = actual length of object in photograph

D1 = apparent length of object on photographic print, mm

D2 = distance from photographic station to object in thousands of ft (distance in ft/1000)

Each of the ten stream segments was divided into a left and a right side (when looking upstream) and maps, with photo station plotted, were enlarged to a final scale of 1 in. ≅ 130 ft (1 cm ≅ 15.6 m). Each flow, with readily discernible boundaries on the outcrop, was mapped on the 1:1560 scale maps. The flow was given an alphanumeric designation such as NR-L3 which stands for N = stream segment N-M, R = right canyon wall, L = recognizable feature designated "L", and 3 = third flow in the "L" area. The thicknesses (or heights) of the flow at apparent length 0.05, 0.1, 0.2, 0.3, 0.4, 0.5, 0.6, 0.7, 0.8, and 0.9 ft from the upstream end, were measured for 92 flows. The maximum height, normal to the outcrop, and the apparent length of an additional 280 flows were measured.

The core study, discussed previously, could only correlate the basalt characteristics at isolated points in a three-dimensional continuum. A basis for how the characteristics vary, is shown by the two most closely spaced wells in the data set.

Wells 76-4 and 76-4A are located near the southcentral portion of the RWMC with well collars separated by only 26 ft. Appreciable differences in the flow characteristics are discernible even at this small distance (Figure 38). The interwell variations noted in the core study indicate a heterogeneous vadose zone at the RWMC. Only a limited amount of data is

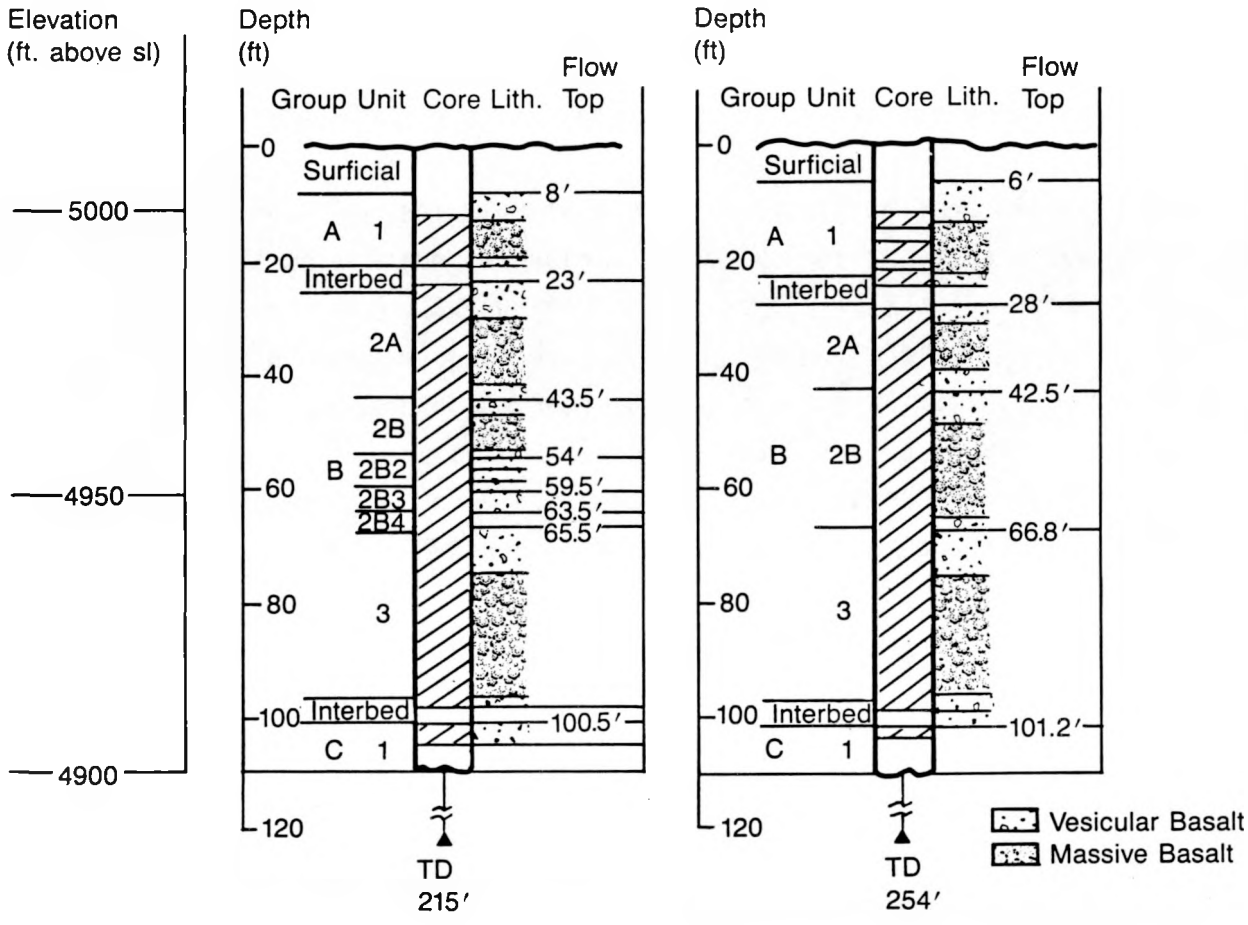

Figure 38. Wells 76-4 and 76-4A located 26 ft apart.

available from the core. Thus, it is best to use outcrop data to develop the geostatistical parameter distributions needed for stochastic modeling.

Box Canyon exhibits a medial/distal flow morphology. Flow group A is a distal configuration at the RWMC. However, the medial/distal configuration is typical of that found in flow groups B and C, and is probably the best analog for the bulk of the vadose zone basalt at the RWMC (see Figure 4).

Analysis of the flow geometry (from vertical cross sections) displayed by the 372 measured flows in Box Canyon yielded a median flow thickness, or height, of about 12 ft (3.7 m), as shown in Figure 39. This compares with the 15-ft (4.6-m) median flow height from core data (Figure 36 and Table 9). The maximum height from the Box Canyon outcrop and the RWMC core data are respectively 60 and 76 ft (18.3 and 23.2 m). Thus, a reasonable analog exists at Box Canyon, although it may be a somewhat less distal flow location than is found in flow group B and deeper RWMC flows.

The apparent length distribution for Box Canyon is presented in Figure 40. The median apparent length is about 65 ft (19.8 m). The distribution for the ratio apparent length (La) divided by maximum height (Hmax), or La/Hmax distribution, is presented as Figure 41. The median La/Hmax ratio is about 6, with a maximum of about 35.

The morphology of the flow cross sections is shown in a photo of a typical Box Canyon outcrop in Figure 42, and a typical scaled flow-boundary tracing of the type used for the statistical outcrop cross section studies is displayed in Figure 43.

The typical flow cross section is a complex lensoidal shape and flow frequently occurs by viscous fingering. The flow lobes typically display an elongation in the flow direction (Figure 6). This preferred orientation or flow direction may be determined by evaluating the relationship between La/Hmax ratio and outcrop cross section orientation.

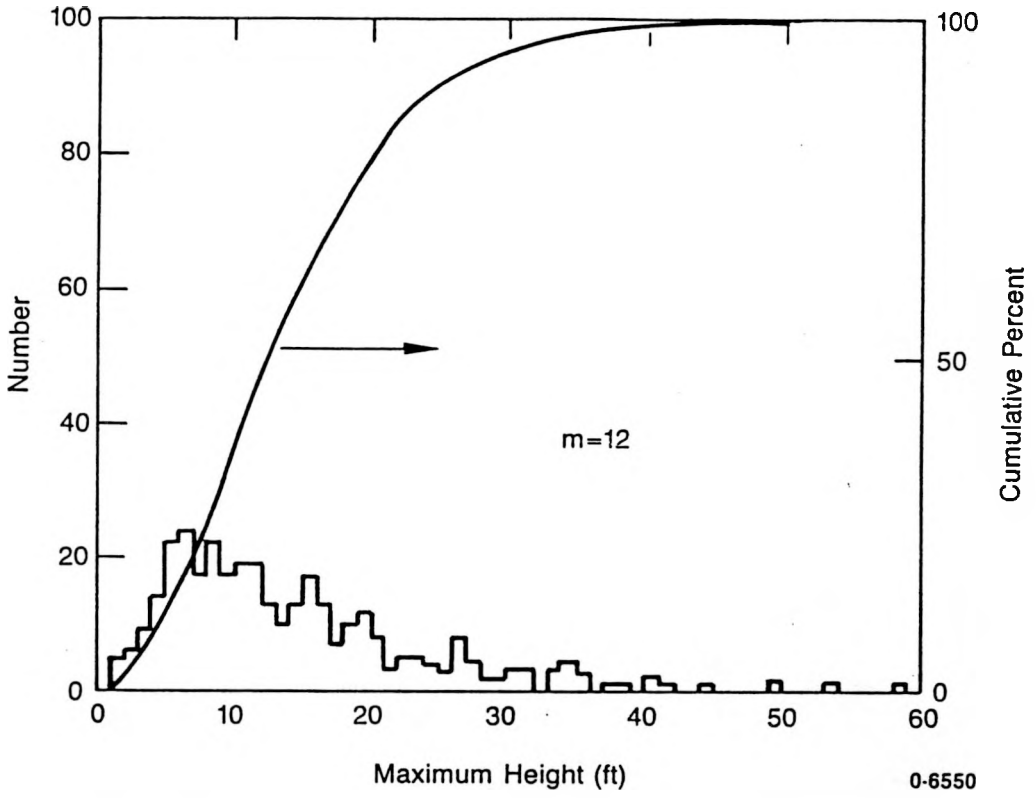

Figure 39. Box Canyon basalt flow geometry, Hmax (m = median value).

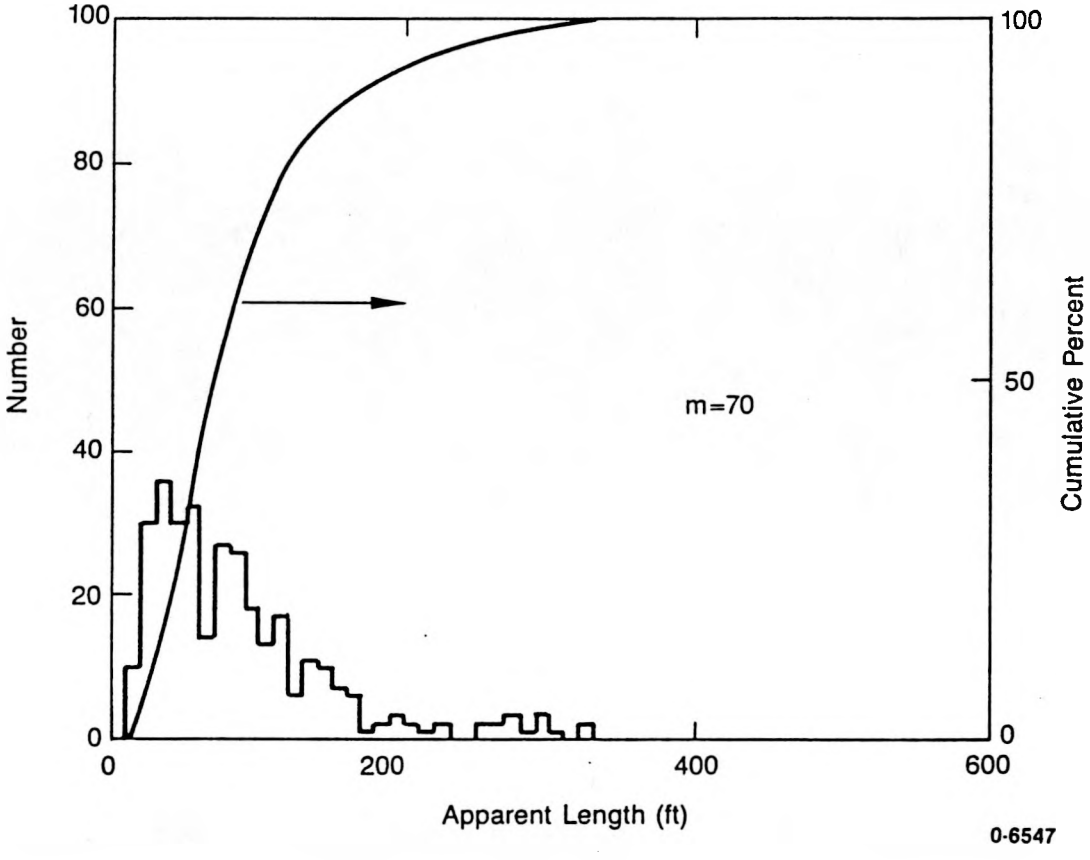

Figure 40. Box Canyon basalt flow geometry, La (m = median value).

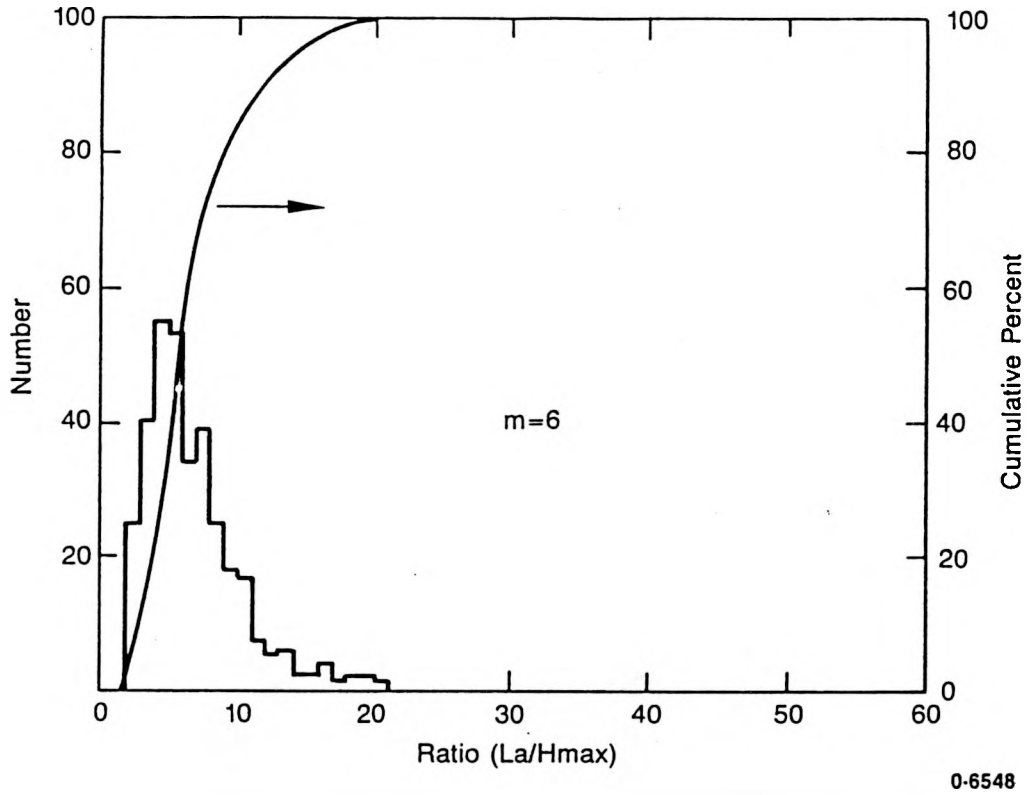

Figure 41. Box Canyon basalt flow geometry, La/Hmax (m = median value).

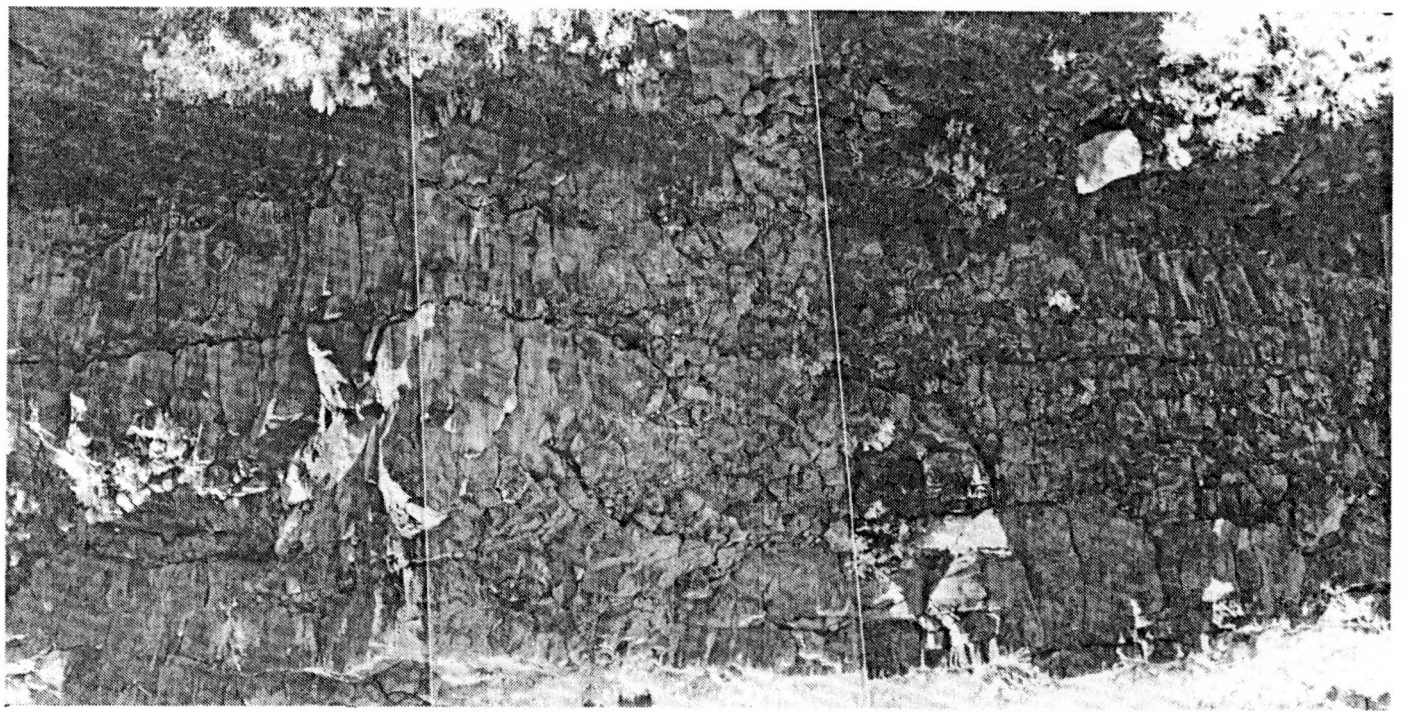

0-6916

Figure 42. Photo panorama of a portion of the north wall of Box Canyon (distance from top to bottom of wall is approximately 50 ft).

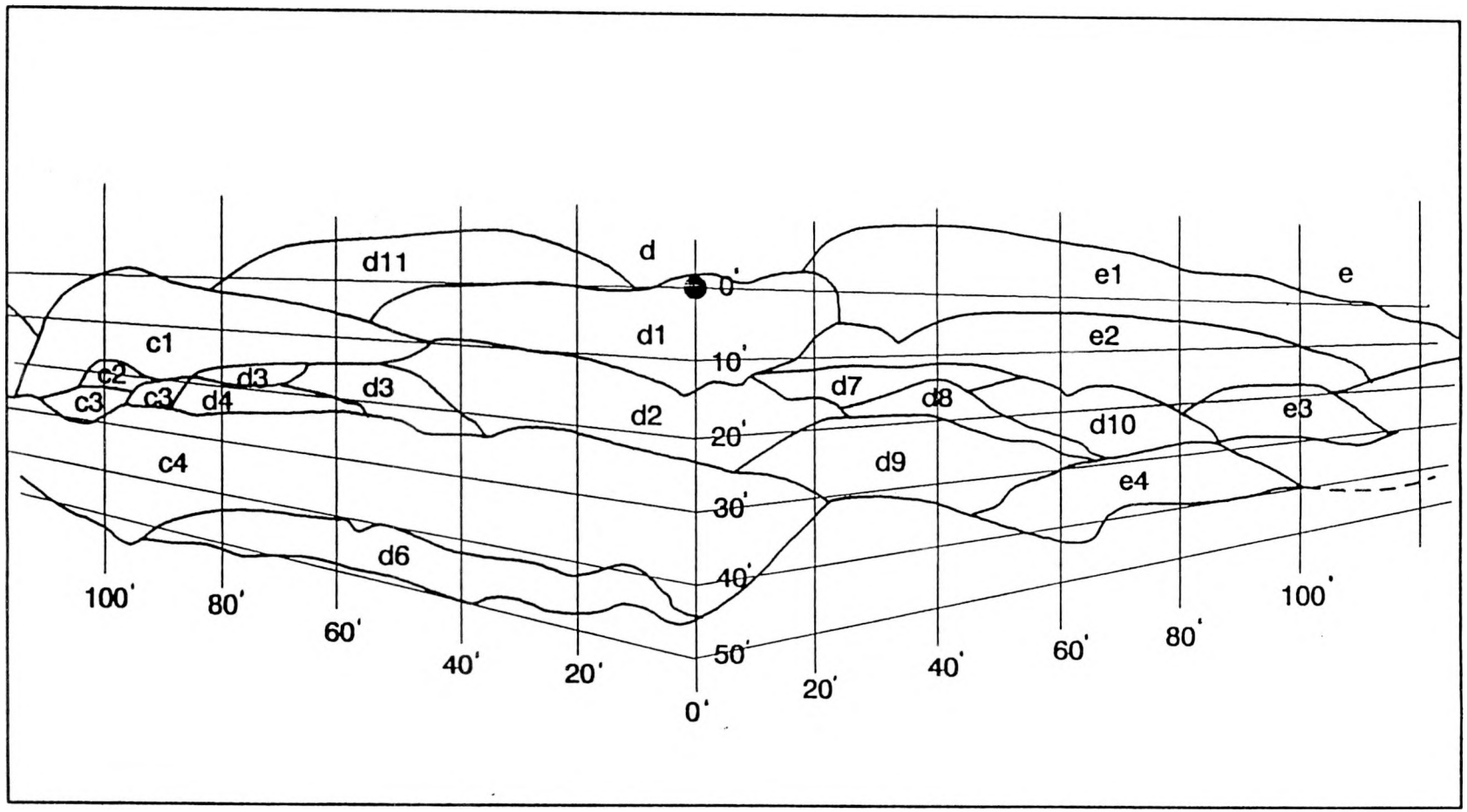

Figure 43. Tracing from a Box Canyon photo panorama with flow boundaries and scale (the notation c1, d10, e3, etc., is the flow name in the LNC3 nomenclature system).

The Big Lost River has a meandering trace in the Box Canyon study area (Figure 37). Thus, the outcrop cross sections cover a broad spectrum of orientations. If the La/Hmax ratio is plotted as a function of the orientation of the normal to the outcrop (the direction in which the cross section is being viewed), then, for a complex series of flow lobes generally oriented in the flow direction, La/Hmax ratios should be a minima when looking directly at the cross section. La/Hmax ratios should be maxima along cross sections cut parallel to the flow directions. Plotting La/Hmax ratio medians as a function of orientation in a rose diagram, Figure 44, shows a narrow lens when viewing in the northeast/southwest directions and an elongated lens when viewing in the northwest/southeast directions.

A simplified model of a single flow provides insight into its three-dimensional configuration. The single lobe model of Figure 45, together with the orientation developed in Figure 44, yield a length/width/height ratio of >8.7:4.6:1.

For well bores encountering a median single lobe, more than half of the penetrations will be in a region near the edge of a flow (half the time within a distance less than 2.3 Hmax and one quarter of the time within a distance of less than 1.15 Hmax), see Figure 46. Figure 46 is a simple illustration. In reality the flow lobes have a more complex geometry (Figure 5).

Hell's Half Acre Flow

Hell's Half Acre flow was chosen for the plan-view geometry study because it is probably the best representative in this area of the general morphology and surface of the basalt flows at the RWMC; the flow is relatively fresh (about 5 Ka), and is covered by little surficial sedimentation. The area of study on the Hell's Half Acre flow lies southeast of the INEL in the Southwest 1/4, Section 34, Range 34 East, Township 2 North and is located on the Kettle Butte SW USGS Quadrangle map

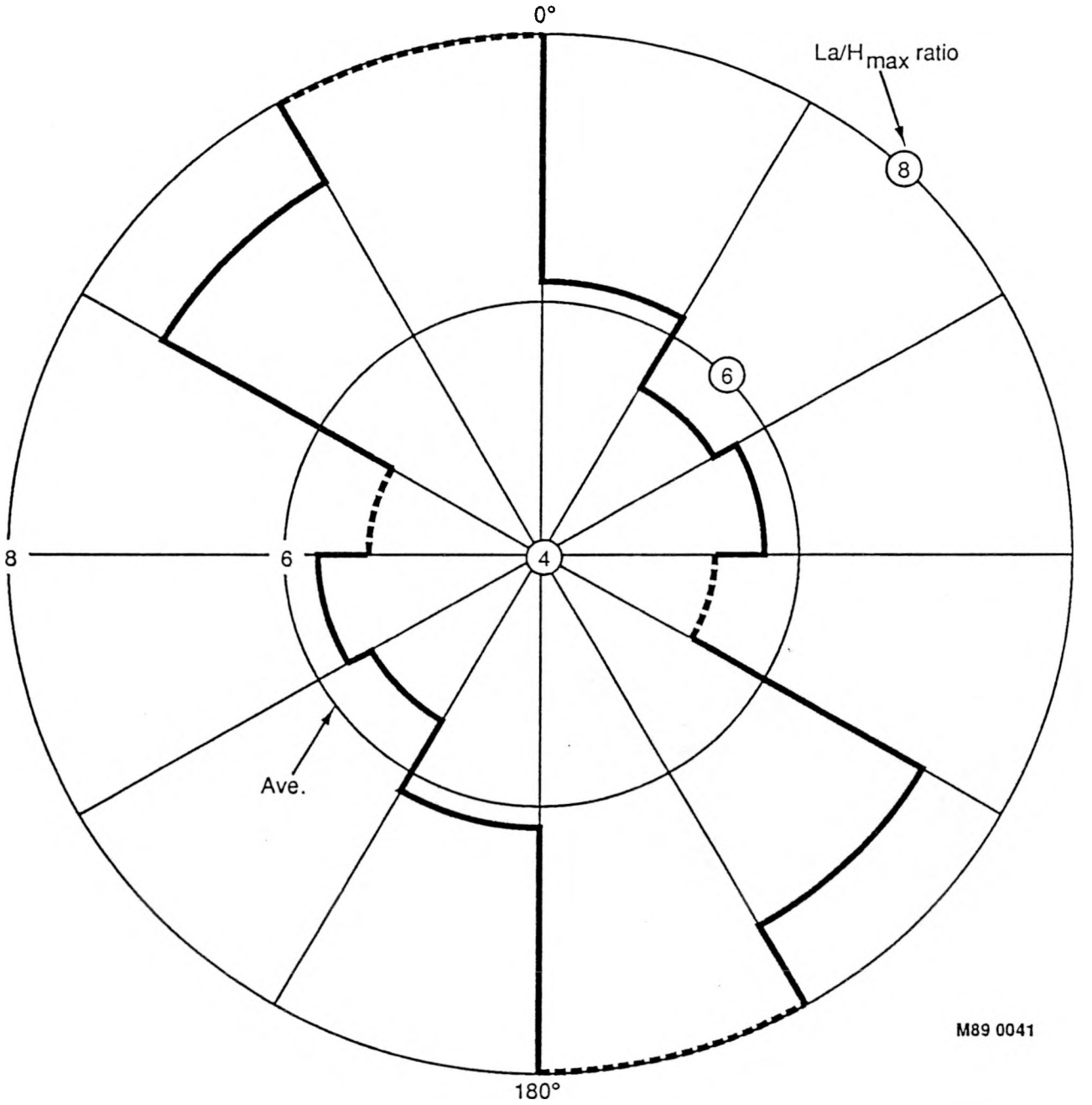

Figure 44. Median La/Hmax ratio as a function of the orientation of the normal to the apparent length direction (dashed sectors are those with less than 10% of the measurements).

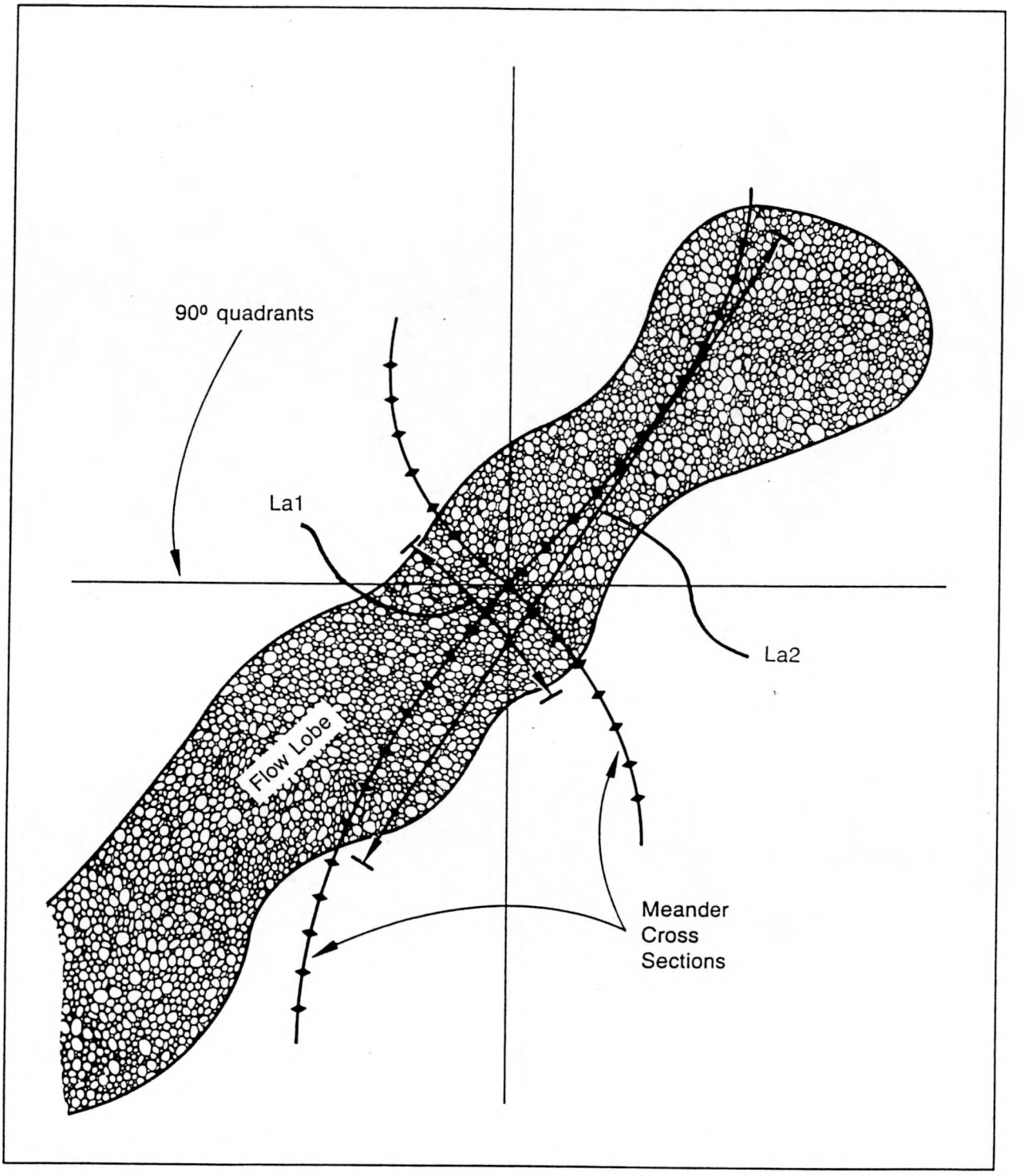

Figure 45. The La/Hmax ratio for the flow lobe measured in the canyon wall [the La/Hmax ratio for the canyon wall, viewed in a northeast-southwest direction, would be small (La1/Hmax), while the La/Hmax ratio for the lobe in the canyon wall, viewed from a northwest-southeast direction (La2/Hmax), would be much larger (La2/Hmax > La1/Hmax)].

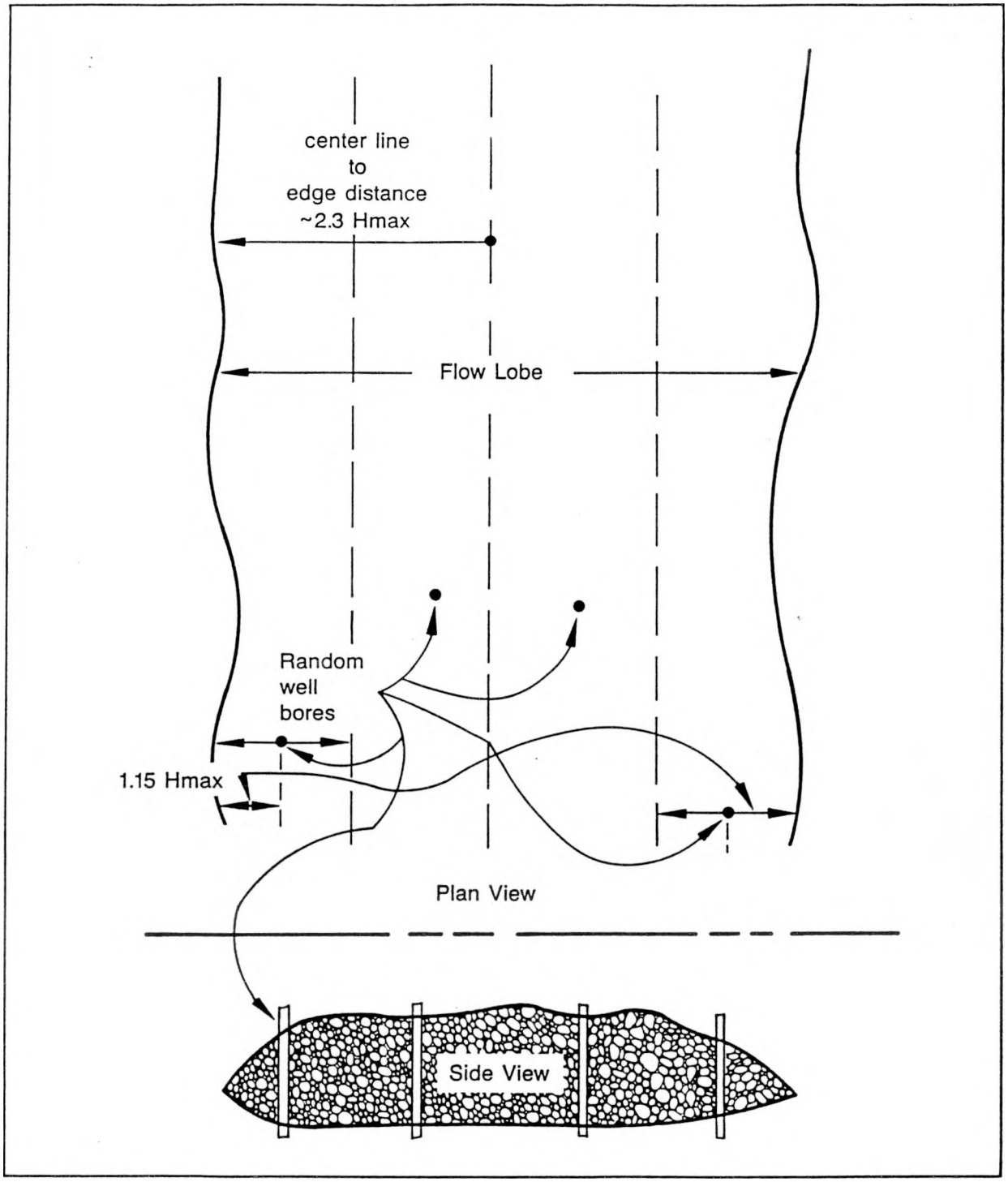

0-6866

Figure 46. Plan and side view of a flow lobe (from a probability standpoint, one-quarter of the time a random well bore will encounter the flow within a distance of 1:15 Hmax of a flow edge).

(see Figure 2). Access to this area starts at a dirt road south of U.S. Highway 20, just west of mile marker 287, between Idaho Falls and Arco (Figure 47). At the study area, four separate stations for the transit were set up and 104 grid point elevations were shot across a flow lobe and collapse structure (Figure 48). The grid was formed on a 10- or 20-pace spacing, except for the first 15 locations, spaced at 2 or 5 paces, and a randomly located 3 x 3, 2-pace grid. The purpose of this approach was to generate a sample set of elevations and surface descriptions across the flow with small to large distances between sample points. These elevation and location data were compiled in the EPA GEO-EAS (Geostatistical Environmental Assessment Software) program, version 1.1, to generate variogram plots and Kriged structure maps. To format location data, an arbitrary origin was chosen and locations were given x-y coordinates (easting and northing, respectively) in feet. Figure 49 is the plot of sample locations on the x-y grid.

Three variograms were generated from these data: one for the top of the flow lobe, one for the collapse structure (bowl), and one for the entire study area. Figures 50 and 51 are variograms of the grid point elevations from the flow top. Initially, true elevation values were used to generate the variogram, but they yielded a negative variance. Subsequently, 5100 was subtracted from the elevation data -- the maximum and minimum values of which are 5155.6 and 5130 feet -- giving a data set with a maximum and minimum of 55.6 and 30.8, respectively. A variogram was generated from these altered values with a calculated variance of 9.8. This new variogram was modeled using a gaussian curve with a lag increment of 46, a nugget of 0, a sill of 12.5, and a range of 125. The resulting variogram and curve are shown in Figure 50. Next, the original variogram with the true elevation values was regenerated and the model that was developed for the first variogram was used to fit a curve to the original data. The resulting variogram and curve are presented in Figure 51. Those points that fall considerably below the curve are probably an effect of the geostatistics program. For the variogram to adequately reflect all the data, the data set for an undulating surface such as this would have to be increased to incorporate perhaps as many as 20 local highs and lows. The problem derives

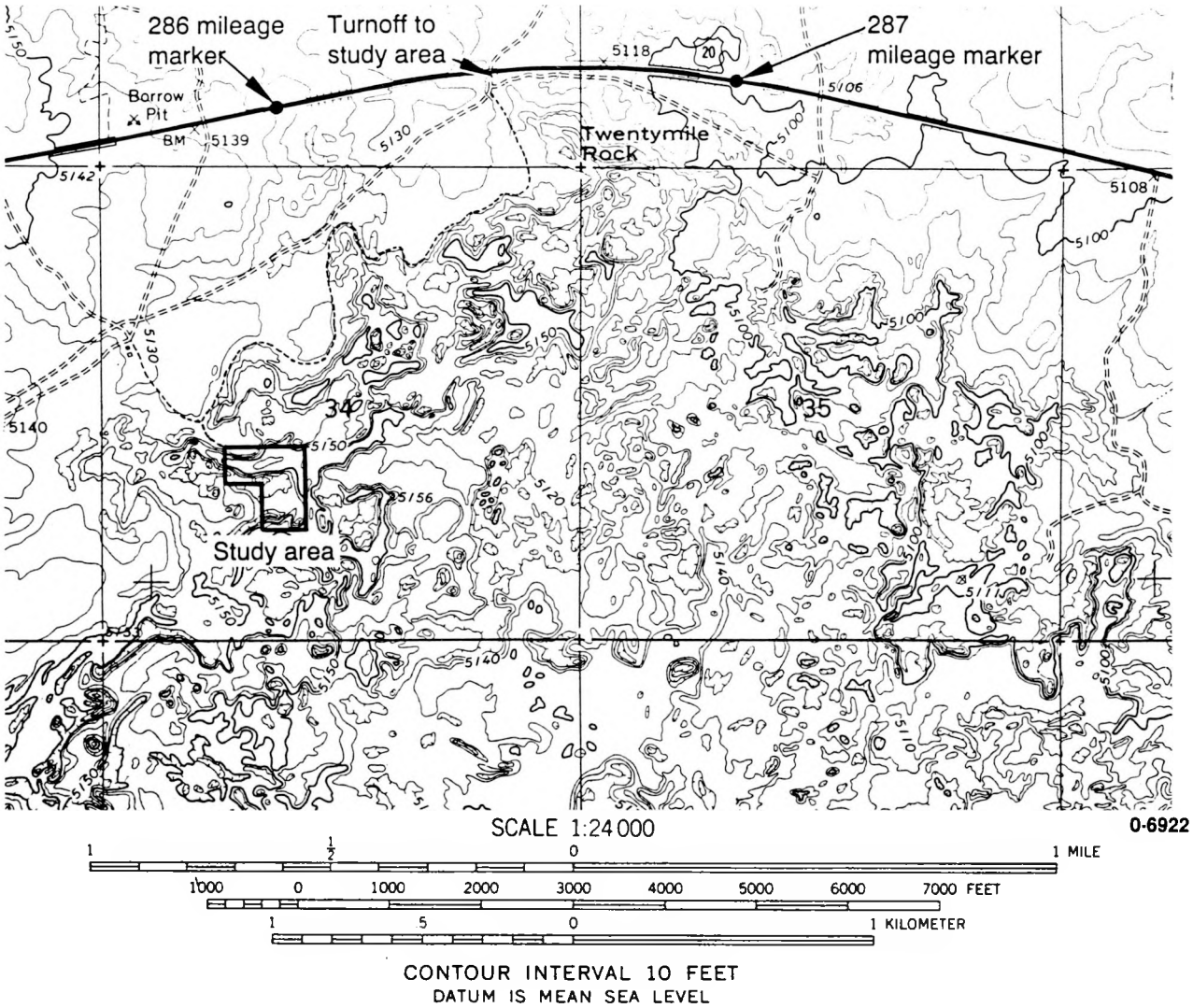

Figure 47. Hell's Half Acre flow, northwestern edge south of U.S. Highway 20 (enlargement of Kettle Butte SW, Idaho Quadrangle).

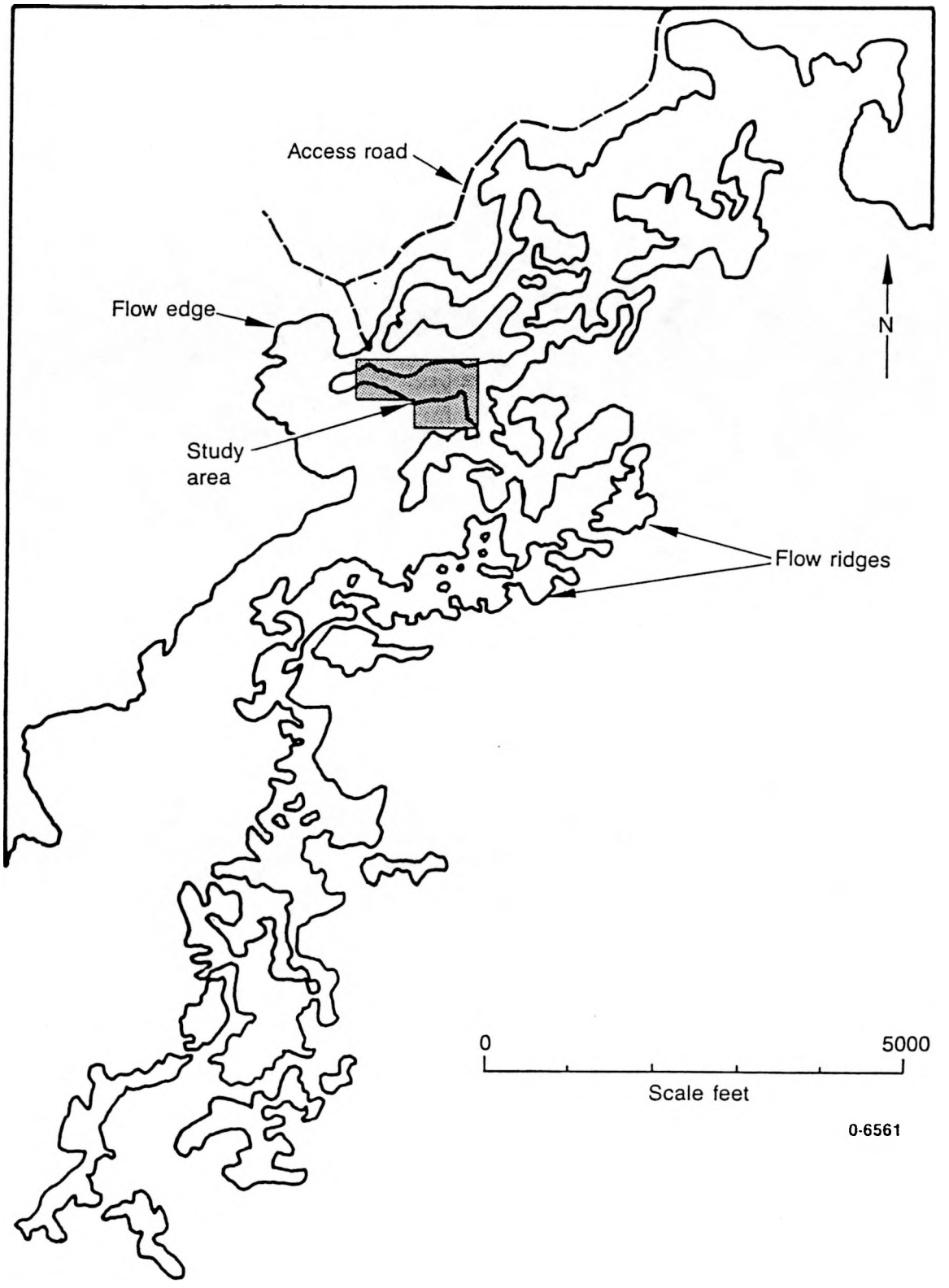

Figure 48. Hell's Half Acre flow south of U.S. Highway 20 showing flow ridges and study area.

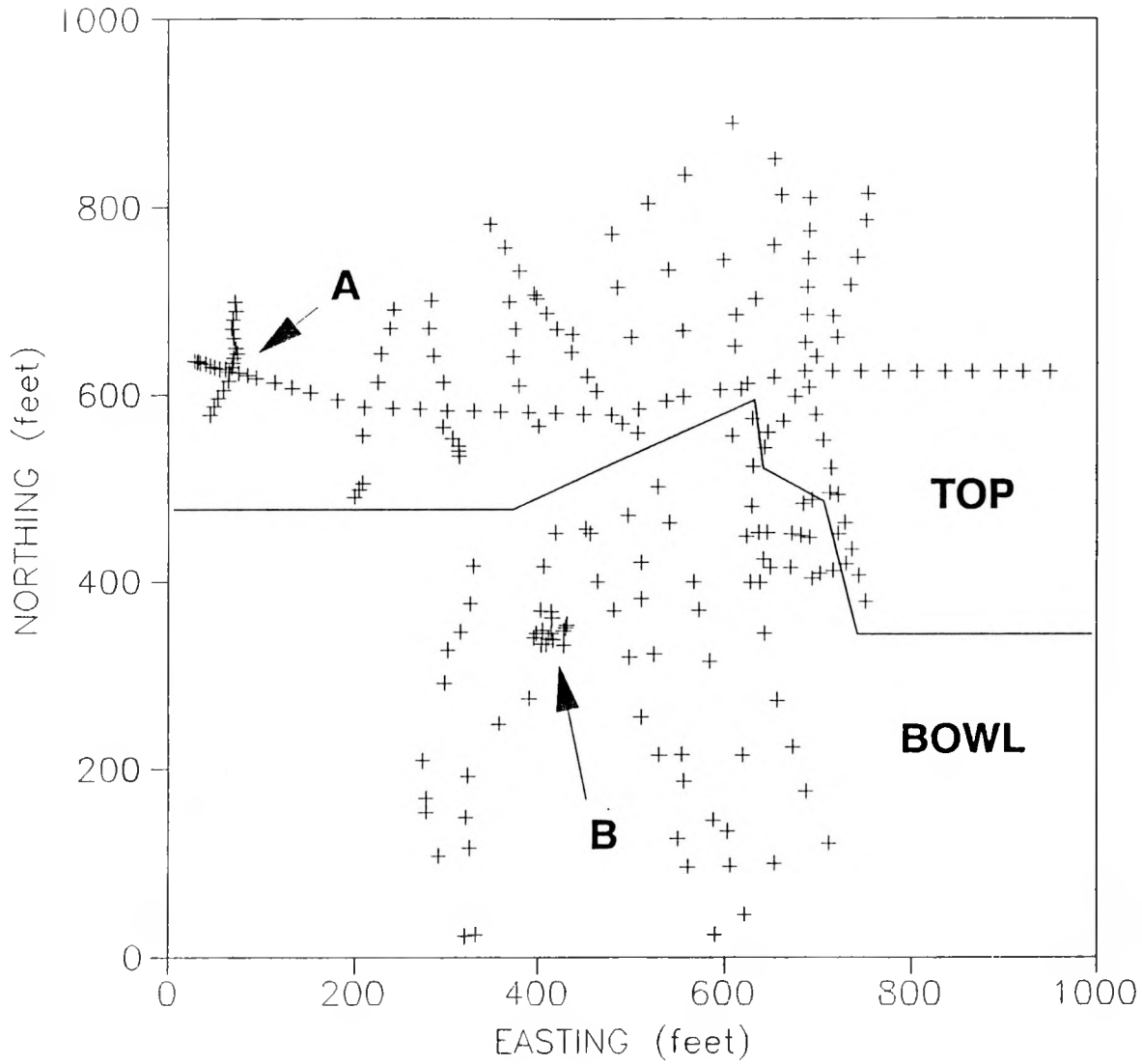

Figure 49. A plot of sample locations on an arbitrary x-y grid (in feet) at Hell's Half Acre flow ("Top" and "Bowl" refer to grid points used for the top of the flow lobe and the deflation structure, respectively). A and B are locations of closely spaced grid points.

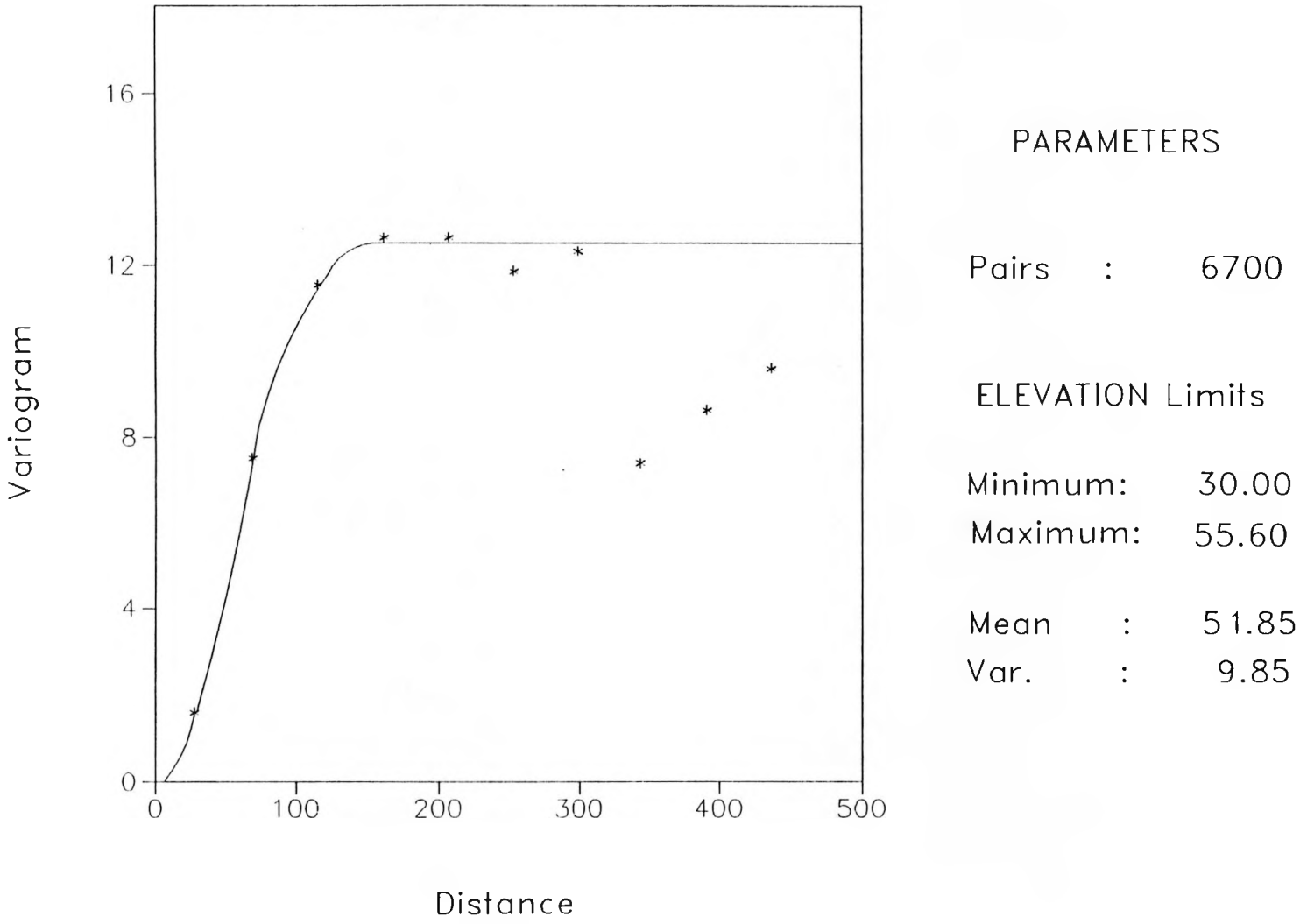

Figure 50. A variogram of grid point elevations (-5100) from the top of the flow.

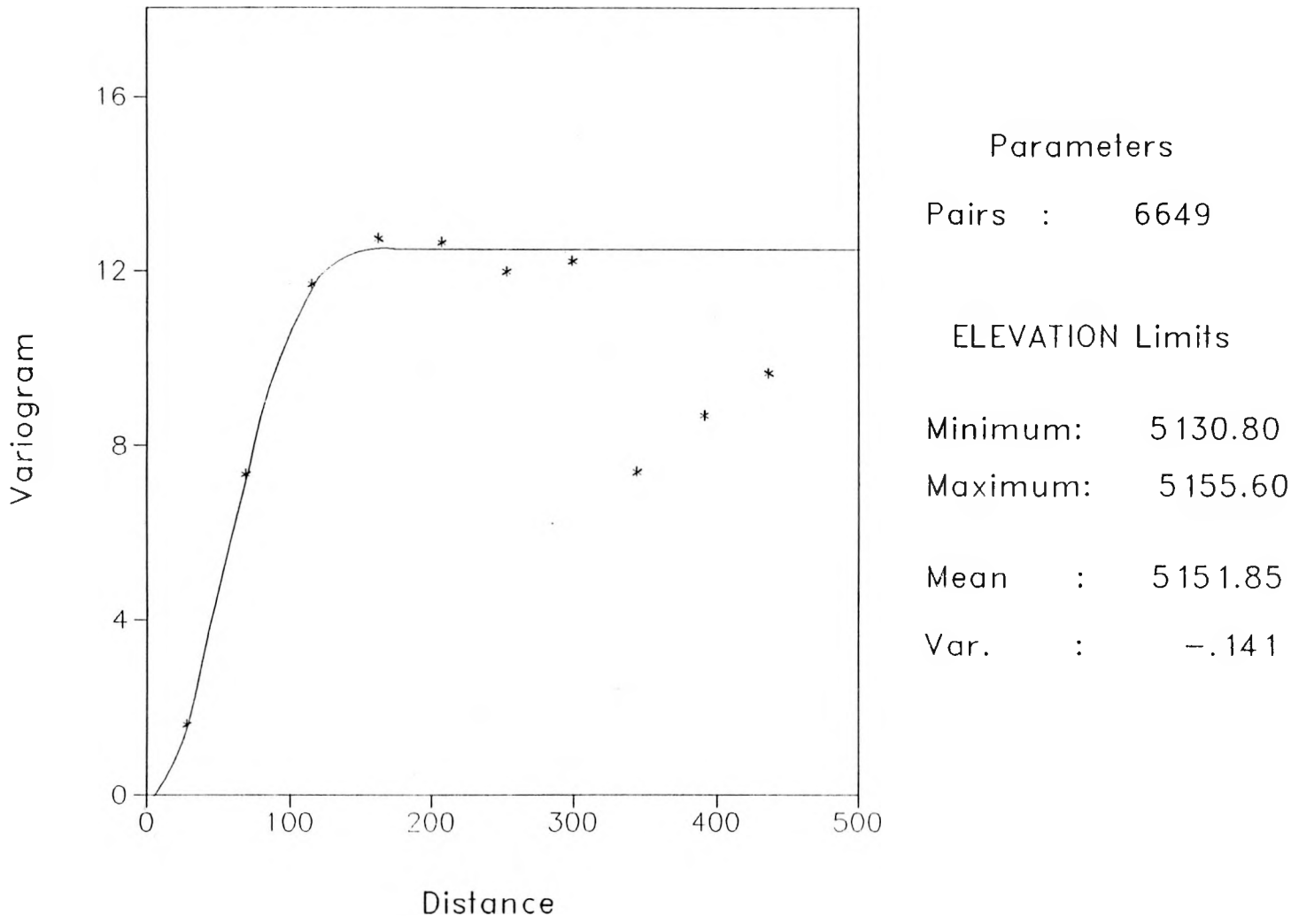

Figure 51. A variogram of grid point elevations from the top of the flow.

from the assumption in geostatistics, called stationarity (Clark, 1984), that all data in a given data set have the same probability distribution. This is not true for data that define a non-horizontal plane. In these cases, the trend surface must be removed from the data set.

The variogram of Figure 51 and the curve modeled from the data of Figure 50 were used to contour the flow top (Figure 52). Figure 52 illustrates the relative flatness of flow tops and the abundance of local highs and lows due to the buckling of the crust as the lava flowed, cooled, and contracted.

The variogram generated from grid point elevations and locations across the collapse structure is presented in Figure 53. The model used to fit the curve to these data is gaussian, with a lag increment of 30, a nugget of 0, a sill of 70, and a range of 55. This curve is believed to be the best fit, despite the considerable scatter on the plot. This again, is likely an effect of the integration of the ridge and bowl data sets. This variogram and curve were used to generate the Kriged structural map of the bowl in Figure 54. The terrain across the bowl is a fairly subdued contour plot up to the edge of the flow (contoured in the northeast corner of the diagram) that bounds the collapse structure on three sides (Figure 49). In this region, the slope becomes very steep. Also, note that few grid point locations were shot for the southcentral area of the bowl [due to the randomness of the sampling (Figure 50)], resulting in a definite lack of detail in the southcentral part of Figure 53. The basic reason for the random pattern of data acquisition was to develop variograms and surface composition probabilities. Hence, this lack of coverage is not a critical factor.

In addition to shooting elevations, the type of surface was described at each location across the bowl, and four surface types were defined: uneven-to-smooth, fracture, rubble, and broken. The uneven-to-smooth surface probably had a pahoehoe texture when fresh, but due to erosion, little trace of the original texture is preserved. Though commonly the

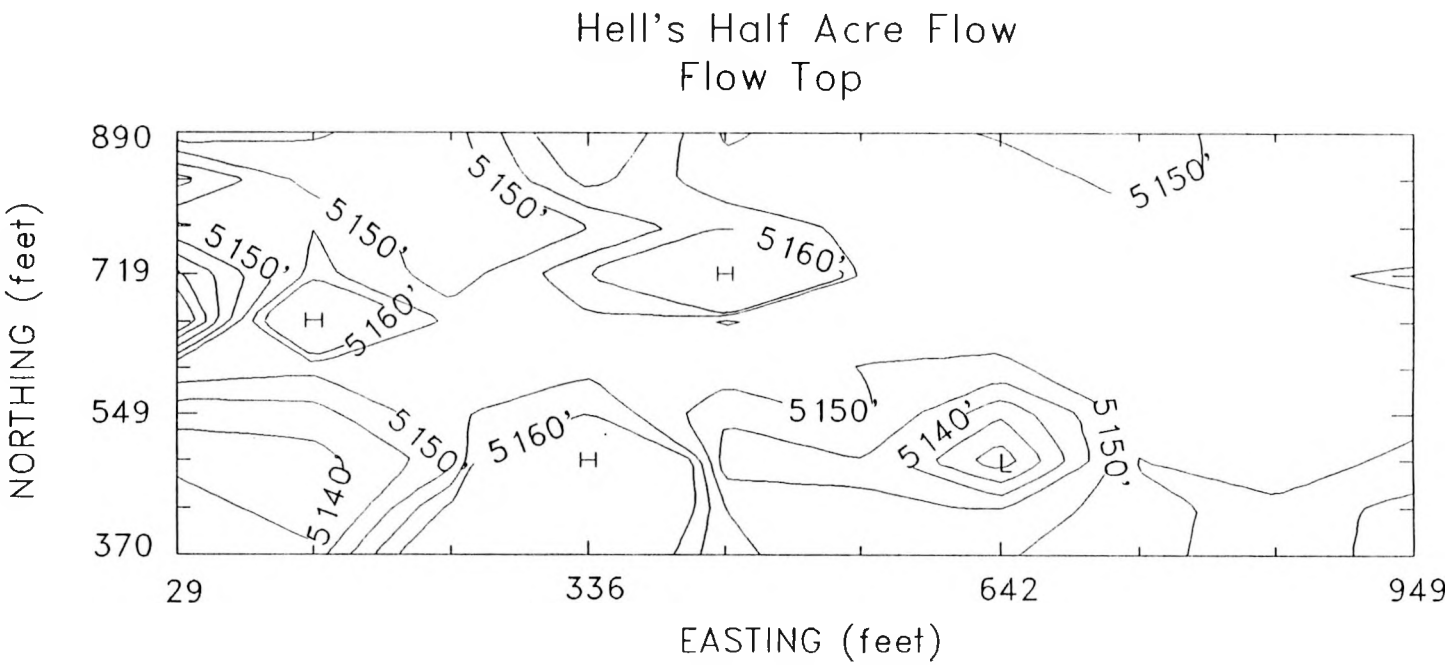

Figure 52. A contour plot of the top of the flow lobe (contour interval is 5 ft; H = local high, L = local low in elevation).

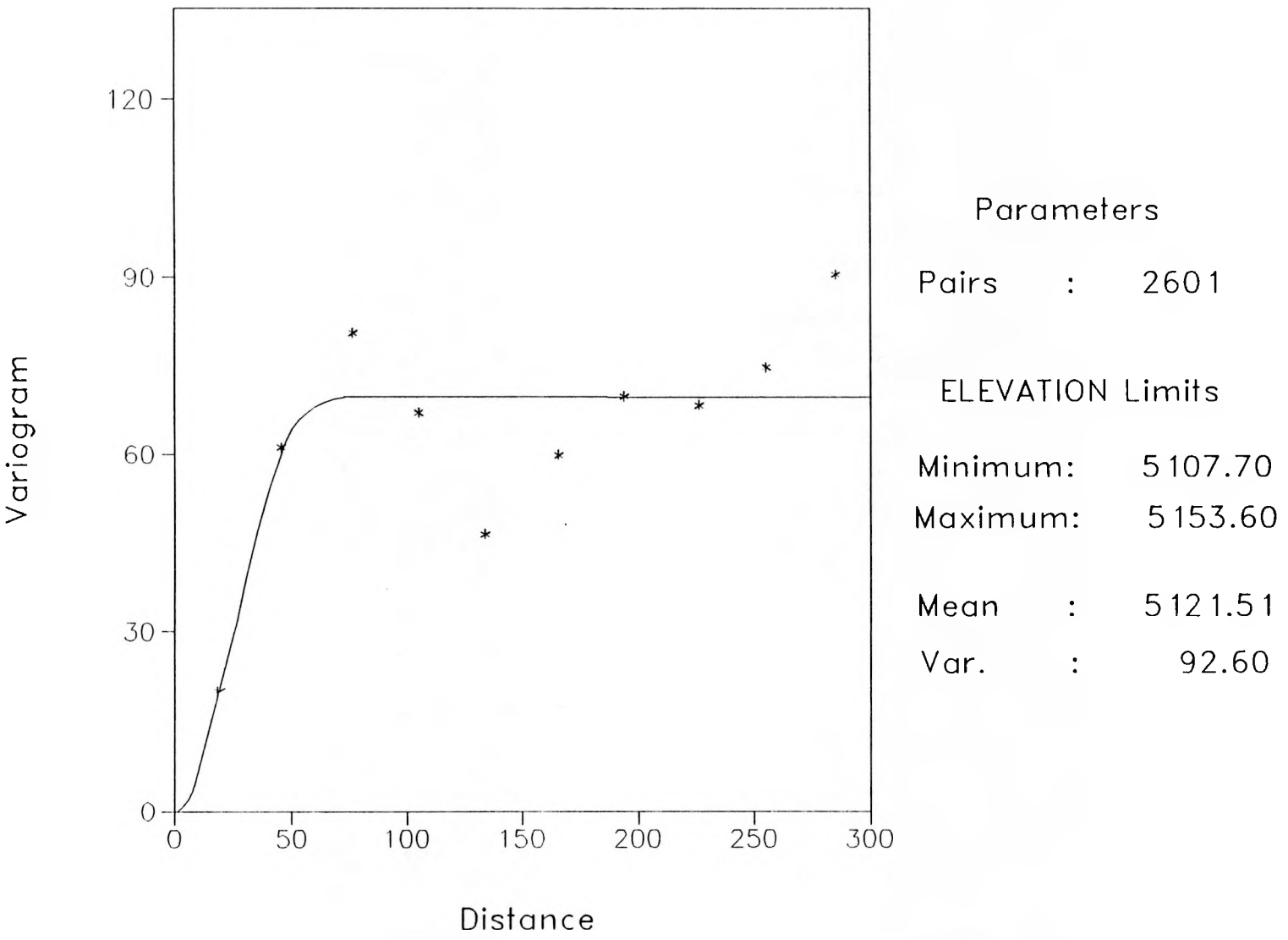

Figure 53. A variogram of grid point elevations from the deflation or bowl structure.

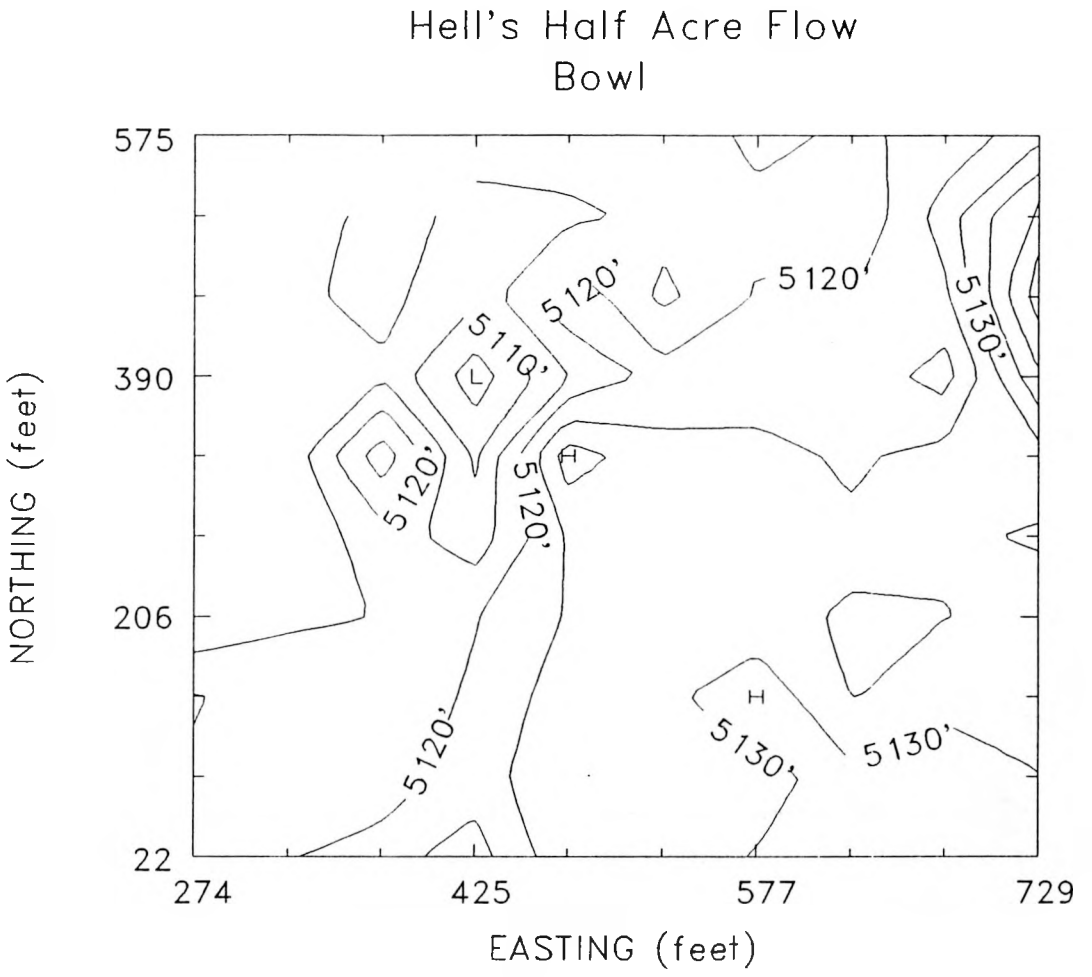

Figure 54. A contour plot of the deflation or bowl structure (contour interval is 5 ft; H = local high, L = local low in elevation).

erosional debris has been transported elsewhere, vegetation such as grass and sage brush is sometimes found on this surface. The fracture category is actually not a surface but literally a fracture or fissure. The minimum depth of these fractures is about 2 ft, with no maximum depth noted. The rubble surface consists of basalt fragments less than or equal to cobble size, but most commonly pebble size. Remnant pahoehoe texture is sometimes seen on this surface, implying that some of these surfaces had a strong pahoehoe texture when fresh. The broken surface typifies flow edges where the slope is steep, and blocks of basalt are boulder size and larger.

The number and frequency of each surface are presented in Table 10. The uneven-to-smooth surface occurs with the greatest frequency (51% of the location points), followed by fracture, rubble, and broken surfaces. Both uneven-to-smooth and at least some of the rubble surfaces were probably pahoehoe, indicating that when fresh, this pahoehoe texture was, as expected, dominant across the flow.

The entire data set (top and collapse depression) was used to generate the variogram presented in Figure 55. The model used to fit a curve to these data is linear, with a nugget of 0, a sill of 350, and a range of 430. However, the maximum interpair distance of 632 had to be decreased to 440 because the maximum number of pairs the program can handle in its data pair calculations had been reached. Due to the larger data set of this variogram, the scatter observed in Figures 50, 51 and 52 is lost. A Kriged structure map of the entire study area was generated from this variogram and fitted curve, and is presented in Figure 56. While the detail of the top and bowl morphology is lost, the steepness of the flow edges is well illustrated, and a general plan-view geometry emerges. This generalized plan-view geometry, along with the surface description data from the deflation structure, will be used in conjunction with the Box Canyon data.

Table 10. Various types of surfaces found on the Hell's Half Acre flow (n = number of grid points, Sum = cumulative number of grid points, n % = number in percent, and Cum % = cumulative percent)

Surface	Uneven-Smooth	Fracture	Rubble	Broken (Collapse, Blocky)
n	47	18	16	12
Sum	47	65	81	93
n %	51	19	17	13
Cum %	51	70	87	100

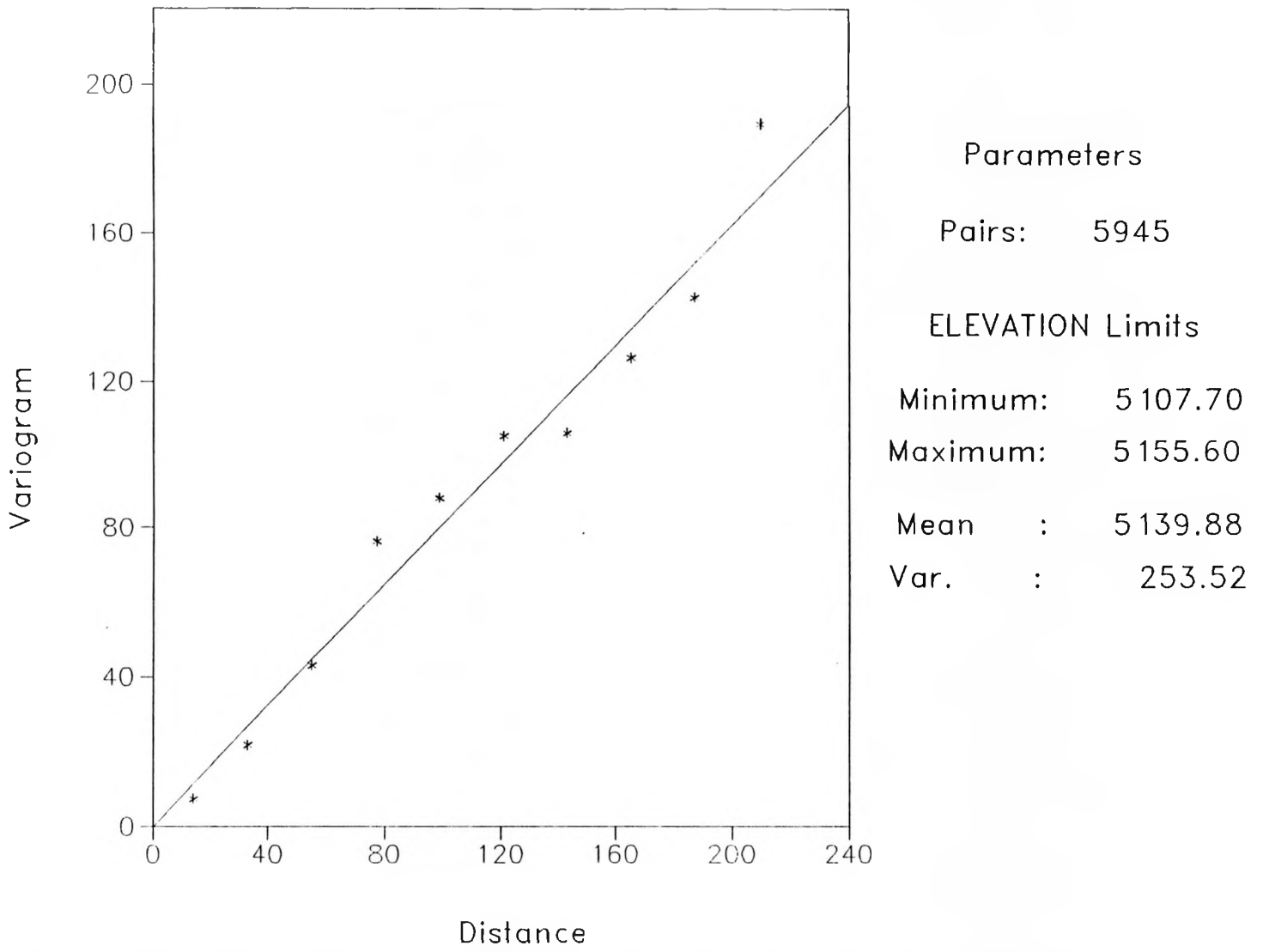

Figure 55. A variogram of grid point elevations from the entire study area (top and bowl).

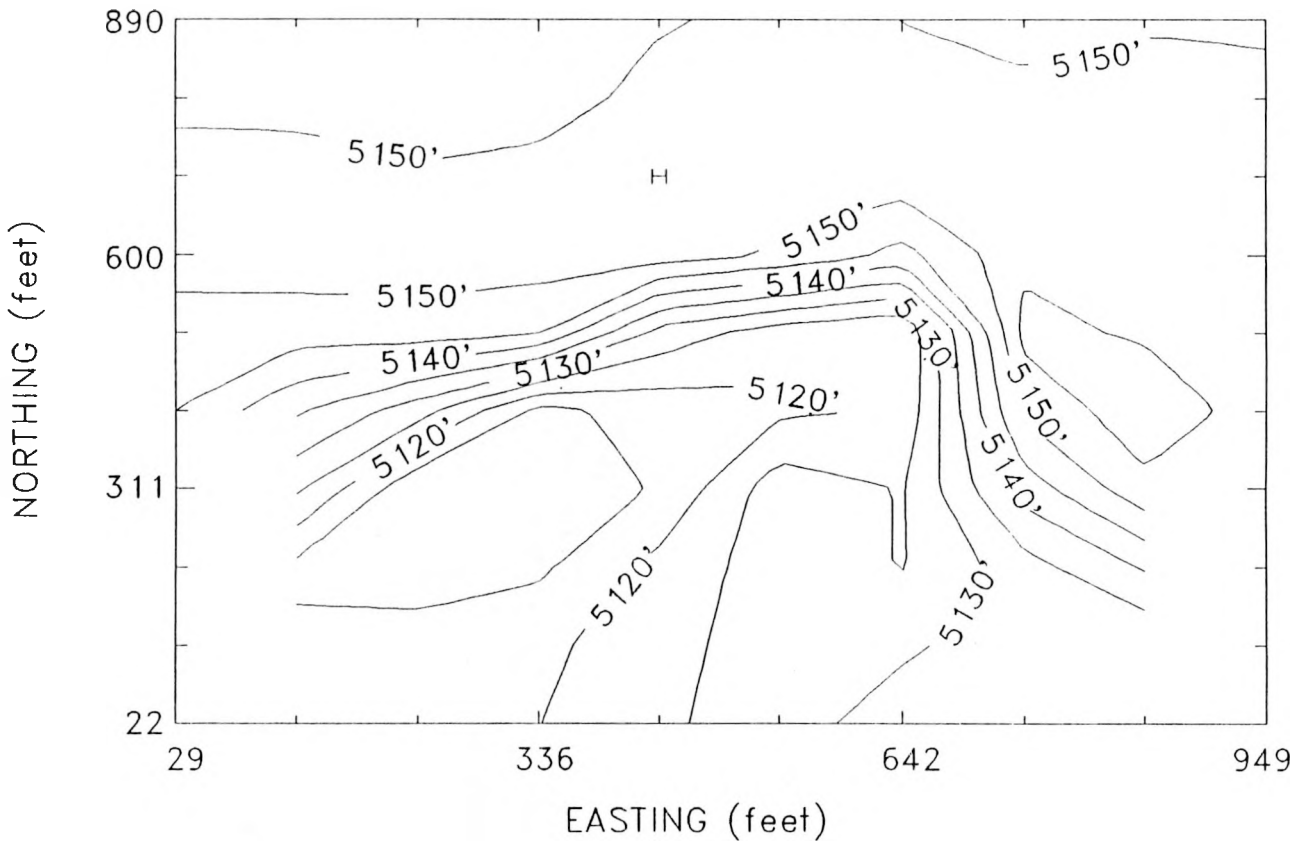

Figure 56. A contour plot of the entire study area (contour interval is 5 ft; H = local high, L = local low in elevation).

SUBSURFACE GEOLOGICAL MODEL OF VADOSE ZONE BASALT

Conceptual Geologic Model

The conceptual model for the basalt of the vadose zone at the RWMC is based on the development of basalt flow groups separated by sedimentary layers. The sediments accumulated over periods of time that are long in relation to the time involved in the deposition of the basalt groups [we are using the USGS flow group/sediment stratigraphic framework of Anderson, Lewis, and coworkers (Anderson and Lewis, 1989), and are endeavoring to provide a conceptual model of the complexity to be found in the basalt flow groups A, B, C, etc.].

The flow groups consist of a complex aggregate of flows and flow units that are very heterogeneous in structure and geometry. The model assumes that:

- A layered, horizontally stratified model is not appropriate.
- The flows form complex assemblies and have many relatively closely-spaced discontinuities, both vertically and laterally. They are also lenticular and display a preferred long-axis orientation.

The RWMC basalts, surficial sediments, and interbeds were deposited in a cyclic glacial-interglacial environment. Current conditions are representative of only the last 5,000 to 6,000 years and a few other relatively brief periods during the last 600 Ka (Figure 57). Hence, the bulk of the time during which sedimentation and basalt emplacement was taking place was colder and sometimes wetter than the present.

The general model is applicable, however, to the basalt flow groups in the RWMC area initially covering an undulating surface where the lows had

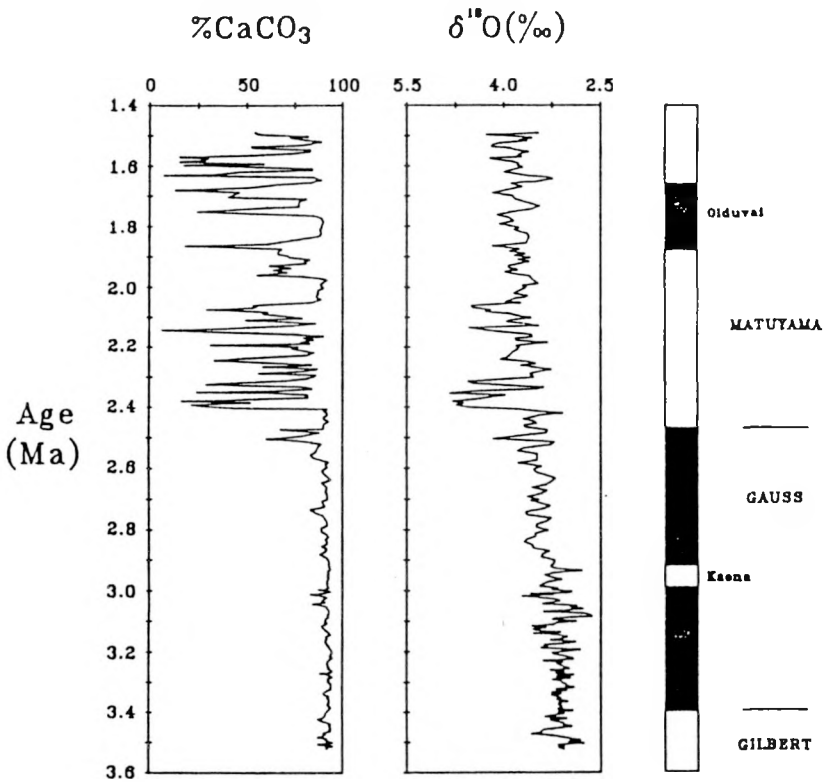

Late-Pliocene and early-Pleistocene records of percent $CaCO_3$ and benthic foraminiferal $\delta^{18}O$ from Site 552 in the North Atlantic at 56°03′N, 23°14′W (after Shackleton and others, 1984; Zimmerman and others, 1985). Abrupt decrease in $CaCO_3$ near 2.55 to 2.4 Ma marks the onset of ice rafting into the North Atlantic brought about by appearance of Northern Hemisphere ice sheets of moderate size.

(after Ruddiman and Wright, 1987)

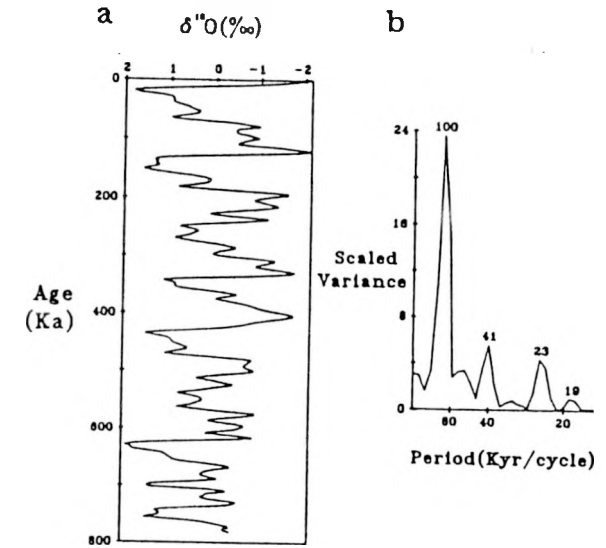

(a) Composite global $\delta^{18}O$ record from Imbrie and others (1984). Units are standard deviations from the mean. (b) Spectral analysis of $\delta^{18}O$ record in Fig. 3a (after Imbrie, 1985).

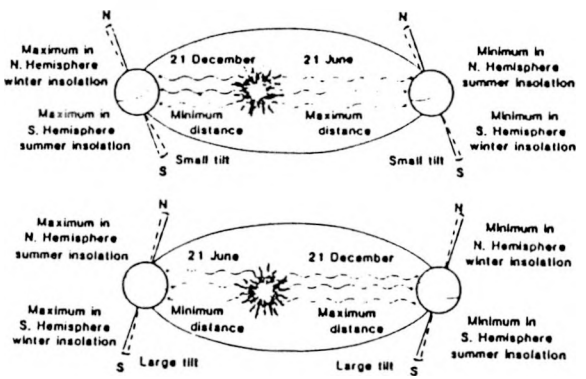

Schematic representation of the earth's orbital elements (eccentricity, tilt, and precession).

Figure 57. Factors controlling glacial-interglacial cycles.

been filled or partially filled with sediments and where topographically high basalt ridges or domes protruded above the sediments. Thus, the variogram developed from the Hell's Half Acre study could be used to krig the base of the surficial layer at the RWMC. The sediment on the north part of the RWMC covering flow group A represents a sedimentation and erosion cycle covering the period 95 Ka, while the southern sediments covering flow group B represent the period about 200 Ka. The resulting structural map (Figure 58) and the structural map on the top of flow group B (Figure 59) show the low in the SDA area filled by post flow group A sediments. Post flow group B to the north of the RWMC was partially filled with sediments and then filled to an even greater extent by flow group A basalts. The current configuration resulted when additional sedimentation covered flow group A, as well as the pre-95 Ka sediments to the south.

The following sections of this report discuss the flow geometries and structural models.

Flow Unit/Flow Geometry

The geometric configuration of the flow units and flows in flow group A is an accumulation of individual flows made up of intercalated flow lobes. The areal extent of these lobes is expected to have a direct relation to flow group thickness.

The basic geological model is one of extremely complex flows that form flow units and flow groups by overlapping and building on the complex undulating topography of previous flow lobes. The median length of the lobes near the Hell's Half Acre study is about 900 ft, with a maximum length of over 3,800 ft. The median length/width (L/W) ratio is about 2.9, with a minimum of 1.3 and a maximum of 8.2. The median L/W ratio from a drawing from stereo pair photographs at Hell's Half Acre is consistent with the >1.9 L/W ratio (>8.7:4.6:1 - length:width:height) that was obtained from the analysis of the Box Canyon data. The distribution of the lengths and length/width ratios is presented as Figure 60. The sketch of the Hell's Half Acre lobes is presented as Figure 48. This complex morphology is consistent with the Box Canyon information and certainly seems consistent

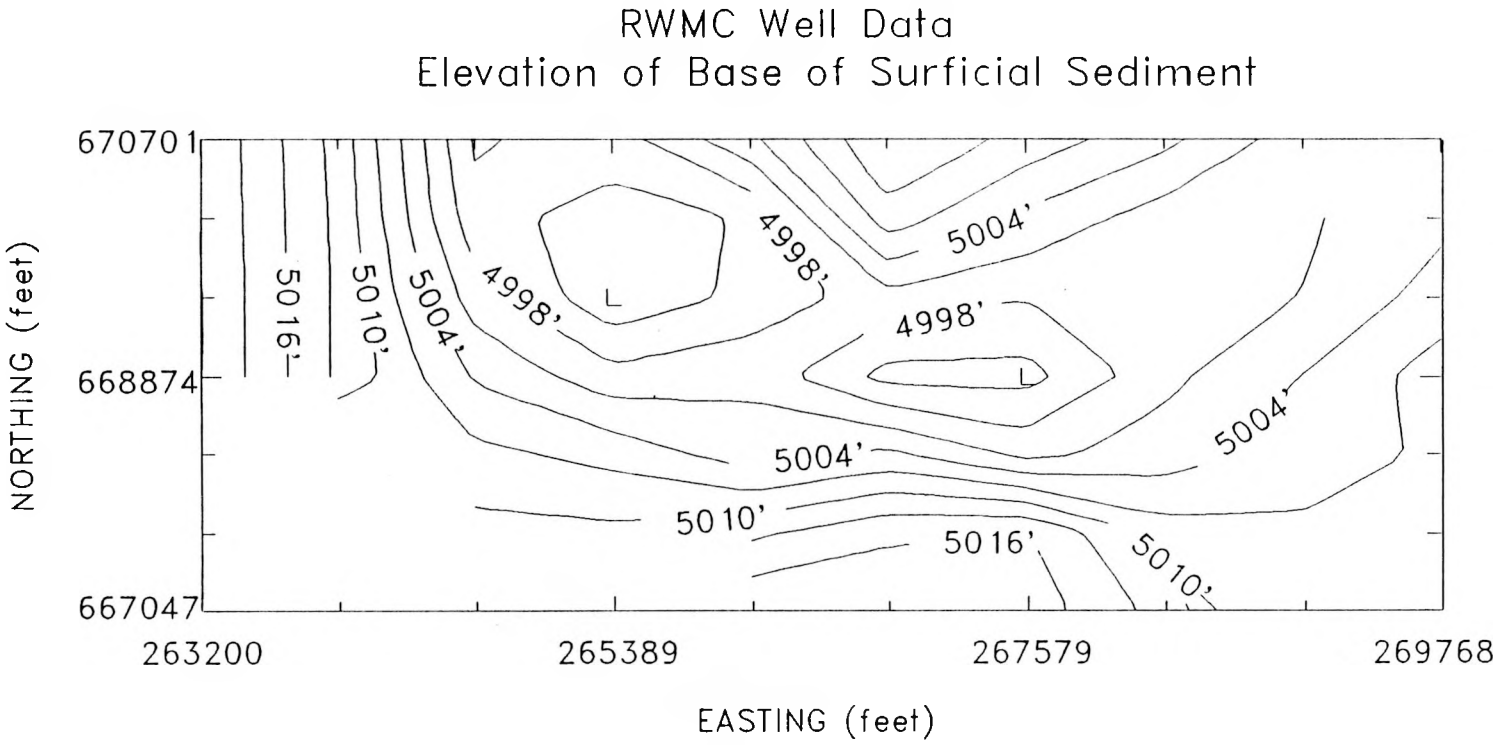

Figure 58. Kriged structural map on bottom of surficial sediment layer (based on Hell's Half Acre survey).

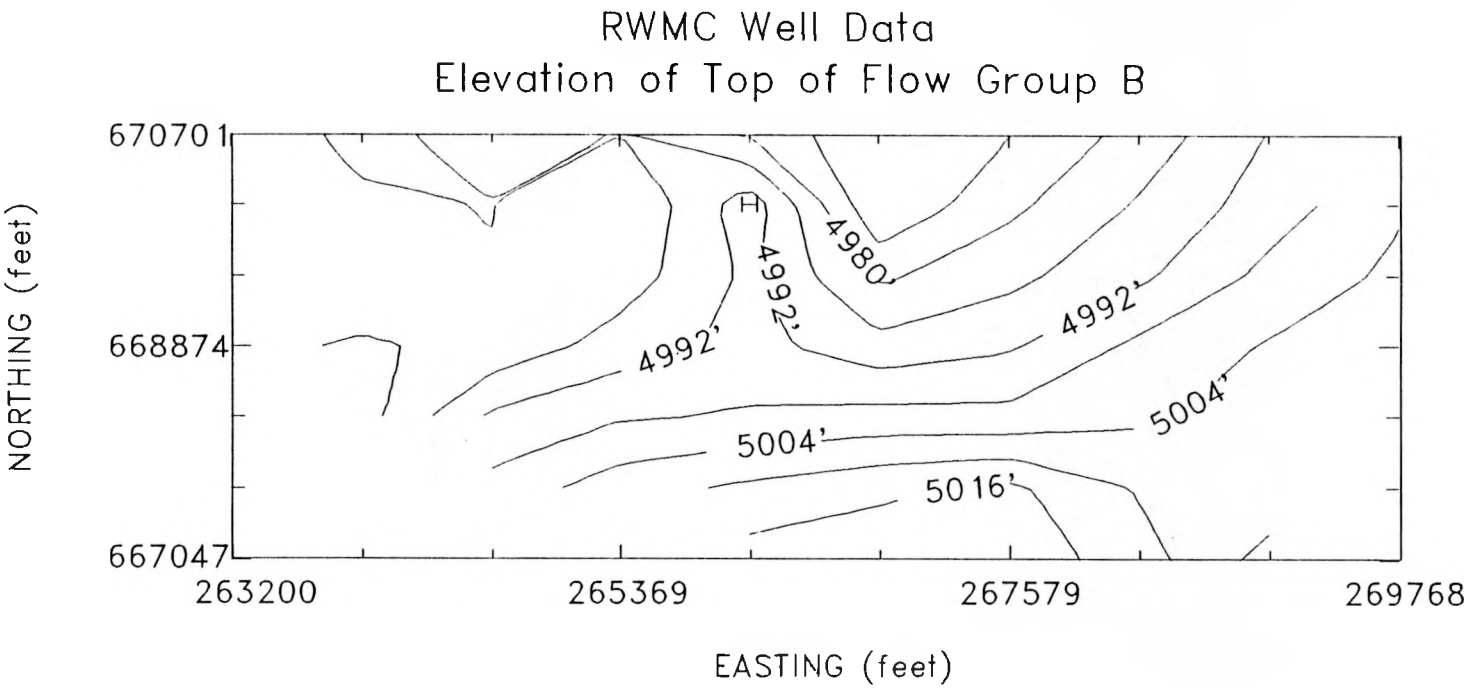

Figure 59. Kriged structural map on top of flow group B.

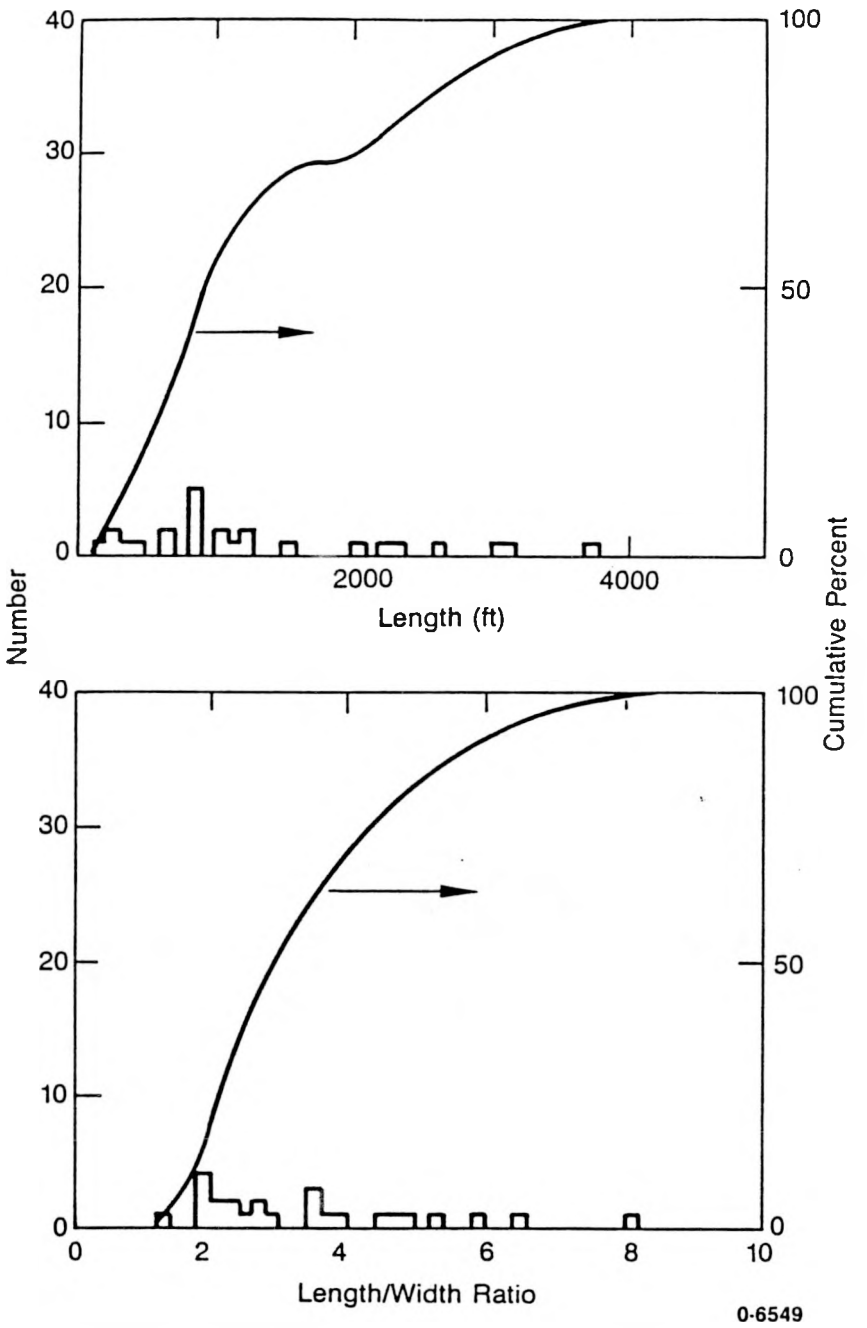

Figure 60. Length and length/width ratio distributions for Hell's Half Acre study area flow ridges.

with the "A" and "B" flows exposed in the SDA pit at the RWMC. A photo of the west pit wall north of the road is presented as Figure 61.

Flow Structure

The typical basalt flow can be divided into 4 horizontal elements: (1) substratum, (2) lower vesicular, (3) central (generally nonvesicular), and (4) upper vesicular. The substratum is a potentially very high transmissivity element and is therefore quite important. This preliminary study reports no quantitative data about this element, because the logs being run are not diagnostic, inadequate core was recovered from this element, and no quantitative outcrop tests were made.

The Hell's Half Acre study provides some statistical information about the expected frequency of a number of substratum types that might be encountered. The ropy surface (pahoehoe) was found approximately 51% of the time. Fracture/fissure surfaces were found to occupy about 19% of the surface substratum, while rubble and broken blocks occupy respectively 17% and 13% of the surface.

The lower vesicular element has a median permeability of 4 md, a median porosity of 21%, a median bulk density of 2.40 g/cm^3, and a median thickness of 1.5 ft (0.46 m), 11% of the total flow thickness. This element is fractured into polygons with a width/height ratio that varies between 0.5 and 1.0. The median joint or fracture is a feature that is roughly perpendicular to the bottom surface of the element, and occurs once every 0.75 to 1.5 ft (0.22 to 0.46 m).

The central element has a median permeability of 8 md, a median porosity of 10%, a median bulk density of 2.73 g/cm^3, and a median thickness of 7.5 ft (2.3 m), 49% of the flow thickness. This element has a joint polygon width/height ratio of a little less than 0.5. Thus, the median joint frequency is one every 3.2 ft (.098 m).

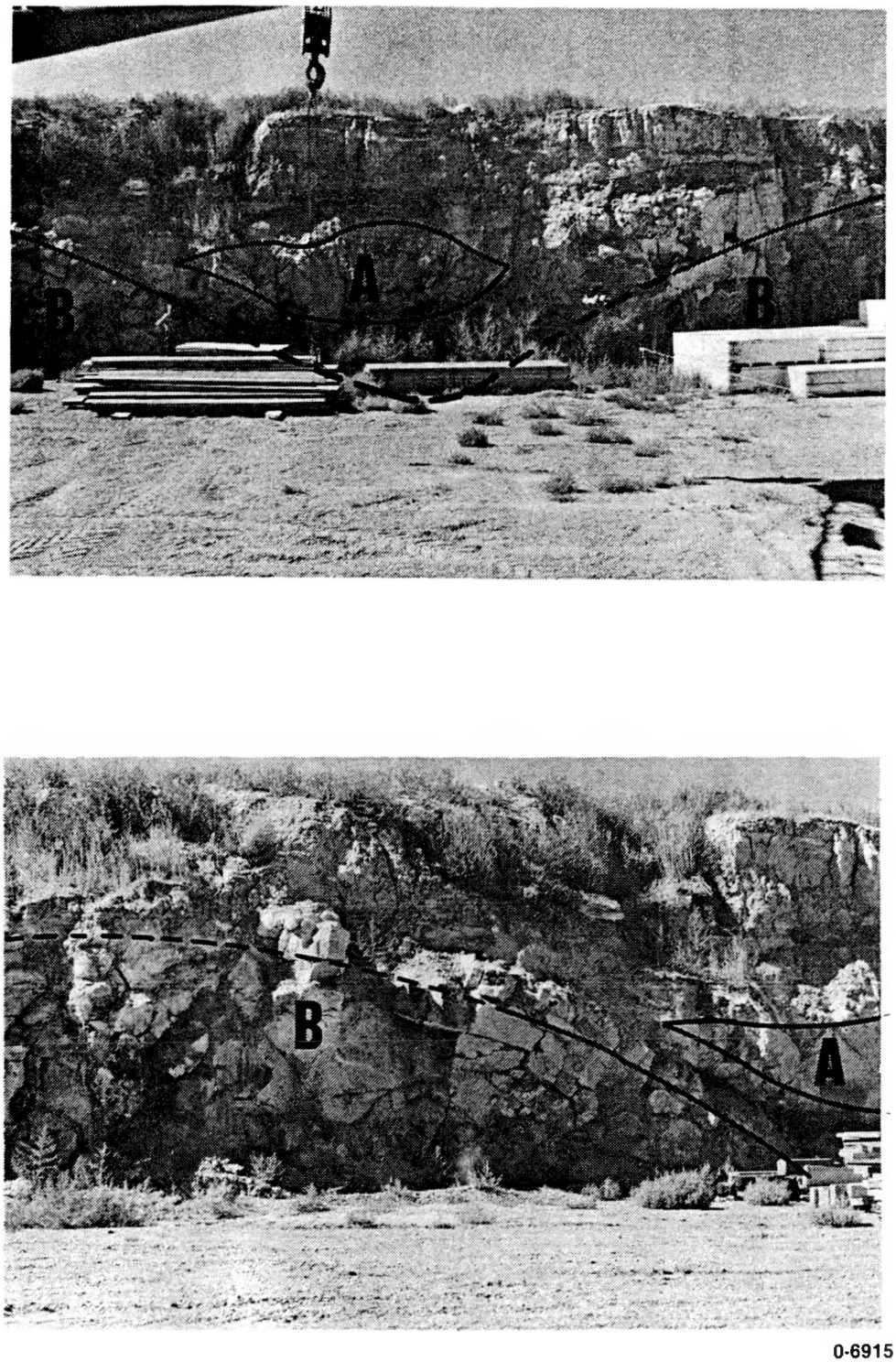

Figure 61. Photographs of flow ridges A and B, bisected by west wall of the RWMC SDA pit (the "A" and "B" flows are outlined).

Lava tubes and collapsed lava tubes that may be found in this element are rare. These essentially two-dimensional features have very high transmissivity and can extend for hundreds of feet.

The upper vesicular element has a median permeability of 7 md, a median porosity of 22%, a median bulk density of 2.4 g/cm^3, a median thickness of 6 ft (35% of the flow thickness), and a joint width/height ratio of about 0.5 (or a joint frequency of one per 3 ft for the element as a whole, and one every 1 1/2 ft for the upper crust of the element). There is frequently a parting parallel to the upper surface of this element. Fissures of appreciable thickness are also a frequent component of this element. They are probably caused by the viscous drag of the still mobile, central element pulling the crust apart, and by the stress in the elongation as the crust falls into a collapsed area. The overlying flow may fill these fissures. However, sometimes it sags into the top of the fissure and a residual, very high transmissive linear feature results.

Mathematical Model

The construction of a mathematical model of the basalt flow parameters in the vadose zone under the RWMC is one the facets of the characterization of this zone. We believe that such a model could be constructed using a hybrid stochastic technique. A stochastic model of this type was constructed for the Cretaceous Mesaverde discontinuous gas reservoirs by the senior author (Knutson, 1976). This model was used in a major DOE study of the enhanced recovery of unconventional gas (Kuuskraa et. al., 1978), a major NPC/NAS tight-gas reservoir study (Baker et. al., 1981), and is being used by DOE-Morgantown.[a] However, such a model is an interpolation technique, and at this point in time, the information at the well bore (the departure point for the interpolation), excluding the lithographic logging of the core, is so poor that it is not reasonable to try modeling it.

---

a. Private communication with Karl Heinz Frohne, Morgantown Energy Technology Center, 1988.

Currently, abundant data for calculating distributions and variograms are available. Data at the well bore should be the springboard from which the three-dimensional subsurface modeling starts; however, this data still needs to be developed.

SUMMARY AND RECOMMENDATIONS

This report is a preliminary step toward the characterization of the RWMC vadose zone basalt. It uses the broad stratigraphic framework developed by the USGS and others (Anderson and Lewis, 1989) and attempts to define a number of parameters that relate to the complex of flows that make up the flow groups (flow group A, B, C, etc.). The geostatistical parameters should be useful in developing a model of the subsurface conditions at the RWMC, as well as other locations at the INEL. A rigorous geologic model is a necessary starting point for fluid flow modeling. This concept of the requirement for an adequate geological model prior to any extensive numerical simulation was developed in petroleum reservoir engineering after many expensive simulation and prediction failures.

The INEL basalts are the results of plains volcanism (Greeley, 1982) modified by the periodic deposition of sedimentary interbeds. The plains volcanism results in an extremely complex and heterogeneous system of basalt flows. The sedimentary interbeds, representing deposition over long time periods and under diverse climatic conditions, add to the complexity of the system.

The RWMC is bounded on three sides by linear volcanic source areas (the Lava Ridge-Hell's Half Acre, the Arco, and the Plains Axis volcanic rift zones, see Figure 2). The resulting basalt sequence consists of a series of flows that:

- Have limited vertical and areal extents;
- Were emplaced during geologically short time periods;
- Emanated from a number of related fissures and low shield volcanoes;

- Have 25-to 100-m-thick flow swarms bounded by sedimentary strata representing, in many cases, protracted time intervals;

- Represent a period of sporadic volcanism ranging from several million to several thousand years before present.

Despite the heterogeneity of the flow morphology, the flows can usually be differentiated into four horizontal elements: (1) substratum, (2) flow base, (3) central zone, and (4) upper zone. The substratum may be a rubble or brecciated layer, a baked sediment, or a covered pahoehoe surface. In many cases, this substratum may be one of the most transmissive elements in the flow sequence. The rubble/breccia layer has a high intra- and inter-block porosity, and is frequently washed out during drilling operations. Since the basalt commonly has a grain density of 3.05 ± 0.02 g/cm^3, this high porosity layer also has a very low bulk density.

Flow bases are generally vesicular and jointed. The moderate degree of vesiculation produces a moderate porosity, median value 20%, and bulk density, median value 2.41 g/cm^3. The jointing is perpendicular to the surface and has a polygon width to height ratio (W/H) of 0.5 to 1. This results in a median distance between fractures of approximately 1.7 ft (0.5 m).

The central zone is generally jointed with a median discontinuity. This zone is massive, with a few bubble plumes or bubble tracks marking the rather plastic internal flow layer boundaries. Thus, it has a low porosity, median value 10%, and high bulk density, median value 2.73 g/cm^3. The jointing is perpendicular to the cooling surfaces and has a polygon W/H ratio of about 0.5, with a median distance between fractures of about 4 ft (1.2 m).

The upper zone generally is layered parallel to the surface, has a vesicular texture, and finely-jointed crust. It has high porosity, median value 21%, and low bulk density, median value 2.40 g/cm^3. One or more partings can develop parallel to the surface and columnar jointing is

common in the crust perpendicular to the surface; a polygon W/H ratio of about 0.5 is common. The most common geometry is a thin crustal element with fracture spacing of about 0.8 ft (0.2 m) and a coarser, more pervasive fracture set with a spacing of about 3 ft (0.9 m).

The cross section of flows measured in the walls of Box Canyon displayed a median apparent length (La) to maximum thickness (Hmax) ratio (R = La/Hmax) of ~6.0. Thus, there is a probability that a well bore will encounter a flow in a location where a flow edge occurs at a distance less than 1.5 times the apparent thickness (H) of the flow. Since there is a high probability that inclined flow surfaces will be encountered, it would seem reasonable to run a dipmeter or other logging device to pick up the dipping surfaces and evaluate pinchout directions.

An evaluation of the La/Hmax ratio as a function of outcrop orientation at Box Canyon indicates that there is a tendency for the northeast/southwest ratios to be smaller, and a northeast/southwest flow elongation is indicated.

Mineralogical and petrophysical information was provided by analyses of plugs and thin sections prepared from representative lithologic samples from each flow encountered in each well.

The rock is predominately crystalline with plagioclase, olivine, and clinopyroxene phenocrysts in a fine-grained (<0.5 mm) crystalline groundmass of the same minerals, plus magnetite, ilmenite, and a number of somewhat oxidized opaques. Plagioclase is the predominate mineral. However, the average grain density is ~3.05 g/cm^3. Thus, the lighter density of the predominate plagioclase (2.7 g/cm^3) is rarely offset by the other denser components (clinopyroxenes ~3.25, olivine ~3.4, ilmenite ~4.7, and magnetite ~5.18 g/cm^3).

The porosity/permeability plots are usually "shotgun" patterns indicating a complex flow mechanism. The petrography provides some insight into this mechanism. The high-permeability vesicular basalt (up to 5000 md) generally has a fine-grained, crystalline matrix and vesicules of irregular

size and shape. The low-permeability vesicular rock (a few millidarcys or less) has glassy or partially oxidized opaque vesicle walls, which are generally regularly shaped and sized. Thus, the permeability is usually controlled by the characteristics of the cavity lining and the rock matrix connecting the vesicles. The lower-permeability, nonvesicular core (a few millidarcys or less) generally has an intergranular matrix with relatively small, regularly sized, nonconnected pores. The more permeable material (5-10 md or higher) has somewhat larger, irregularly sized, more frequently connected pores. There is a close correlation between permeabilities and the percentage of visible pinpoint porosity noted in the core descriptions.

The maximum, minimum, and median permeability (kh, kl, km) and porosity (θh, θl, θm) values for the upper vesicular zone are: kl = 0.1, km = 7, kh = 5000 md, and θl = 11, θm = 22, and θh = 43%. The equivalent values for the central zone are kl <0.05, km = 8, kh = 253 md, and θl = 3, θm = 10, and θh = 17%. The values for intermediate, plus lower vesicular zones are kl <0.05, km = 4, kh = 1649 md, and θl = 12, θm = 21, and θh = 39 md. Thus, the low porosity central zone has the highest median permeability.

There is a relatively good break at 15% between the vesicular zones and the porosities of the central massive zones. A few central zone plugs have bubble trains and some of the vesicular zone plugs contact small nonvesicular areas. However, logging sondes generally detect a volume appreciably larger than the plugs; hence, a porosity cutoff based on valid log data should be more precise.

The highest transmissivity elements are the fractures and fissures, interflow rubble zones, lava tubes, and partially collapsed zones that surround the more competent lower-transmissivity flow ridges.

The geostatistical study of the surface of the recent Hell's Half Acre Flow indicates that the most common surface form to be expected (as the surface for the lower contact) is a ropy pahoehoe layer. This would not yield a highly transmissive interface. The pahoehoe accounts for 51% of the contact area.

The next most common element is a blocky/broken/rubbly surface. This would make a highly porous interflow layer with both intra- and inter-block porosity, and would be highly transmissive. The surface layer is generally highly oxidized. This red oxide coloration might aid in its detection from core or cutting descriptions. Rubble is present on 30% of the Hell's Half Acre surface, displays appreciable continuity (as a fraction of the surface), and is commonly associated with a fracture/fissure component.

The fracture/fissures represent 19% of the surface, and where unfilled by basalt or sediments, could be one of the most transmissive elements encountered (it is only exceeded by open or partially collapsed lava tubes).

The geologic characterization of basalt under the RWMC would be significantly improved using geophysics logs at every well drilled at the INEL. The logging concepts and techniques are extremely sophisticated. If the system being investigated is reasonably well understood, then the integration of state-of-the-art logging with good geological concepts should produce logging suite and techniques that result in first-rate subsurface characterization parameters.

As mentioned previously, a significant amount of geostatistical data were developed during this study, but quantitative information at the departure points is lacking. Our recommendations consider the general tasks and procedures that might produce a more manageable and useful future data set, and also, the specific tasks that might result in a more useful and complete vadose zone characterization within the next two years.

Two deficiencies that caused concern in this study were the lack of quantitative geophysical well log data, and the lack of a comprehensive and readily available database covering subsurface information of activities at the RWMC during the past fifteen or twenty years.

Some actions that could be taken to provide better characterization follow:

- Develop a consistent database and information format for all INEL wells.

- Develop tomographic characterization techniques for INEL waste areas. These would include.
  - X-Y plane analysis,
  - Cross hole analysis, and
  - Analyses utilizing multiple complimentary methods:
    -- Seismic,
    -- Ground-penetrating radar,
    -- Magnetics,
    -- Resistivity.
- Log every hole with a suite of quantitative logging tools.
- Core every well.
- Drill several deep holes, 1000 to 3000 ft (305 to 915 m), and test for:
  - Aquifer thickness,
  - Vertical permeability,
  - Effectiveness of aquatard layers,
  - Transmissivity of high permeability zones.
- Sample all identified surface flows in the INEL area and evaluate the following correlation techniques in order to correlate with subsurface flow units:
  - Petrographic analysis,
  - Elemental evaluation via SEM-trace element analysis,

- Magnetic characterization,

- Age dating,

- Accessory mineral identification.

- Evaluate oriented coring, horizontal drilling and coring, and surface to bore hole sounding in order to help characterize the subsurface fracture/fissure geometry.

REFERENCES

Anderson, S. R., and Lewis, B. D., "Stratigraphy of the Unsaturated Zone at the Radioactive Waste Management Complex, Idaho National Engineering Laboratory, Idaho," USGS WRIR 89-4065, 1989, p. 54.

Baker, C. O., et. al., Tight Gas Reservoirs, Report of the National Petroleum Council/National Academy of Sciences Committee on Unconventional Gas Sources, Vol. V, 1981.

Bates, R. L., and J. A. Jackson, Glossary of Geology, AGI, Falls Church, VA, 1980, p. 751.

Champion, D. E., Lamphere, M. A., and Kuntz, M. A., "Evidence for a New Geomagnetic Reversal from Lava Flows in Idaho: Discussion of Short Polarity Reversals in the Brunhes and Late Matuyama Polarity Chrons," Journal of Geophysical Research, Vol. 93, No. B-10, Oct. 10, 1988, p. 11, 667-11, 680.

Clark, I., Practical Geostatistics, Elsevier Applied Science Publishers, New York, NY, 1984, p. 129.

Daian, J. F., "Condensation and Isothermal Water Transfer in Cement Mortar, Part I-- Pore Size Distribution, Equilibrium Water Condensation and Imbibition," Transport in Porous Media 3, 1988, p. 563-589.

de Boer, A. H., Structure and Properties of Porous Materials, Everett and Stone, editors, Butterworth, London, 1958, p. 68.

Dean, R. S. and C. W. Davis, "Magnetic Concentration of Ores," AIME Transactions, Vol. 112, 1935, p. 509-537.

Dollimore, D. and G. R. Heal, "Pore-Size Distribution in Typical Adsorbent Systems," Journal of Colloid and Interface Science, 33, 4, 1970, p. 508-519.

Eick, P. M. and C. M. Schlinger, "Multi-Frequency Magnetic Susceptibility Variations in Ash-Flow Sheets," 3rd International Symposium in Geophysics, Las Vegas, NV, Oct. 2-5, 1989.

Elphick, R. Y., "Petrophysical Corner," Geobyte, Vol 4., Aug. 1989, p. 25-37.

Greeley, R., "The Style of Volcanism in the Eastern Snake River Plain, Idaho," Idaho Geol. Survey Bull., 26, 1982, p. 407-422.

Gregg, S. J. and K. S. W. Sing, Adsorption, Surface Area and Porosity, 2nd Ed., Academic Press, New York, NY, 1982, p. 303.

Haldorsen, H. H., and Damsleth, E., Stochastic Modeling JPT, April 1990, p. 404-412.

Knutson, C. F., 1974, "Modeling of Non-Continuous Fort Unio and Mesaverde Sandstone Reservoirs, Piceance Basin, Northwestern Colorado," SPE Jour., August, 1976.

Kuntz, M. A., Dalrymple, G. B., Champion, D. E., and Doherty, D. J., "An Evaluation of Potential Volcanic Hazards at the Radioactive Waste Management Complex, Idaho National Engineering Laboratory, Idaho," USGS OFR 80-388, 1980, p. 63.

Kuntz, M. A., Spiker, E. C., Rubin, M., Champion, D. E., and Lafebre, R. H., "Radiocarbon Studies of Latest Pleistocene and Holocene Lava Flows of the Snake River Plain, Idaho: Data, Lessons, Interpretations," Quat. Res., Vol. 25, 1986, pp. 163-176.

Kuuskraa, V., et al., Enhanced Recovery of Unconventional Gas, Vol. I, II, and III, DOE HCP/T2705, Oct. 1978.

Smith, R. P., Hackett, W. R., and Rodgers, D. W., 1989a, "Surface Deformation Along the Arco Rift Zone, Eastern Snake River Plain, Idaho," GSA Bul., Vol. 21, No. 5, 1989, p. 146.

Smith, R. P., Hackett, W. R., and Rodgers, D. W., 1989b, Geologic Aspects of Seismic Hazards Assessment at INEL, Southeastern Idaho," Proc. 2nd DOE Natural Hazard Phenomena Mitigation Conference, Knoxville, TN, Oct. 1989, p. 282-289.

Worm, H. N., S. K. Benerjer, and P. J. Ryan, "Magnetic Domains," EOS, August 29, 1989, p. 803.

APPENDIX A

CORE LOGGING

A.1 Logger [tm] Procedures

A.2 Logger [tm] Logs

A.3 Characterization and Stratigraphy of RWMC Lava Flows

APPENDIX A.1

LOGGER[tm] PROCEDURES

APPENDIX A.1

LOGGER[tm] PROCEDURES

The Rockware Incorporated Logger[tm] version 3.99 was used to transform fifteen field core logs from RWMC drill holes into Logger[tm] logs (this Appendix). Figure A-1 illustrates the basic format used for the core data text file. The data included in the Logger[tm] logs are depth, lithology, fracture location, alteration, percent vesicles, maximum vesicle size (mm), phenocryst size range, intergranular void space in the matrix, percent of plagioclase, olivine, and oxidized minerals of each core and laboratory and field porosity and permeability measurements.

Procedure

Above the start flag, START:, in the core data text file of each well log all information unique to the particular log, such as the well log and the person who described the core, is recorded (Figure A-1). (Being above the start flag, these remarks will be ignored by the program when compiling the core data.). Below the start flag are the interval settings. Except for initial- and final-depth, the interval settings remain the same for each well log (Figure A-1), but can be easily changed as desired. The values for the initial- and final-depth settings are dictated by the depth each field core log starts and ends. Generally the initial- and final-depths are set at least five feet above and below the starting and ending logged depths, respectively (both settings are rounded to the nearest five-foot interval) (Figure A-2).

Figure A-2, the Logger[tm] core data file for well log 76-4, illustrates the format used for the RWMC core logs (this Appendix). The three data flags used to enter lithology, porosity, permeability, and structures (i.e., fractures) are LITHOLOGY:, which can be abbreviated L:; COMMENT:; and INTERBED:. All data flags must be followed by a colon-space, and each lithologic description, comment, and interbed (e.g., structure) description must be enclosed by quotation marks.

COREDATA.TXT

This is a listing of the file which is used to plot the RWMC core logging information.CFK 2/1/89.

START:

LOG-TYPE: "SETUP_03.TXT"
LOG-SCALE: 10
LABEL-INTERVAL: 5
DIVISION-INTERVAL: 1
INITIAL-DEPTH: 0
FINAL-DEPTH: 250

L: 0 0 0

CURVES: 9

	1	2	3	4	5	6	7	8	9
-1	0.0	0.0	0.0	0.0	0.0	0.0	0.0	0.0	0.0
0	0.0	0.0	0.0	0.0	0	0	0	0	0
1	0.0	0.0	0.0	0.0	0	0	0	0	0
2	0.0	0.0	0.0	0.0	0	0	0	0	0
3	0.0	0.0	0.0	0.0	0	0	0	0	0
4	0.0	0.0	0.0	0.0	0	0	0	0	0
5	0.0	0.0	0.0	0.0	0	0	0	0	0
6	0.0	0.0	0.0	0.0	0	0	0	0	0
7	0.0	0.0	0.0	0.0	0	0	0	0	0
8	0.0	0.0	0.0	0.0	0	0	0	0	0
9	0.0	0.0	0.0	0.0	0	0	0	0	0
10	0.0	0.0	0.0	0.0	0	0	0	0	0
11	0.0	0.0	0.0	0.0	0	0	0	0	0
12	0.0	0.0	0.0	0.0	0	0	0	0	0
13	0.0	0.0	0.0	0.0	0	0	0	0	0
14	0.0	0.0	0.0	0.0	0	0	0	0	0
15	0.0	0.0	0.0	0.0	0	0	0	0	0
16	0.0	0.0	0.0	0.0	0	0	0	0	0
17	0.0	0.0	0.0	0.0	0	0	0	0	0
18	0.0	0.0	0.0	0.0	0	0	0	0	0
19	0.0	0.0	0.0	0.0	0	0	0	0	0
20	0.0	0.0	0.0	0.0	0	0	0	0	0
21	0.0	0.0	0.0	0.0	0	0	0	0	0
22	0.0	0.0	0.0	0.0	0	0	0	0	0
23	0.0	0.0	0.0	0.0	0	0	0	0	0
24	0.0	0.0	0.0	0.0	0	0	0	0	0
25	0.0	0.0	0.0	0.0	0	0	0	0	0
26	0.0	0.0	0.0	0.0	0	0	0	0	0
27	0.0	0.0	0.0	0.0	0	0	0	0	0
28	0.0	0.0	0.0	0.0	0	0	0	0	0
29	0.0	0.0	0.0	0.0	0	0	0	0	0
30	0.0	0.0	0.0	0.0	0	0	0	0	0
31	0.0	0.0	0.0	0.0	0	0	0	0	0
32	0.0	0.0	0.0	0.0	0	0	0	0	0
33	0.0	0.0	0.0	0.0	0	0	0	0	0
34	0.0	0.0	0.0	0.0	0	0	0	0	0
35	0.0	0.0	0.0	0.0	0	0	0	0	0
36	0.0	0.0	0.0	0.0	0	0	0	0	0
37	0.0	0.0	0.0	0.0	0	0	0	0	0
38	0.0	0.0	0.0	0.0	0	0	0	0	0
39	0.0	0.0	0.0	0.0	0	0	0	0	0
40	0.0	0.0	0.0	0.0	0	0	0	0	0
41	0.0	0.0	0.0	0.0	0	0	0	0	0
42	0.0	0.0	0.0	0.0	0	0	0	0	0
43	0.0	0.0	0.0	0.0	0	0	0	0	0
44	0.0	0.0	0.0	0.0	0	0	0	0	0
45	0.0	0.0	0.0	0.0	0	0	0	0	0
46	0.0	0.0	0.0	0.0	0	0	0	0	0
47	0.0	0.0	0.0	0.0	0	0	0	0	0
48	0.0	0.0	0.0	0.0	0	0	0	0	0
49	0.0	0.0	0.0	0.0	0	0	0	0	0
50	0.0	0.0	0.0	0.0	0	0	0	0	0
51	0.0	0.0	0.0	0.0	0	0	0	0	0
52	0.0	0.0	0.0	0.0	0	0	0	0	0
53	0.0	0.0	0.0	0.0	0	0	0	0	0

Figure A-1

54	0.0	0.0	0.0	0.0	0	0	0	0	0
55	0.0	0.0	0.0	0.0	0	0	0	0	0
56	0.0	0.0	0.0	0.0	0	0	0	0	0
57	0.0	0.0	0.0	0.0	0	0	0	0	0
58	0.0	0.0	0.0	0.0	0	0	0	0	0
59	0.0	0.0	0.0	0.0	0	0	0	0	0
60	0.0	0.0	0.0	0.0	0	0	0	0	0
61	0.0	0.0	0.0	0.0	0	0	0	0	0
62	0.0	0.0	0.0	0.0	0	0	0	0	0
63	0.0	0.0	0.0	0.0	0	0	0	0	0
64	0.0	0.0	0.0	0.0	0	0	0	0	0
65	0.0	0.0	0.0	0.0	0	0	0	0	0
66	0.0	0.0	0.0	0.0	0	0	0	0	0
67	0.0	0.0	0.0	0.0	0	0	0	0	0
68	0.0	0.0	0.0	0.0	0	0	0	0	0
69	0.0	0.0	0.0	0.0	0	0	0	0	0
70	0.0	0.0	0.0	0.0	0	0	0	0	0
71	0.0	0.0	0.0	0.0	0	0	0	0	0
72	0.0	0.0	0.0	0.0	0	0	0	0	0
73	0.0	0.0	0.0	0.0	0	0	0	0	0
74	0.0	0.0	0.0	0.0	0	0	0	0	0
75	0.0	0.0	0.0	0.0	0	0	0	0	0
76	0.0	0.0	0.0	0.0	0	0	0	0	0
77	0.0	0.0	0.0	0.0	0	0	0	0	0
78	0.0	0.0	0.0	0.0	0	0	0	0	0
79	0.0	0.0	0.0	0.0	0	0	0	0	0
80	0.0	0.0	0.0	0.0	0	0	0	0	0
81	0.0	0.0	0.0	0.0	0	0	0	0	0
82	0.0	0.0	0.0	0.0	0	0	0	0	0
83	0.0	0.0	0.0	0.0	0	0	0	0	0
84	0.0	0.0	0.0	0.0	0	0	0	0	0
85	0.0	0.0	0.0	0.0	0	0	0	0	0
86	0.0	0.0	0.0	0.0	0	0	0	0	0
87	0.0	0.0	0.0	0.0	0	0	0	0	0
88	0.0	0.0	0.0	0.0	0	0	0	0	0
89	0.0	0.0	0.0	0.0	0	0	0	0	0
90	0.0	0.0	0.0	0.0	0	0	0	0	0
91	0.0	0.0	0.0	0.0	0	0	0	0	0
92	0.0	0.0	0.0	0.0	0	0	0	0	0
93	0.0	0.0	0.0	0.0	0	0	0	0	0
94	0.0	0.0	0.0	0.0	0	0	0	0	0
95	0.0	0.0	0.0	0.0	0	0	0	0	0
96	0.0	0.0	0.0	0.0	0	0	0	0	0
97	0.0	0.0	0.0	0.0	0	0	0	0	0
98	0.0	0.0	0.0	0.0	0	0	0	0	0
99	0.0	0.0	0.0	0.0	0	0	0	0	0
100	0.0	0.0	0.0	0.0	0	0	0	0	0
101	0.0	0.0	0.0	0.0	0	0	0	0	0
102	0.0	0.0	0.0	0.0	0	0	0	0	0
103	0.0	0.0	0.0	0.0	0	0	0	0	0
104	0.0	0.0	0.0	0.0	0	0	0	0	0
105	0.0	0.0	0.0	0.0	0	0	0	0	0
106	0.0	0.0	0.0	0.0	0	0	0	0	0
107	0.0	0.0	0.0	0.0	0	0	0	0	0
108	0.0	0.0	0.0	0.0	0	0	0	0	0
109	0.0	0.0	0.0	0.0	0	0	0	0	0
110	0.0	0.0	0.0	0.0	0	0	0	0	0
111	0.0	0.0	0.0	0.0	0	0	0	0	0
112	0.0	0.0	0.0	0.0	0	0	0	0	0
113	0.0	0.0	0.0	0.0	0	0	0	0	0
114	0.0	0.0	0.0	0.0	0	0	0	0	0
115	0.0	0.0	0.0	0.0	0	0	0	0	0
116	0.0	0.0	0.0	0.0	0	0	0	0	0
117	0.0	0.0	0.0	0.0	0	0	0	0	0
118	0.0	0.0	0.0	0.0	0	0	0	0	0
119	0.0	0.0	0.0	0.0	0	0	0	0	0
120	0.0	0.0	0.0	0.0	0	0	0	0	0
121	0.0	0.0	0.0	0.0	0	0	0	0	0
122	0.0	0.0	0.0	0.0	0	0	0	0	0
123	0.0	0.0	0.0	0.0	0	0	0	0	0
124	0.0	0.0	0.0	0.0	0	0	0	0	0
125	0.0	0.0	0.0	0.0	0	0	0	0	0
126	0.0	0.0	0.0	0.0	0	0	0	0	0
127	0.0	0.0	0.0	0.0	0	0	0	0	0
128	0.0	0.0	0.0	0.0	0	0	0	0	0
129	0.0	0.0	0.0	0.0	0	0	0	0	0
130	0.0	0.0	0.0	0.0	0	0	0	0	0
131	0.0	0.0	0.0	0.0	0	0	0	0	0
132	0.0	0.0	0.0	0.0	0	0	0	0	0

133	0.0	0.0	0.0	0.0	0	0	0	0	0
134	0.0	0.0	0.0	0.0	0	0	0	0	0
135	0.0	0.0	0.0	0.0	0	0	0	0	0
136	0.0	0.0	0.0	0.0	0	0	0	0	0
137	0.0	0.0	0.0	0.0	0	0	0	0	0
138	0.0	0.0	0.0	0.0	0	0	0	0	0
139	0.0	0.0	0.0	0.0	0	0	0	0	0
140	0.0	0.0	0.0	0.0	0	0	0	0	0
141	0.0	0.0	0.0	0.0	0	0	0	0	0
142	0.0	0.0	0.0	0.0	0	0	0	0	0
143	0.0	0.0	0.0	0.0	0	0	0	0	0
144	0.0	0.0	0.0	0.0	0	0	0	0	0
145	0.0	0.0	0.0	0.0	0	0	0	0	0
146	0.0	0.0	0.0	0.0	0	0	0	0	0
147	0.0	0.0	0.0	0.0	0	0	0	0	0
148	0.0	0.0	0.0	0.0	0	0	0	0	0
149	0.0	0.0	0.0	0.0	0	0	0	0	0
150	0.0	0.0	0.0	0.0	0	0	0	0	0
150	0.0	0.0	0.0	0.0	0	0	0	0	0
151	0.0	0.0	0.0	0.0	0	0	0	0	0
152	0.0	0.0	0.0	0.0	0	0	0	0	0
153	0.0	0.0	0.0	0.0	0	0	0	0	0
154	0.0	0.0	0.0	0.0	0	0	0	0	0
155	0.0	0.0	0.0	0.0	0	0	0	0	0
156	0.0	0.0	0.0	0.0	0	0	0	0	0
157	0.0	0.0	0.0	0.0	0	0	0	0	0
158	0.0	0.0	0.0	0.0	0	0	0	0	0
159	0.0	0.0	0.0	0.0	0	0	0	0	0
160	0.0	0.0	0.0	0.0	0	0	0	0	0
161	0.0	0.0	0.0	0.0	0	0	0	0	0
162	0.0	0.0	0.0	0.0	0	0	0	0	0
163	0.0	0.0	0.0	0.0	0	0	0	0	0
164	0.0	0.0	0.0	0.0	0	0	0	0	0
165	0.0	0.0	0.0	0.0	0	0	0	0	0
166	0.0	0.0	0.0	0.0	0	0	0	0	0
167	0.0	0.0	0.0	0.0	0	0	0	0	0
168	0.0	0.0	0.0	0.0	0	0	0	0	0
169	0.0	0.0	0.0	0.0	0	0	0	0	0
170	0.0	0.0	0.0	0.0	0	0	0	0	0
171	0.0	0.0	0.0	0.0	0	0	0	0	0
172	0.0	0.0	0.0	0.0	0	0	0	0	0
173	0.0	0.0	0.0	0.0	0	0	0	0	0
174	0.0	0.0	0.0	0.0	0	0	0	0	0
175	0.0	0.0	0.0	0.0	0	0	0	0	0
176	0.0	0.0	0.0	0.0	0	0	0	0	0
177	0.0	0.0	0.0	0.0	0	0	0	0	0
178	0.0	0.0	0.0	0.0	0	0	0	0	0
179	0.0	0.0	0.0	0.0	0	0	0	0	0
180	0.0	0.0	0.0	0.0	0	0	0	0	0
181	0.0	0.0	0.0	0.0	0	0	0	0	0
182	0.0	0.0	0.0	0.0	0	0	0	0	0
183	0.0	0.0	0.0	0.0	0	0	0	0	0
184	0.0	0.0	0.0	0.0	0	0	0	0	0
185	0.0	0.0	0.0	0.0	0	0	0	0	0
186	0.0	0.0	0.0	0.0	0	0	0	0	0
187	0.0	0.0	0.0	0.0	0	0	0	0	0
188	0.0	0.0	0.0	0.0	0	0	0	0	0
189	0.0	0.0	0.0	0.0	0	0	0	0	0
190	0.0	0.0	0.0	0.0	0	0	0	0	0
191	0.0	0.0	0.0	0.0	0	0	0	0	0
192	0.0	0.0	0.0	0.0	0	0	0	0	0
193	0.0	0.0	0.0	0.0	0	0	0	0	0
194	0.0	0.0	0.0	0.0	0	0	0	0	0
195	0.0	0.0	0.0	0.0	0	0	0	0	0
196	0.0	0.0	0.0	0.0	0	0	0	0	0
197	0.0	0.0	0.0	0.0	0	0	0	0	0
198	0.0	0.0	0.0	0.0	0	0	0	0	0
199	0.0	0.0	0.0	0.0	0	0	0	0	0
200	0.0	0.0	0.0	0.0	0	0	0	0	0
201	0.0	0.0	0.0	0.0	0	0	0	0	0

202	0.0	0.0	0.0	0.0	0	0	0	0	0
203	0.0	0.0	0.0	0.0	0	0	0	0	0
204	0.0	0.0	0.0	0.0	0	0	0	0	0
205	0.0	0.0	0.0	0.0	0	0	0	0	0
206	0.0	0.0	0.0	0.0	0	0	0	0	0
207	0.0	0.0	0.0	0.0	0	0	0	0	0
208	0.0	0.0	0.0	0.0	0	0	0	0	0
209	0.0	0.0	0.0	0.0	0	0	0	0	0
210	0.0	0.0	0.0	0.0	0	0	0	0	0
211	0.0	0.0	0.0	0.0	0	0	0	0	0
212	0.0	0.0	0.0	0.0	0	0	0	0	0
213	0.0	0.0	0.0	0.0	0	0	0	0	0
214	0.0	0.0	0.0	0.0	0	0	0	0	0
215	0.0	0.0	0.0	0.0	0	0	0	0	0
216	0.0	0.0	0.0	0.0	0	0	0	0	0
217	0.0	0.0	0.0	0.0	0	0	0	0	0
218	0.0	0.0	0.0	0.0	0	0	0	0	0
219	0.0	0.0	0.0	0.0	0	0	0	0	0
220	0.0	0.0	0.0	0.0	0	0	0	0	0
221	0.0	0.0	0.0	0.0	0	0	0	0	0
222	0.0	0.0	0.0	0.0	0	0	0	0	0
223	0.0	0.0	0.0	0.0	0	0	0	0	0
224	0.0	0.0	0.0	0.0	0	0	0	0	0
225	0.0	0.0	0.0	0.0	0	0	0	0	0
226	0.0	0.0	0.0	0.0	0	0	0	0	0
227	0.0	0.0	0.0	0.0	0	0	0	0	0
228	0.0	0.0	0.0	0.0	0	0	0	0	0
229	0.0	0.0	0.0	0.0	0	0	0	0	0
230	0.0	0.0	0.0	0.0	0	0	0	0	0
231	0.0	0.0	0.0	0.0	0	0	0	0	0
232	0.0	0.0	0.0	0.0	0	0	0	0	0
233	0.0	0.0	0.0	0.0	0	0	0	0	0
234	0.0	0.0	0.0	0.0	0	0	0	0	0
235	0.0	0.0	0.0	0.0	0	0	0	0	0
236	0.0	0.0	0.0	0.0	0	0	0	0	0
327	0.0	0.0	0.0	0.0	0	0	0	0	0
328	0.0	0.0	0.0	0.0	0	0	0	0	0
239	0.0	0.0	0.0	0.0	0	0	0	0	0
240	0.0	0.0	0.0	0.0	0	0	0	0	0
241	0.0	0.0	0.0	0.0	0	0	0	0	0
242	0.0	0.0	0.0	0.0	0	0	0	0	0
243	0.0	0.0	0.0	0.0	0	0	0	0	0
244	0.0	0.0	0.0	0.0	0	0	0	0	0
245	0.0	0.0	0.0	0.0	0	0	0	0	0
246	0.0	0.0	0.0	0.0	0	0	0	0	0
247	0.0	0.0	0.0	0.0	0	0	0	0	0
248	0.0	0.0	0.0	0.0	0	0	0	0	0
249	0.0	0.0	0.0	0.0	0	0	0	0	0
250	0.0	0.0	0.0	0.0	0	0	0	0	0
-99									

HISTOGRAMS: 2

		10	11
0	1	0.0	0.0
1	2	0.0	0.0
2	3	0.0	0.0
3	4	0.0	0.0
4	5	0.0	0.0
5	6	0.0	0.0
6	7	0.0	0.0
7	8	0.0	0.0
8	9	0.0	0.0
9	10	0.0	0.0
10	11	0.0	0.0
11	12	0.0	0.0
12	13	0.0	0.0
13	14	0.0	0.0
14	15	0.0	0.0
15	16	0.0	0.0
16	17	0.0	0.0
17	18	0.0	0.0
18	19	0.0	0.0
19	20	0.0	0.0
20	21	0.0	0.0
21	22	0.0	0.0
22	23	0.0	0.0
23	24	0.0	0.0
24	25	0.0	0.0
25	26	0.0	0.0
26	27	0.0	0.0
27	28	0.0	0.0
28	29	0.0	0.0
29	30	0.0	0.0
30	31	0.0	0.0
31	32	0.0	0.0
32	33	0.0	0.0
33	34	0.0	0.0
34	35	0.0	0.0
35	36	0.0	0.0
36	37	0.0	0.0
37	38	0.0	0.0
38	39	0.0	0.0
39	40	0.0	0.0
40	41	0.0	0.0
41	42	0.0	0.0
42	43	0.0	0.0
43	44	0.0	0.0
44	45	0.0	0.0
45	46	0.0	0.0
46	47	0.0	0.0
47	48	0.0	0.0
48	49	0.0	0.0
49	50	0.0	0.0
50	51	0.0	0.0
51	52	0.0	0.0
52	53	0.0	0.0
53	54	0.0	0.0
54	55	0.0	0.0
55	56	0.0	0.0
56	57	0.0	0.0
57	58	0.0	0.0
58	59	0.0	0.0
59	60	0.0	0.0
60	61	0.0	0.0
61	62	0.0	0.0
62	63	0.0	0.0
63	64	0.0	0.0
64	65	0.0	0.0
65	66	0.0	0.0
66	67	0.0	0.0
67	68	0.0	0.0
68	69	0.0	0.0
69	70	0.0	0.0
70	71	0.0	0.0
71	72	0.0	0.0
72	73	0.0	0.0
73	74	0.0	0.0
74	75	0.0	0.0
75	76	0.0	0.0
76	77	0.0	0.0
77	78	0.0	0.0
78	79	0.0	0.0
79	80	0.0	0.0
80	81	0.0	0.0
81	82	0.0	0.0
82	83	0.0	0.0
83	84	0.0	0.0
84	85	0.0	0.0
85	86	0.0	0.0
86	87	0.0	0.0
87	88	0.0	0.0
88	89	0.0	0.0
89	90	0.0	0.0
90	91	0.0	0.0
91	92	0.0	0.0
92	93	0.0	0.0
93	94	0.0	0.0
94	95	0.0	0.0
95	96	0.0	0.0
96	97	0.0	0.0
97	98	0.0	0.0
98	99	0.0	0.0
99	100	0.0	0.0
100	101	0.0	0.0
101	102	0.0	0.0
102	103	0.0	0.0
103	104	0.0	0.0
104	105	0.0	0.0
105	106	0.0	0.0
106	107	0.0	0.0
107	108	0.0	0.0
108	109	0.0	0.0
109	110	0.0	0.0
110	111	0.0	0.0
111	112	0.0	0.0
112	113	0.0	0.0
113	114	0.0	0.0
114	115	0.0	0.0
115	116	0.0	0.0
116	117	0.0	0.0
117	118	0.0	0.0
118	119	0.0	0.0
119	120	0.0	0.0
120	121	0.0	0.0
121	122	0.0	0.0
122	123	0.0	0.0
123	124	0.0	0.0
124	125	0.0	0.0
125	126	0.0	0.0
126	127	0.0	0.0
127	128	0.0	0.0
128	129	0.0	0.0
129	130	0.0	0.0
130	131	0.0	0.0
131	132	0.0	0.0
132	133	0.0	0.0
133	134	0.0	0.0
134	135	0.0	0.0
135	136	0.0	0.0
136	137	0.0	0.0
137	138	0.0	0.0
138	139	0.0	0.0
139	140	0.0	0.0
140	141	0.0	0.0
141	142	0.0	0.0
142	143	0.0	0.0
143	144	0.0	0.0
144	145	0.0	0.0
145	146	0.0	0.0
146	147	0.0	0.0
147	148	0.0	0.0
148	149	0.0	0.0
149	150	0.0	0.0
150	151	0.0	0.0
151	152	0.0	0.0
152	153	0.0	0.0
153	154	0.0	0.0
154	155	0.0	0.0

```
155 156     0.0 0.0
156 157     0.0 0.0
157 158     0.0 0.0
158 159     0.0 0.0
159 160     0.0 0.0
160 161     0.0 0.0
161 162     0.0 0.0
162 163     0.0 0.0
163 164     0.0 0.0
164 165     0.0 0.0
165 166     0.0 0.0
166 167     0.0 0.0
167 168     0.0 0.0
168 169     0.0 0.0
169 170     0.0 0.0
170 171     0.0 0.0
171 172     0.0 0.0
172 173     0.0 0.0
173 174     0.0 0.0
174 175     0.0 0.0
175 176     0.0 0.0
176 177     0.0 0.0
177 178     0.0 0.0
178 179     0.0 0.0
179 180     0.0 0.0
180 181     0.0 0.0
181 182     0.0 0.0
182 183     0.0 0.0
183 184     0.0 0.0
184 185     0.0 0.0
185 186     0.0 0.0
186 187     0.0 0.0
187 188     0.0 0.0
188 189     0.0 0.0
189 190     0.0 0.0
190 191     0.0 0.0
191 192     0.0 0.0
192 193     0.0 0.0
193 194     0.0 0.0
194 195     0.0 0.0
195 196     0.0 0.0
196 197     0.0 0.0
197 198     0.0 0.0
198 199     0.0 0.0
199 200     0.0 0.0
200 201     0.0 0.0
201 202     0.0 0.0
202 203     0.0 0.0
203 204     0.0 0.0
204 205     0.0 0.0
205 206     0.0 0.0
206 207     0.0 0.0
207 208     0.0 0.0
208 209     0.0 0.0
209 210     0.0 0.0
210 211     0.0 0.0
211 212     0.0 0.0
212 213     0.0 0.0
213 214     0.0 0.0
214 215     0.0 0.0
215 216     0.0 0.0
216 217     0.0 0.0
217 218     0.0 0.0
218 219     0.0 0.0
219 220     0.0 0.0
220 221     0.0 0.0
221 222     0.0 0.0
222 223     0.0 0.0
223 224     0.0 0.0
224 225     0.0 0.0
225 226     0.0 0.0
226 227     0.0 0.0
227 228     0.0 0.0
228 229     0.0 0.0
229 230     0.0 0.0
230 231     0.0 0.0
231 232     0.0 0.0
232 233     0.0 0.0
233 234     0.0 0.0
234 235     0.0 0.0
235 236     0.0 0.0
236 237     0.0 0.0
237 238     0.0 0.0
238 239     0.0 0.0
239 240     0.0 0.0
240 241     0.0 0.0
241 242     0.0 0.0
242 243     0.0 0.0
243 244     0.0 0.0
244 245     0.0 0.0
245 246     0.0 0.0
246 247     0.0 0.0
247 248     0.0 0.0
248 249     0.0 0.0
249 250     0.0 0.0
-99

END:
```

This is data from well log 76-4 described by J.P. O'Brien and includes laboratory and field porosity and permeability measurements. KAM 9/29/89

START:

```
LOG-TYPE:           "SETUP_03.TXT"
LOG-SCALE:          10
LABEL-INTERVAL:     5
DIVISION-INTERVAL:  1
INITIAL-DEPTH:      5
FINAL-DEPTH:        120

L: 11 13 10 "BASALT: VESICULAR  (11.4' S,L-p=16.60,k=3.74)"
INTERBED: 11 13 "FRACTURE: MOD ANGLE"
L: 13 20 13 "BASALT  (18.2' S,ts L-p=10.08,k=0.92)"
COMMENT: 12 50 "15.0' p=10.52"
COMMENT: 13 50 "15.2' k=1.50"
COMMENT: 15 50 "18.1' p=9.22"
COMMENT: 16 50 "18.4' k=6.74"
COMMENT: 18 50 "19.2' p=13.49"
COMMENT: 19 50 "19.6' k=11.56"
INTERBED: 13 14 "FRACTURE: SILT FILL"
INTERBED: 16 17 "FRACTURE: LOW ANGLE"
L: 20 30 20 "BASALT: VESICULAR  (20.0' S,L-p=22.94,k=9.44; 25.3'
S,L-p=23.98,k=3.32; 28.5' S,L-p=22.75,k=3.44)"
COMMENT: 20 50 "FLOW TOP @ 21.2'"
COMMENT: 22 50 "24.0' p=21.06"
COMMENT: 23 50 "24.3' k=6.17"
COMMENT: 25 50 "26.8' p=22.86"
COMMENT: 26 45 "USGS Sample @ 26.3-26.8'"
COMMENT: 27 50 "27.1' k=7.67"
COMMENT: 28 50 "28.0' p=23.74"
COMMENT: 30 50 "28.2' k=1.09"
INTERBED: 20 23 "CINDERS"
INTERBED: 24 26 "FRACTURE: LOW ANGLE"
INTERBED: 27 28 "FRACTURE: SILT FILL"
INTERBED: 28 30 "FRACTURE: LOW ANGLE"
L: 30 42 30 "BASALT  (31.5' S,L-p=11.63,k=27.11; 36.2' S,ts
L-p=4.63,k=0.18; 38.7' S,L-p=10.73,k=3.34"
COMMENT: 32 50 "31.7' p=10.20"
COMMENT: 33 50 "32.0' k=28.75"
COMMENT: 35 50 "32.2' p=7.45"
COMMENT: 36 50 "32.6' k=1.54"
COMMENT: 38 50 "36.4' p=0.60"
COMMENT: 39 50 "36.7' k=0.48"
COMMENT: 41 50 "38.4' p=7.80"
COMMENT: 42 50 "38.6' k=1.00"
INTERBED: 30 31 "FRACTURE: SILT FILL"
INTERBED: 32 33 "FRACTURE: LOW ANGLE"
INTERBED: 33 36 "FRACTURE: MOD ANGLE"
INTERBED: 37 38 "FRACTURE: MOD ANLGE"
INTERBED: 38 39 "FRACTURE: LOW ANLGE"
INTERBED: 40 42 "FRACTURE: LOW ANGLE"
L: 42 47 42 "BASALT: VESICULAR  (42.3' S,L-p=19.09,k=1.72; 44.9'
S,L-p=22.22,k=29.91)"
COMMENT: 43 47 "FLOW TOP @ 43.5'"
COMMENT: 44 50 "41.6' p=17.79"
COMMENT: 46 50 "42.0' k=4.68"
INTERBED: 42 43 "FRACTURE: LOW ANGLE"
INTERBED: 44 46 "OXIDATION , FRACTURE: LOW ANGLE"
INTERBED: 44 45 "CINDERS"
INTERBED: 45 46 "CINDERS"
L: 47 53 46 "BASALT  (49.0' S,ts L-p=5.20,k=0.14)"
COMMENT: 48 47 "USGS Sample @ 48-48.7'"
INTERBED: 47 48 "FRACTURE: LOW ANGLE"
INTERBED: 50 52 "FRACTURE: LOW ANGLE"
L: 53 57 52 "BASALT: VESICULAR  (53.7' S,L-p=32.96,k=105.12;
56.1' S,L-p=38.36,k=5000.26)"
COMMENT: 52 47 "FLOW TOP @ 54'"
COMMENT: 54 50 "55.9' p=33.99"
COMMENT: 55 50 "56.1' k=3815.49"
INTERBED: 54 55 "BASALT: BRECCIA , OXIDATION"
INTERBED: 56 57 "CINDERS , OXIDATION"
```

Figure A-2

```
L: 57 59 56 "BASALT (57.4' S,ts L-p=14.47,k=4.49)"
COMMENT: 57 50 "57.6' p=15.86"
COMMENT: 58 50 "57.9' k=7.36"
INTERBED: 57 59 "FRACTURE: LOW ANGLE"
L: 59 75 60 "BASALT: VESICULAR  (60.5' S,L-p=21.66,k=4.08; 63.7'
S,L-p=21.61,k=1.89; 65.2' S,L-p=21.84,k=1.46; 67.5' S,ts
L-p=21.64,k=4.61; 71.5' S,L-p=16.06,k=113.65"
COMMENT: 59 47 "FLOW TOP @ 59.5'?"
COMMENT: 60 50 "59.9' p=23.78"
COMMENT: 62 50 "60.2' k=11.18"
COMMENT: 63 47 "FLOW TOP @ 63.5'?"
COMMENT: 65 50 "63.9' p=23.99"
COMMENT: 66 50 "64.1' k=20.62"
COMMENT: 67 47 "FLOW TOP @ 65.5'"
COMMENT: 68 50 "64.4' p=22.78"
COMMENT: 70 50 "64.7' k=8.54"
COMMENT: 72 50 "67.0' p=22.06"
COMMENT: 73 50 "67.1' k=1.27"
COMMENT: 75 50 "68.6' p=20.06"
COMMENT: 76 50 "68.9' k=1.13"
INTERBED: 59 61 "OXIDATION"
INTERBED: 59 60 "BASALT: BRECCIA"
INTERBED: 61 63 "FRACTURE: SILT FILL"
INTERBED: 63 64 "BASALT: BRECCIA"
INTERBED: 64 64 "FRACTURE: SILT FILL"
INTERBED: 65 66 "BASALT: BRECCIA"
INTERBED: 66 67 "OXIDATION , FRACTURE: SILT FILL , CINDERS"
INTERBED: 67 69 "FRACTURE: LOW ANGLE"
INTERBED: 69 73 "FRACTURE: SILT FILL"
INTERBED: 74 75 "FRACTURE: LOW ANGLE"
L: 75 97 75 "BASALT  (76.6' S,L-p=11.76,k=18.56; 83.5' S,ts
L-p=9.46,k=10.52; 91.5' S,L-p=12.22,k=18.20)"
COMMENT: 79 50 "74.8' p=13.19"
COMMENT: 80 50 "75.3' k=8.77"
COMMENT: 82 50 "76.0' p=10.66"
COMMENT: 83 50 "76.3' k=12.85"
COMMENT: 84 50 "82.2' p=7.78"
COMMENT: 86 50 "82.5' k=4.53"
COMMENT: 88 50 "88.7' p=45.47"
COMMENT: 89 50 "88.9' k=39.90"
INTERBED: 75 76 "FRACTURE: SILT FILL"
INTERBED: 76 77 "FRACTURE: MOD ANGLE"
INTERBED: 77 78 "FRACTURE: LOW ANGLE"
INTERBED: 78 80 "FRACTURE: SILT FILL"
INTERBED: 80 82 "FRACTURE: HIGH ANGLE"
INTERBED: 82 83 "FRACTURE: LOW ANGLE"
INTERBED: 84 85 "FRACTURE: SILT FILL"
INTERBED: 87 88 "FRACTURE: LOW ANGLE"
INTERBED: 89 90 "FRACTURE: LOW ANGLE"
INTERBED: 94 96 "FRACTURE: SILT FILL"
L: 97 114.4 96 "BASALT: VESICULAR  (101.0' S,L-p=22.98,k=0.36;
105.4' S,ts L-p=15.71,k=26.32; 113.0' S,L-p=12.05,k=37.85;
113.9' S,L-p=14.58,k=38.67)"
COMMENT: 98 47 "FLOW TOP @ 100.5'"
COMMENT: 100 50 "101.8' p=22.54"
COMMENT: 102 50 "102.0' k=6.66"
COMMENT: 104 50 "104.0' p=15.82"
COMMENT: 105 50 "104.2' k=73.02"
COMMENT: 107 50 "107.1' p=13.45"
COMMENT: 108 50 "107.5' k=18.96"
COMMENT: 110 50 "110.8' p=9.30"
COMMENT: 111 50 "111.3' k=1.67"
INTERBED: 98 101 "SILT"
INTERBED: 100 103 "OXIDATION"
INTERBED: 101 105 "FRACTURE: LOW ANGLE"
INTERBED: 106 108 "FRACTURE: LOW ANGLE"
INTERBED: 109 110 "FRACTURE: LOW ANGLE"
INTERBED: 111 112 "FRACTURE: LOW ANGLE"
INTERBED: 113 114.4 "FRACTURE: LOW ANGLE"


CURVES: 9
     1   2   3   4   5   6   7   8   9

 5  0.0 0.0 0.0 0.0  0   0   0   0   0
 6  0.0 0.0 0.0 0.0  0   0   0   0   0
 7  0.0 0.0 0.0 0.0  0   0   0   0   0
 8  0.0 0.0 0.0 0.0  0   0   0   0   0
 9  0.0 0.0 0.0 0.0  0   0   0   0   0
10  0.0 0.0 0.0 0.0  0   0   0   0   0
```

11	8.0	8.0	1.5	12	0	2	4	1	0
12	9.0	8.0	1.5	12.5	0	2	4	1	0
13	5.0	4.0	1.5	11	0	2	5	1	0
14	3.0	1.0	1.5	7.0	0	2	5	1	0
15	0.0	0.0	0.0	0.0	0	0	0	0	0
16	9.0	2.0	2.0	7.0	0	2	2.5	1	0
17	3.0	1.0	2.0	3.0	0	2	2.5	1	0
18	4.0	2.0	2.0	3.0	0	2	3	1	0
19	4.0	2.0	2.0	5.0	0	2	2.5	2	0
20	9.0	4.0	2.0	7.0	0	2	3	2	0
21	12	5.0	1.5	4.0	0	2.5	2	4	0
22	0.0	0.0	0.0	0.0	0	0	0	0	0
23	0.0	0.0	0.0	0.0	0	0	0	0	0
24	23	5.0	2.0	3.0	0	6	4	1	0
25	28	4.0	2.0	2.0	0	6	4	1	0
26	25	4.0	2.0	2.5	0	6	4	2	0
27	0.0	0.0	0.0	0.0	0	0	0	0	0
28	23	6.0	2.5	8.0	0	6	5	2	0
29	18	15	2.5	6.0	0	6	5	2	0
30	11	11	2.5	5.0	0	6	5	2	0
31	7.0	4.0	2.5	4.0	0	6	5	2	0
32	5.0	2.0	2.5	3.0	0	6	5	1	0
33	3.0	1.0	2.5	10	0	6	5	1	0
34	2.0	1.0	2.5	6.0	0	7	5	1	0
35	1.0	1.0	2.5	3.0	0	6	5	1	0
36	2.0	1.0	2.5	1.0	0	6	5	1	0
37	1.0	2.0	2.5	1.0	0	7	5	1	0
38	2.0	2.0	2.5	2.0	0	8	5	1	0
39	3.0	2.0	3.0	3.0	0	10	3	2	0
40	3.0	1.0	3.0	8.0	0	10	2.5	2	0
41	4.0	1.0	3.0	6.0	0	10	2.5	2	0
42	10	2.0	2.0	3.0	0	8	2	1	0
43	21	2.0	2.0	7.0	0	7	2	2	0
44	0.0	0.0	0.0	0.0	0	0	0	0	0
45	19	7.0	2.0	4.0	0	7	1	4	0
46	10	10	2.0	3.0	0	7	2	5	0
47	4.0	22	2.5	4.0	0	7	2	5	0
48	3.0	5.0	2.5	2.0	0	8	2.5	3	0
49	0.0	0.0	0.0	0.0	0	0	0	0	0
50	4.0	1.0	2.5	2.0	0	9	3	1	0
51	2.0	1.0	2.5	3.0	0	9	4	1	0
52	2.0	1.0	2.5	2.5	0	9	4	1	0
53	2.0	1.0	2.5	3.0	0	9	4	1	0
54	21	1.0	2.5	12	0	8	1	8	0
55	22	1	1	12	0	8	1	7.5	0
56	27	2.0	1.0	11	0	9	1	7	0
57	28	2.0	1.0	11	0	9	1	7	0
58	7.0	2.0	2.5	0.0	0	9	1	1	0
59	2.0	2.0	2.5	4.0	0	10	1	1	0
60	10	2.0	1.0	5.0	0	10	2	4	0
61	13	7.0	2.0	5.0	0	9	2	6	0
62	9.0	11	2.0	3.0	0	9	2	2	0
63	8.0	3.0	2.0	4.0	0	2	2	2	0
64	9.0	12	1.0	4.0	0	1	3	7	0
65	18	9.0	2.0	7.0	0	8	2	5	0
66	12	3.0	1.0	6.0	0	1	2	5	0
67	9.0	3.0	1.0	5.0	0	1	1	2	0
68	5.0	2.0	1.0	3.0	0	2	1	1	0
69	14	9.0	1.0	3.0	0	2	1	1	0
70	13	20	1.0	4.0	0	2	1	1	0
71	12	6.0	1.0	7.0	0	2	1	1	0
72	11	15	1.0	8.0	0	2	1	1	0
73	9.0	19	1.0	8.0	0	2	2	1	0
74	0.0	10	0.0	0.0	0	4	1	1	0
75	8.0	20	1.0	11	0	5	1	1	0
76	12	13	1.0	11	0	5	1	1	0
77	4.0	13	1.0	11	0	5	2	1	0
78	4.0	12	1.0	11	0	5	2	2	0
79	10	5.0	1.0	12	0	5	2	2	0
80	5.0	2.0	1.0	12	0	4	2	1	0
81	4.0	2.0	1.0	13	0	4	2.5	1	0
82	10	2.0	1.0	12	0	5	2	1	0
83	4.0	2.0	1.0	12	0	5	3	1	0
84	4.0	2.0	1.0	12	0	4.5	3	1	0
85	10	4.0	1.0	6.0	0	4.5	3	1	0
86	2.0	2.0	1.5	5.0	0	5	3	1	0
87	2.0	1.0	1.5	10	0	5	3	1	0
88	2.0	1.0	1.5	10	0	5	3	1	0
89	2.0	1.0	1.5	9.0	0	5	3	2	0

90	9.0	2.0	1.5	10	0	4	3	2	0
91	3.0	1.0	1.5	10	0	4.5	3	2	0
92	3.0	1.0	1.5	10	0	5	3	2	0
93	3.0	1.0	1.5	10	0	5	3	2	0
94	4.0	2.0	1.5	10	0	5	3	2	0
95	4.0	2.0	1.5	10	0	5	3	2	0
96	3.0	2.0	1.5	10	0	5	3	2.5	0
97	4.0	2.0	1.0	10	0	5	2	4	0
98	10	2.0	1.0	6.0	0	1	1	6	0
99	0.0	0.0	0.0	0.0	0	0	0	0	0
100	0.0	0.0	0.0	0.0	0	0	0	0	0
101	0.0	0.0	0.0	0.0	0	0	0	0	0
102	12	2.0	1.0	2.0	0	1	1	7	0
103	11	15	1.0	3.0	0	1	1	8	0
104	18	27	1.0	7.0	0	1	2	6	0
105	11	25	1.0	8.0	0	1	2	2	0
106	12	28	2.0	10	0	2	5	3	0
107	15	28	2.0	13	0	2	6	4	0
108	10	18	2.0	13	0	1	6	2.5	0
109	8.0	19	2.0	14	0	2	6	1	0
110	6.0	18	2.0	13	0	2	6	1	0
111	4.0	13	2.0	13	0	2	6	1	0
112	4.0	16	2.0	12	0	2	6	1	0
113	4.0	12	2.0	12	0	2	5	1	0
114	3.0	9.0	2.0	13	0	2	6	1	0
115	7.0	2.0	2.0	12	0	2	7	2	0
116	0.0	0.0	0.0	0.0	0	0	0	0	0
117	0.0	0.0	0.0	0.0	0	0	0	0	0
118	0.0	0.0	0.0	0.0	0	0	0	0	0
119	0.0	0.0	0.0	0.0	0	0	0	0	0
120	0.0	0.0	0.0	0.0	0	0	0	0	0

-99

HISTOGRAMS: 2

		10	11
5	6	0.0	0.0
6	7	0.0	0.0
7	8	0.0	0.0
8	9	0.0	0.0
9	10	0.0	0.0
10	11	0.0	0.0
11	12	0.0	0.0
12	13	0.0	0.0
13	14	0.0	0.0
14	15	0.0	0.0
15	16	0.0	0.0
16	17	0.0	0.0
17	18	0.0	0.0
18	19	0.0	0.0
19	20	0.0	0.0
20	21	0.0	0.0
21	22	0.0	0.0
22	23	0.0	0.0
23	24	0.0	0.0
24	25	0.0	0.0
25	26	0.0	0.0
26	27	0.0	0.0
27	28	0.0	0.0
28	29	0.0	0.0
29	30	0.0	0.0
30	31	0.0	0.0
31	32	0.0	0.0
32	33	0.0	0.0
33	34	0.0	0.0
34	35	0.0	0.0
35	36	0.0	0.0
36	37	0.0	0.0
37	38	0.0	0.0
38	39	0.0	0.0
39	40	0.0	0.0
40	41	0.0	0.0
41	42	0.0	0.0
42	43	0.0	0.0
43	44	0.0	0.0
44	45	0.0	0.0
45	46	0.0	0.0
46	47	0.0	0.0

```
 47  48    0.0 0.0
 48  49    0.0 0.0
 49  50    0.0 0.0
 50  51    0.0 0.0
 51  52    0.0 0.0
 52  53    0.0 0.0
 53  54    0.0 0.0
 54  55    0.0 0.0
 55  56    0.0 0.0
 56  57    0.0 0.0
 57  58    0.0 0.0
 58  59    0.0 0.0
 59  60    0.0 0.0
 60  61    0.0 0.0
 61  62    0.0 0.0
 62  63    0.0 0.0
 63  64    0.0 0.0
 64  65    0.0 0.0
 65  66    0.0 0.0
 66  67    0.0 0.0
 67  68    0.0 0.0
 68  69    0.0 0.0
 69  70    0.0 0.0
 70  71    0.0 0.0
 71  72    0.0 0.0
 72  73    0.0 0.0
 73  74    0.0 0.0
 74  75    0.0 0.0
 75  76    0.0 0.0
 76  77    0.0 0.0
 77  78    0.0 0.0
 78  79    0.0 0.0
 79  80    0.0 0.0
 80  81    0.0 0.0
 81  82    0.0 0.0
 82  83    0.0 0.0
 83  84    0.0 0.0
 84  85    0.0 0.0
 85  86    0.0 0.0
 86  87    0.0 0.0
 87  88    0.0 0.0
 88  89    0.0 0.0
 89  90    0.0 0.0
 90  91    0.0 0.0
 91  92    0.0 0.0
 92  93    0.0 0.0
 93  94    0.0 0.0
 94  95    0.0 0.0
 95  96    0.0 0.0
 96  97    0.0 0.0
 97  98    0.0 0.0
 98  99    0.0 0.0
 99 100    0.0 0.0
100 101    0.0 0.0
101 102    0.0 0.0
102 103    0.0 0.0
103 104    0.0 0.0
104 105    0.0 0.0
105 106    0.0 0.0
106 107    0.0 0.0
107 108    0.0 0.0
108 109    0.0 0.0
109 110    0.0 0.0
110 111    0.0 0.0
111 112    0.0 0.0
112 113    0.0 0.0
113 114    0.0 0.0
114 115    0.0 0.0
115 116    0.0 0.0
116 117    0.0 0.0
117 118    0.0 0.0
118 119    0.0 0.0
119 120    0.0 0.0
120 121    0.0 0.0

-99

END:
```

The numbers following each flag locate the description and/or comment vertically and horizontally on the Logger^{tm} log. The three numbers following the lithology flag indicate depth to the top of the interval being described, depth to the bottom of the interval, and depth at which the textural description will begin, respectively. These numbers are entered as whole numbers; the Logger^{tm} program will arbitrarily round the number up or down anyway when printing the log. The lithology of the defined interval is in quotation marks. In parentheses following the lithology are the laboratory porosity and permeability measurements and corresponding depths at which each analyzed sample was taken, where S=sample, ts-thin section made, L=laboratory, p=porosity in percent, and k=permeability in millidarcy.

The comment flag is used to present field porosity and permeability data, indicate flow tops, and note where the USGS sampled the core (Figure A-2). The two numbers following the comment flag designate the depth at which the comment will appear and where at that depth (measured from the left) it will begin, respectively, on the Logger^{tm} log (compare Figures A-1 with A-2). When using the comment flag care must be taken that the information being entered is not overwritten on the printout of the Logger^{tm} log. The program stacks these comments and if the comments are defined at consecutive depths (e.g., 34′, 35′, 36′,..) they will overlap. Following the numbers, in quotation marks, is the depth at which the porosity and permeability measurements were taken and the actual values.

The interbed flag is used to indicate any alteration, type of structure, or minor lithology within the interval defined after L: (Figure A-2). The two numbers following this flag designate depth to top and bottom of the interbed, respectively. The type of alteration, structure, or minor lithology for the interbed must be in quotation marks. If more than one type of descriptor (e.g., alteration and structure) occur over the same interval, each description can be written within the same set of quotation marks provided they are separated by a space-comma-space (see interbed at 44′ in Figure A-2). Fractures are common in these cores, and both type of fracture fill (such as calcite or silt) and the angle of fracture (measured from horizontal; 0-30 degrees is low angle, 30-60 degrees, moderate angle, and 60 or greater is high angle) are recorded. However,

when a fracture fill (such as silt or secondary calcite) is noted on the field core log, this descriptor is used preferentially over angle of fracture.

The number of curves is defined by the curves flag, CURVES:, followed by the number of curve columns needed. Nine curves are defined in the core data text file for the RWMC well logs (Figure A-1), but only curves 1-4 and 6-8 are used. The columns not used, 5 and 9, and any places in the other columns where data is not available, must contain the value zero; the Logger^{tm} program does not read a space as a zero value (Figure A-2). The rows are numbered beginning at the initial-depth (except where the initial-depth is zero, in which case a -1 row containing only zeros must be added), and each row represents a one-foot interval as defined in the interval setting (Figures A-1, A-2).

For the RWMC Logger^{tm} logs, column 1 represents the percent of macroscopic vesicles; column 2, the maximum vesicle size in millimeters; column 3, the vesicle size range; column 4, the matrix void space; column 6 (P), the percent plagioclase; column 7 (S1), the percent olivine; and column 8 (S2), the percent oxidized minerals over the given interval of core (see Characterization and Stratigraphy of the RWMC Basalt Flows, this Appendix, for a detailed discussion of the determination of these values). The phenocryst size range (column 3) is given as actual number on the field core logs and is translated directly into Logger^{tm} at each one-foot interval. The percent vesicles, maximum vesicle size range, matrix void space, and percent plagioclase, olivine and oxidized minerals values are recorded as curves of the field core logs. To translate these curves into numbers for the Logger^{tm} program, the most representative value over each one-foot interval is used-- this value is taken as either an average or a maximum or minimum depending on the shape and trend of the curve above and below the interval. Each row in the core data file, then, represents the one-foot core interval above the equivalently numbered grid line on the field core log. The Logger^{tm} log curves regenerated from these numbers adequately mimic those recorded on the filed core log.

Histograms are used to graphically indicate the amount of core that is currently available (percent of the indicated foot, Column 9), and the percentage of core originally recovered (Column 10).

APPENDIX A.2

LOGGER[tm] LOGS

Logger[tm] Logs

The computerized logs that are the output of the previously described Logger[tm] program follow:

INEL
Idaho National Engineering Lab, Box 1625, Idaho Falls, ID. 83415

Organization EG&G.....
Well Name 76-2.....
Location
Cord. System N669352.3',E266117.8'.....
Descriptive.....
County Butte.....State Idaho.....

Drilling Supervisor
.....

Reference Elevation
for Geophysical Logs
Ref.....
Gl 5010.5'.....

Dates:
Start.....
Completion .....

Total Depth:
Driller 249'.....
Logger .....

Surveyed By.....

Geophysical Logs
...Gamma, Neutron....
..Density, Caliper...
.....

Core Log By: J.P. O'Brien.....Date: 4/89.....
Org...EG&G.....Stored.CF-649.....
.....

INDEX TO SYMBOLS

CLAY: SANDY	SAND: CLAYEY	SAND: SILTY	SILT: CLAYEY
BASALT	BENTONITE	CINDERS	CLAY
FAULT	GRAVEL	LOESS	OXIDATION
RHYOLITE	SAND	SILT	ALT.CALC.
ALT.CHLR.	ALT.IDDS.	BAS.BX.	BAS.VES.
FLT.BX.	FRAC.CALC.FL	FRAC.CLY.FL	FRAC.PYR.FL
FRAC.SLT.FL	FRAC.HI ANG	FRAC.MOD ANG	FRAC.LO ANG

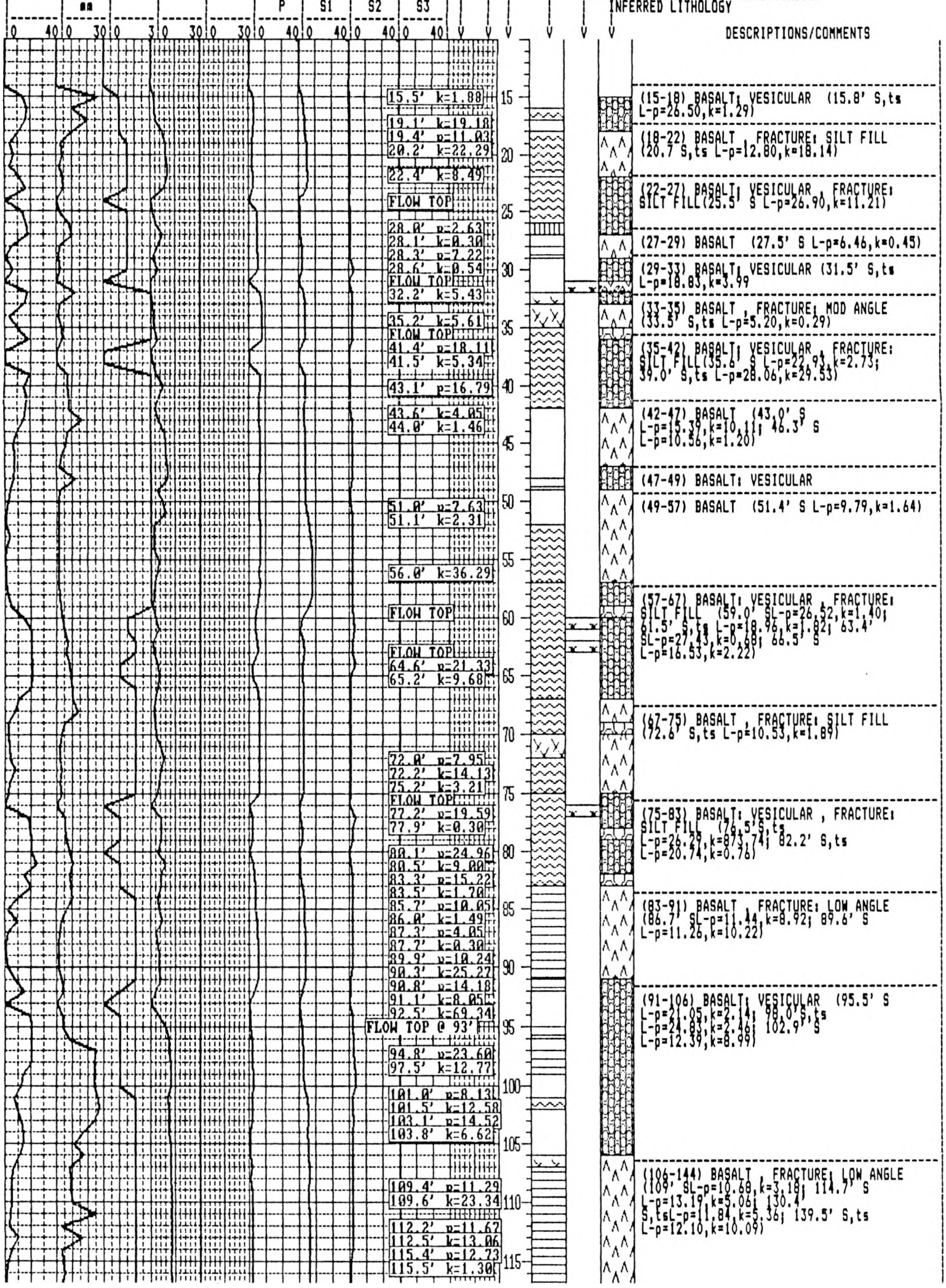

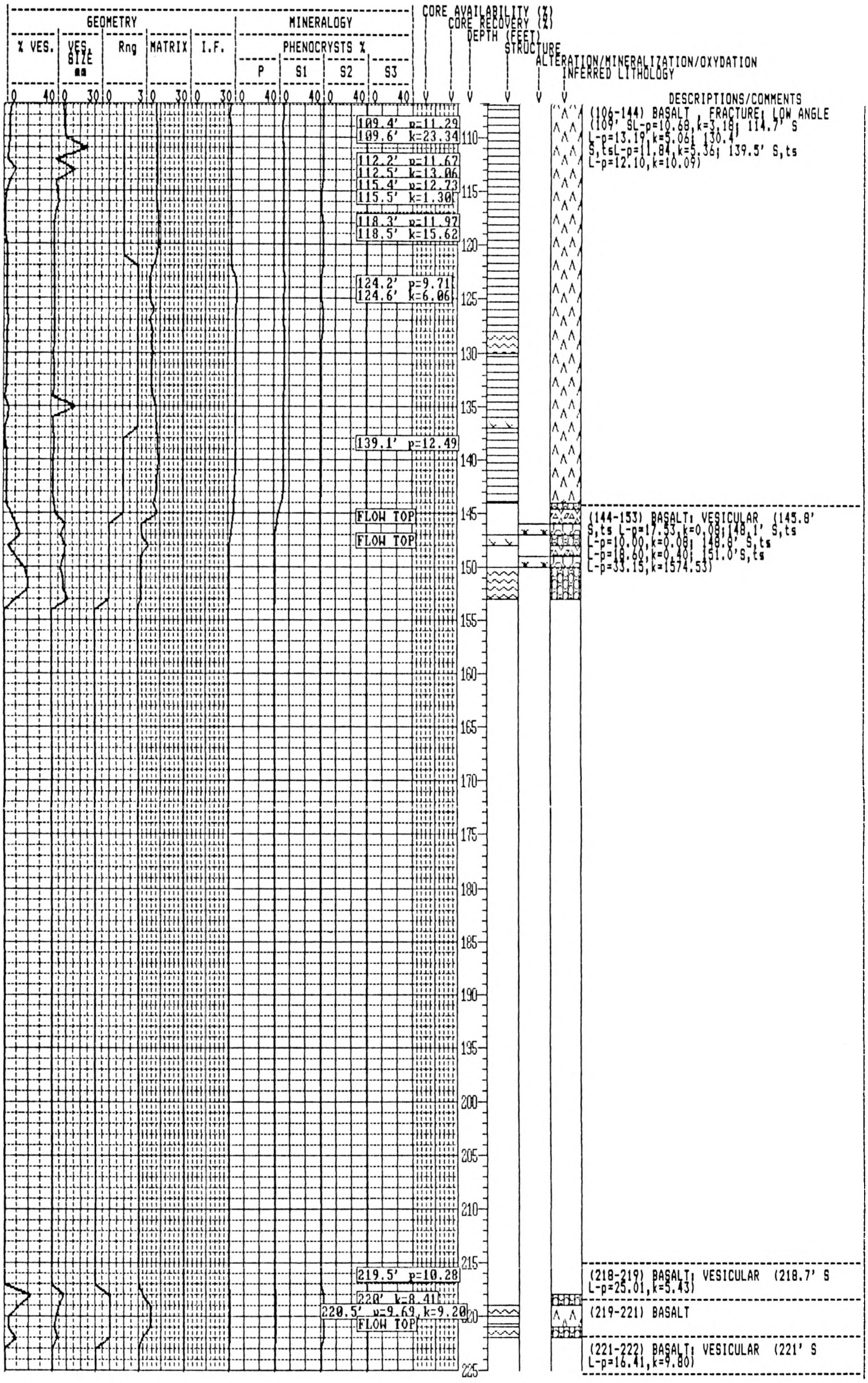

(Well 76-2, continued)

INEL
Idaho National Engineering Lab, Box 1625, Idaho Falls, ID. 83415

Organization EG&G.....
Well Name 76-3.....
Location
Cord. System N669286.4',E265160.9'.....
Descriptive.....
County Butte.....State Idaho.....

Drilling Supervisor
.....

Reference Elevation
for Geophysical Logs
Ref.....
Gl 5010'.....

Dates:
Start.....
Completion .....

Total Depth:
Driller 223'.....
Logger .....

Surveyed By.....

Geophysical Logs
..Gamma, Neutron....
..Density, Caliper...
.....

Core Log By: J.P. O'Brien.....Date: 4/89.....
Org...EG&G.....Stored.CF-649.....
.....

INDEX TO SYMBOLS

CLAY: SANDY
SAND: CLAYEY
SAND: SILTY
SILT: CLAYEY
BASALT
BENTONITE
CINDERS
CLAY
FAULT
GRAVEL
LOESS
OXIDATION
RHYOLITE
SAND
SILT
ALT.CALC.
ALT.CHLR.
ALT.IDDS.
BAS.BX.
BAS.VES.
FLT.BX.
FRAC.CALC.FL
FRAC.CLY.FL
FRAC.PYR.FL
FRAC.SLT.FL
FRAC.HI ANG
FRAC.MOD ANG
FRAC.LO ANG

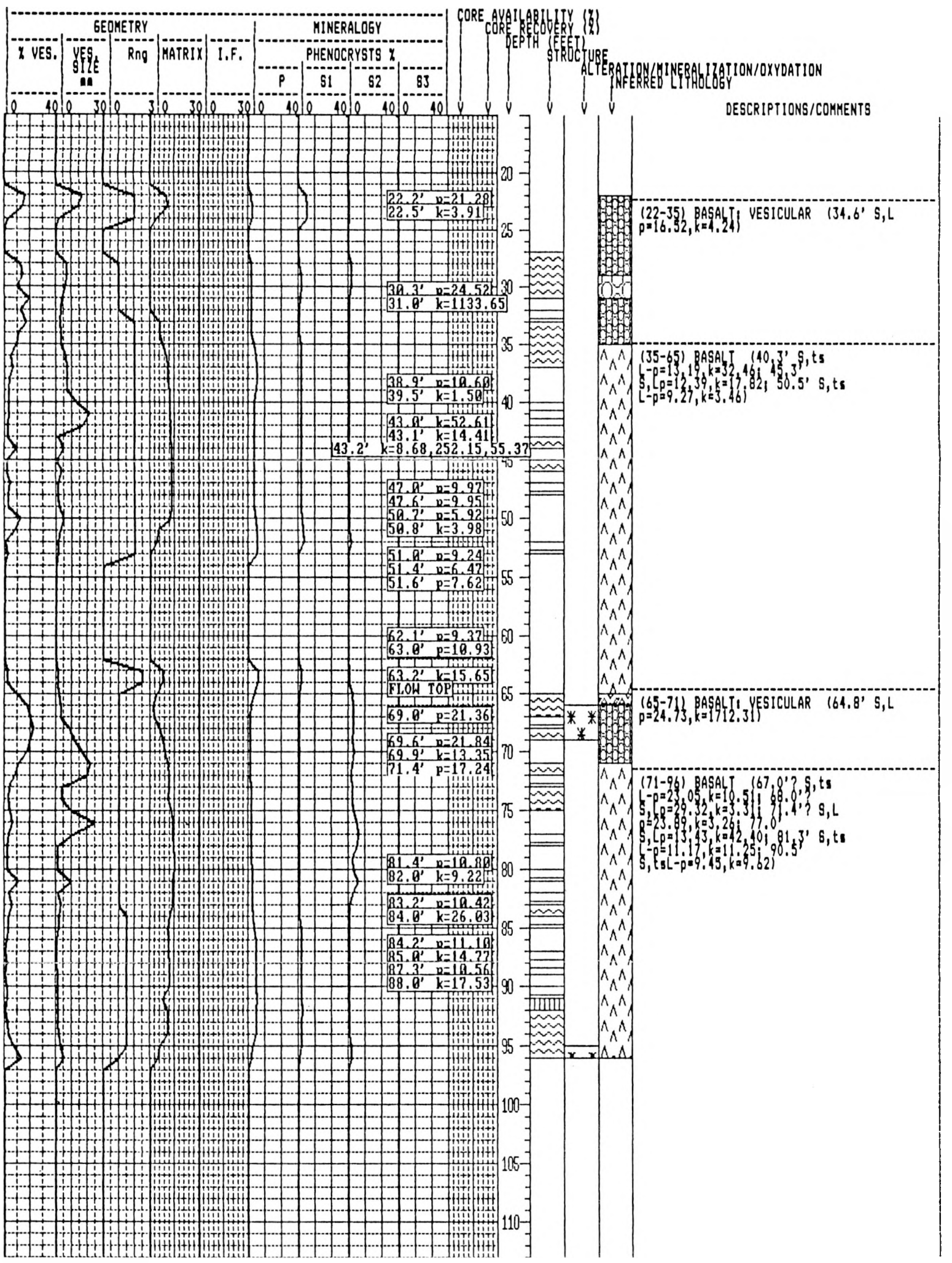

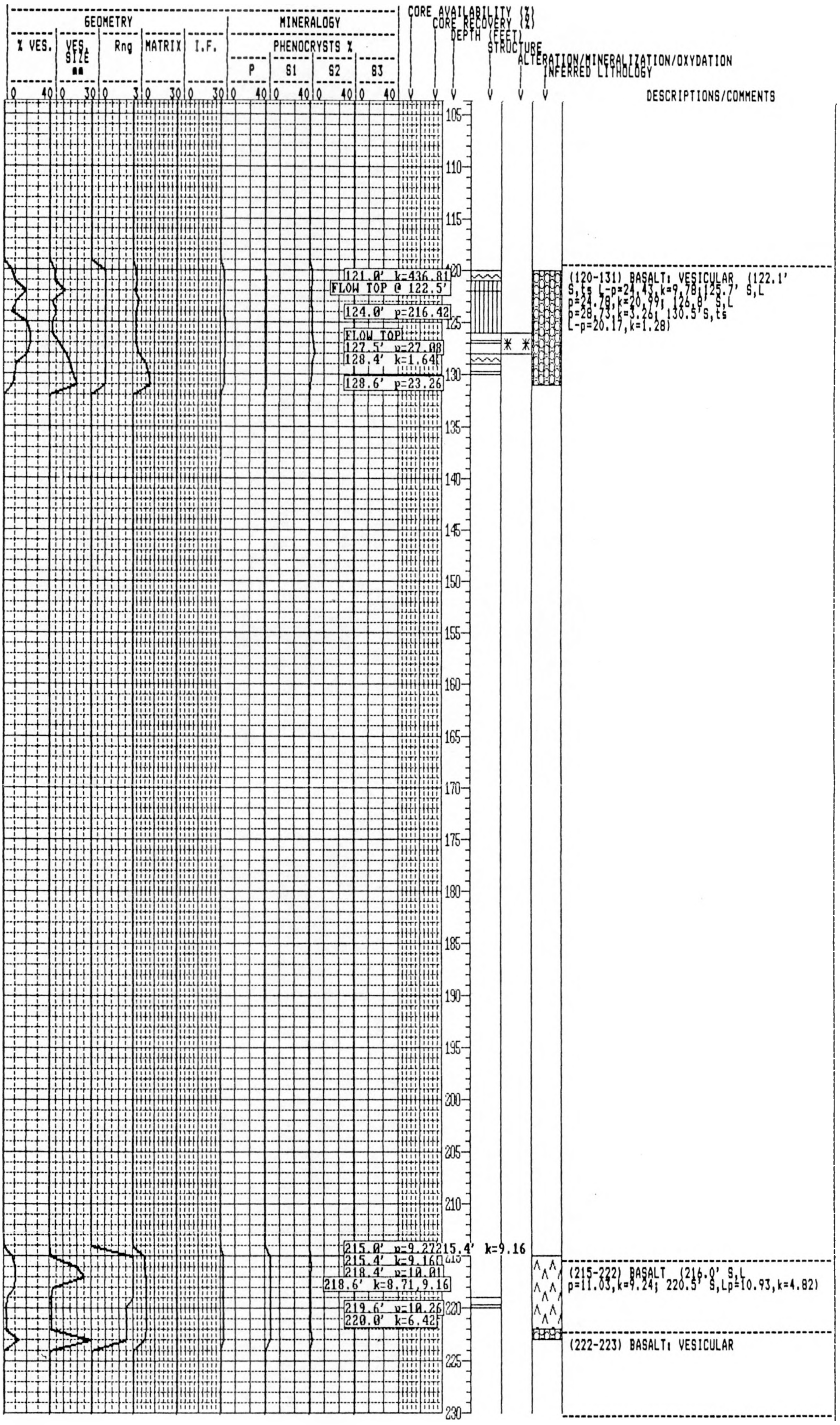

(Well 76-3, continued)

INEL
Idaho National Engineering Lab, Box 1625, Idaho Falls, ID. 83415

Organization EG&G.....
Well Name 76-4.....
Location
Cord. System N668889.3',E266520.2'.....
Descriptive.....
County Butte.....State Idaho.....

Drilling Supervisor
.....

Reference Elevation
for Geophysical Logs
Ref.....
GL 5010.6'.....

Dates:
Start.....
Completion .....

Total Depth:
Driller 114.4'.....
Logger .....

Surveyed By.....

Geophysical Logs
..Gamma, Neutron....
..Density, Caliper...
.....

Core Log By: J.P. O'Brien.....Date: 4/89.....
Org...EG&G.....Stored.CF-649.....
.....

INDEX TO SYMBOLS

CLAY; SANDY	SAND; CLAYEY	SAND; SILTY	SILT; CLAYEY
BASALT	BENTONITE	CINDERS	CLAY
FAULT	GRAVEL	LOESS	OXIDATION
RHYOLITE	SAND	SILT	ALT.CALC.
ALT.CHLR.	ALT.IDDS.	BAS.BX.	BAS.VES.
FLT.BX.	FRAC.CALC.FL	FRAC.CLY.FL	FRAC.PYR.FL
FRAC.SLT.FL	FRAC.HI ANG	FRAC.MOD ANG	FRAC.LO ANG

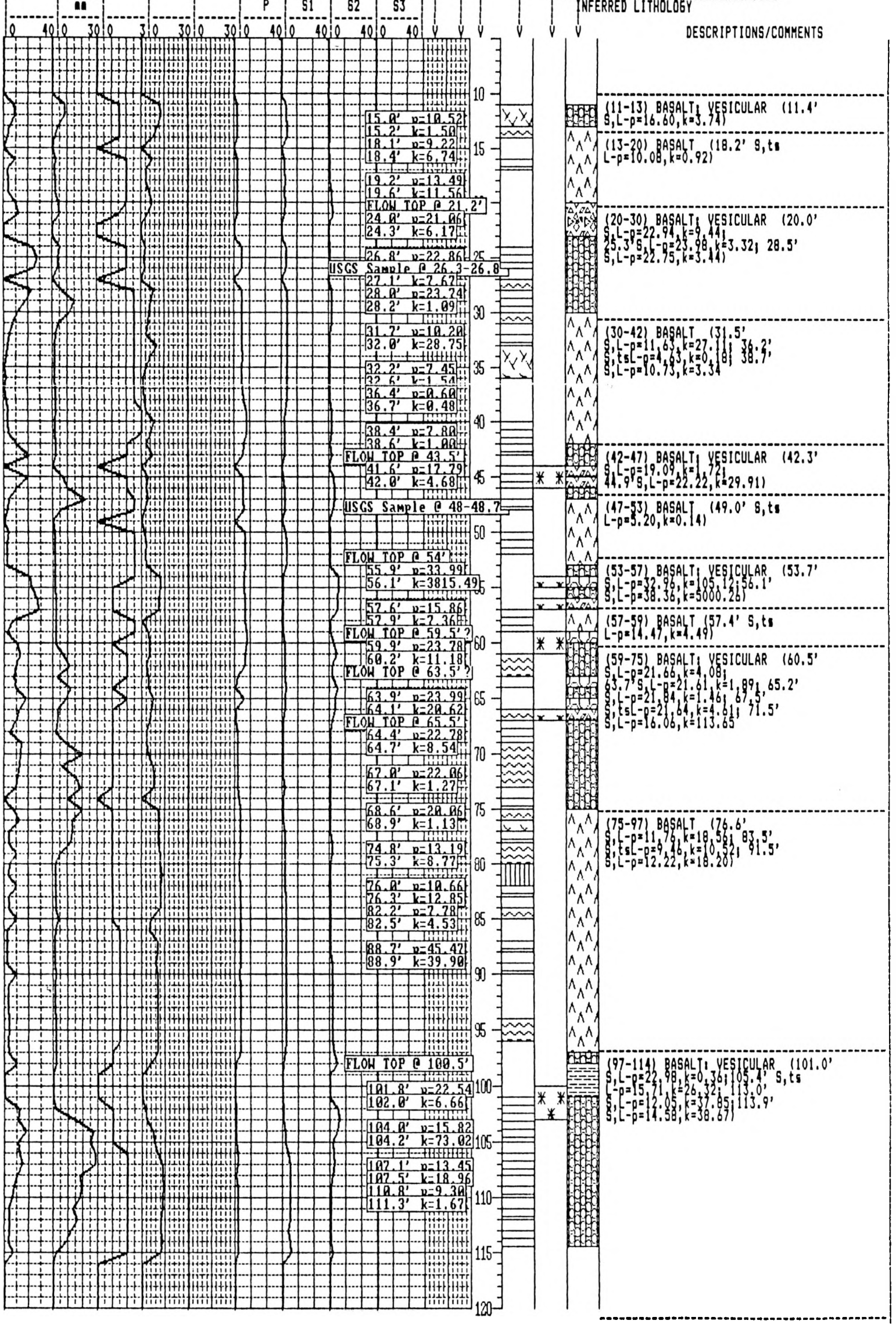

INEL
Idaho National Engineering Lab, Box 1625, Idaho Falls, ID. 83415

Organization EG&G.....
Well Name 76-4A.....
Location
Cord. System N668896.1',E266495.1'.....
Descriptive.....
County Butte.....State Idaho.....

Drilling Supervisor
.....

Reference Elevation
for Geophysical Logs
Ref.....
GL 5010.9'.....

Dates:
Start.....
Completion .....

Total Depth:
Driller 241'.....
Logger .....

Surveyed By.....

Geophysical Logs
..Gamma, Neutron....
..Density, Caliper...
.....

Core Log By: J.P. O'Brien.....Date: 4/89.....
Org...EG&G.....Stored.CF-649.....
.....

INDEX TO SYMBOLS

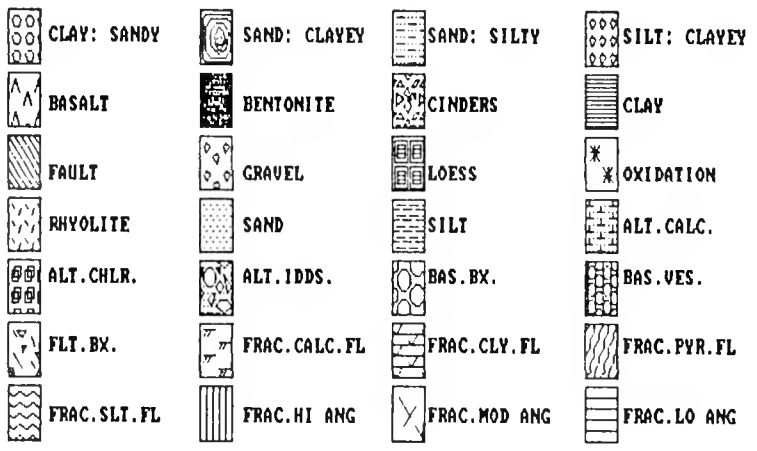

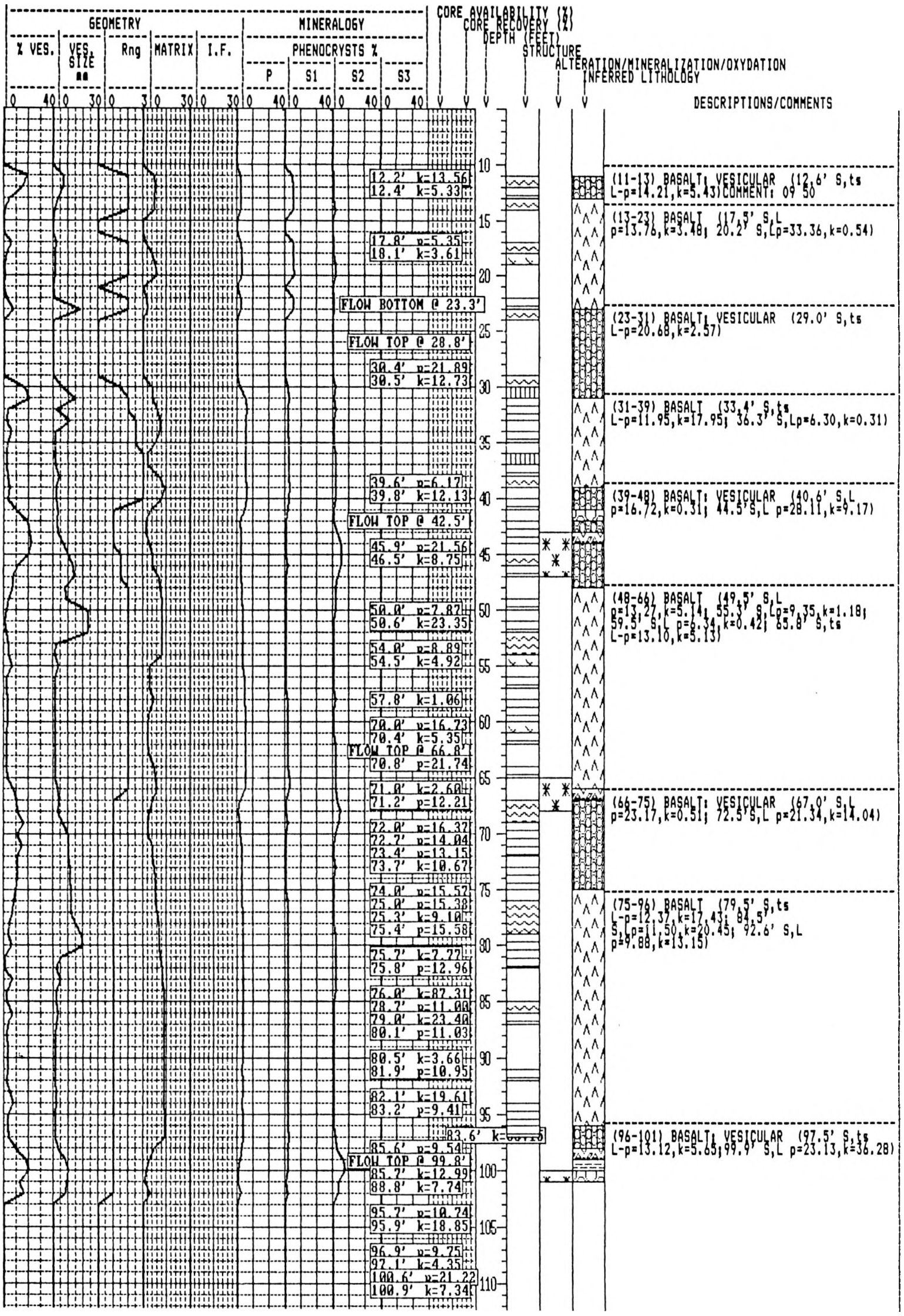

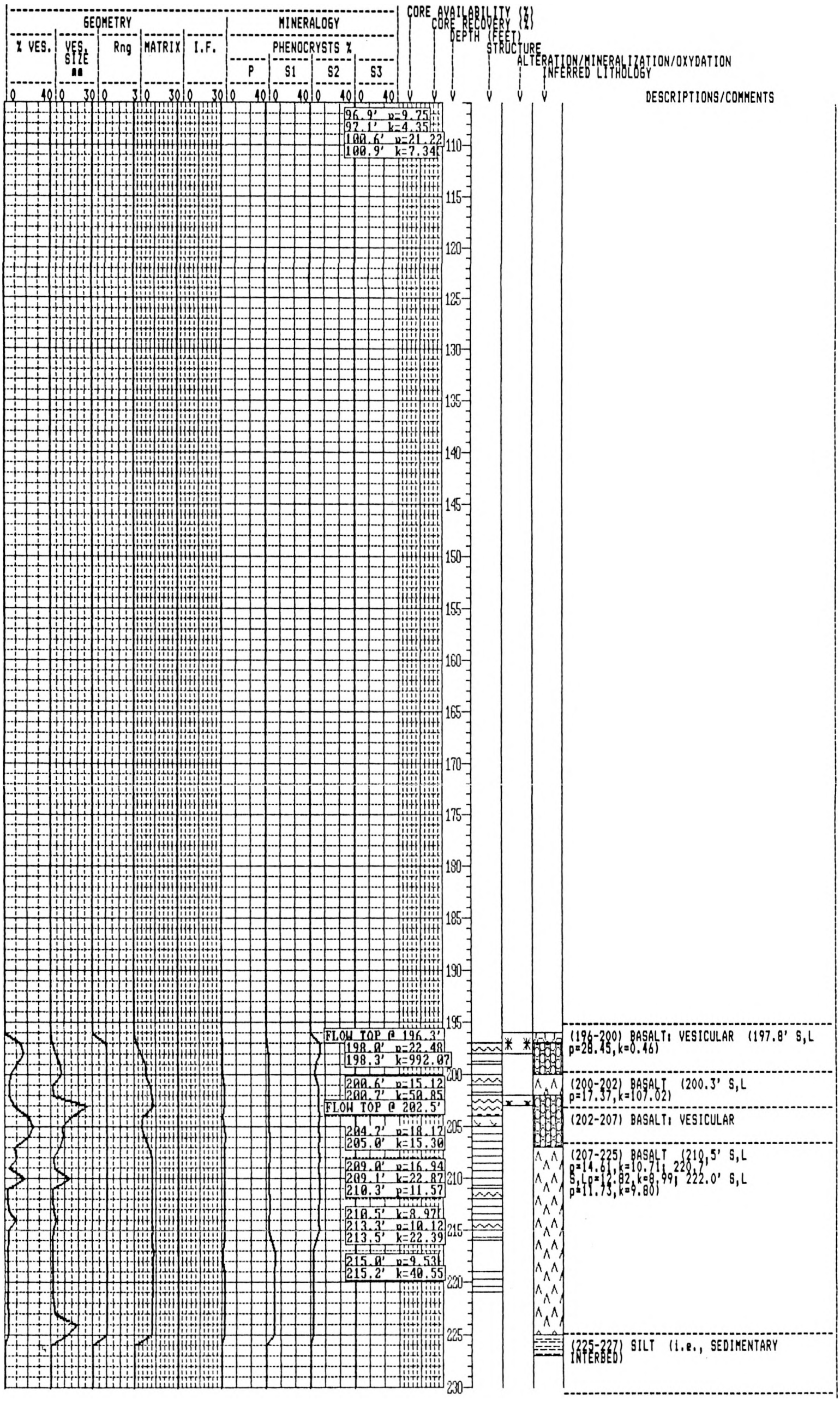

(Well 76-4A, continued)

INEL
Idaho National Engineering Lab, Box 1625, Idaho Falls, ID. 83415

Organization EG&G.....
Well Name 76-6.....
Location
Cord. System N668734',E268425.5'.....
Descriptive.....
County Butte.....State Idaho.....

Drilling Supervisor
.....

Reference Elevation
for Geophysical Logs
Ref.....
Gl 5011.2'.....

Dates:
Start.....
Completion .....

Total Depth:
Driller 240'.....
Logger .....

Surveyed By.....

Geophysical Logs
..Gamma, Neutron....
..Density, Caliper...
.....

Core Log By: J.P. O'Brien.....Date: 6/89.....
Org...EG&G.....Stored.CF-649.....
.....

INDEX TO SYMBOLS

CLAY: SANDY
SAND: CLAYEY
SAND: SILTY
SILT: CLAYEY
BASALT
BENTONITE
CINDERS
CLAY
FAULT
GRAVEL
LOESS
OXIDATION
RHYOLITE
SAND
SILT
ALT.CALC.
ALT.CHLR.
ALT.IDDS.
BAS.BX.
BAS.VES.
FLT.BX.
FRAC.CALC.FL
FRAC.CLY.FL
FRAC.PYR.FL
FRAC.SLT.FL
FRAC.HI ANG
FRAC.MOD ANG
FRAC.LO ANG

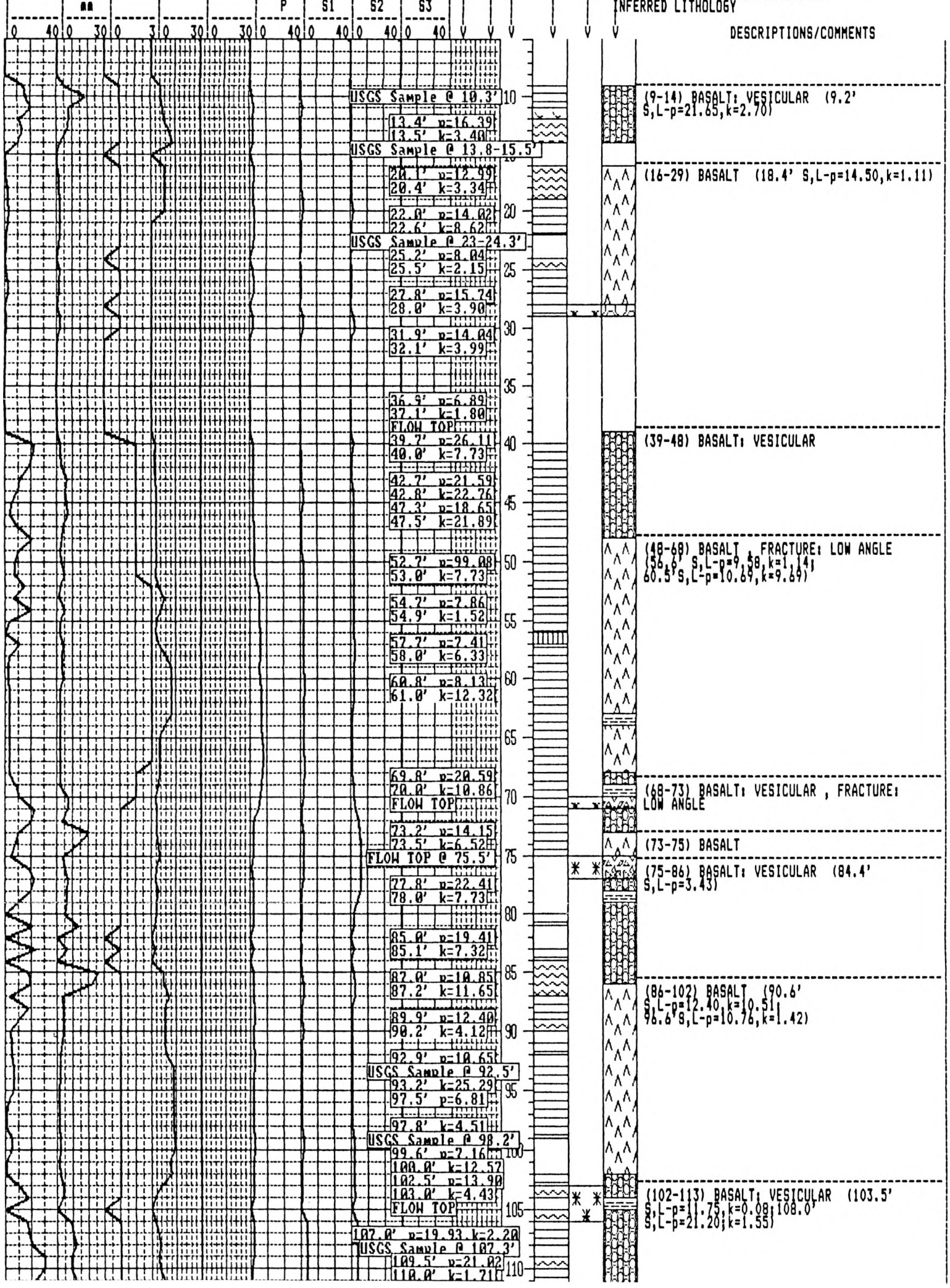

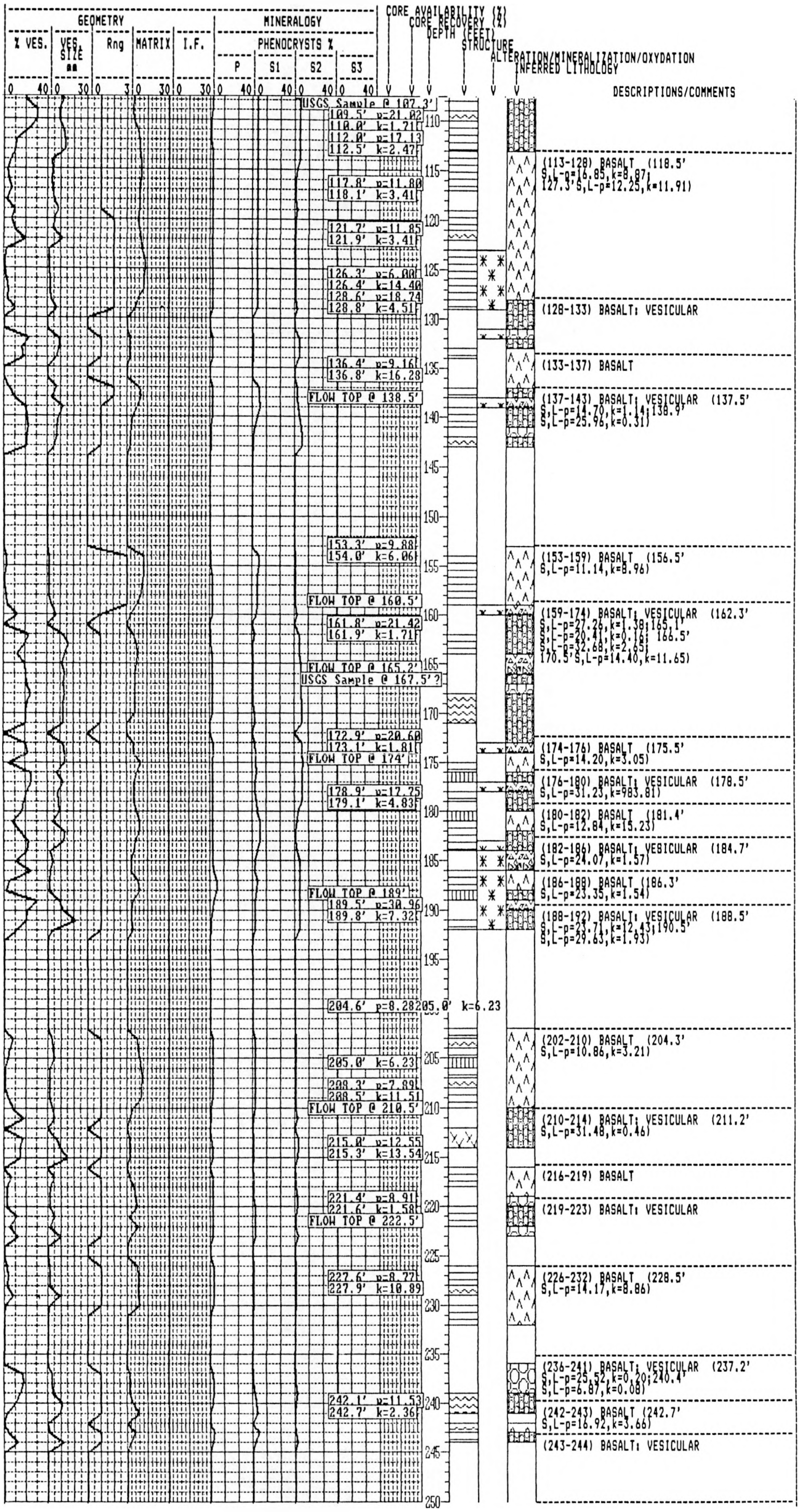

(Well 76-6, continued)

INEL
Idaho National Engineering Lab, Box 1625, Idaho Falls, ID. 83415

Organization EG&G.....
Well Name 77-2.....
Location
Cord. System N669579.4',E265632.6'.....
Descriptive.....
County Butte.....State Idaho.....

Drilling Supervisor
.....

Reference Elevation
for Geophysical Logs
Ref.....
Gl 5014.4'.....

Dates:
Start.....
Completion .....

Total Depth:
Driller 203'.....
Logger 50'.....

Surveyed By.....

Geophysical Logs
..... Neutron.....
.....
.....

Core Log By: J.P. O'Brien.....Date: 5/89.....
Org...EG&G.....Stored.CF-649.....
.....

INDEX TO SYMBOLS

CLAY: SANDY	SAND: CLAYEY	SAND: SILTY	SILT: CLAYEY
BASALT	BENTONITE	CINDERS	CLAY
FAULT	GRAVEL	LOESS	OXIDATION
RHYOLITE	SAND	SILT	ALT.CALC.
ALT.CHLR.	ALT.IDDS.	BAS.BX.	BAS.VES.
FLT.BX.	FRAC.CALC.FL	FRAC.CLY.FL	FRAC.PYR.FL
FRAC.SLT.FL	FRAC.HI ANG	FRAC.MOD ANG	FRAC.LO ANG

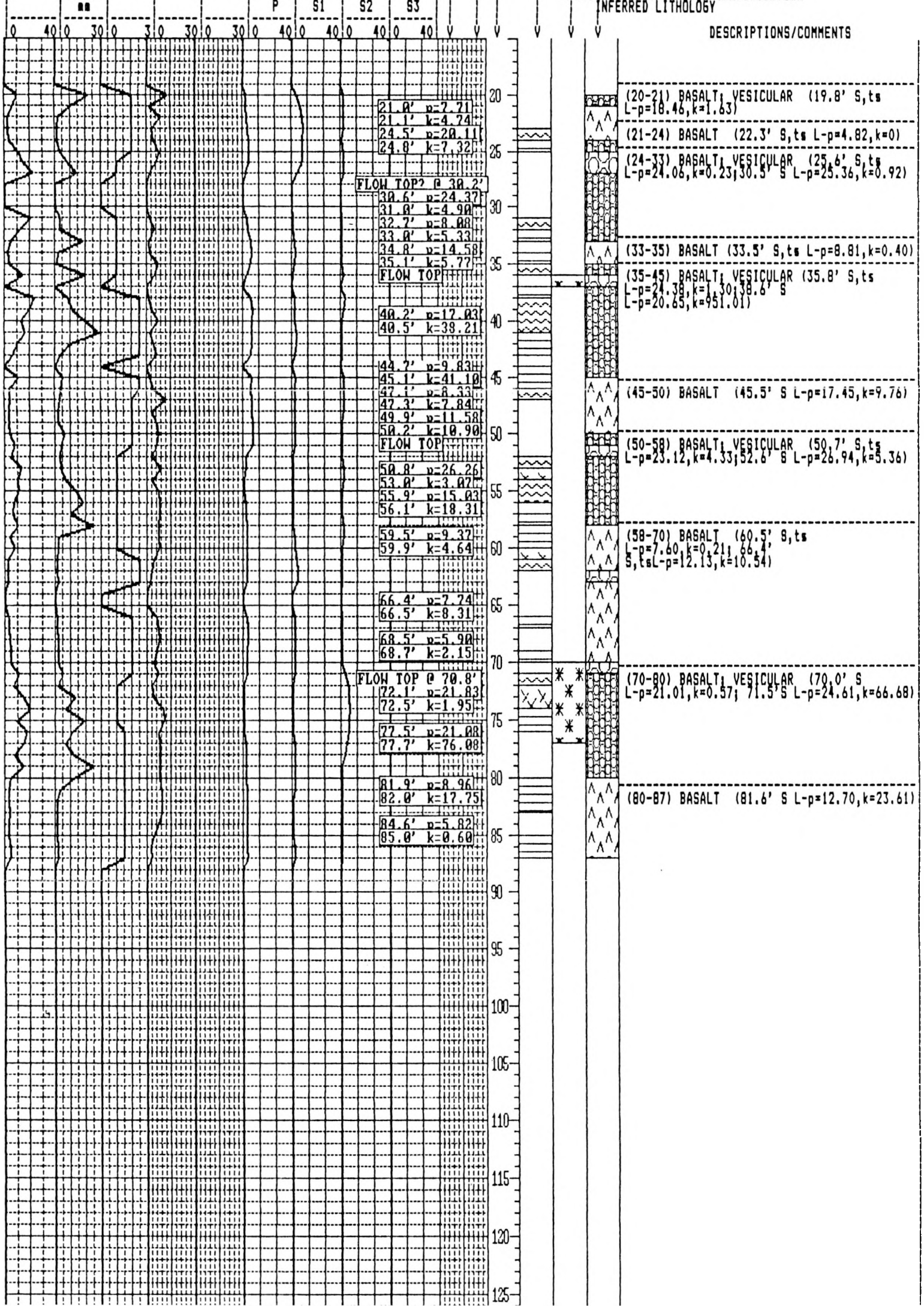

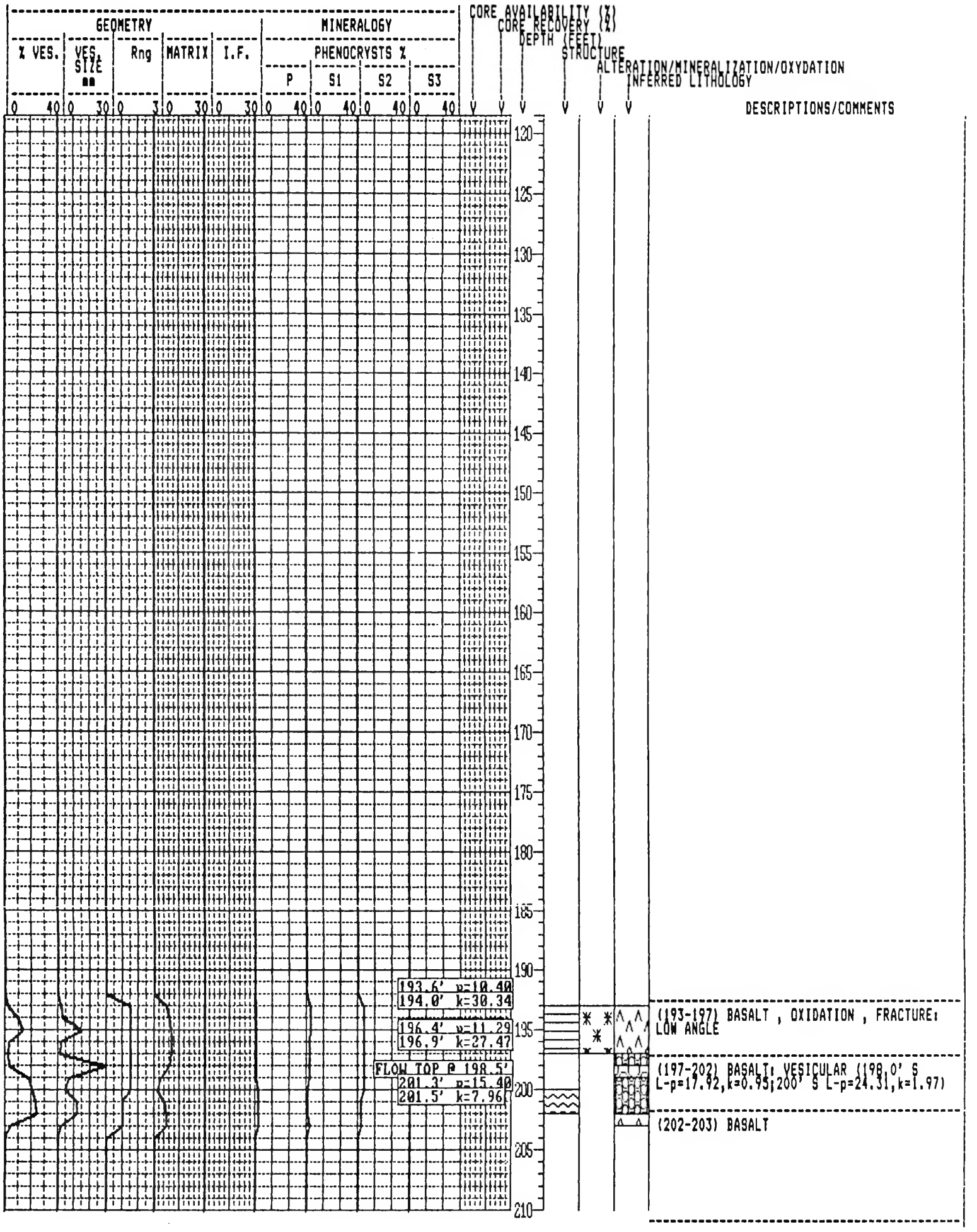

(Well 77-2, continued)

INEL
Idaho National Engineering Lab, Box 1625, Idaho Falls, ID. 83415

Organization EG&G.....
Well Name 78-1.....
Location
Cord. System N669032.9',E267306'.....
Descriptive.....
County Butte.....State Idaho.....

Drilling Supervisor
.....

Reference Elevation
for Geophysical Logs
Ref.....
G1 5010'.....

Dates:
Start.....
Completion .....

Total Depth:
Driller 82'.....
Logger .....

Surveyed By.....

Geophysical Logs
.....Gamma.....
.....
.....

Core Log By: R.L. Smith.....Date: 6/88.....
Org...EG&G.....Stored.CF-649.....
.....

INDEX TO SYMBOLS

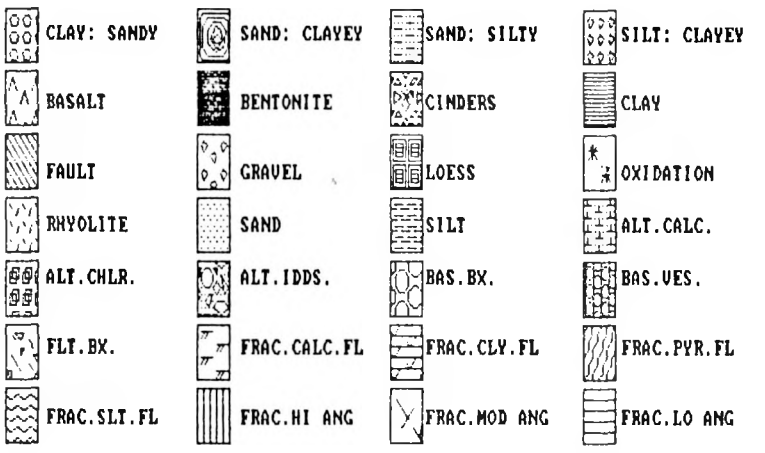

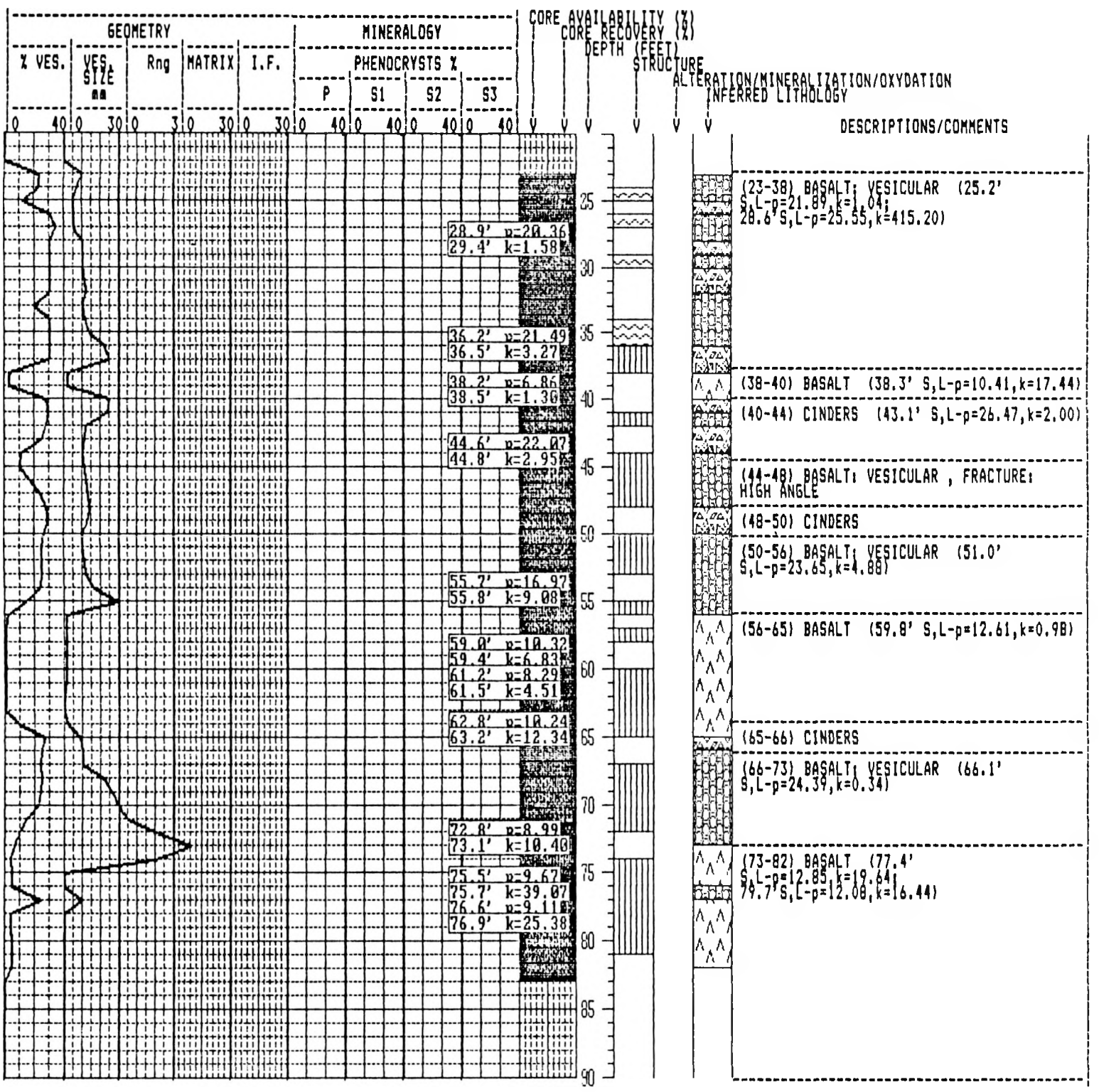

INEL
Idaho National Engineering Lab, Box 1625, Idaho Falls, ID. 83415

Organization EG&G.....
Well Name 78-2.....
Location
Cord. System N669781.7',E268098.9'.....
Descriptive.....
County Butte.....State Idaho.....

Drilling Supervisor
.....

Reference Elevation
for Geophysical Logs
Ref.....
Gl 5007'.....

Dates:
Start.....
Completion .....

Total Depth:
Driller 234'.....
Logger .....

Surveyed By.....

Geophysical Logs
..Gamma, Neutron....
..Density, Caliper...
.....

Core Log By: J.P. O'Brien.....Date: 3/89.....
Org...EG&G.....Stored.CF-649.....
.....

INDEX TO SYMBOLS

CLAY: SANDY	SAND: CLAYEY	SAND: SILTY	SILT: CLAYEY
BASALT	BENTONITE	CINDERS	CLAY
FAULT	GRAVEL	LOESS	OXIDATION
RHYOLITE	SAND	SILT	ALT.CALC.
ALT.CHLR.	ALT.IDDS.	BAS.BX.	BAS.VES.
FLT.BX.	FRAC.CALC.FL	FRAC.CLY.FL	FRAC.PYR.FL
FRAC.SLT.FL	FRAC.HI ANG	FRAC.MOD ANG	FRAC.LO ANG

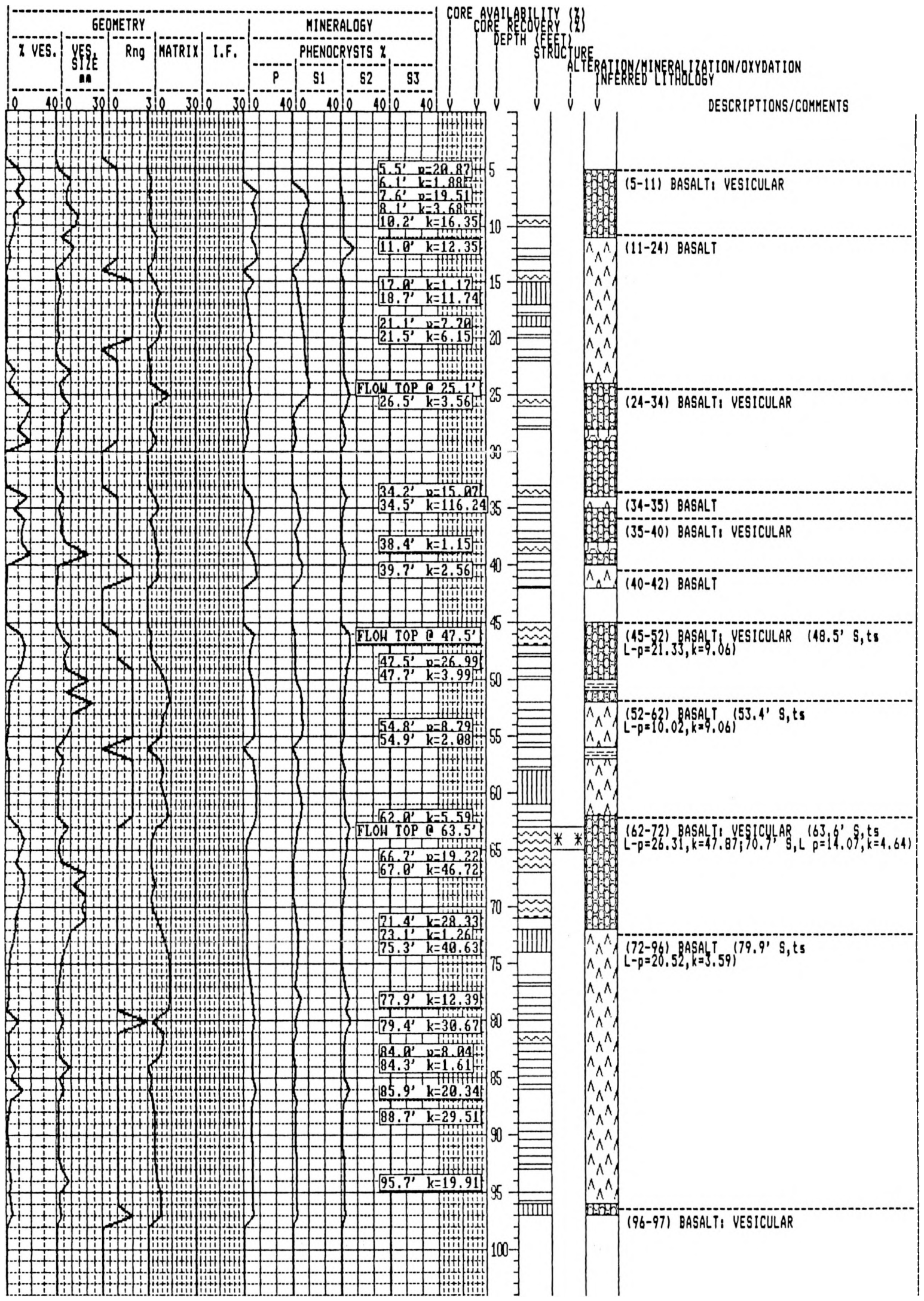

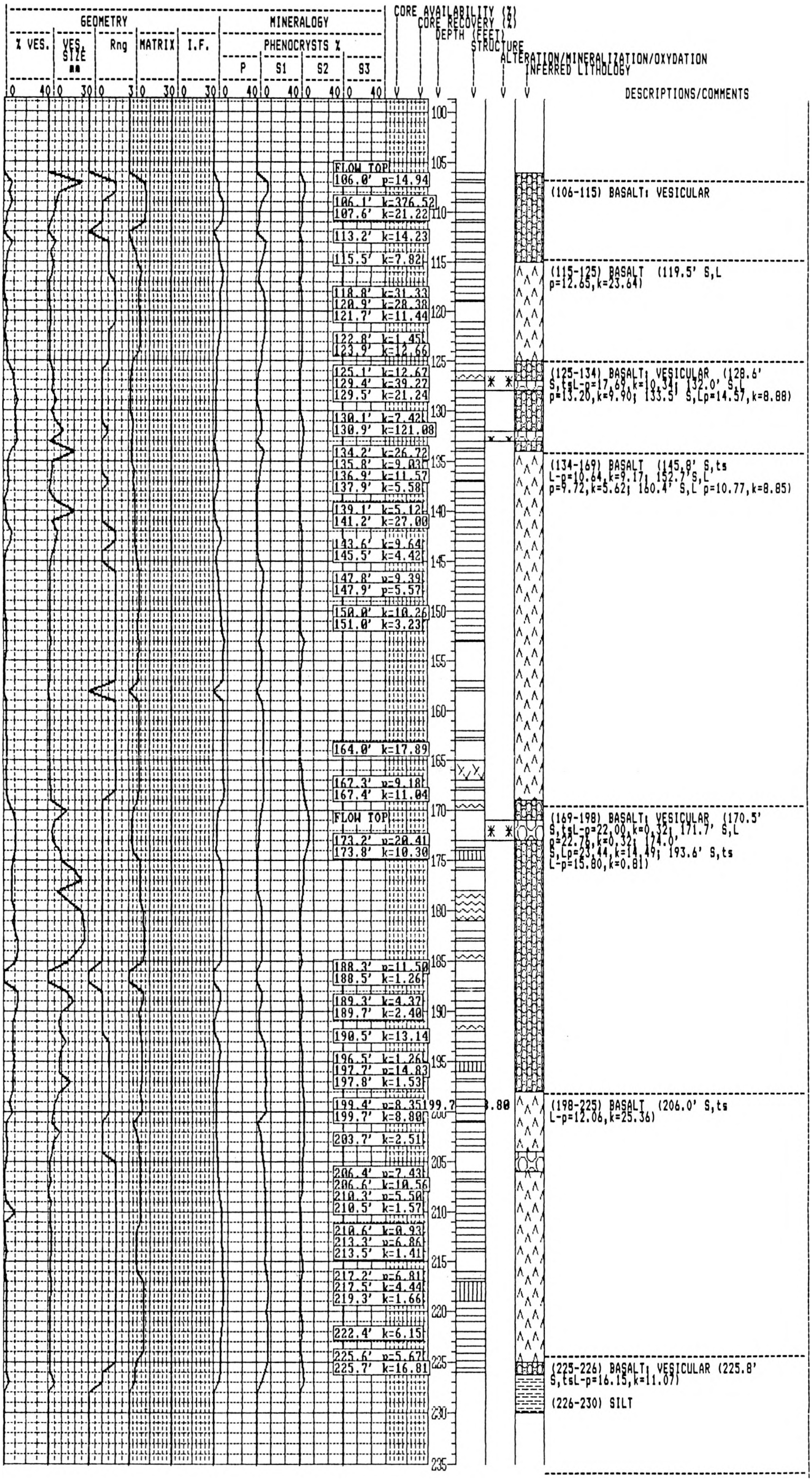

(Well 78-2, continued)

INEL
Idaho National Engineering Lab, Box 1625, Idaho Falls, ID. 83415

Organization EG&G.....
Well Name 78-3.....
Location
Cord. System N669787.6',E266151.1'.....
Descriptive.....
County Butte.....State Idaho.....

Drilling Supervisor
.....

Reference Elevation
for Geophysical Logs
Ref.....
GL 5011'.....

Dates:
Start.....
Completion .....

Total Depth:
Driller 225'.....
Logger 166'.....

Surveyed By.....

Geophysical Logs
..Gamma, Neutron....
..Density, Caliper...
.....

Core Log By: J.P. O'Brien.....Date: 3/89.....
Org...EG&G.....Stored.CF-649.....
.....

INDEX TO SYMBOLS

CLAY: SANDY	SAND: CLAYEY	SAND: SILTY	SILT: CLAYEY
BASALT	BENTONITE	CINDERS	CLAY
FAULT	GRAVEL	LOESS	OXIDATION
RHYOLITE	SAND	SILT	ALT.CALC.
ALT.CHLR.	ALT.IDDS.	BAS.BX.	BAS.VES.
FLT.BX.	FRAC.CALC.FL	FRAC.CLY.FL	FRAC.PYR.FL
FRAC.SLT.FL	FRAC.HI ANG	FRAC.MOD ANG	FRAC.LO ANG

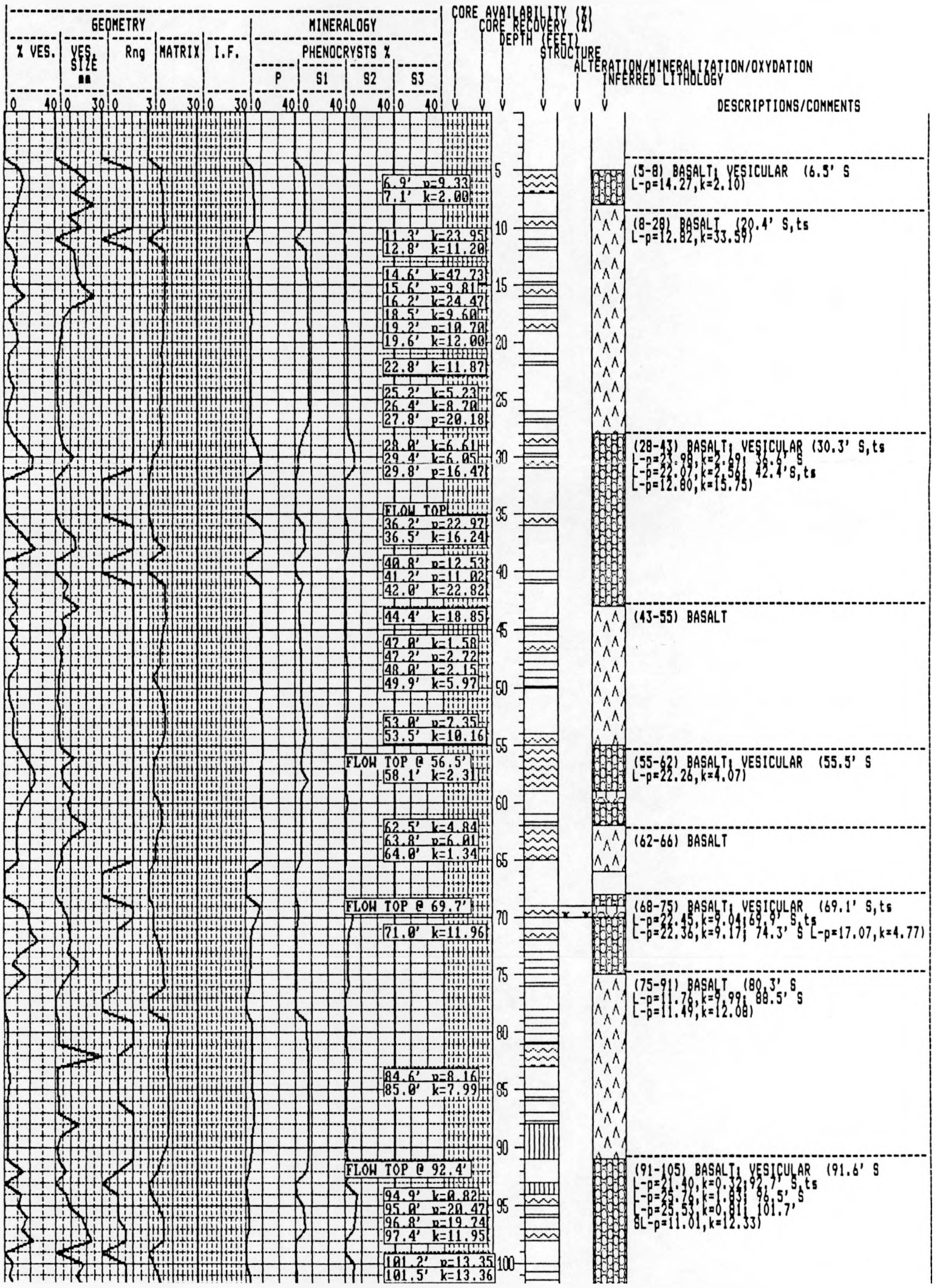

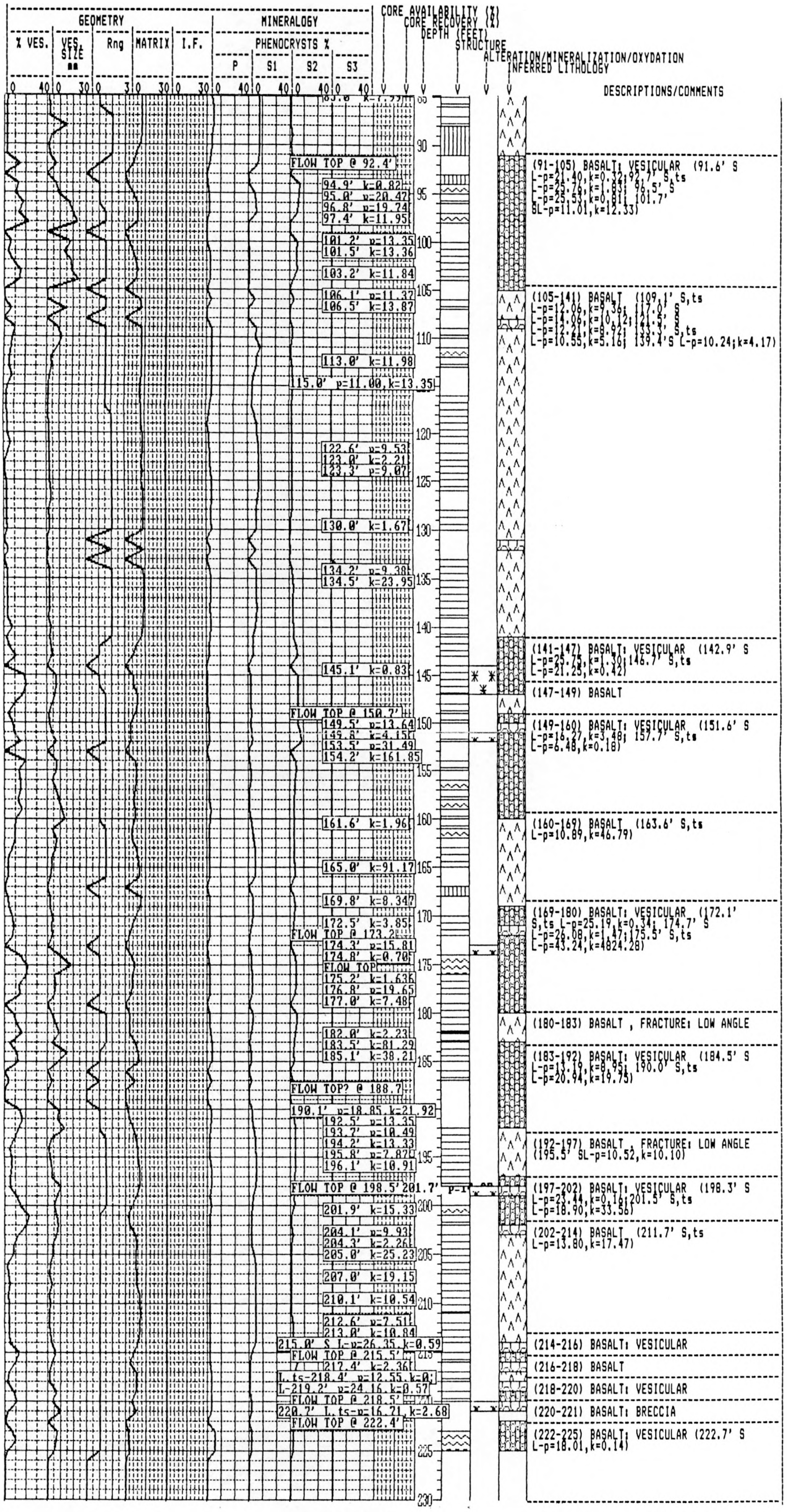

(Well 78-3, continued)

INEL
Idaho National Engineering Lab, Box 1625, Idaho Falls, ID. 83415

Organization EG&G.....
Well Name 78-5.....
Location
Cord. System N669365',E265931'.....
Descriptive.....
County Butte.....State Idaho.....

Drilling Supervisor
.....

Reference Elevation
for Geophysical Logs
Ref.....
GL 5010'.....

Dates:
Start.....
Completion .....

Total Depth:
Driller 225'.....
Logger .....

Surveyed By.....

Geophysical Logs
.....
.....
.....

Core Log By: J.P. O'Brien.....Date: 3/89.....
Org...EG&G.....Stored.CF-649.....
.....

INDEX TO SYMBOLS

CLAY: SANDY
SAND: CLAYEY
SAND: SILTY
SILT: CLAYEY
BASALT
BENTONITE
CINDERS
CLAY
FAULT
GRAVEL
LOESS
OXIDATION
RHYOLITE
SAND
SILT
ALT.CALC.
ALT.CHLR.
ALT.IDDS.
BAS.BX.
BAS.VES.
FLT.BX.
FRAC.CALC.FL
FRAC.CLY.FL
FRAC.PYR.FL
FRAC.SLT.FL
FRAC.HI ANG
FRAC.MOD ANG
FRAC.LO ANG

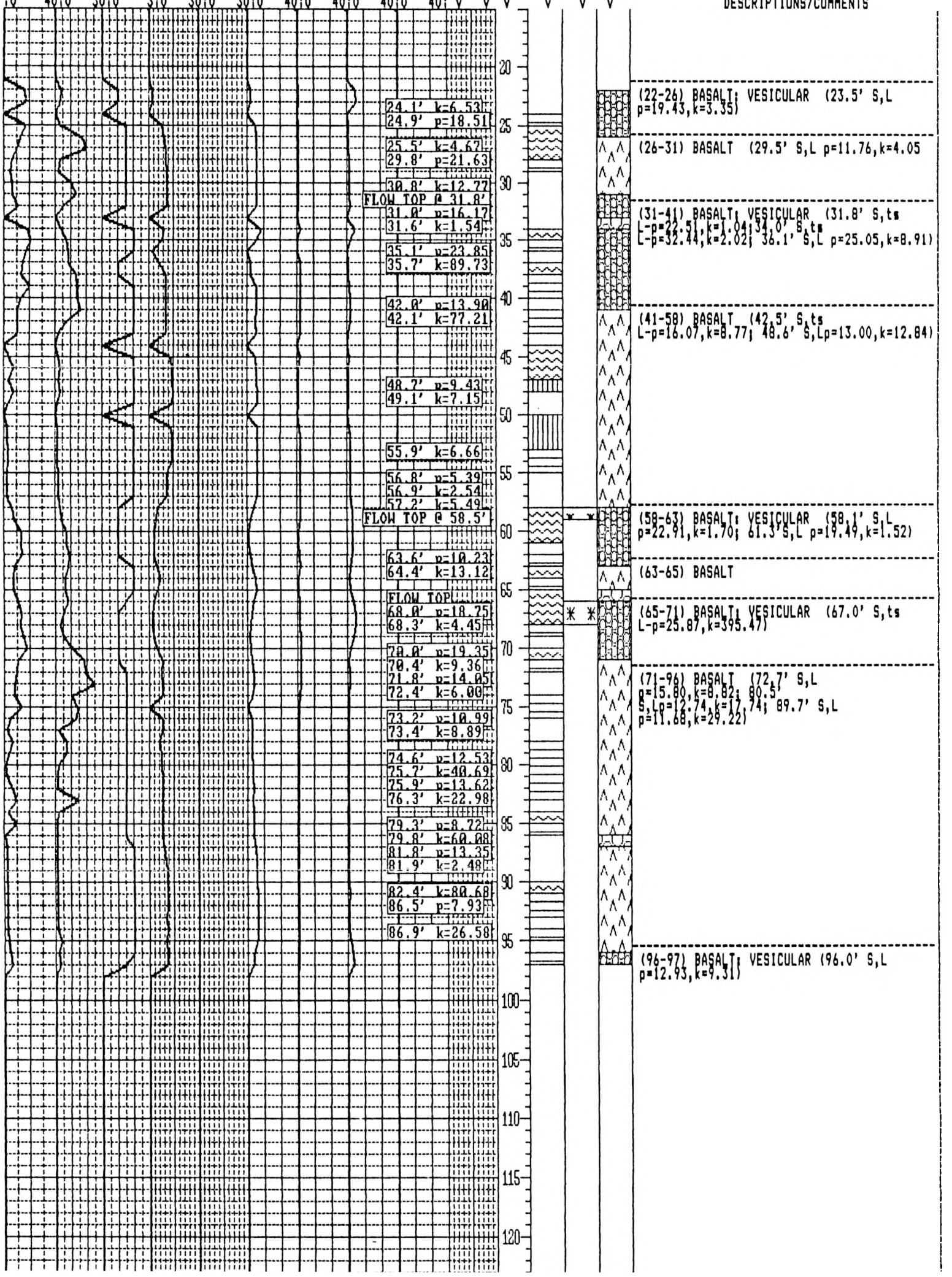

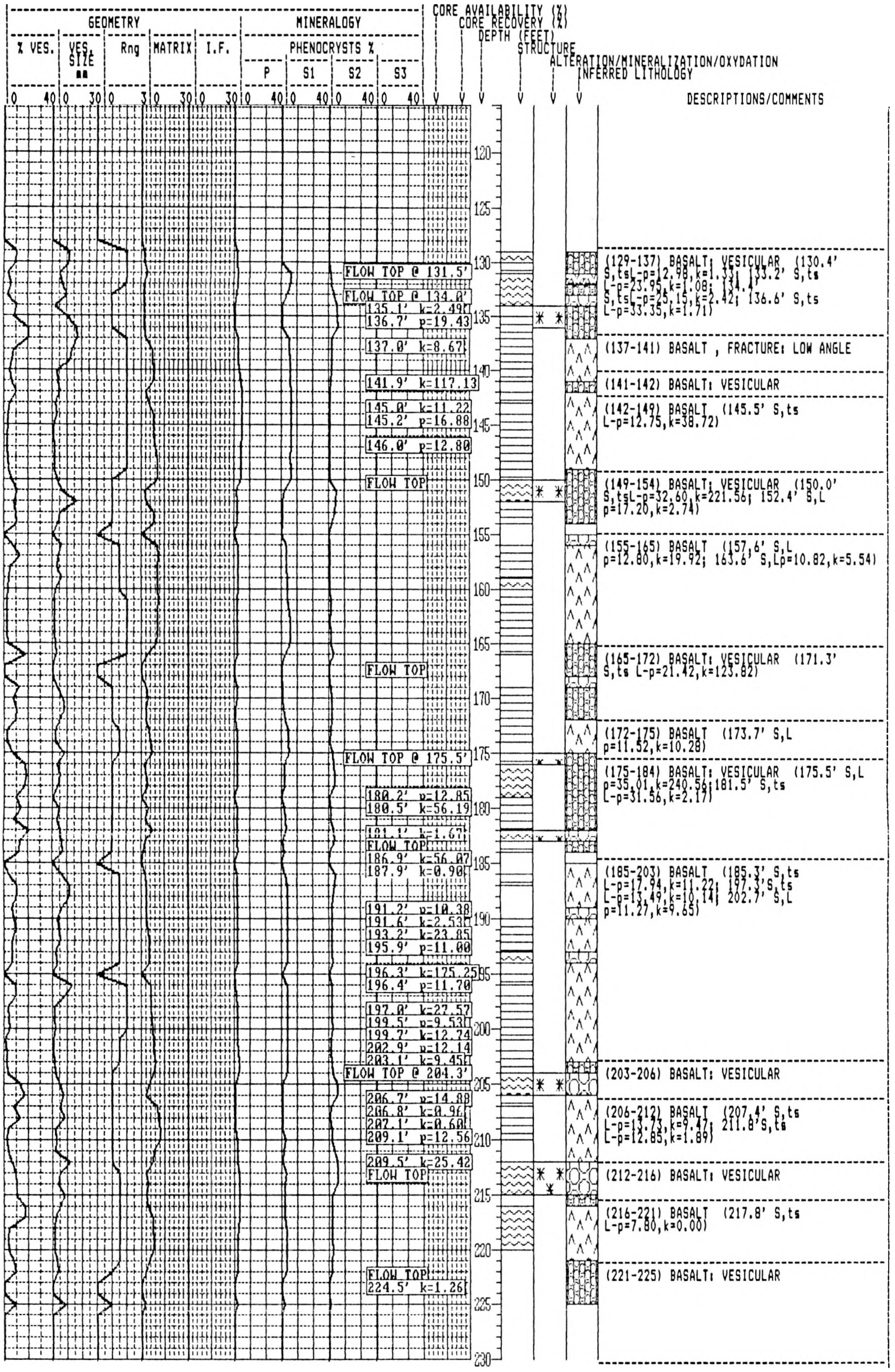

(Well 78-5, continued)

INEL
Idaho National Engineering Lab, Box 1625, Idaho Falls, ID. 83415

Organization EG&G.....
Well Name 79-1.....
Location
Cord. System N668789.4',E269768.3'.....
Descriptive.....
County Butte.....State Idaho.....

Drilling Supervisor
.....

Reference Elevation
for Geophysical Logs
Ref.....
GL 5018'.....

Dates:
Start.....
Completion .....

Total Depth:
Driller 240'.....
Logger .....

Surveyed By.....

Geophysical Logs
.....Gamma.....
.....
.....

Core Log By: J.P. O'Brien.....Date: 3/89.....
Org...EG&G.....Stored.CF-649.....
.....

INDEX TO SYMBOLS

CLAY: SANDY
SAND: CLAYEY
SAND: SILTY
SILT: CLAYEY
BASALT
BENTONITE
CINDERS
CLAY
FAULT
GRAVEL
LOESS
OXIDATION
RHYOLITE
SAND
SILT
ALT.CALC.
ALT.CHLR.
ALT.IDDS.
BAS.BX.
BAS.VES.
FLT.BX.
FRAC.CALC.FL
FRAC.CLY.FL
FRAC.PYR.FL
FRAC.SLT.FL
FRAC.HI ANG
FRAC.MOD ANG
FRAC.LO ANG

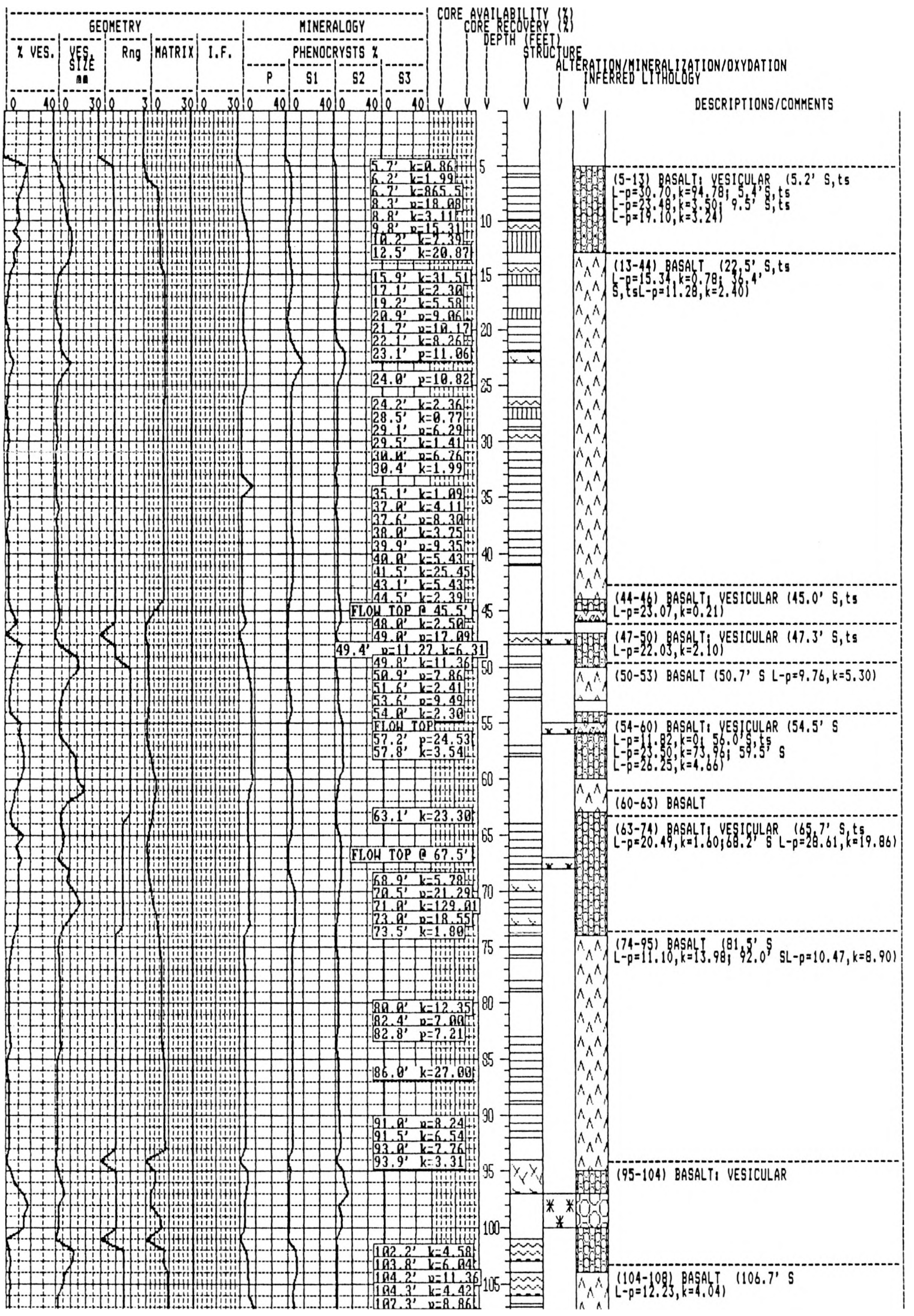

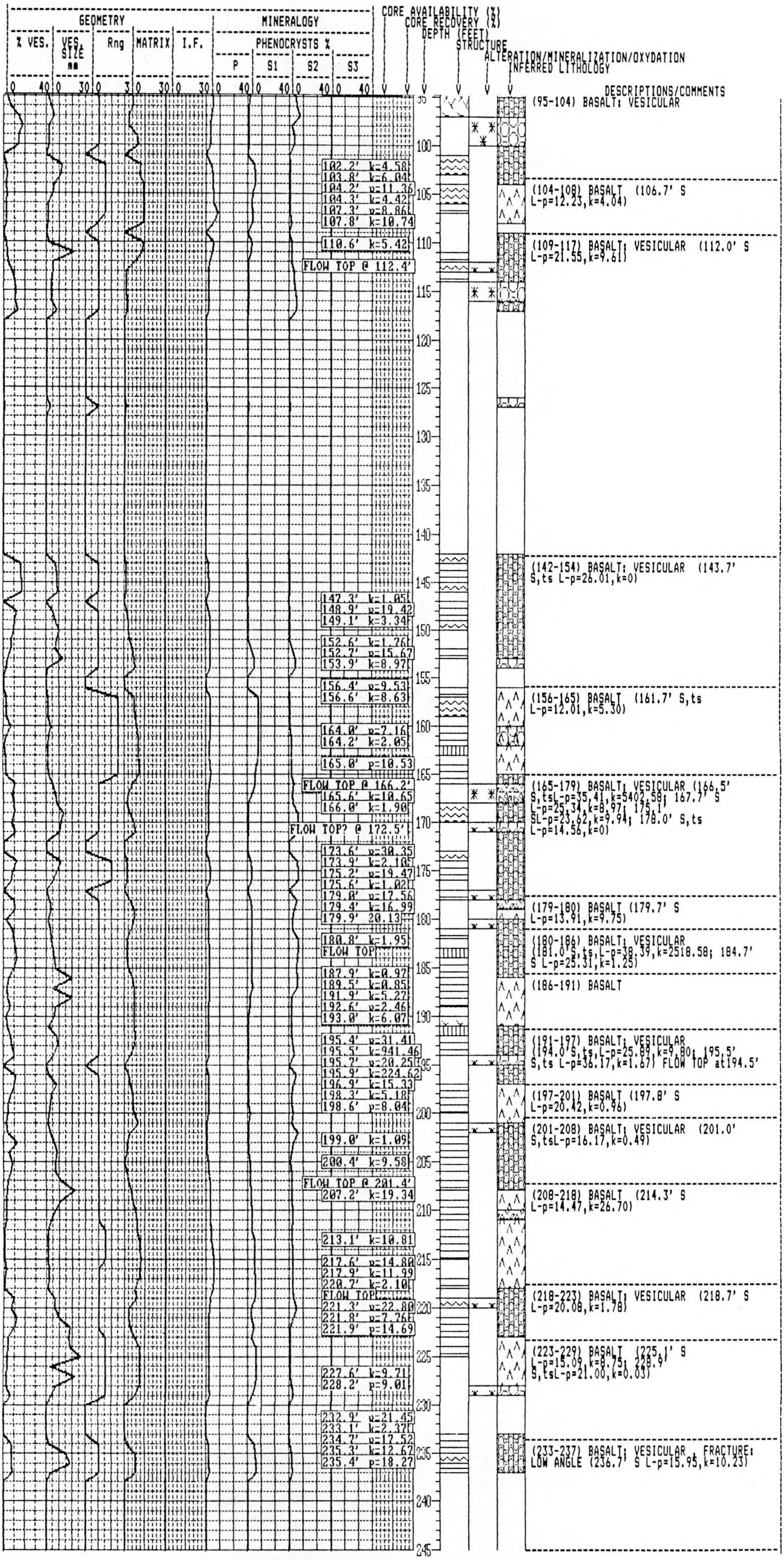

(Well 79-1 continued)

INEL
Idaho National Engineering Lab, Box 1625, Idaho Falls, ID. 83415

Organization EG&G.....
Well Name 79-2.....
Location
Cord. System N669689.5',E267160.5'.....
Descriptive.....
County Butte.....State Idaho.....

Drilling Supervisor
.....

Reference Elevation
for Geophysical Logs
Ref.....
GL 5011'.....

Dates:
Start.....
Completion .....

Total Depth:
Driller 222.9'.....
Logger .....

Surveyed By.....

Geophysical Logs
Gamma, Neutron....
Density, Caliper...
.....

Core Log By: J.P. O'Brien.....Date: 2/89.....
Org...EG&G.....Stored.CF-649.....
.....

INDEX TO SYMBOLS

CLAY: SANDY	SAND: CLAYEY	SAND: SILTY	SILT: CLAYEY
BASALT	BENTONITE	CINDERS	CLAY
FAULT	GRAVEL	LOESS	OXIDATION
RHYOLITE	SAND	SILT	ALT.CALC.
ALT.CHLR.	ALT.IDDS.	BAS.BX.	BAS.VES.
FLT.BX.	FRAC.CALC.FL	FRAC.CLY.FL	FRAC.PYR.FL
FRAC.SLT.FL	FRAC.HI ANG	FRAC.MOD ANG	FRAC.LO ANG

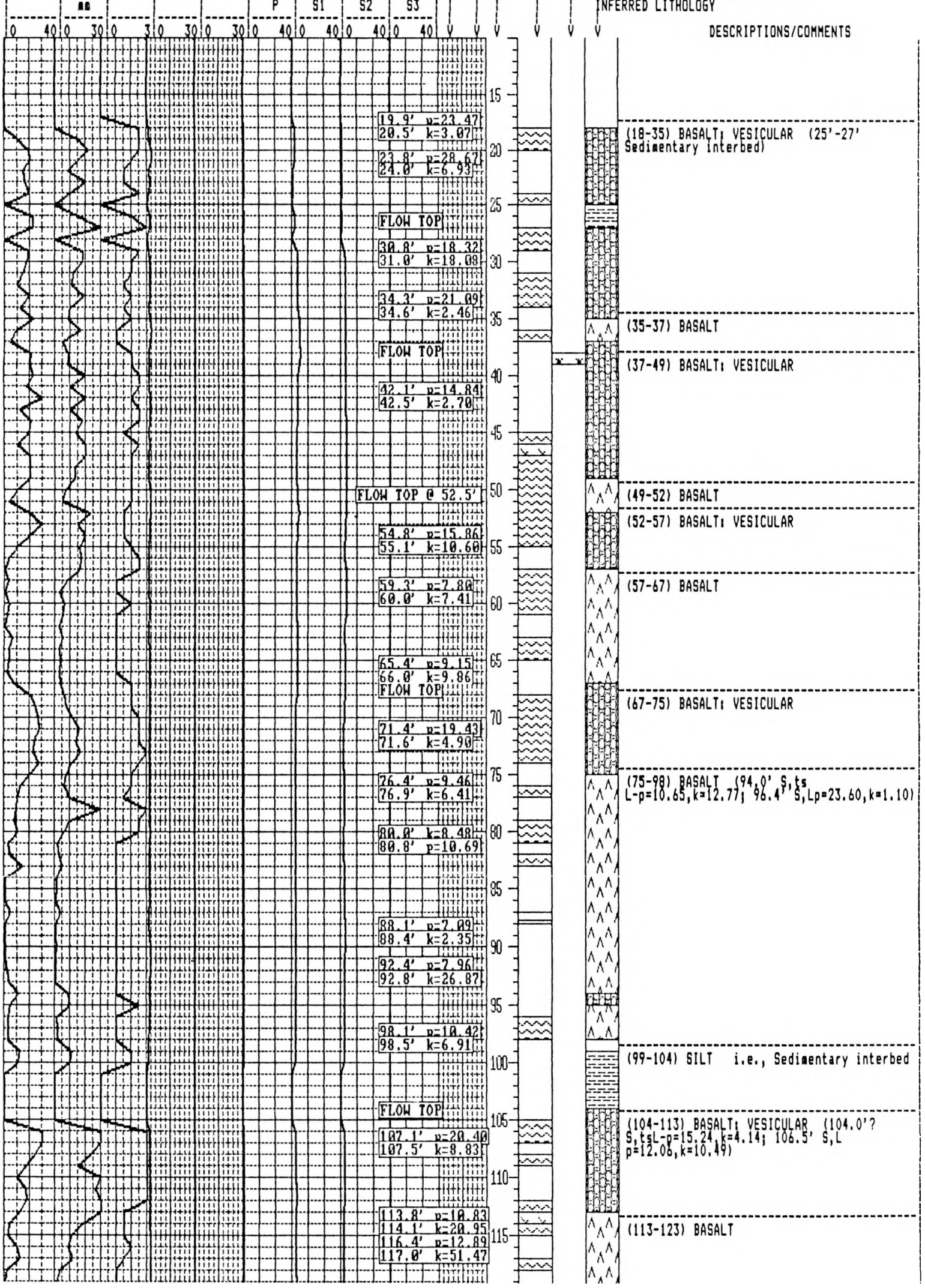

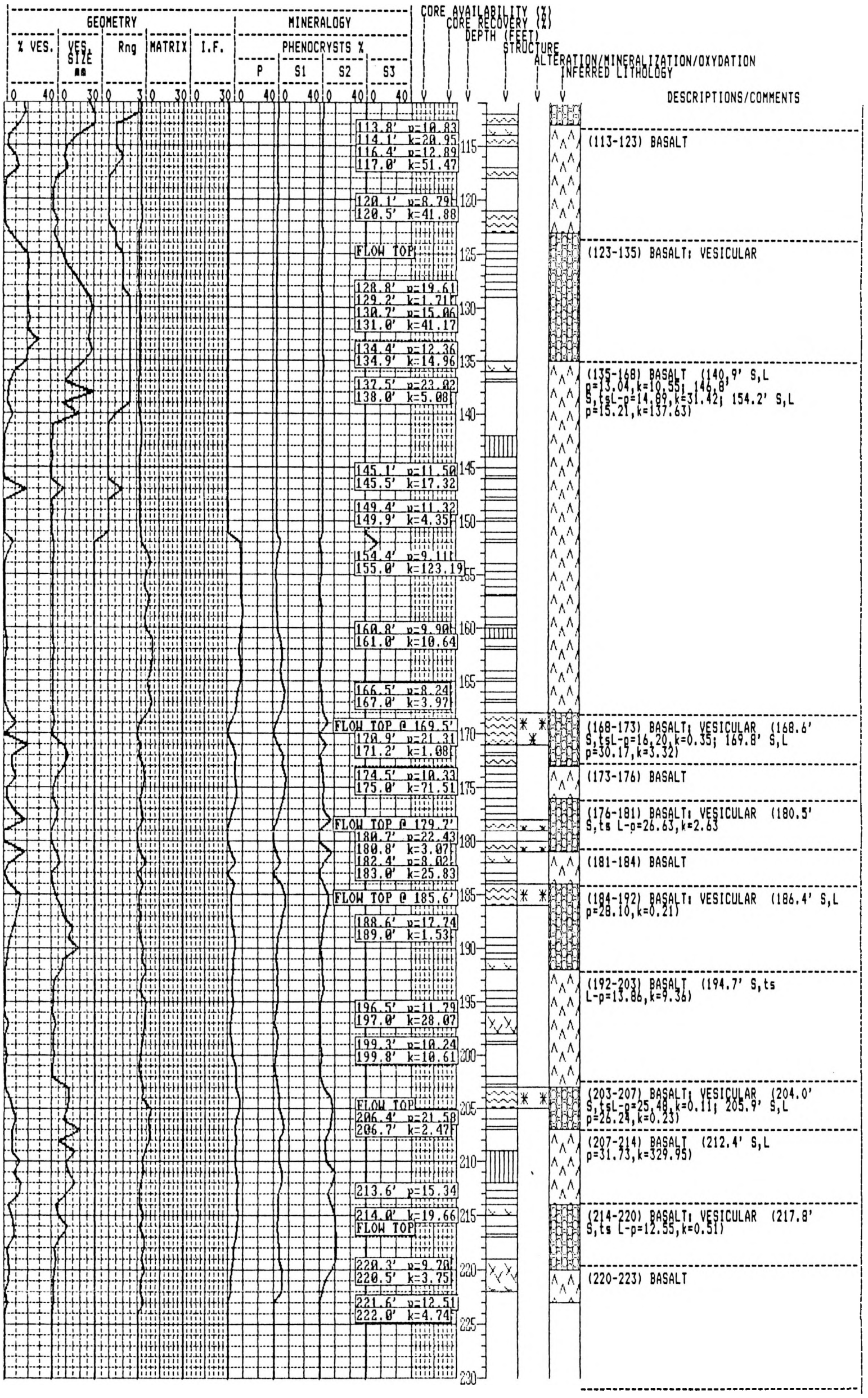

(Well 79-2, continued)

INEL
Idaho National Engineering Lab, Box 1625, Idaho Falls, ID. 83415

Organization EG&G.....
Well Name 79-3.....
Location
Cord. System N668243',E267806.7'.....
Descriptive.....
County Butte.....State Idaho.....

Drilling Supervisor
.....

Reference Elevation
for Geophysical Logs
Ref.....
Gl 5008'.....

Dates:
Start.....
Completion .....

Total Depth:
Driller 257'.....
Logger .....

Surveyed By.....

Geophysical Logs
.....Gamma.....
.....
.....

Core Log By: J.P. O'Brien.....Date: 4/89.....
Org...EG&G.....Stored.CF-649.....
.....

INDEX TO SYMBOLS

CLAY: SANDY
SAND: CLAYEY
SAND: SILTY
SILT: CLAYEY
BASALT
BENTONITE
CINDERS
CLAY
FAULT
GRAVEL
LOESS
OXIDATION
RHYOLITE
SAND
SILT
ALT.CALC.
ALT.CHLR.
ALT.IDDS.
BAS.BX.
BAS.VES.
FLT.BX.
FRAC.CALC.FL
FRAC.CLY.FL
FRAC.PYR.FL
FRAC.SLT.FL
FRAC.HI ANG
FRAC.MOD ANG
FRAC.LO ANG

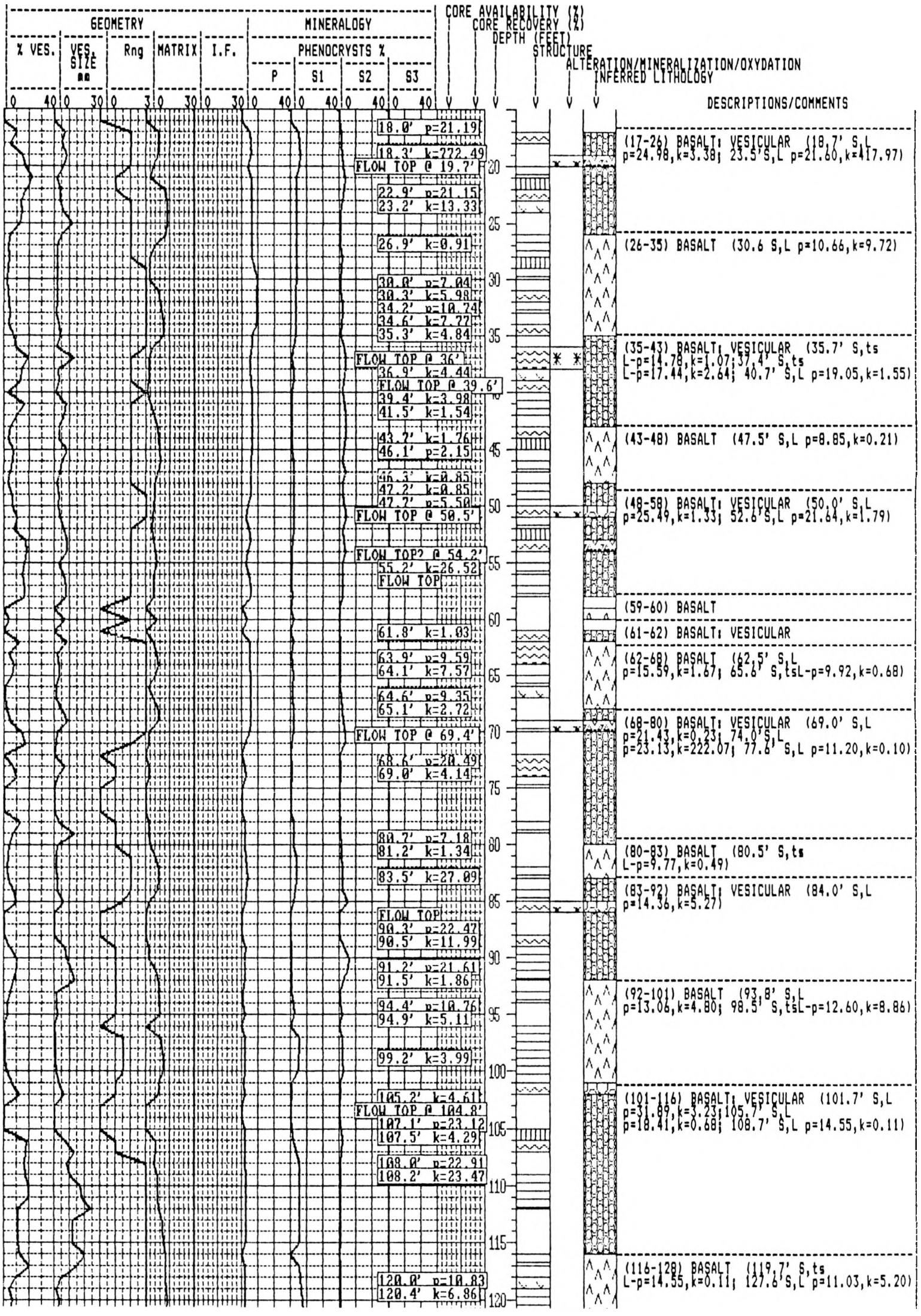

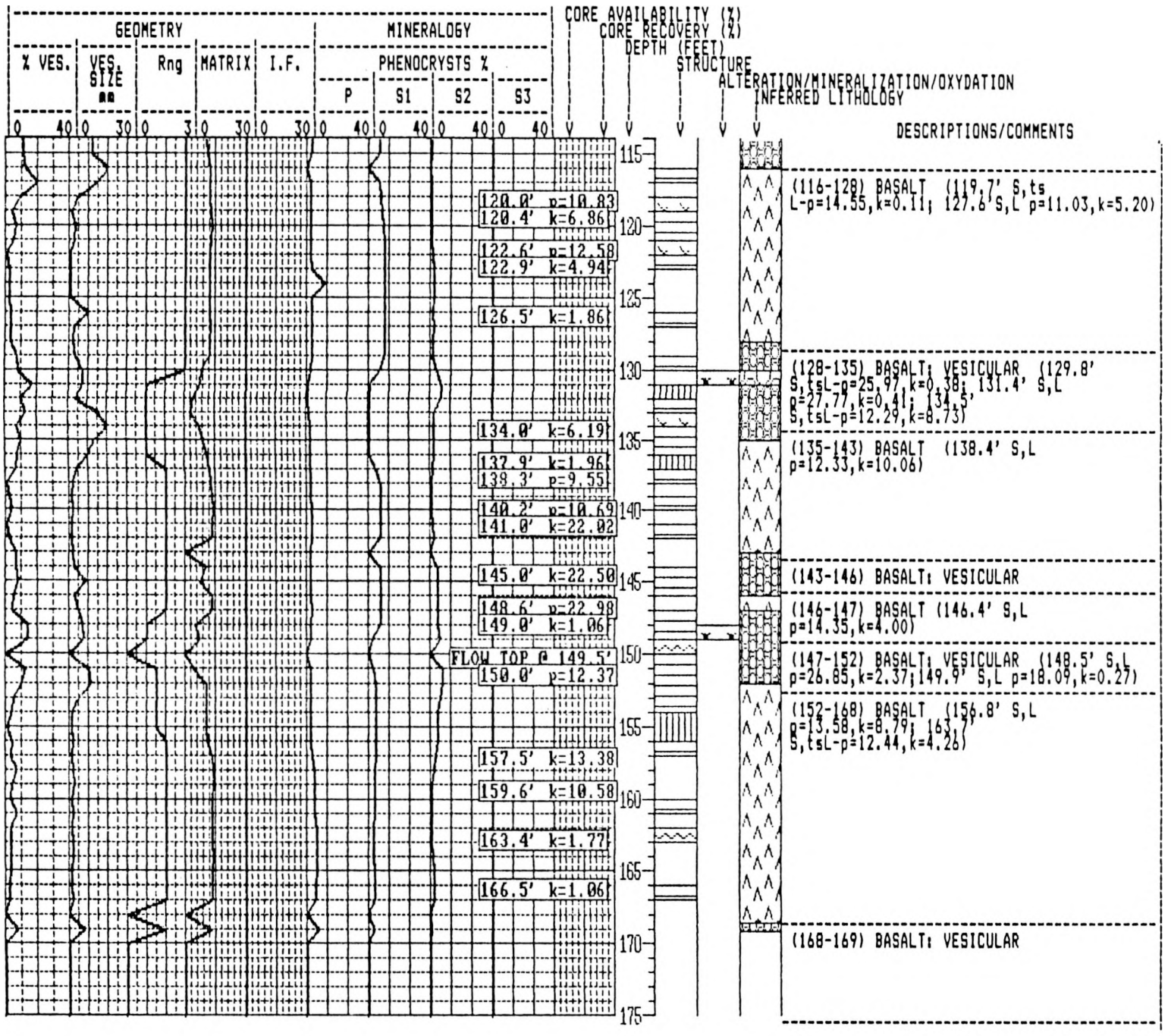

(Well 79-3, continued)

INEL
Idaho National Engineering Lab, Box 1625, Idaho Falls, ID, 83415

Organization EG&G.....
Well Name 93-A.....
Location
Cord. System N669566',E265066.8'.....
Descriptive.....
County Butte.....State Idaho.....

Drilling Supervisor
.....

Reference Elevation
for Geophysical Logs
Ref.....
GL 5010'.....

Dates:
Start.....
Completion .....

Total Depth:
Driller 231'.....
Logger .....

Surveyed By.....

Geophysical Logs
...Gamma, Neutron....
.....Density.....
.....

Core Log By: J.P. O'Brien.....Date: 5/89.....
Org...EG&G.....Stored.CF-649.....
.....

INDEX TO SYMBOLS

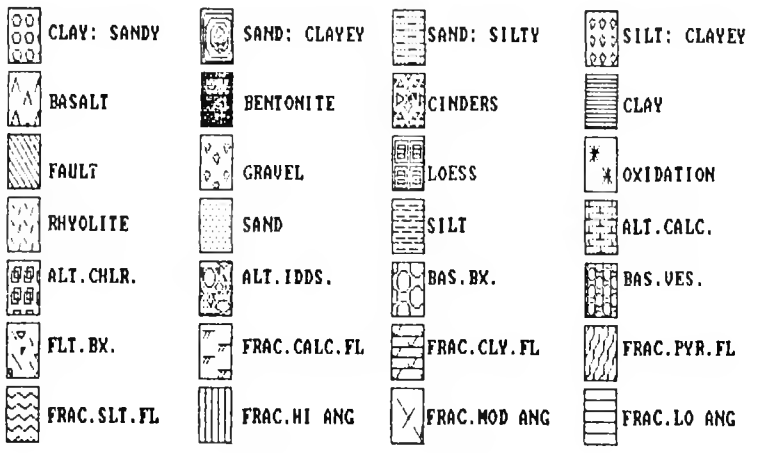

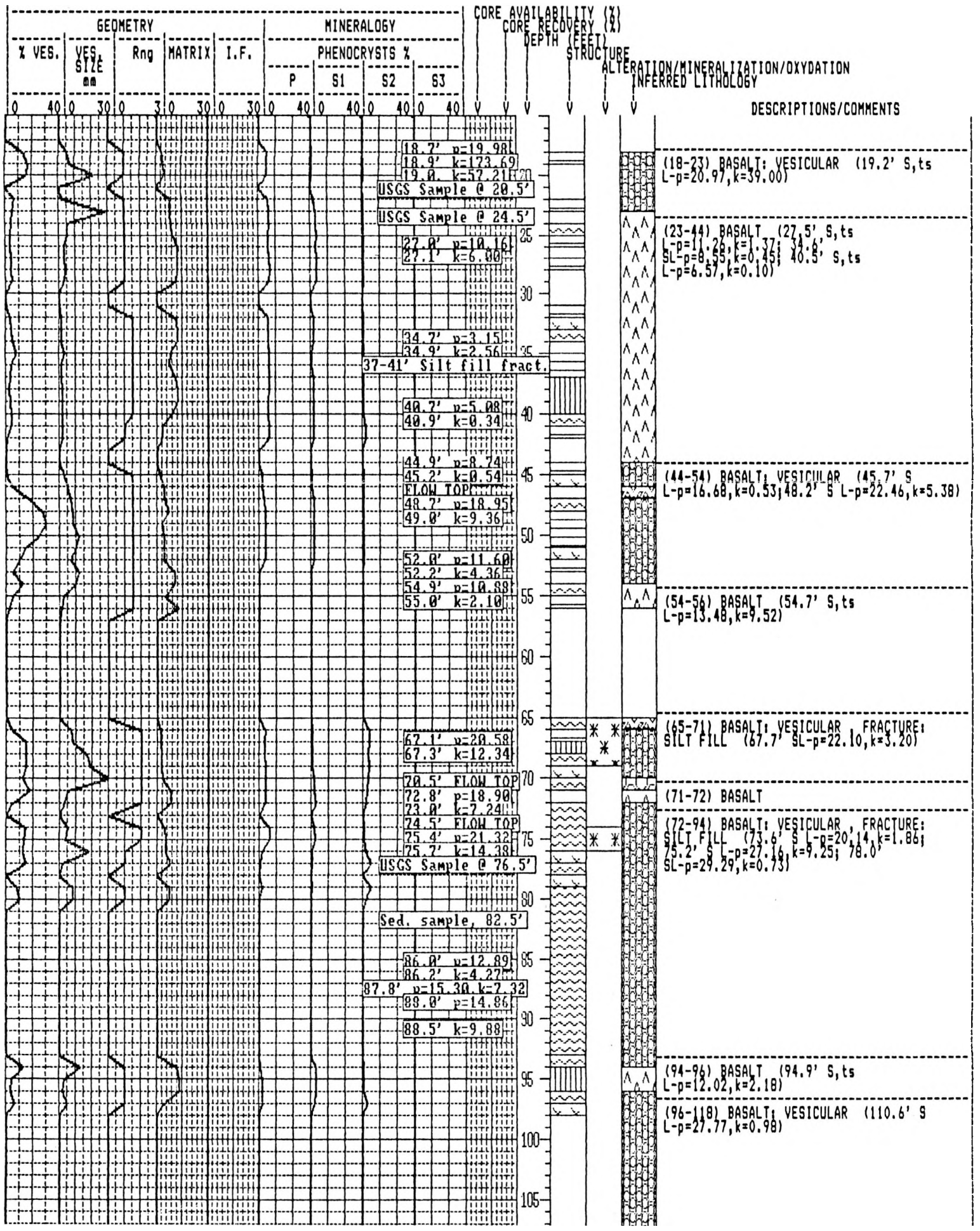

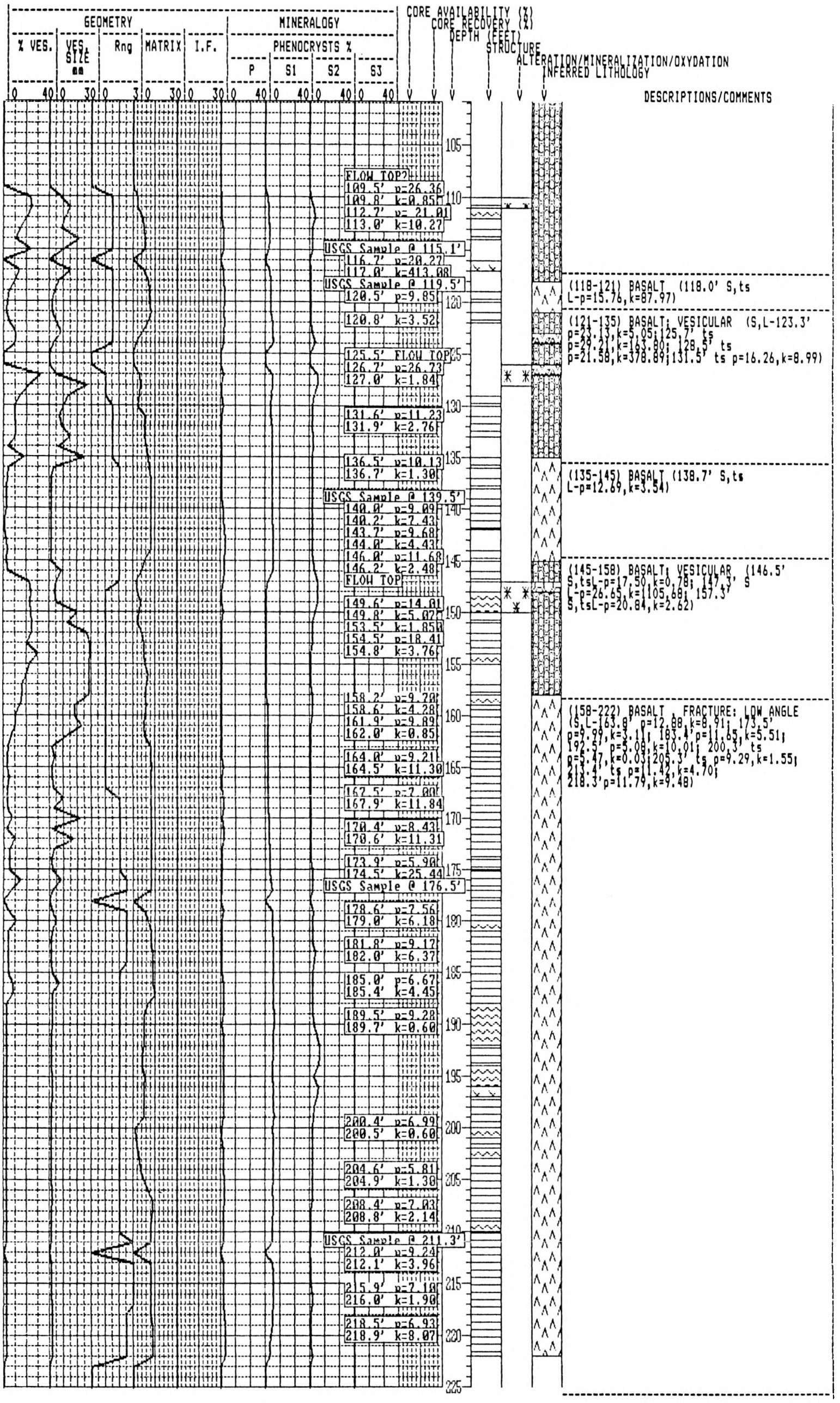

(Well 93-A, continued)

INEL
Idaho National Engineering Lab, Box 1625, Idaho Falls, ID. 83415

Organization EG&G.....
Well Name 96-A.....
Location
Cord. System N669750',E265700'.....
Descriptive.....
County Butte.....State Idaho.....

Drilling Supervisor
.....

Reference Elevation
for Geophysical Logs
Ref.....
Gl 5007'.....

Dates:
Start.....
Completion .....

Total Depth:
Driller 118.2'.....
Logger .....

Surveyed By.....

Geophysical Logs
.....
.....
.....

Core Log By: J.P. O'Brien.....Date: 4/89.....
Org...EG&G.....Stored.CF-649.....
.....

INDEX TO SYMBOLS

CLAY: SANDY
SAND: CLAYEY
SAND: SILTY
SILT: CLAYEY
BASALT
BENTONITE
CINDERS
CLAY
FAULT
GRAVEL
LOESS
OXIDATION
RHYOLITE
SAND
SILT
ALT.CALC.
ALT.CHLR.
ALT.IDDS.
BAS.BX.
BAS.VES.
FLT.BX.
FRAC.CALC.FL
FRAC.CLY.FL
FRAC.PYR.FL
FRAC.SLT.FL
FRAC.HI ANG
FRAC.MOD ANG
FRAC.LO ANG

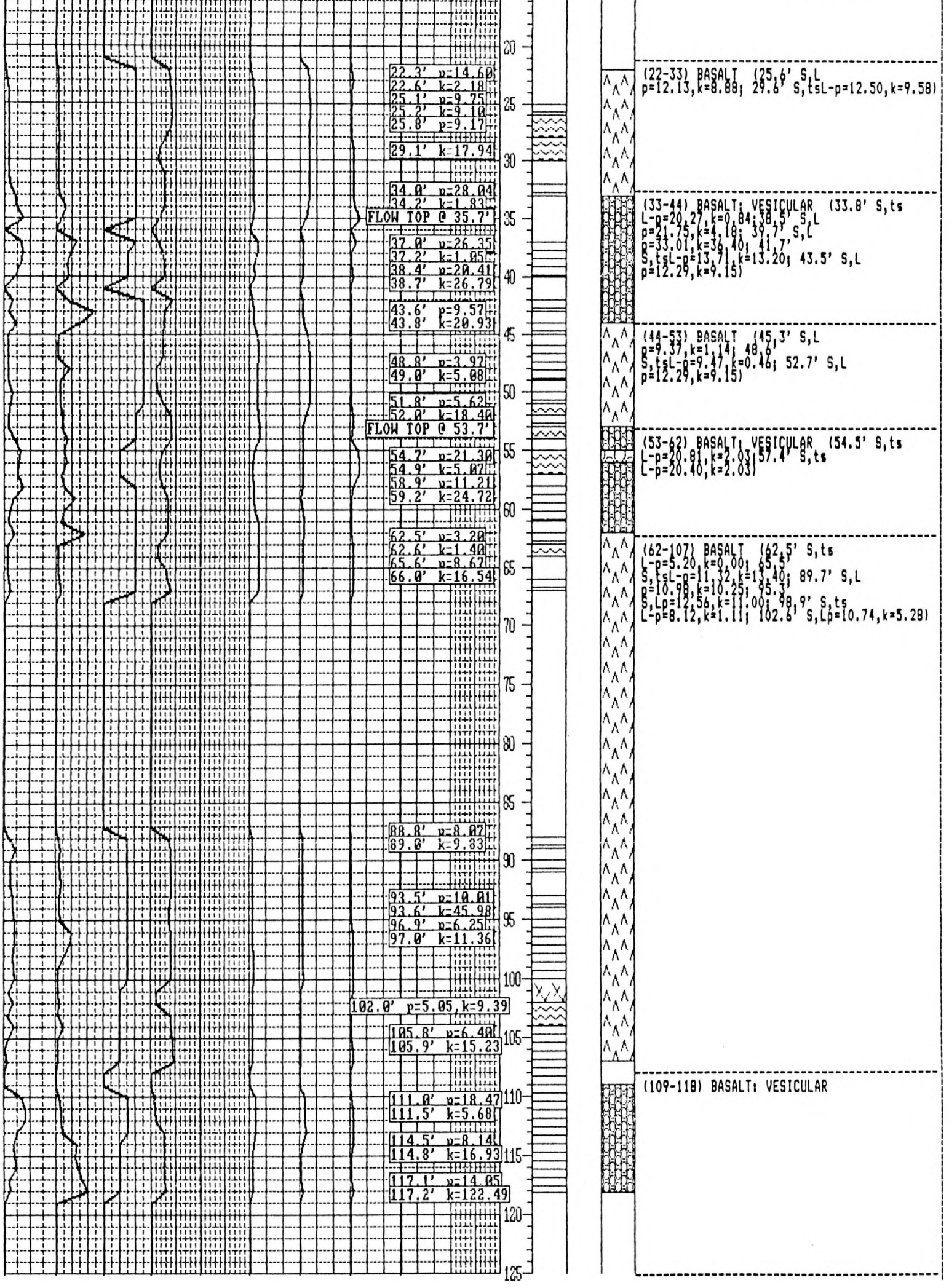

APPENDIX A.3

CHARACTERIZATION AND STRATIGRAPHY OF RWMC LAVA FLOWS

James P. O'Brien

September 5, 1989

CONTENTS

---

a. Figures modified from: U.S. Geological Survey Water Resources Investigations Report 89-4065.

INTRODUCTION

From approximately February 15th to June 10th of 1989 the following drill holes from the RWMC were logged by J. P. O'Brien: 76-2, 76-3, 76-4, 76-4A, 76-6, 77-2, 78-2, 78-3, 78-5, 79-1, 79-2, 79-3, 93A, and 96A. Approximately 2900 feet of hole was logged from these drill holes.

Pieces of the basalt drill core were fitted together on a 12-foot core trough and marked at one-foot intervals. A lithologic log was then prepared for each drill hole. Logs indicate vesicular and nonvesicular zones, fractures and fracture angles, and the presence of silt or sedimentary interbeds. Flow boundaries or breaks were placed in appropriate areas where core displayed oxidized (erosional), scoriaceous, chilled, or sediment zones. These breaks are displayed on the logs with a heavy line, and in graphs one through four with symbols. At one foot intervals an estimate was made of the percent of vesicles present, the maximum vesicle size, the (nonvesicular) porosity of the matrix, and the size and composition of phenocrysts. Approximately 100 to 125 feet of core was logged during a ten hour day.

METHODS: LOG LEGEND

Information obtained from the RWMC basalt cores was recorded on 11x17 inch log sheets provided by EG&G. Pieces of core were taken from marked, unmarked, and sometimes mismarked boxes that contained approximately 3 to 5 feet of core. Efforts were made to reorient and relabel obviously incorrectly boxed core. To properly fit the core back together, several methods were employed: physically matching (fitting) ends together; looking for up-down indicators, such as silt resting on the bottom of vesicles; and the proper stratigraphic position of interflow intervals, such as large vesicles and oxidized zones on top, massive "flat" zones in the middle, and glassy or chilled portions with pipe vesicles on the bottom. The following legend describes notations on the log sheets and the procedure that was used to derive them.

The far left hand column on the log sheets has a scale of 1 inch equals ten feet; numbers indicate depth and measurements of "gaps" in the core. All

decimal numbers in this column are in tenths of feet. Measurements were obtained from a scale on the side of the core trough.

The second column to the right labeled "Rx" has checks, circles of varying sizes, and solid intervals of varying lengths. The checks indicate "massive" or "flat" nonvesicular basalt, the circles indicate vesicular zones. Vesicle size is scaled and indicated graphically. Solid intervals represent missing core or sedimentary interbeds where specially noted.

The third and fourth columns to the right are labeled "Struct". The third column graphically indicates the orientation and position of bubble trains, large vesicles, and pipe vesicles. Bubble trains are indicated graphically with the symbols:  . These symbols are scaled to show the size of vesicles, orientation of the train, and thickness of the train. Large vesicles are noted with the symbol:  , which is scaled to the size of the vesicle. Pipe vesicles are denoted with the symbol:  , which also indicates the orientation, and relative size of the pipe vesicle. The fourth column was used to label these features and any additional ones. Additional remarks might include USGS sample locations, oxidized or cindery (scoriaceous) zones, the presence of silt in fractures, and sometimes the angle of these fractures.

The fifth and sixth columns, labeled "Fracture Filling" describe the angle of fractures both graphically and quantitatively. The fifth column is solid where core is missing; lines indicate position and azimuth of fractures. The angle of fractures is noted in the following way:
horizontal lines indicate fractures at or near 90 degrees from the core axis, inclined lines indicate fractures at less than 90 degrees (fracture angles are noted exactly the opposite way in the Logger^{tm} logs:
0° is a horizontal fracture and 90° is a vertical fracture).
Numbers between ten and ninety represent degrees measured from the core axis and are placed in the fourth and sixth columns where measurements were taken. The sixth column is somewhat analogous to the fourth, describing silt filling in fractures, oxidized zones, cindery (scoriaceous) zones, and zones that consist primarily of rubble (fist and smaller sized chunks of core).

The first column from the left with a grid pattern, labeled "% Ves", indicates a macroscopic percentage estimate of vesicles at any interval down the core. This is displayed in the form of a line graph. Each grid box represents 10%, thus percentage estimates range from 0 to 40%. The estimate of percent vesicles was derived by a comparison of the outer core surface with comparison charts for estimating percentage composition from the Journal of Sedimentary Petrography (v. 25, n. 3, p. 229-234, 1955).

The second column from the left with a grid is labeled "Max. Ves. Size (mm)". This column represents maximum vesicle size in mm at any given spot along the core, represented graphically in the form of a line graph. The scale for this column is in 5 mm increments, measurements range from 0 to 30 mm. Very large vesicles (< 8 mm) were measured with a ruler; along the long axis if the vesicle was not spherical. Vesicles smaller than 8 mm were measured by comparison with a graph for determining the size of sedimentary particles from the AGI Data Sheet Committee (1982).

The next grid column to the right labeled "Rng", contains numbers corresponding to a phenocryst size range. Phenocrysts are composed of plagioclase, olivine, or oxidized accessory minerals. Often the measured phenocrysts were "clumps" of the minerals mentioned above. Phenocrysts were measured with a ruler. The numbers (1 through 3) represent the following phenocryst sizes:

1 = phenocrysts less than 1 mm in diameter.

1.5 = more than 50% of phenocrysts present are less than 1 mm in diameter, but more than 10% are greater than 1 mm in diameter.

2 = phenocrysts are greater than 1 mm in diameter but less than 3 mm in diameter.

2.5 = more than 50% of phenocrysts present are greater than 1 mm in diameter but less than 3 mm in diameter, and more than 10% are greater than 3 mm in diameter.

3 = 80% of phenocrysts are greater than 3 mm in diameter.

Note: if phenocrysts are elongate, the maximum dimension (length) was measured.

Further to the right, the next column is labeled "Matrix". The "Matrix" column describes the percentage of porosity, or void space present in core intervals that is not related to vesicle content. The matrix porosity is displayed graphically in line graph form. Pores are much smaller than vesicles, ~.5 mm, and were counted with a 10x handlens. A comparison was then made between the number of voids counted and the number of particles found in a percentage range, using comparison charts for estimating percentage composition (Journal of Sedimentary Petrography, v. 25, n. 3, p. 229-234, 1955). Total porosity of the core is calculated by adding the matrix porosity value to the % vesicle value. Each grid block in this column represents 5%, so matrix porosity can vary from 0 to 15%.

The next three columns to the right labeled "I.F." and "Alteration" were not used.

The next four columns under the heading of "Phenocrysts" represent a percentage estimate of phenocrysts present in the core. The first column labeled "P" under this category represents the amount of plagioclase phenocrysts present. The second column under this category labeled "S1" represents the amount of olivine present. The third column under this category labeled "S2" represents the amount of oxidized minerals present, oxidized minerals can include iddingsite, ilmenite, and olivine. The fourth column under this category labeled "S3" represents the amount of accessory mineral phenocrysts present, examples of accessory minerals are pyrite, pigeonite, and augite. Often the plagioclase, olivine, and accessory minerals were aggregates by mineral type. These aggregates were treated as a single phenocryst. A comparison was then made between the number of phenocrysts counted and the number of particles found in a percentage range, using comparison charts for estimating percentage composition (Journal of Sedimentary Petrography, v. 25, n. 3, p. 229-234, 1955).

NOTE: THE SCALE ON THESE GRIDS IS 5%, 10%, AND 15%; NOT 10%, 20%, AND 30% AS INDICATED ON SOME OF THE LOGS.

The next two columns to the right marked "A" and "R" were not used.

The next ruled section labeled "Remarks" indicates any unusual findings: sedimentary interbeds or drilling mud, breaks (or boundaries) between flow units, zones of large phenocrysts or glass, color changes, or exceptionally long bubble trains. Further to the right of this column, the ruled section contains numbers and captions to indicate intervals or exact locations in the core where "Basalt", "Basalt; Vesicular", and "Flow Top" are located.

Black lines drawn horizontally across the log sheet indicate approximate flow boundaries. Black lines are dashed where there is uncertainty in placing a flow boundary. Flow boundaries commonly exhibit scoriaceous and oxidized zones at the top of flows and somewhat glassy, perhaps chilled areas on flow bottoms. Flow tops usually display a five to ten foot vesicular zone, and the largest vesicles are usually found in the upper portion of a flow unit. The middle portion of a flow is commonly massive or "flat", and bubble trains are often found in this middle portion. Flow bottoms commonly exhibit a zone of one or two feet of small (~.5 cm) vesicles, cindery zones, pipe vesicles, and in a few instances, rounded cobble-sized basalt inclusions of a different origin than the surrounding flow unit.

The far right column labeled "Samples" indicates the depth at which samples were taken, and any interesting feature the sample possesses. At least three samples were taken from the top, middle, and lower portions of each flow unit. Often more than three samples were taken if the flow was especially thick, or contained an interesting feature. The top sample was always taken at or near the flow boundary, the middle sample was commonly taken from the massive or "flat" zone, the lower sample was always taken at or near the bottom flow margin.

RESULTS: GRAPHS

Well positions on the RWMC site are shown in Figure 1. Four cross sections were constructed across the RWMC site, a northern west-east line (A-A′), a southern west-east line (B-B′), an eastern south-north line (C-C′), and a western south-north line (D-D′). Cross-section (x-section) lines A-A′ and B-B′ are shown in Figure 2. X-section lines C-C′ and D-D′ are shown in Figure 3. Flow break depth graphs (graphs one through four), and flow unit thickness graphs (graphs five through twelve) were constructed along these lines. Flow groups and the individual flows that comprise them were also correlated between boreholes (graphs five through eight) along these x-section lines. Table 1 lists depths of flow groups and the individual flow units that comprise them.

The compound flow groups are defined or separated from each other by identifying intervening soils, erosion surfaces, and sediments. A hiatus of unknown deration unquestionably exists between deposition of the flow groups. The flow units that comprise a flow group are correlated on the basis of composition and mineralogy, grain/phenocryst size, thickness, and color. The flow breaks separating the flow units within a flow group unquestionably exist but correlations between holes are tentative, pending further investigation. Exact correlation was hindered by lack of precise topographic control on elevation at the top of each hole. Correlations are shown assuming a datum for the top of each hole, and disregarding the possible effects of erosion on the uppermost flow.

In graphs one through four, blocks represent the first flow break down each hole, crosses the second, diamonds the third, triangles the fourth, x's the fifth, and inverted triangles the sixth. Flow breaks are not always correlatable from hole to hole in these graphs; their purpose is to show the relative distribution of the first six flow breaks in each hole.

The correlation graphs, five through nine, display flow units that have been correlated between drill holes along the two west-east and two south-north lines, A-A′ B-B′ and C-C′ D-D′, respectively. Absolute

identification of individual flows from the same event or flow group is beyond the scope of this report, therefore correlations are primarily of eruptive events. However, when possible, individual flow units were identified between the 30 and 100 foot interbeds and below the 100 foot interbed. Three flow groups were identified: flow group one lies above the 30 foot interbed, flow group two lies below the 30 foot interbed and above the 100 foot interbed, and flow group three lies below the 100 foot interbed. The 30 foot and 100 foot interbeds are named thus because they are consistently found at approximately this depth when they are encountered. The 30 foot and 100 foot interbeds are shown with a heavy dark line in graphs five through eight. The precise lithologic description, depositional environment, and amount of time represented by these sedimentary interbeds is beyond the scope of this report.

Event correlations do not always coincide with the flow breaks represented in graphs one through four. Some breaks were omitted because they were thought to represent flows that were very closely spaced, nearly continuous in time, or gas laden horizons. Conversely, some tentative breaks were added at the 100 foot interbed level because of mineralogical differences. These tentative breaks are indicated on the logs (see log 79-3 for example). The missing physical evidence for the break is attributed to erosion. The absence of flow group one in some holes was based upon mineralogical differences and the presence or absence of the 30 foot sedimentary interbed. Flow 2-1 of group two was absent in some holes (see Logs 96A, 79-4, and 76-4A) based on mineralogical differences.

All correlations were hampered by missing core intervals in several holes, therefore correlation lines often have "gaps" in them where a correlation cannot be made.

The primary purpose of graphs nine through twelve is to represent the thickness of flow units. The 30 foot and 100 foot interbeds are indicated with heavy lines. Numbers inside the bar graph segments indicate the thickness of the segment below the number. The datum for these graphs is the first basalt flow, therefore the Y-axis (depth in feet to bottom of flow) does not coincide with the Y-axis of graphs one through eight. Often

approximately 20 feet consisted of unconsolidated material and was not suitable for storage in core boxes. Whatever the case, this missing upper interval is responsible for the decrease in depth observed in these stacked bar graphs. It should also be noted that graphs 11 and 12 (C-C' & D-D') are drawn from north to south, not south to north as in graphs 7 and 8.

DISCUSSION:

The original proposal for this job listed five tasks that were to be completed. Since the job was subsequently split between John Crocker and myself some of the tasks are to be completed by him.

Task one, descriptive logging of the core is summarized in this report. Objectives one through seven of task one were completed and are displayed in the original log sheets. In addition to these objectives, the core was marked at one foot intervals, a size range for phenocrysts was made (column labeled Rng), and a percentage of each type of phenocryst present was made.

Task two is to be carried out by John Crocker.

Task three was split between us. Information on the fracture locations, orientations, and fillings is summarized here. All further quantitative work with this data is to be done by John Crocker.

Tasks four and five are to be performed by John Crocker.

The results show that the RWMC area received lava and sediment in a somewhat uniform manner through the time represented between flow group three and the 100 foot sedimentary interbed. During the period represented by flow group two and certainly during flow group one the area had developed an irregular topography or experienced eruptive events of a smaller magnitude. This is represented by the lack of, and variation in thickness of the younger flow groups/units.

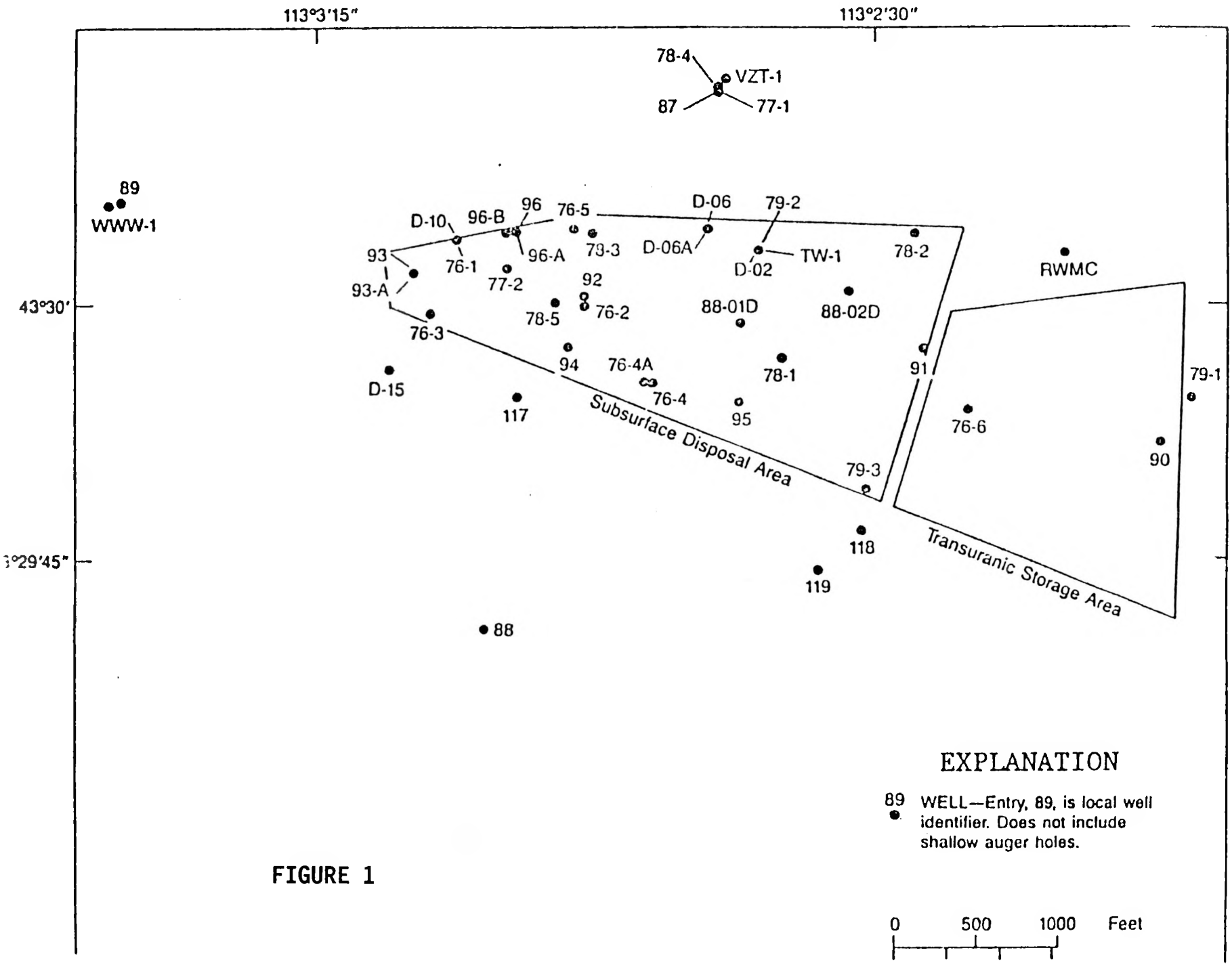
113°3'15"
113°2'30"
43°30'
43°29'45"
78-4
VZT-1
87
77-1
89
WWW-1
D-10
96-B
96
76-5
D-06
79-2
93
76-1
96-A
79-3
D-06A
TW-1
78-2
93-A
77-2
92
D-02
RWMC
78-5
76-2
88-01D
88-02D
76-3
94
76-4A
78-1
91
79-1
D-15
117
76-4
95
76-6
90
Subsurface Disposal Area
79-3
118
Transuranic Storage Area
119
88
EXPLANATION
89 WELL—Entry, 89, is local well identifier. Does not include shallow auger holes.
0
500
1000
Feet

FIGURE 1

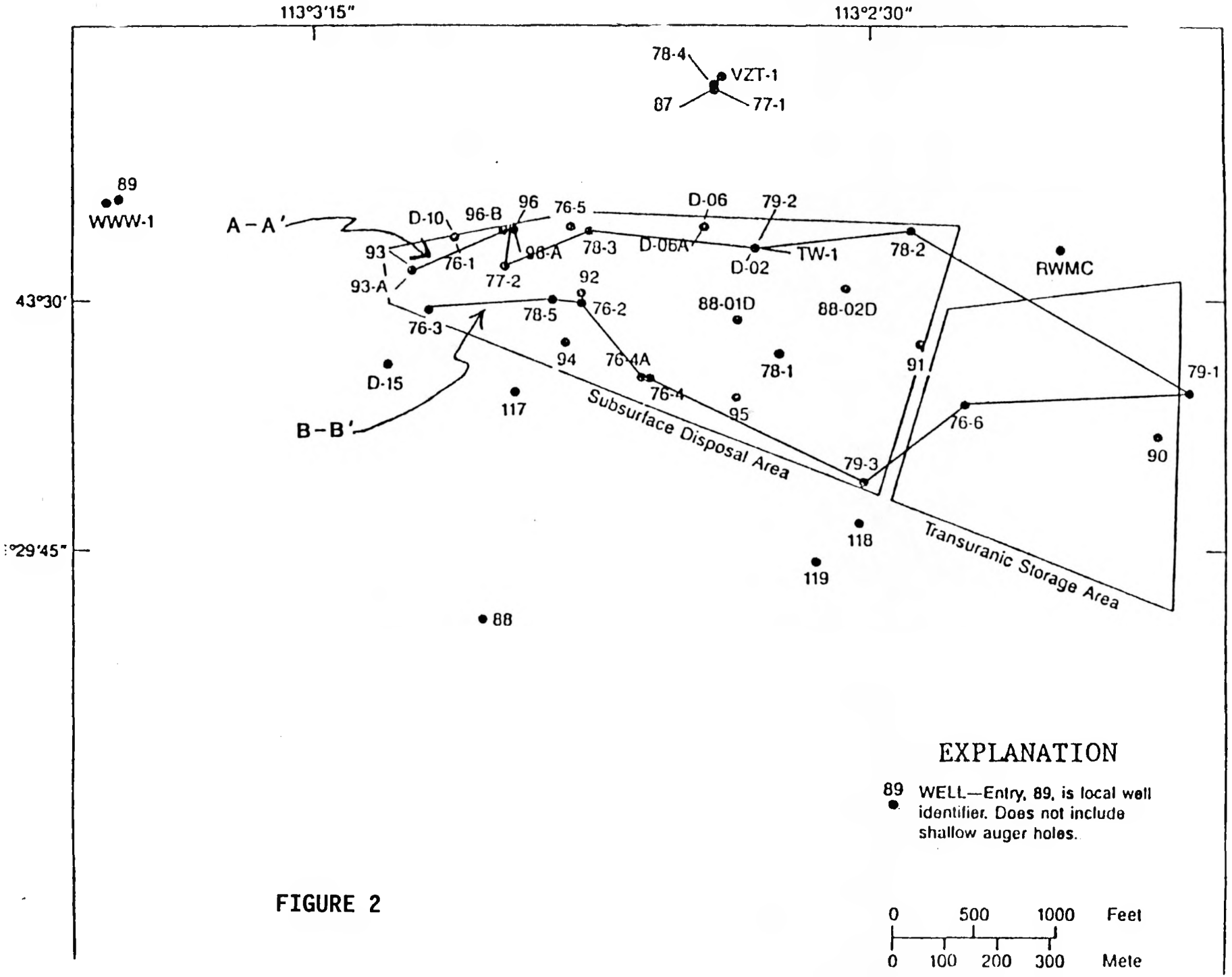
113°3'15"
113°2'30"
43°30'
29'45"
78-4
VZT-1
87
77-1
89
WWW-1
A – A'
D-10
96-B
96
76-5
D-06
79-2
93
76-1
98-A
78-3
D-06A
D-02
TW-1
78-2
RWMC
93-A
77-2
92
88-01D
88-02D
76-3
78-5
76-2
94
76-4A
78-1
91
79-1
D-15
117
76-4
95
B – B'
Subsurface Disposal Area
76-6
90
79-3
118
Transuranic Storage Area
119
88
EXPLANATION
89
WELL—Entry, 89, is local well identifier. Does not include shallow auger holes.
0
500
1000
Feet
0
100
200
300
Mete

FIGURE 2

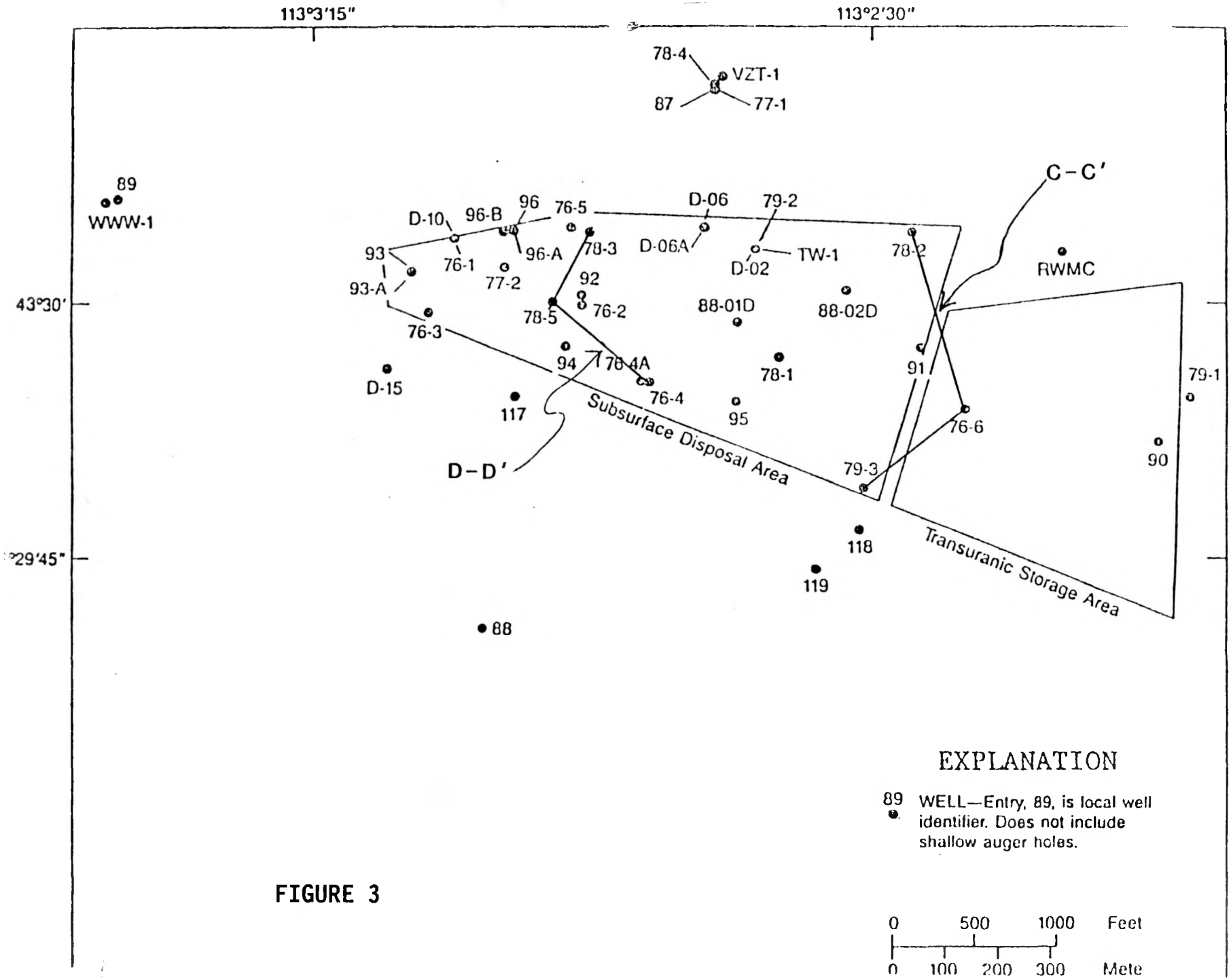
113°3'15"
113°2'30"
43°30'
29'45"
78-4
VZT-1
87
77-1
89
WWW-1
C-C'
D-10
96-B
96
76-5
D-06
79-2
93
76-1
96-A
78-3
D-06A
D-02
TW-1
78-2
RWMC
93-A
77-2
92
78-5
76-2
88-01D
88-02D
76-3
94
78-4A
78-1
91
79-1
D-15
117
76-4
95
76-6
90
D-D'
Subsurface Disposal Area
79-3
118
Transuranic Storage Area
119
88
EXPLANATION
89 WELL—Entry, 89, is local well identifier. Does not include shallow auger holes.
0 500 1000 Feet
0 100 200 300 Mete

FIGURE 3

DATA TABLE NUMBER ONE

BASALT FLOW INFORMATION TAKEN FROM LOGS (APPENDIX TWO).
ALL INFORMATION IS PLOTTED ON GRAPHS 1 THROUGH 12.
BOREHOLE DEPTH INDICATES DEPTH TO BOTTOM OF FLOW UNITS.
ALL MEASUREMENTS IN FEET.

NORTHERN WEST-EAST CROSS SECTION A-A'

COORDINATES IN FEET EAST 260000 +			5066	5337	5632	6151	7160	8098	9768
HOLE NUMBER			93	96	77-2	78-3	79-2	78-2	79-1
	FLOW GROUP	FLOW UNIT							
BOREHOLE DEPTH	1	1-1	0	34	27	0	25	25	0
THICKNESS			0	12	7	0	7	20	0
B.D.	2	2-1	46	34	36	30	38	48	45
T.			28	0	9	25	13	23	40
B.D.	2	2-2	80	54	51	56	68	64	55
T.			34	20	15	26	30	16	10
B.D.	2	2-3			71	70			68
T.					20	14			13
B.D.	2	2-4	109	118		92	100	105	98
T.			29	64		22	32	41	30
B.D.	3	3-1	125			151	124	128	112
T.			16			59	24	23	14
B.D.	3	3-2	147			175	169	171	166
T.			22			24	45	43	54
B.D.	3	3-3	222						
T.			75						

SOUTHERN WEST-EAST CROSS SECTION B-B'

COORDINATES IN FEET EAST 260000 +			5160	5931	6117	6495	6520	7806	8425	9768
HOLE NUMBER			76-3	78-5	76-2	76-4	76-4	79-3	76-6	79-1
	FLOW GROUP	FLOW UNIT								
BOREHOLE DEPTH	1	1-1	0	0	23	23	21	0	0	0
THICKNESS			0	0	7	11	10	0	0	0
B.D.	2	2-1	24	32	36	23	21	20	29	45
T.			1	10	13	0	0	3	20	40
B.D.	2	2-2	65	66	60	43	43	36	71	55
T.			41	34	24	20	22	16	42	10
B.D.	2	2-3			76	67	66	70		68
T.					16	24	23	34		13
B.D.	2	2-4	96		93	99	98	103	104	98
T.			31		17	32	32	33	33	30
B.D.	3	3-1	126	134	146			131	138	112
T.			30	68	53			28	34	14
B.D.	3	3-2		150					165	166
T.				16					27	54
B.D.	3	3-3		167					185	
T.				17					20	
B.D.	3			183						
T.				16						

DATA TABLE ONE (continued)

EASTERN SOUTH-NORTH CROSS SECTION C-C'

COORDINATES IN FEET NORTH 660000 +			9781	8734	8243
HOLE NUMBER			78-2	76-6	79-3
	FLOW GROUP	FLOW UNIT			
BOREHOLE DEPTH	1	1-1	25	0	0
THICKNESS			20	0	0
B.D.	2	2-1	48	29	20
T.			23	20	3
B.D.	2	2-2			36
T.					16
B.D.	2	2-3	64	71	70
T.			16	42	34
B.D.	2	2-4	105	104	103
T.			41	33	33
B.D.	3	3-1	128	138	131
T.			23	34	28
B.D.	3	3-2	171	165	
T.			43	27	
B.D.	3	3-3		185	
T.				20	

WESTERN SOUTH-NORTH CROSS SECTION D-D'

COORDINATES IN FEET NORTH 660000 +			9787	9365	8889
HOLE NUMBER			78-3	78-5	76-4
	FLOW GROUP	FLOW UNIT			
BOREHOLE DEPTH	1	1-1	0	0	21
THICKNESS			0	0	10
B.D.	2	2-1	30	32	21
T.			25	10	0
B.D.	2	2-2	56	66	43
T.			26	34	22
B.D.	2	2-3	70		66
T.			14		23
B.D.	2	2-4	92	100	98
T.			22	34	32
B.D.	3	3-1		134	
T.				68	
B.D.	3	3-2	151	150	
T.			59	16	
B.D.	3	3-3	175	167	
T.			24	17	
B.D.	3			183	
T.				16	

GRAPH 1. X-SECTION A-A′: FLOW BREAK DEPTHS

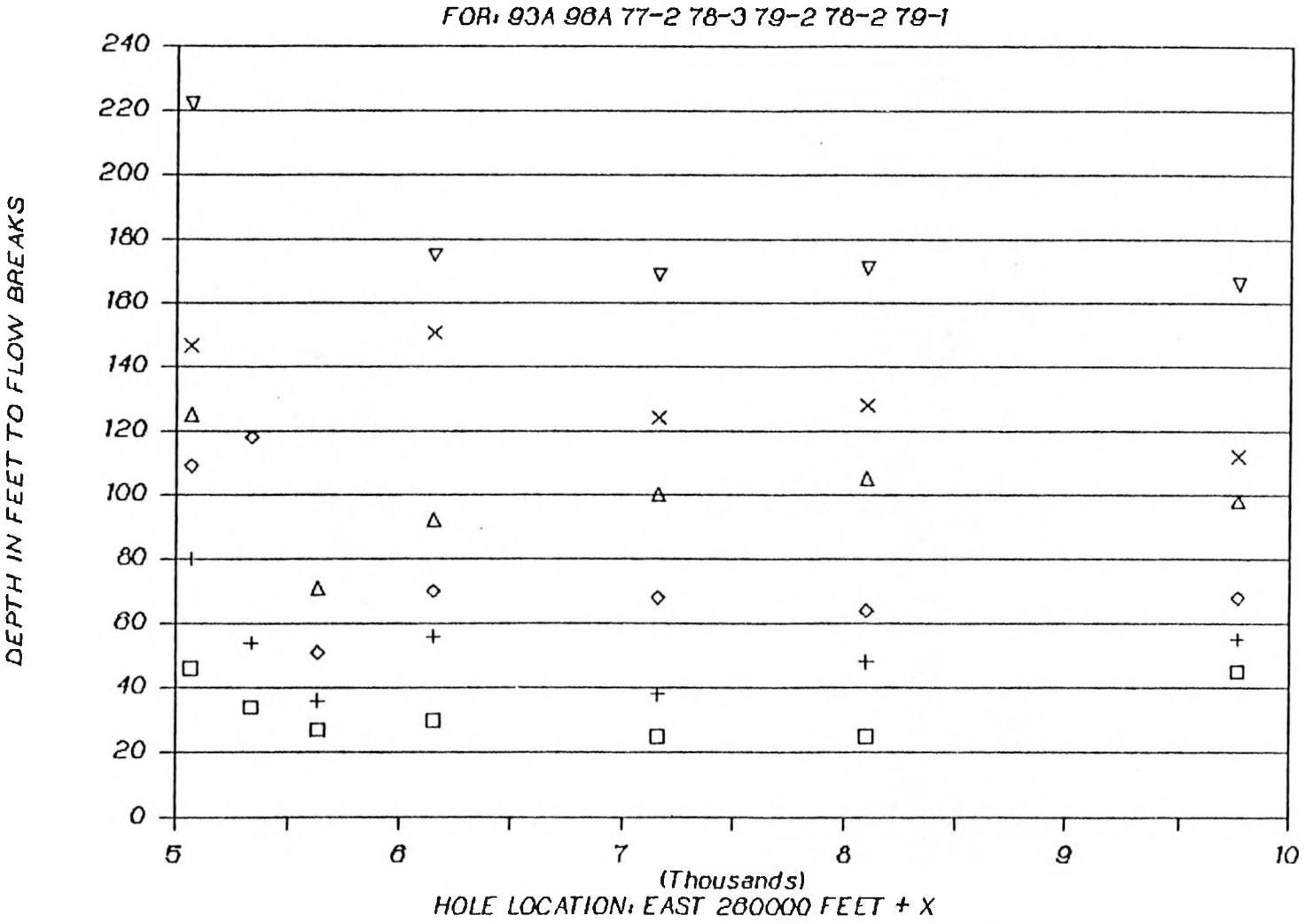

GRAPH 2. X-SECTION B-B′: FLOW BREAK DEPTHS

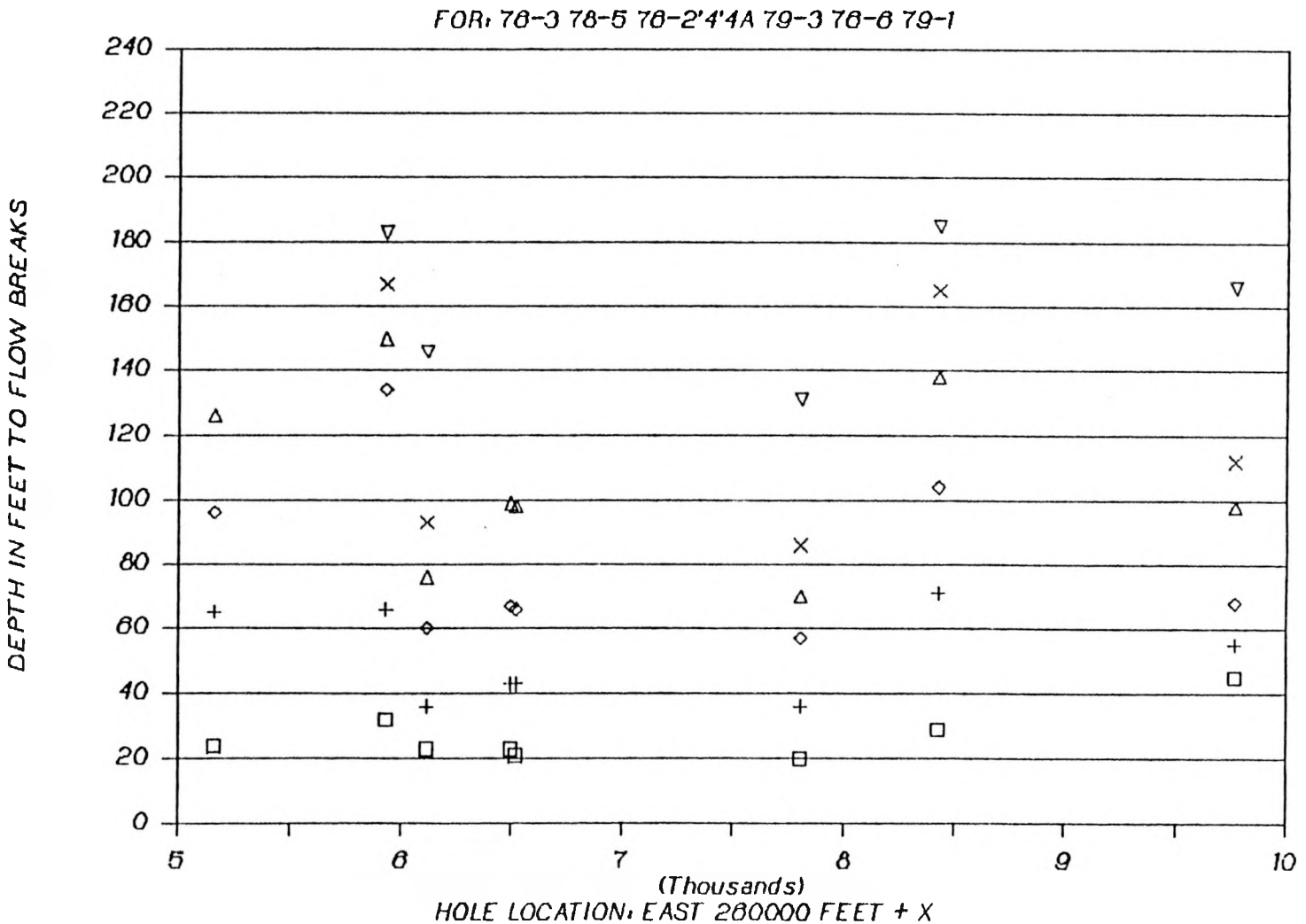

GRAPH 3. X-SECTION C-C′: FLOW BREAK DEPTHS

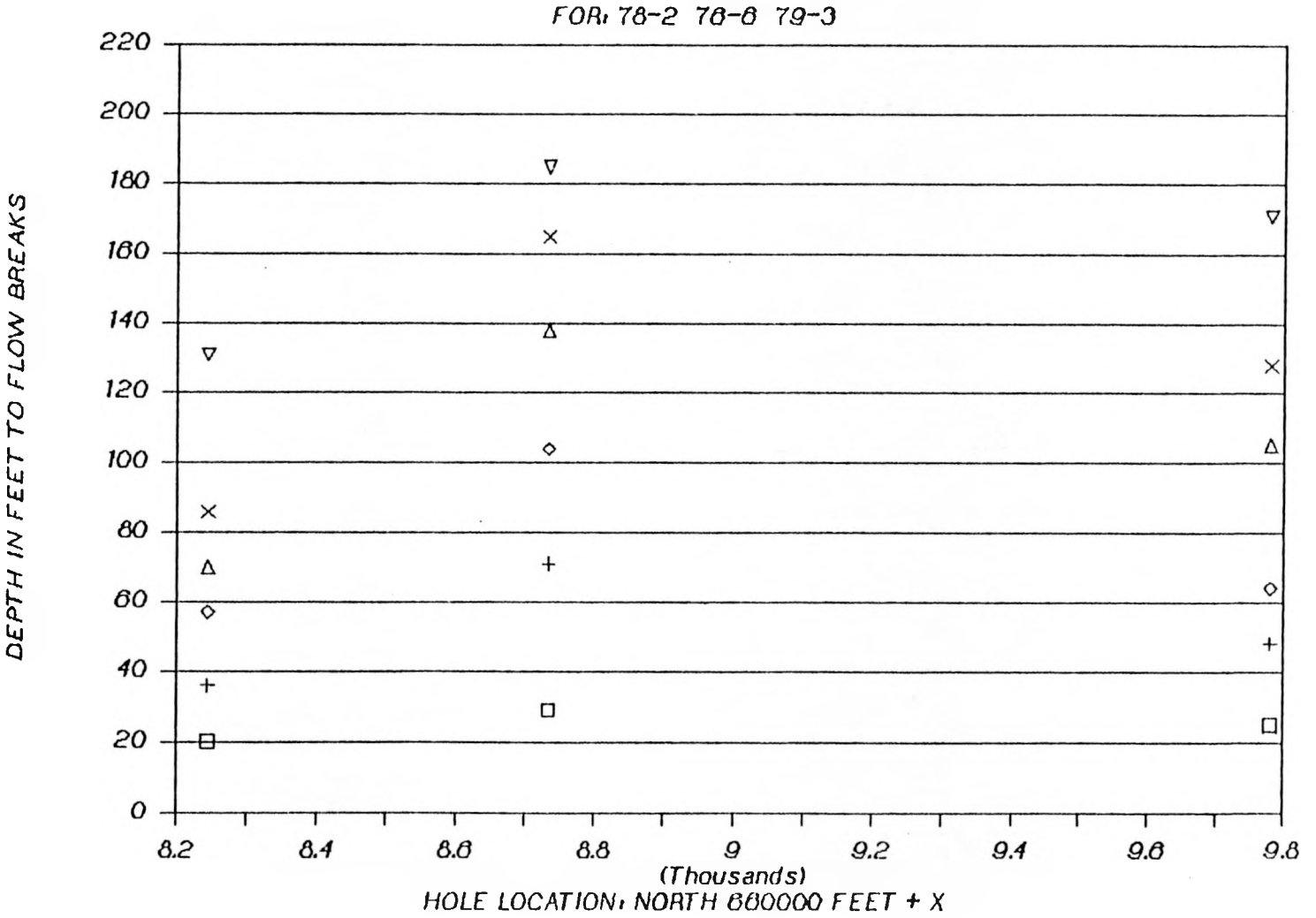

GRAPH 4. X-SECTION D-D′: FLOW BREAK DEPTHS

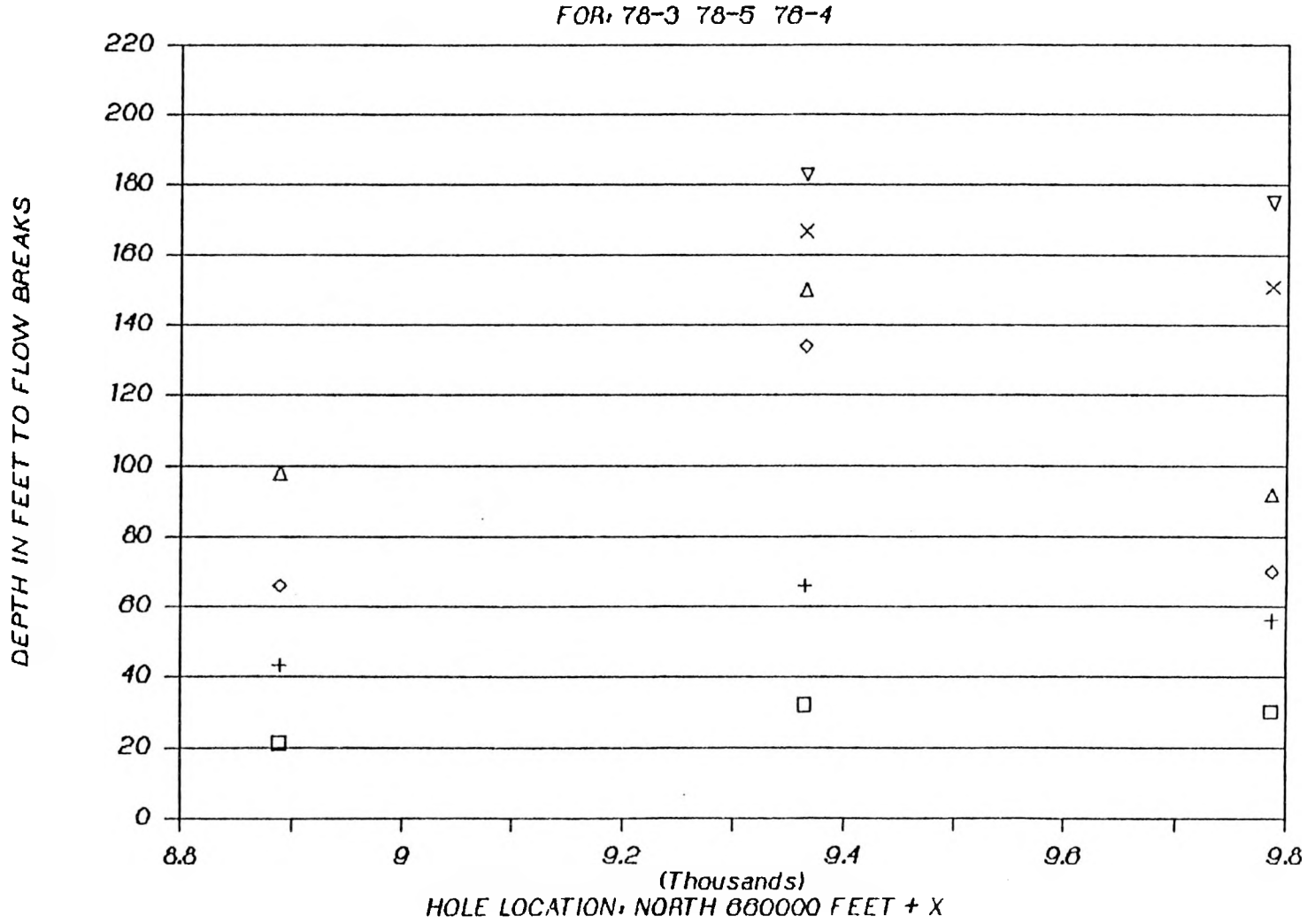

GRAPH 5. CORRELATION X-SECTION A-A'

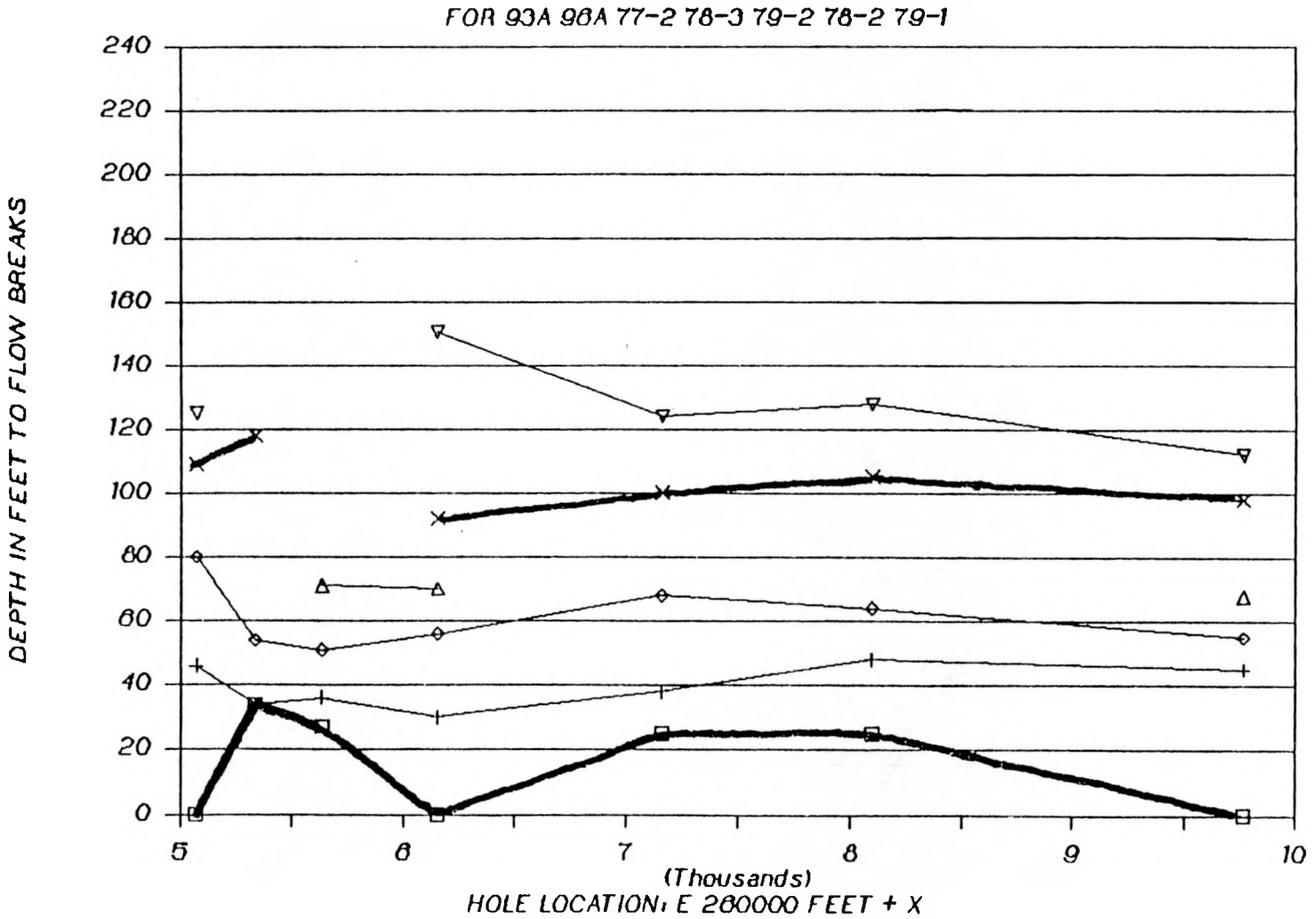

GRAPH 6. CORRELATION X-SECTION B-B′

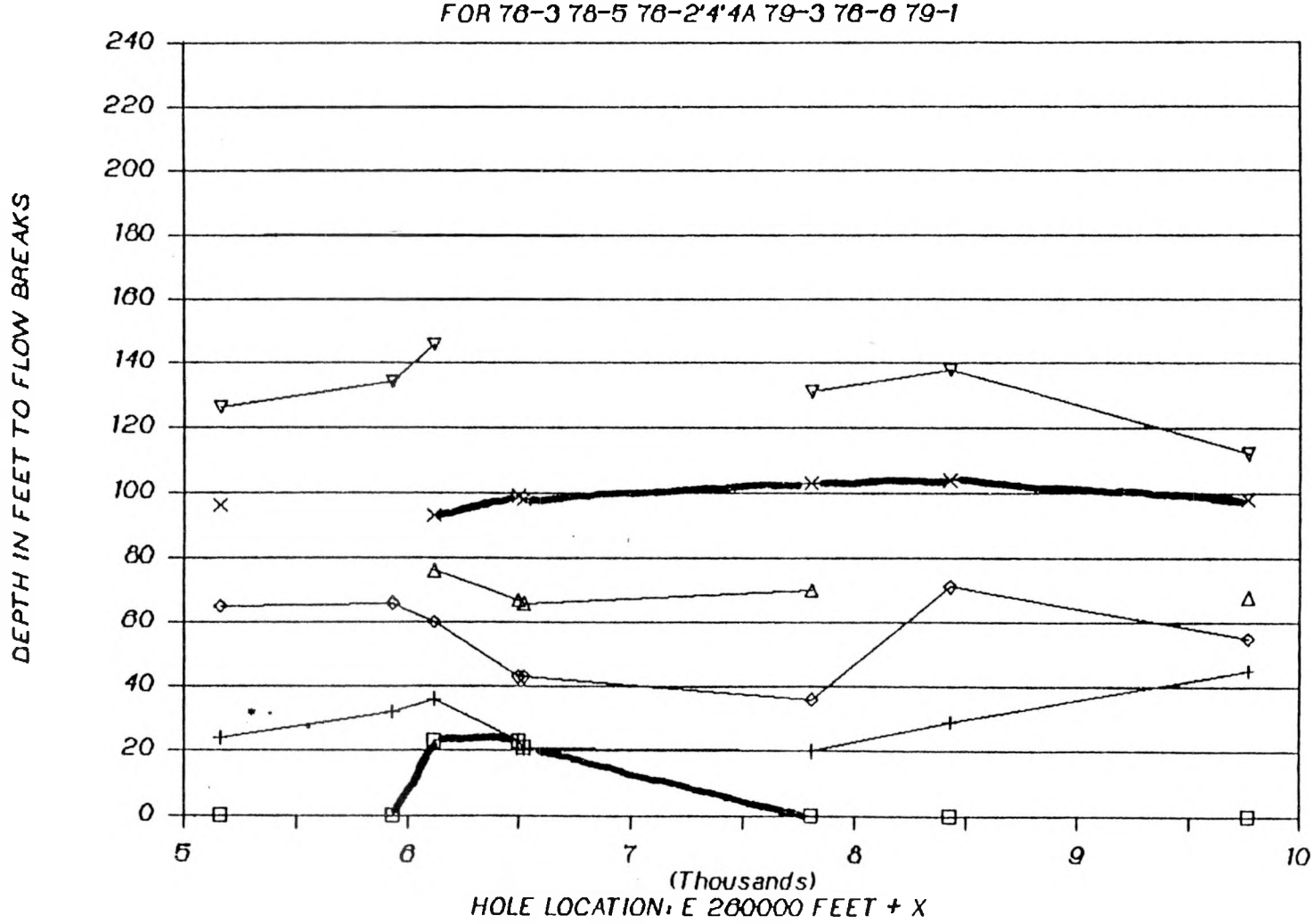

GRAPH 7. CORRELATION X-SECTION C-C′

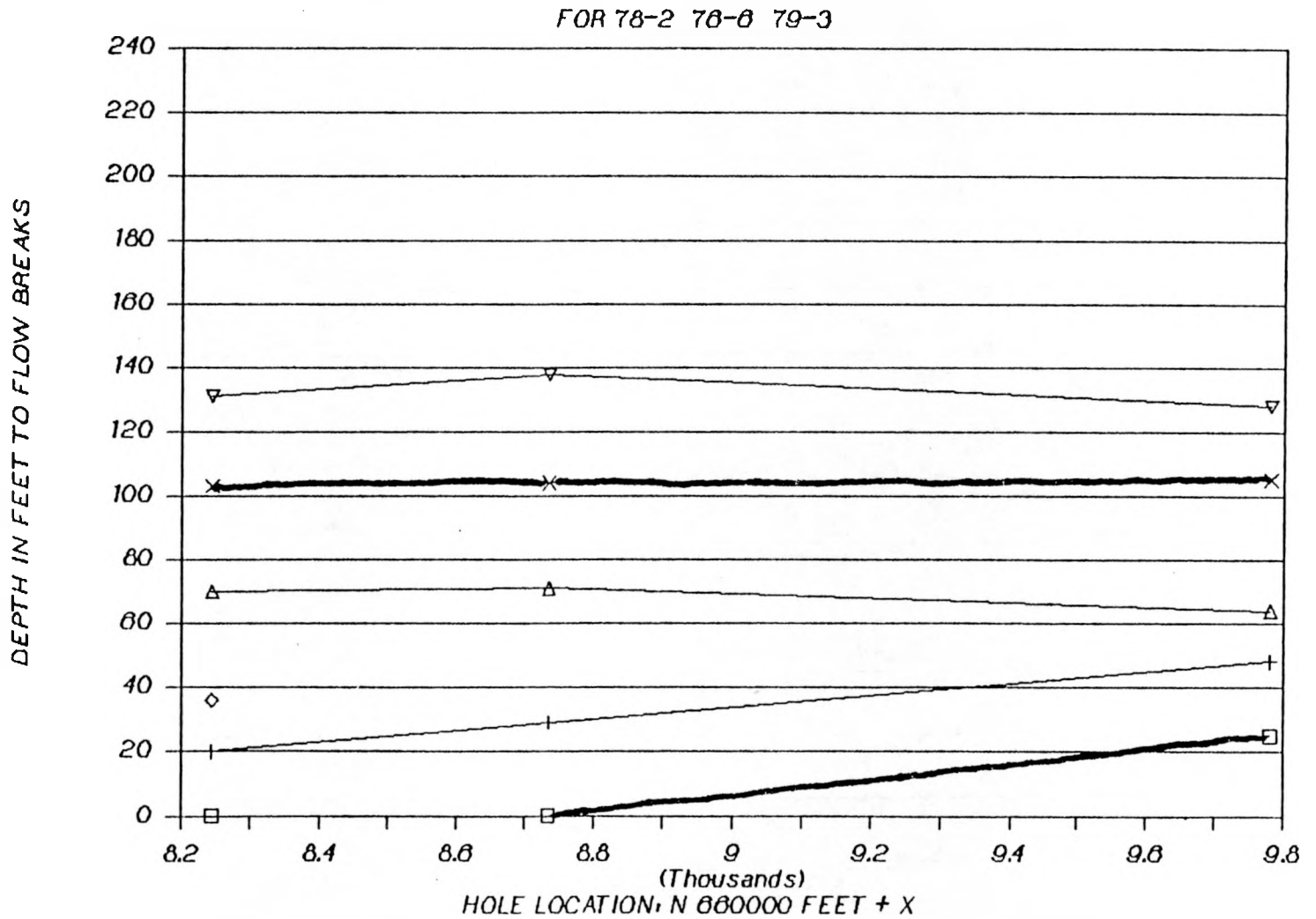

GRAPH 8. CORRELATION X-SECTION D-D'

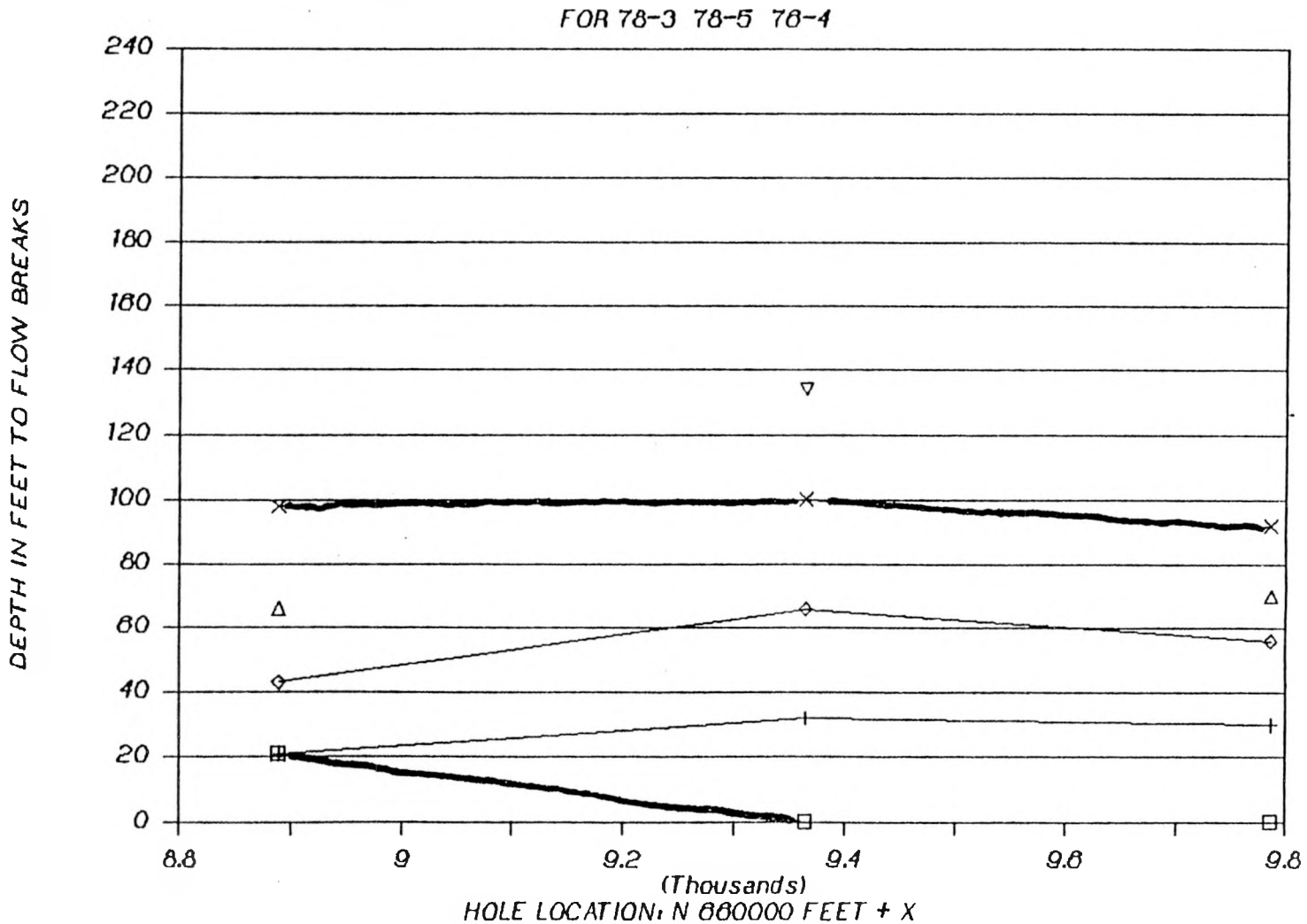

GRAPH 9. FLOW THICKNESS GRAPH ALONG A-A′

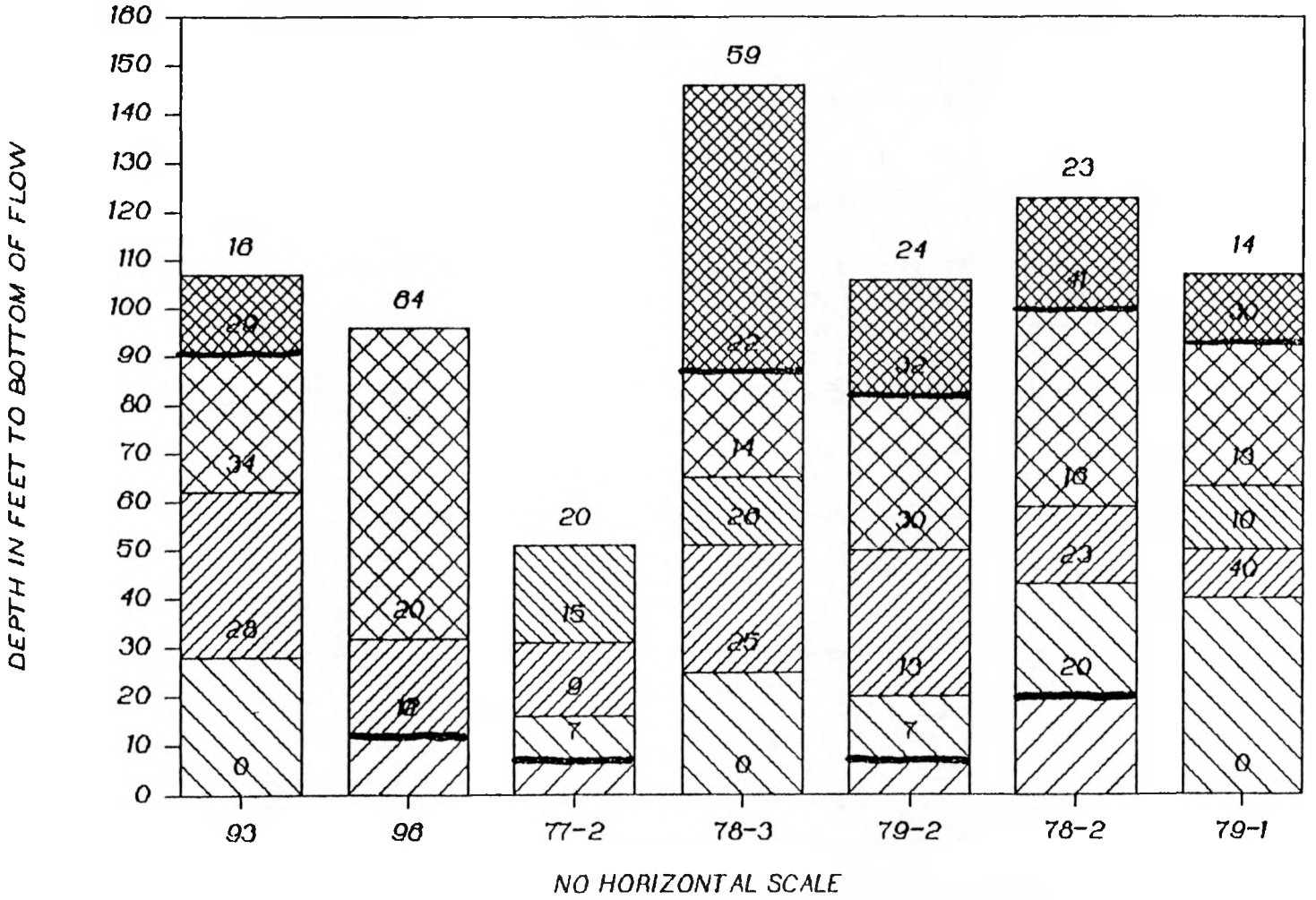

GRAPH 10. FLOW THICKNESS GRAPH ALONG B-B′

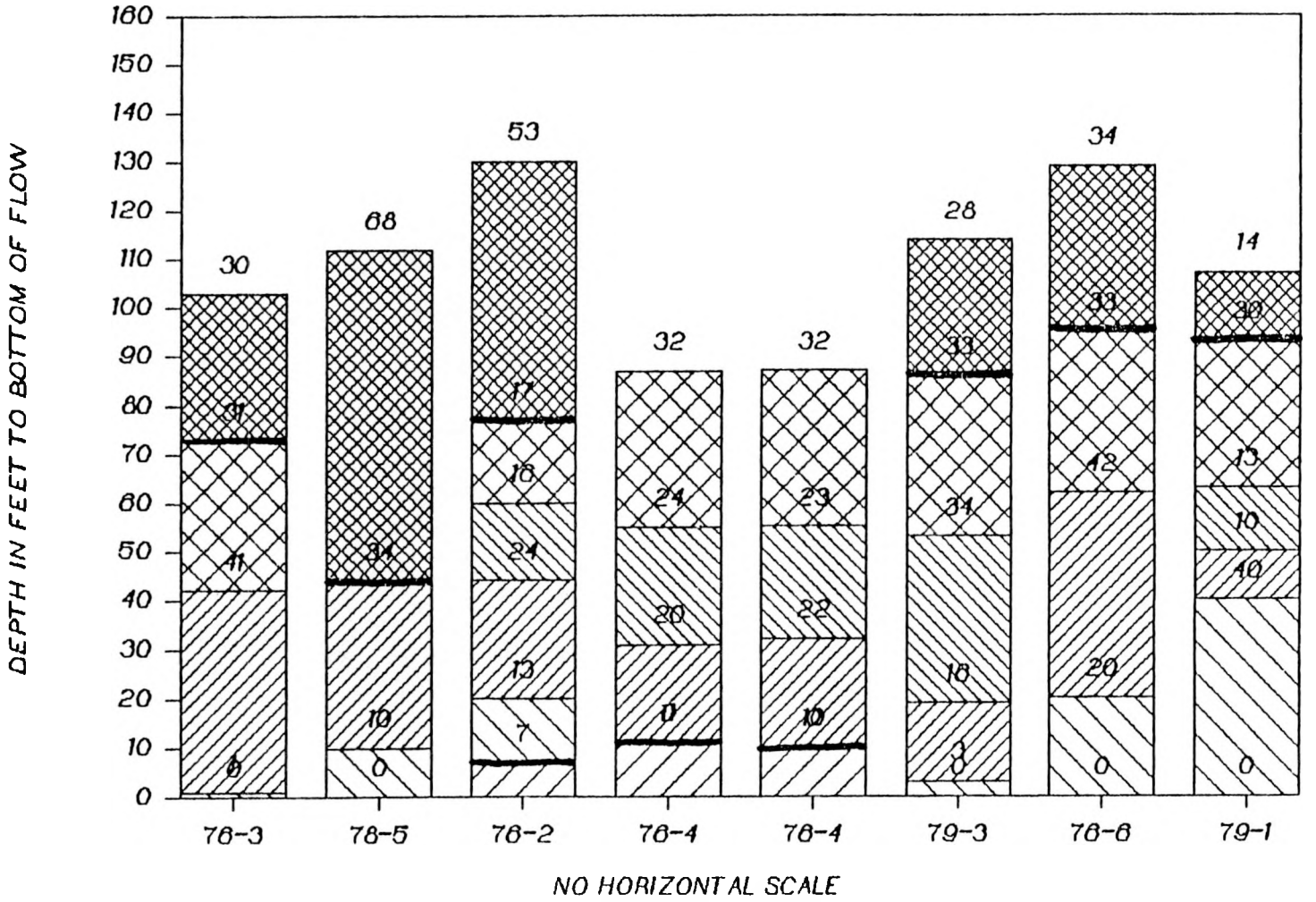

GRAPH 11. FLOW THICKNESS GRAPH ALONG C-C′

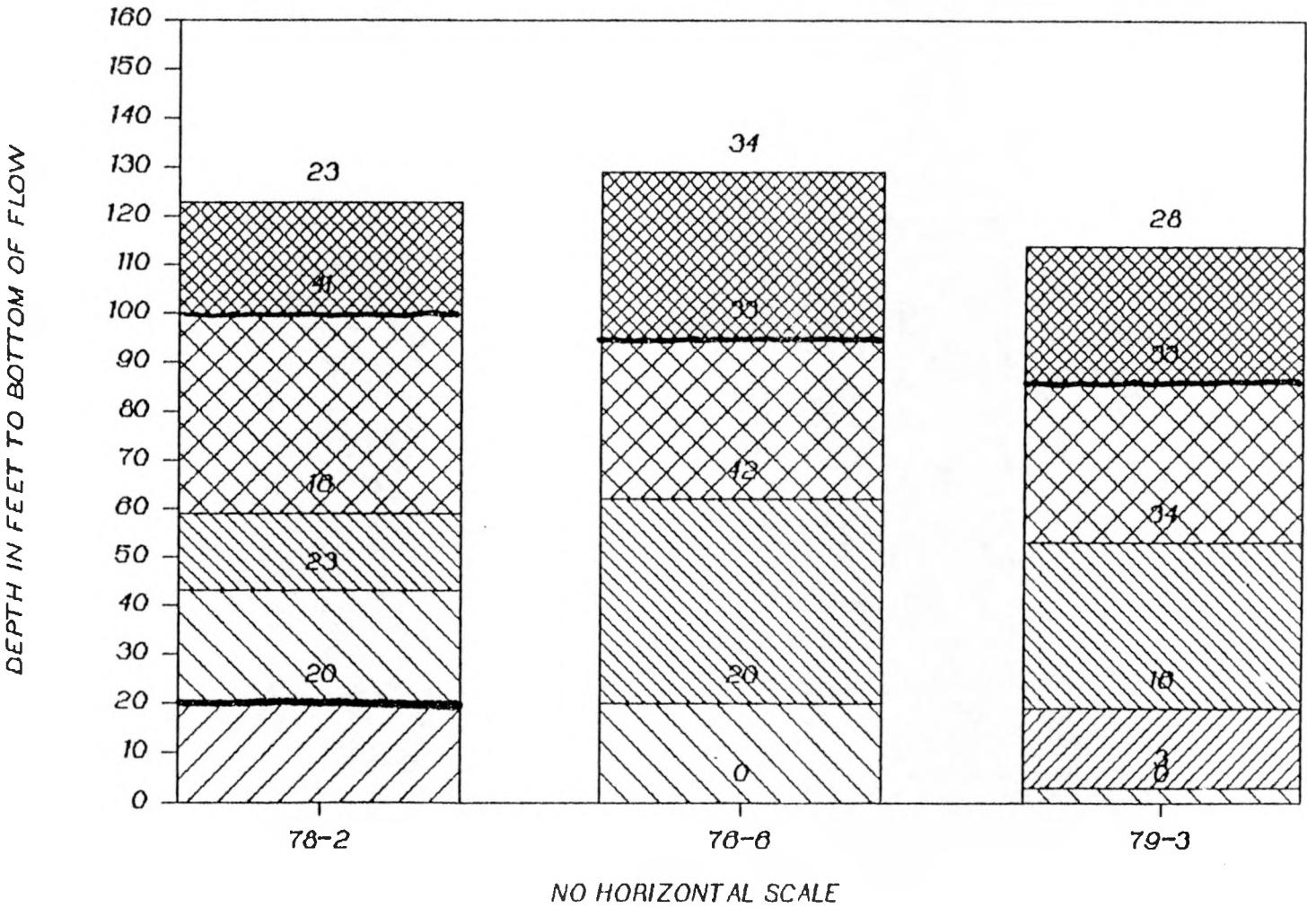

GRAPH 12. FLOW THICKNESS GRAPH ALONG D-D′

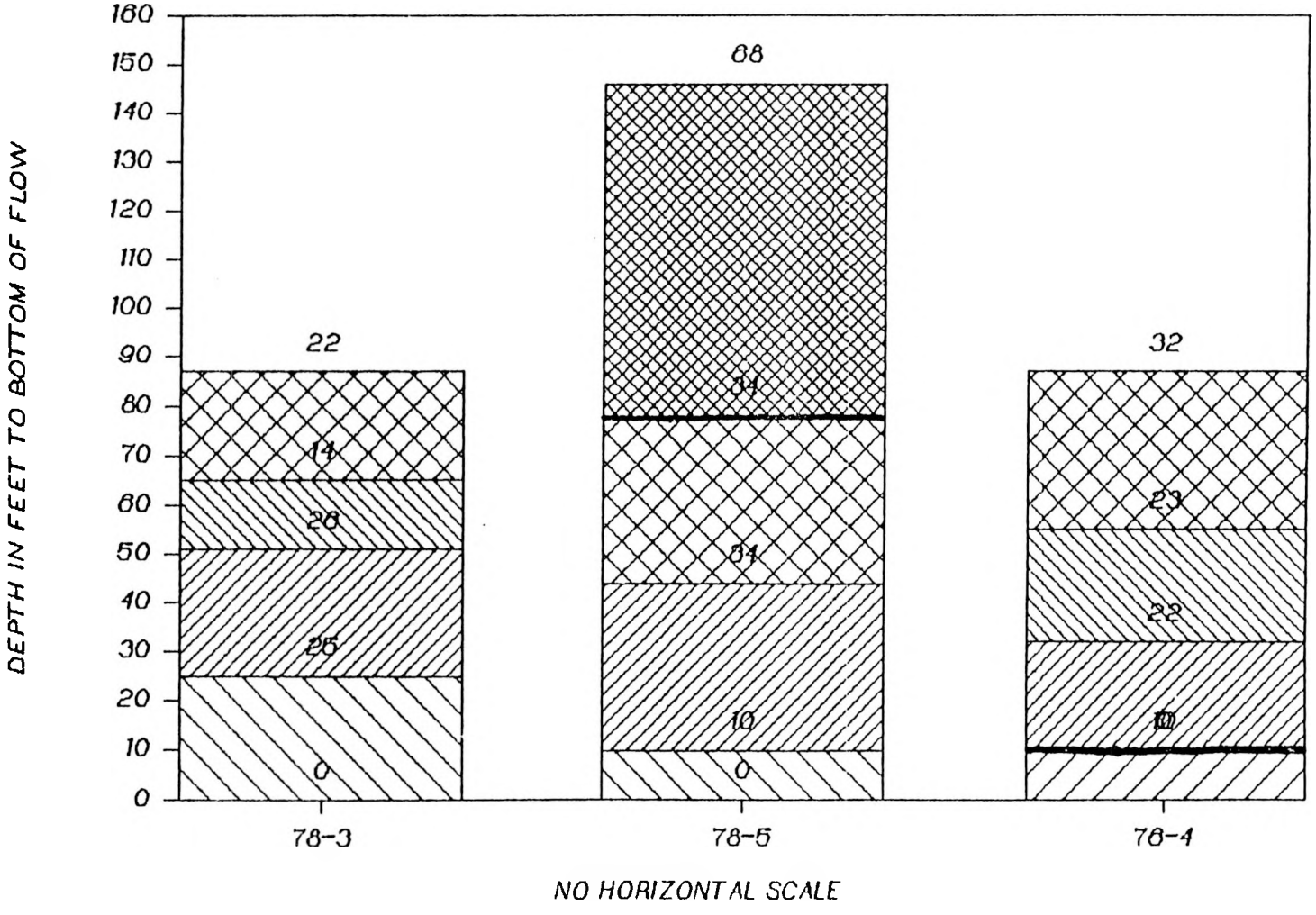

08-A/80

APPENDIX B

PHYSICAL AND PETROGRAPHIC VARIABILITY OF SNAKE RIVER PLAIN BASALT LAVA FLOWS BENEATH THE RADIOACTIVE WASTE MANAGEMENT COMPLEX AT THE IDAHO NATIONAL ENGINEERING LABORATORY

PHYSICAL AND PETROGRAPHIC VARIABILITY OF SNAKE RIVER PLAIN BASALT LAVA FLOWS BENEATH THE RADIOACTIVE WASTE MANAGEMENT COMPLEX AT THE IDAHO NATIONAL ENGINEERING LABORATORY

John C. Crocker

Published September 1989

Department of Geology
Idaho State University
Pocatello, Idaho 83209

CONTENTS

APPENDICES

LIST OF TABLES

LIST OF FIGURES

PHOTOMICROGRAPHS

1. INTRODUCTION.

The physical and petrographic characteristics of Snake River Plain (SRP) basalt lava flows beneath the Radioactive Waste Management Complex (RWMC) in the southwest portion of the Idaho National Engineering Laboratory (INEL) were examined. Macroscopic data were collected from core logs and samples removed from cores, and petrographic data were collected from standard thin sections. These data were used to describe the physical and petrographic characteristics of the lava flows.

This study defines the subsurface lava flow stratigraphy beneath the RWMC to a depth of about 150 feet. Within this stratigraphic framework the lithology and petrography of individual lava flows and of packages of lava flows is described. The relationships between characteristics observed in hand samples and thin section and the porosity and permeability of the basalt samples are also discussed.

1.1 Results.

All quantitative data and lithologic diagrams are found in the appendices at the end of the report, and in figures and tables within the text.

1.2 Terminology.

The following terms are used frequently in the text, and have specific meanings.

Lava flow or flow unit is defined as a single body of basalt that represents a single out pouring of lava from a vent. Such bodies of basalt have distinct upper and lower contacts and probably cooled as single cooling units.

Compound flows are multiple lava flows with poorly defined contacts between them. The flows erupted from the same source vent over a short period of time and cooled as a single cooling unit.

A flow group is defined as a collection of lava flows or compound lava flows that are bounded above and below by sedimentary interbeds.

A phenocryst is defined as any subhedral to euhedral crystal that is significantly larger than the surrounding ground mass. This definition is appropriate for both hand samples and thin sections. The intent is to make

the quantitative phenocryst percentages collected from thin sections readily used with hand samples.

The term porphyritic is only used when discussing samples where the largest, most prominent phenocrysts are plagioclase feldspar. The term is defined to eliminate the potential for confusion between samples that are porphyritic with large olivine phenocrysts rather than plagioclase.

Opaque is used in tables to denote those samples in which the groundmass of the rock is almost completely dark as a result of large quantities of opaque, iron-titanium oxide minerals. Such minerals are referred to collectively as opaque oxides.

Intergranular voids are those void spaces that occupy the areas between grains in the sample. The quantified value is a reflection of how open textured a sample is. Vesicles are not counted as intergranular voids.

2. NATURE AND SCOPE OF WORK.

The study area is shown in Figure 1. Only the cores indicated in the figure were examined and the applicability of the data beyond the area covered by the cores is unknown.

Approximately 2900 feet of basalt core from 15 wells were logged and sampled by J.P. O'Brien of the Idaho State University geology department prior to June 1989 and several hundred feet of core from additional wells were logged by R. P. Smith or C. F. Knutson. Core logs include depths to flow breaks, and information about vesicle sizes, percentages, and location. Also logged were fracture locations, orientations and fracture-fill materials. For details about the exact logging procedure see the sub-task report by O'Brien, 1989 (Appendix A.3 of main report). Data from the core logs and from hand-sample examination were used by the author to define a flow group and lava flow stratigraphy to a depth of about 150 feet beneath the surface at the RWMC.

Thin sections from 11 of the wells were examined for textural descriptions and to determine the quantitative percentages of phenocrysts and intergranular voids. This information was further used to determine the petrographic variability of flows and flow groups. The petrographic data were then compared with permeability and porosity data (Carroll Knutson, personal

communication 1989) to examine the relationship between porosity, permeability, and petrographic characteristics.

3. METHODS.

The nature of the data and methods of data collection are given. Criteria for the definition of flow groups and individual flows are also given.

3.1 Petrographic data collection.

Samples collected from the subsurface cores (O'Brien, 1989) were selected from 11 wells for preparation of 150 thin sections for petrographic examination. Quantitative phenocryst mineralogies and matrix percentages were determined by making counts of no less than 1000 points from 75 of the 150 thin sections. The subset was selected to include petrographic and mineralogic end members and representative samples from all flows.

Point counts of thin sections were made using a John Swift automated electronic point counter. Thin sections were impregnated with blue dyed epoxy to aide in void space identification. Point counts quantified phenocryst mineral, intergranular void space percentages, and total void space percentages for slides. Samples that were counted for total voids are noted in Appendix D with an asterisk.

Textures were noted for all 150 thin sections as were the maximum sizes of vesicles in the thin sections. Textural information includes the relationship between phenocrysts and groundmass and the textures observed for clinopyroxene. In addition, the maximum size of plagioclase and olivine phenocrysts were measured for each thin section.

3.2 Porosity and permeability data collection.

Porosity and permeability data (Carroll Knutson, personal communication, 1989) were measured for all samples that were thin sectioned. Permeability data are gas permeabilities and are always listed in millidarcys. Porosity values are always listed as percentages of rock volume. Permeability and porosity data were compared with the thin section petrographic data to assess relationships and to establish correlations between petrography, porosity and permeability.

3.3 Criteria for flow and flow group definition.

The following section discusses the definition of flow groups and criteria used for the correlation of flows within flow groups. Sources of data used for the definition of flow groups and flow correlation are from core logs, hand sample examination and thin sections. Also used were reports by Anderson and Lewis (1989) and Kuntz and others (1980). Both reports define flow groups in the same manner as will be used in this report.

3.3.1 Flow group definition.

As previously defined in the terminology section of this report, a flow group is enclosed by upper and lower bounding sedimentary interbeds or surficial sediment. Three interbeds establish the boundaries of the three flow groups in this study. These interbeds are located at depths of about 30, 100, and 220 feet beneath the surface in the study are. These interbeds are not always noted in the core logs of O'Brien (1989).

Where these interbeds are not noted in the core logs of O'Brien (1989) the following criteria were used to locate them. In most cases gaps between lava flows are present in the core logs at the levels where the interbeds were expected. If the basalt above and below these gaps was vesicular, scoriaceous, and oxidized (characteristics of flow tops or flow bottoms) the break was inferred to be the location of the sedimentary interbed.

The 30-foot interbed is everywhere associated with the uppermost flow group, and is noted in most of the core logs. The presence of a consistent gap in the core logs at the 30 ft depth, together with flow bottoms and tops on either side of the break were the criteria used to infer the presence of the 30 ft interbed.

In cores 79-1 and 96-A the 100-foot interbed is absent. For these two cores the location of the interbed was inferred from flow breaks beneath basal lava flows of a flow group. These two flow breaks occurred at the approximate level where the interbed was expected and the lithologies on either side of the break did not contradict the choices for flow group boundaries.

The 220-foot interbed is identified only in the core logs from wells 76-4A and 78-2 (O'Brien, personal communication, 1989); other wells do not reach sufficient depth. Thus, the total thickness of the flow group overlying the 220-foot interbed is poorly defined.

3.3.2 Criteria for flow correlation between cores.

Correlations of flows between cores are based on hand sample lithologies and on flow breaks at comparable levels. Within groups, the samples may be very similar in appearance and visual correlation using hand samples should not be the sole criterion for correlation of flows.

Within flow groups the number of flows present between the interbeds is fairly consistent and the flow breaks from the core logs can be correlated with few problems for the flow groups above the 100-foot interbed. Where correlations were possible with more than one flow break in another core, the break that most closely maintained the thickness of the flow was used. All correlations were then compared with the hand samples to check for possible problems in the stratigraphy.

Queried flow breaks in the core logs were used in correlation when they were consistent between wells. Those queried flow breaks that could not be correlated between wells were not included in the final stratigraphy and it is assumed that the flow they are found in may be compound or has a zone of oxidation within it.

3.4 Characteristics examined for variability within flow groups and individual flows.

Discussion of the variability within flow groups will include variation in 1) phenocryst mineral percentages; 2) matrix percentages; 3) intergranular void space percentages; 4) porosity and permeability values; 5) maximum vesicle sizes; 6) range of textures observed within a group and 7) thickness ranges within a group. Individual flow variability will include the above ranges of variability and the following data: 1) fracture density variability; 2) ranges in fracture orientation, and 3) fracture filling material. The end of each variability discussion will detail the important characteristics for the identification of that flow in hand sample and core.

4. Stratigraphy and petrography beneath the RWMC.

The following section is patterned after that used in Kuntz and others (1980). The format is efficient for conveyance of the pertinent data and especially suited to this paper which deals with the variability of the lava flows. All data, unless cited otherwise, is from the present study.

Basalts and sediments of the study area can be broken down into three lava flow groups that are separated by sedimentary interbeds. Textures of the flows across the interbeds are often very similar and identification of the interbeds therefore is crucial in establishing the group boundaries.

Figure 2 is a cross section of the RWMC along its northern boundary, showing the complete flow stratigraphy defined in this study. Flows are numbered according to the flow group they belong to and their position within the group. The uppermost flow of the second flow group is named 2-1. The next lowest flow is named 2-2, etc.

The interbed at 30 feet separates the first and second flow groups. The 30-foot interbed is present everywhere flow group 1 is present. Where flow group 1 is missing, the top of flow group 2 is covered by sediments.

The 100-foot interbed is present in all cores except 96A and 79-1. This interbed separates flow groups 2 and 3 from one another. In all other cores, the interbed is either noted in the logs or there is a break in flows across a gap in the core record at the 100-foot level.

4.1 Petrographic overview.

4.1.1 Minerals present.

Phenocryst compositions were not determined in this study. Mineral compositions are given in Kuntz and others (1980) and the reader is referred to that report.

Plagioclase:

Plagioclase feldspar is present in all samples as both a phenocryst mineral and as a constituent of the matrix. Plagioclase occurs as individual laths, crosses, radially arranged laths with interstitial olivine and equant crystals. Plagioclase is always subhedral to euhedral in form and the majority of the grains are elongated. Measurements indicate that the average plagioclase has length:width ratio no greater than 11:1.

Olivine:

Olivine occurs as both phenocrysts and as a constituent of the matrix. Phenocrysts are equant to elongated, with length:width ratios as great as about 2:1. Phenocrysts are nearly all subhedral.

Phenocrysts of olivine occur as individual grains, aggregates, and in association with plagioclase phenocrysts. Larger subhedral and euhedral phenocrysts are usually square, rectangular or rhombic in form.

Many olivine phenocrysts have opaque inclusions within them. These inclusions are blocky in shape and a spinel phase (Kuntz and others, 1980). Other olivine phenocrysts are completely free of inclusions. The presence or absence of inclusions is not consistent within any given flow.

Olivine of the matrix is always anhedral to subhedral. Small olivine grains are present as intergranular matrix components and also commonly as interstitial grains adjacent to plagioclase phenocrysts.

Clinopyroxene:

Clinopyroxene is almost exclusively an anhedral constituent of the matrix. Intergranular and subophitic textures are observed in all samples that are not opaque from oxide minerals. Where masses of clinopyroxene are large or where the grain size of the rock is fine, ophitic textures are observed. The development of ophitic and subophitic textures in the samples seems to be best developed in the mid-flow samples and the thicker flows.

In two samples clinopyroxene is present as phenocrysts. In sample F-6 and sample J-5 subhedral clinopyroxene is present. As a component of the rock, these samples have less than one percent clinopyroxene phenocrysts.

Accessory minerals.

Magnetite:

Square to rectangular magnetite grains are ubiquitous as matrix components in the samples. Most magnetite grains are <<0.5 mm in their longest dimension. Some magnetite grains were observed greater than 0.5 mm in some samples.

Glass:

Glass is not a major component of any of the samples examined. In samples from the tops and bottoms of flows, vesicles are lined with a thin opaque coating that is most likely devitrified glass.

Glass is present most often as small blebs within the oxides along vesicle walls. Glass is opaque under crossed polars and brownish in plain polarized light.

Others:

Ilmenite is present as a matrix component in most samples as small needles << 0.5 mm in length. Along vesicle walls ilmenite is common.

Apatite was noted as a possible accessory mineral by Kuntz and others (1980). The mineral was not observed in this study.

A "feathery" mineral was noted by Kuntz and others (1980). This mineral was also noted in samples of this study. The mineral occurred in association with opaque oxide linings in nearly all instances.

4.1.2 Textures in thin section.

Hand sample and thin section examinations of basalt samples show that there are two general textural types of lava flows in the three flow groups examined. Present in all groups are intergranular-equigranular flows. A typical example of the coarser grained variety of this texture is shown in photomicrograph 1. This sample is from flow 2-3 and shows a typically equigranular matrix with phenocrysts of olivine. Scattered throughout are large plagioclase phenocrysts. The texture is most clearly seen in hand samples where few phenocrysts of plagioclase are visible. Also from group three is photomicrograph 2, showing the fine grained variety of the intergranular texture. The fine-grained intergranular texture is commonly associated with the tops and bottoms of intergranular flows.

The porphyritic flows are restricted to flows of group 2. These samples characteristically have fine-grained intergranular groundmasses that are dark to light grey in color, with large laths of plagioclase feldspar, often reaching lengths greater than 4.0 mm. This texture is also vaguely observable in the tops of some flows in group 3. In these samples the porphyritic appearance is as much a function of the matrix grain size as it is the size of the plagioclase grains.

Within this textural class are two subdivisions which reflect the grain size of the matrix. In samples with a coarse-grained matrix the texture is defined as porphyritic-intergranular (photomicrograph 3). Those samples with a very fine-grained matrix or flow top samples that have basically opaque matrices are defined as being porphyritic-aphanitic. This texture is shown in photomicrograph 4.

PHOTOMICROGRAPHS OF REPRESENTATIVE TEXTURE

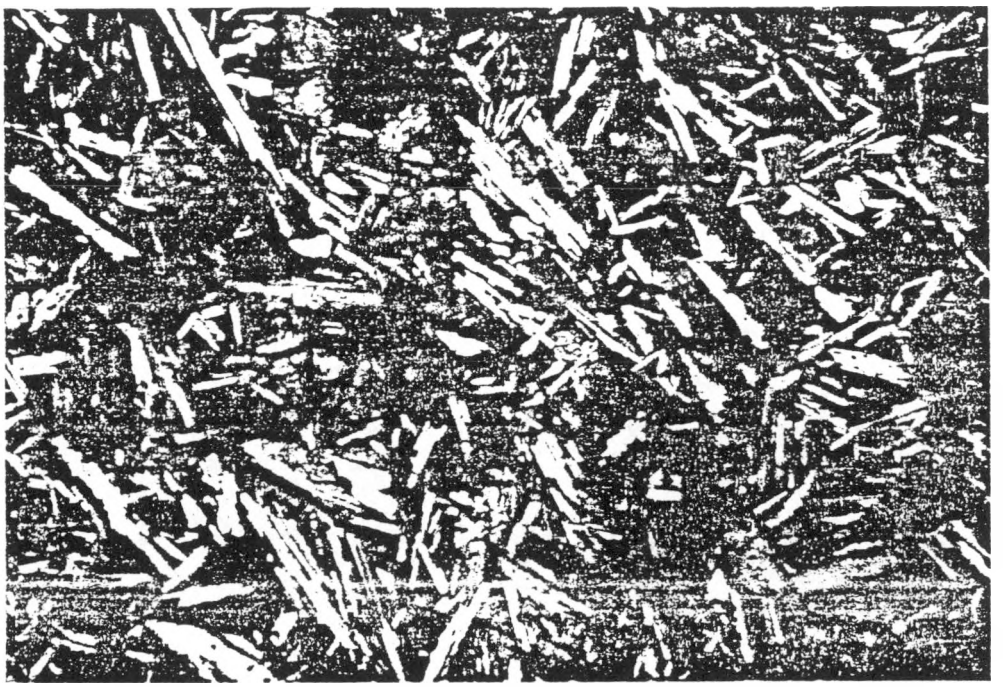

PM 1. Representative area of an intergranular-coarse sample. Long dimension of photograph is 4.0 mm. Sample is from flow 2-3.

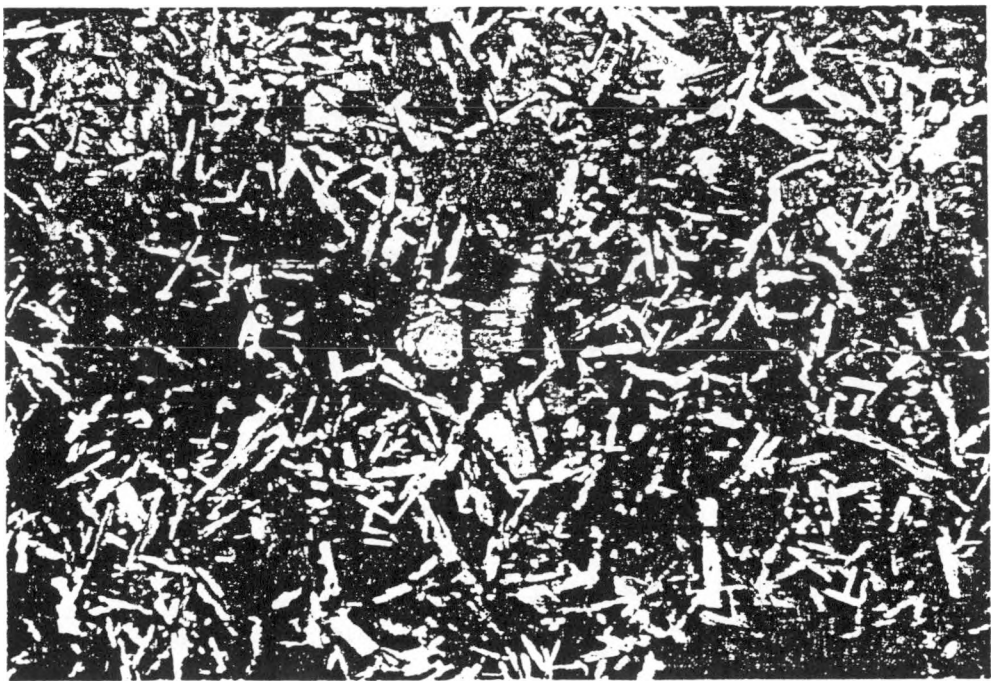

PM 2. Representative area of an intergranular-fine thin section. Long dimension of photograph represents 4.0 mm. Sample is from flow 3-3.

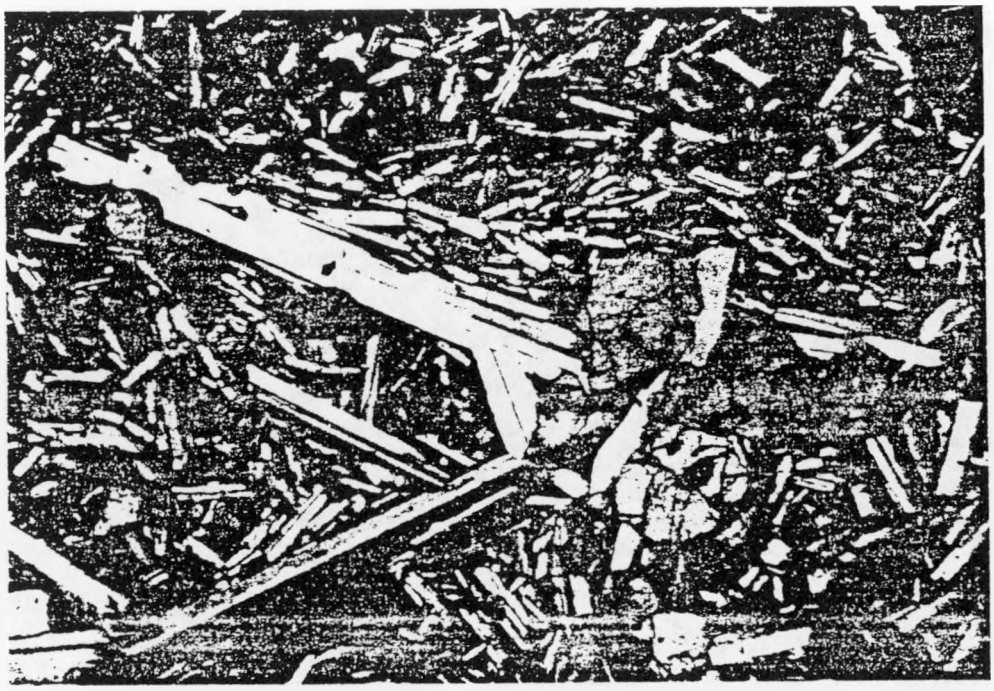

PM 3. Representative area of a porphyritic-intergranular sample. Long dimension of the photograph represents 4.0 mm. Sample is from flow 2-2b.

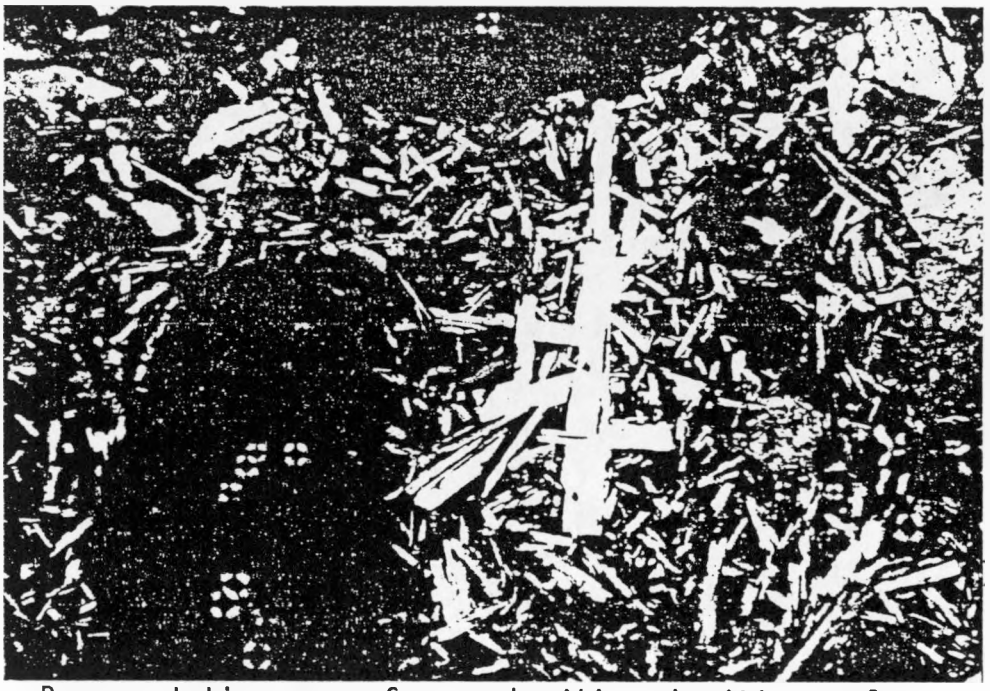

PM 4. Representative area of a porphyritic-aphanitic sample. Long dimension of the photograph represents 4.0 mm. Sample is from flow 3-2.

4.2 Lava flow descriptions.

The following section describes the hand sample and petrographic characteristics of individual flows within flow groups. Ranges in measured characteristics will be presented in tables at the end of each flow description to eliminate repetitive descriptions. The group variability discussion will be left until all flow data have been discussed to eliminate repetition.

The positions of flows are given in the lithologic logs of Appendix A. The correlation diagram from Kuntz and others (1980) is included in Appendix B for reference.

4.2.1 Flow 1.

Flow 1 is also flow group 1. This flow is the equivalent of flow 1 of group A in the stratigraphy of Kuntz and others (1980). Flow 1 is present at the surface or beneath the surficial sediments of the RWMC. The flow rests directly on the interbed located at a depth of about 30 feet beneath the surface.

In the stratigraphy of Kuntz and others (1980), two flows are present in group 1. In all but one core, group 1 is made up of a single flow. Flow 1a in the Kuntz and others (1980) stratigraphy is the lower of the two flows and is described as being heavily oxidized. Heavy oxidation is not present in any samples from flow 1 of this study and is the basis for the correlation with flow 1.

Flow 1 is restricted to the cores from the northern end of the site, and wells 76-4 and 76-4a. Anderson and Lewis show the distribution of flow 1 (Group A in the stratigraphy used in their study) and this is shown in Figure 3. The presence of this flow was not established until after all thin section samples were sent out. Thus, data discussed for this flow is from a limited number of observations and should not be considered representative of the flow's total variability.

In hand sample the flow is very fine grained to medium grained and light grey in color. The flow is of the equigranular textural type and phenocrysts are not a major component of the rock. Locally small olivine phenocrysts can be seen in the hand samples as aggregates and individual grains. The flow is never porphyritic in appearance.

As noted above, the flow is not heavily oxidized and where oxidation is observed it is limited to the vesicle walls and intergranular void spaces.

The flow is only lightly fractured in all cores and the fractures are at a low angle. Only a few fractures are logged as reaching to 60 degrees. Silt fracture filling is not heavy in any of the cores except for 76-4A. In this core silt filling is common and locally heavy.

In thin section, flow tops and bottoms are characteristicly fine grained and intergranular. Small unaltered phenocrysts of plagioclase and olivine are set in a dark, fine grained, intergranular matrix with much opaque oxides.

Mid-flow samples are intergranular-fine to intergranular-coarse textured and diktytaxitic. Plagioclase phenocrysts are usually individual laths, with only a few crosses and star-shaped aggregates present. Matrix plagioclase is < 0.5 mm in length and intergranular with olivine, clinopyroxene and opaque minerals. The largest plagioclase grains are found towards the middle of the flow.

Olivine phenocrysts of the mid-flow occur primarily as individual grains, and also in aggregates with matrix plagioclase and plagioclase phenocrysts. Matrix olivine grains are all <<0.5 mm in length and are intergranular with plagioclase and clinopyroxene. Where plagioclase phenocrysts form crosses small interstitial olivine grains are common.

Clinopyroxene of the matrix is intergranular and subophitic. Locally, ophitic textures are observed where large clinopyroxene masses are present.

Diktytaxitic texture is often well developed in mid-flow samples. Percentages of intergranular voids reflect the range of development of the texture. The range is listed in Table 1 as are all other ranges in measured values.

The best criteria for the identification of this flow is the presence of the 30-foot interbed at the flow base. Where the interbed is absent, this flow has the highest stratigraphic position and is present at the surface or beneath surficial sediments. The flow has few phenocrysts of olivine or plagioclase compared to other flows between the surface and the 220-foot interbed. The flow can be differentiated from flows of group 2 because it never has large plagioclase phenocrysts.

Table 1. Ranges and averages for measured values for flow group 1.

	GROUP 1		
	MINIMUM	MAXIMUM	MEAN
% PLAGIOCLASE (2)	2.7	2.5	2.6
% OLIVINE (2)	4.3	5.8	5.1
% MATRIX (2)	91.5	93.2	92.4
% VOIDS (2)	8.6	15.7	12.2
% POROSITY (8)	4.8	26.5	14.5
PERMEABILITY (8)	0.0	18.0	4.53
Maximum sizes in mm.			
MAX PLAGIOCLASE (8)	1.6	2.7	2.1
MAX OLIVINE (8)	1.15	4.15	2.0
MAX VESICLE (8)	3.6	5.2	4.5

Values in parentheses are total number of samples measured.

4.2.2 Group 2 flows.

Four individual flows are present in group 2. Two of the flows are identical in appearance and are part of a compound flow. Within the group, flows are defined by laterally correlative flow breaks between the 30- and 100-foot interbeds which define the group. Correlations within the group were facilitated by the differences in textures between the flows.

4.2.2.1 Flow 2-1.

In most cases, flow 2-1 is absent when flow 1 is present. The exception to this is in core 77-2 where both flows are found.

In hand sample flow 2-1 is light grey in color, fine to medium grained and equigranular. The upper part of this flow is not oxidized greatly and very closely resembles flow 1. From top to bottom of the flow there is a trend towards becoming more porphyritic in appearance. The increase in the porphyritic appearance is a result of an increase in the number of larger plagioclase phenocrysts.

Fracturing of this flow is moderate to heavy in all cores with no specific portion of the flow being more fractured than another. Most fractures are low angle (horizontal to 30 degrees) with a few fractures logged as reaching angles to 60 degrees. Silt fracture filling is found in all cores, but the majority of the fractures are logged as being free of silt filling.

In thin section the flow tops have an intergranular fine to porphyritic-aphanitic appearance depending on if there is a large plagioclase phenocryst present in the field of view. Phenocryst percentages in the flow tops are universally low and the matrix accounts for over ninety percent of the rock volume in some samples.

The matrix of the flow top samples is dark and has a high percentage of opaque oxides. Matrix plagioclase and olivine are all <0.5 mm in length and are unaltered. Clinopyroxene is only rarely present and occurs only as small oxidized intergranular grains when present. Except for the presence of larger phenocrysts of plagioclase and olivine, flow bottoms have the same texture as the flow tops.

Mid-flow samples have a coarse grained intergranular texture in thin section and are distinctly diktytaxitic in most samples. Thin sections show the same trend towards becoming more porphyritic towards the flow base.

The matrix of the intergranular portions of the flow are made up of intergranular olivine, plagioclase, intergranular to subophitic clinopyroxene and opaque minerals, all less than 0.5 mm in length. Ophitic clinopyroxene is present in most samples, but is not a major constituent of the matrix.

In the lower porphyritic portions of the flow the matrix is intergranular as described above and less diktytaxitic. Clinopyroxene is subophitic and intergranular in the matrix with the development of ophitic textures less common in this part of the flow.

Flow 2-1 can be identified by it's intergranular to porphyritic texture and position beneath the 30-foot interbed. The flow can also be identified by the fact that it rests directly on the top of the very porphyritic flow 2-2.

Table 2. Ranges in measured values for flow 2-1.

	FLOW 2-1		
	MINIMUM	MAXIMUM	MEAN
% PLAGIOCLASE (17)	6.4	24.5	14.6
% OLIVINE (17)	0.4	10.0	3.5
% MATRIX (17)	70.9	92.9	81.8
% VOIDS (17)	0.1	12.2	5.3
% POROSITY (22)	5.2	30.7	17.1
PERMEABILITY (22)	0.1	6.8	9.8
(Maximum sizes in mm.)			
MAX PLAGIOCLASE (22)	1.2	6.8	2.5
MAX OLIVINE (22)	0.3	2.1	0.9
MAX VESICLE (22)	2.8	11.2	5.7

Values in parentheses are the number of samples measured.

4.2.2.2 Flow 2-2.

Flow 2-2 is a compound lava flow in all cores except 76-3. In all other cores two flows (2-2a and 2-2b) make up the compound flow. The flows are separated by both definite and queried flow breaks. These breaks can be correlated between cores and the division into flow units in the stratigraphy was made to indicate the compound nature of the flow. In the following discussion, the flows will be treated as a single flow because they are essentially identical.

In hand sample flow 2-2 is distinctly porphyritic in appearance. The matrix of the rock is dark grey to purplish grey in color and aphanitic, with prominent plagioclase phenocrysts clearly visible. Locally, phenocrysts of olivine are present as individual grains and in aggregates. Individual grains of olivine as large as 1.5 mm were measured in hand samples.

Flow tops in both flow units are lightly oxidized. The oxidation lends a reddish tint to the hand samples. Below about 1 meter from the upper surfaces of the flow units, the color change is lost and oxidation is limited to vesicle walls and matrix voids. Fracturing of the flow is locally heavy and in these locations heavy silt filling is common.

In thin section, samples of flow 2-2 are either porphyritic-aphanitic or porphyritic-intergranular in texture. Porphyritic-aphanitic samples are from the tops of flows and the porphyritic-intergranular samples are from the middle of the flow.

As with the previously described flows, the samples from the flow tops have very dark matrices with high percentages of opaque oxides. The matrix is made up of opaque oxides, plagioclase, olivine, opaque minerals, and oxidized clinopyroxene. The matrix is intergranular and very fine grained in the flow top and bottom samples. With rare exception, clinopyroxene is intergranular in the flow tops.

In all samples, plagioclase phenocrysts occur as individual laths, in sub-parallel bundles, crosses and radially arranged crystals with ubiquitous interstitial olivine and clinopyroxene. The latter two textures are the most distinctive feature of flow 2-2 in thin section (photomicrograph number 3).

Olivine phenocrysts are present in all thin sections examined. Olivine occurs as individual grains in the matrix, aggregates and in close association with plagioclase crosses and radially arranged aggregates of plagioclase.

The matrix of the mid-flow samples is coarser grained than the flow top and flow bottom samples that were examined. The matrix lacks the significant opaque oxide presence seen in the flow top samples. The most important difference in the matrix is the presence of significant amounts of clinopyroxene in the matrix. Clinopyroxene is present in all mid-flow samples as intergranular grains. Approximately one half of the samples have significant amounts of subophitic clinopyroxene. Ophitic textures are not prominent in most samples and where present, represent the presence of a large isolated mass of clinopyroxene in the sample.

Phenocryst morphology is the same as in the flow tops and bottoms.

Flow 2-2 is easily identified in the samples examined. The porphyritic texture is diagnostic, as are the prominent crosses and radially arranged plagioclase phenocrysts seen in thin section. This flow is always situated between intergranular flows in the stratigraphy (either flow 1 or 2-1 and flow 2-3).

Table 3. Ranges in measured values for flow 2-2B.

	FLOW 2-2B		
	MINIMUM	MAXIMUM	MEAN
% PLAGIOCLASE (7)	9.0	21.4	16.6
% OLIVINE (7)	3.1	7.5	5.4
% MATRIX (7)	72.8	87.9	77.9
% VOIDS (7)	0.9	10.5	5.1
% POROSITY (9)	5.2	26.3	15.0
PERMEABILITY (9)	0.0	4448.0	414.0
(Maximum size in mm.)			
MAX PLAGIOCLASE (9)	2.3	5.8	4.4
MAX OLIVINE (9)	0.9	2.3	1.4
MAX VESICLE (9)	1.7	8.4	4.4

Values in parentheses are the number of samples measured.

Table 4. Ranges in measured values for flow 2-2A.

	FLOW 2-2A		
	MINIMUM	MAXIMUM	MEAN
% PLAGIOCLASE (7)	10.3	26.7	17.5
% OLIVINE (7)	2.3	8.2	5.3
% MATRIX (7)	69.8	87.4	77.2
% VOIDS (7)	0.0	13.9	7.6
% POROSITY (8)	4.6	32.4	16.5
PERMEABILITY (8)	0.2	18.0	5.0
(Maximum size in mm.)			
MAX PLAGIOCLASE (8)	3.2	6.3	4.3
MAX OLIVINE (8)	0.9	1.8	1.5
MAX VESICLE (8)	1.1	16.0	5.8

Values in parentheses represent number of samples measured.

4.2.2.3 Flow 2-3.

Flow 2-3 is present in all cores examined in this study and is a single lava flow. Flow 2-3 lies directly beneath flow 2-2 and rests directly on the 100-foot interbed where it is present.

Flow 2-3 is distinctly different from flow 2-2. In hand sample the flow is light grey in color and is very much equigranular and intergranular in appearance. Tops of flows are oxidized in hand sample and have a distinctive orange color. Vesicles in the oxidized flow top samples commonly have caliche in them.

In all core logs, flow 2-3 is moderately to highly fractured. No specific interval of the flow is more fractured than another. Fractures range from horizontal to angles as high as 60 degrees. In general, fractures are free of silt filling.

In hand sample this flow is vaguely porphyritic in the upper portions of the flow. This porphyritic appearance is not present in all hand samples, which may be a result of where the samples were taken from the core.

The matrix of the upper parts of the flow is very fine grained and phenocrysts of plagioclase are much smaller than in the lower part of flow 2-2. Olivine phenocrysts are present in the upper part of the flow and occur as individual grains and in aggregates that are as large as three or four mm in size.

In thin sections from the flow tops, opaque oxides make the matrix nearly completely dark. Clinopyroxene is present as intergranular grains that are oxidized. Plagioclase and olivine of the matrix are small (<0.5 mm), intergranular grains that are unaltered except for local oxidation on the crystal faces of olivine. The remainder of the matrix is comprised of amorphous, opaque oxides and opaque minerals.

Thin sections from the mid-flow samples reflect the intergranular texture that can be seen in hand samples. Most of the samples fall into the intergranular-coarse textural category. Plagioclase occurs primarily as individual laths and subparallel bundles; less frequently as crosses and radially arranged aggregates. Olivine is present as both individual phenocrysts and in aggregates. Olivine phenocrysts are commonly associated with plagioclase phenocrysts.

The matrix of the mid-flow is intergranular and made up of plagioclase, olivine, clinopyroxene and opaque minerals. Subophitic clinopyroxene is present in most samples and ophitic textures are well developed in about one half of the samples.

While samples from the flow bottom are finer grained than samples from the flow tops, the textures present are similar. The major difference between the two parts of the flow is the lack of well developed ophitic textures and an increase in the amount of opaque oxides. Oxidation may be apparent adjacent to vesicle walls.

Identification of flow 2-3 is ideally based on the presence of the 100-foot interbed. If the interbed is missing, textural similarity to flow 3-1 can make correlations difficult. Phenocrysts minerals of this flow are of different size than those of flow 3-1. Plagioclase is larger in flow 2-3 and olivine is smaller in flow 2-3. Aggregates of olivine in flow 2-3 are not as prominent as in flows of group 3.

Table 5. Ranges in measured values for flow 2-3.

	FLOW 2-3		
	MINIMUM	MAXIMUM	MEAN
% PLAGIOCLASE (8)	6.9	27.1	18.5
% OLIVINE (8)	4.0	6.0	5.1
% MATRIX (8)	67.4	89.1	76.5
% VOIDS (8)	2.2	16.2	9.2
% POROSITY (13)	7.6	25.9	14.9
PERMEABILITY (13)	0.2	39.5	33.1
(Maximum size in mm.)			
MAX PLAGIOCLASE (13)	1.3	6.9	3.3
MAX OLIVINE (13)	0.7	3.4	1.3
MAX VESICLE (13)	1.6	8.6	4.4

Values in parentheses are the number of samples measured.

4.2.3 Group 3 flows.

Flow group 3 is present in all cores examined in the study. Correlations have been made for the uppermost two flows of the group (3-1 and 3-2). Flows below this stratigraphic level have not been correlated with confidence because of large gaps in the core record. The lack of continuous core in adjacent wells makes flow correlations difficult.

The flow group is immediately beneath the interbed located at a depth of about 100 feet beneath the surface. Group three rests on a sedimentary interbed that is at a depth of approximately 220 feet. Only two cores contain this interbed (76-4a and 78-2).

Textures within the flow group are monotonous. Each flow is intergranular in appearance and have very few plagioclase phenocrysts visible in hand sample. Olivine phenocrysts are present as individual grains and in aggregates in all samples. Individual flows differ primarily in the average grain size of the matrix and the degree to which olivine phenocrysts are oxidized.

4.2.3.1 Flow 3-1

Flow 3-1 is equigranular and intergranular with textural classification ranging from intergranular-fine to intergranular coarse. In samples where larger plagioclase grains are present textures tend to be porphyritic-intergranular. Flow 3-1 is present in all cores with recovery from immediately below the 100-foot interbed.

In hand samples, flow tops are locally oxidized and orange in color. Samples with this color change commonly have silt and caliche as vesicle fill materials. Grain size in oxidized flow tops is very fine to aphanitic. These portions of the flow may be mildly porphyritic in appearance.

The mid-flow portions are fine to medium grained and have prominent individual grains and aggregates of olivine present in all samples. Olivine of flow 3-1 are larger than those in flow 2-3.

The matrix of samples from the bottoms of flows are aphanitic in hand sample. In these samples, the matrix of the rock is very tight. The color change observed in the flow top samples is not present in samples from flow bottoms.

In most cores, flow 3-1 is highly fractured throughout it's thickness. Fractures in flow 3-1 are almost free of silt.

In thin section, flow tops and bottoms usually appear dark due to the presence of much opaque oxides in the matrix. Diktytaxitic textures are not present because of the opaque oxides. The matrix of the flow tops is comprised of unaltered plagioclase, olivine, opaque minerals, and small intergranular grains of oxidized clinopyroxene. Olivine grains are locally oxidized along fractures surfaces and crystal faces in flow top and flow bottom samples.

In the mid-flow samples, the basalt is intergranular-fine to intergranular-coarse in texture. The matrix of the rock is diktytaxitic, equigranular and made up of plagioclase, olivine, and opaque minerals <0.5 mm in length. About one third of the samples examined have well developed ophitic textures. Intergranular and subophitic clinopyroxene is common in all mid-flow samples.

Plagioclase phenocrysts in mid-flow samples occur as individual grains, crosses, and sub-parallel bundles. Crosses commonly have small interstitial grains of olivine and are also associated with olivine phenocrysts.

Olivine phenocrysts occur as large individual grains in the matrix as well as in aggregates. In thin section these aggregates may take up the entire field of view at low power (approximately 5.0 mm). These large aggregates of olivine represent the greatest change in texture from flow 2-3 to flow 3-1.

Large aggregates of olivine are diagnostic of the group in general. Olivine phenocrysts of flow 3-1 are generally unoxidized which differentiates this flow from flows 3-3 and 3-4. This flow has smaller plagioclase grains than flow 3-2 which it rests directly upon. Differentiating flow 3-1 from 2-3 has been previously discussed.

Table 6. Range in measured values for flow 3-1.

	FLOW 3-1		
	MINIMUM	MAXIMUM	MEAN
% PLAGIOCLASE (12)	2.3	17.5	11.3
% OLIVINE (12)	2.0	8.9	5.0
% MATRIX (12)	76.9	95.7	83.8
% VOIDS (12)	10.0	12.0	10.2
% POROSITY (14)	10.0	33.1	17.0
PERMEABILITY (14)	0.1	1575.0	133.0
Maximum size in mm.			
MAX PLAGIOCLASE (14)	1.3	3.0	2.2
MAX OLIVINE (14)	0.8	4.0	2.3
MAX VESICLE (10)	1.7	8.1	4.0

Value in parentheses is the number of values measured.

4.2.3.2 Flow 3-2.

Flow 3-2 is an intergranular-coarse lithology in most samples examined. The notable exceptions are those samples that are very close to the flow tops. In hand sample, large aggregates of olivine stand out against a coarse grained matrix with plagioclase laths that can be easily identified with the unaided eye. The size and number of intergranular voids is noticeably greater in hand samples from flow 3-2. The larger plagioclase laths of the matrix lend a mildly porphyritic appearance to many of the samples from this flow.

While flow 3-2 has large plagioclase grains, the flow is not as porphyritic in appearance as flow 2-2. This is due to the smaller plagioclase size and the lighter colored matrix of flow 3-2.

Oxidation of the flow tops is present, but lacks a pronounced color change. In vesicular samples from the upper and lower parts of the flow there is a slight red tint to oxidized samples. Out of the vesicular zone, oxidation is limited to vesicle walls and in matrix voids.

In thin section, flow top and flow bottom samples have abundant opaque oxides present. Clinopyroxene in the flow tops is altered and limited to small, oxidized, intergranular, grains of the matrix. Plagioclase of the matrix is less than 1.0 mm in length for most grains. Matrix olivine is less than 0.5 mm in size. Diktytaxitic textures are present in the flow tops and bottoms, but are not well developed except in the mid-flow.

Mid-flow samples are intergranular-coarse for the majority of samples examined in thin section and all mid-flow samples are diktytaxitic. Plagioclase of the matrix is usually less than 1.0 mm in length and olivine of the matrix is less than 0.5 mm in size. Matrix clinopyroxene is generally subophitic and intergranular. Ophitic clinopyroxene is present in most samples but is not a dominant texture in most thin sections.

Plagioclase phenocrysts occur as individual laths, subparallel bundles, crosses and occasional radially arranged aggregates. Olivine phenocrysts are present as large individual crystals and in aggregates that can occupy the entire field of view at low power (approximately 5.0 mm). Phenocrysts of olivine are often associated with plagioclase phenocrysts of the samples.

Flow 3-2 can be differentiated from flow 3-1 by the coarser grained matrix of the rock, with plagioclase laths that are much more prominent. The

flow can be differentiated from flow 3-3 because olivine phenocrysts are not greatly oxidized.

Table 7. Range of measured values for flow 3-2.

	FLOW 3-2		
	MINIMUM	MAXIMUM	MEAN
% PLAGIOCLASE (10)	3.1	17.2	10.8
% OLIVINE (10)	0.2	10.9	5.0
% MATRIX (10)	75.0	96.7	84.2
% VOIDS (TOTAL) (10)	8.3	26.7	18.7
% POROSITY (13)	12.7	33.4	12.7
PERMEABILITY (13)	0.0	379.0	53.9
Maximum size in mm.			
MAX PLAGIOCLASE (13)	1.9	3.1	2.4
MAX OLIVINE (13)	0.7	3.7	2.2
MAX VESICLE (13)	0.5	13.0	4.8

Value in parentheses is the number of samples measured.
Total denotes that all void space vales measured are for total void space (vesicles and intergranular granular voids).

4.2.3.3 Flow 3-3.

Correlations of flow 3-3 between cores have been made with a low level of confidence. Because of the lack of continuous core and the basically generic intergranular texture of the flows of group 3, it is uncertain whether the correlations are correct. In their stratigraphic breakdown of the lava flows beneath the RWMC Kuntz and others (1980) show two flows at most in the interval between flow 3-2 and the 220-foot interbed. Examination of the core logs and hand samples show that at least four flows are present below flow 3-2 in some cores.

Because of the correlation problems, quantitative point counts were made of only two samples from the flow. These were made to check to see if there was any distinctive phenocryst mineralogy that might be used for correlation purposes. The point counts showed that the selected samples fall well within the range of diversity of the overlying flows in the group. More point counts were not made because of the correlation uncertainty.

Textures within the flow are much the same as in the flows above. In contrast to flow 3-2, this flow has a finer grained matrix; the decrease in the plagioclase size being the major contributor to the finer grain texture. The rock ranges from intergranular-fine to intergranular coarse-textured.

The upper parts of the flow are oxidized and have a distinctive orange color. Vesicles of these flow top samples have both clay and caliche as fill materials. Plagioclase is not an obvious phenocryst mineral in hand samples. Olivine occurs as large individual grains and in aggregates as in the flows described above. In this flow olivine phenocrysts frequently have a brassy appearance due to an oxidation on the surface of grains.

Flow bottom samples do not show the color change observed in the flow top samples. The most heavily oxidized samples from flow bottoms take on a rusty coloration. Grain size in flow bottom samples is aphanitic to very fine, and these samples are not pronouncedly diktytaxitic.

Samples from flow 3-3 were all examined for texture classification. All samples are intergranular in texture, with the majority being in the intergranular fine category. Some mid-flow samples were classified as intergranular coarse. Two samples from flow tops were very fine grained and should not be included in the intergranular-fine category. Photomicrograph number 5 shows an example of this texture.

Clinopyroxene of the matrix is more commonly ophitic in these samples than in those from flows 3-1 or 3-2. This reflects on the finer matrix grain size in these samples. Subophitic and intergranular clinopyroxene are common in all samples except for the heavily oxidized flow top samples. Olivine of the matrix is less than 0.5 mm in size as are the plagioclase grains of the matrix.

PHOTOMICROGRAPHS OF REPRESENTATIVE AREAS

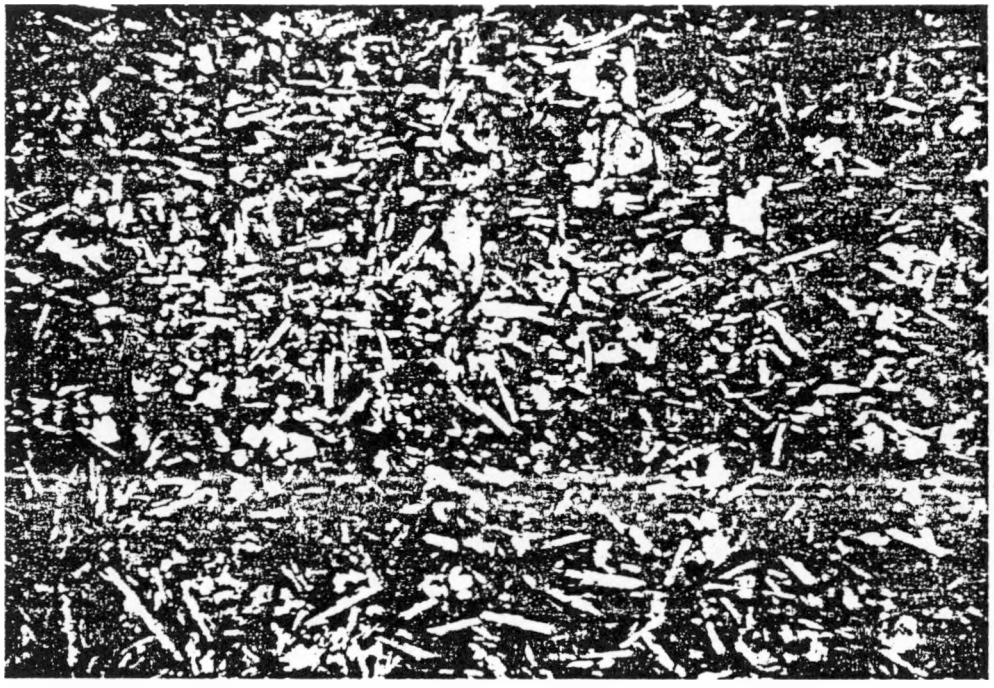

PM 5. Representative area of a very fine grained sample from near the top of a flow.

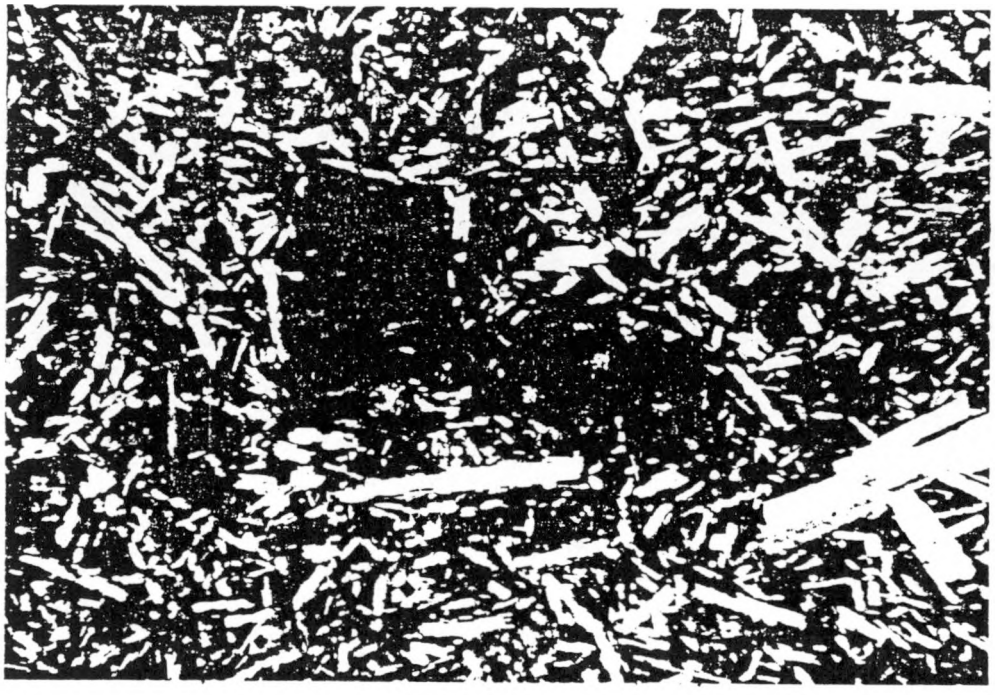

PM 6. Example of oxidized olivine phenocrysts found in flows 3-3 and 3-4. Long dimension of photograph represents 4.0 mm.

Diktytaxitic textures are well developed in mid-flow samples, and flow tops are partly diktytaxitic.

Plagioclase phenocrysts occur as individual laths, crosses and in subparallel bundles in the mid-flow samples examined. The average maximum size for plagioclase phenocrysts is 1.5 mm and ranges from 1.0 mm to 2.7 mm.

Olivine occurs as individual phenocrysts and in prominent aggregates as described above. Oxidation can be seen on the crystal faces and fractures of most phenocrysts. Locally, oxidation of the olivines is so heavy that their presence in the sample is known only because of the presence of a rhombic opaque mass. (Photomicrograph number 6). Olivine phenocrysts reach a maximum size of 4.3 mm in the samples examined. Average maximum size for olivine phenocrysts is 2.0 mm.

5. Discussion.

5.1 Flow group variability.

Within each of the flow groups all correlated flows have been described. Textures within any flow of a given group is consistent throughout the study area. Thus, the discussion will center on the variation of textures between flows within each group, the variation in thickness of each group and the mineralogic variability of the group.

5.1.1 Flow group 1.

Because of the limited distribution of flow group 1 and the incomplete recovery of the flow group in two of six cores, trends in lateral variation are difficult to define. The distribution of flow group 1 as shown by Anderson and Lewis (1989) is shown in Figure 3. This study finds flow 1 to be thickest in wells at the north end of the site. In wells 76-2 and 78-2 The group is 15.4 and 20.1 feet thick respectively. In wells 77-2, 76-4 and 76-4a, which are either in isolated pockets of the flow or on the very edge of the flow, the thickness ranges from 7.0 to 12.1 feet and averages 9.6 feet in thickness.

In all flows where upper and lower flow surfaces were recovered, oxidation is very light or completely lacking. Textures within the flow are consistently fine to medium grained and equigranular. No comment can be made

on the relationship between the grain size and the flow thickness because samples were not taken from the thickest flows and the thicknesses of other flows is not known. The thickness data for this and the other flow groups can be found in Appendix C.

5.1.2 Group 2.

Group 2 recovery is much more complete than either flow group 1 or flow group 3. The group is completely penetrated in all cores. Discussion of this group is most important because it represents the greatest range of textures and mineralogy of the three groups examined in the study. Problems that can arise in group definition are also discussed.

The most pronounced variations within group 2 are the changes in texture seen in the vertical section of the flow group. Flow 2-1 is an equigranular lithology that becomes vaguely porphyritic towards it's base. Flow 2-2 is pronouncedly porphyritic throughout it's thickness, with large plagioclase feldspar grains set in an intergranular matrix that ranges from dark grey to light grey with increasing matrix grain size. Flow 2-3 is vaguely porphyritic at the top of the flow and is equigranular towards the base. Textures within each flow of group 2 are laterally monotonous.

Thickness of the group is greatest in the wells along the northern end of the study area, and thin slightly to the south. From west to east the flow group thickens, thins and thickens again between wells 93a and 79-1. The thickest part of the flow group is in wells 76-6 and 79-1 which are both approximately 93 feet thick. In the wells west of 76-6 the minimum complete thickness is 62 feet.

The presence or absence of flow 2-1 in a given well does not seem to have any effect on the total thickness of the group. In those cores where flow group 1 is present, the group averages 72 feet in thickness. In the cores where flow group 1 is missing the thickness of group 2 averages about 67 feet in thickness. This difference is quite small when compared to the thickness variation possible within a single flow.

The limits of variability for phenocryst mineralogy is almost completely encompassed by flow 2. Plagioclase percentages range from 6.4 to as much as 27.1 percent. Olivine ranges from <1.0 to 10.0 percent. Average values for plagioclase and olivine in group 2 are 16.7 and 4.76 respectively. These

average values for phenocryst percentages are within 2.0 percent of the average values for each of the three flows of the group.

Maximum plagioclase size for group 2 ranges from 1.2 mm to 6.9 mm in length. Maximum olivine size ranges from 0.3 mm to 3.4 mm in the group. Average values for the maximum size of plagioclase and olivine are 3.6 mm and 1.2 mm respectively.

In flow 2-1 the average values for maximum length of plagioclase and olivine are 2.5 mm and 0.85 mm respectively. These values reflect the more intergranular nature of the flow. For flow 2-2a the averages for plagioclase and olivine maximum lengths are 4.3 mm and 1.5 mm respectively and reflect the porphyritic nature of the flow. For 2-2b the plagioclase and olivine maximum lengths average 4.4 mm and 1.4 mm respectively. The values for the two flow units of flow 2-2 help to show the similarity in characteristics between the two flows. In the intergranular flow 2-3 the average values for maximum plagioclase and olivine are 3.3 mm and 1.3 mm respectively.

Criteria for identification of flow group 2.

Two factors greatly help in the identification of flow group 2. First, the textural changes within the group are distinctive and consistent. Where the complete package is present, the change from an intergranular flow to a porphyritic lithology and back into an intergranular lithology is consistent and diagnostic. Second, the location of the bounding interbeds is fairly consistent in the study area.

If the bounding interbeds cannot be identified, problems might arise in the definition of the flow group. This is especially true when it is uncertain as to whether flow group 1 is present or not. It is possible that flow 2-1 might not be present in a core and the presence of the 30-foot interbed can not be confirmed. In this situation it would be very easy to mistake flow 1 for flow 2-1. This situation arose in the study and the presence or absence of flow 1 was then determined by the presence of gaps in the core logs at the 30-foot level associated with flow breaks, and comparison of the core logs with the flow- group stratigraphy of Anderson and Lewis (1989).

Identification of the flow group base relies on the identification of the 100-foot interbed. If the 100-foot interbed is absent, the base of the

first intergranular flow beneath the porphyritic flow 2-2 should be used. Differences in the sizes of olivine and plagioclase phenocrysts might be useful for differentiating the basal flow 2-2 from flow 3-1.

5.1.3 Flow group 3.

Individual flows of group 3 are laterally monotonous. Differences between adjacent flows within this group are subtle and reflect slight changes in the matrix grain size and the degree of oxidation of olivine. This discussion will deal with the flows that have been correlated with some degree of confidence. Phenocryst percentages for flows 3-3 and 3-4 will not be included in this discussion because of the complete lack of confidence in correlations between wells.

Flows 3-1 and 3-2 are both intergranular lava flows with prominent olivine phenocrysts that occur as individual grains and in aggregates in the fine- to medium-grained matrix. Average plagioclase and olivine phenocryst percentages for the two flows together are 11.2 and 5.0 percent respectively. In flow 3-1 the average percentages for plagioclase and olivine are 11.3 and 5.0 percent respectively. In flow 3-2 average values for plagioclase and olivine phenocryst percentages are 10.8 and 5.0 percent respectively.

Maximum plagioclase and olivine phenocryst sizes average 2.0 mm and 2.2 mm for the two flows. Flow 3-1 averages 2.2 mm for maximum plagioclase length and 2.3 mm for maximum olivine lengths. In flow 3-2 the average maximum lengths for plagioclase and olivine are 2.4 mm and 2.2 mm respectively. These two flows are identical in terms of their phenocryst minerals.

Thickness at the west and east end of the RWMC range from 52 feet thick in the west (core 93A) to 61 feet and 65 feet in the east (cores 79-3 and 78-2 respectively). In core 78-3 the flows total thickness is 80 feet.

The total thickness for the package of flows 3-1 through 3-3 is at least 127 feet in core 93A. In core 78-3 the package is 123 feet thick. In cores 78-2 and 79-3 the thickness of the package of three flows is 120 feet and 72.3 feet respectively.

The vertical variation within flow 3-1 and 3-2 is very minor. Flow tops and flow bottoms of these two flows are finer grained than the main body of the flows. Locally there is a porphyritic appearance to flow top samples where the matrix is aphanitic. There is no observed change in the olivine or

plagioclase phenocryst percentages. In flow 3-3 sequential samples were not all point counted so quantitative percentage variations from top to bottom of the flow can not be documented. However, hand sample examination does not show any obvious trend in the percentages of phenocrysts in the samples.

Group identification.

Identification of flow group 3 is best based on the presence of the 100-foot and 220-foot interbeds. Where the 100-foot interbed is not present in the cores, differences between flow 2-3 and flow 3-1 can be used. Flow 3-1 has larger individual and aggregates of olivine phenocrysts than flow 2-3, and flow 2-3 has larger plagioclase phenocrysts than flow 3-1. These differences in phenocrysts should be checked for across a flow break at approximately the 100-foot depth. Completion of the package of flows in flow group 2 as discussed above gives a good first choice for which flow breaks to check across.

5.2 Model flow.

The intent of this section is to show how the physical characteristics of a SRP lava flow vary within the study area.
Within the study area, each individual lava flow is homogeneous in terms of lateral variability. This is not surprising in as much as all of these flows appear to be far enough away from their source vents that no facies changes occur within the study area. Kuntz's (1980) statement that there is no evidence for there ever having been a volcanic vent within the RWMC supports this.

Core log examination shows that a typical flow beneath the RWMC may range in thickness from under 10 feet to over 40 feet. The tops and bottoms of the flows studied are usually vesicular, sintered, oxidized and frequently have silt within fractures and vesicles. Where two flows are in direct contact, the top of the lower flow may be highly oxidized and show a color change to a reddish or orange color.

Pipe vesicles are frequently noted in the core logs near the base of flows. Vertical vesicle trains and horizontal layers of vesicles are found in the dense parts of flows.

Figure 4 shows the variation in thickness of flow 2-3 in a northwest to southeast line of cores (96A, 76-2, 76-4A and 79-3). Also shown in the figure are the thickness of the vesicular zones in these flows, percent vesicles in flow tops and bottoms, maximum vesicle size in the vesicular zones and the fracture density within the vesicular zones and dense portions of the flows.

Fracture densities have been calculated for the 220 feet of logged core from well 78-2. These data are in Appendix A. All other lithologic logs in Appendix A have vesicular zone and thickness data only.

In Figure 4 the tops of the flows have been brought up to the same level so that thickness variations can easily be seen. A typical flow within the study area may double in thickness between adjacent cores. These thickness variations appear to be local in most individual flows. The variations in thickness probably result from flows filling in local topographic depressions.

Vesicular zones of a typical lava flow in the study area vary in thickness from flow to flow. There does not seem to be any correlation between the thickness of the lava flows and the thickness of the vesicular zones. In most flows the flow tops have the thickest vesicular zones and the largest vesicles. Vesicle size in the vesicular zones increases toward the base of the vesicular zones. Vesicularity increases toward the top of the vesicular zones in the flow tops. These trends are best seen in the core log columns for vesicle percentage and maximum vesicle size.

Flow bottom vesicular zones have the highest percentage of vesicles in the flow base and the largest vesicles toward the top of the vesicular zone. Most vesicular zones are less than three feet thick. Some flows, however, are essentially vesicular from top to bottom.

Fracture density in the flow tops in the cores of Figure 4 range from 1.3 fractures per foot to 2.3 fractures per foot. Fracture density of the mid-flow portion ranges from 0.3 fractures per foot to 1.1 fractures per foot. In the flow bottom fracture density ranges from 0.0 to 1.6 fractures per foot. The presence of vesicles reduces the competence of the basalt.

In all flows this general trend towards being more fractured in the vesicular zones is observed to varying degrees. At any given level in a flow there may be a rubble zone present. Frequently, these rubble zones and regions of increased fracture density are filled with silt, and may represent cooling breaks in compound flows.

Unfortunately, fracture orientations in the core logs provide limited information. Most fractures are nearly horizontal or have no orientations noted. Occasionally, fractures logged are as steep as 60 degrees from horizontal. In some flows, however, there are no fracture orientations noted at all.

5.3 Porosity and permeability of basalt samples.

Porosity and permeability data for the basalt samples thin sectioned is listed in the tables of Appendix D. Values for porosity range from under ten percent to over forty percent. Permeability values range from less than 0.005 millidarcys to nearly 5000 millidarcys. In the discussion to follow it has been assumed that the very high values of permeability are related to defects in the samples being tested. To avoid any problems with these extremely high values for permeability, the data set has been restricted to values no greater than 74 millidarcys, and for a given graph the range in permeability or porosity values have been restricted to the value ranges shown. The 74 millidarcy cut off was chosen because of the gap in permeability values below this value. The next lowest value is over 30 millidarcys less.

Figure 5 is a plot of all permeability (log axis) and porosity data received from EG&G (Carroll Knutson, personal communication, 1989) for permeability less than 100 millidarcys. From this graph it can be seen that no direct relationship exists between porosity and permeability. Further restriction of permeability values yield similar shotgun plots. This is true even for permeability values less than 1.0 millidarcy.

Point count-determined intergranular void percentages reflect the development of the diktytaxitic texture in a sample. Plots for all values less than 100 millidarcys show no correlation between permeability and development of the diktytaxitic texture. Figure 6 is a plot of intergranular void space percentage versus permeability for permeability less than 1.0 millidarcys. The straight line on the graph is the best fit straight line to the data generated by the statistics package SPSSX. While a general trend of the data can be seen in the graph no conclusions can be drawn from it.

Figure 7 is a plot of total void space (vesicles and intergranular voids) percentage versus permeability. Total void space data are from thin

sections point counted for total voids and thin sections with no vesicles. In this graph a general trend can be identified between total porosity and permeability. This is especially true for the nonvesicular samples (open circles). A good deal of scatter, however, is still present in the plot. The four data points near the center of the graph with void space percentages greater than 20 percent indicate that thin sections may not be representative of samples with porosities greater than 20 percent.

Figure 8 is a plot of measured porosity versus total voids. The line passing through the origin has a slope of one and is the theoretical slope of the plot if thin section determinations of total void space perfectly predicted rock porosity. Nearly all points plot above this line and show that point count porosity values consistently underestimate the actual porosity of the rock. The underestimation of porosity by thin section is expected. The plain of the thin section slide will, most often, cut a vesicle off short of its maximum diameter. Thus, the apparent diameter of the vesicle will always be smaller than the actual diameter, causing the underestimation of porosity.

Figures 9 and 10 are plots of measured porosity and intergranular void space. The former is for measured porosity less than 15 percent. The second of the two plots is for values of measured porosity less than 20 percent. Intergranular void space seems to be the major component of the rock porosity for porosity values less than about 15%. For values of porosity above 20%, considerable scatter is introduced.

5.4 Petrographic controls on basalt permeability.

From the discussion above it is apparent that porosity and permeability do not have any direct relationship in the basalt samples examined. From the porosity measurements it is known that all samples have some known percentage of void space. In some samples these voids are not connected. An example is sample A-18 which has a measured porosity of 26.0 percent and permeability less than 0.005 millidarcys. Examination of the data in Appendix D shows that the opposite case is also true.

The plot of intergranular void space versus permeability shows that the development of diktytaxitic textures is not the primary control over basalt permeability in all samples. Examination of hand samples and thin sections

show that the matrix of samples with very high permeability may be either tight or open textured.

Thin section examinations of the samples shows that the walls of vesicles in those samples with high (>74 millidarcys) permeability may or may not be coated with opaque oxides. Glassy walled vesicles were not observed in the samples.

The average of the maximum vesicle size measured in thin sections is 6.1 mm for samples with permeability higher than 74 millidarcys. The average maximum vesicle size for those samples with lower permeability is 4.6 mm. In general, vesicles of the very high permeability samples are irregular in shape and are connected together by small holes in their walls. These observations were made on hand samples; this type of three dimensional examination cannot be made of thin sections.

In the lower permeability samples the vesicle form tends to be more rounded. The connecting holes in vesicle walls have been noted in some of the lower permeability samples.

The measured porosity of the lower permeability group is less than that of the high permeability group. This, and observations just discussed, imply that the high permeability group has vesicles spaced close enough together that high permeability paths through the samples are established between vesicles. In the lower permeability samples the vesicles are spaced far enough apart that connections are not continuous through the samples.

Thin sections were not useful in predicting the permeability of a given sample. The main problem is that the thin section is essentially a two dimensional view of the sample. How interconnected the void spaces in the basalts actually are is a three dimensional quality of the rocks that the thin sections cannot show.

The development of diktytaxitic textures are not homogeneous within a sample. This is especially true for areas adjacent to vesicles where the matrix of the basalt is often very tight. Even in dense samples the distribution of matrix voids tends to be localized. These data agree with the data in Figure 7, which show the greatest scatter of points for vesicular samples. Scatter of points in the data set for dense samples is attributed to inhomogeneous development of diktytaxitic texture in the samples. This localized development of diktytaxitic texture may limit the application of

thin sections in some slides. More non-vesicular samples need to be point counted to determine if the trend of points shown by the dense samples is consistent. Further examination of thin sections and hand samples is also called for to assess the role vesicles play in the development or destruction of diktytaxitic textures.

For those samples with permeability < 0.005 millidarcys, there are essentially no intergranular voids present. This can best be seen on the cut surfaces of the hand samples. In these samples, porosity may be as great as 26 percent, but the vesicles are isolated from each other by the tight matrix between them.

Above these essentially zero permeability values, no clear relationship can be found between the petrography of the samples and their permeability. Samples of similar texture and vesicularity may have very different permeabilities. The development of diktytaxitic textures are different for samples with similar permeabilities. The same is true for samples of all degrees of vesicularity.

6. Conclusions.

From the data collected for this report the following conclusions can be made:

1) Flow groups may have similar textural characteristics for all flows (group 3), or may show distinct textural variations between flows (group 2).

2) Within any given flow, textures may vary from top to bottom, but the vertical trends are laterally continuous.

3) The range of phenocryst mineral percentages for flows within a group are all similar and any one flow may reflect the range of variability for the group.

4) Phenocryst mineralogies between groups may be similar and are not diagnostic.

5) Changes in the maximum sizes of phenocrysts may be diagnostic of flow group boundaries.

6) Textural similarity between adjacent flows within a flow group make continuous core necessary for confident correlations of individual flows. This is especially true for the flows beneath the 100-foot interbed.

7) For samples with total porosity of less that 15 percent, intergranular void spaces account for most of the porosity in a sample and can be used as approximations of true porosities.

8) Samples with porosity as great as about 25 percent can be estimated by thin section point counts for total void space. These values almost always underestimate the total porosity of the rock. A clear relationship between vesicle size and when a thin section is no longer representative of a basalt sample has not been determined.

9) None of the measured characteristics of the basalt samples is predictive of how permeable a sample will be. Only dense samples with very poorly developed diktytaxitic textures give consistent prediction of essentially no permeability for a sample. For dense thin sections, permeability predictions may be possible using intergranular void space percentages. More samples need to be point counted to test the correlation between intergranular void space and permeability implied by the trend seen in Figure 7.

10) Scatter in the plots of porosity versus total void percentages indicate that thin sections may not always be representative of the sample used for porosity and permeability measurements.

11) The development or destruction of diktytaxitic textures may be related to the presence of vesicles in the basalt. Further thin section and hand sample examination will be required to address this hypothesis.

7. Epilogue

The relationships between porosity, permeability and the petrographic character of basalts from beneath the RWMC are complex. Some very general trends have been identified in the study. More thin sections need to be point counted for intergranular void space percentages and total void space percentages for specific populations based on vesicle size and development of intergranular void space in the rock.

Time limitations for manuscript preparation did not allow for point counting very many thin sections after receipt of the porosity and permeability data. Further investigation is suggested and may prove to be more productive now that a porosity and permeability data base are available for the thin sections.

Other areas that should be investigated further is in the development of methods that more clearly identify individual lava flow and flow groups. Discussions of the flow and flow group variability highlight the differences between the groups and individual flows. In the field, where exposures may be poor, it would be extremely difficult to locate the stratigraphic position of an exposure from hand sample or thin section. Some form of geochemistry may be the best method for identification of flows and flow groups in the area of the RWMC.

REFERENCES CITED

Anderson, S. and Lewis, B., "Stratigraphy of the Unsaturated Zone at the Radioactive Waste Management Complex, Idaho National Engineering Laboratory, Idaho", USGS Water-Resources Investigations Report 89-4065, 1989, p. 54.

Kuntz, M., Dalrymple, G., Champion, D. and Doherty, D., "An Evaluation of Potential Volcanic Hazards at the Radioactive Waste Management Complex, Idaho National Engineering Laboratory, Idaho", USGS Open File Report 80-388, 1980, p. 63.

O'Brien, J.P., Unpublished contract report to EG&G Idaho, Inc., 1989, np.

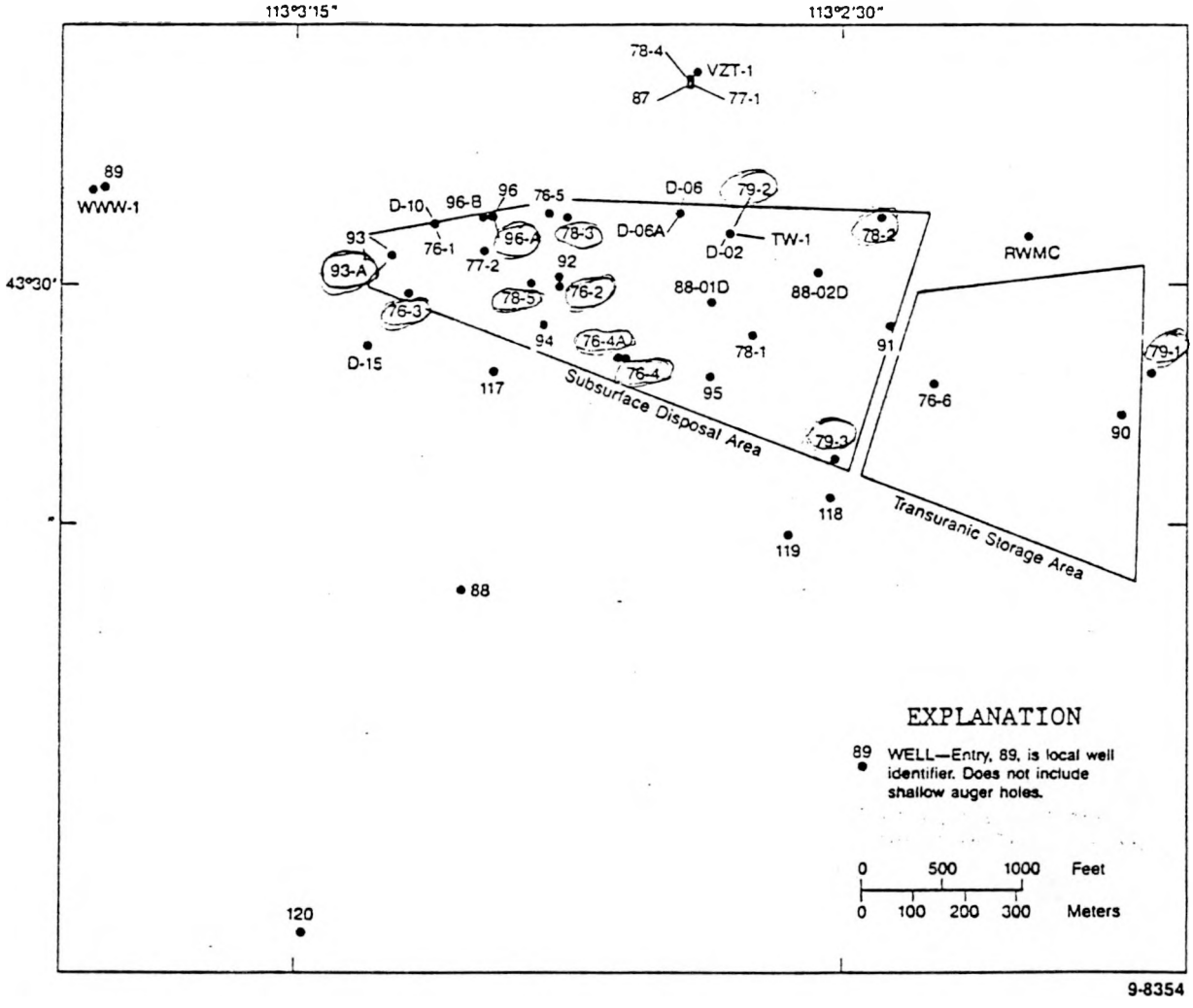

Figure 1. Location of wells at the Radioactive Waste Management Complex (from Anderson and Lewis 1989).

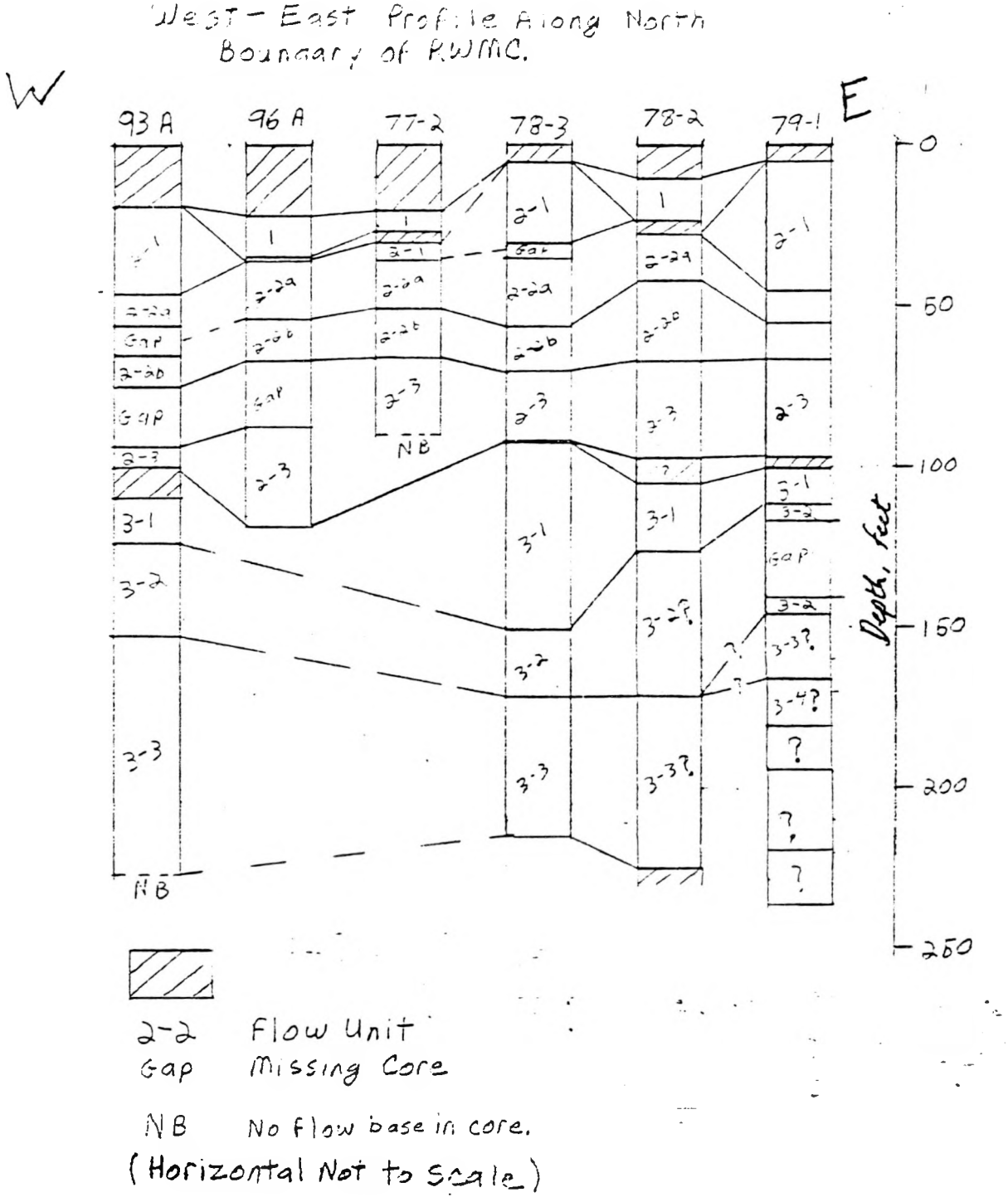

Figure 2. Stratigraphy of RWMC (see Figure 1 for well locations).

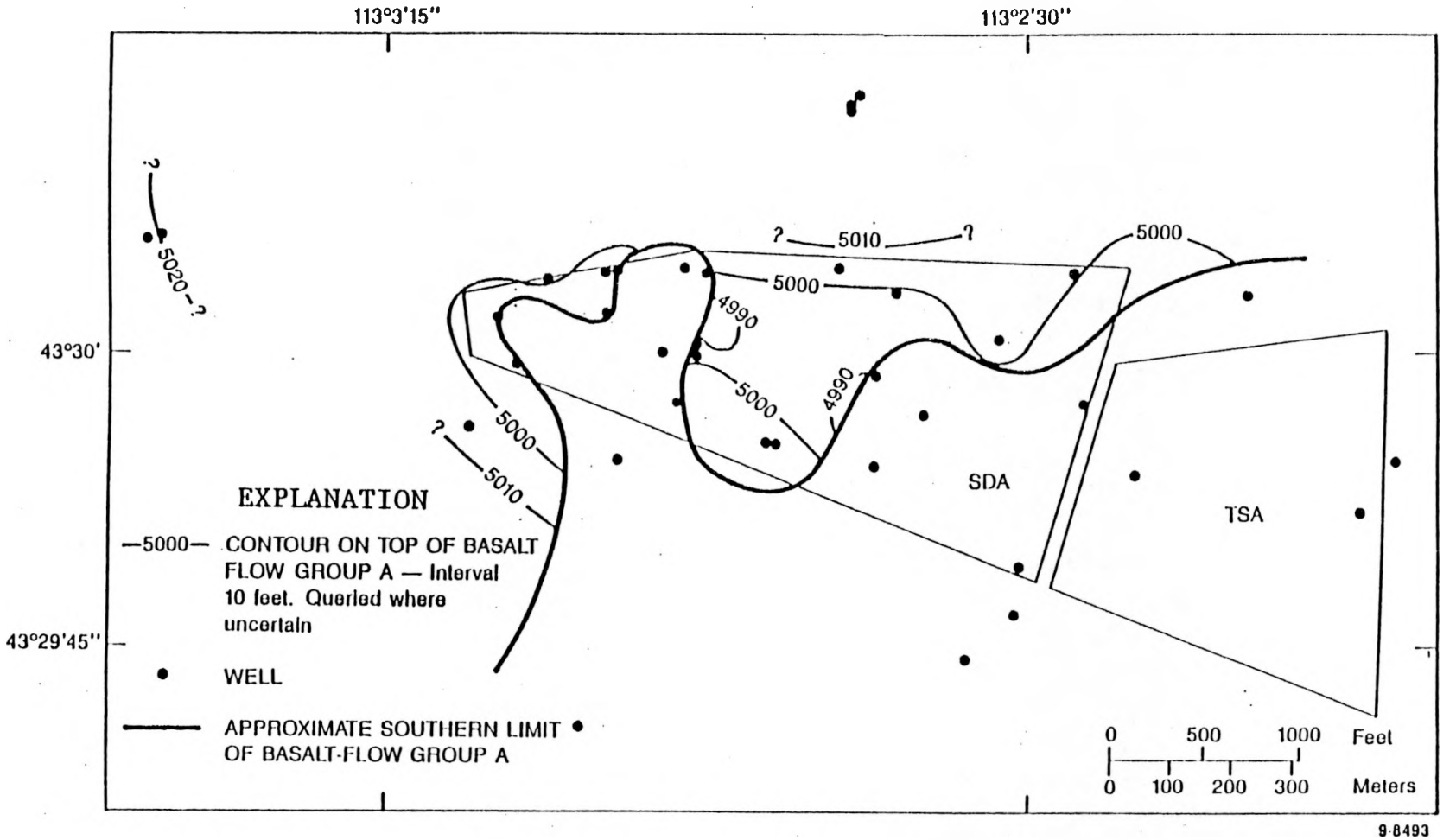

Figure 3. Altitude of the top of basalt-flow group at the Radioactive Waste Management Complex (modified from Anderson and Lewis, 1989)[a]

a. Flow group A in this Figure is Flow 1 of the stratigraphy proposed by this study.

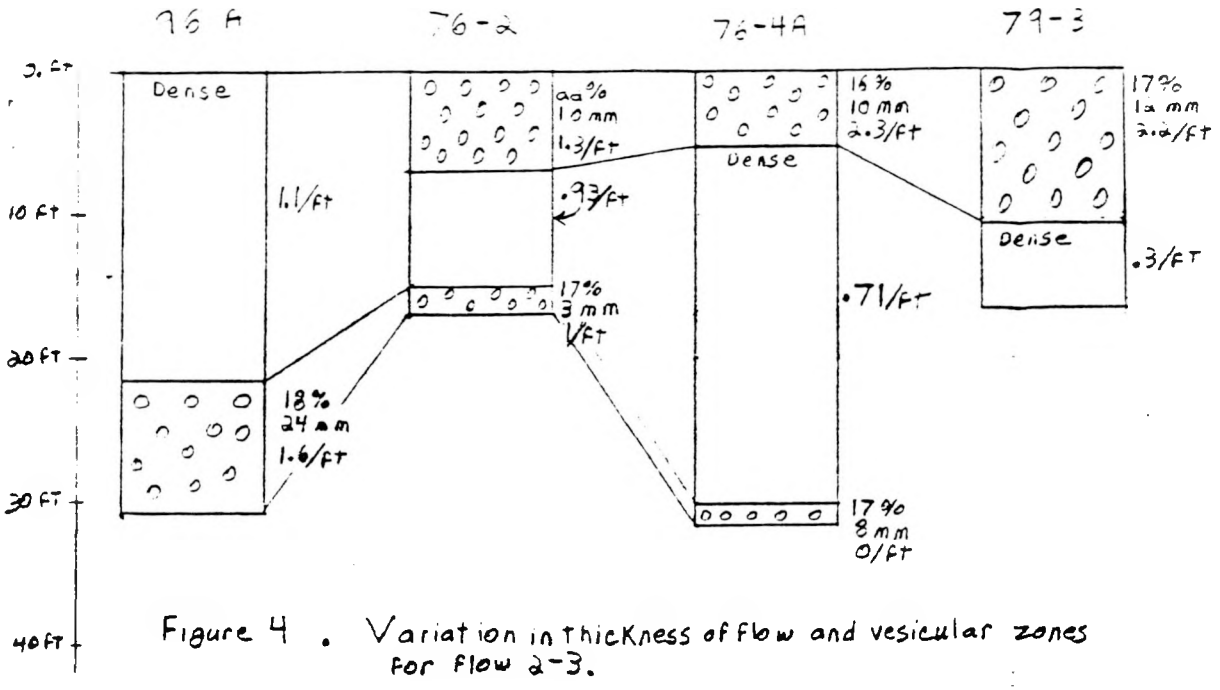

Figure 4 . Variation in thickness of flow and vesicular zones for flow 2-3.

Numbers per foot are fracture densities for vesicular zones and dense mid-flows.

Vesicular Zones

22% - Percen Vesicles from core logs

10 mm - Maximum Vesicle size from core logs

1.3/ft - Fracture density (Number of fractures per foot)

Figure 4. Variation in thickness of Flow 2-3 including fracture and vesicular zone data.

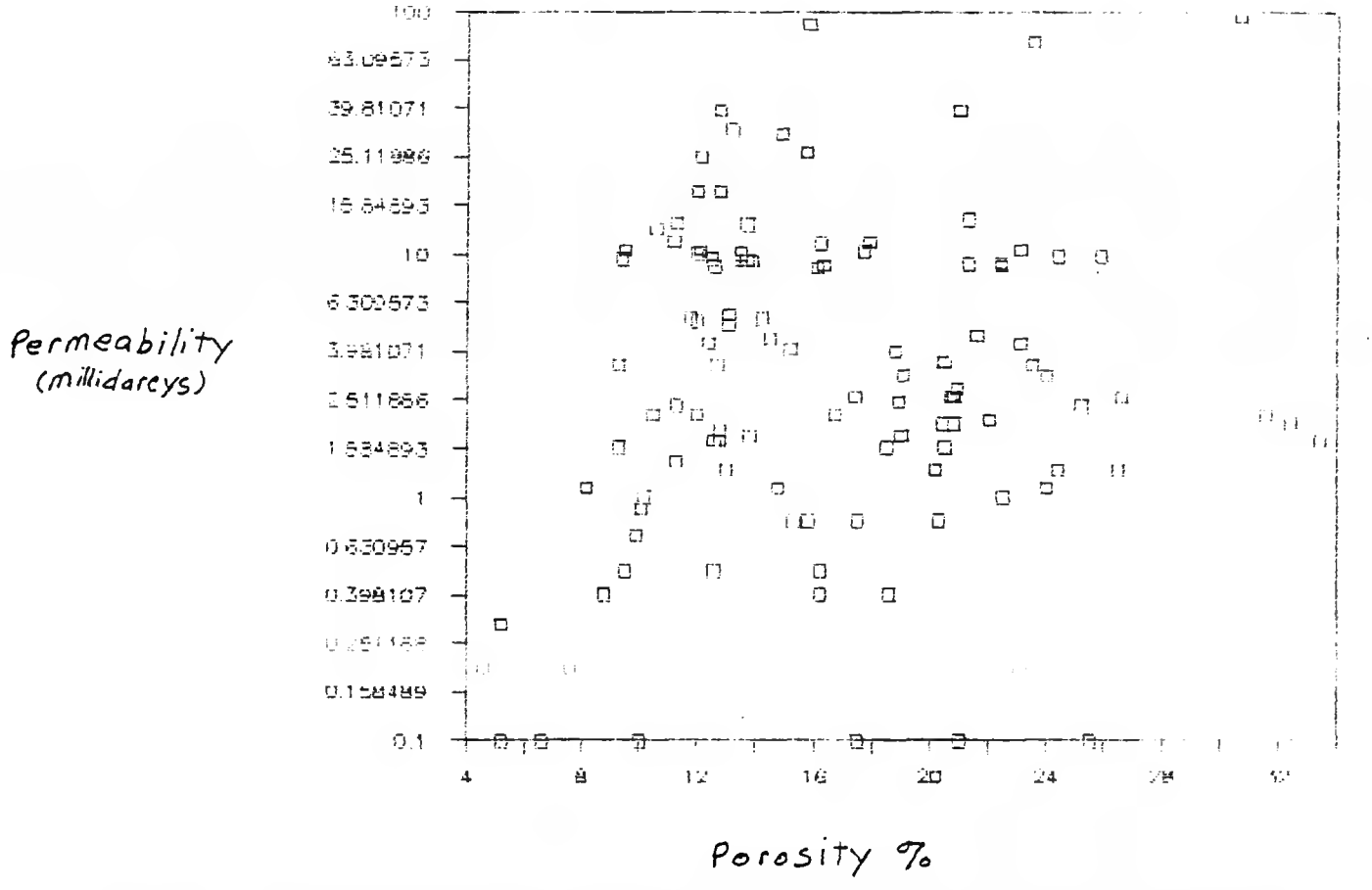

Figure 5. Plot of permeability vs porosity for permeability <100 millidarcys.

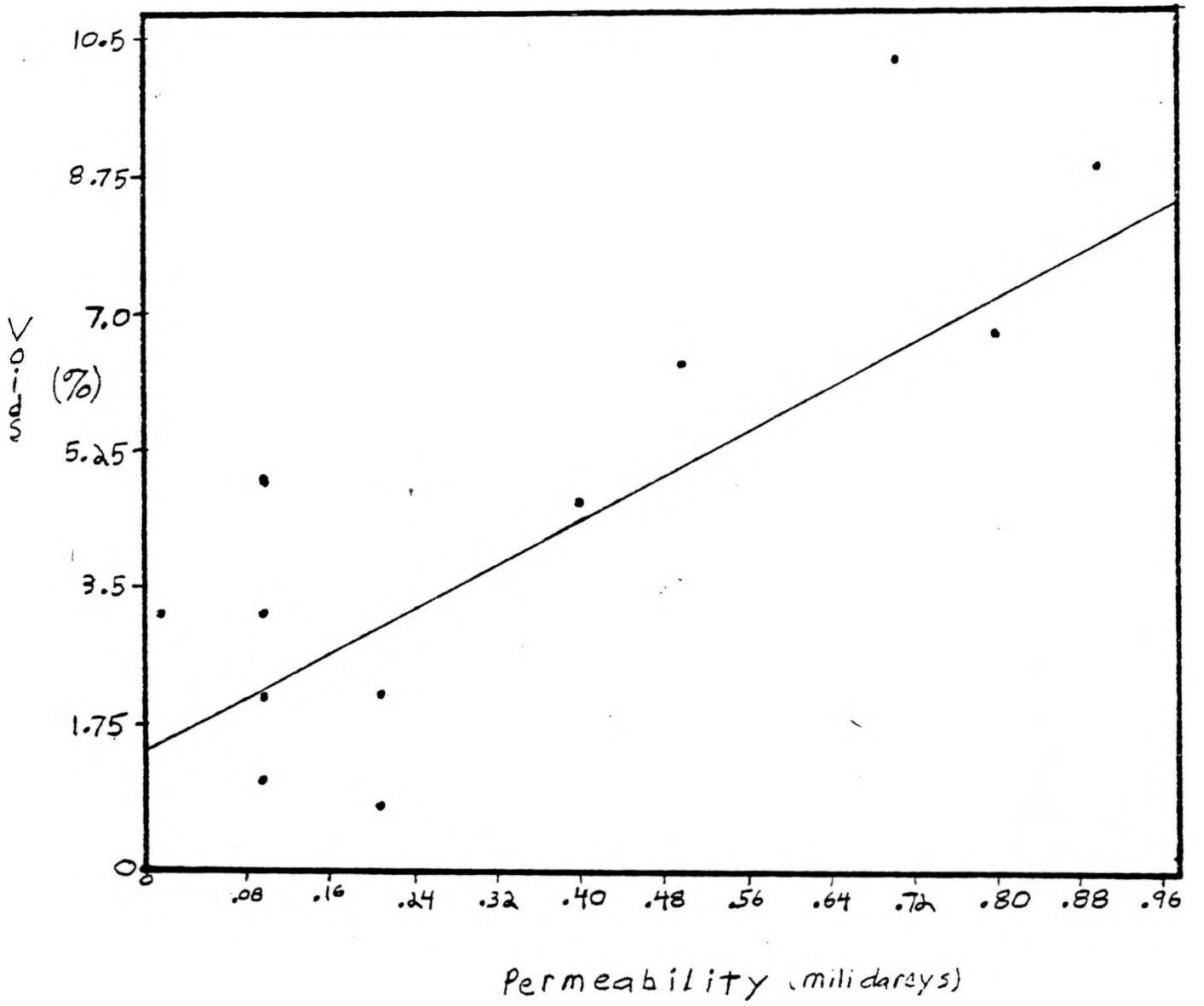

Figure 6. Intergranular void space vs permeability (permeability < 1.0).

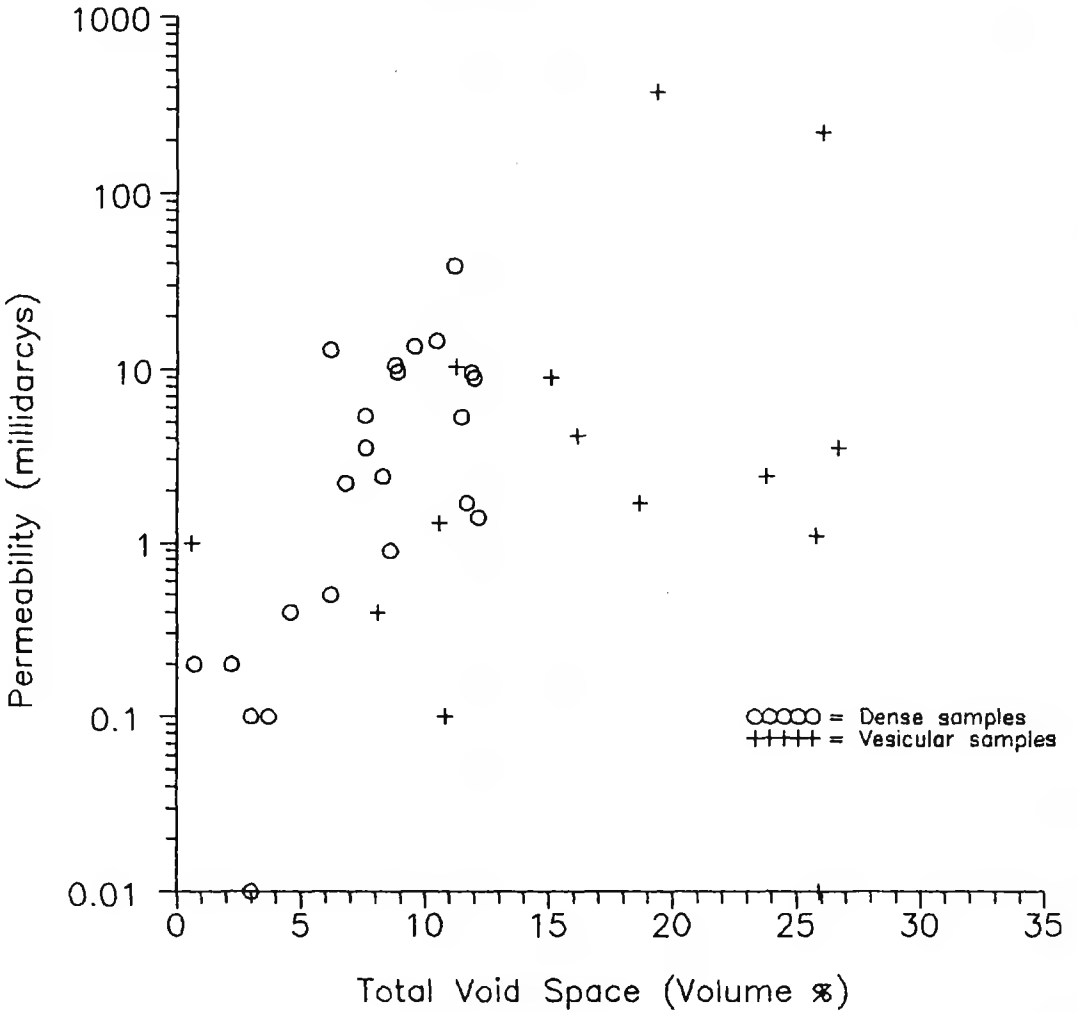

Figure 7. Permeability vs void space percentage determined by thin section point counts.

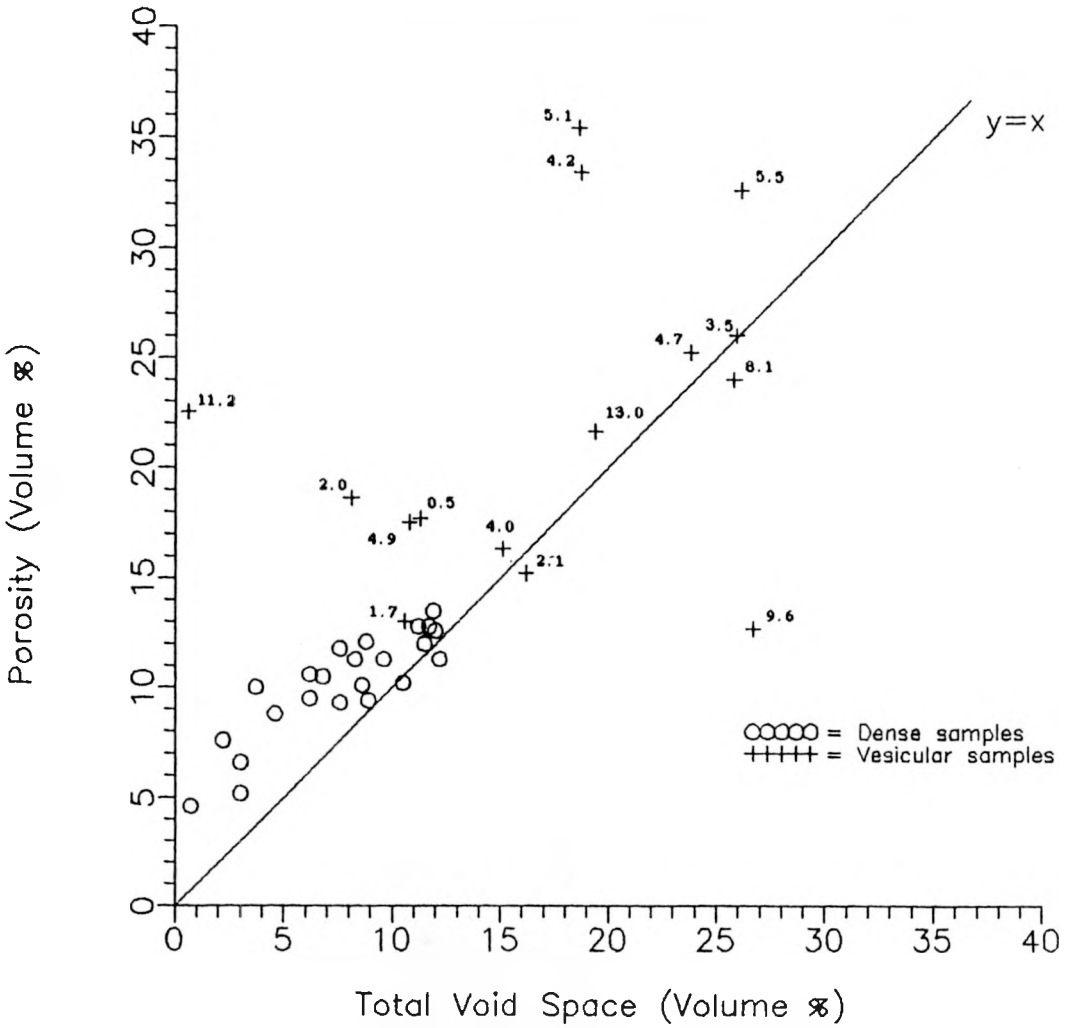

Figure 8. Measured porosity vs total void space. Numbers next to points are maximum vesicle size (in millimeters).

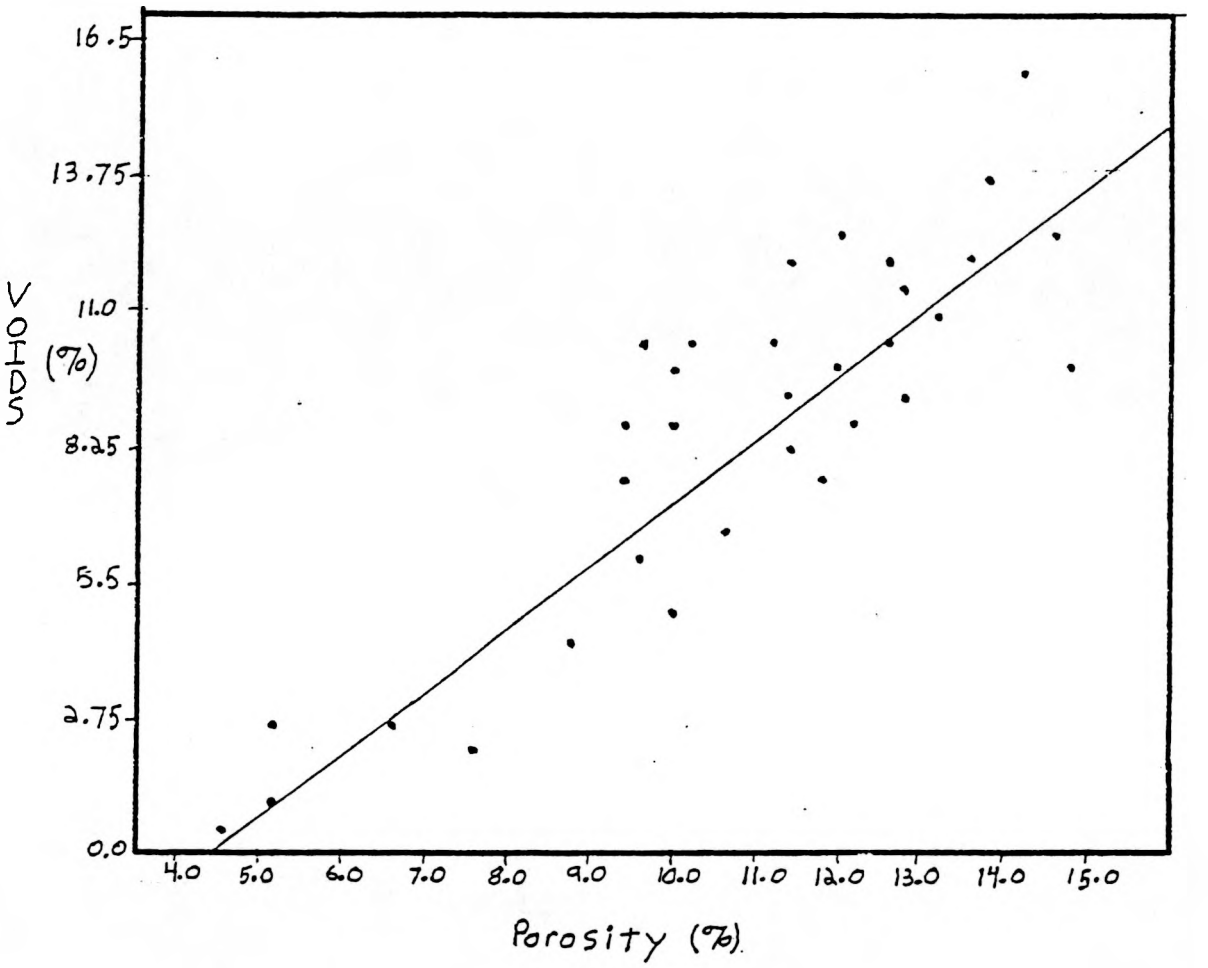

Figure 9. Intergranular void space vs porosity (porosity < 15.0%).

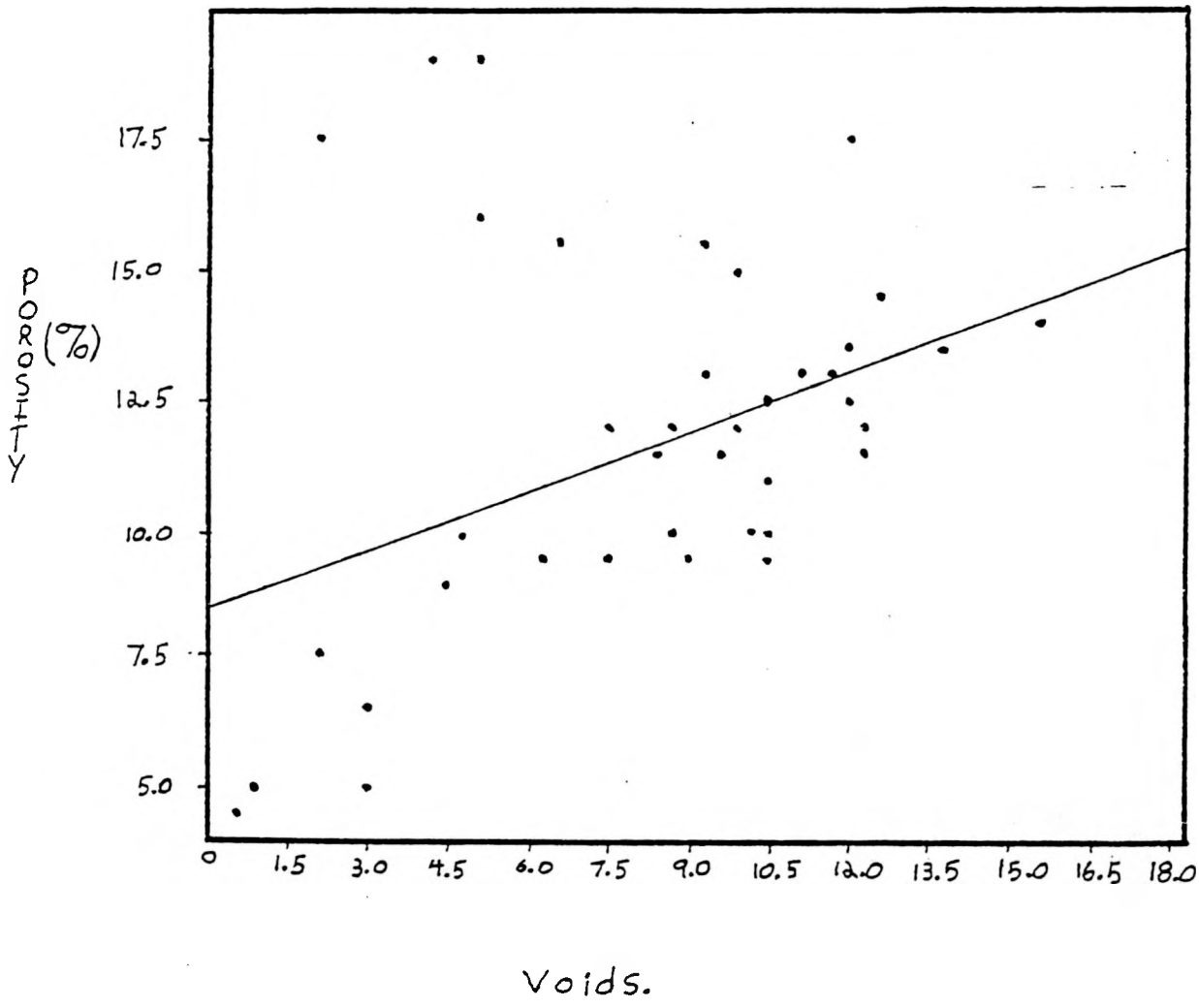

Figure 10. Porosity vs intergranular void space (porosity < 20%).

Appendix A:
Lithologic Logs

Each of the logs in this section shows the thickness of flows that have been correlated with confidence in the cores of this study. Selected cores show representative fracture density information for vesicular zones and the dense mid-flow portions of each flow. The key below applies to all lithologic logs in the appendix.

Vesicular zones.

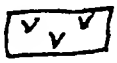

Dense Mid-flow
P= Porphyritic lithology
I = Intergranular Lithology

IB = Interbed
Sed = Surficial sediment/interbed
Gap = Gap in core

sediment, either interbed or surficial

Key for all lithologic Logs of Appendix A.

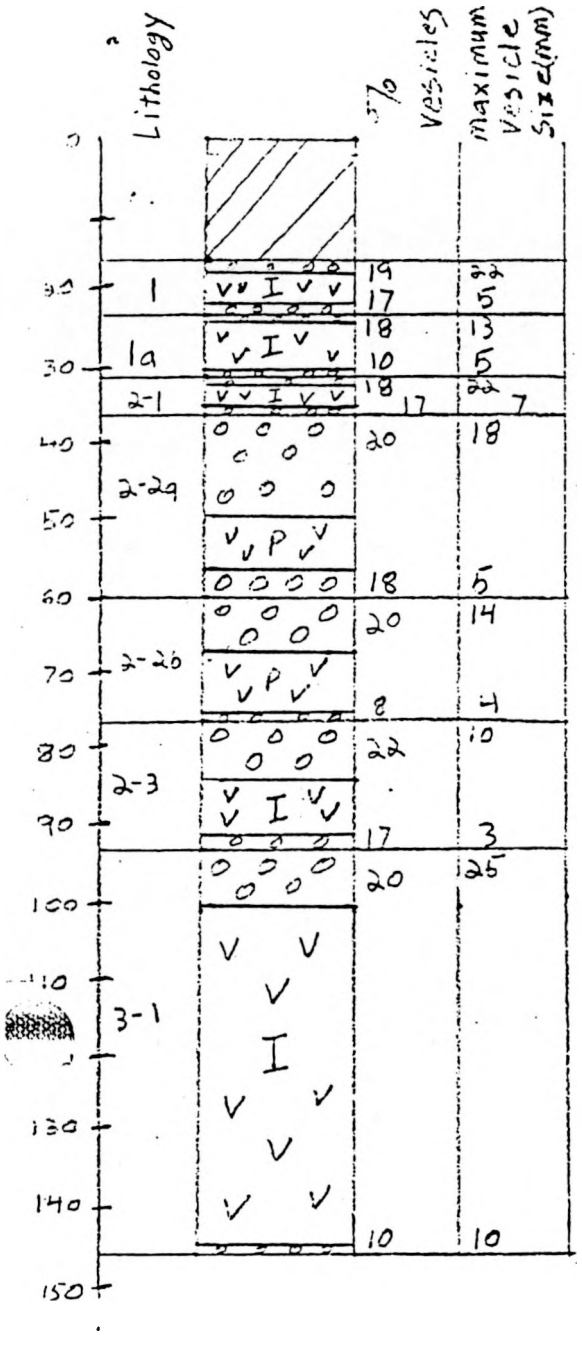

Lithologic log for Well 76-2

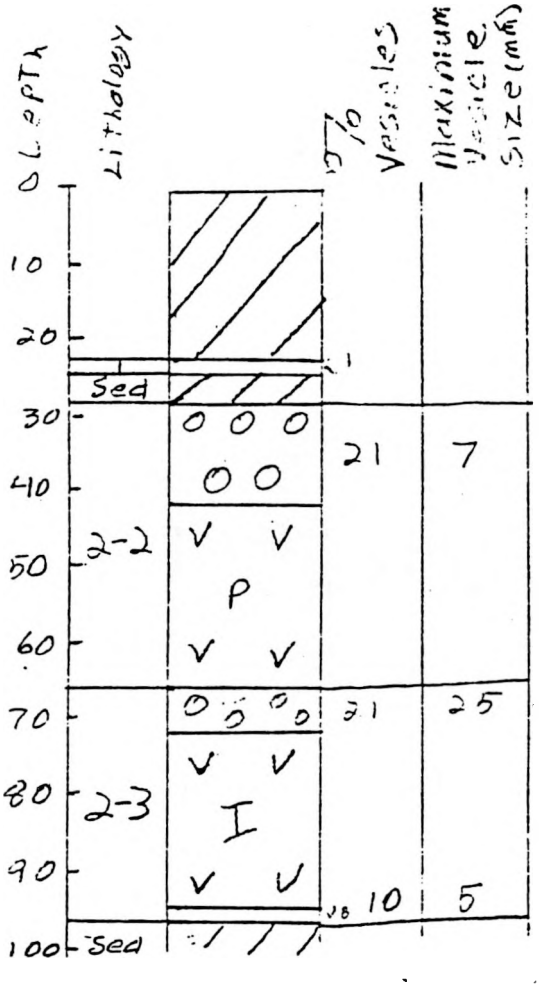

Lithologic log for Well 76-3

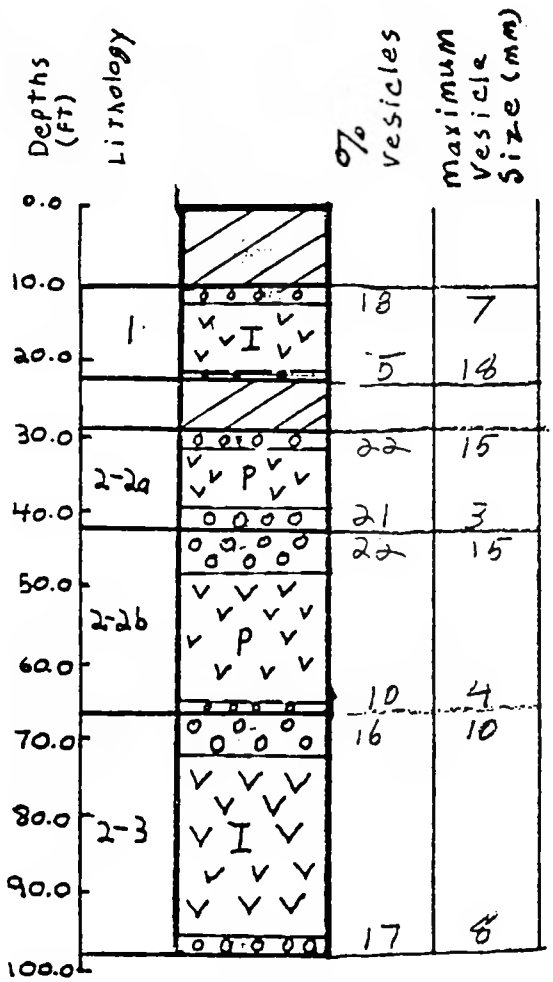

Lithologic log for Well 76-4

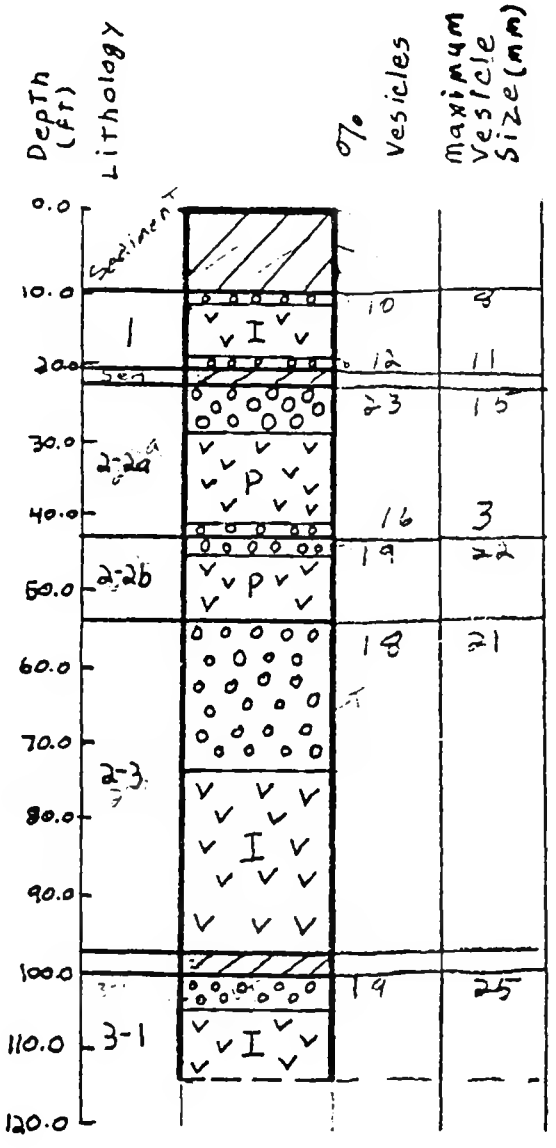

Lithologic log for Well 76-4A

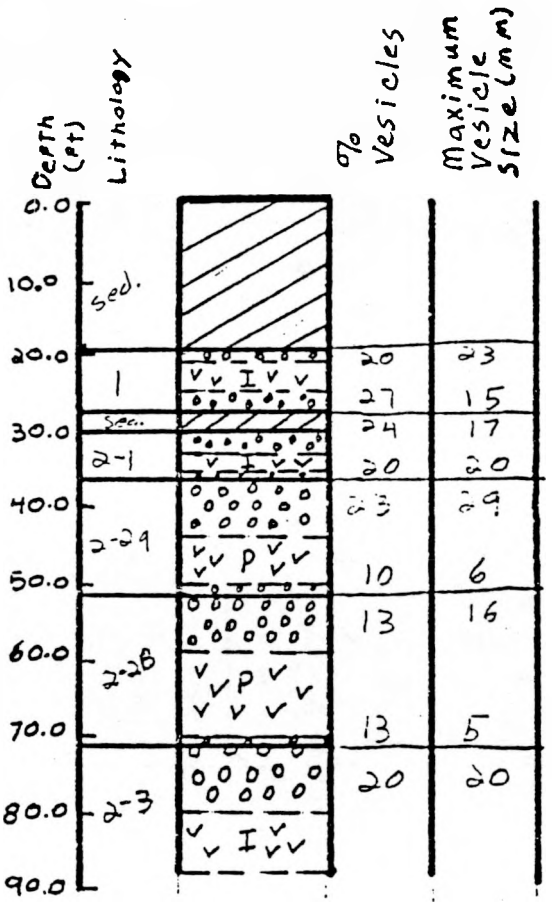

Lithologic log for Well 77-2

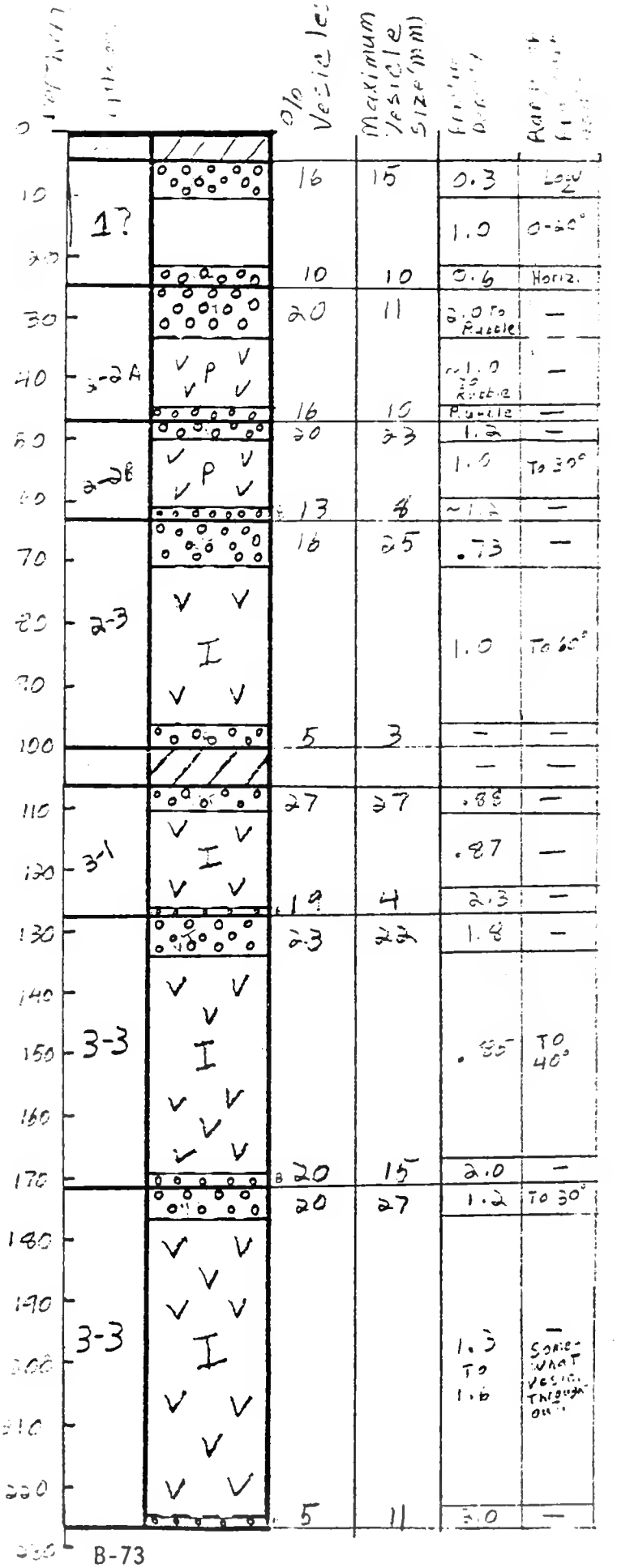

Lithologic log for Well 78-2

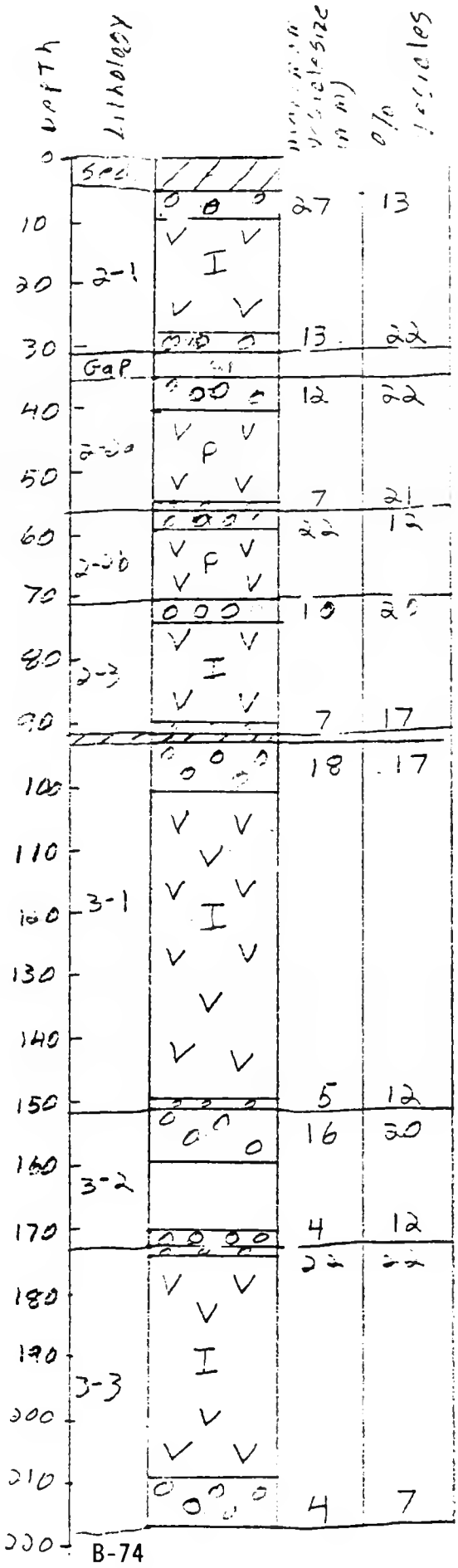

Lithologic log for Well 78-3

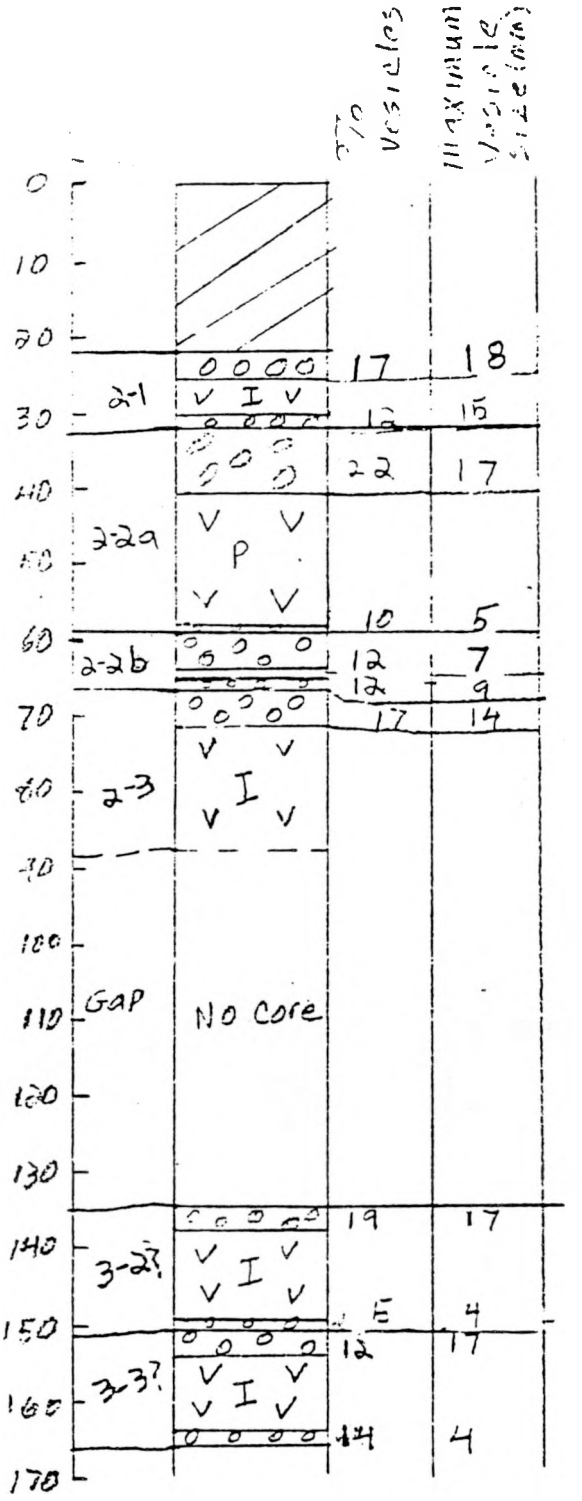

Lithologic log for Well 78-5

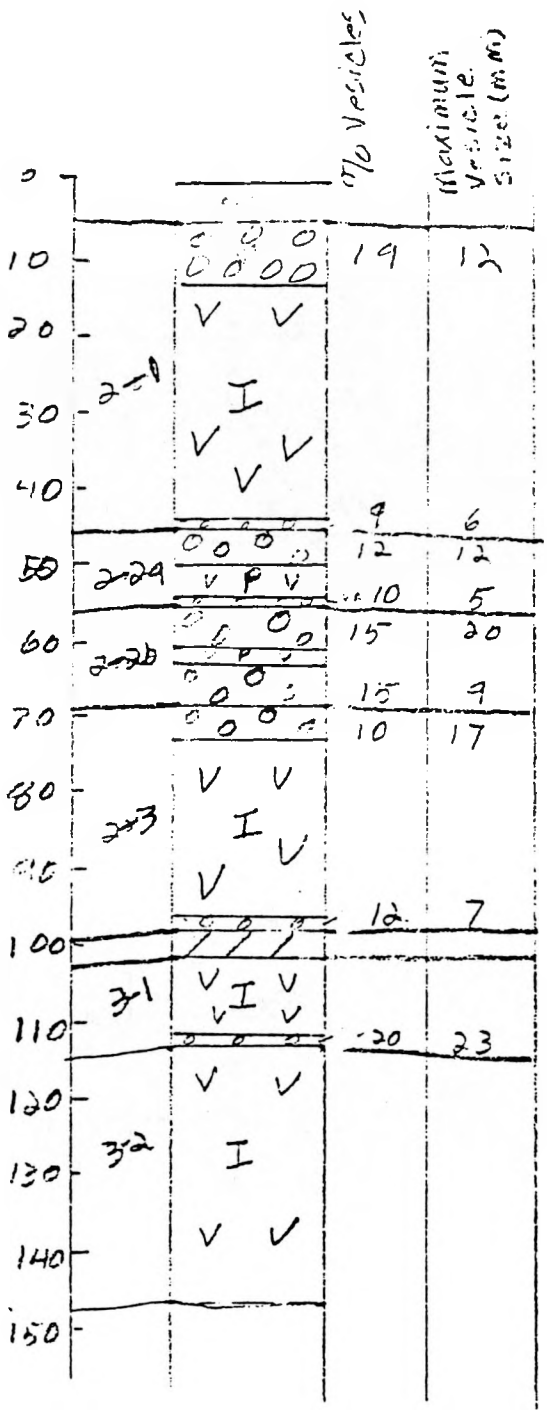

Lithologic log for Well 79-1

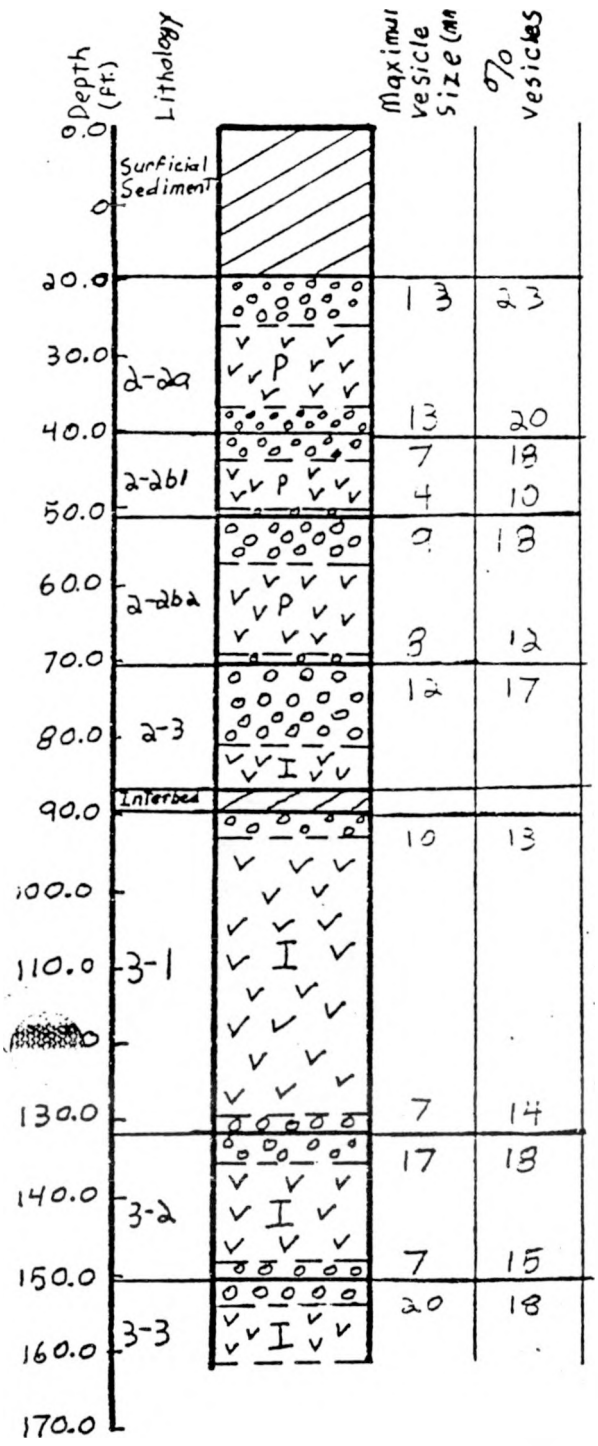

Lithologic log for Well 79-3

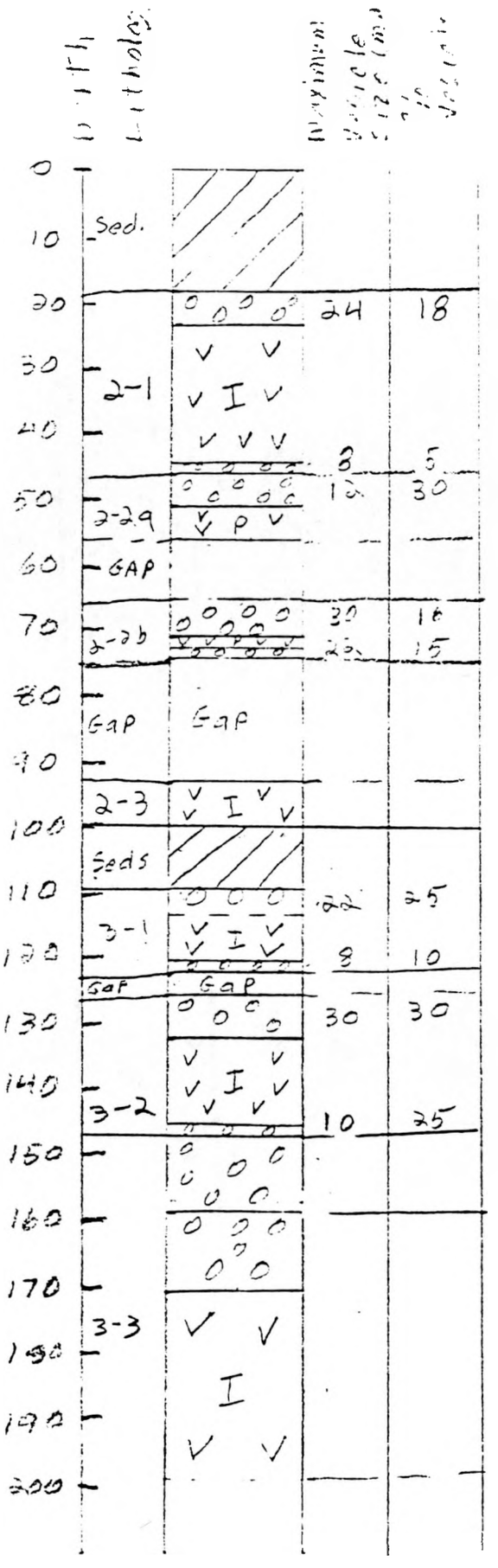

Lithologic log for Well 93A

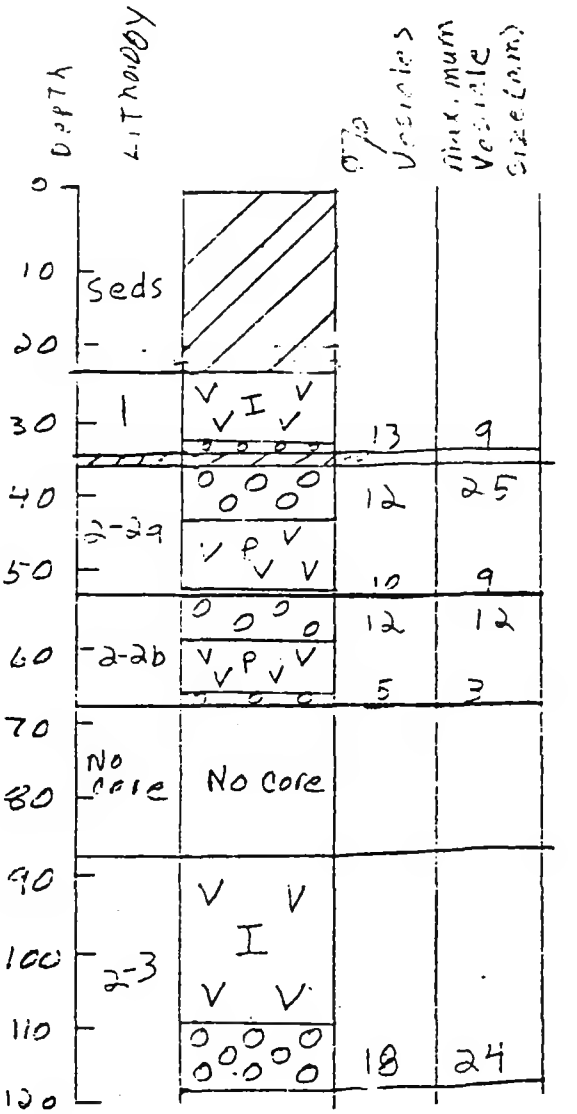

Lithologic log for Well 96A

APPENDIX B

Stratigraphy proposed by Kuntz and others (1980).

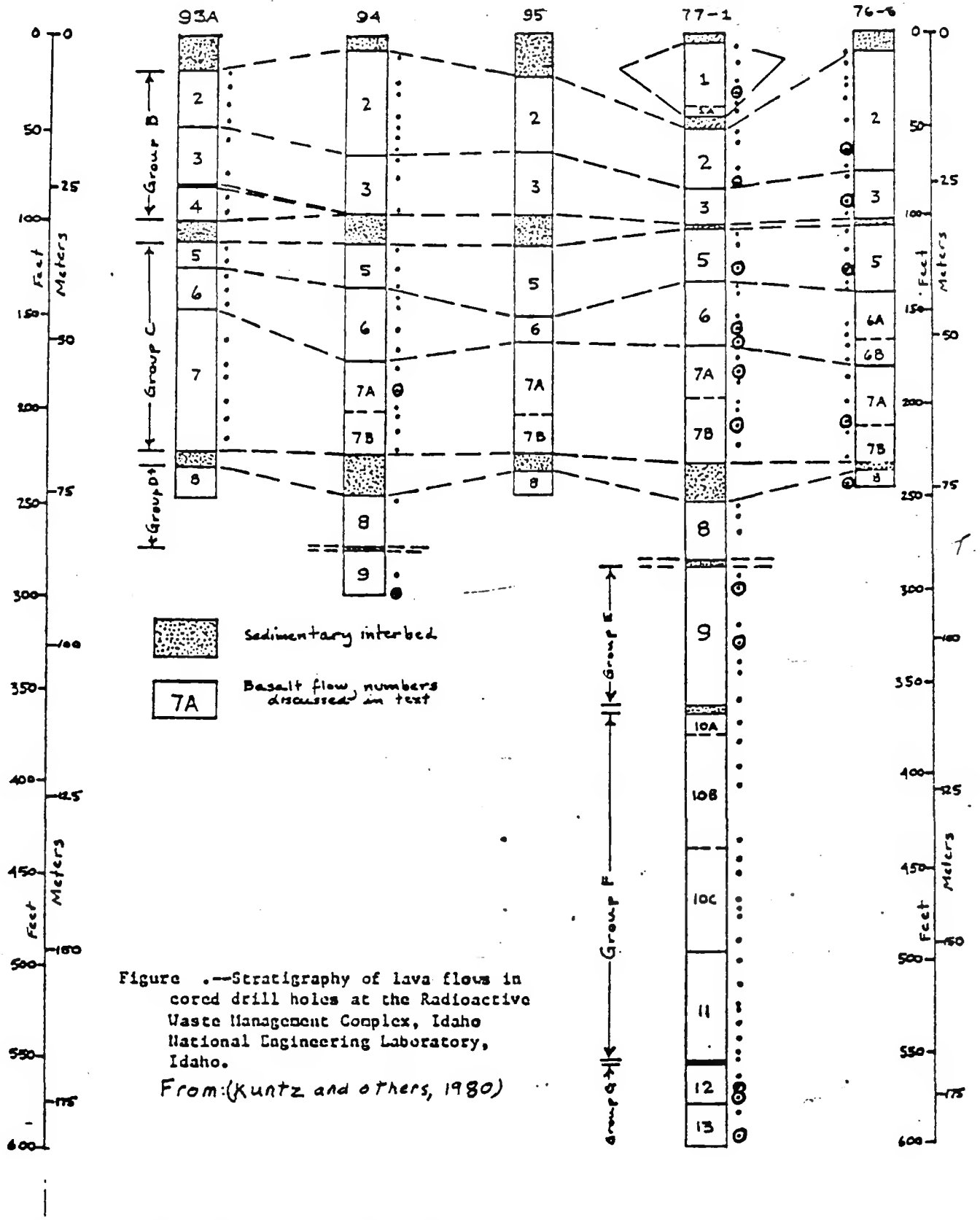

Figure .--Stratigraphy of lava flows in cored drill holes at the Radioactive Waste Management Complex, Idaho National Engineering Laboratory, Idaho.

From:(Kuntz and others, 1980)

Figure 1. Stratigraphy of lava flows in cored drill holes at the Radioactive Waste Management Complex, Idaho National Engineering Laboratory, Idaho. From: (Kuntz and others, 1980).

APPENDIX C

Flow Group thickness by core.

FLOW THICKNESS AND VESICULAR ZONE THICKNESS DATA
CORE 76-3

FLOW	FLOW TOP	FLOW BASE	TOP VES.	BASE VES.	FLOW THICKNESS
1	22.0	23.5	-	-	>1.3
2-2	27.5	65.0	7.5	-	37.5
2-3	65.0	95.5	6.0	1.5	30.5

FLOW THICKNESS AND VESICULAR ZONE THICKNESS DATA
CORE 76-4

FLOW	FLOW TOP	FLOW BASE	TOP VES.	BASE VES.	FLOW THICKNESS
1	11.2	21.0	1.3	1.5	9.8
2-2A	23.0	43.5	6.0	2.0	20.5
2-2B	43.5	54.0	2.5	-	10.5
2-3	54.0	98.1	20.0	-	44.1
3-1	100.5	>114.4	4.5	-	>13.9

FLOW THICKNESS AND VESICULAR ZONE THICKNESS DATA
CORE 76-4A

FLOW	FLOW TOP	FLOW BASE	TOP VES.	BASE VES.	FLOW THICKNESS
1	11.2	23.3	1.3	0.3	12.1
2-2A	28.8	42.5	2.2	3.5	13.7
2-2B	42.5	66.8	5.5	1.3	24.3
2-3	66.9	98.5	5.2	2.5	31.7

FLOW THICKNESS AND VESICULAR ZONE THICKNESS DATA
77-2

FLOW	FLOW TOP	FLOW BASE	TOP VES.	BASE VES.	FLOW THICKNESS
1	19.7	26.7	1.3	2.7	7.0
2-1	30.0	36.0	3.0	1.0	6.0
2-2A	36.0	51.0	7.2	1.5	15.0
2-2B	51.0	70.8	7.0	0.8	19.8
2-3	70.8	-	8.2	-	-

FLOW THICKNESS AND VESICULAR ZONE THICKNESS DATA
CORE 78-2

FLOW	FLOW TOP	FLOW BASE	TOP VES.	BASE VES.	FLOW THICKNESS
1?	5.0	25.1	6.0	3.1	20.1
2-2A?	25.1	47.0	3.9	2.0	21.9
2-2B	47.0	63.5	2.5	2.0	16.5
2-3	63.5	100.0	7.5	4.0	36.5
3-1	106.0	127.5	4.0	1.5	21.5
3-2	127.5	171.0	6.5	2.0	43.5
3-3	171.0	226.0	5.0	1.0	55.0

FLOW THICKNESS AND VESICULAR ZONE THICKNESS DATA
CORE 78-3

FLOW	FLOW TOP	FLOW BASE	TOP VES.	BASE VES.	FLOW THICKNESS
2-1	5.5	31.0	4.5	3.0	25.5
2-2A	35.0	56.5	5.0	1.5	21.5
2-2B	56.5	69.7	2.5	-	13.2
2-3	69.7	91.8	3.3	1.3	21.1
3-1	92.4	150.7	7.6	1.7	58.3
3-2	150.7	172.3	8.3	2.3	21.6
3-3	172.3	215.5	1.0	2.7	42.2

FLOW THICKNESS AND VESICULAR ZONE THICKNESS DATA
CORE 78-5

FLOW	FLOW TOP	FLOW BASE	TOP VES.	BASE VES.	FLOW THICKNESS
2-1	22.0	31.8	3.5	1.3	8.5
2-2A	31.8	58.5	8.2	1.5	26.7
2-2B	58.5	66.0	5.5	1.0	7.5
2-3	66.0	>86.7	4.5	-	>20.7
3-2?	134.0	150.0	3.0	1.0	15.0
3-3?	150	165.9	3.0	1.9	15.9

FLOW THICKNESS AND VESICULAR ZONE THICKNESS DATA
CORE 79-1

FLOW	FLOW TOP	FLOW BASE	TOP VES.	BASE VES.	FLOW THICKNESS
2-1	5.0	45.5	8.0	1.0	40.5
2-2A	45.5	55.0	4.5	1.0	9.5
2-2B	55.0	67.5	5.0	4.5	12.5
2-3	67.5	97.5	4.5	2.5	30.0
3-1	100.8	112.4	-	1.4	11.6
3-2	112.4	145.8	-	-	>33.4

FLOW THICKNESS AND VESICULAR ZONE THICKNESS DATA
CORE 79-3

FLOW	FLOW TOP	FLOW BASE	TOP VES.	BASE VES.	FLOW THICKNESS
2-2A	19.7	39.6	6.3	3.6	19.9
2-2B1	39.6	50.5	3.4	1.0	10.9
2-2B2	50.5	69.5	6.5	1.0	19.0
2-3	69.4	86.0	10.6	-	16.6
3-1	88.7	130.5	3.3	2.5	41.5
3-2	130.5	149.5	3.5	2.5	19.0
3-3	149.5	161.0	3.0	-	11.5

FLOW THICKNESS AND VESICULAR ZONE THICKNESS DATA
CORE 93

FLOW	FLOW TOP	FLOW BASE	TOP VES.	BASE VES.	FLOW THICKNESS
2-1	18.1	46.1	4.9	1.1	28.0
2-2A	46.1	55.7	4.9	-	9.6
2-2B	65.1	74.5	5.4	1.7	9.4
3-1?	93.0	123.5	-	1.5	30.5
3-2?	125.5	146.9	6.5	1.4	21.4
3-3?	146.9	221.7	12.1	-	>74.8

FLOW THICKNESS AND VESICULAR ZONE THICKNESS DATA
96A

FLOW	FLOW TOP	FLOW BASE	TOP VES.	BASE VES.	FLOW THICKNESS
1	22.3	34.5	-	1.5	>12.2
2-2A	35.7	53.7	6.8	0.7	18.0
2-2B	53.7	67.2	5.3	1.7	13.5
2-3	87.4	118.2	-	9.2	30.8

APPENDIX D

QUANTIFIED DATA.

SAMPLE	PLAG	OLIVINE	MATRIX	VOIDS	FLOW	POROS.	PERM.	M.PL.	M.OL.	M.VES	OXIDE.
A-1	6.4	0.4	93.2	2.5	2-1	30.7	94.8	1.2	0.5	7.2	NO
A-2	8.2	1.2	90.6	3.2	2-1	23.5	3.5	2.6	0.5	5.6	NO
A-3					2-1	19.1	3.2	2.1	0.4	3.0	L
A-4	13.4	1.1	85.5	6.7	2-1	15.3	0.8	2.7	0.6	4.0	L
A-5*	16.4	1.8	81.8	8.3	2-1	11.3	2.4	1.8	0.7	0.0	-
A-6					2-1	23.1	0.2	2.9	0.3	6.8	H
A-7					2-2A	22.0	2.1	3.5	1.7	6.1	H
A-10	17.9	7.1	75.0	3.2	2-2B	23.5	74.0	5.8	2.1	4.6	NO
A-12					2-2B	20.5	1.6	4.8	1.3	6.8	H
A-18*	9.1	2.3	88.6	25.9	3-2	26	0.0	1.9	1.3	3.5	NO
A-19*	12.8	5.5	81.7	11.5	3-3	12.0	5.3	2.7	3.0	0.0	-
A-20*	9.4	7.5	83.1	18.6	3-3	35.4	5403	2.4	2.6	5.1	H
A-23					3-4	14.6	0.0	2.1	1.2	6.6	L
A-25					3-4	38.4	2518	1.4	0.6	5.5	H
A-27					3-4	25.9	9.8	2.0	2.3	3.8	NO
A-30					3-4	16.2	0.5	1.8	1.3	5.6	L
A-34					3-4	21.0	0.1	1.7	1.2	4.8	H
B-1*	15.6	4.3	80.1	6.2	2-3	10.6	12.8	2.9	0.9	0.0	-
B-3*	6.9	4.0	89.1	16.2	2-3	15.2	4.1	1.3	1.2	2.1	NO
B-5					3-2	14.9	31.4	3.0	1.3	0.8	NO
B-7					3-2	16.2	0.4	3.1	1.3	1.3	NO
B-9					3-3	26.6	2.6	1.7	1.3	7.2	H
B-11					3-3	13.9	9.4	1.4	1.8	2.0	L
B-12					3-3	25.5	0.1	1.7	2.7	5.0	-
B-15					3-3	12.6	0.5	1.4	1.4	1.6	L
C-5	16.5	6.7	76.8	10.0	2-1	14.8	1.1	3.6	1.8	1.1	L
C-6	14.8	3.1	82.1	11.9	2-1	17.4	2.6	5.6	1.8	4.2	NO
C-15	21.4	5.6	73.0	10.1	2-2B	9.9	0.7	4.1	1.4	2.0	NO
C-24*	10.6	3.4	86.0	12.0	3-1	12.6	8.9	1.3	2.5	0.0	-
C-38					3-3	12.4	4.3	3.0	2.5	2.1	NO
D-1					1	26.5	1.3	2.1	1.6	5.2	NO
D-2					1	12.8	18.0	2.0	4.1	0.0	-
D-5	16.5	5.9	77.6	4.3	2-1	18.8	4.0	5.0	1.4	8.0	NO
D-6	24.5	4.6	70.9	0.1	2-1	5.2	0.3	6.8	1.4	0.0	-
D-8					2-1	18.8	4.0	3.6	1.5	0.0	-
D-13	19.7	7.5	72.8	5.2	2-2A	19.0	1.8	5.0	1.6	3.8	NO
D-16*	19.3	6.3	74.4	6.8	2-2B	10.5	2.2	7.2	1.4	0.0	-
D-17	15.9	3.4	80.7	1.9	2-2B	26.3	874	3.3	0.9	5.0	H
D-26*	14.2	6.2	79.6	7.6	3-1	11.8	5.4	2.5	3.2	0.0	-
D-27	17.5	5.6	76.9	10.0	3-1	12.0	10.1	2.6	1.9	1.8	NO
D-28*	8.9	5.1	86.0	18.4	3-1	----	---	2.2	2.4	5.4	L
D-29*	13.4	7.1	79.5	10.8	3-1	17.5	0.1	1.6	2.8	4.9	L
D-30*	10.9	3.4	85.7	3.7	3-1	10.0	0.1	2.4	4.0	0.0	-
D-31*	7.4	2.2	90.5	8.1	3-1	18.6	0.4	3.0	1.4	2.0	L
D-32	2.3	2.0	95.7	24.5	3-1	33.1	1575	1.6	0.8	5.6	H
E-2*	12.1	7.0	80.9	11.7	2-1	12.8	1.7	1.9	1.4	0.0	-
E-4					2-1	24.0	3.2	2.5	0.6	6.8	H
E-6	26.7	3:5	69.8	9.2	2-2A	12.8	1.7	4.4	1.1	6.2	NO
E-8	13.2	4.8	82.0	1.5	2-2B	----	---	4.1	1.2	8.4	L
E-9					2-2B	22.4	9.0	7.3	1.8	3.7	H
E-10					2-2B	22.4	9.2	2.0	0.8	4.4	L
E-30					3-3	43.2	4824	1.0	1.3	6.4	L

SAMPLE	PLAG.	OLIVINE	MATRIX	VOIDS	FLOW	POROS.	PERM.	M.PLAG.	M.OLIV.	M.VES.	OXIDE.
E-32					3-3	20.9	2.8	1.5	1.8	4.4	NO
E-35					3-3	18.9	2.5	1.4	2.0	4.0	NO
E-36					3-3	13.8	1.8	1.5	2.5	0.0	-
E-38					3-4	12.6	1.7	1.8	1.8	8.4	H
E-40					3-4	16.7	2.2	1.8	1.3	1.6	NO
F-3*	16.1	3.0	80.9	0.6	2-1	22.5	1.0	1.6	1.0	11.2	NO
F-4	10.3	2.3	87.4	0.0	2-2A	32.4	2.0	3.8	1.6	5.0	L
F-6	14.7	2.7	82.4	5.2	2-2A	16.1	8.8	3.2	0.9	16.0	L
F-10					2-3	25.9	395	2.3	0.7	6.4	H
F-15*	10.7	8.9	80.4	10.6	3-1	13.0	1.3	2.1	2.4	1.7	NO
F-16*	10.5	8.0	81.5	25.8	3-1	24.0	1.1	2.7	3.2	8.1	H
F-17*	9.0	5.2	85.8	23.8	3-2	25.2	2.4	2.0	2.1	4.7	H
F-18*	12.2	7.5	80.3	18.7	3-2	33.4	1.7	3.0	2.8	4.2	L
F-19*	17.2	7.8	75.0	11.2	3-2	12.8	38.7	2.8	2.2	0.0	-
F-20*	3.1	0.2	96.7	26.1	3-2	32.6	222	2.2	0.7	5.5	L
F-27					3-4	31.6	2.2	1.0	1.2	8.2	L
F-28					3-4	17.9	11.2	1.4	1.4	4.2	NO
F-29					3-4	13.5	10.1	1.4	4.1	0.0	-
F-31					3-4	----	----	0.8	2.2	5.8	H
F-32					3-4	13.7	9.5	1.7	1.4	0.9	NO
F-33					3-4	12.8	1.9	1.3	3.0	0.9	NO
F-34					3-4	7.8	0.0	1.4	1.8	1.1	H
F-35					3-4	----	---	1.8	2.5	7.9	H
F-36					3-4	----	---	2.0	1.8	13.0	H
F-37					3-4	----	---	1.8	1.7	5.4	H
G-2*	16.4	3.3	80.3	12.2	2-1	11.3	1.4	1.6	0.4	0.0-	
G-4*	18.1	3.3	78.7	3.0	2-1	6.6	0.1	2.4	1.1	0.0	-
G-7*	15.8	6.4	77.8	11.9	2-2	13.5	9.5	3.6	1.5	0.0	-
G-1					2-1	21.0	39.0	2.0	0.8	4.8	NO
G-11					3-1	12.0	2.2	3.0	0.8	0.0	-
G-13					3-1	15.8	88.0	1.6	1.9	3.6	NO
G-15*	7.2	2.6	90.2	26.7	3-2	12.7	3.5	2.8	3.7	9.6	L
G-16*	12.2	2.4	85.4	19.4	3-2	21.6	379	2.1	1.6	13.0	NO
G-17*	14.0	6.2	79.8	15.1	3-2	16.3	9.0	2.2	2.9	4.0	L
G-18*	10.3	10.9	78.8	11.3	3-2	17.7	10.3	2.4	2.2	0.5	L
G-19					3-3	17.5	0.8	2.0	2.5	0.0	-
G-22					3-3	20.8	2.6	1.1	1.0	6.4	L
G-29					3-3	9.3	1.6	1.3	1.6	0.0	-
H-2	9.5	10.0	80.5	10.5	1	12.5	9.6	1.8	2.1	2.8	NO
H-3	11.9	2.0	85.9	4.6	1	20.3	0..8	3.6	0.8	6.8	NO
H-6	20.1	8.2	71.7	13.9	2-2A	13.7	13.2	3.9	1.4	3.6	NO
H-9*	18.8	80.	73.2	6.2	2-2A	9.5	0.5	5.0	1.5	0.0	-
H-11					2-2B	20.8	2.0	4.6	1.3	5.2	H
H-12					2-2B	20.4	2.0	4.4	1.3	7.2	L
H-13*	20.4	4.8	74.8	3.0	2-2B	5.2	0.0	4.7	1.4	0.0	-
H-14*	15.7	5.1	79.2	9.6	2-2B	11.3	13.4	4.0	1.3	0.0	-
H-17					2-3	8.2	1.1	3.0	1.0	0.0	-
I-2	25.0	4.2	70.8	11.2	2-2	13.2	32.5	4.5	1.0	3.5	NO
I-4*	20.1	9.5	70.4	7.6	2-2	9.3	3.5	3.8	1.4	0.0	-
I-5	13.7	2.4	83.9	4.7	2-2	23.1	10.5	2.8	0.7	2.8	L
I-6	17.7	7.0	75.3	2.0	2-2	24.7	1712	6.4	1.6	2.3	L
I-10	22.0	4.1	73.9	10.4	2-3	11.2	11.3	4.5	0.8	1.6	NO

SAMPLE	PLAG	OLIVINE	MATRIX	VOIDS	FLOW	POROS.	PERM.	M.PL.	M.OL.	M.VES	OXIDE.
I-11*	19.8	6.0	74.2	8.9	2-3	9.4	9.6	3.6	1.1	0.0	-
I-12	15.2	4.4	80.4	27.3	3-1	24.4	9.8	1.6	2.9	3.6	NO
I-15	13.4	4.9	81.4	8.3	3-1	20.2	1.3	2.1	3.6	6.2	NO
J-1					2-2	21.3	9.1	5.0	1.0	4.1	NO
J-2*	15.7	4.7	79.6	10.5	2-2	10.2	14.4	1.7	0.0	-	
J-3	9.0	3.1	87.9	2.0	2-2	26.3	4448	2.3	0.9	6.0	L
J-5					2-3	20.5	3.6	3.4	8.6	NO	
J-17					3-3	----	---	1.3	0.9	2.4	NO
J-18					3-3	15.8	0.8	1.3	1.9	5.0	NO
J-19					3-3	12.1	25.0	1.3	1.8	0.0	-
J-20					3-3	16.2	11.1	1.6	4.3	4.0	NO
K-1	2.5	4.3	93.2	15.7	1	14.2	5.4	2.7	1.2	4.7	NO
K-4	16.8	4.3	78.9	5.6	2-1	20.7	2.6	3.4	1.7	3.8	NO
K-5	21.7	6.2	71.4	12.4	2-1	12.0	18.0	4.6	1.6	3.6	NO
K-13					2-2	13.1	5.1	4.4	2.3	2.2	NO
K-15					2-3	21.3	14.0	2.6	0.9	7.2	NO
K-19					2-3	13.1	5.6	2.5	0.8	1.6	NO
L-2*	2.7	5.8	91.5	8.6	1	10.1	0.9	1.6	1.6	0.0	-
L-7*	17.7	5.6	76.7	0.7	2-1	4.6	0.2	5.8	1.6	0.0	-
L-11	16.7	5.9	77.4	0.9	2-2	5.2	0.1	4.6	1.1	1.7	NO
L-14	22.2	4.6	73.2	12.6	2-3	14.5	4.5	5.0	2.1	3.2	L
L-18	13.4	4.3	82.3	7.2	2-3	21.6	4.6	2.0	-	4.2	NO
L-21	20.4	7.9	71.7	10.5	2-3	9.5	10.5	2.9	1.4	0.0	-
L-25	13.7	3.4	82.9	9.4	3-1	15.7	26.3	2.3	1.5	3.4	NO
M-1					1	18.5	1.6	2.1	1.8	3.6	NO
M-2					1	4.8	0.0	1.9	1.9	0.0	-
M-5*	14.3	1.6	84.1	4.6	2-1	8.8	0.4	1.7	0.6	0.0	-
M-6	18.4	2.5	79.1	1.0	2-1	24.4	1.3	2.5	0.7	2.8	H
M-9	15.5	6.6	77.9	4.5	2-2A	23.1	4.3	6.3	1.8	8.4	L
M-11*	27.1	5.5	67.4	2.2	2-3	7.6	0.2	4.8	1.3	0.0	-
M-12*	18.7	5.0	76.3	8.8	2-3	12.1	10.5	6.9	1.3	0.0	-

APPENDIX C

BIBLIOGRAPHY FROM LITERATURE SEARCH OF DATA BASES

APPENDIX C

BIBLIOGRAPHY

1. (NASA, Office of Space Science and Applications, USA). NASA Technical Memorandum; 1988: 376-378; CODEN: NATMA4; ISSN: 0499-9320.
Note: English.

2. Allmendinger, R. W.; Bonnichsen, B. (EDITOR); Breckenridge, R. M. (EDITOR) (Cornell Univ., Dep. Geol. Sci., Ithaca, NY, USA Idaho Bur. Mines and Geol., Moscow, ID, USA). <Analytic> Sequence of late Cenozoic deformation in the Blackfoot Mountains, southeastern Idaho <Monographic> Cenozoic geology of Idaho. Bulletin - Idaho Bureau of Mines and Geology 26; 1982: 505-516; ISSN: 0073-442X.
Note: DIALOG GEOREF FILE 89 English illus., sketch maps.

3. Anderson, Alfred Leonard. <Analytic> Lava Creek Vents, Butte County, Idaho. Northwest Sci. vol. 3, no. 1, pp. 13-19, 1 fig. geol. map, March; 1929.
Note: DIALOG GEOREF FILE 89.

4. Armstrong, R. L. (Univ. B.C. Geol. Sci., Vancouver, B.C., CAN). <Analytic> Volcanic-tectonic evolution of the Snake River Plain. EOS (Am. Geophys. Union, Trans.) 56: 12; 1974: 1189; CODEN: EOSTAJ.
Note: DIALOG GEOREF FILE 89 English.

5. Armstrong, R. L.; Leeman, William P.; Malde, Harold E. (Yale Univ., Dep. Geol. Geophys., New Haven, Conn., USA; Univ. Oreg). <Analytic> K-Ar dating, Quaternary and Neogene volcanic rocks of the Snake River Plain, Idaho. Am. J. Sci. 275: 3; 1975: 225-251; CODEN: AJSCAP.
Note: DIALOG GEOREF FILE 89 English illus., tables, geol. sketch map.

6. Birkett, T. C.; Stout, M. Z.; Nicholls, J. (Ecole Polytech. Montreal, Dep. Genie Min., Montreal, Que., CAN; Univ Calgary, CAN). <Analytic> Mineralogy and petrology of Quaternary lavas from the Snake River Plain, Idaho discussion and reply. Can. J. Earth Sci. 15: 5; 1978: 859-862; CODEN: CJESAP.
Note: DIALOG GEOREF FILE 89 English for reference to paper by Stout, M. Z., and Nicholls, J., see Can. J. Earth Sci., vol. 14, p. 2140, 1977 table.

7. Bisdorf, R. J. (U.S. Geol. Surv., Denver, CO, USA). <Monographic> Schlumberger sounding results near Twin Falls, Idaho. Open-File Report (United States Geological Survey. 1978); 1987: 90; CODEN: XGROAG; ISSN: 0196-1497.
Note: DIALOG GEOREF FILE 89 English illus., sketch map.

8. Bishop, D. T. (Univ. of Idaho, Moscow, Idaho, USA). <Monographic> Petrology and geochemistry of the Purcell sills, Boundary County, Idaho and adjacent areas; 1974: 147.
Note: DIALOG GEOREF FILE 89 English.

9. Bretches, J. E. (State Univ. of New York, Buffalo, NY, USA). <Monographic> A geologic study of East Butte, a rhyolitic volcanic dome on the eastern Snake River Plain, Idaho; 1984: 113.
Note: DIALOG GEOREF FILE 89 English 12 plates; 1:6,200; geol. map.

10. Bretchs, J. E.; King, J. S. (State Univ. N.Y. at Buffalo, Dep. Geol. Sci., Amherst, NY, USA). <Analytic> The geology of East Butte, a rhyolitic volcanic dome on the eastern Snake River Plain, Idaho <Monographic> Reports of Planetary Geology and Geophysics Program; 1984. NASA Technical Memorandum 87563; 1985: 269-271; CODEN: NATMA4; ISSN: 0499-9320.
Note: DIALOG GEOREF FILE 89 English.

11. Champion, D. E.; Dalrymple, G. B.; Kuntz, M. A. (U.S. Geol. Surv., Menlo Park, CA, USA). <Analytic> Radiometric and paleomagnetic evidence for the Emperor reversed polarity event at 0.46 + or - 0.05 m.y. in basalt lava flows from the eastern Snake River Plain, Idaho. Geophysical Research Letters 8: 10; 1981: 1055-1058; CODEN: GPRLAJ; ISSN: 0094-8276.
Note: DIALOG GEOREF FILE 89 English illus., 1 table.

12. Chase, George H. <Analytic> Potassium-argon ages from whole-rock analyses of igneous rocks in the area of the National Reactor Testing Station, Idaho. U.S. Geol. Surv., Prof. Pap. No. 800-D, p. D123-D126, sketch maps; 1972; CODEN: XGPPA9.
Note: DIALOG GEOREF FILE 89 English.

13. Creighton, D. N.; Beus, Stanley S. (EDITOR) (Chevron U.S.A., Houston, TX, USA North. Ariz. Univ., Dep. Geol., Flagstaff, AZ, USA). <Analytic> Menan Buttes, southeastern Idaho <Monographic> Rocky Mountain Section of the Geological Society of American <Collective> Centennial field guide volume; 1987: 109-111.
Note: DIALOG GEOREF FILE 89 English The Decade of North American Geology Project series; Vol. 6 sect., geol. sketch map.

14. Duffy, C. J.; Harrison, J. (Utah State Univ., Dep. Civ. and Environ. Eng., Logan, UT, USA). <Analytic> The statistical structure and filter characteristics of tritium fluctuations in fractured basalt. Water Resources Research 23: 5; 1987: 894-902; CODEN: WRERAQ; ISSN: 0043-1397.
Note: DIALOG GEOREF FILE 89 English illus., 1 table, sketch map.
The statistical structure and spectral-covariance characteristics of tritium fluctuations are examined from injection of low-level radioactive waste in a fractured basalt aquifer. The tritium fluctuations are the result of a time-varying injection well concentration. The integral scale of the fluctuations increases with distance from the source and the observation well spectra are characteristic of attenuation characteristics, a theoretical filter is constructed and transport parameters are estimated. The analysis indicates that environmental tracers may provide a useful extension to controlled tests over large length scales (>100m). Although current research has concentrated on the importance of intrinsic variability such as porous media heterogeneities, the present study addresses the control exerted by extrinsic variability as exhibited by source strength fluctuations.--Journal abstract.

15. Evans, John Richard (Princeton Univ., Princeton, NJ, USA). <Monographic> Restricted-array seismic tomography; 1988: 181.
Note: DIALOG GEOREF FILE 89 English.

16. Faye, Gordon H.; Miller, Roy M. <Analytic> "Blue Dragon" Basalt from Craters of the Moon National Monument, Idaho; Origin of Color. Am. Mineral. Vol. 58, No. 11-12, p. 1048-1051, illus; 1973; CODEN: AMMIAY.
Note: DIALOG GEOREF FILE 89 English Reflection from titanian magnetite particles, electron transfer processes.

17. Fiesinger, D. W.; Perkins, W. D.; Puchy, B. J.; Bonnichsen, B. (EDITOR); Breckenridge, R. M. (EDITOR) (Utah State Univ., Dep. Geol., Logan, UT, USA; Andover Oil, USA Idaho Bur. Mines and Geol., Moscow, ID, USA). <Analytic> Mineralogy and petrology of Tertiary-Quaternary volcanic rocks in Caribou County, Idaho <Monographic> Cenozoic geology of Idaho. Bulletin - Idaho Bureau of Mines and Geology 26; 1982: 465-488; ISSN: 0073-442X.
Note: DIALOG GEOREF FILE 89 English illus., 12 tables, sketch maps.

18. Fountain, J. C.; Spear, D. B. (State Univ. N.Y. at Buffalo, Dep. Geol. Sci., Amherst, N.Y., USA). <Analytic> Geochemistry of ferrobasalt, ferrolatite, and rhyolite lavas from the Cedar Butte area, eastern Snake River Plain, Idaho. Geol. Soc. Am., Abstr. Programs 11: 6; 1979: 272-273; CODEN: GAAPBC; ISSN: 0016-7592.
Note: DIALOG GEOREF FILE 89 English.

19. Fowler, Claude S. (Washington State Univ., Pullman, WA, USA). <Monographic> Radial columnar structure in Columbia River Basalt; 1931: unknown.
Note: DIALOG GEOREF FILE 89 English.

20. Fuller, Richard E. <Analytic> The Asotin craters of the Columbia River basalt. Jour. Geology vol. 36, no. 1, pp. 56-74, 7 figs., January-February; 1928.
Note: DIALOG GEOREF FILE 89.

21. Gibson, Ian L. <Analytic> Crustal flexures and flood basalts. Tectonophysics Vol. 3, No. 5, p. 447-456, illus. (incl. geol. sketch maps); 1966.
Note: DIALOG GEOREF FILE 89 English.
The published accounts of five major downwarps in the earth's crust are summarized with respect to related thick sequences of flood basalts extruded from long linear fissure systems. The Lebombo flexure involving a succession of basic and acidic volcanics, 9000 m thick in the western border of Mozambique; the Penvel flexure involving 2000 m of basic lavas covering 500,000 km 2 on the Deccan plateau of India; the thick flood basalt (20 km) in the Snake River downfaulted downwarp in western United States; the Shugra basalts of the Red Sea and Gulf of Aden region; and the 7000 m of basic lavas in the east Greenland flexure exhibit a number of common features. Extrusion of the lavas, intrusion of dikes, and the flexures developed contemporaneously.

Each has a dike swarm parallel to, or coincident with, the length of the flexure. The features studied are believed to represent part of the major crustal pattern of the earth's surface rather than simply constituting features of regional significance.

22. Goldstein, F. J.; Weight, W. D. (U.S. Geol. Surv., Idaho Falls, ID, USA). <Monographic> Subsurface information from eight wells drilled at the Idaho National Engineering Laboratory. Open-File Report (United States Geological Survey, 1978); 1982: 34; CODEN: XGROAG; ISSN: 0196-1497.
Note: DIALOG GEOREF FILE 89 English illus., 1 table, sketch maps.

23. Greeley, R. (Ariz. State Univ., Dep. Geol., Tempe, AZ, USA). <Analytic> The Snake River Plain, Idaho; representative of a new category of volcanism <Monographic> Yellowstone-Snake River plain symposium. JGR. Journal of Geophysical Research. B 87: 4; 1982: 2705-2712; ISSN: 0196-6936.
Note: DIALOG GEOREF FILE 89 English illus., sketch map.

24. Greeley, Ronald; Martel, Linda (Ariz. State Univ., Dep. Geol., Tempe, AZ, USA). <Analytic> Radar observations of basaltic lava flows, Craters of the Moon, Idaho. International Journal of Remote Sensing 9: 6; 1988: 1071-1085; ISSN: 0143-1161.
Note: DIALOG GEOREF FILE 89 English illus., 2 tables, geol. sketch maps.

25. Hamilton, Warren. <Analytic> Petrology of rhyolite and basalt, northwestern Yellowstone Plateau <Monographic> in Geological Survey Research 1963. U.S. Geol. Survey Prof. Paper 475-C p. C78-C81, table, geol. map; 1963.
Note: DIALOG GEOREF FILE 89.

26. Hamilton, Warren. <Analytic> Geology and petrogenesis of the Island Park caldera of rhyolite and basalt, eastern Idaho. U.S. Geol. Survey Prof. Paper 504-C p. C1-C37, illus., table, geol. map; 1965.
Note. DIALOG GEOREF FILE 89.
The Island Park caldera, in the northeastern part of the Snake River Plain, is an elliptical collapse structure 18 by 23 mi in diameter, formed by collapse during Pleistocene time of a shield volcano of rhyolite tuff. Rhyolite domes and lava flows were extruded along the western rim during and after the period of collapse. The caldera was filled by rhyolite and basalt from interspersed vents. Uniform highly silicic rhyolite magma lay upon uniform low-alkali olivine basalt magma in the large magma chamber. The contrasting magmas may be liquid fractionates from primary tholeiitic magma.

27. Hamilton, Warren; Myers, W. Bradley. <Analytic> Menan Buttes, cones of glassy basalt tuff in the Snake River Plain, Idaho <Monographic> in Geological Survey Research 1962. U.S. Geol. Survey Prof. Paper 450-E p. E114-E118, illus; 1963.
Note: DIALOG GEOREF FILE 89.

28. Harper, G. D.; Link, P. K. (State Univ. N.Y., Dep. Geol. Sci., Albany, NY, USA; Idaho State Univ., USA). <Analytic> Geochemistry of upper Proterozoic rift-related volcanics, northern Utah and southeastern Idaho. Geology (Boulder) 14: 10; 1986: 864-867; CODEN: GLGYBA; ISSN: 0091-7613.
Note: DIALOG GEOREF FILE 89 English illus., sketch map.

29. Hart, W. K. (Case Western Reserve Univ., Cleveland, OH, USA). <Monographic> Chemical, geochronologic and isotopic significance of low K, high-alumina olivine tholeiite in the northwestern Great Basin, U.S.A.; 1982: 431.
Note: DIALOG GEOREF FILE 89 English.

30. Hart, W. K.; Aronson, J. L.; Mertzman, S. A. (Case West. Reserve Univ., Cleveland, OH, USA; Franklin and Marshall Coll., USA). <Analytic> Areal distribution and age of low-K, high-alumina olivine tholeiite magmatism in the northwestern Great Basin. Geological Society of American Bulletin 95: 2; 1984: 186-195; CODEN: BUGMAF; ISSN: 0016-7606.
Note: DIALOG GEOREF FILE 89 English illus., 290 anal., 3 tables, sketch maps.
The time period over which high-alumina olivine tholeiite (HAOT) lavas were erupted extends from late Miocene to Holocene. Overlap with the timing of Snake River, Cascade, and northwestern Basin and Range volcanism, but distinguished from the main pulse of Columbia River volcanism. Three major pulses of HAOT magmatism. Distinctive holocrystalline, nonporphyritic, and diktytaxitic texture, low incompatible-element concentrations.--Modified journal abstract.

31. Heiss, H. <Analytic> Regional geology; Part VI. Water well Journal 32: 7; 1978: 73-75; CODEN: WWJOA9; ISSN: 0043-1443.
Note: DIALOG GEOREF FILE 89 English sketch map.

32. Higgs, N. B. <Analytic> Slaking basalts. Assoc. Eng. Geol., Bull. 13: 2; 1976: 151-162; CODEN: ENGEA9.
Note: DIALOG GEOREF FILE 89 English tables.

33. Hoffer, Jerry M. <Analytic> Compositional variations of plagioclase feldspar from a basaltic lava flow. Am. Mineralogist v. 51, nos. 5-6, p. 807-813, illus., table; 1966.
Note: DIALOG GEOREF FILE 89.
A detailed study of the Rock Creek basalt flow reveals significant relationships between chemical composition of the plagioclase feldspar and texture. The An content of the groundmass plagioclase varies inversely with size and directly with the amount of associated glass. The rate of cooling, after extrusion, determined the composition of the groundmass plagioclase. The plagioclase phenocrysts, averaging 20 percent more calcic than the corresponding groundmass plagioclase, are intratelluric.

34. Hoffer, Jerry M. <Analytic> Order-disorder relationships of plagioclase in a porphyritic basalt flow. Am. Mineralogist v. 53, nos. 5-6, p. 908-916, illus; 1968.
Note: DIALOG GEOREF FILE 89.
The structural state of phenocryst and groundmass plagioclase from a thick prophyritic flow of the Columbia River Basalt ranges from high to intermediate disorder. Two groups have been differentiated: (1) Groundmass plagioclase in a lower structural state than phenocrysts; the groundmass plagioclase is more calcic than the An 50 and of small size. (2) Groundmass plagioclase in a higher structural state than phenocrysts; groundmass plagioclase generally less calcic than An 50 and of large size. The latter group contains smaller amounts of glass than those of group one. The reversal in structural state relationship between the phenocryst and groundmass plagioclase of (2) is probably due to the sluggishness of the transformation from disorder to order in plagioclase less calcic than An 50.

35. Honjo, N. (Rice Univ., Houston, TX, USA). <Monographic> Petrology and geochemistry of the Magic Reservoir eruptive center, Snake River Plain, Idaho; 1986: 511.
Note: DIALOG GEOREF FILE 89 English 5 plates.

36. Honjo, N.; Leeman, W. P. (Rice Univ., Kieth-Wiess Geol. Lab., Houston, TX 77251, USA). <Analytic> Origin of hybrid ferrolatite lavas from Magic Reservoir eruptive center, Snake River Plain, Idaho. Contributions to Mineralogy and Petrology 96: 2; 1987: 163-177; CODEN: CMPEAP; ISSN: 0010-7999.
Note: DIALOG GEOREF FILE 89 English illus., 14 anal., 7 tables, geol. sketch map, charts.

37. Ireton, M. F.; Rea, G. T. (EDITOR) (Gem State Grotto, Box 256, Mountain Home, ID, USA). <Analytic> Vulcanospeleology of the lower Snake River basin <Monographic> Proceedings of the Annual meeting of the National Speleological Society. The NSS Bulletin 45: 1; 1983: unpaginated; ISSN: 0146-9517.
Note: DIALOG GEOREF FILE 89 English.

38. Ireton, M. F.; Wilson, M. D. (Boise State Univ., Dep. Geol. and Geophys., Boise, Idaho, USA). <Analytic> Relationship of a lava tube cave system to lava flow development Lincoln County, Idaho. Geol. Soc. Am., Abstr. Programs 9: 7; 1977: 1033; CODEN: GAAPBC.
Note: DIALOG GEOREF FILE 89 English.

39. Jacobson, N. D. (investigator). <Analytic> Ground-water conditions in the Michaud Flats area, Fort Hall Indian Geological Survey Professional Paper 1375; 1982: 97-98; CODEN: XGPPA9; ISSN: 0096-0446.
Note: DIALOG GEOREF FILE 89 English.

40. Jeanloz, R.; Schleicher, D. (U.S. Geol. Surv., Denver, United States). <Analytic> A bimodal rhyolite-basalt sequence on the north margin of the eastern Snake River Plain, Idaho. Geol. Soc. Am., Abstr. Programs 7: 5: Rocky Mountain Section, 28th annual meeting; 1975: 615; CODEN: GAAPBC.
Note: DIALOG GEOREF FILE 89 English.

41. Jobin, Daniel A.; Schroeder, Marvin L. <Analytic> Geology of the Conant Valley Quadrangle, Bonneville County, Idaho. U.S. Geol. Survey Mineral Inv. Field Studies Map MF-277, scale 1:24,000, with text,; 1964.
Note: DIALOG GEOREF FILE 89.
The principal mineral resources of the Conant Valley Quadrangle are riprap, available from talus slopes of basalt of the Snake River and Pine Creek; sand and gravel from islands and banks of the Snake River; limestone principally from the Wells and Mission Canyon Formations; and phosphate mainly from the Meade Peak Phosphatic Shale Member of the Phosphoria Formation. Included is a table of the chemical analyses of the aforementioned Member.

42. Johnson, Arnold I. <Analytic> Determination of hydrologic and physical properties of volcanic rocks by laboratory methods <Monographic> in Dr. D. N. Wadia Commemorative Volume. Calcutta, India, Mining, Geol. and Metall. Inst. India p. 49-66, illus., tables; 1965.
Note: DIALOG GEOREF FILE 89.
Analytical methods used in the Denver, Colo., Hydrologic Laboratory of the U.S. Geological Survey are briefly described, and hydrologic and physical properties data presented for samples of volcanic rock from near Los Alamos, N. Mex., Arco, Idaho, Mercury, Nev., and Eniwetok, Marshall Islands. In a thick formation of considerable areal extent characteristics such as joints, fractures, interflow sediments, and open spaces between flows may have great influence on the quantitative hydrology even though the permeability and effective porosity of the rocks themselves are low. However, for the analysis of a hydrologic problem, it is important to know these properties of the rocks as well as of the formational unit.

43. Jones, R. W.; Buffa, J. W. (Univ. Idaho, Dep. Geol., Moscow, Idaho, USA; Union Carbide). <Analytic> Chemistry of early Tertiary age Challis Volcanics in south half of the Twin Peaks Quandrangle, East-central Idaho. Geol. Soc. Am., Abstr. Programs 9: 6; 1977: 737; CODEN: GAAPBC.
Note: DIALOG GEOREF FILE 89 English.

44. Jones, Robert W. <Analytic> Comparison of Columbia River basalts and the Snake River Plain basalts <Monographic> in Columbia River Basalt Symposium, 2nd, 1969, p. 209-221, illus. (incl. sketch maps). East. Wash. State Coll. Press Cheney; 1970.
Note: DIALOG GEOREF FILE 89 English.

45. Jorgenson, D. B.; Karlo, J. F.; Fountain, J. C. (Cent. Mich. Univ., Dep. Geol., Mt. Pleasant, Mich., USA; State Univ. N.Y. at Buffalo, USA). <Analytic> Tertiary high-alumina basalts of the Snake River volcanic province, Idaho. Geol. Soc. Am., Abstr. Programs 11: 6; 1979: 276; CODEN: GAAPBC; ISSN: 0016-7592.
Note: DIALOG GEOREF FILE 89 English.

46. Karlo, J. F.; Clemency, C. V. (Cent. Mich. Univ., Geol. Dep., USA; State Univ. NY, Buffalo, NY, USA). <Analytic> Picrite xenoliths from the eastern Snake River Plain, Idaho. Contrib. Mineral. Petrol.--Beitr. Mineral. Petrol. 73: 2; 1980: 173-178; CODEN: CMPEAP; ISSN: 0010-7999.
Note: DIALOG GEOREF FILE 89 English illus., tables, geol. sketch map.

47. Kellogg, Karl S.; Marvin, Richard F. (U.S. Geol. Surv., USA). <Monographic> New potassium-argon ages, geochemistry, and tectonic setting of upper Cenozoic volcanic rocks near Blackfoot, Idaho. Geological Survey Bulletin (Washington); 1988: 19; CODEN: XDIGAS; ISSN: 0364-4510.
Note: DIALOG GOEREF FILE 89 English illus., 2 tables, geol. sketch map.

48. Kimbrell, A. F.; Miller, W. O.; Farmer, I. W. (EDITOR); Daemen, J. J. K. (EDITOR); Desai, C. S. (EDITOR); Glass, C. E. (EDITOR); Neuman, S. P. (EDITOR) (U.S. Army Waterw. Exp. Stn., Geotech. Lab., Vicksburg, MS, USA Univ. Ariz., Tucson, AZ, USA). <Analytic> A laboratory and field assessment of non-linear pressure flow relationships <Monographic> Rock mechanics; proceedings of the 28th U.S. symposium. Proceedings - Symposium on Rock Mechanics 28; 1987: 517-524; CODEN: PSRMA6; ISSN: 0586-3031.
Note: DIALOG GEOREF FILE 89 English.

49. Klauss, T. E. (Idaho State). <Monographic> Petrographic variations along the Portneuf Valley lava flow; 1969: unpaginated.
Note: DIALOG GEOREF FILE 89 English.

50. Knowles, Charles R. <Analytic> Chemical and mineralogic variations within a single basalt flow [abstr.]. Geol. Soc. Am., Abstr. Vol. 5, No. 7, p. 696; 1973; CODEN: GAAPBC.
Note: DIALOG GOEREF FILE 89 English.

51. Kuntz, M. A. (investigator); Dalrymple, G. B. (investigator); Kork, J. O. (investigator). <Analytic> Volcanic recurrence intervals and volcanic hazards in the eastern Snake River Plain in Idaho. U.S. Geol. Surve., Prof. Pap. 1150; 1979: 71-72; CODEN: XGPPA9.
Note: English.

52. Kuntz, M. A.; Champion, D. E.; Spiker, E. C.; Lefebvre, R. H.; McBroome, L. A.; Bonnichsen, B. (EDITOR); Breckenridge, R. M. (EDITOR) (U.S. Geol. Surv., Denver, CO, USA; Grand Valley State Coll., Dep. Geol., USA Idaho Bur. Mines and Geol., Moscow, ID, USA). <Analytic> The Great Rift and the evolution of the Craters of the Moon lava field, Idaho <Monographic> Cenozoic geology of Idaho. Bulletin - Idaho Bureau of Mines and Geology 26; 1982: 423-437; ISSN: 0073-442X.
Note: DIALOG GEOREF FILE 89 English 1 table, sketch map.

53. Leeman, W. P.; Olsen, K. H. (convener); Chapin, C. E. (chairperson) (Rice Univ., Geol. Dep., Houston, TX, USA Los Alamos Sci. Lab., Geosci. Div., Los Alamos, NM, USA). <Analytic> Petrology and geochemistry of volcanic rocks from the Snake River Plain - Yellowstone province <Monographic> 1978 International symposium on the Rio Grande Rift; program and abstract. Conf. Proc. - Los Alamos Sci. Lab., LA-C 7487; 1978: 50-51.
Note: DIALOG GEOREF FILE 89 English.

54. Leeman, W. P.; Vitaliano, C. J.; Prinz, M. (U. S. Geol. Surv., Fed. Cent., Denver, Colo., USA; Indiana Univ., United States). <Analytic> Petrology and origin of "evolved" lavas from Craters of the Moon lava field, Snake River Plain (SRP). Geol. Soc. Am., Abstr. Programs 7: 5: Rocky Mountain Section, 28th annual meeting; 1975: 622; CODEN: GAAPBC.
Note: DIALOG GEOREF FILE 89 English.

55. Leeman, W. P.; Vitaliano, C. J. (Oreg. State Univ., Dep. Geol., Corvallis, Oreg., USA; Indiana Univ., United States). <Analytic> Petrology of McKinney Basalt, Snake River Plain, Idaho. Geol. Soc. Am., Bull. 87: 12; 1976: 1777-1792; CODEN: BUGMAF.
Note: DIALOG GEOREF FILE 89 English. See also this Bibliography, Leeman, W. P., 02 illus., tables, sketch map.

56. Mansfield, George Rogers, 1875-1947. <Analytic> Geography, geology, and mineral resources of the Ammon and Paradise Valley quadrangles, Idaho. U.S. Geol. Survey Prof. Paper 238 v. 92 p., illus. incl. geol. map; 1952.
Note: DIALOG GEOREF FILE 89

57. Matzner, R. A.; Anonymous (Benham Group, Oklahoma City, OK, USA). <Analytic> Hydrogeologic and geophysical investigations of the Springfield/Blackfoot area, Idaho <Monographic> International water well exhibition; abstracts of papers to be presented at the Ground-Water Technology Division's Education Session. Ground Water 21: 4; 1983: 518-519; CODEN: GRWAAP; ISSN: 0017-467x.
Note: DIALOG GEOREF FILE 89 English

58. Mazierski, P. F.; King, J. S. (State Univ. N.Y. at Buffalo, Dep. Geol. Sci., Amherst, NY, USA). <Analytic> The geology of Pine and Crater buttes; two basaltic constructs on the far eastern Snake River Plain. NASA Technical Memorandum 89810; 1987: 368-370; CODEN: NATMA4; ISSN: 0499-9320.
Note: DIALOG GEOREF FILE 89 English Reports of the Planetary Geology and Geophysics Program, 1986 illus.

59. Mazierski, Paul F.; King, John S. (State Univ. N.Y. at Buffalo, Dep. Geol. Sci., Amherst, NY, USA). <Analytic> Basaltic plains volcanism on the eastern Snake River Plain, Idaho; a geologic and petrologic study of Pine and Crater buttes <Monographic> Reports of Planetary Geological and Geophysics Program.
Note: DIALOG GEOREF FILE 89.

60. McBroome, L. A.; Doherty, D. J.; Kuntz, M. A.; Riddihough, R. P. (chairperson); Johnson, S. (chairperson) (U.S. Geol. Surv., Denver, CO, USA; Oreg. State Univ., USAPac. Geosci. Cent., CAN). <Analytic> Geological interpretation of INEL-1, the deepest well on the eastern Snake River Plain, Idaho <Monographic> American Geophysical Union; Twenty-sixth annual meeting of Pacific Northwest AGU. Eos, Transactions, American Geophysical Union 61: 6; 1980: 66, 67; CODEN: EOSTAJ; ISSN: 0096-3941.
Note: DIALOG GEOREF FILE 89 English.

61. McCaslin, J. C. (Oil and Gas J., Tulsa, OK, USA). <Analytic> Snake River test renews interest in Idaho. Oil and Gas Journal 81: 25; 1983: 145-146; CODEN: OIGJAV; ISSN: 0030-1388.
Note: DIALOG GEOREF FILE 89 English sketch map.

62. McKee, Edwin H.; Mark, Robert K. <Analytic> Strontium isotopic composition of two basalts representative of the southern Snake River volcanic province. U. S. Geol. Surv., Prof. Pap. No. 750B, p. B92-B95, sketch map; 1971; CODEN: XGPPA9.
Note: DIALOG GEOREF FILE 89 English Sr-87/Sr-86, Pliocene, Sheep Creek range, Great Basin, Nevada.

63. McNary, S. W. (Univ. of Idaho, Moscow, Idaho USA). <Monographic> Petrography and field studies of late Cenozoic basalt flows and intrusions in the Orofino-Elk River area, Idaho; 1976: 135.
Note: DIALOG GEOREF FILE 89 English.

64. Menzies, M. A.; Leeman, W. P.; Hawkesworth, C. J.; Moorbath, S. (EDITOR); Thompson, R. N. (EDITOR); Oxburgh, E. R. (EDITOR) (Open Univ. Milton Keynes, Dep. Earth Sci., Milton Keynes, GBR; Imp. Coll. Sci. and Technol., Dep. Geol., GBRUniv. Oxford, Dep. Geol. and Mineral., Oxford, GBR). <Analytic> Geochemical and isotopic evidence for the origin of continental flood basalts with particular reference to the Snake River Plain, Idaho, U.S.A. <Monographic> The relative contributions of mantle, oceanic crust and continental crust to magma genesis. Philosophical Transactions of the Royal Society of London, Series A: Mathematical and Physical Sciences 310: 1514; 1984: 643-660; CODEN: PTRMAD; ISSN: 0080-4614.
Note: DIALOG GEOREF FILE 89 English with discussion by Pankhurst, R. J. illus., sketch maps.

65. Morgenstern, Karl A.; Syverson, Tim L. (Ecol. and Environ., Seattle, WA, USAAssociation of Ground Water Scientists and Engineers, Dublin, OH, USA). <Analytic> Determination of contaminant migration in vertical faults and basalt flows with electromagnetic conductivety techniques <Monographic> Proceedings of the Second national outdoor action conference on Aquifer restoration, ground water monitoring and geophysical methods. Proceedings of the National Outdoor Action Conference on Aquifer Restoration, Ground Water Monitoring and Geophysical Methods 2; 1988: 597-616.
Note: DIALOG GEOREF FILE 89 English 2 tables, sketch maps.

66. Muehlenbachs, K.; Stone, G. T. (Carnegie Inst., Washington, D. C., USA). <Analytic> Oxygen isotope compositions of some basaltic lavas from the Snake River Plain. Carnegie Inst. Wash., Yearb. 72; 1973: 598-601; CODEN: CIWYAO.
Note: DIALOG GEOREF FILE 89 English.

67. Muller, S. C. (Idaho State Univ., Dep. Geol., Pocatello, Idaho, USA). <Analytic> Distribution and genesis of a copper mineralization near Pocatello, Idaho. Geol. Soc. Am., Abstr. Programs 7: 5: Rocky Mountain Section, 28th annual meeting; 1975: 632-633; CODEN: GAAPBC.
Note: DIALOG GEOREF FILE 89 English.

68. Nace, R. L.; Voegeli, P. T.; Jones, J. R.; Deutsch, M.; Subitzky, S. (EDITOR) (U.S. Geol. Surv., USA). <Monographic> Generalized geologic framework of the National Reactor Testing Station, Idaho. U.S. Geol. Surv., Prof. Pap. 725-B; 1975: 49; CODEN: XGPPA9.
Note: DIALOG GEOREF FILE 89 English Geology, hydrology, and waste management at the National Reactor Testing Station, Idaho illus., ; 1:48,000; colored geol. map.

69. Newcomb, R. C. (investigator). <Analytic> Structural control of ground water in basalt. Geological Survey Professional Paper 525A; 1965: A169; CODEN: XGPPA9; ISSN: 0096-0446.
Note: DIALOG GEOREF FILE 89 English.

70. Newcomb, R. C.; Powar, K. B. (EDITOR); Thigale, S. S. (EDITOR) (Consult. Geol., Portland, OR, USAUniv. Poona, Dep. Geol., Poona, IND). <Analytic> Groundwater in the Columbia River Basalt <Monographic> Hydrogeology of volcanic terrains; 1986: 1-19.
Note: DIALOG GEOREF FILE 89 English illus., sketch map.

71. Niccum. M. R. (Idaho State). <Monographic> Geology and permeable structures in basalts of the east central Snake River Plain; 1969: unpaginated.
Note: DIALOG GEOREF FILE 89 English.

72. Niccum, Marvin R. <Analytic> Geology and permeable structures in basalts (Pleistocene-recent) of the east central Snake River Plain near Atomic City, Idaho; 1969.
Note: DIALOG GEOREF FILE 89 English.

73. Niccum, Marvin R. <Analytic> The construction and subsurface geology of the PBF waste seepage wells <Monographic> in Engineering geology and soils engineering, p. 65-84; illus., Idaho Dep. Highw. Boise; 1970.
Note: DIALOG GEOREF FILE 89 English Soil composition and properties, basalt, x-ray diffraction analysis, National Reactor Testing Station, Idaho.

74. Page, Oliver. <Analytic> Feasibility of subsurface correlation at the National Reactor Testing Station, Idaho [abs.] Geol. Soc. America Spec. Paper 87 p. 298; 1966.
Note: DIALOG GEOREF FILE 89.

75. Perkins, W. D.; Fiesinger, D. W. (Utah State Univ., Dep. Geol., Logan, Utah, USA). <Analytic> Mineralogy and chemistry of the Quaternary basalts from Gem Valley (Caribou Co.), Idaho. Geol. Soc. Am., Abstr. Programs 11: 6; 1979: 299; CODEN: GAAPBC; ISSN: 0016-7592.
Note: DIALOG GEOREF FILE 89 English.

76. Peterson, Donald William. <Analytic> The prebasalt surface in the vicinity of Peck, Idaho. Northwest Science v. 29, no. 1, p. 1-9, illus., Feb; 1955.
Note: DIALOG GEOREF FILE 89

77. Pitz, C. F.; Thiessen, R. L.; Aldrich, M. J., Jr. (EDITOR); Laughlin, A. W. (EDITOR) (327 NW 54th St., Seattle, WA, USA: Wash. State Univ., USALos Alamos Natl. Lab., Los Alamos, NM, USA). <Analytic> Lineament analysis and structural mapping of the Trans-Idaho Discontinuity and their implications for regional tectonic models <Monographic> Proceedings of the Sixth international conference on basement tectonics; 1986: 16-24.
Note: DIALOG GEOREF FILE 89 English geol. sketch maps.

78. Powers, Howard Adorno. <Analytic> A distinctive chemical characteristic of Snake River basalts of Idaho. Art. 137 in U. S. Geol. Survey Prof. Paper 400-B p. B298 incl. diagram; 1960.
Note: DIALOG GEOREF FILE 89

79. Prieto, C.; Perkins, C.; Berkman, E. (Integr. Geophys. Corp., Houston, TX, USA; Emerald Explor. Consult., USA). <Analytic> Columbia River Basalt plateau, an integrated approach to interpretation of basalt-covered areas. Geophysics 50: 12; 1985: 2709-2719; CODEN: GPYSA7; ISSN: 0016-8033.
Note: DIALOG GEOREF FILE 89 English illus., 1 table, sects., strat. cols., sketch maps.

80. Prinz, Martin. <Analytic> Volcanic geology of the American Falls area <Monographic> in Structures and origin of volcanic rocks, Montana-Wyoming-Idaho--Natl. Sci. Found. Summer Field Course 1968, Guidebook. Detroit, Mich., Wayne State Univ. p. 56-63, illus; 1968.
Note: DIALOG GEOREF FILE 89.
This one-day field trip has been added in the 1968 revision of the original 1965 guidebook. A stratigraphic section along the Snake River south of American Falls Dam, Idaho, and the lavas of King's Bowl Rift are examined. The section represents Pliocene to Holocene rocks of the Eastern Snake River Plain, including rhyolitic and basaltic tuffs, Quaternary basalt flows, many other types of basaltic rocks, and intercalated fluvial and lake sediments. The formations are described and the sequence of geologic events outlined, including volcanism, faulting, erosion, deposition, and drainage changes. Lavas of the King's Bowl, entirely of Holocene age, are symmetrically related to an open rift zone, a sourthward extension of the Great Rift of the Craters of the Moon lava field. Geologic sketch maps and a columnar section are included.

81. Prostka, H. J.; McIntyre, D. H.; Skipp, B. (U. S. Geol. Surv., Denver, Colo., USA). <Analytic> Interrelations of lower Tertiary volcanic fields in northwestern interior United States. Geol. Soc. Am., Abstr. Programs 9: 6; 1977: 755-756; CODEN: GAAPBC.
Note: DIALOG GEOREF FILE 89 English.

82. Russell, J. K.; Nicholls, J. (Univ. Calgary, Dep. Geol. and Geophys., Calgary, AB, CAN). <Analytic> Application of Duhem's theorem to the estimation of extensive and intensive properties of basaltic magmas. The Canadian Mineralogist 23, Part 3; 1985: 479-488; CODEN: CAMIA6; ISSN:0008-4476.
Note: DIALOG GEOREF FILE 89 English <Summary> French Geochemistry of mineral deposits illus., 4 tables.

83. Schmalz, Bruce L.; Keys, W. Scott. <Analytic> Retention and migration of radioactive isotopes in the lithosphere at the National Reactor Testing Station, Idaho <Monographic> in La retention et la migration des ions radioactifs dans les sols--Colloque international, Saclay, France, 1962. Paris, Presses Universitaires de France p. 243-256, illus., tables; 1963.
Note: DIALOG GEOREF FILE 89 with French abs.

84. Scott, W. E.; Pierce, K. L.; Bradbury, J. P.; Forester, R. M.; Bonnichsen, B. (EDITOR); Breckenridge, R. M. (EDITOR) (U.S. Geol. Surv., Denver, CO, USAIdaho Bur. Mines and Geol., Moscow, ID, USA). <Analytic> Revised Quaternary stratigraphy and chronology in the American Falls area, southeastern Idaho <Monographic> Cenozoic geology of Idaho. Bulletin - Idaho Bureau of Mines and Geology 26; 1982: 581-595; ISSN: 0073-442X.
Note: DIALOG GEOREF FILE 89 English illus., 3 tables, sect., strat. cols., sketch maps.

85. Siems, P. L.; Jones, R. W. (Univ. Idaho, Dep. Geol., Moscow, Idaho, USA). <Analytic> The Challis volcanic field; a review. Geol. Soc. Am., Abstr. Programs 9: 6; 1977: 762-763; CODEN: GAAPBC.
Note: DIALOG GEOREF FILE 89 English.

86. Spear, D. B. (State Univ. N.Y., Dep. Geol. Sci., Amherst, N.Y., USA). <Analytic> Evidence for the mixing of rhyolite and basalt magmas at East Butte, eastern Snake River Plain, Idaho. Geol. Soc. Am., Abstr. Programs 11: 6; 1979: 303; CODEN: GAAPBC; ISSN: 0016-7592.
Note: DIALOG GEOREF FILE 89 English.

87. Spear, D. B. (State Univ. of New York, Buffalo, Amherst, N.Y., USA). <Monographic> The geology and volcanic history of the Big Southern Butte-East Butte area, eastern Snake River Plain, Idaho; 1979: 198.
Note: DIALOG GEOREF FILE 89 English.

88. Spear, D. B.; King, J.S.; Bonnichsen, B. (EDITOR); Breckenridge, R. M. (EDITOR) (Arco Explor. Co., Houston, TX, USA: State Univ. N.Y. at Buffalo, USA Idaho Bur. Mines and Geol., Moscow, ID, USA). <Analytic>

The geology of Big Southern Butte, Idaho <Monographic> Cenozoic geology of Idaho. Bulletin - Idaho Bureau of Mines and Geology 26; 1982: 395-403; ISSN: 0073-442X.
Note: DIALOG GEOREF FILE 89 English illus., 1 table, strat. col., sketch maps.

89. Spendlove, E. <Analytic> Field trip; Gooding geodes. Rock Gem 10: 4; 1980: 64-67; ISSN: 0048-8453.
Note: DIALOG GEOREF FILE 89 English illus., sketch map.

90. Stearns, Harold Thornton. <Analytic> Causes of basaltic explosions. Geol. Soc. America Bull. v. 64, no. 5, p. 599, May; 1953.
Note: DIALOG GEOREF FILE 89.

91. Stout, M. Z. (Calgary). <Monographic> Mineralogy and petrology of Quaternary lavas, Snake River Plain, Idaho and the cation distribution in natural titanomagnetites; 1975: unpaginated.
Note: DIALOG GEOREF FILE 89 English.

92. Stout, M. Z.; Nicholls, J. <Analytic> Mineralogy and pertrology of Quaternary lavas from the Snake River Plain, Idaho. Geol. Soc. Am., Abstr. Programs 7: 5: Rocky Mountain Section, 28th annual meeting; 1975: 644; CODEN: GAAPBC.
Note: DIALOG GEOREF FILE 89 English.

93. Stout, M. Z.; Nicholls, J. <Analytic> Mineralogy and petrology of Quaternary lavas from the Snake River Plain, Idaho. Can. J. Earth Sci. 14: 9; 1977: 2140-2156; CODEN: CJESAP.
Note: DIALOG GEOREF FILE 89 English <Summary> French illus., tables, sketch map.

94. Swanson, D. A.; Wright, T. L.; Armentrout, J. M. (EDITOR); Cole, M. R. (EDITOR); TerBest, H., Jr. (EDITOR) (U.S. Geol. Surv., Menlo Park, Calif., USA: U.S. Geol. Surv., Reston, VA., USA). <Analytic> Paleogeography of southeast Washington during the middle and late Miocene based on the distribution of intracanyon basalt flows <Monographic> Cenozoic paleogeography of the western United States. Pac. Coast Paleogeogr. Symp. 3; 1979: 331.
Note: DIALOG GEOREF FILE 89 English.

95. Theilig, E.; Holt, H.E. (COMPILER) (Ariz. State Univ., Dep. Geol., Tempe, AZ, USA NASA Off. Space Sci. and Appl., Washington, D.C., USA). <Analytic> Ridges on basalt flows <Monographic> Reports of Planetary Geology Program; 1983. NASA Technical Memoradum 86246; 1984: 147-148; CODEN: NATMA4; ISSN: 0499-9320.
Note: DIALOG GEOREF FILE 89 English.

96. Thomspon, R. N. <Analytic> Primary basalts and magma genesis; II, Snake River Plain, Idaho, U.S.A. Contrib. Mineral. Petrol.--Beitr. Mineral. Petrol. 52: 3; 1975: 213-232; CODEN: CMPEAP.
Note: DIALOG GEOREF FILE 89 English for reference to part 1, see Thompson, R. N., Contrib. Mineral. Petrol., Vol. 45, p. 317, 1974 illus., tables.

97. Thompson, Robert N. <Analytic> Titanian chromite and chromian titanomagnetite from a Snake River Plain basalt, a terrestrial analogue to lunar spinels. Am. Mineral. Vol. 58, No. 9-10, p. 826-830, illus; 1973; CODEN: AMMIAY.
Note: DIALOG GEOREF FILE 89 English Microphenocrysts, formed by direct precipitation from basaltic magma, rapid quenching, electron microprobe analysis; Idaho.

98. Toth, M. I.; Martin, R. A.; Moyle, P. R.; Winters, R. A. (U.S. Bur. Mines, USAU. S. Geol. Surv., USA). <Monographic> Mineral resources of the Hell's Half Acre Wilderness Study Area, Bingham and Bonneville counties, Idaho. Geological Survey Bulletin (Washington) 1718-A; 1987; A1-A10; CODEN: XDIGAS; ISSN: 0364-4510.
Note: DIALOG GEOREF FILE 89 English mineral resources of wilderness study areas; southeastern Idaho 1 table, sketch maps; 1:50,000; colored econ. geol. map.

99. Viglienzone, L.; Greeley, R. (Ariz. State Univ., Dep. Geol., Tempe, AZ, USA). <Analytic> Remote sensing of fissure-fed basalt flows and their source areas; Craters of the Moon volcanic field, Idaho. NASA Technical Memorandum 84211; 1981: 443-445; CODEN: NATMA4; ISSN: 0499-9320.
Note: DIALOG GEOREF FILE 89 English sketch map.

100. Warner, M. M.; Tucker, T. E. (EDITOR); Aram, R. B. (EDITOR); Brinker, W. F. (EDITOR); Grabb, R. F., Jr. (EDITOR) (Boise State Univ., Dep. Geol., Boise, ID, USA). <Analytic> Cenozoic marker beds of southern Idaho <Monographic> Montana Geological Society field conference and symposium guidebook to Southwest Montana; 1981: 121-124.
Note: DIALOG GEOREF FILE 89 English strat. col., sketch maps.

101. White, R. W.; Sarcia, C. <Analytic> Natural and artifical weathering of basalt, northwestern United States. Fr., Bur. Rech. Geol. Minieres, Bull, (Ser. 2), Sect. 2 1; 1978: 1-29; ISSN: 0300-9351.
Note: DIALOG GEOREF FILE 89 English <Summary> French illus., tables.

102. Whitehead, R. L. (U.S. Geol. Surv., USA). <Monographic> Geohydrologic framework of the Snake River Plain, Idaho and eastern Oregon. Hydrologic Investigations Atlas HA-0681; 1986: 3 sheets; CODEN: XGHAAQ; ISSN: 0375-7978.
Note: DIALOG GEOREF FILE 89 English Supersedes Open-file report 84-51 1:1,000,000; hydrogeol. map.

103. Whitehead, R. L. (investigator); Lindholm, G. F. (investigator). <Analytic> Geologic mapping on the Snake River Plain in southern Idaho <Monographic> Geological Survey research 1982. Geological Survey Professional Paper 1375; 1982: 107; CODEN: XGPPA9; ISSN: 0096-0446.
Note: DIALOG GEOREF FILE 89 English.

104. Winkelmaier, Joseph R. (Univ. of Idaho, Moscow, ID, USA). <Monographic> Ground water flow characteristics in fractured basalt in a zero order basin; 1987: 128.
Note: DIALOG GEOREF FILE 89 English.

105. Womer, M. B.; Greeley, R.; King, J. S.; Bonnichsen, B. (EDITOR); Breckenridge, R. M. (EDITOR) (Amoco Int. Oil Co., Houston, TX, USA: Ariz. State Univ., Dep. Geol., USA Idaho Bur. Mines and Geol., Moscow, ID, USA). <Analytic> Phreatic eruptions of the eastern Snake River Plain of Idaho <Monographic> Cenozoic geology of Idaho. Bulletin - Idaho Bureau of Mines and Geology 26; 1982: 453-464; ISSN: 0073-442X.
Note: DIALOG GEOREF FILE 89 English illus., sketch maps.

106. Wright, Thomas L. (Hawaii. Volc. Obs., Hawaii Natl. Park, HI, USA). <Monographic> Chemical analyses used to compute the average chemical composition of rocks and glasses for geochemical units defined in the Yakima Basalt Subgroup, Columbia River Basalt Group, Washington, Oregon, and Idaho. Open-File Report (United States Geological Survey. 1978); 1988: 69; CODEN: XGROAG; ISSN: 0196-1497.
Note: DIALOG GEOREF FILE 89 English 7 tables.

107. Wright, Thomas L.; Mangan, Margaret; Swanson, David A. (U. S. Geol. Surv., USA). <Monographic> Chemical data for flows and feeder dikes of the Yakima Basalt Subgroup, Columbia River Basalt Group, Washington, Oregon, and Idaho, and their bearing on a petrogenetic model. Geological Survey Bulletin (Washington); 1989: 71; CODEN: XDIGAS; ISSN: 0364-4510.
Note: DIALOG GEOREF FILE 89 English illus., 17 tables, sketch map.

APPENDIX D

LABORATORY/FIELD--INSTRUMENT/EQUIPMENT PROCEDURES AND CALCULATION PROGRAMS

D.1--CORE PERMEABILITY

D.2--CORE POROSITY/BULK DENSITY

D.3--LABORATORY PERMEABILITY

D.4--LABORATORY POROSITY

D.5--EQUILIBRIUM SATURATION

APPENDIX D.1

CORE PERMEABILITY

APPENDIX D.1

CORE PERMEABILITY

Instrument: Field Core Test Air Permeameter

References: Pirson, S. J.; "Oil Reservoir Engineering," McGraw-Hill New York, 1958, p. 56-96 (also contains extensive background bibliography).

Hill, W. N.; "Permeability Measuring Device," U.S. Patent 3,102,416, Sept. 3, 1963, p. 4.

API, "Recommended Practice for Determining Permeability of Porous Media," API RP 27, Sept. 1952, p. 27.

API, "API Recommended Practice for Core-Analysis Procedure," API RP 40, Aug. 1960, p. 55.

Description:

Types of data collected: Well name, sample location (ft below G.L.), ambient temperature (°C), flowmeter and flowmeter reading pressure drop (psi), core diameter (cm), and brief description of rock being analyzed.

Example:

Well Name

Core Diameter (cm)	Depth (ft below G.L.)	Temperature (°C)	Pressure (psi)	Rotometer (meter#/readings)	Remarks and Core Description

Principle of operation: A deformable stopper is held tightly against the side of the core and air is caused to flow from/to a hole in the stopper to/from the surface of the core. The air flow rate and pressure differential are measured and used to calculate the air permeability of the portion of the core under and near the stopper location.

Limitations: The permeameter must be free of leaks, the flow meters must be clean and operating correctly, and the gauges must be in calibration. In addition, (1) the stopper must seal against the surface of the core, hence areas with large vesicles cannot be measured, and (2) the core surface must be dry and free of dried mud or other material which would impede the flow of air.

Equipment Needs:

1. Permeameter
2. Core holder and stopper of correct geometry
3. Pressure or vacuum source
4. Brushes and rags to clean surface of core
5. Safety glasses
6. Lab notebook

Precautions:

Safety Considerations: Make sure pressure source is securely tethered and safety glasses are worn when system is pressured.

Transportation Considerations: Subject permeameter to a minimum of jarring or bumps.

Special Training Requirements: Operator should be checked out on equipment before using.

Calibration/Standardization:

Frequency: Calibrate gauges and flow meters once a year.

Who Performs: EG&G Calibration lab.

Criteria for Timing: Allow 2 months.

Procedures: Contact Cal lab @ 6-2468.

Installation: Permeameter, pressure/vacuum source, and core holder should be located conveniently close so that operator can reach all controls without delay. Equipment should be secured so that permeameter cannot be bumped or tipped over and pressure/vacuum source cannot be inadvertently moved so as to strain or break connection to permeameter.

Operating Procedures:

Pre-operation

1. Check for leaks between pressure/vacuum source and permeameter at maximum anticipated pressure differential.
2. Check that pressure/vacuum gauges are zeroed and needles are not binding.
3. Check that flow meter floats are at zero flow position, are free, and that interior of tubes appear to be clean.
4. Check for leaks in permeameter by (a) closing valve to core holder, (b) opening number 1 flowmeter, (c) slowly applying maximum anticipated pressure differential to system, and (d) verifying that flow is zero and no leaks are apparent in the connections between flowmeters and pressure/vacuum source.
5. Check for stopper seal by measuring permeability of a short section of plastic or iron pipe the same diameter as the core. If permeability is not zero, we are in trouble. Replace stopper and verify lack of perm.
6. Clean core with stiff bristle brush to remove excess mud and dirt.

Operation

1. Open flowmeter 5 and (a) close valve to stopper, (b) apply pressure differential to permeameter, (c) regulate pressure at about 10 psi, (d) check appropriate pressure valve to ascertain that it is reading correct pressure, (e) place section of core in holder, (f) clamp stopper in place hard enough so that stopper develops a noticeable bulge.
2. Open valve to stopper. If the flowmeter returns to zero, successively try smaller flowmeters until meter is open with measurable (preferably above 10) reading.
3. Tighten clamp on stopper until flowmeter reading stops declining.
4. Record (a) well name, (b) sample depth, (c) temperature, (d) pressure, (e) flow meter number, and (f) flowmeter reading.
5. Close valve to stopper, open flowmeter 5, and remove sample from holder
6. Start measuring operation on next sample.

Common Problems and Solutions:

1. Flowmeter floats exhibit jerky movements. Flowmeter tubes are dirty or damp and require cleaning and drying. (Use "pipe cleaner" to clean/dry inside of tube. Access provided by bolts on top and bottom of flowmeter housing.)
2. Stopper won't seal. Stopper either scarred, cracked, deformed, or stiffened. Replace with new stopper assemblage.

Special Maintenance:

Data Recorded In Lab: Data recorded in field using using previously indicated format.

Data Reduction: Permeability in millidarcys (~μm2) is calculated using a basic PC program having the name PERM + CORE DIAMETER (in cm), i.e., for 3.2 inch core program it is "PERM82.BAS," 1.77 inch core "PERM44.BAS," etc. The permeability has been corrected for Klinkenberg effect and is the "calculated specific" permeability.

Data Reporting: Computer program reports:

WELL NAME _____

Depth (ft. below G.L.)	Temp. (°C)	Press. (psi)	Rate (scc/min)	PERM (md)

Units: Units are as indicated above.

Accuracy: Gauges - 0.1%; Flowmeters - 1-10%; Instrument permeability accuracy far exceed precision of evaluation.

Precision: Because of heterogeneity of rock, reproducibility is $\pm$ a factor of ~2.

Comments: Repeat measurements of the same location on the same sample yielded a standard deviation of about 100%, i.e., actual value is within range of (calculated value/2) <value> (calculated value*2) with a probability of ~ 0.66.

General QA/QC Considerations: The four control samples 1, 2, 3, and 4 should be measured every couple of days. The stopper should be placed on the indicated area and the flowmeter reading should approximate the indicated value. If the reading varies widely, the permeameter should be re-calibrated. (Control samples are kept in desiccator to maintain low water saturation. A relatively small amount of adsorbed water can change the air permeability.)

Program 1-A

A. PERM 82.BAS Operating Instructions:

1. Turn on computer and printer.
2. At the prompt, type BASICA and enter.
3. At OK, hit F3 -- type PERM82 and enter.
4. At OK, hit F2 (you are now in the program).
5. Respond to question on Caps Lock and enter.
6. Type in well name and enter.
7. Type in sample depth and enter (enter in a similar manner all the other questions about the sample properties).
8. After inputting all the sample data, the program will ask if you want to change any input. Compare the input on the screen with the appropriate values in the lab book. If everything looks OK, answer with a cap "N", and go on to the next calculation. If there is an error, answer with a cap "Y", and answer the questions correctly.
9. After you have a good data set and answer with a "N", the program will calculate the perm values, display them on the monitor screen, and type them out on the printer, prior to asking for the input on the next sample.
10. After you have entered all the data for the samples for one well, terminate that set of calculations by entering a "-99" for the next sample depth (and enter, of course).
11. You will get a message about naming the data set you have just finished, and a line that looks like--

    880 NAME "P$" AS "PERM_.DBF"

    with the cursor under the 8. Move the cursor over until it coincides with the underline after the M in PERM, and type in the well's code, (being certain that the file name is enclosed in quotes). Hit enter, then type "RUN 880" and hit enter again.

12. You will then be asked if you want to calculate the porosities for another well. If you answer "Y", you will cycle back to Well Name ----. Continue with the next well as with the first one (follow the previous instructions). If you are through with the calculations, type "N" in answer to question on continuing. You will then be back in basic with an OK prompt.
13. Type "SYSTEM" and enter.
14. You will be back in DOS with the C:\DOS> prompt. Type "PARK" and enter.
15. You are now ready to close up shop. Turn off computer and printer.

B. Listing of basic program PERM82.BAS.

```
10 PRINT ,"* THIS IS A PROGRAM TO CALCULATE PERMEABILITY *"
20 PRINT "          * FOR USE WITH 5 ROTOMETER , 50 PSI BENCHTOP PERMEAMETER *
30 PRINT "         * BASED ON MAR. 2,'90. CALIBRATION AND LITERATURE CONSTANT *
40 REM * PROGRAM BY C F KNUTSON , 3/25/89 *
45 REM * FLOWMETER CALIBRATION ON MARCH 2, 1990
50 PRINT
60 PRINT
70 PRINT "TOGGLE - CAP LOCK - ( USE CAP Y/N FOR OPTION ANSWERS )"
80 PRINT
90 PRINT
110 PRINT
120 LPRINT
130 LPRINT
140 INPUT "WELL NAME...";N$
150 LPRINT
160 LPRINT
170 PRINT
180 LPRINT "WELL NAME...";N$
190 LPRINT
200 LPRINT
210 LPRINT ," SAMPLE DEPTH","   PRESSURE  ","     RATE"," PERMEABILITY"
220 LPRINT ,"(FT BELOW GL)","     (PSI) ","  (SCC/MIN)"," (MILLIDARCY)"
230 LPRINT
240 PRINT "TO END CALCULATIONS, INSERT -99 FOR SAMPLE DEPTH."
250 PRINT
260 WHILE ELEV >-8
265 OPEN "PS" FOR APPEND AS 1
270 INPUT "SAMPLE DEPTH (FT BELOW GL)";ELEV
280 IF ELEV < -9 THEN 800
300 INPUT "TEMPERATURE (DEG C)";T
310 INPUT "PRESSURE (PSI)";P
320 INPUT "ROTORMETER NUMBER";RN
330 INPUT "ROTOMETER READING";RD
340 INPUT "DO YOU WISH TO CHANGE ABOVE INPUT (Y/N)";A$
350 IF A$ = "Y" THEN 270
360 REM * CALCULATE RATE *
365 DP = (P+14.7)
370 ON RN GOTO 400,420,440,460,480
380 PRINT "IMPROPER ROTORMETER DESIGNATION AT";ELEV
390 GOTO 320
400 QSC = -.1481+(.1243*RD)+(.0009003*RD^2)
410 GOTO 490
420 QSC = -.5274+(.2271*RD)-(.002626*RD^2)+(3.243E-05*RD^3)-(9.575001E-08*RD^4)
430 GOTO 490
440 QSC = 21.1739+(1.2879*RD)-(.01462*RD^2)+(.0004054*RD^3)-(1.894E-06*RD^4)
450 GOTO 490
460 QSC = 105.1835+(13.281*RD)
470 GOTO 490
480 QSC = -148.2321+(80.3888*RD)
490 CON = (((T+273.15)/293.15)*(24.7/DP))^.5
500 PRINT "QSC=...";QSC,
510 PRINT "CON=...";CON,
520 Q = QSC/CON
530 REM * CALCULATE PERMEABILITY *
540 VIS = (17+(.03*T))/1000
550 DP = (P+14.7)
560 AP = (DP+14.7)/2
```

```
630 KA = KG
640   FOR N = 1 TO 20
650   KL = KG/(1+(.777*KA^-.39)/AP)
660   X = (KA-KL)
670   IF X < .0001 GOTO 710
680   KA = KL
690   PRINT KL
700   NEXT N
710 PRINT "KL=...";KL
720 X=1
730 REM * PRINT CALCULATIONS FOR THIS SAMPLE DEPTH *
740 LPRINT " ",
750 LPRINT USING U$;ELEV,
760 LPRINT USING U$;P,
770 LPRINT USING U$;Q,
780 LPRINT USING V$;KL
790 PRINT #1,ELEV,KG.KL
800 CLOSE 1
810 WEND
820 PRINT
830 PRINT
840 PRINT "ASSIGN A NAME TO PERM DATA FROM THIS WELL. NAME = PERM + WELL NAME..
        EXAMPLE -- PERM78_1"
850 PRINT
860 PRINT "AFTER CHANGING NAME, HIT ENTER - THEN TYPE 'RUN 880' AND HIT ENTER AG
AIN."
870 EDIT 880
880 NAME "P$" AS "PERM765A"
890 PRINT
895 LPRINT CHR$(12)
900 PRINT
910 INPUT "DO YOU WANT TO CALCULATE PERMS FOR ANOTHER WELL (Y/N)";A$
920 IF A$ = "Y" THEN 940
930 END
940 CLS
950 RUN
```

APPENDIX D.2

CORE POROSITY/BULK DENSITY

APPENDIX D.2

CORE POROSITY/BULK DENSITY

GEOSCIENCES UNIT
STANDARD PROCEDURES MANUAL FORMAT

Instrument: Field Core Porosity/Bulk Density

References: API, "Recommended Practice for Core-Analysis Procedures," API-RP-40, Aug. 1960, P 55.

Description:

Type of data collected: Well name, sample location (ft. below G.L for core sample top and bottom), core diameters, core lengths, core weight, and brief description of core rock characteristics.

Example:

Well Name:

Depth (core top-bottom) (ft. below G.L.)	Weight (g)	Diameter (cm) (01) (02)	Length (cm) L1 L2 L3 L4

Principle of Operation: A dry piece of core with smooth ends, a relatively regular shape, and a weight less then ~5 kg is selected for analysis. The weight, the average diameter, and the average length are determined. The bulk volume is calculated from the weight and dimensional measurements.

$$BD = WT/(3.1416*(D/2)^2*L) \quad (1)$$

Where:

BD = bulk density, g/cm^3
WT = weight, g
D = average diameter, cm
L = average length, cm

The grain density of basalt core is generally 3.05 + .03 g/cm^3. Thus, the porosity can be calculated + 1%, using this value and the calculated bulk density:

$$\theta = 100 * (BV-GV)/BV \quad (2)$$

Where:

θ = porosity, %
BV = bulk volume, cm^3
GV = grain volume, WT/3.05, cm^3

Limitations: The core sample must be dry, clean, of regular dimensions, and weigh less than 5 kg. In addition: (1) the scale must be in calibration, (2) the sample must not lose any fragments during the measurement procedures, and (3) the scale pan must remain clean and the scale should come to a zero reading before each measurement.

Equipment Needs:

1. 5-kg scale (electronic/automatic zero)
2. 10-cm scale or caliper 30-cm ruler
3. brush and rags to clean core surface
4. compressed air source to final clean core surface
5. safety glasses
6. lab notebook and pen

Precautions:

Safety Considerations: Operator must wear safety glasses and direct compressed air stream away from all personnel.

Transportation Requirements: Scale should be subjected to a minimum of jarring and bumps.

Special Training Requirements: Operator must be able to operate scale and adequately describe core sample.

Calibration/Standardization:

Frequency: Calibrate scale once a year or after any rough handling.

Who Performs: EG&G Calibration Laboratory.

Criteria for Timing: Allow two weeks.

Procedure: Contact EG&G Calibration Laboratory (6-2468) and arrange for pickup and delivery.

Installation: Plug scale to electric socket and check, and arrange compressed air hose so that core samples can be cleaned without subjecting scale to excessive dust.

Operating Procedures:

Pre-Operation:

1. Select appropriate sample.
2. Clean by brushing off mud and blow surface clean with compressed air.
3. Record elevation of top and bottom of core (under correct well heading) in lab notebook.
4. Weigh core sample on electronic scale and record weight in lab notebook.
5. Measure four lengths at representative and equally spaced quadrants on core and record in lab notebook (use metric scale or caliper).
6. Measure two diameters at representative perpendicular locations on core and record in lab notebook.
7. Return sample to original location in core tray or box.

Common Problems and Solutions:

1. Scale does not return to zero after measurement. Usually caused by fragments on pan (clean pan, rezero, and reweigh).

Special Maintenance: None

Date Recorded in Field: (Outlined on page 1).

Data Reduction: Porosity and bulk density are calculated with a PC program having the name POROFLD.BAS.

The listing for POROFLD.BAS and instructions for use are found in section labeled Program 1B.

Program 1-B

A. POROFLD.BAS Operating Instructions:

1. Turn on computer and printer.
2. At the prompt, type BASICA and enter.
3. At OK, hit F3 -- type POROFLD and enter.
4. At OK, hit F2 (you are now in the program).
5. Respond to question on Caps Lock and enter.
6. Type in well name and enter.
7. Type in sample depth and enter (enter in a similar manner all the other questions about the sample properties).
8. After inputting all the sample data, the program will ask if you want to change any input. Compare the input on the screen with the appropriate values in the lab book. If everything looks OK, answer with a cap "N", and go on to the next calculation. If there is an error, answer with a cap "Y", and answer the questions correctly.
9. After you have a good data set and answer with a "N", the program will calculate the perm values, display them on the monitor screen, and type them out on the printer, prior to asking for the input on the next sample.
10. After you have entered all the data for the samples for one well, terminate that set of calculations by entering a "-99" for the next sample depth (and enter, of course).
11. You will get a message about naming the data set you have just finished, and a line that looks like--

    720 NAME "B$" AS "PORO_.DBF"

    with the cursor under the 7. Move the cursor over until it coincides with the underline after the O in PORO, and type in the well's code, (being certain that the file name is enclosed in quotes). Hit enter, then type "RUN 72" and hit enter again.

12. You will then be asked if you want to calculate the porosities for another well. If you answer "Y", you will cycle back to Well Name ----. Continue with the next well as with the first one (follow the previous instructions). If you are through with the calculations, type "N" in answer to question on continuing. You will then be back in basic with an OK prompt.
13. Type "SYSTEM" and enter.
14. You will be back in DOS with the C:\DOS> prompt. Type "PARK" and enter.
15. You are now ready to close up shop. Turn off computer and printer.

B. Listing for basic program POROFLD.BAS.

```
10 CLS
20 PRINT
30 PRINT
40 PRINT
50 PRINT ,"THIS IS A PROGRAM TO CALCULATE POROSITY/DENSITY"
60 PRINT ,"       FOR USE WITH THE FIELD POROSIMETER"
70 REM * PROGRAM BY C F KNUTSON, 6/12/89. *
80 PRINT
90 PRINT
100 PRINT
110 PRINT ,"ACTIVATE CAPS LOCK - ( Y/N ANSWERS MUST BE IN CAPS )"
120 PRINT
130 PRINT
140 PRINT
150 PRINT
160 PRINT
170 PRINT
180 LPRINT
190 INPUT "WELL NAME...";N$
200 LPRINT "     WELL NAME...";N$
210 LPRINT
220 LPRINT
230 LPRINT "            SAMPLE DEPTH   BULK DENSITY  GRAIN DENSITY     POROSITY
 VOID VOL"
240 LPRINT "            (FT BELOW GL)     (GM/CC)       (GM/CC)           (%)
   (CC)"
250 LPRINT
260 PRINT
270 PRINT "TO END CALCULATIONS, INSERT -99 FOR SAMPLE DEPTH."
280 PRINT
290 PRINT
300 WHILE ELEV >-8
310 OPEN "B$" FOR APPEND AS 1
320 PRINT
330 PRINT
340 INPUT "TOP OF SAMPLE INTERVAL (FT BELOW GL).....";ELEV
350 IF ELEV < -9 THEN 630
360 REM * INPUT OF DATA FOR A SINGLE SAMPLE *
365 INPUT "SAMPLE WEIGHT (GM).........";WT
370 INPUT "DIAMETER 1 (CM)....";D1
380 INPUT "DIAMETER 2 (CM)....";D2
390 INPUT "LENGTH 1 (CM)..";L1
400 INPUT "LENGTH 2 (CM)..";L2
410 INPUT "LENGTH 3 (CM)..";L3
420 INPUT "LENGTH 4 (CM)..";L4
460 PRINT
470 INPUT "DO YOU WISH TO CHANGE ABOVE INPUT (Y/N).............";A$
480 IF A$ = "Y" THEN 320
490 VOL = 3.1416*(((D1+D2)/4)^2)*((L1+L2+L3+L4)/4)
505 CVOL = WT/3.05
506 IF CVOL > VOL THEN VOL = CVOL
510 BDEN = WT/VOL
520 POR = (VOL-CVOL)/VOL
530 VVOL = VOL-CVOL
540 PRINT
550 PRINT
560  PRINT ,"BULK DEN";BDEN,"GRAIN DENSITY";WT/CVOL,"POROSITY";POR*100,"VOID VOL
.";VVOL
570 V$ = "####.#       "
580 U$ = "######.##     "
585 W$ = "######.##"
590 LPRINT " ",
600 LPRINT USING V$;ELEV,
610 LPRINT USING U$;BDEN,WT/CVOL,POR*100,
615 LPRINT USING W$;VVOL
620 PRINT #1,ELEV,BDEN,WT/CVOL,POR*100,VVOL
630 CLOSE 1
640 WEND
650 PRINT
660 PRINT
670 PRINT "ASSIGN A NAME TO POROSITY DATA FROM THIS WELL. NAME = PORO + WELL NUM
BER,  I.E.   PORO78 1"
680 PRINT "AFTER CHANGING NAME, HIT ENTER - THEN TYPE 'RUN 720' - AND HIT ENTER
AGAIN."
690 PRINT
700 PRINT
710 EDIT 720
720 NAME "B$"AS "PORO____"
730 PRINT
735 LPRINT CHR$(12)
740 PRINT
750 INPUT "DO YOU WANT TO CALCULATE POROSITIES FOR OTHER WELLS (Y/N)....";A$
760 IF A$ = "Y" THEN 780
770 END
780 PRINT
790 PRINT
800 CLS
810 GOTO 140
820 IF CVOL <0 THEN CVOL = VOL
830 APOR = (VOL-AVOL)/VOL
840 AVOL = AVOL*(1-APOR*.02)
```

OUTPUT

WELL NAME...TEST

SAMPLE DEPTH (FT BELOW GL)	BULK DENSITY (GM/CC)	GRAIN DENSITY (GM/CC)	POROSITY (%)	VOID VOL (CC)
10.0	2.62	3.05	13.95	71.88
20.0	2.58	3.05	15.30	97.75
30.0	2.60	3.05	14.86	232.59

APPENDIX D.3

LABORATORY PERMEABILITY

APPENDIX D.3

LABORATORY PERMEABILITY

GEOSCIENCES UNIT
STANDARD PROCEDURES MANUAL FORMAT

Instrument: Laboratory Air Permeameter

References: Pirson, S. J.; "Oil Reservoir Engineering," McGraw-Hill New York, 1958, p. 56-96 (also contains extensive background bibliography).

Hill, W. N.; "Permeability Measuring Device," U.S. Patent 3,102,416, Sept. 3, 1963, p. 4.

API, "Recommended Practice for Determining Permeability of Porous Media," API RP 27, Sept. 1952, p. 27.

API, "API Recommended Practice for Core-Analysis Procedure," API RP 40, Aug. 1960, p. 55.

Description:

Types of data collected: Well name, sample location (ft below G.L.), ambient temperature (°C), flowmeter and flowmeter reading (#/###) pressure drop (psi), core diameter (cm), and brief description of rock being analyzed.

Example:

Well Name

Depth (ft. below G.L.)	Lab Code (alphanumeric)	Diameters (D1) (D2)	Lengths (L1) (L2)	Temperature (°C)	Pressure (psi)	Rotometer (#/read)	Remarks and Core Description

Principle of operation: The sample's diameter and length are measured and then the sample is placed in a Hassler holder. Gas is forced through the sample and the gas pressure differential and flow rate are measured. The measured data are recorded and subsequently used to calculate the gas and Klinkenberg permeabilities of the sample, utilizing a basic computer program.

Limitations: The permeameter must be free of leaks, the flow meters must be clean and operating correctly, and the rotometers and gauges must be in calibration. In addition, (1) the Hassler holder must seal against the surface of the core, and (2) the gas must be able to flow across the upper and lower faces of the sample.

Equipment Needs:

1. Permeameter
2. Core holder
3. Pressure or vacuum source
4. Digital caliper to measure sample diameter and length
5. Safety glasses
6. Lab notebook and pen

Precautions:

Safety Considerations: Make sure pressure source is securely tethered and safety glasses are worn when system is pressured.

Transportation Considerations: Subject permeameter to a minimum of jarring or bumps.

Special Training Requirements: Operator should be checked out on equipment before using.

Calibration/Standardization:

Frequency: Calibrate gauges and flow meters twice a year.

Who Performs: EG&G Calibration lab.

Criteria for Timing: Allow 2 weeks.

Procedures: Contact Cal lab @ 6-2468.

Installation: Permeameter, pressure/vacuum source, and core holder should be located conveniently close so that operator can reach all controls without delay. Equipment should be secured so that permeameter cannot be bumped or tipped over and pressure/vacuum source cannot be inadvertently moved so as to strain or break connection to permeameter.

Operating Procedures:

Pre-operation

1. Check for leaks between pressure source and permeameter at maximum anticipated pressure differential.
2. Check that pressure gauges are zeroed and needles are not binding.
3. Check that flow meter floats are at zero flow position, are free, and that interior of tubes appear to be clean.
4. Check for leaks in permeameter by (a) closing valve to core holder, (b) opening number 1 flowmeter, (c) slowly applying maximum anticipated pressure differential to system, and (d) verifying that flow is zero and no leaks are apparent in the connections between flowmeters and pressure source.
5. Check holder for adequate seal by inserting an aluminum cylinder the size of the core sample into the holder and verify that zero flow occurs at maximum pressure differential. If flow occurs, replace holder sleeve and verify lack of flow with zero permeability plug.

Operation

1. Record sample identification information in lab notebook and verify that lab identification code (alphanumeric value) is written on side of sample plug in India ink and is legible.
2. Measure plug diameter 4 times and length twice with digital caliper and record values in lab notebook.
3. Insert sample in Hassler holder, place holder in press, and apply confining pressure.
4. Open flowmeter 5 and (a) close valve to holder, (b) apply pressure differential to permeameter, (c) regulate pressure at about 10 psi, (d) check appropriate pressure gage to ascertain that it is reading correct pressure.
5. Open valve to holder. When flowmeter returns to zero, successively try smaller flowmeters until meter is open with measurable (preferable above 10) reading.
6. Record (a) temperature, (b) pressure, (c) flow meter number, and (d) flowmeter reading.
7. Close valve to holder, open flowmeter 5, change confining pressure on holder to atmospheric pressure or vacuum, remove holder from press and sample from holder.
8. Start measuring operation on next sample.

Common Problems and Solutions:

1. Flowmeter floats exhibit jerky movements. Flowmeter tubes are dirty or damp and require cleaning and drying. (Use "pipe cleaner" to clean/dry inside of tube. Access provided by bolts on top and bottom of flowmeter housing.)
2. Holder won't seal. Sleeve either scarred, cracked, punctured, or stiffened. Replace with new sleeve assemblage (check sleeve after every ten measurements by verifying zero flow using zero permeability aluminum plug).

Special Maintenance:

None required.

Data Recorded In Lab: Data is recorded in lab notebook using previously indicated format.

Data Reduction: Permeability in millidarcys (md) is calculated with a basic PC program having name PERMLAB.BAS if only permeability is to be calculated, or LABCALC.BAS if both permeability and porosity are to be calculated at same time. (Both permeability and porosity calculations require dimensional data. Thus, if both parameters are calculated at the same time, the 4 diameters and the 2 lengths need only be entered once.)

The PERMLAB.BAS and LABCALC.BAS listings and instructions for use are found in the section labeled PROGRAM 1-C.

The calculated permeability has been corrected for Klinkenberg effect and is the calculated specific permeability.

Data Reporting: The PERMLAB.BAS computer program reports:

WELL NAME _____

Sample Depth (ft. below G.L.)	Press. (psi)	Rate (scc/min)	PERM (md)
_____	_____	_____	_____

In addition an ASCII computer file is established with a file name PERM plus the well's lab code, e.g. PERM, plus .DBF (e.g., PERMA.DBF). This file is a matrix with the sample depth, gas permeability, and Klinkenberg permeability for each sample analyzed for well A.

The LABCALC.BAS computer program reports:

Sample Depth (ft. below G.L.)	Bulk Den (g/cm^3)	Grain Den (g/cm^3)	Porosity (%)	Air Perm (md)	Klink Perm (md)

Units: Units are as indicated above.

Accuracy: Gauges - 0.1%; Flowmeters - 10%; Instrument permeability accuracy far exceed precision of evaluation, because of the variability in the rock and the small sample size.

Precision: Reproducibility is $\pm$ ~ 10%.

Comments: The permeability measurements are representative of only the small sample plug (2.5 cm diameter 2.8 cm length) that is being measured. The vesicular basalt core frequently has vesicles that are large compared to the sample plug, hence the permeability measurement does not contain a representative sample of the porous elements in the rock and thus does not constitute a statistically significant representation of the rock's permeability.

General QA/QC Considerations: Several control plugs are kept in a desiccator, and should be measured after every few days of operation. If the flow rate is > $\pm$ 10% of control value (at a pressure differential of 10 psi), the system should be checked for leaks, obstructions, or other defects. If the readings cannot be brought within the 10% range, the system should be recalibrated.

Program 1-C

A. PERMLAB.BAS Operating Instructions:

1. Turn on computer and printer.
2. At the prompt, type BASICA and enter.
3. At OK, hit F3 -- type PERMLAB and enter.
4. At OK, hit F2 (you are now in the program).
5. Respond to question on Caps Lock and enter.
6. Type in well name and enter.
7. Type in sample depth and enter (enter in a similar manner all the other questions about the sample properties).
8. After inputting all the sample data, the program will ask if you want to change any input. Compare the input on the screen with the appropriate values in the lab book. If everything looks OK, answer with a cap "N", and go on to the next calculation. If there is an error, answer with a cap "Y", and answer the questions correctly.
9. After you have a good data set and answer with a "N", the program will calculate the perm values, display them on the monitor screen, and type them out on the printer, prior to asking for the input on the next sample.
10. After you have entered all the data for the samples for one well, terminate that set of calculations by entering a "-99" for the next sample depth (and enter, of course).
11. You will get a message about naming the data set you have just finished, and a line that looks like--

    940 NAME "P$" AS "PERM_.DBF"

    with the cursor under the 9. Move the cursor over until it coincides with the underline after the M in PERM, and type in the well's code (being certain that the file name is enclosed in quotes). Hit enter, then type "RUN 940" and hit enter again.

12. You will then be asked if you want to calculate the permeabilities for another well. If you answer "Y", you will cycle back to Well Name ----. Continue with the next well as with the first one (follow the previous instructions). If you are through with the calculations, type "N" in answer to question on continuing. You will then be back in basic with an OK prompt.
13. Type "SYSTEM" and enter.
14. You will be back in DOS with the C:\DOS> prompt. Type "PARK" and enter.
15. You are now ready to close up shop. Turn off computer and printer.

B. Listing for basic program PERMLAB.BAS.

```
10 PRINT ,"* THIS IS A PROGRAM TO CALCULATE PERMEABILITY *"
20 PRINT "           * FOR USE WITH 5 ROTOMETER , 50 PSI BENCHTOP PERMEAMETER *
30 REM * BASED ON JAN. 1989 CALIBRATION AND LITERATURE CONSTANT *
40 REM * PROGRAM BY C F KNUTSON , 3/25/89 *
50 PRINT
60 PRINT
70 PRINT "TOGGLE - CAP LOCK - ( USE CAP Y/N FOR OPTION ANSWERS )"
80 PRINT
90 PRINT
100 KILL "P$"
110 PRINT
120 LPRINT
130 LPRINT
140 INPUT "WELL NAME...";N$
150 LPRINT
160 LPRINT
170 PRINT
180 LPRINT "WELL NAME...";N$
190 LPRINT
200 LPRINT
210 LPRINT ," SAMPLE DEPTH","   PRESSURE  ","     RATE"," PERMEABILITY"
220 LPRINT ,"(FT BELOW GL)","     (PSI)  ","   (SCC/MIN)"," (MILLIDARCY)"
230 LPRINT
240 PRINT "TO END CALCULATIONS, INSERT -99 FOR SAMPLE DEPTH."
250 PRINT
260 WHILE ELEV >-8
270 INPUT "SAMPLE DEPTH (FT BELOW GL)";ELEV
280 IF ELEV < -9 THEN 970
290 OPEN "P$" FOR APPEND AS 1
300 INPUT "TEMPERATURE (DEG C)";T
310 INPUT "PRESSURE (PSI)";P
320 INPUT "ROTORMETER NUMBER";RN
330 INPUT "ROTOMETER READING";RD
340 INPUT "DIAMETER 1 (CM)...";D1
350 INPUT "DIAMETER 2 (CM)...";D2
360 INPUT "DIAMETER 3 (CM)...";D3
370 INPUT "DIAMETER 4 (CM)...";D4
380 INPUT "LENGTH 1 (CM)...";L1
390 INPUT "LENGTH 2 (CM)...";L2
400 INPUT "DO YOU WISH TO CHANGE ABOVE INPUT (Y/N)";A$
410 IF A$ = "Y" THEN 270
420 REM * CALCULATE RATE *
430 ON RN GOTO 460,480,500,520,540
440 PRINT "IMPROPER ROTORMETER DESIGNATION AT";ELEV
450 GOTO 320
460 QSC = .5+(.1*RD)
470 GOTO 550
480 QSC = .993+.0304*RD+(.000605*(RD)^2)
490 GOTO 550
500 QSC = 18.26+.28*RD+(.00693*(RD)^2)
510 GOTO 550
520 QSC = 2.129+11.77*RD-(.013*(RD)^2)
530 GOTO 550
540 QSC = -310.7+62.04*RD-(.0206*(RD)^2)
550 CON = (((T+273.15)/293.15)*(14.7/P))^.5
560 PRINT "QSC=...";QSC,
570 PRINT "CON=...";CON,
580 Q = QSC/CON
590 REM * CALCULATE PERMEABILITY *
600 VIS = (17+(.03*T))/1000
610 DP = (P/14.7)
620 AP = (DP+21)/2
630 U$ = "######.#      "
640 V$ = "#####.##"
650 K = (.02122*Q*VIS*(L1+L2))/((D1+D2+D3+D4)*AP*DP)
660 PRINT "AIR PERM=...";K*1000,
670 REM * CHANGE AIR PERM TO MILLIDARCY AND CALCULATE KLINKENBERG PERM *
680 KG = 1000*K
690 KA = KG
```

```
700   FOR N = 1 TO 20
710   KL = KG/(1+(.777*KA^-.39)/AP)
720   X = (KA-KL)
730   IF X < .0001 GOTO 770
740   KA = KL
750   PRINT KL
760   NEXT N
770 PRINT "KL=...";KL
780 X=1
790 REM * PRINT CALCULATIONS FOR THIS SAMPLE DEPTH *
800 LPRINT " ",
810 LPRINT USING U$;ELEV,
820 LPRINT USING U$;P,
830 LPRINT USING U$;Q,
840 LPRINT USING V$;KL
850 PRINT #1,ELEV,KG.KL
860 CLOSE 1
870 WEND
880 PRINT
890 PRINT
900 PRINT "ASSIGN A NAME TO PERM DATA FROM THIS WELL. NAME = PERM + LAB LETTER.
          EXAMPLE -- PERMA.DBF"
910 PRINT
920 PRINT "AFTER CHANGING NAME, HIT ENTER - THEN TYPE 'RUN 940' AND HIT ENTER AG
AIN."
930 EDIT 940
940 NAME "P$" AS "PERM_.DBF"
950 PRINT
960 PRINT
970 INPUT "DO YOU WANT TO CALCULATE PERMS FOR ANOTHER WELL (Y/N)";A$
980 IF A$ = "Y" THEN 1000
990 END
1000 RUN
```

C. LABCALC.BAS Operating Instructions:

1. Turn on computer and printer.
2. At the prompt, type BASICA and enter.
3. At OK, hit F3 -- type PERMLAB and enter.
4. At OK, hit F2 (you are now in the program).
5. Respond to question on Caps Lock and enter.
6. Type in well name and enter.
7. Type in sample depth and enter (enter in a similar manner all the other questions about the sample properties).
8. After inputting all the sample data, the program will ask if you want to change any input. Compare the input on the screen with the appropriate values in the lab book. If everything looks OK, answer with a cap "N", and go on to the next calculation. If there is an error, answer with a cap "Y", and answer the questions correctly.
9. After you have a good data set and answer with a "N", the program will calculate the perm values, display them on the monitor screen, and type them out on the printer, prior to asking for the input on the next sample.
10. After you have entered all the data for the samples for one well, terminate that set of calculations by entering a "-99" for the next sample depth (and enter, of course).
11. You will get a message about naming the data set you have just finished, and a line that looks like--

    1230 NAME "P$" AS "CALC_.DBF"

    with the cursor under the 1. Move the cursor over until it coincides with the underline after the C in CALC, and type in the well's code (being certain that the file name is enclosed in quotes). Hit enter, then type "RUN 1230" and hit enter again.

12. You will then be asked if you want to calculate the permeabilities for another well. If you answer "Y", you will cycle back to Well Name ----. Continue with the next well as with the first one (follow the previous instructions). If you are through with the calculations, type "N" in answer to question on continuing. You will then be back in basic with an OK prompt.
13. Type "SYSTEM" and enter.
14. You will be back in DOS with the C:\DOS> prompt. Type "PARK" and enter.
15. You are now ready to close up shop. Turn off computer and printer.

D. Listing for basic program LABCALC.BAS.

```
10 CLS
20 PRINT ,"THIS IS A PROGRAM TO CALCULATE POROSITY AND PERMEABILITY"
30 PRINT ,"        FOR USE WITH THE LABORATORY EQUIPMENT"
35 PRINT
36 PRINT "        FOR USE DURING PERIOD 12/14/89 TO 7/4/90"
37 PRINT
40 REM * PROGRAM BY C F KNUTSON, 5/25/89. *
50 PRINT
60 PRINT
70 PRINT
80 PRINT ,"ACTIVATE CAPS LOCK - ( Y/N ANSWERS MUST BE IN CAPS )"
90 PRINT
100 PRINT
110 PRINT
120 INPUT "IS CAPS LOCK ON...(Y/N)...";A$
130 IF A$ <> "Y" THEN 80
140 LPRINT
150 LPRINT
160 CLS
180 PRINT
190 PRINT
200 PRINT
210 LPRINT
220 INPUT "WELL NAME...";N$
230 LPRINT "      WELL NAME...";N$
240 LPRINT
250 LPRINT
260 LPRINT "SAMPLE DEPTH  BULK DEN    GDEN    POR     VVOL   APERM    LPERM"
270 LPRINT " FT BELOW GL  (GM/CC)   (GM/CC)   (%)     (CC)    (MD)     (MD)"
280 LPRINT
290 PRINT
300 PRINT "TO END CALCULATIONS, INSERT -99 FOR SAMPLE DEPTH."
310 PRINT
320 WHILE ELEV >-8
330 OPEN "B$" FOR APPEND AS 1
340 INPUT "SAMPLE DEPTH (FT BELOW GL)";ELEV
350 IF ELEV < -9 THEN 1160
351 PRINT
352 PRINT
353 PRINT "INPUT SAMPLE DIMENSIONAL INFO..."
354 PRINT
355 PRINT
370 INPUT "DIAMETER 1 (MM)...";D1
380 INPUT "DIAMETER 2 (MM)...";D2
390 INPUT "DIAMETER 3 (MM)...";D3
400 INPUT "DIAMETER 4 (MM)...";D4
410 INPUT "LENGTH 1 (MM)...";L1
420 INPUT "LENGTH 2 (MM)...";L2
425 INPUT "SAMPLE WEIGHT (GM)...";WT
430 PRINT
440 PRINT
450 PRINT "HELIUM POROSIMETER READINGS"
460 PRINT
470 INPUT "PRESSURE 1 (HIGH PRESSURE READING--IN PSI)";P1
480 INPUT "PRESSURE 2 (LOW PRESSURE READING--IN PSI)";P2
490 PRINT
500 PRINT "LAB PERMEAMETER READINGS"
510 PRINT
520 INPUT "TEMPERATURE (DEG C)...";T
530 INPUT "PRESSURE (PSI)...";P
540 INPUT "ROTOMETER NUMBER...";RN
550 INPUT "ROTOMETER READING...";RD
560 PRINT
570 PRINT
580 INPUT "DO YOU WISH TO CHANGE ABOVE INPUT (Y/N)...";A$
582 PRINT
584 PRINT
590 IF A$ = "Y" THEN 340
600 REM * CALCULATE POROSITY *
610 VOL = 3.1416*(((D1+D2+D3+D4)/80)^2)*((L1+L2)/20)
620 BDEN = WT/VOL
630 CVOL = 39.9945-(18.54254*P1/P2)
635 IF CVOL > VOL THEN CVOL = VOL
637 VVOL = VOL-CVOL
640 POR = VVOL/VOL
650 REM * CALCULATE PERMEABILITY *
660 REM * CALCULATE RATE FIRST *
670 ON RN GOTO 740,760,780,800,820
680 PRINT
690 PRINT
```

```
680 PRINT
690 PRINT
700 PRINT "IMPROPER ROTORMETER DESIGNATION AT";ELEV
710 PRINT
720 PRINT
730 GOTO 540
740 QSC = -.5301+.1589*RD-.001907*(RD^2)+3.219E-05*(RD^3)
750 GOTO 830
760 QSC = -7.487+.6512*RD-.01151*(RD^2)+.0001038*(RD^3)-2.885E-07*(RD^4)
770 GOTO 830
780 QSC = 72.463-1.523*RD+.04294*(RD^2)-.0001356*(RD^3)
790 GOTO 830
800 QSC = 3.7972+12.226*RD-.01433*(RD^2)
810 GOTO 830
820 QSC = -211.3+59.79*RD
830 CON = (((T+273.15)/293.15)*(14.7/P))^.5
840 PRINT "QSC=";QSC,
850 PRINT "CON=";CON,
860 Q = QSC/CON
863 IF Q < 0 THEN Q=.01
865 PRINT "Q=";Q
870 REM * CALCULATE PERMEABILITY *
880 VIS = (17+(.03*T))/1000
890 DP = (P+14.6)/14.6
900 AP = (DP+1)/2
910 U$ = "######.#      "
920 V$ = "#####.##"
930 K = (1.6976*Q*VIS*(L1+L2))/((D1+D2+D3+D4)^2*AP*(DP-1))
940 PRINT "AIR PERM (MD) =";K*1000
950 REM * CHANGE AIR PERM TO MILLIDARCY AND CALCULATE KLINKENBERG PERM *
960 KG = 1000*K
970 KA = KG
980   FOR N = 1 TO 20
990   KL = KG/(1+(.777*KA^(-.39))/AP)
1000  X = (KA-KL)
1010  IF X < .0001 GOTO 1050
1020  KA = KL
1030  PRINT KL
1040   NEXT N
1050 PRINT "KL=";KL
1060 X=1
1065 PRINT
1070 REM * PRINT CALCULATIONS FOR THIS SAMPLE DEPTH *
1080 LPRINT USING U$;ELEV,
1090 LPRINT USING V$;BDEN,
1100 LPRINT USING V$;WT/CVOL,
1110 LPRINT USING V$;POR*100,
1115 LPRINT USING V$;VVOL,
1120 LPRINT USING V$;KG,
1130 LPRINT USING V$;KL
1140  PRINT ,"BULK DEN";BDEN,"GRAIN DENSITY";WT/CVOL,"POROSITY";POR*100,"AIR PER
M";KG,"LIQ PERM";KL
1150 PRINT #1,ELEV,BDEN,WT/CVOL,POR*100,KG,KL
1160 CLOSE 1
1161 PRINT
1162 PRINT
1170 WEND
1180 PRINT
1190 PRINT
1200 PRINT "ASSIGN A NAME TO LABORATORY DATA FROM THIS WELL. NAME = CALC + LAB L
ETTER, I.E. CALCA"
1210 PRINT "AFTER CHANGING NAME, HIT ENTER THEN TYPE 'RUN 1230' AND HIT ENTER AG
AIN."
1220 EDIT 1230
1230 NAME "B$" AS "CALC_.DBF"
1240 PRINT
1250 PRINT
1260 INPUT "DO YOU WANT TO CALCULATE LAB DATA FOR OTHER WELLS (Y/N)...";A$
1270 IF A$ = "Y" THEN 1290
1280 END
1290 PRINT
1300 PRINT
1310 PRINT
1320 GOTO 160
```

APPENDIX D.4

LABORATORY POROSITY

APPENDIX D.4

LABORATORY POROSITY

GEOSCIENCES UNIT
STANDARD PROCEDURES MANUAL FORMAT

Instrument: Laboratory Helium Porosimeter

References: Pirson, S. J.; "Oil Reservoir Engineering" McGraw-Hill New York, 1958, p. 56-96 (also contains extensive background bibliography).

API, "API Recommended Practice for Core Analysis Procedure", API RP 40, Aug. 1960, p. 53.

Description:

Types of data collected: Well name, sample location (ft below G.L.), sample designation, diameters (4 measurements - mm), lengths (2 measurements - mm), sample weight (g), initial pressure (psi), and final pressure (psi).

Example:

Well Name	Depth (GL)	Lab Code	Diameter(mm) D1	D2	D3	D4	Length (mm) L1	L2	Weight (gm)	Pressure (psi) P1	P2

Principle of operation: Helium gas under pressure is introduced into a volume in the porosimeter, V1, and the pressure, P1, is noted. This volume of gas is then allowed to expand into a second chamber and the pressure, P2, is noted. The volume of the second chamber is determined from the Boyle's Law relationship:

$$P1 * V1 = P2 * V2 \quad (1)$$

where

P1 = pressure at initial conditions, psi
V1 = volume of initial configuration , cm^3
P2 = pressure under total volume configuration, psi
V2 = volume of total configuration, cm^3

If the bulk volume of the sample is carefully measured and the sample weights determined, the sample porosity, densities, and void volume can be determined with the following relationships

$$BD = VM/WT \quad (3)$$
$$GD = VS/WT \quad (4)$$
$$VV = VM - VS \quad (5)$$
$$\phi = (VV/VM) * 100 \quad (6)$$

where:

BD = bulk density, g/cm^3
GD = grain density, g/cm^3
VV = void volume, cm^3
ϕ = porosity, %
VM = measured sample bulk volume, cm^3
WT = sample weight, g
VS = grain volume, cm^3

Limitations: The porosimeter volumes must remain constant and free of leaks. The gage must be accurate. The samples must be of a regular shape, so that the measured bulk volume can be accurately determined.

Equipment Needs:

1. Porosimeter
2. Digital caliper
3. Pressure source (He)
4. Safety glasses
5. Lab notebook and pen

Precautions:

Safety Considerations: Make sure pressure source is securely tethered and safety glasses are worn when system is pressured.

Transportation Considerations: Subject porosimeter to a minimum of jarring or bumps.

Special Training Requirements: Operator should be checked out on equipment before using.

Calibration/Standardization:

Frequency: Calibrate gauges and flow-regulators twice a year.

Who Performs: EG&G Calibration Lab.

Criteria for Timing: Allow 2 weeks.

Procedures: Contact Cal Lab @ 6-2468.

Installation: Porosimeter and pressure source should be located conveniently close so that operator can reach all controls without delay. Equipment should be secured so that the porosimeter cannot be bumped or tipped over and the pressure source cannot be inadvertently moved so as to strain or break connection to the porosimeter.

Operating Procedures:

Pre-operation

1. Check for leaks by determining that no loss in pressure occurs when V1 and subsequently V2 are shut in at maximum pressure for several minutes.
2. Cycle through the operation and verify that P2/P1 is a correct value.
3. Set the helium pressure regulator at 100 psi.

Operation

1. Carefully measure the sample with a digital caliper (measure four representative diameters and two lengths), and record values (in mm) in the lab notebook.
2. Open valve 1, (I), to pressure up volume V1, (valve 2, (II) is in vent position and valve 3, (III), is closed).
3. Open the cell, if it's not already open, and place the sample in the holders. Close the cell (close the cover to the same point each time).
4. Close I, tap gage and record pressure P1.
5. Check for loss of pressure by verifying that the gage reading remains constant for about 30 seconds.
6. Open II to measure position, tap the gage and record the pressure, P2, when the reading stabilizes.
7. Check for leaks by leaving the system shut to obtain pressure of V2-VS. Determine that the pressure remains constant during the minute or more required to complete the measurement on the next sample.
8. Return II to vent position, open the cell, and remove the sample.
9. Continue with the measurements by completing operation 2-8 for each sample.
10. When all measurements are complete
    a) shut the valve on the helium tank, and
    b) open I and vent II and III.

Common Problems and Solutions:

1. Sample cell may leak. If this occurs replace "O" ring.
2. Gage may not produce correct P2/P1 ratio. If this occurs check for leaks. If none are found, recalibrate gage and system.

Special Maintenance:

None required.

Data Recorded: Data is recorded in a lab notebook. Record values for well name, depth, lab code, diameters, lengths, weight, and pressures, using the previously displayed format.

Data Reduction: The densities and porosity are calculated with a basic computer program POROHE.BAS or with the general calculation program LABCALC.BAS, which calculates both porosity and permeability.

Operating instructions for these programs and program listings are found in section PROGRAM 1-D.

Data Reporting: Computer programs reports either:

1. POROHE.BAS

Well Name_____

Sample Depth (ft. below G.L.)	Bulk Den (g/cm^3)	Grain Den (g/cm^3)	Porosity (%)	Void Volume (cm^3)

2. LABCALC.BAS

Well Name_____

Sample Depth (ft. below G.L.)	Bulk Den (g/cm^3)	Grain Den (g/cm^3)	Porosity (%)	Void Volume (cc)	Air Perm (MD)	Klink Perm (MD)

3. In both cases files are created and a data matrix is set up in the computer memory.

The POROHE.BAS names the file PORO, plus the lab code, plus .DBF, e.g. POROA.DBF.

The LABCALC.BAS names the file CALC, plus the lab code, plus .DBF, e.g. CALCA.DBF.

Units: Units are as indicated above.

Accuracy: Gauges - 0.1%;

Precision: The precision of the porosity measurements was determined by repeatedly analyzing a suite of samples ranging from about 1/2 to 39% in porosity. The standard deviation for porosity was about 0.305% and about 0.038 cm^3 for void volume.

Comments: None

General QA/QC Considerations: The precision of measurements will be determined at the start of each field season, utilizing a broad suite of samples and the statistical analysis of repeat measurements.

Program 1-D

A. POROHE.BAS Operating Instructions:

1. Turn on computer and printer.
2. At the prompt, type BASICA and enter.
3. At OK, hit F3 -- type POROHE.BAS and enter.
4. At OK, hit F2 (you are now in the program).
5. Respond to question on Caps Lock and enter.
6. Type in well name and enter.
7. Type in sample depth and enter (enter in a similar manner all the other questions about the sample properties).
8. After inputting all the sample data, the program will ask if you want to change any input. Compare the input on the screen with the appropriate values in the lab book. If everything looks OK, answer with a cap "N", and go on to the next calculation. If there is an error, answer with a cap "Y", and answer the questions correctly.
9. After you have a good data set and answer with a "N", the program will calculate the porosity values, display them on the monitor screen, and type them out on the printer, prior to asking for the input on the next sample.
10. After you have entered all the data for the samples from one well, terminate that set of calculations by entering a "-99" for the next sample depth (and enter, of course).
11. You will get a message about naming the data set you have just finished, and a line that looks like--

    610 NAME "B$" AS "PORO_.DBF"

    with the cursor under the 6. Move the cursor over until it coincides with the underline after the O in PORO, and type in the well's code (being certain that the file name is enclosed in quotes). Hit enter, then type "RUN 610" and hit enter again.

12. You will then be asked if you want to calculate the permeabilities for another well. If you answer "Y", you will cycle back to Well Name ----. Continue as above to complete the porosity calculation.
13. If you wish to stop, then type "N" and enter. You will then get an OK prompt. Type SYSTEM and enter.
14. You will be back in DOS with the C:\DOS> prompt. Type PARK and enter.
15. You are now ready to close up shop. Turn off computer and printer.

B. Listing for basic program POROHE.BAS.

```
5 CLS
6 PRINT
7 PRINT
8 PRINT
10 PRINT ,"THIS IS A PROGRAM TO CALCULATE POROSITY/DENSITY"
20 PRINT ,"       FOR USE WITH THE HELIUM POROSIMETER"
30 REM * PROGRAM BY C F KNUTSON, 5/31/89, USING 2/90 GAGE CALIBRATION *
40 PRINT
50 PRINT
60 PRINT
70 PRINT ,"ACTIVATE CAPS LOCK - ( Y/N ANSWERS MUST BE IN CAPS )"
80 PRINT
90 PRINT
100 PRINT
110 PRINT
120 PRINT
130 PRINT
140 LPRINT
150 INPUT "WELL NAME...";N$
160 LPRINT "      WELL NAME...";N$
170 LPRINT
180 LPRINT
190 LPRINT "            SAMPLE DEPTH   BULK DENSITY  GRAIN DENSITY     POROSITY
 VOID VOL"
200 LPRINT "            (FT BELOW GL)      (GM/CC)       (GM/CC)           (%)
   (CC)"
210 LPRINT
220 PRINT
230 PRINT "TO END CALCULATIONS, INSERT -99 FOR SAMPLE DEPTH."
231 PRINT
240 PRINT
250 WHILE ELEV >-8
255 OPEN "B$" FOR APPEND AS 1
256 PRINT
257 PRINT
260 INPUT "SAMPLE DEPTH (FT BELOW GL).....";ELEV
270 IF ELEV < -9 THEN 540
280 REM * INPUT OF DATA FOR A SINGLE SAMPLE *
300 INPUT "DIAMETER 1 (MM)....";D1
310 INPUT "DIAMETER 2 (MM)....";D2
320 INPUT "DIAMETER 3 (MM)....";D3
330 INPUT "DIAMETER 4 (MM)....";D4
340 INPUT "LENGTH 1 (MM)..";L1
350 INPUT "LENGTH 2 (MM)..";L2
355 INPUT "SAMPLE WEIGHT (GM).........";WT
360 INPUT "PRESSURE 1 (HIGH PRESSURE READING--IN PSI)...";P1
370 INPUT "PRESSURE 2 (LOW PRESSURE READING--IN PSI)....";P2
375 PRINT
380 INPUT "DO YOU WISH TO CHANGE ABOVE INPUT (Y/N).............";A$
390 IF A$ = "Y" THEN 256
400 VOL = 3.1416*(((D1+D2+D3+D4)/80)^2)*((L1+L2)/20)
410 BDEN = WT/VOL
420 CVOL = 39.9945-(18.54254*P1/P2)
425 IF CVOL > VOL THEN CVOL = VOL
430 APOR = (VOL-AVOL)/VOL
440 AVOL = AVOL*(1-APOR*.02)
450 POR = (VOL-CVOL)/VOL
460 VVOL = VOL-CVOL
462 PRINT
464 PRINT
470  PRINT ,"BULK DEN";BDEN,"GRAIN DENSITY";WT/CVOL,"POROSITY";POR*100,"VOID VOL
.";VVOL
480 V$ = "####.#       "
490 U$ = "######.##      "
495 W$ = "######.##"
500 LPRINT " "
510 LPRINT USING V$;ELEV,
520 LPRINT USING U$;BDEN,WT/CVOL,POR*100,VVOL
530 PRINT #1,ELEV,BDEN,WT/CVOL,POR*100,VVOL
540 CLOSE 1
550 WEND
560 PRINT
570 PRINT
580 PRINT "ASSIGN A NAME TO POROSITY DATA FROM THIS WELL. NAME = PORO + LAB LETT
ER, I.E. POROA.DBF"
590 PRINT "AFTER CHANGING NAME, HIT ENTER THEN TYPE 'RUN 610' AND HIT ENTER AGAI
N."
600 EDIT 610
610 NAME "B$"AS "PORO_.DBF"
620 PRINT
630 PRINT
640 INPUT "DO YOU WANT TO CALCULATE POROSITIES FOR OTHER WELLS (Y/N)?";A$
650 IF A$ = "Y" THEN 670
660 END
670 PRINT
680 PRINT
690 PRINT
700 GOTO 100
```

C. LABCALC.BAS Operating Instructions:

1. Turn on computer and printer.
2. At the prompt, type BASICA and enter.
3. At OK, hit F3 -- type PERMLAB and enter.
4. At OK, hit F2 (you are now in the program).
5. Respond to question on Caps Lock and enter.
6. Type in well name and enter.
7. Type in sample depth and enter (enter in a similar manner all the other questions about the sample properties).
8. After inputting all the sample data, the program will ask if you want to change any input. Compare the input on the screen with the appropriate values in the lab book. If everything looks OK, answer with a cap "N", and go on to the next calculation. If there is an error, answer with a cap "Y", and answer the questions correctly.
9. After you have a good data set and answer with a "N", the program will calculate the perm values, display them on the monitor screen, and type them out on the printer, prior to asking for the input on the next sample.
10. After you have entered all the data for the samples for one well, terminate that set of calculations by entering a "-99" for the next sample depth (and enter, of course).
11. You will get a message about naming the data set you have just finished, and a line that looks like--

    1230 NAME "P$" AS "CALC_.DBF"

    with the cursor under the 1. Move the cursor over until it coincides with the underline after the C in CALC, and type in the well's code (being certain that the file name is enclosed in quotes). Hit enter, then type "RUN 1230" and hit enter again.

12. You will then be asked if you want to calculate the permeabilities for another well. If you answer "Y", you will cycle back to Well Name ----. Continue as above to complete the porosity calculation.
13. If you wish to stop, then type "N" and enter. You will then get an OK prompt. Type SYSTEM and enter.
14. You will be back in DOS with the C:\DOS> prompt. Type "PARK" and enter.
15. You are now ready to close up shop. Turn off computer and printer.

D. Listing for basic program LABCALC.BAS.

```
10 CLS
20 PRINT ,"THIS IS A PROGRAM TO CALCULATE POROSITY AND PERMEABILITY"
30 PRINT ,"        FOR USE WITH THE LABORATORY EQUIPMENT"
35 PRINT
36 PRINT "        FOR USE DURING PERIOD 12/14/89 TO 7/4/90"
37 PRINT
40 REM * PROGRAM BY C F KNUTSON, 5/25/89. *
50 PRINT
60 PRINT
70 PRINT
80 PRINT ,"ACTIVATE CAPS LOCK - ( Y/N ANSWERS MUST BE IN CAPS )"
90 PRINT
100 PRINT
110 PRINT
120 INPUT "IS CAPS LOCK ON...(Y/N)...";A$
130 IF A$ <> "Y" THEN 80
140 LPRINT
150 LPRINT
160 CLS
180 PRINT
190 PRINT
200 PRINT
210 LPRINT
220 INPUT "WELL NAME...";N$
230 LPRINT "      WELL NAME...";N$
240 LPRINT
250 LPRINT
260 LPRINT "SAMPLE DEPTH  BULK DEN    GDEN    POR     VVOL   APERM    LPERM"
270 LPRINT " FT BELOW GL  (GM/CC)   (GM/CC)   (%)     (CC)    (MD)     (MD)"
280 LPRINT
290 PRINT
300 PRINT "TO END CALCULATIONS, INSERT -99 FOR SAMPLE DEPTH."
310 PRINT
320 WHILE ELEV >-8
330 OPEN "B$" FOR APPEND AS 1
340 INPUT "SAMPLE DEPTH (FT BELOW GL)";ELEV
350 IF ELEV < -9 THEN 1160
351 PRINT
352 PRINT
353 PRINT "INPUT SAMPLE DIMENSIONAL INFO..."
354 PRINT
355 PRINT
370 INPUT "DIAMETER 1 (MM)...";D1
380 INPUT "DIAMETER 2 (MM)...";D2
390 INPUT "DIAMETER 3 (MM)...";D3
400 INPUT "DIAMETER 4 (MM)...";D4
410 INPUT "LENGTH 1 (MM)...";L1
420 INPUT "LENGTH 2 (MM)...";L2
425 INPUT "SAMPLE WEIGHT (GM)...";WT
430 PRINT
440 PRINT
450 PRINT "HELIUM POROSIMETER READINGS"
460 PRINT
470 INPUT "PRESSURE 1 (HIGH PRESSURE READING--IN PSI)";P1
480 INPUT "PRESSURE 2 (LOW PRESSURE READING--IN PSI)";P2
490 PRINT
500 PRINT "LAB PERMEAMETER READINGS"
510 PRINT
520 INPUT "TEMPERATURE (DEG C)...";T
530 INPUT "PRESSURE (PSI)...";P
540 INPUT "ROTOMETER NUMBER...";RN
550 INPUT "ROTOMETER READING...";RD
560 PRINT
570 PRINT
580 INPUT "DO YOU WISH TO CHANGE ABOVE INPUT (Y/N)...";A$
582 PRINT
584 PRINT
590 IF A$ = "Y" THEN 340
600 REM * CALCULATE POROSITY *
610 VOL = 3.1416*(((D1+D2+D3+D4)/80)^2)*((L1+L2)/20)
620 BDEN = WT/VOL
630 CVOL = 39.9945-(18.54254*P1/P2)
635 IF CVOL > VOL THEN CVOL = VOL
637 VVOL = VOL-CVOL
640 POR = VVOL/VOL
650 REM * CALCULATE PERMEABILITY *
660 REM * CALCULATE RATE FIRST *
670 ON RN GOTO 740,760,780,800,820
```

```
680 PRINT
690 PRINT
700 PRINT "IMPROPER ROTORMETER DESIGNATION AT";ELEV
710 PRINT
720 PRINT
730 GOTO 540
740 QSC = -.5301+.1589*RD-.001907*(RD^2)+3.219E-05*(RD^3)
750 GOTO 830
760 QSC = -7.487+.6512*RD-.01151*(RD^2)+.0001038*(RD^3)-2.885E-07*(RD^4)
770 GOTO 830
780 QSC = 72.463-1.523*RD+.04294*(RD^2)-.0001356*(RD^3)
790 GOTO 830
800 QSC = 3.7972+12.226*RD-.01433*(RD^2)
810 GOTO 830
820 QSC = -211.3+59.79*RD
830 CON = (((T+273.15)/293.15)*(14.7/P))^.5
840 PRINT "QSC=";QSC,
850 PRINT "CON=";CON,
860 Q = QSC/CON
863 IF Q < 0 THEN Q=.01
865 PRINT "Q=";Q
870 REM * CALCULATE PERMEABILITY *
880 VIS = (17+(.03*T))/1000
890 DP = (P+14.6)/14.6
900 AP = (DP+1)/2
910 U$ = "######.#      "
920 V$ = "#####.##"
930 K = (1.6976*Q*VIS*(L1+L2))/((D1+D2+D3+D4)^2*AP*(DP-1))
940 PRINT "AIR PERM (MD) =";K*1000
950 REM * CHANGE AIR PERM TO MILLIDARCY AND CALCULATE KLINKENBERG PERM *
960 KG = 1000*K
970 KA = KG
980   FOR N = 1 TO 20
990   KL = KG/(1+(.777*KA^(-.39))/AP)
1000  X = (KA-KL)
1010  IF X < .0001 GOTO 1050
1020  KA = KL
1030  PRINT KL
1040   NEXT N
1050 PRINT "KL=";KL
1060 X=1
1065 PRINT
1070 REM * PRINT CALCULATIONS FOR THIS SAMPLE DEPTH *
1080 LPRINT USING U$;ELEV,
1090 LPRINT USING V$;BDEN,
1100 LPRINT USING V$;WT/CVOL,
1110 LPRINT USING V$;POR*100,
1115 LPRINT USING V$;VVOL,
1120 LPRINT USING V$;KG,
1130 LPRINT USING V$;KL
1140  PRINT ,"BULK DEN";BDEN,"GRAIN DENSITY";WT/CVOL,"POROSITY";POR*100,"AIR PER
M";KG,"LIQ PERM";KL
1150 PRINT #1,ELEV,BDEN,WT/CVOL,POR*100,KG,KL
1160 CLOSE 1
1161 PRINT
1162 PRINT
1170 WEND
1180 PRINT
1190 PRINT
1200 PRINT "ASSIGN A NAME TO LABORATORY DATA FROM THIS WELL. NAME = CALC + LAB L
ETTER, I.E. CALCA"
1210 PRINT "AFTER CHANGING NAME, HIT ENTER THEN TYPE 'RUN 1230' AND HIT ENTER AG
AIN."
1220 EDIT 1230
1230 NAME "B$" AS "CALC_.DBF"
1240 PRINT
1250 PRINT
1260 INPUT "DO YOU WANT TO CALCULATE LAB DATA FOR OTHER WELLS (Y/N)...";A$
1270 IF A$ = "Y" THEN 1290
1280 END
1290 PRINT
1300 PRINT
1310 PRINT
1320 GOTO 160
```

APPENDIX D.5

EQUILIBRIUM SATURATION

APPENDIX D.5

STANDARD OPERATING PROCEDURES
FOR EQUILIBRIUM WATER SATURATION ANALYSIS

Instruments: 45.7 x 76.2 x 71.1 cm stainless steel glove box with loading chamber, top and side windows, and power outlet; 36.5 x 30 x 49 cm Sanplatec Corp. "Dry Keeper" desiccating cabinet; two 0 to 100 scale hygrometers; a temperature probe; an EC bridge; a low rpm fan; and a Sartorius digital readout scale.

References: Daian, J.F., "Condensation and Isothermal Water Transfer in Cement Mortar Part I--Pore Size Distribution, Equilibrium Water Condensation and Imbibition", Transport in Porous Media 3, 1988, p. 563-589.

(A complete reference list is at the back of the report.)

Description:

Types of data recorded: Well name, sample location (depth, feet to tenths), salt type and concentration (M), time, temperature (°C), and initial and equilibrium water saturation weight of sample (g) (Figure D-1).

Types of data calculated: Relative humidity (%), capillary pressure (water potential, matric potential; bar), water content (cm^3), pore-size distribution, and surface area.

Principle of operation: The glove box is wrapped in Celotex (foil-covered foam insulation). The insulation will (1) reflect room lights, thus preventing a greenhouse effect from developing in the glove box and (2) prevent cold spots from developing due to temperature variations around the glove box. The scale is placed inside the box and plugged in.

Date and time experiment begins: _____ _____

Direction of experiment: Adsorption Desorption

Well Name _____ Sample No.: _____ Depth below G.L. (ft) _____
SALT: type _____ Concentration (M)_____ Ambient temp.(°C) _____
h_r(%) _____ -Pc(Bar) _____ Initial wt of sample(g) _____

Weighing History

Date	Time	Weight (g)	Weight change (g)
____	____	_____	_____
____	____	_____	_____
____	____	_____	_____
____	____	_____	_____
____	____	_____	_____
____	____	_____	_____

Equilibrium water saturation wt of sample (g) _____
Water content (g) _____

Figure D-1. Format for types of data recorded.

A number of approximately 2.8 cm long by 2.5 cm diameter basalt plugs are oven dried at 105°C for 24 hours, cooled for 30 minutes, individually weighed, and placed on racks in the insulated glove box. A salt solution of a specified concentration is mixed and poured into a tray, which is set at the bottom of the box. The basalt plugs are allowed to come to equilibrium with the vapor pressure over the salt solution. As the experiment progresses, the water vapor pressure is incrementally increased, i.e., the capillary pressure is decreased, resulting in increased adsorption of water by the basalt plugs.

For the highest capillary pressure, i.e., the starting point of the analysis, a saturated solution of LiCl is used. For incrementally lower capillary pressures (P_c), saturated solution of $MgCl_2$ and NaCl are used, respectively. When using the saturated solutions, the P_c has to be calculated from the fixed relative humidity (Table D-1) using Equation (1). For lower P_c, dilute NaCl is used. P_c for dilute NaCl are given in a concentration versus pressure table (Table D-2). For $P_c = 0$, pure water is used.

The plugs are individually weighed approximately every day inside the glove box, as necessary, until equilibrium water saturation (the point at which there is no change in weight from the last weighing) is reached. The equilibrium water saturation weight is measured and recorded. The experiment is repeated at the next lower P_c.

If time allows, this process will be reversed: after equilibration over pure water, the water vapor pressure is incrementally decreased causing increases in capillary pressure and the subsequent desorption of the basalt plugs. This will allow a hysteresis curve of P_c to be plotted.

(For a theoretical evaluation of the condensation and water transfer process, see Appendix α.)

Limitations: The glove box and desiccating cabinet should be free of hygroscopic materials such as wood. The glove box should seal around the gloves, the sample chamber doors, the gas inlet and outlet, and the windows. The desiccator door should seal when the door is closed.

Distilled water and chemically pure salts should be used when mixing the solutions. The basalt plugs should be oven dried, initially, and free of dirt and other particles. If the experiment is not to begin immediately, the oven dried samples should be placed in the desiccator cabinet to keep them dry. The scale used in weighing the samples should be in calibration, as should the temperature probe, the EC bridge, and the two hygrometers. The tables used to determine relative humidity and capillary pressure should be accurate.

Equipment needs:

1. Glove box
2. Celotex insulation
3. Desiccating cabinet with hygrometer for glove box
4. Hygrometers
5. Scale
6. Two beakers (500 ml and 1000 ml) to mix the solutions
7. Distilled water
8. Chemically pure LiCl, $MgCl_2$, and NaCl
9. Fume hood under which to mix the LiCl and $MgCl_2$
10. Tables that relate salt solution concentration to capillary pressure and/or relative humidity
11. Several racks to hold the samples and the scale
12. A pyrex 2 quart baking dish less than 10 in. in diameter (to fit into the glove box from the round port)
13. An EC bridge (optional) to measure conductivity (i.e., salinity) of the solutions inside the box
14. A low-rpm fan to circulate air across the solution
15. Shelves to suspend samples above the salt solution
16. Forceps

17. Safety glasses
18. Lab coat
19. Notebook

Precautions:

Safety considerations: Care should be taken in handling the salt solutions; when concentrated, they cause irritation to the skin and eyes. A fume hood should be used when mixing the LiCl and $MgCl_2$ solutions. Also, when mixing the LiCl, care should be taken in handling the beaker due to the great quantity of heat given off during mixing (i.e., LiCl + H_2O is very exothermic). Safety glasses should be worn at all times. To dispose of a liter or less LiCl + H_2O or $MgCl_2 \cdot 6H_2O$ + H_2O, pour it down the drain with copious amounts of water. If there are questions, call Clint Graden at 6-0817.

Transportation considerations: The glove box is large, awkward, and heavy. If it needs to be moved within a building, a large, strong lab cart should be used. If it is to be transported by motor vehicle, a truck is necessary.

Special training requirements: The analyst must be familiarized with the procedures of the experiment, as well as possible reactions that any of the salts may have when mixed with water. A qualified professional should demonstrate the experimental procedures to the technician, if a lab technician is to perform the routine weighing operation.

Calibration/Standardization:

Frequency: Calibrate hygrometers and scale once a year.

Who performs: EG&G Calibration Lab.

Procedures: Contact Calibration Lab at 6-2656 or Larry Demming at 6-2468.

Installation: The glove box should be placed near a power outlet and situated for easy access (i.e., about elbow-high) for hygrometer, temperature, and weight readings. The scale, baking dish, forceps and samples should be inside the box and easily manipulated using the gloves. All equipment needing power should be hooked up to the power outlet inside the box. The desiccator cabinet should be located near the box for quick transfer of samples from a dry environment to the set humidity of the box if the experiment is not started immediately. The salts should be stored where they will not be spilled.

Operating Procedures:

Pre-operation

1. Check for poor sealing of the glove box and the desiccator.
2. Check for dirt/debris inside the glove box and desiccator.
3. Check that the temperature probe and hygrometers are calibrated and the scale is zeroed.
4. Check for loose dirt/debris on the basalt plugs.

Operation

1. Oven-dry the basalt plugs at 105°C for 24 hours.
2. Cool the plugs for 30 minutes, then weigh each basalt plug and record its sample number and initial dry weight.
3. If the experiment is not to be started immediately, place the dry samples in the desiccator to keep them dry.
4. Make sure the scale and fan are plugged in; also place small sealed containers of salt and de-ionized water in the box at this time (useful when working with the saturated salt solutions).
5. Mix a saturated solution of LiCl in a beaker (Table D-1), taking the precautions stated under Safety Considerations. Pour the solution in baking dish and place it on the bottom of the glove box.
6. If the humidity has to be lowered or raised a great amount to obtain the correct setting, it may be desirable to close the box

at this time and let the humidity adjust. If this is done, Step 3 must be taken.

7. Place the basalt plugs on the racks inside the box above the salt solution. If Step 6 was taken, this must be accomplished quickly so that the humidity is not changed by the influence of the room humidity. This may be done by setting all samples on a tray, setting the tray in the sample chamber, and closing the door. Then, using the gloves, open the chamber door into the main box, place the samples on the racks, and reseal the door.
8. Make sure the humidity reaches the desired value and remains there. More salt or water can be added from the sealed containers in the box when working with the saturated solutions to maintain saturation (from Step 4).
9. Approximately every day, weigh each of the basalt plugs and, across from the sample number, record the date, time, weight, and change of weight from the starting weight of the sample. (The time it takes for equilibration will vary, and the intervals at which the samples are weighed should vary accordingly.) Make sure the scale is zeroed before each plug is weighed.
10. Repeat Step 9 until no change in weight is observed (the plugs are now in equilibrium). Record the weight of each plug under "equilibrium water saturation weight of sample."
11. Clean the dish and rinse it with distilled water.
12. Repeat Steps 5 through 11, using a saturated $MgCl_2$ solution (Table D-1).
13. Repeat Steps 5 through 11, using a saturated NaCl solution (Table D-1).
14. Repeat Steps 5 through 11, using the dilute NaCl solutions listed in Table D-2. Begin with the <u>most</u> concentrated NaCl solution and, each time Step 11 is completed, decrease the concentration according to Table D-2.
15. Repeat Steps 5 through 11 using pure water.
16. Repeat Steps 5 through 11 using the dilute NaCl solutions. Begin with the <u>least</u> concentrated NaCl solution, and each time Step 11 is completed, increase the concentration according to Table D-2.
17. Repeat Steps 5 through 11 using a saturated NaCl solution.
18. Repeat Steps 5 through 11 using a saturated $MgCl_2$ solution.
19. Repeat Steps 5 through 11 using a saturated LiCl solution.

Table D-1. Relative humidities of saturated solutions of LiCl, $MgCl_2$ and NaCl at 22°C (modified from Wexler and Hasegawa, 1954)

Saturated Solutions	Concentration (M)	Relative Humidity (%)	Calculated - P_c (bar)
LiCl	15.0	12.24	2.9×10^3
$MgCl_2$	5.7	33.44	1.5×10^3
NaCl	6.1	75.62	3.8×10^2

Table D-2. Concentration of NaCl versus capillary pressure at 22°C (extrapolated from Daian, 1988; J. Harris)

Dilute NaCl (M)	-Pc (bar)
2	96.8
1.7	80.7
1.3	60.4
1	46.7
0.72	31.8
0.5	22.3
0.31	13.6
0.2	9.0
0.1	4.6
0.05	2.3

Common Problems and Solutions: If the relative humidity has to be lowered or raised any amount greater than about 5%, the concentration of the solution will probably change. If a saturated solution is to be used, the solution must be over-saturated to compensate for any great quantity of water vapor that has to be removed from or released to the atmosphere. The solutions should then be closely monitored to make sure that there are still crystals present. A sealed container of the salt can be placed in the box prior to beginning the experiment in the event that more salt has to be added. If a dilute solution is used (necessary for higher water saturation), the EC bridge can be used to determine the concentration of the solution at equilibrium.

If the temperature is fluctuating greater than 2°C, more insulation can be added (e.g., throw a couple of blankets over the glove box). The salts chosen for this analysis are fairly temperature independent, but temperature fluctuations greater than a few degrees celsius will be a factor and should be avoided when possible.

Special Maintenance: None

Date Recorded: Types of data and format reported as in Figure D-1.

Date Reduction: Water volume (cm^3), water content (% PV), capillary pressure (bar) for known relative humidity are calculated with a basic PC program having the name "EQWSAT.BAS" (Appendix β). Pore-size distribution and surface area are calculated with a basic PC program having the name "PORSFC.BAS" (Appendix γ).

Date Reporting: Examples of the format used by the computer for each program follow.

EQWSAT.BAS

Well name: _____

Sample No	H (%)	Pore Vol (cm^3)	Water Vol (cm)	Water Content (% PV)	-Pc (bar)	Water V.P. (bar)

PORSFC.BAS

Well name: _____

Sample No.: _____

Sample Depth (ft below G.L.): _____

Pore radius (mm)	Pore sfc (m^2/g)	Pore volume (mm^3/g)	Calculated Sfc (m^2/g)

Units: Units are as indicated above.

Accuracy: The accuracy of the non-measured values, such as relative humidity, water saturation vapor pressure, and most of the capillary pressures, are limited to the accuracy of the tables and/or instruments from which they were taken. The accuracy of the scale is 0.001 g up to 60 g and 0.01 g up to 600 g.

Precision: Precision will be determined by the following process:

1. Choose a few samples that are not used in the analysis and that represent the range of porosities typical of the basalts. Oven-dry them at 105°C for 24 hr and let them cool for 30 minutes, or use a vacuum oven.
2. Weigh the samples and record the weight of each.

3. Place them in a glove box at a set relative humidity/salt solution concentration (preferably the initial saturation step to reduce the time it takes to reach equilibrium).
4. Allow the samples to come to equilibrium by the methods presented in the Operation section.
5. Weigh and record the weight of each sample.
6. Repeat Steps 1 through 6 several times, using the same salt and concentration each time.
7. Calculate the change of weight for each sample and for each experiment run. From these data, small sample statistics can be used to generate the variance and standard deviation for one step of the technique.

Comments: Different water content values are expected depending on whether the process is one of adsorption or desorption (see Principle of Operation section). The water content values are direction dependent.

Equations:

$$-Pc = RT(\rho_w \times 10^6) \ln(h_r)/(m \times 10^5) \quad (1)$$

$$V_w = (W_{s+w} - W_s)/P_w \quad (2)$$

$$\% PV = V_w/PV_{total} * 100 \quad (3)$$

where:

$-Pc$ = capillary pressure in bar

R = gas constant = 8.3144 J/K-mol

T = temperature in °K; °K = °C + 273

m = molecular weight of water = 18 g/mol

ρ_w = density of water in g/cm^3 at temperature T

h_r = relative humidity = p/po =

$$\frac{\text{(partial water v.p. over the solution)}}{\text{(water saturation v.p. over pure water at temperature T)}}$$

PV_{total} = total pore volume

% PV = $[(\text{water volume})/(PV_{total})] \times 100$

W_{s+w} = weight of sample at equilibrium water saturation in grams

W_s = initial weight of oven-dried sample in grams

V_w = volume of water in cm^3

10^6 is a conversion factor = 10^6 cm^3/m^3

10^5 is a conversion factor = 10^{-5}bar/Pa

v.p. = abbreviation for vapor pressure

Sfc = surface area

mol = abbreviation for one mole

M = molarity = mol solute/1 solution or mol solute/dm^3 solution

General QA/QC Considerations: It is assumed that labeling is correct on the samples taken from the labeled boxes; the procedures used during sampling were designed to minimize the chance of a labeling mistake. The sampling procedure was the following:

One well was processed at a time, and the samples were placed in labeled boxes for shipping. In the lab, the samples were taken out of the boxes, fitted together using geophysical logs, recorded well depths, lithology, etc., and the best estimate of the precise location and footage was marked on the

core. Samples were selected from the cores at this time and were labeled with the well name and depth to the nearest tenth of a foot. They were then placed in 3 ft x 4 in. x 4 in. boxes for transport to an area to be drilled. The cores were taken out of the boxes, placed in the correct sequence, and 2.5 x 6.4 cm plugs were drilled out of them. The individual plugs were assigned a lab letter and number. All of this information was recorded in a bound laboratory notebook. Specific plugs were selected, and the ends trimmed to yield a final cylindrical plug with dimensions of approximately 2.5 x 2.6 cm. These plugs were also permanently marked with India ink. This designation was used consistently throughout the above process, so unless a wrong number is recorded on an individual plug, there should be no error in assigning results to the correct well and location.

The quality of all procedures used in the water saturation analysis falls under Analytical Level III (see EG&G DIRC draft report, November 28, 1988).

APPENDIX α

APPENDIX α

Appendix α: A brief theoretical evaluation of adsorption and capillary condensation during water adsorption in an initially dry porous media.

Hysteresis

For a given value of relative humidity, h, and assuming the pore geometry of an open-ended cylinder, all pores of the same size or class will be filled with capillary water only when a cylindrical meniscus of the adsorbed layer reaches the radius of curvature of the capillary interface:

$$r - e_a(h) < R(h) \qquad (\alpha\text{-}1)$$

where:

r = pore radius, μm
$e_a(h)$ = thickness of adsorbed layer as a function of the humidity, μm
$R(h)$ = radius of curvature of a capillary interface as a function of humidity, μm, (Daian, 1988).

Within this domain, no capillary water is present and, assuming the adsorbed water is inert, only vapor diffusion takes place (Daian, 1988). At the capillary condensation threshold, however, i.e., at the point $h = h_c$ (point D in Figure α-1), capillary water will begin to appear in all pores of the smallest radius. As the meniscus of the adsorbed layer becomes larger, the capillary water will appear in an increasingly larger class of pores (Gregg and Sing, 1982; Daian, 1988). "Nearly discontinuous" capillary islands that are subsequently formed are provided by both direct capillary migration of liquid water and vapor diffusion. This process is dominant in the range of intermediate water contents.

For large degrees of water saturation, capillary invasion of the medium involves a viscous flow of migrating liquid water and simultaneous vapor diffusion (Daian, 1988).

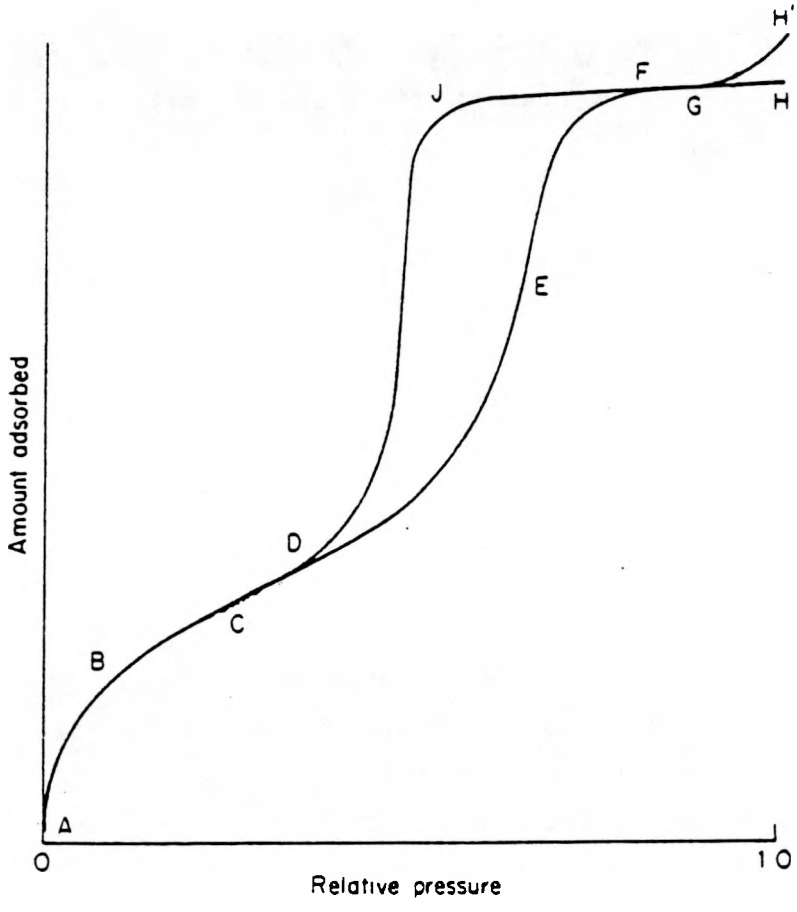

Figure α-1. Vapor adsorbed versus relative humidity plot at constant T for a mesoporous solid (type IV isotherm in the BDDT classification) (from Gregg and Sing, 1982).

APPENDIX β

APPENDIX β

Dollimore and Heal's (1970) method assumes a cylindrical pore geometry. The pore radius is taken as the independent variable, and the pore system is divided into groups of pores. Dollimore and Heal used a maximum pore radius of 10μm and a minimum of $5 \times 10^{-4}\mu$m with $5 \times 10^{-3}\mu$m steps from 1×10^{-2} to $2.5 \times 10^{-3}\mu$m and $10^{-4}\mu$m steps from 5 to $25 \times 10^{-4}\mu$m, but the choice of these values vary considerably in the literature as do the increments between pore groups; they have not yet been chosen for this study. This method is applied to the desorption curve, thus at the initiation of the calculation, all pores are filled.

During desorption, water is initially lost from the largest class of pores; this first small, but finite, loss of a volume of water is stage i = 1 (stage i = 0 is the point at which all pores are filled). At the next small, but finite, lost volume of water, stage i = 2, the second largest class of pores loses a minute volume of water, while the largest class of pores loses an additional increment. In stage i = 3, a third class of pores is affected in addition to the first two, and so on for stages i = 4, 5, ... n. In order to calculate pore-size distribution and surface area, however, adsorbed layer thickness and volume of condensate have to first be calculated at each stage for each class of pores that loses a volume of water.

The thickness of the adsorbed layer, t, can be calculated if the thickness and cross-sectional area of a single water molecule and the specific surface area of water absorbent is known. The equation for t used in the computer program follows:

$$t = s(n/N_m) \quad (4)$$

where

t = thickness of adsorbed layer, μm
s = thickness of single water monolayer, ~$2 \times 10^{-4} \mu m$
n = amount of adsorbed water, mol/g of medium
N_m = monolayer capacity of surface, moles water per gram of sample[a]

and

$$n = m * q_i/W_s \quad (5)$$

where

q_i = weight of water adsorbed (g) at the given relative humidity
W_s = dry weight of sample, g
m = molecular weight of water, mol/g

Thus, the molecular capacity, N_m, is

$$N_m = \frac{(3.03\ m^2/g)(10^{12}\mu m^2/m^2)}{(10.6 \times 10^{-8}\mu m^2)(6.02 \times 10^{23}/mol)} = 4.75 \times 10^{-5} mol/g \quad (6)$$

(Leutkenhans, 1988).

For the condensate, the volume of water lost over a small, but finite, step i, can be calculated by the following equation:

---

a. Specific surface area is ~3.03 m^2/g, calculated from the cross sectional area of a water molecule [$10.6 \times 10^{-8} \mu m^2$ and Avagadro's Number (6.02×10^{23}/mol)].

$$\delta\nu^f(>r_i) = A(>r_i)\delta t_i - 2\pi L(>r_i)t_i\delta t_i \quad (7)$$

where

$\delta\nu^f(>r_i)$ = the decrease in volume of the multilayer film on the walls of all pores with a radius greater than r_i

t_i = the thickness of the adsorbed layer

δt_i = the minute thickness loss of the adsorbed layer

$L(>r_i)$ = the total length of all pores having a radius greater than r_i.

(Gregg and Sing, 1982)

It is known that:

$$r_ik = r_i^p - t_i \quad (8)$$

where

r_ik = the core radius for a given class of pores, i

r_i^p = the total pore radius for the class of pores, i

t_i = the thickness of the adsorbed layer for the class of pores, i.

Now, let δV_i be the total amount of water (experimentally measured) which is lost during stage i. Then the decrease in volume, $\delta\nu_i^k$, of cores is:

$$\delta\nu_i^k = \delta V_i - \delta\nu_i^f \quad (9)$$

and the corresponding change in pore volume, $\delta\nu_i^p$, during stage i is:

$$\delta\nu_i^p = Q_i(\delta V_i - \delta\nu_i^f). \quad (10)$$

Q_i is a conversion factor:

$$Q_i = [r_i^p/(r_i^p - t_i)]^2 \quad (11)$$

where

i = a given class of pores

r_i^p = the mean radius of the group, i, of pores; the actual radii of which cover a small, but finite range.

The calculation of $\delta\nu_i^p$ is carried out for each stage, i, beginning with i = 0. At this point there is as yet no loss of water in the pores and, thus $\delta\nu^f = 0$, $A(>r_i) = 0$, and $L(>r_i) = 0$. For stage i = 1, the volume of the first (largest) group of pores is:

$$\delta\nu_i^p = Q_i\delta\nu^f. \tag{12}$$

For the next value of $\delta\nu^f$, stage 2:

$$A_1 = 2(\delta\nu_i^p/r_i^p) \tag{13}$$

where:

A_1 = the wall area of pore group one

and

$$L_1 = A_1/(2\pi r_i^p) \tag{14}$$

where

L_1 = the length of pore group one.

For the core volume of pore group 2, the next largest class:

$$\delta\nu_2^k = \delta V_2 - \delta\nu_2^f \tag{15}$$

and

$$\delta\nu_2^p = Q_2\delta\nu_2^k. \tag{16}$$

Equations (13), (14), (15), and (16) are used in each stage for each class of pores. For example, for stage 3:

$$\delta\nu_3^f = \delta t_3(A_1 + A_2) - 2\pi t_3(L_1 + L_2) \quad (17)$$

where

$$A_2 = 2(\delta\nu 2^p/r_2^p)$$

$$L_2 = A_2/(2\pi r_2^p)$$

and

$$\delta\nu_3^p = Q_3(\delta V_3 - \delta\nu_3^f) = [r_3^p/(r_3^p - t_3)]^2(\delta V_3 - \delta\nu_3^f) \quad (18)$$

(Gregg and Sing, 1982, p. 149). The pores-size distribution is the plot of $\delta^p/\delta r^p$ against r^p.

The surface area, δA, for each group of pores and the cumulated surface area, $\Sigma(\delta A)$, are calculated from the pore-size distribution using the equation:

$$\delta A = 2 \times 10^{-3}(\delta v^p/r^p) \quad (19)$$

where

10^{-3} = a conversion factor $mm^3/\mu m \times 10^{-3} = m^2$.

A. EQWSAT.BAS Operating Instructions:

1. Turn on computer and printer.
2. At the prompt, type BASIC and enter.
3. At OK, hit F3 -- type the disk drive, colon, EQWSAT.BAS and enter.

   For example: B:EQWSAT.BAS

4. At OK, hit F2 (you are now in the program).
5. Make sure the Caps Lock is on.
6. Type in well name and enter.
7. Type in sample label and enter.
8. Respond to pore volume, weight of water, density of water, and average temperature prompts in a similar manner.
9. If no mistakes have been made answering the above questions, type N (for No) and return.
10. If capillary pressure (Pc) is known, type Y and enter. Type the absolute value of the Pc and enter. Type N and enter if Pc is not known.
11. If relative humidity (H) is known, type Y and enter. Type the value of H in percent and enter. Type N and enter if H is not known.
12. If you answer N to both Pc and H, type in Y and enter in the NaCl solution is saturated. If it's not saturated, type in N and enter and then type in the solution concentration in molarity and enter.
13. Type in the next sample label and answer the questions at the prompts or type STOP and enter to start a new well or to quit the program.
14. If STOP is entered, type Y and enter to start a new well and repeat Steps 6 through 12. Type N and return to end the program.
15. When the program is ended type SYSTEM and enter.
16. Type PARK and enter.
17. Turn off the computer and printer.

B. Listing for the PC program EQWSAT.BAS.

```
10 CLS
20 '
30 '**THIS PROGRAM, EQWSAT.BAS, COMPUTES Pc, WATER CONTENT (%PV) AND WATER V.P.*
*
40 '
50 PRINT
60 PRINT
70 PRINT
80 PRINT
90 PRINT "TOGGLE-CAP LOCK- (USE CAP Y/N FOR OPTION ANSWERS)"
100 OPEN "A",1,"EWSFILE1.DAT"
110 E=1
120 PRINT
130 PRINT "OPENING EWSFILE1.DAT"
140 PRINT
150 INPUT "Enter Well Name";A$
160 LPRINT "Well Name:  "A$
170 LPRINT
180 LPRINT
190 LPRINT "Sample";TAB(11);"h";TAB(16);"Pore Vol";TAB(27);"Water Vol.";TAB(38);
"Water Content";TAB(55);"-Pc";TAB(64);"Water V.P."
200 LPRINT TAB(3);"No.";TAB(10);"(%)";TAB(17);"(cc)";TAB(30);"(cc)";TAB(43);"(%)
";TAB(54);"(bar)";TAB(67);"(bar)"
210 LPRINT "______";TAB(9);"_____";TAB(16);"________";TAB(25);"___________";TAB(
38);"_____________";TAB(53);"________";TAB(62);"_____________"
220 LPRINT
230 PRINT
240 PRINT #1,"WELL NAME:  ";A$
250 PRINT #1,
260 PRINT #1,"Sample";TAB(11);"h";TAB(16);"Pore Vol";TAB(27);"Water Vol.";TAB(38
);"Water Content";TAB(55);"-Pc";TAB(64);"Water V.P."
270 PRINT #1,TAB(3);"No.";TAB(10);"(%)";TAB(17);"(cc)";TAB(30);"(cc)";TAB(43);"(
%)";TAB(54);"(bar)";TAB(67);"(bar)"
280 PRINT #1,"______";TAB(9);"_____";TAB(16);"________";TAB(25);"___________";TA
B(38);"_____________";TAB(53);"________";TAB(62);"_____________"
290 PRINT #1,
300 PRINT "**    **    **    **    **    **    **    **    **"
310 PRINT "TO END DATA INPUT, TYPE 'STOP' AT SAMPLE LABEL PROMPT."
320 PRINT
330 WHILE SL$<>"STOP"
340 INPUT "Enter Sample Label";SL$
350 IF SL$="STOP" THEN 950
360 PRINT
370 INPUT "Enter Pore Vol in cc";V
380 PRINT
390 INPUT "Enter wt. of water in g";W
400 PRINT
410 IF E>1 THEN 440
420 INPUT "Enter Density of Water in g/cm3";P2
430 PRINT
440 IF E>1 THEN 470
450 INPUT "Enter Avg. Temperature in degrees C";T
460 PRINT
470 INPUT "Do you want to change any of the above values (Y or N)";U$
480 IF U$="Y" THEN 340
490 V3=INT(V*100+.5)/100
500 W1=INT(W*1000+.05)/1000
510 D1=P2*1000000!
520 T1=INT(T*100+.5)/100
530 IF T>=15 AND T<=30 THEN GOTO 560
540 PRINT
550 PRINT "WARNING:  All water saturation v.p.'s within this program are for the
 range T=15-30 degrees C"
560 K=T+273
570 M=18!:R=8.3144
580 PRINT
590 PRINT
600 IF E>1 THEN 630
610 INPUT "Do you know capillary pressure (N or Y)";B$
620 PRINT
630 IF B$="N" OR E>1 THEN 660
640 INPUT "Enter Capillary Pressure (absolute value) in bar";P1
645 P1=INT(P1*100+.5)/100
650 PRINT
660 IF E>1 THEN 680
670 INPUT "Do you know relative humidity (N or Y)";D$
680 IF D$="N" THEN 760
690 PRINT
700 IF E>1 THEN 760
710 INPUT "Enter Rel. Humidity in %";H
720 'CALCULATING -Pc FROM HUMIDITY
730 N=H/100
740 P9=ABS(((D1*R*K)/(M*(100000!)))*LOG(N))
750 P1=INT(P9*100+.5)/100
760 GOSUB 1040
770 IF D$="Y" THEN 840
780 IF D$="N" THEN LET P9=P5
790 P1=INT(P9*100+.5)/100
```

```
800 'CALCULATING HUMIDITY FROM Pc
810 L=((-1)*P1*M*(100000!))/(R*K*D1)
820 H1=(2.71828^L)*100
830 H=INT(H1*100+.5)/100
840 'CALCULATING % WATER SATURATION
850 V4=W1/P2
860 V9=(V4/V)*100
870 V2=INT(V9*100+.5)/100
880 GOSUB 1470
890 PRINT #1,SL$;TAB(8);H;TAB(15);V3;TAB(24);V4;TAB(40);V2;TAB(52);P1;TAB(62);S1

900 LPRINT SL$;TAB(8);H;TAB(15);V3;TAB(24);V4;TAB(40);V2;TAB(52);P1;TAB(62);S1
910 PRINT
920 RESTORE
930 E=E+1
940 WEND
950 INPUT "DO YOU WANT TO CALCULATE VALUES FOR ANOTHER WELL (Y OR N)";G$
960 IF G$="Y" THEN GOTO 990
970 CLOSE
980 END
990 LPRINT
1000 LPRINT
1010 PRINT #1,
1020 PRINT #1,
1030 RUN
1040 '**SUBROUTINE FOR CONC. VS. PC TO CALC H**
1050 PRINT
1055 IF D$="Y" OR E>1 THEN C$="N":GOTO 1070
1060 INPUT "IS THIS A SATURATED NaCl SOLUTION (Y or N)";C$
1070 PRINT
1080 IF C$="N" THEN 1110
1090 P5=379.7*K/293
1100 GOTO 1120
1110 IF D$<>"Y" THEN INPUT "Enter NaCl concentration in molarity";C
1120 IF E>1 THEN 1140
1130 DIM Z(17,2)
1140 DATA 6.1,379.7,2.0,96,1.7,80,1.3,60,1.0,45,.88,40.9,.79,36.2,.69,31.6
1150 DATA .59,27,.5,22,.4,17.9,.3,13.5,.2,9,.099,4.54,.05,2.3,0,0
1160 FOR I=1 TO 16 STEP 1
1170 FOR J=1 TO 2 STEP 1
1180 READ Z(I,J)
1190 NEXT J
1200 IF C$="Y" THEN 1230
1210 IF C<>Z(I,1) THEN GOTO 1230
1220 P5=Z(I,2)*(K/293)
1230 NEXT I
1240 IF C$="Y" THEN 1460
1250 'EXTRAPOLATING BETWEEN KNOWN CONC. VS. Pc VALUES
1260 FOR I=1 TO 16 STEP 1
1270 IF C=Z(I,1) THEN 1450
1280 IF I<2 THEN 1450
1290 Q=I-1
1300 IF NOT (C<Z(Q,1) AND C>Z(I,1)) THEN 1450
1310 B1=Z(Q,1)-Z(I,1)
1320 F1=C-Z(I,1)
1330 B3=Z(I,2)
1340 F2=F1/B1
1350 B2=Z(Q,2)
1360 B3=Z(I,2)
1370 F2=F1/B1
1380 F3=B2-B3
1390 F4=F2*F3
1400 B=F4+B3
1410 P5=B*K/293
1420 H9=100*EXP((P5*M)/((100000!)*D1*R*K))
1430 IF H9>=100 THEN LET H=INT(H9):GOTO 1460
1440 H=INT(H9*100+.5)/100
1450 NEXT I
1460 RETURN
1470 '**SUBROUTINE T (C) VS. WATER SATURATION V.P.**
1480 IF E>1 THEN 1500
1490 DIM V(19,2)
1500 FOR I=1 TO 18 STEP 1
1510 FOR J=1 TO 2 STEP 1
1520 READ V(I,J)
1530 DATA 14,1.1987,15,1.2788,16,1.3634,17,1.4530,18,1.5477,19,1.6477,20,1.7535,
21,1.8650,22,1.9827,23,2.1068,24,2.2377,25,2.3756,26,2.5209,27,2.6739,28,2.8349,
29,3.0043,30,3.1824,31,3.3695
1540 NEXT J
1550 IF INT(T1)<>V(I,1) THEN 1590
1560 Z5=V(I,2)
1570 D=I+1
1580 Q=I
1590 NEXT I
1600 X1=(T1-INT(T1))
1610 V(Q,2)=(X1*(V(D,2)-Z5))+Z5
1620 S=V(Q,2)*.0133322
1630 IF T<15 THEN LET S=V(1,2)*.0133322
1640 IF T>30 THEN LET S=V(19,2)*.0133322
1650 S1=S*(H/100)
1660 RETURN
```

APPENDIX γ

C. PORSFC.BAS Operating Instructions

1. Turn on computer and printer.
2. At the prompt, type BASIC and enter.
3. At OK, hit F3--type the disk drive, colon, PORSFC.BAS and enter. For example: B:PORSFC.BAS
4. At OK, hit F2 (you are now in the program).
5. Make sure the Caps Lock is on.
6. Type in well name and enter.
7. Type in sample label and enter; type STOP at this prompt to end program.
8. Type in sample depth and enter.
9. Type in the initial dry weight of the sample and enter.
10. Type in the maximum power radius chosen for the calculations and enter.
11. Type in the minimum pore radius chosen for the calculations and enter.
12. Type in the pore volume and enter.
13. If no mistakes have been made answering the above prompts, type N (for No) and enter. (Answering with a Y loops you back up to the sample depth prompt and Steps 8 through 13 are repeated.)
14. Type in the quantity of water for the relative humidity (H) of .998 and enter.
15. Type in the quantity of water corresponding to the maximum H as determined by the maximum pore radius.
16. Type in the next lower H, enter, then type in the quantity of water corresponding to this H. Repeat this step until minimum relative humidity, as determined by the minimum pore radius, is reached.
17. Type -99 to end the data entry.

18. If no mistakes have been made answering the above prompts, type N (for No) and enter. (Answering with a Y loops you back up to Step 14.)
19. Type in water density at the average temperature of the experiment.
20. Computing the pore-size distribution and surface area takes a couple of minutes. At the end of the calculations, the sample label prompt will re-appear. Repeat Steps 7 through 20 to continue with the same well.
21. Type STOP at the sample label.
22. Type Y to start a new well. Type N to end the program.
23. When the program is ended type SYSTEM and enter.
24. Type PARK and enter.

D. Listing for the PC program PORSFC.BAS.

```
10 CLS
20 '**THIS PROGRAM, porsfc.bas, CALCULATES PORE-SIZE DISTRIBUTION AND SFC AREA**

30 '**THE CALCULATIONS IN THIS PROGRAM ARE BASED ON THE BJH METHOD**
40 PRINT
50 PRINT "**** This procedure is based on an imaginary emptying of the pores by
the"
60 PRINT "step-wise lowering of relative humidity ****
70 OPEN "A",1,"PORFILE1.DATA"
80 PRINT
90 E=1
100 INPUT "Enter Well Name";WN$
110 PRINT
120 PRINT "**    **    **    **    **    **    **    **    **
130 PRINT
140 PRINT "TYPE 'STOP' AT SAMPLE LABEL TO END DATA ENTRY"
150 PRINT
160 WHILE SL$<>"STOP"
170 PRINT
180 PRINT "TYPE 'STOP' AT SAMPLE LABEL TO END DATA ENTRY FOR THIS WELL"
190 PRINT
200 INPUT "Enter Sample Label";SL$
210 IF SL$="STOP" THEN 2590
220 PRINT
230 INPUT "Enter Sample Depth in feet below ground level";SD$
240 PRINT
250 INPUT "Enter initial dry wt. of sample in g";F
260 LPRINT "Well Name:  ";WN$
270 LPRINT
280 LPRINT "Sample No.:  ";SL$;"    Sample Depth (ft below g.l.):  ";SD$
290 LPRINT
300 LPRINT "Pore Radius";TAB(15);"Sfc Area";TAB(26);"Pore Vol";TAB(37);"Cumulate
d Sfc Area";TAB(57);"Cumulate Pore Vol"
310 LPRINT TAB(3);"(angs)";TAB(16);"(m2/g)";TAB(26);"(mm3/g)";TAB(42);"(m2/g)";T
AB(62);"(mm3/g)"
320 LPRINT "___________";TAB(15);"________";TAB(26);"________";TAB(37);"________
_________";TAB(57);"_________________"
330 LPRINT
340 PRINT #1,"Well Name:  ";WN$
350 PRINT #1,
360 PRINT #1,"Sample No.:  ";SL$;"    Sample Depth (ft below g.l.):  ";SD$
370 PRINT #1,
380 PRINT #1,"Pore Radius";TAB(15);"Sfc Area";TAB(26);"Pore Vol";TAB(37);"Cumula
ted Sfc Area";TAB(57);"Cumulate Pore Vol"
390 PRINT #1,TAB(3);"(angs)";TAB(16);"(m2/g)";TAB(26);"(mm3/g)";TAB(42);"(m2/g)"
;TAB(62);"(mm3/g)"
400 PRINT #1,"___________";TAB(15);"________";TAB(26);"________";TAB(37);"______
___________";TAB(57);"_________________"
410 PRINT #1,
420 PRINT
430 IF E>1 THEN 540
440 INPUT "Enter maximum pore radius in angstroms (for cylindrical pores)";R1
450 PRINT
460 INPUT "Enter minimum pore radius in angstroms";R2
470 Q8=-10.555/R1
480 X8=2.7182818#^Q8
490 Q7=-10.555/R2
500 X7=2.7182818#^Q7
510 R3=R1+100
520 Q9=-10.555/R3
530 X9=2.7182818#^Q9
540 PRINT
550 INPUT "Enter the pore volume of this sample (in cm3)";Y9
560 PRINT
570 INPUT "Do you wish to change any of the above information";AN$
580 IF AN$="Y" THEN 230
590 '**** p/po vs. q ****
600 Z=1
610 IF E>1 OR Z>1 THEN 640
620 OPTION BASE 1
630 DIM Z(20,2)
640 K=1
650 PRINT
660 INPUT "Enter quantity of water adsorbed in g for rel. humidity of 0.998";Z8
670 Z9=Z8/F
680 PRINT
690 PRINT K
700 Z(1,1)=INT(X9*100+.5)/100
710 PRINT "FOR THE CHOSEN MAXIMUM PORE RADIUS, THE MAXIMUM HUMIDITY IS";Z(1,1)
```

```
720 PRINT
730 INPUT "Enter quantity of water in g adsorbed at the max. rel. humidity";F1
740 Z(1,2)=F1/F
750 PRINT
760 X6=INT(X7*100+.5)/100
770 PRINT
780 PRINT "FOR THE CHOSEN MINIMUM PORE RADIUS, THE MINIMUM HUMIDITY IS";X6
790 PRINT
800 PRINT "ENTER -99 AT THE REL. HUMIDITY PROMPT WHEN YOU WANT TO STOP ENTERING"

810 PRINT
820 K=K+1
830 PRINT
840 PRINT K;")"
850 INPUT "Enter next lower rel. humidity (as a fraction)";Z(K,1)
860 IF Z(K,1)<-1 THEN 900
870 PRINT
880 INPUT "Enter corresponding quantity of water adsorbed in g";F1
890 Z(K,2)=F1/F
900 IF Z(K,1)>-1 THEN 820
910 J=K-1
920 PRINT
930 INPUT "Do you want to change any of the above values";B$
940 IF B$="Y" THEN Z=Z+1:GOTO 610
950 IF E>1 THEN 1010
960 OPTION BASE 1
970 DIM T(J),C(J),A1(K),A2(J),Q1(J),D1(K),D2(J),D3(J),V1(J),V(J)
980 DIM B(J),C5(J),D9(J),V2(J),D4(J),S1(J),S2(J),D5(K),A3(J),S3(J),X1(J),X2(J)
990 DIM D6(J),A(J),L1(J),D7(J),S4(J),X3(J),S5(J),X4(K),R(K),N1(J)
1000 DIM M(K),N(K),P(K),Q(K),S(K),D(J)
1010 PRINT
1020 PRINT
1030 '**** core radius, C1, (angstroms) ****
1040 X=Z9
1050 C1=-10.555/LOG(X)
1060 FOR L=1 TO J STEP 1
1070 X=Z(L,1)
1080 IF X=1 THEN LET X=.999
1090 C(L)=-10.555/LOG(X)
1100 NEXT L
1110 '**** (avg) thickness of adsorbed film layer (T), pore radius (R), angs ***
*
1120 T1=(2!*(Z9/18.0152)/4.748E-05)
1130 FOR L=1 TO J STEP 1
1140 T(L)=2!*((Z(L,2)/18.0152)/4.748E-05)
1150 R(L)=C(L)+T(L)
1160 NEXT L
1170 '**** avg pore radius A1 (angs) ****
1180 IF R1>R(1) THEN A1(1)=((R1-R(1))/2)+R(1):GOTO 1220
1190 R1=R(1)
1200 R5=R(1)-R(2)+R(1)
1210 A1(1)=((R5-R(1))/2)+R1
1220 FOR L=2 TO J STEP 1
1230 P=L-1
1240 A1(L)=((R(P)-R(L))/2)+R(L)
1250 NEXT L
1260 '**** avg core radius A2(J) (angs) ****
1270 C1=(C(1)-C(2))/2
1280 A2(1)=C1+C(1)
1290 FOR L=2 TO J STEP 1
1300 P=L-1
1310 A2(L)=((C(P)-C(L))/2)+C(L)
1320 NEXT L
1330 '**** avg thickness (A3), calc Q, dt (D2), drp (D1) (angs) ****
1340 D1(1)=R5-R1
1350 FOR L=2 TO J STEP 1
1360 P=L-1
1370 D1(L)=R(P)-R(L)
1380 NEXT L
1390 A3(1)=(D1(1)/2)+T(1)
1400 X=A1(1)/(A1(1)-T(1))
1410 Q1(1)=X*X
1420 D2(1)=ABS(T1-T(1))
1430 FOR L=2 TO J STEP 1
1440 P=L-1
```

```
1450 A3(L)=((T(P)-T(L))/2)+T(L)
1460 X=A1(L)/(A1(L)-T(L))
1470 Q1(L)=X*X
1480 D2(L)=ABS(T(P)-T(L))
1490 NEXT L
1500 PRINT
1510 PRINT
1520 INPUT "Enter water density for the given temperature in g/cm3";R9
1530 FOR L=1 TO J STEP 1
1540 V1(L)=1000*((Z(L,2)*F)/R9)
1550 V(L)=INT(V1(L)*100+.5)/100
1560 NEXT L
1570 '**** calculate dV (mm3) ****
1580 D3(1)=0
1590 FOR L=2 TO J STEP 1
1600 P=L-1
1610 D3(L)=V(P)-V(L)
1620 NEXT L
1630 '**** calculate dvp (D) (mm3) from A (cm2), L (cm), and dvf(mm3) ****
1640 D(1)=0:D4(1)=0:A(1)=0:L1(1)=0:D2(1)=0
1650 A(2)=(2*D(1)/A1(1))*100000!
1660 A9=A(1)+A(2)
1670 L1(2)=(A(2)/(2*3.14159265#*R(1)))*1E+08
1680 L9=L1(1)+L1(2)
1690 D4(2)=((A9*D2(1)*1E-08)-(2*3.14159265#*D2(1)*T(1)*L9*1E-16))*1000
1700 D(2)=Q1(2)*D3(2)
1710 FOR L=3 TO J STEP 1
1720 P=L-1
1730 A(L)=(2*D(P)/A1(P))*100000!
1740 L1(L)=(A(L)/(2*3.14159265#*R(P)))*1E+08
1750 A9=A9+A(L)
1760 L9=L9+L1(L)
1770 D4(L)=((A9*D2(P)*1E-08)-(2*3.14159265#*D2(P)*T(P)*L9*1E-16))*1000
1780 D(L)=Q1(L)*(D3(L)-D4(L))
1790 NEXT L
1800 '**** calculate dA and Sum(dA) (for D) in cm2 ****
1810 S1(1)=0:D6(1)=0
1820 FOR L=2 TO J STEP 1
1830 P=L-1
1840 D6(L)=(20*D(L)/A1(L))*100000!
1850 S1(L)=S1(P)+D6(L)
1860 NEXT L
1870 '**** calculate dA/rmp and Sum(dA/rmp) in cm2/angs (for D)
1880 X1(1)=0:S3(1)=0
1890 FOR L=2 TO J STEP 1
1900 P=L-1
1910 X1(L)=D6(L)/A1(L)
1920 S3(L)=S3(P)+X1(L)
1930 NEXT L
1940 '**** calculating the B (mm3), C (angs), D (mm3) values ****
1950 '**** recalc dvp, D5 in mm3, and Sum(dvp), S2(L) in mm3 ****
1960 '**** dA(D7), Sum(dA) (S4(L), dA/rmp and Sum(dA/rmp) ****
1970 Y2=Y9*1000/F
1980 C5(1)=0:D9(1)=0:B(1)=0:D5(1)=0:S2(1)=0
1990 S4(1)=0:D7(1)=0:X3(1)=0:S5(1)=0
2000 E1=0
2010 FOR L=2 TO J STEP 1
2020 P=L-1
2030 B(L)=.1*D2(L)*1E-08*S1(P)
2040 C5(L)=.1*D2(L)*A3(L)*1E-08*S3(L)
2050 D9(L)=D3(L)-(B(L)*1000)+(C5(L)*1000)
2060 D5(L)=Q1(L)*D9(L)
2070 P(L)=D5(L)/F
2080 S2(L)=S2(P)+D5(L)
2090 S(L)=S2(L)/F
2100 D7(L)=20*D5(L)*.001/(A1(L)*1E-08)
2110 N(L)=D7(L)*.0001/F
2120 S4(L)=S4(P)+D7(L)
2130 Q(L)=S4(L)*.0001/F
2140 X3(L)=D7(L)/A1(L)
2150 S5(L)=S5(P)+X3(L)
2160 NEXT L
2170 GOSUB 2640
2180 '**** calculate dvp/drp (mm3/angs) for D5 (X4 in mm3) ****
```

```
2190 X2(1)=0:X4(1)=0
2200 FOR L=2 TO K STEP 1
2210 X4(L)=D5(L)/D1(L)
2220 NEXT L
2230 FOR L=1 TO K STEP 1
2240 IF R(L)>.01 THEN M(L)=INT(R(L)*100+.5)/100
2250 IF N(L)>.01 THEN N(L)=INT(N(L)*100+.5)/100
2260 IF P(L)>.01 THEN P(L)=INT(P(L)*100+.5)/100
2270 IF Q(L)>.01 THEN Q(L)=INT(Q(L)*100+.5)/100
2280 IF S(L)>.01 THEN S(L)=INT(S(L)*100+.5)/100
2290 PRINT #1,M(L);TAB(15);N(L);TAB(26);P(L);TAB(38);Q(L);TAB(58);S(L)
2300 LPRINT M(L);TAB(15);N(L);TAB(26);P(L);TAB(38);Q(L);TAB(58);S(L)
2310 NEXT L
2320 PRINT
2330 PRINT #1,
2340 LPRINT
2350 PRINT #1,
2360 LPRINT
2370 PRINT #1,"For Pore Size Distribution, plot:  change in pore vol/change in p
ore radius vs. mean pore radius (in mm3/angs):
2380 LPRINT "For Pore Size Distribution, plot:   change in pore vol/change in po
re radius vs. mean pore radius (in mm3/angs):
2390 PRINT #1,
2400 LPRINT
2410 PRINT #1,TAB(20);"dvp/drp";TAB(45);"mean pore radius"
2420 LPRINT TAB(20);"dvp/drp";TAB(45);"mean pore radius"
2430 PRINT #1,TAB(20);"_______";TAB(45);"_________________"
2440 LPRINT TAB(20);"_______";TAB(45);"_________________"
2450 PRINT #1,
2460 LPRINT
2470 IF E>1 THEN 2500
2480 OPTION BASE 1
2490 DIM U(J),W(J)
2500 FOR L=1 TO K STEP 1
2510 IF X4(L)>.01 THEN U(L)=INT(X4(L)*100+.5)/100
2520 IF A1(L)>.01 THEN W(L)=INT(A1(L)*100+.5)/100
2530 PRINT #1,TAB(20);U(L);TAB(45);W(L)
2540 LPRINT TAB(20);U(L);TAB(45);W(L)
2550 NEXT L
2560 E=E+1
2570 WEND
2580 PRINT
2590 INPUT "DO YOU WANT TO CALCULATE VALUES FOR ANOTHER WELL (Y or N)";G$
2600 IF G$="Y" THEN 2630
2610 CLOSE
2620 END
2630 RUN
2640 '**** SUBROUTINE TO DEAL WITH THE FINAL dvf ****
2650 E1=0:E2=0:G=0:K=0:P=0
2660 FOR L=1 TO J STEP 1
2670 IF R2<R(L) THEN 2690
2680 E1=E1+1
2690 IF S(L)<Y2 THEN 2710
2700 E2=E2+1
2710 NEXT L
2720 IF E1>E2 THEN G=E1:GOTO 2740
2730 G=E2
2740 P=J-G
2750 K=P+1
2760 R(K)=R2
2770 D1(K)=R2-0
2780 P(K)=Y2-S(P)
2790 A1(K)=((R(P)-R2)/2)+R2
2800 S(K)=P(K)+S(P)
2810 D5(K)=P(K)*F
2820 D7(K)=20*D5(K)*.001/(A1(K)*1E-08)
2830 N(K)=D7(K)*.0001/F
2840 Q(K)=Q(P)+N(K)
2850 RETURN
```

REFERENCES

Anderson, W. G., "Wettability Literature Survey--Part 4: Effect of Wettability on Capillary Pressure," JPT, 1987, p. 1282-1300.

Campbell, G. S., An Introduction to Environmental Biophysics, New York: Springer-Verleg, 1977, p. 21-31.

Cole, K. M. and J. A. Reger, "Humidity Calibration Techniques," Instruments and Control System, 1970.

CRC, Handbook of Chemistry and Physics 55th ed., CRC Press, Inc., 1974, p. 63-B156, D159, D224-D225.

Daian, J. F., "Condensation and Isothermal Water Transfer in Cement Mortar Part I--Pore Size Distribution, Equilibrium Water Condensation and Imbibition," Transport in Porous Media 3, 1988, p. 563-589.

Dumore, J. M. and R. S. Schols, "Drainage Capillary-Pressure Functions and Their Computation from One Another," Soc. of Petrol. Eng. of AIME, 1972, p. 12.

EG&G Idaho, Inc., Standard Practice Buried Waste Program Data Integrity Review Committee, EG&G DIRC Draft Report, 1988, p. 9.

Franklin, J. A., "Suggested Methods for Determining H_2O Content, Porosity Density, Absorption, and Related Properties and Swelling and Slake-Durability Index Properties," Int. Soc. Rock Mech. Comm. on Lab. Tests., Doc. 2, 1972, p. 36.

Gregg, S. J. and K. S. W. Sing, Adsorption, Surface Area and Porosity, 2nd ed., Academic Press, New York, NY, 1982, p. 303.

Harris, J., SC-10A Thermocouple Psychrometer Sample Changer Operator's Manual, Decagon Devices, Inc., Table 2.

Hoel, P. G. Introduction to Mathematical Statistics, 5th ed., John Wiley & Sons, Inc., New York, 1984, p. 435.

Katz, D. L., D. Cornell, R. Kobayashi, F. H. Poettmann, J. A. Vary, J. R. Elenbaas, and C. G. Weinaug, Handbook of Natural Gas Engineering, McGraw-Hill, 1959, p. 33-68.

Livington, H. K. "Cross-sectional Areas of Molecules Adsorbed on Solid Surfaces," Journal of the Amer. Chem. Soc., v. 66, 1944, p. 569-573.

Luetkehans, J., A Laboratory Investigation of Steam Adsorption in Geothermal Reservoir Rocks, paper SGP-TR-115, Stanford University, Stanford, CA, 1988, p. 188.

Storer, R. A., et al., eds., ASTM Standards, Sect. 4, 1988, p. C-97.

Wexler, A. and W. G. Brombacher, "Methods of Measuring Humidity and Testing Hygrometers, a Review and Bibliography," NBS 51 no. 2, 1951, p. 263-280.

Wexler, A. and S. Hasegawa, "Relative Humidity-Temperature Relationships of Some Saturated Salt Solutions in the Temperature Range 0° to 50°," NBS 53 no. 1, 1954, p. 287-294.

Yuan, H. H. and B. F. Swanson, "Resolving Pore-Space Characteristics by Rate-Controlled Porosimetry," Soc. Pertrol. Eng. Paper SOE 14892, 1989, p. 17-24.